DOPAMINE NEURON DIVERSITY IN CIRCUITS AND DISEASES

EDITED BY: Jean-Francois Poulin, Talia Newcombe Lerner and Mark Howe

PUBLISHED IN: Frontiers in Neural Circuits

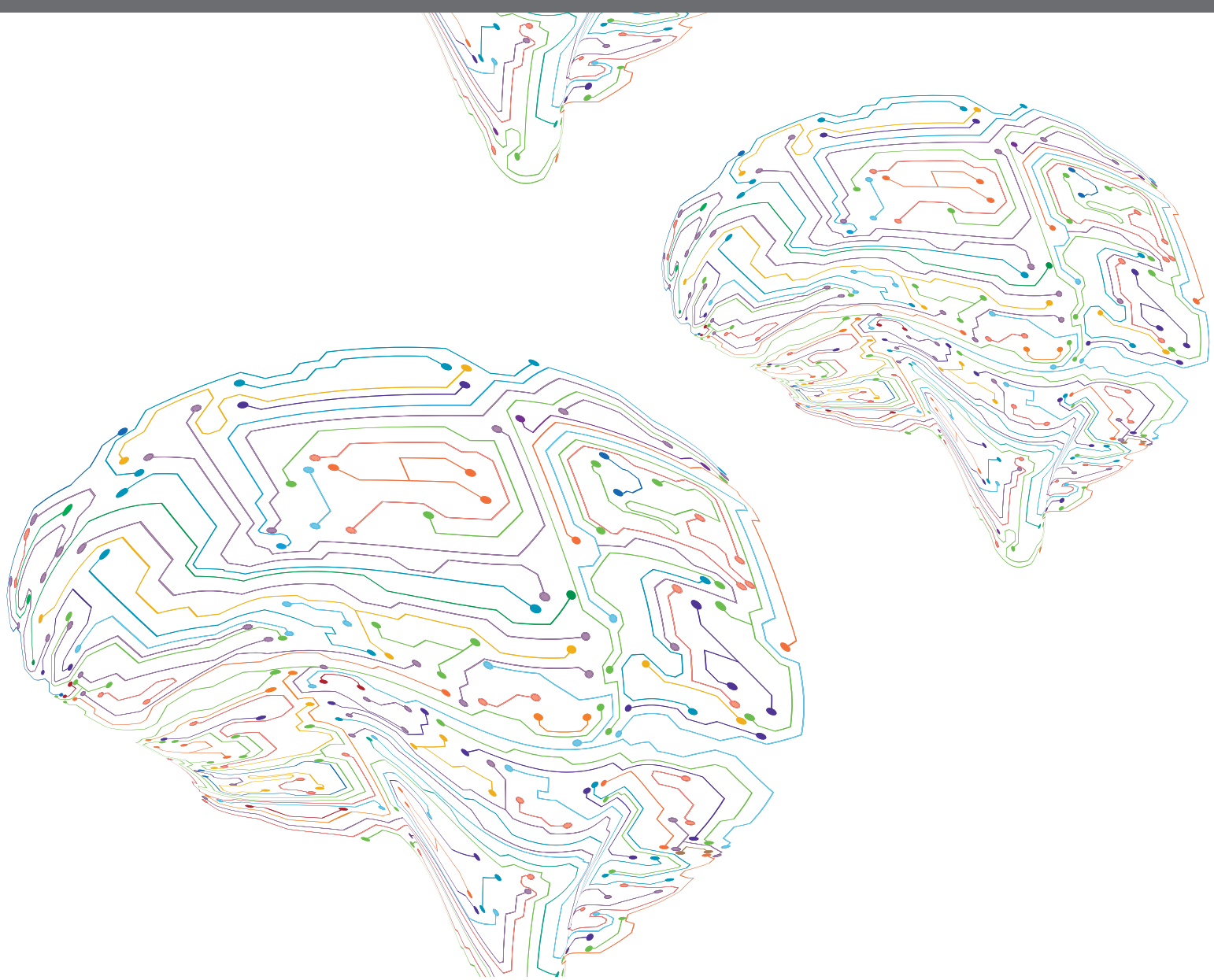

frontiers Research Topics

Frontiers eBook Copyright Statement

The copyright in the text of individual articles in this eBook is the property of their respective authors or their respective institutions or funders. The copyright in graphics and images within each article may be subject to copyright of other parties. In both cases this is subject to a license granted to Frontiers.

The compilation of articles constituting this eBook is the property of Frontiers.

Each article within this eBook, and the eBook itself, are published under the most recent version of the Creative Commons CC-BY licence. The version current at the date of publication of this eBook is CC-BY 4.0. If the CC-BY licence is updated, the licence granted by Frontiers is automatically updated to the new version.

When exercising any right under the CC-BY licence, Frontiers must be attributed as the original publisher of the article or eBook, as applicable.

Authors have the responsibility of ensuring that any graphics or other materials which are the property of others may be included in the CC-BY licence, but this should be checked before relying on the CC-BY licence to reproduce those materials. Any copyright notices relating to those materials must be complied with.

Copyright and source acknowledgement notices may not be removed and must be displayed in any copy, derivative work or partial copy which includes the elements in question.

All copyright, and all rights therein, are protected by national and international copyright laws. The above represents a summary only. For further information please read Frontiers' Conditions for Website Use and Copyright Statement, and the applicable CC-BY licence.

ISSN 1664-8714
ISBN 978-2-88974-753-5
DOI 10.3389/978-2-88974-753-5

About Frontiers

Frontiers is more than just an open-access publisher of scholarly articles: it is a pioneering approach to the world of academia, radically improving the way scholarly research is managed. The grand vision of Frontiers is a world where all people have an equal opportunity to seek, share and generate knowledge. Frontiers provides immediate and permanent online open access to all its publications, but this alone is not enough to realize our grand goals.

Frontiers Journal Series

The Frontiers Journal Series is a multi-tier and interdisciplinary set of open-access, online journals, promising a paradigm shift from the current review, selection and dissemination processes in academic publishing. All Frontiers journals are driven by researchers for researchers; therefore, they constitute a service to the scholarly community. At the same time, the Frontiers Journal Series operates on a revolutionary invention, the tiered publishing system, initially addressing specific communities of scholars, and gradually climbing up to broader public understanding, thus serving the interests of the lay society, too.

Dedication to Quality

Each Frontiers article is a landmark of the highest quality, thanks to genuinely collaborative interactions between authors and review editors, who include some of the world's best academicians. Research must be certified by peers before entering a stream of knowledge that may eventually reach the public - and shape society; therefore, Frontiers only applies the most rigorous and unbiased reviews.
Frontiers revolutionizes research publishing by freely delivering the most outstanding research, evaluated with no bias from both the academic and social point of view. By applying the most advanced information technologies, Frontiers is catapulting scholarly publishing into a new generation.

What are Frontiers Research Topics?

Frontiers Research Topics are very popular trademarks of the Frontiers Journals Series: they are collections of at least ten articles, all centered on a particular subject. With their unique mix of varied contributions from Original Research to Review Articles, Frontiers Research Topics unify the most influential researchers, the latest key findings and historical advances in a hot research area! Find out more on how to host your own Frontiers Research Topic or contribute to one as an author by contacting the Frontiers Editorial Office: frontiersin.org/about/contact

DOPAMINE NEURON DIVERSITY IN CIRCUITS AND DISEASES

Topic Editors:
Jean-Francois Poulin, McGill University, Canada
Talia Newcombe Lerner, Northwestern University, United States
Mark Howe, Boston University, United States

Citation: Poulin, J.-F., Lerner, T. N., Howe, M., eds. (2022). Dopamine Neuron Diversity in Circuits and Diseases. Lausanne: Frontiers Media SA.
doi: 10.3389/978-2-88974-753-5

Table of Contents

frontiers in Neural Circuits

EDITORIAL
published: 02 March 2022
doi: 10.3389/fncir.2022.856716

Editorial: Dopamine Neuron Diversity in Circuits and Diseases

Jean-Francois Poulin[1]*, *Talia Newcombe Lerner*[2] and *Mark W. Howe*[3]

[1] Montreal Neurological Institute, McGill University, Montreal, QC, Canada, [2] Department of Physiology, Feinberg School of Medicine, Northwestern University, Chicago, IL, United States, [3] Department of Psychological and Brain Sciences, Boston University, Boston, MA, United States

Keywords: dopamine, circuit, mesocortical dopamine system, addiction, Parkinson's Disease, Autism Spectrum Disorder (ASD)

Editorial on the Research Topic

Dopamine Neuron Diversity in Circuits and Diseases

In 1957–1958, Arvid Carlsson demonstrated that dopamine (DA) acts as a neurotransmitter in the brain and pinpointed its crucial role in Parkinson's Disease (PD; Carlsson et al., 1957, 1958). This ground-breaking discovery, which won the Nobel Prize in 2000, led to the adoption of the DA precursor L-DOPA as a life-changing treatment for PD. Further technological developments such as the Falck-Hillarp fluorescence histochemical method (Dahlstrom and Fuxe, 1964), which allowed the visualization of monoamines in histological sections, and the discovery of the neurotoxin 6-hydroxydopamine (Uretsky and Iversen, 1970), which selectively targets DAergic and noradrenergic neurons, enabled identification of the three major ascending DAergic pathways of the mammalian brain: the nigrostriatal, mesocortical, and mesolimbic pathways (Moore and Bloom, 1978). In the last several decades, it has become increasingly apparent that diverse DA neuron populations exist within and across these three pathways which differ in their molecular signatures, developmental origins, physiological characteristics, anatomical connections, and functional roles during behavior. New sequencing approaches are revealing significant molecular diversity in DA neurons that has led to classifications of new subtypes with unique physiology and connectivity. Advances in *in-vivo* monitoring approaches are demonstrating that different DA neuron populations and their projections in the striatum transmit signals related to diverse aspects of rewarding and aversive outcomes, sensory stimuli, and behavior.

How DA neuron diversity impacts downstream striatal or cortical circuits, and how dysfunction in particular DA neurons subpopulations generates the symptoms of neurological and psychiatric disorders as disparate as PD, autism spectrum disorder, and addiction are currently Research Topics of intense investigation. Here, we present a Research Topic that contains a collection of both original and review articles illustrating the diversity of the midbrain DAergic system. This Research Topic of nine articles highlights key topics in the neuroanatomical, molecular, developmental, and functional determinants of DA diversity.

Fundamental differences in the physiological and wiring properties of DA neurons within individual neuroanatomical structures such as the substantia nigra pars compacta (SNc) and ventral tegmental area (VTA) are increasingly appreciated. The work of Montero et al. demonstrates such differences by characterizing the dendritic architecture and firing properties of DA neurons located within these structures. Their results suggest dendritic morphology shapes both the physiological properties and connectivity of DA neurons within a single neuroanatomical structure. Similarly, the article from Derdeyn et al. illustrates the diversity of synaptic input to VTA neurons and provides an in-depth analysis of rabies-based circuit mapping studies of the VTA. In addition, Eskenazi et al.

OPEN ACCESS

Edited and reviewed by:
Jochen Roeper,
Goethe University Frankfurt, Germany

***Correspondence:**
Jean-Francois Poulin
j-francois.poulin@mcgill.ca

Received: *17 January 2022*
Accepted: *31 January 2022*
Published: *02 March 2022*

Citation:
Poulin JF, Lerner TN and Howe MW (2022) Editorial: Dopamine Neuron Diversity in Circuits and Diseases. Front. Neural Circuits 16:856716. doi: 10.3389/fncir.2022.856716

provide a systematic review of DA neurons expressing the glutamate vesicular transporter Vglut2, which includes the synaptic properties and connectivity of these neurons.

Abnormal development of the DAergic system has a broad impact on behavior and vulnerability to neuropsychiatric diseases. Two articles provide an in-depth review of the early development and the maturation of the mesocortical pathway, contributed by Islam et al. and Reynolds and Flores, respectively. These articles summarize the current state of the field but also highlight windows of vulnerability to psychiatric and neurological conditions.

The DAergic system is particularly vulnerable and can be hacked by drugs of abuse to produce self-destructive behavioral patterns. The role of diverse DA pathways in substance abuse and addiction is expertly reviewed by Poisson et al., not an easy task due to the long history of this literature. In addition, the implications of DA neuron diversity in response to the drug of abuse amphetamine was investigated by Serra et al. focussing on a medial VTA subpopulation that expresses the gene *TrpV1*. Among other findings, Serra et al. demonstrate that removing the ability of TrpV1+ neurons to package and release DA leads to sensitization of the response to amphetamine.

Finally, the role of DA neuron diversity in neurological diseases is the Research Topic of two excellent articles. Kosillo and Bateup provide a nice overview of the DAergic dysfunction observed in genetic mouse models of Autism Spectrum Disorders (ASD). Although it is increasingly clear that DA plays a significant role in symptoms of ASD, the authors conclude that more investigations are needed if a complete picture of the role of diverse DA populations is to emerge. On the other hand, the picture of DA diversity in PD is clearer as a subtype of DA neuron, defined by the expression of *Aldh1a1* and located in the SNc, appears to be selectively vulnerable in PD. Carmichael et al. review what is currently known about this DA neuron population and its role in motor control and PD.

Overall, tremendous progress has been made since the pioneering work of Carlsson. Discoveries regarding the rich diversity within the midbrain DA system are both fascinating and necessary for the further development of treatments for an array of neurological and psychiatric disorders. We are indebted to the authors for their contributions to this Research Topic and hope you'll enjoy reading these articles as much as we did.

AUTHOR CONTRIBUTIONS

All authors listed have made a substantial, direct, and intellectual contribution to the work and approved it for publication.

ACKNOWLEDGMENTS

J-FP would like to acknowledge funding from Parkinson's Canada, HBHL, Azrieli foundation, Brain Canada, and NSERC. TL would like to acknowledge funding from the NIH (DP2MH122401, P50DA044121, and R01DK090625), and Aligning Science Across Parkinson's (ASAP). MH would like to acknowledge funding from the Klingenstein-Simons Foundation, Whitehall Foundation, Parkinson's Foundation, ASAP, the NIH (R01MH125835-01), and Boston University's Centers for Neurophotonics and Systems Neuroscience.

REFERENCES

Carlsson, A., Lindqvist, M., and Magnusson, T. (1957). 3,4-Dihydroxyphenylalanine and 5-hydroxytryptophan as reserpine antagonists. *Nature* 180:1200. doi: 10.1038/1801200a0

Carlsson, A., Lindqvist, M., Magnusson, T., amd Waldeck, B. (1958). On the presence of 3-hydroxytyramine in brain. *Science* 127:471. doi: 10.1126/science.127.3296.471

Dahlstrom, A., and Fuxe, K. (1964). Localization of monoamines in the lower brain stem. *Experientia* 20, 398–399. doi: 10.1007/BF02147990

Moore, R. Y., and Bloom, F. E. (1978). Central catecholamine neuron systems: anatomy and physiology of the dopamine systems. *Annu. Rev. Neurosci.* 1, 129–169. doi: 10.1146/annurev.ne.01.030178.001021

Uretsky, N. J., and Iversen, L. L. (1970). Effects of 6-hydroxydopamine on catecholamine containing neurones in the rat brain. *J. Neurochem.* 17, 269–278. doi: 10.1111/j.1471-4159.1970.tb02210.x

Conflict of Interest: The authors declare that the research was conducted in the absence of any commercial or financial relationships that could be construed as a potential conflict of interest.

Publisher's Note: All claims expressed in this article are solely those of the authors and do not necessarily represent those of their affiliated organizations, or those of the publisher, the editors and the reviewers. Any product that may be evaluated in this article, or claim that may be made by its manufacturer, is not guaranteed or endorsed by the publisher.

Copyright © 2022 Poulin, Lerner and Howe. This is an open-access article distributed under the terms of the Creative Commons Attribution License (CC BY). The use, distribution or reproduction in other forums is permitted, provided the original author(s) and the copyright owner(s) are credited and that the original publication in this journal is cited, in accordance with accepted academic practice. No use, distribution or reproduction is permitted which does not comply with these terms.

frontiers in Neural Circuits

REVIEW
published: 17 May 2021
doi: 10.3389/fncir.2021.644776

Function and Regulation of ALDH1A1-Positive Nigrostriatal Dopaminergic Neurons in Motor Control and Parkinson's Disease

*Kathleen Carmichael[1,2], Rebekah C. Evans[3,4], Elena Lopez[1], Lixin Sun[1], Mantosh Kumar[1], Jinhui Ding[5], Zayd M. Khaliq[4] and Huaibin Cai[1]**

[1] Transgenic Section, Laboratory of Neurogenetics, National Institute on Aging, National Institutes of Health, Bethesda, MD, United States, [2] The Graduate Partnership Program of NIH and Brown University, National Institutes of Health, Bethesda, MD, United States, [3] Department of Neuroscience, Georgetown University Medical Center, Washington, DC, United States, [4] Cellular Neurophysiology Section, National Institute of Neurological Disorders and Stroke, National Institutes of Health, Bethesda, MD, United States, [5] Computational Biology Group, Laboratory of Neurogenetics, National Institute on Aging, National Institutes of Health, Bethesda, MD, United States

Dopamine is an important chemical messenger in the brain, which modulates movement, reward, motivation, and memory. Different populations of neurons can produce and release dopamine in the brain and regulate different behaviors. Here we focus our discussion on a small but distinct group of dopamine-producing neurons, which display the most profound loss in the ventral *substantia nigra pas compacta* of patients with Parkinson's disease. This group of dopaminergic neurons can be readily identified by a selective expression of aldehyde dehydrogenase 1A1 (ALDH1A1) and accounts for 70% of total nigrostriatal dopaminergic neurons in both human and mouse brains. Recently, we presented the first whole-brain circuit map of these ALDH1A1-positive dopaminergic neurons and reveal an essential physiological function of these neurons in regulating the vigor of movement during the acquisition of motor skills. In this review, we first summarize previous findings of ALDH1A1-positive nigrostriatal dopaminergic neurons and their connectivity and functionality, and then provide perspectives on how the activity of ALDH1A1-positive nigrostriatal dopaminergic neurons is regulated through integrating diverse presynaptic inputs and its implications for potential Parkinson's disease treatment.

Keywords: ALDH1A1, dopamine, Parkinson's disease, connectivity, motor learning, *substantia nigra*

OPEN ACCESS

Edited by:
Talia Newcombe Lerner, Northwestern University, United States

Reviewed by:
Yoshikazu Isomura, Tokyo Medical and Dental University, Japan
Jean-Francois Poulin, McGill University, Canada

****Correspondence:***
Huaibin Cai
caih@mail.nih.gov

Received: *21 December 2020*
Accepted: *26 April 2021*
Published: *17 May 2021*

Citation:
Carmichael K, Evans RC, Lopez E, Sun L, Kumar M, Ding J, Khaliq ZM and Cai H (2021) Function and Regulation of ALDH1A1-Positive Nigrostriatal Dopaminergic Neurons in Motor Control and Parkinson's Disease. Front. Neural Circuits 15:644776. doi: 10.3389/fncir.2021.644776

INTRODUCTION

Parkinson's disease (PD), the most common degenerative movement disorder, particularly affects basal ganglia dopamine transmission (Sulzer and Surmeier, 2013; Vogt Weisenhorn et al., 2016). One of the most prominent pathological hallmarks of the disease is a preferential degeneration of dopaminergic neurons (DANs) located in the ventrolateral tier of *substantia nigra pars compacta* (SNc) (Fearnley and Lees, 1991; Kordower et al., 2013). While a member of aldehyde dehydrogenase family genes termed murine class 1 (cytosolic) aldehyde dehydrogenase (AHD2) or aldehyde dehydrogenase 1A1 (ALDH1A1) was reported some time ago to be selectively expressed by a subpopulation of DANs in the rodent ventral SNc (McCaffery and Drager, 1994), it is until 20 years

later that research in post-mortem human brains demonstrates a conserved topological distribution of ALDH1A1-positive DANs in the human SNc as well as a more severe loss of ALDH1A1-positive nigrostriatal DANs (ALDH1A1$^+$ nDANs) in PD patients compared to the ALDH1A1-negative ones (Liu et al., 2014). ALDH1A1 is a key enzyme to mediate the biosynthesis of retinoic acids (McCaffery and Drager, 1994) and catabolism of reactive dopamine metabolites (Marchitti et al., 2007; Burke, 2010) in DANs. The reduction of ALDH1A1 expression may contribute to the etiopathogenesis of PD (Galter et al., 2003; Mandel et al., 2007; Werner et al., 2008; Grunblatt et al., 2017), whereas an increase of ALDH1A1 levels protects against dopaminergic neurodegeneration (Cai et al., 2014; Liu et al., 2014). Although the expression and biochemical function of ALDH1A1 protein is extensively documented, less is known regarding the molecular, electrophysiological, anatomical, and physiological properties of ALDH1A1$^+$ nDANs. We believe that a further in-depth study of ALDH1A1$^+$ nDANs will bridge the gap toward a cell-type specific understanding of neural circuit mechanisms and treatment of PD.

ALDH1A1 DEFINES AND PROTECTS A NIGROSTRIATAL DOPAMINERGIC NEURON SUBPOPULATION

The nigrostriatal DANs are diverse in nature and can be categorized into groups of distinct subpopulations based on location, gene expression profiles, electrophysiological properties, morphology, projection pattern, physiological functions, and vulnerabilities to various diseases (Liu et al., 2014; Poulin et al., 2014; Lerner et al., 2015; Menegas et al., 2015; Evans et al., 2017; Hook et al., 2018). Traditionally, midbrain DANs can be divided into three main subgroups, retrorubral field (RRF, A8), SNc (A9), and ventral tegmental area (VTA, A10), in human and rodents (Bentivoglio and Morelli, 2005; Vogt Weisenhorn et al., 2016). In the post-mortem brains of PD patients, the most profound loss of DANs has been seen in the ventral tier of SNc (Fearnley and Lees, 1991; Kordower et al., 2013). Further studies have demonstrated that these ventral DANs can be molecularly defined by a selective expression of ALDH1A1 (Cai et al., 2014; Liu et al., 2014). ALDH1A1 belongs to ALDH superfamily genes, which consist of 19 members in human genome (Koppaka et al., 2012) and 20 members in mouse genome (Cai et al., 2014). ALDH1A1 is predominantly and highly expressed by the ventral DANs in human and mouse SNc, suggesting its distinctive role in the function and survival of ventral DANs (Cai et al., 2014; Liu et al., 2014). As a multifunctional enzyme in DANs, ALDH1A1 mediates the synthesis of retinoic acids important for the differentiation of DANs during development (Jacobs et al., 2007). ALDH1A1 is also suggested to conduct the alternative synthesis of inhibitory transmitter GABA in DANs (Kim et al., 2015). More importantly, ALDH1A1 oxidizes the highly reactive dopamine catabolic intermediate dopamine-3,4-dihydroxyphenylacetaldehyde (DOPAL) and protects ALDH1A1$^+$ nDANs against DOPAL-induced cytotoxicity (Marchitti et al., 2007; Burke, 2010). A recent study suggests that DOPAL can be actively produced in DANs when the monoamine oxidase (MAO)-mediated dopamine oxidation is employed in ATP production in mitochondria (Graves et al., 2019). DOPAL is highly reactive and a lack of ALDH1A1 may lead to accumulation of DOPAL, which has been shown to promote cytotoxic polymerization of PD-related α-synuclein and compromise the functions of proteins important in the activity and survival of DANs (Rees et al., 2009). Accordingly, ALDH1A1$^+$ nDANs are less vulnerable to α-synuclein–mediated neurodegeneration compared with the ALDH1A1-negative ones in α-synuclein transgenic mice, while genetic deletion of *Aldh1a1* exacerbates DAN loss (Liu et al., 2014). Downregulation of *ALDH1A1* mRNA and protein levels along with severe loss of DANs has also been reported in the ventral SNc of post-mortem PD brains (Galter et al., 2003; Mandel et al., 2007; Werner et al., 2008). The reduction of ALDH1A1 expression in PD may weaken the protective function of ALDH1A1 in the ventral tier of SNc and predispose these neurons to degeneration at the later stages of disease (Cai et al., 2014). Therefore, a profound reduction of ALDH1A1 expression may represent the turning point toward pathogenicity of ventral SNc DANs undergoing neurodegeneration in PD and ALDH1A1 expression level and activity may be extrapolated as a useful biomarker to monitor the progression of the disease as well as potential therapeutic targets (Cai et al., 2014).

The ALDH1A1$^+$ DANs account for 63% of SNc, 32% of VTA and 5% of RRF DANs in mouse brains (Wu et al., 2019). The ALDH1A1$^+$ DANs also make up for 72% of SNc DANs in human brains (Liu et al., 2014), while the percentages in other midbrain brain regions remain to be determined. The ALDH1A1$^+$ DANs in VTA regions exhibit distinct connectivity patterns compared to their counterparts in SNc (Wu et al., 2019); however, little is known about their functional contribution to any behavioral phenotypes. Therefore, we focused the present review on the SNc ALDH1A1$^+$ DANs only.

MOLECULAR CHARACTERISTICS OF ALDH1A1-POSITIVE NIGROSTRIATAL DOPAMINERGIC NEURONS

The ALDH1A1$^+$ nDANs are closely clustered in the ventral tier of SNc (Wu et al., 2019). The most distinctive genetic markers for this subtype of DANs in rodents are *Aldh1a1* (McCaffery and Drager, 1994; Liu et al., 2014; Poulin et al., 2014) and *Aldh1a7* (Cai et al., 2014). The *Aldh1a7* gene is located next to the *Aldh1a1* in the mouse chromosome 19 and is highly homologous to the *Aldh1a1*. *Aldh1a7* gene is absent in the human genome, which may contribute to the higher sensitivity of human DANs to dopamine-related cytotoxicity and PD-related genetic insults (Cai et al., 2014; Liu et al., 2014). Recently, single-cell RNA-sequencing (scRNA-seq) in combination with various mRNA fluorescence *in situ* hybridization methods provide unprecedented molecular details for diverse DAN subpopulations at different developmental stages (Poulin et al., 2014; La Manno et al., 2016; Hook et al., 2018;

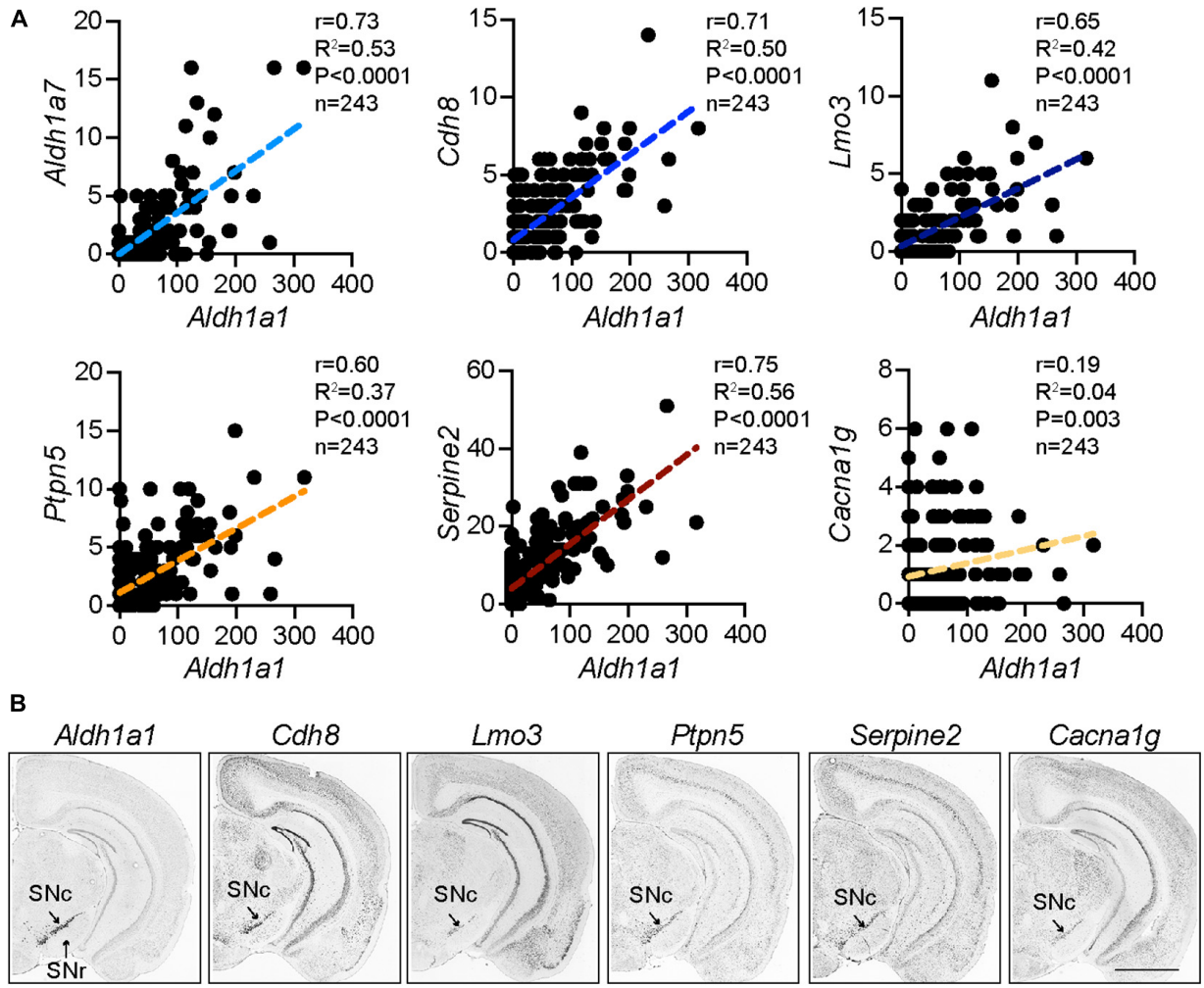

FIGURE 1 | Distinct molecular signature of ALDH1A1$^+$ nDANs. **(A)** Correlation of *Aldh1a1* expression with a selective set of genes in mature mouse DANs from a single cell RNA sequencing study (La Manno et al., 2016). **(B)** *In situ* hybridization of *Aldh1a1* and correlated genes in the SNc of adult mouse brains (Allen Brain Atlas).

Tasic, 2018; Tiklova et al., 2019). A number of genes are highly correlated with the *Aldh1a1* expression in the rodent DANs (La Manno et al., 2016), including *Lmo3*, *Cdh8*, *Serpine2*, *Ptpn5*, and *Aldh1a7* (**Figure 1A**), which also display a similarly restricted expression pattern in the ventral SNc as *Aldh1a1* mRNAs in mouse brains (Allen Brain Atlas) (**Figure 1B**), indicating these genes are among the molecular signature of ALDH1A1$^+$ nDANs. By contrast, there is no or extremely low expression of *calbindin* in the ALDH1A1$^+$ nDANs (Poulin et al., 2014; La Manno et al., 2016), which may serve as a useful marker for ALDH1A1-negative nigrostriatal DANs. In a recent scRNA-seq study with postnatal day 60 to 70 mouse brain, *Vglut2*, *Cbln4*, *Neurod6*, and *Tacr3* were added as additional markers for the mature ALDH1A1$^+$ nDANs (Saunders et al., 2018). Moreover, based on the unique expression of *Vcan*, *Anxa1*, and *Grin2C*, the ALDH1A1$^+$ nDANs can be further divided into three subpopulations (Saunders et al., 2018). The gene expression studies lay the foundation for later functional characterization of distinct ALDH1A1$^+$ nDANs subpopulations under normal and disease-related conditions.

ELECTROPHYSIOLOGICAL PROPERTIES OF ALDH1A1-POSITIVE NIGROSTRIATAL DOPAMINERGIC NEURONS

ALDH1A1$^+$ nDANs exhibit distinct electrophysiological properties and rebound more readily from hyperpolarization (Evans et al., 2017). To interrogate the electrophysiological properties of ALDH1A1$^+$ nDANs, we performed whole-cell recoding of tdTomato-labeled neurons in SNc slices of 2–5-month-old *Aldh1a1*$^{+/CreERT2}$/Ai9 mouse brains (**Figure 2A**). The ALDH1A1$^+$ nDANs fired spontaneous action potentials (APs) at a rate of 0.5–6 Hz (1.8 ± 0.4 Hz, n = 15). They had characteristically broad APs (1.9 ± 0.1 ms, n = 15) with a height

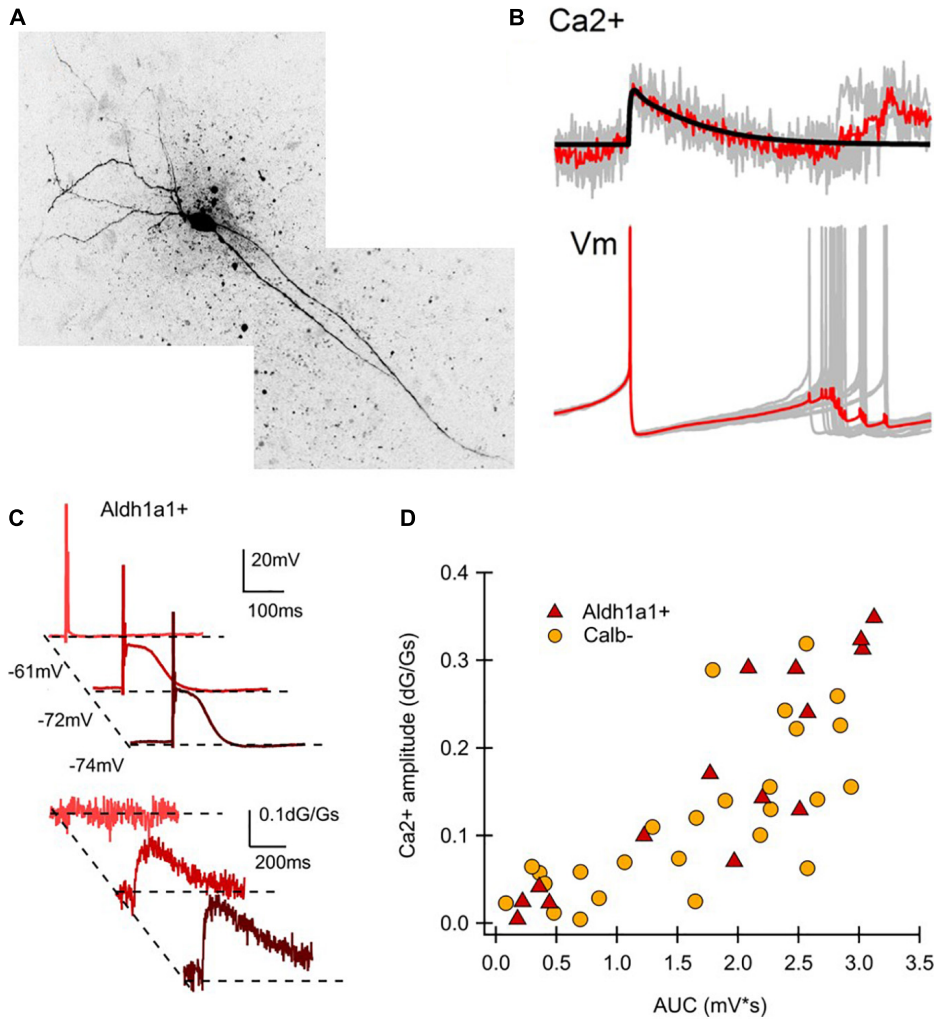

FIGURE 2 | Electrophysiological characteristics of ALDH1A1$^+$ nDANs. **(A)** Two-photon image of a ALDH1A1$^+$ nDAN. **(B)** Average calcium transient (above) and action potential (below) shape during tonic firing for a ALDH1A1$^+$ nDAN. **(C)** Hyperpolarization-dependent after depolarizations (above) and corresponding dendritic calcium transients (below) for a ALDH1A1$^+$ nDAN. **(D)** Amplitude of the calcium transient from a potential of −80 mV graphed by the area under the curve (AUC) for the corresponding low-threshold depolarization. Calb$^-$, Calbindin-negative population (data re-graphed from Evans et al., 2017, **(D)**, adult heated calbindin-negative population).

of 68.5 ± 2.5 mV, an input resistance of 327.5 ± 26.2 MΩ, and a capacitance of 63.3 ± 5.23. During each AP, a calcium transient of 0.033 ± 0.005 dG/Gs (n = 12) was apparent in the dendrites (**Figure 2B**). Furthermore, the ALDH1A1$^+$ nDANs shared many characteristics with the calbindin-negative neurons, which populate the ventral tier of the SNc (Evans et al., 2017). Specifically, the ALDH1A1$^+$ nDANs had a large voltage "sag" during hyperpolarization (17 ± 1.6 mV) indicative of a strong hyperpolarization cation current (I_h, **Figure 2C**). In addition, these neurons demonstrated large low-threshold depolarizations [area under the curve (AUC) from −80 mV membrane potential: 1.8 ± 0.28 mV *s, n = 15], indicative of strong T-type calcium channel activity. Using two-photon calcium imaging (see Evans et al., 2017 for methods), we found that these low-threshold depolarizations were accompanied by large dendritic calcium transients (0.17 ± 0.032 dG/Gs, n = 15) (**Figure 2C**). When graphing the size of the low threshold depolarization (AUC) by the calcium amplitude for each cell, labeled neurons from the *Aldh1a1*$^{+/CreERT2}$ mouse show a strong similarity to unlabeled (calbindin-negative) neurons from the calbindin-Cre mouse (**Figure 2D**), indicating that these neurons represent overlapping populations. Compared to the calbindin-positive DANs in the dorsal tier of SNc, the calbindin-negative DANs exhibit increased sensitivity to excitatory inputs following dopamine-mediated autoinhibitory stimulation, which then trigger large dendritic calcium transients likely through T-type calcium channels (Evans et al., 2017). The ventral DANs also display distinct rebound activity in response to the inhibitory inputs from striatal projection neurons (SPNs) (Evans et al., 2020; **Figure 3A**). Therefore, the ALDH1A1$^+$ nDANs appear to differ substantially in their responses to both excitatory and inhibitory presynaptic inputs compared to the calbindin-positive DANs,

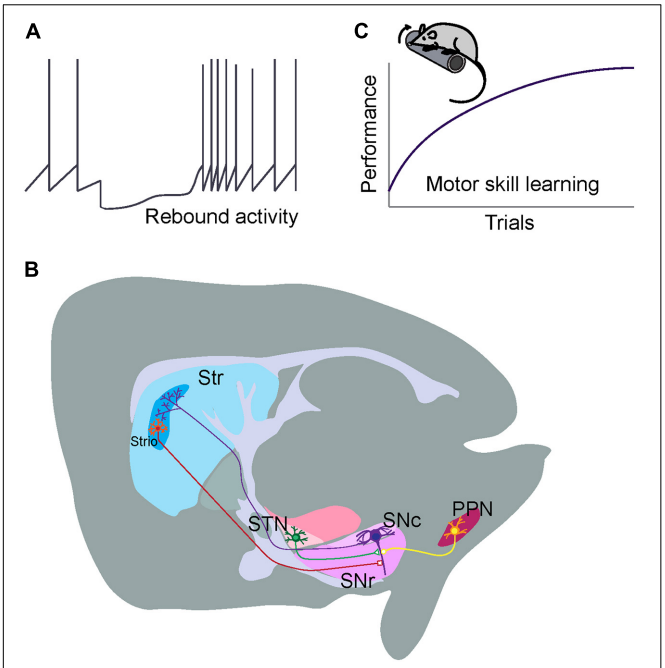

FIGURE 3 | Distinct electrophysiology, connectivity, and functionality of ALDH1A1$^+$ nDANs. **(A)** Rebound activity of ALDH1A1$^+$ nDANs following dSPN inhibition. **(B)** Major inhibitory and excitatory presynaptic inputs to the ALDH1A1$^+$ nDANs. **(C)** A critical involvement of ALDH1A1$^+$ nDANs in regulating the vigor of movement during the acquisition of motor skills.

which may contribute to their distinct physiological functions in motor control and learning. This absence of calbindin in the more PD-vulnerable ALDH1A1$^+$ nDANs also suggests the relevance of calcium buffering in PD pathophysiology (Surmeier and Schumacker, 2013).

PROJECTION PATTERN OF ALDH1A1-POSITIVE NIGROSTRIATAL DOPAMINERGIC NEURONS

The ALDH1A1$^+$ nDANs exhibit a distinct projection pattern in the rostral and dorsal portions of dorsal striatum (DS), including both the dorsomedial striatum (DMS) and dorsolateral striatum (DLS) (Sgobio et al., 2017; Poulin et al., 2018; Pan et al., 2019; Wu et al., 2019). In parallel with the location of their cell bodies in the SNc, the projection of ALDH1A1-positive axon fibers is arranged along the same medial to lateral axis in the DS (Wu et al., 2019). By contrast, ALDH1A1-positive nigrostriatal DANs in the more caudal SNc regions tend to innervate the more rostral striatal regions (Wu et al., 2019). In DS, the densities of ALDH1A1$^+$ nDAN axon fibers display a gradient change along the dorsal to ventral and rostral to caudal axes (Poulin et al., 2018; Wu et al., 2019). Noticeably, the ALDH1A1$^+$ nDANs project heavily to the dorsal portion of DS, the striatal region that is also heavily innervated by the sensorimotor cortices (Hintiryan et al., 2016); as well as the rostral striatal regions, which also receive mixed innervations from both associative and sensorimotor cortices (Hintiryan et al., 2016). The convergence of diverse cortical glutamatergic and midbrain dopaminergic inputs in the rostral DS indicates the functional importance of this striatal region in motor control and learning. Additionally, a small fraction of ALDH1A1-positive axon fibers converges to the striosome (or called patch) compartments in DS (Sgobio et al., 2017; Poulin et al., 2018; Wu et al., 2019; **Figure 3B**). The functional significance of this specific innervation remains to be determined. It needs be pointed out that ALDH1A1-positive DANs are also comprised of heterogenous subtypes and an individual subtype may possess distinct connectivity and functionality. With the increasing availability of single cell RNAseq data, we expect additional genetic markers could be identified to further molecularly define different subpopulations of ALDH1A1-positive DANs for more in-depth circuit studies.

MONOSYNAPTIC INPUTS ONTO ALDH1A1-POSITIVE NIGROSTRIATAL DOPAMINERGIC NEURONS

ALDH1A1-positive DANs receive the majority of monosynaptic inputs from the striatum (Wu et al., 2019). Compared to the non-specified nigrostriatal DAN total populations (Watabe-Uchida et al., 2012), ALDH1A1$^+$ nDANs receive more innervations from ventral striatum and hypothalamus, but less from cerebral cortices, pallidum, amygdala, and midbrain regions (Wu et al., 2019). Furthermore, ALDH1A1$^+$ nDANs appear to form reciprocal innervation with SPNs in the dorsal regions of DS (Wu et al., 2019). This reciprocal connection between ALDH1A1$^+$ nDANs and SPNs may constitute a feedback loop for timely regulating the dopamine release and neuron activity in motor control. Both striosome and matrix SPNs innervate ALDH1A1$^+$ nDANs in the ventral SNc (Wu et al., 2019). Some of the striosome SPN axons are intermingled with the dendrites of ventral ALDH1A1$^+$ nDANs perpendicularly protruding in the *substantia nigra pars reticulata* (SNr) and form this so-called striosome-dendron bouquet structure (Crittenden et al., 2016; Evans et al., 2020; **Figure 3B**), which may establish a unique striatonigral circuit for unspecified physiological functions. Besides the inhibitory presynaptic inputs from SPNs, ALDH1A1$^+$ nDANs receive the majority of excitatory monosynaptic inputs from subthalamus nucleus (Wu et al., 2019). The impact of both inhibitory and excitatory presynaptic inputs on the function and regulation of ALDH1A1$^+$ nDANs will be discussed in the later sections.

DOPAMINE RELEASE DYNAMICS OF ALDH1A1-POSITIVE NIGROSTRIATAL DOPAMINERGIC NEURONS

There has been no direct quantification of dopamine release from the axon terminals of ALDH1A1$^+$ nDAN in DS. Since ALDH1A1-positive dopaminergic axons converge onto striosome compartments in the DLS (Sgobio et al., 2017), afferent stimulus-evoked dopamine release was compared

between striosome and surrounding matrix compartments by fast scan cyclic voltammetry in a line of striosome reporter mice (Salinas et al., 2016; Sgobio et al., 2017), in which the green fluorescent protein-marked striosomes can be readily identified under epifluorescence microscope (Davis and Puhl, 2011; Sgobio et al., 2017). The amplitude of evoked dopamine release is lower in striosome compared to matrix compartments (Salinas et al., 2016; Sgobio et al., 2017). Genetic deletion of *Aldh1a1* selectively enhances dopamine release in striosomes, suggesting that ALDH1A1 actively regulates dopamine release in ALDH1A1–positive fibers projecting to the DLS striosomes, but not the surrounding matrix area (Sgobio et al., 2017). In addition, pharmacological inhibition of dopamine reuptake also leads to more dopamine release in the striosomes than in the proximal matrix areas (Davis and Puhl, 2011; Sgobio et al., 2017), correlated with a higher dopamine transporter (DAT) level in the ALDH1A1-positive axon terminals in the striosomes (Sgobio et al., 2017). DAT mediates the uptake of 1-methyl-4-phenyl-1,2,3,6-tetrahydropyridine (MPTP)-derived neurotoxin cation 1-methyl-4-phenylpyridinium (MPP^+) in DANs (Frim et al., 1994; Langston, 2017). The higher content of DAT in $ALDH1A1^+$ nDANs might be attributable to the increased sensitivity of $ALDH1A1^+$ nDANs to MPTP-mediated cytotoxicity (Poulin et al., 2014). By contrast, neither dopamine D2 autoreceptors nor nicotinic acetylcholine receptors appear to differentially regulate dopamine release in striosome and matrix compartments (Sgobio et al., 2017). The differential expression of ALDH1A1 and other proteins for dopamine synthesis, packaging, reuptake, and degradation in $ALDH1A1^+$ nDANs may contribute to the distinct dopamine release dynamics (Sgobio et al., 2017). With the availability of Cre mouse lines that specifically target gene expression in the $ALDH1A1^+$ DANs (Poulin et al., 2018; Wu et al., 2019) and genetically encoded dopamine sensors (Patriarchi et al., 2018; Sun et al., 2018), a direct measurement of dopamine release from $ALDH1A1^+$ nDANs in live behaving mice may provide new insight into how the dynamic of dopamine release contributes to the physiological function of $ALDH1A1^+$ nDANs.

PHYSIOLOGICAL FUNCTION OF ALDH1A1-POSITIVE NIGROSTRIATAL DOPAMINERGIC NEURONS

It has been generally accepted that the nigrostriatal DAN-mediated dopamine transmission is essential in regulating the vigor of movement (Mazzoni et al., 2007; Dudman and Krakauer, 2016). Movement vigor represents a key element of movement manifested with speed, amplitude, or frequency; while motor motivation drives movement vigor (Mazzoni et al., 2007; Dudman and Krakauer, 2016). The nigrostriatal DAN-mediated dopamine transmission is proposed to signal the motor motivation (Dudman and Krakauer, 2016), which provides the theoretical framework to explain why the degeneration of nigrostriatal DANs in PD patients leads to reduced movement vigor (Mazzoni et al., 2007; Dudman and Krakauer, 2016). A causal relationship has been established in rodents between the activity of nigrostriatal DANs before movement initiation and the probability and vigor of future movements (da Silva et al., 2018). However, a selective ablation of $ALDH1A1^+$ nDANs in mouse brains only moderately reduces the occurrence of high-speed walking when the mice are free to choose movement speed in Open-field test (Wu et al., 2019). Compared to a modest reduction in high-speed walking, the $ALDH1A1^+$ nDAN-ablated mice display much more severe impairments in accelerating rotarod test, in which the mice have to move at an instructed and gradually increased speed. These observations suggest that $ALDH1A1^+$ nDANs play a more critical role in supporting goal-oriented actions that demand strong motor motivation.

$ALDH1A1^+$ nDANs are also implicated in motor skill learning (Wu et al., 2019). Motor skill is regarded as the ability to select and execute goal-directed actions and act over a range of vigor (Dudman and Krakauer, 2016). Motor skill learning, a product of both learning actions and the capacity to flexibly parameterize their execution, is required for optimizing movements in every aspect of life (Kantak and Winstein, 2012; Dudman and Krakauer, 2016). The associate cortex-DMS and sensorimotor cortex-DLS circuits function coordinately during the acquisition of skilled movements (Corbit et al., 2017; Kupferschmidt et al., 2017), in which dopamine dynamically modulates synaptic strength of cortical and striatal neurons and serves as a reinforcement learning signal in the DS (Valentin et al., 2016). The repeated rotarod test is a well-adopted motor training paradigm to examine the motor skill learning in rodents (Sommer et al., 2014), which includes both the initial acquisition phase to optimize the foot placement on the rotating rod and the later retention phase to maintain the optimal stepping practice (Cao et al., 2015). The ablation of $ALDH1A1^+$ nDAN in mouse brains completely abolish the improvement of motor performance in the rotarod motor skill learning tests (Wu et al., 2019). Further study demonstrates that $ALDH1A1^+$ nDAN are essential in the acquisition of skilled movements, but not for the maintenance of acquired motor skills (Wu et al., 2019). These observations support the notion that nigrostriatal dopamine released from $ALDH1A1^+$ nDANs functions as a key feedback signal for the cortico-striatal network-mediated reinforcement learning (Valentin et al., 2016). Together, we hypothesize that $ALDH1A1^+$ nDAN-mediated dopamine transmission provides the implicit motor motivation and means to gain new motor skills through improvement of movement vigor during the learning phase (**Figure 3C**).

Systemic administration of levodopa or dopamine receptor agonists allows the $ALDH1A1^+$ nDAN-ablated mice to walk faster but fail to improve the motor skill learning (Wu et al., 2019). Similarly, dopamine replacement therapy is also less effective in treating the PD patients with learning and memory deficiency (Emre, 2003; Heremans et al., 2016). These findings suggest that dynamic dopamine release from $ALDH1A1^+$ nDANs is a key requirement for the learning process (Helie et al., 2015). $ALDH1A1^+$ nDANs may integrate diverse presynaptic inputs from basal ganglion and other brain regions to dynamically regulate the neuronal activity and dopamine release during the learning process.

FUNCTIONAL REGULATION OF ALDH1A1-POSITIVE NIGROSTRIATAL DOPAMINERGIC NEURONS

ALDH1A1$^+$ nDANs receive monosynaptic inhibitory GABAergic inputs from DS, external globus pallidus (GPe) and other brain regions (Wu et al., 2019). Both striosome and matrix direct pathway SPNs (dSPNs) innervate ALDH1A1$^+$ nDANs (Wu et al., 2019). However, striosome dSPNs may supply a higher ratio of direct inputs on nigrostriatal DANs compared to matrix dSPNs (McGregor et al., 2019). Striosome dSPNs can induce a pause-rebound firing pattern exclusively in ventral nigrostriatal DANs through GABA-B receptors on dendron bouquets as a potential mechanism to control plasticity of dopamine secretion (Evans et al., 2020). The GPe, however, does not exhibit a similar firing pattern when stimulating GABA-A receptors on ventral nigrostriatal DANs (Evans et al., 2020), suggesting a differential functional output of GABA signaling in subpopulations of nigrostriatal DANs depending on the origin of the signal. Since the ventral nigrostriatal DANs may not necessarily be all ALDH1A1-positive, future studies will be needed to further elucidate the synaptic transmission of ALDH1A1$^+$ nDANs by taking advantage of recently developed *Aldh1a1*-Cre knock-in mouse lines (Poulin et al., 2018; Wu et al., 2019). Selective ablation of dSPNs in mice also completely prevents the improvement in performing rotarod motor skill learning task (Durieux et al., 2012), suggesting that the dSPN-ALDH1A1$^+$ nDAN circuit is essential for motor skill learning (**Figure 3B**). Partial ablation of μ-opioid receptor (MOR1)-positive striosome SPNs with the toxin dermorphin-saporin seems to mainly affect the motor improvement in the later training sections (Lawhorn et al., 2009). The role of striosome dSPNs in motor skill learning, however, remains to be determined.

The subthalamic nucleus (STN), cortex, and pedunculopontine nucleus (PPN) all provide excitatory inputs to the ALDH1A1$^+$ nDANs, but the major source of excitatory input to ALDH1A1$^+$ nDANs comes from neurons projecting from the STN (Wu et al., 2019; **Figure 3B**). While the role of glutamatergic input to ALDH1A1$^+$ nDANs in regulating dopamine signaling and ALDH1A1$^+$ nDAN activity has not been well-characterized, the nature of glutamatergic input in the central nervous system as a whole and its role in synaptic plasticity suggests it is important for learning and adapting behavior. Treatment for PD patients that involves deep brain stimulation of the STN suggests that STN input in particular plays an important role in regulating at least some of the behaviors that are disrupted in PD (Dayal et al., 2017), emphasizing the importance of understanding the role of glutamatergic input. Similar to the lack of work investigating the effect of glutamatergic regulation on ALDH1A1$^+$ nDAN activity and signaling, there is also insufficient work isolating the behavioral effects of pharmacologically or genetically altering glutamatergic input to ALDH1A1 + nDANs. For example, although behavioral work with mice suggests that impaired glutamatergic input to midbrain DANs disrupts performance in tasks related to effort and incentive but not motor coordination or reward learning (Hutchison et al., 2018), the behavioral consequences of glutamatergic input onto ALDH1A1$^+$ nDAN in particular is not clear. This inability to discriminate the effects of different types of DANs is extremely prevalent in studies investigating the role of glutamatergic input onto midbrain DANs. Although many experiments leave us unable to decipher the role of glutamatergic input to ALDH1A1$^+$ nDANs in isolation, the findings from such experiments can still give us insight into how glutamatergic input to midbrain DANs in general is important. Hopefully in the future we can use that knowledge to see how ALDH1A1$^+$ nDAN activity and their glutamatergic regulation work in support or in opposition to other neurons with respect to motor skill learning and other PD-related behaviors.

CONCLUSION AND FUTURE PERSPECTIVES

Previous studies demonstrate that ALDH1A1$^+$ nDANs are preferentially degenerated in PD, the most common degenerative movement disorder (Cai et al., 2014; Liu et al., 2014). Further studies in rodent models reveal distinct molecular composition, electrophysiological properties, connectivity and functionality of this DAN subpopulation (Poulin et al., 2014, 2018; La Manno et al., 2016; Evans et al., 2017, 2020; Sgobio et al., 2017; Pan et al., 2019; Wu et al., 2019). There is still much to learn about the physiological function and regulation of ALDH1A1$^+$ nDANs and how to compensate for the lost function of those neurons as occurred in PD. While the inputs to ALDH1A1$^+$ nDANs have been well-characterized (Watabe-Uchida et al., 2012; Wu et al., 2019), how the relevant inputs from each of the identified brain areas regulate the activity and physiological function of ALDH1A1$^+$ nDANs has not been completely elucidated. Parsing out these specific anatomical sources of presynaptic inputs and their relative functional contributions in regulating ALDH1A1$^+$ nDANs will allow us to better understand the ALDH1A1$^+$ nDAN-mediated circuit mechanism of motor control.

The importance of regulated dopamine release by nigrostriatal DANs, particularly ALDH1A1$^+$ nDANs, may explain why so many therapies for PD that largely focus on simply supplementing lost dopamine fail to fully restore behavioral deficits in patients, including learning and memory deficits (Emre, 2003; Rochester et al., 2010; Beeler et al., 2012). While dopamine levels alone may help with alleviating or reversing some symptoms, evidence now seems to suggest that more complex or demanding tasks such as motor learning not only require dopamine release but need tightly regulated dopamine release as learning occurs. A better understanding of how ALDH1A1$^+$ nDANs integrate diverse presynaptic inputs to regulate dopamine release may also provide insight into which behavioral tests are most effective at studying the more nuanced and complex symptoms of nigrostriatal dopamine loss and seeing which treatment interventions most fully restore those symptoms in PD.

The revelation of preferential vulnerability of ALDH1A1$^+$ nDANs in PD promotes ongoing efforts in understanding cell-type and neural circuit specific mechanism of the disease. By taking advantage of newly developed single cell

RNA sequencing, CRISPR/Cas9 gene editing, optogenetics, chemogenetics, and live imaging with genetically encoded indicators techniques, we expect that increasing knowledge will be gained on how different subtypes of DANs contribute to different aspects of behavioral phenotypes. A further emphasis on system and behavioral neuroscience may provide new mechanistic insights into designing novel therapeutic strategies for PD treatment.

AUTHOR CONTRIBUTIONS

HC outlined the article, wrote the introduction, physiology, function, and perspectives sections, as well as prepared the figures. KC wrote the main regulation and conclusion sections. EL contributed to the regulation section. MK contribute to introduction section. LS wrote the molecule section. JD contributed to the gene expression analyses. RCE and ZMK contributed to the electrophysiology analyses. All authors contributed to the article and approved the submitted version.

FUNDING

This work was supported by the Intramural Research Programs of National Institute on Aging, NIH (HC, ZIA AG000944, AG000928).

ACKNOWLEDGMENTS

We are indebted to the suggestions and comments from other Cai lab members.

REFERENCES

Beeler, J. A., Frank, M. J., McDaid, J., Alexander, E., Turkson, S., Bernardez Sarria, M. S., et al. (2012). A role for dopamine-mediated learning in the pathophysiology and treatment of Parkinson's disease. *Cell Rep.* 2, 1747–1761. doi: 10.1016/j.celrep.2012.11.014

Bentivoglio, M., and Morelli, M. (2005). The organization and circuits of mesencephalic dopaminergic neurons and the distribution of dopamine receptors in the brain. *Dopamine* 21, 1–107. doi: 10.1016/S0924-8196(05)80005-3

Burke, R. E. (2010). Intracellular signalling pathways in dopamine cell death and axonal degeneration. *Progress Brain Res.* 183, 79–97. doi: 10.1016/S0079-6123(10)83005-5

Cai, H., Liu, G., Sun, L., and Ding, J. (2014). Aldehyde Dehydrogenase 1 making molecular inroads into the differential vulnerability of nigrostriatal dopaminergic neuron subtypes in Parkinson's disease. *Transl. Neurodegener.* 3:27. doi: 10.1186/2047-9158-3-27

Cao, V. Y., Ye, Y., Mastwal, S., Ren, M., Coon, M., Liu, Q., et al. (2015). Motor learning consolidates Arc-Expressing neuronal ensembles in secondary motor cortex. *Neuron* 86, 1385–1392. doi: 10.1016/j.neuron.2015.05.022

Corbit, V. L., Ahmari, S. E., and Gittis, A. H. (2017). A corticostriatal balancing act supports skill learning. *Neuron* 96, 253–255. doi: 10.1016/j.neuron.2017.09.046

Crittenden, J. R., Tillberg, P. W., Riad, M. H., Shima, Y., Gerfen, C. R., Curry, J., et al. (2016). Striosome-dendron bouquets highlight a unique striatonigral circuit targeting dopamine-containing neurons. *Proc. Natl. Acad. Sci. U.S.A.* 113, 11318-11323 doi: 10.1073/pnas.1613337113

da Silva, J. A., Tecuapetla, F., Paixao, V., and Costa, R. M. (2018). Dopamine neuron activity before action initiation gates and invigorates future movements. *Nature* 554, 244–248. doi: 10.1038/nature25457

Davis, M. I., and Puhl, H. L. III (2011). Nr4a1-eGFP is a marker of striosome-matrix architecture, development and activity in the extended striatum. *PLoS One* 6:e16619. doi: 10.1371/journal.pone.0016619

Dayal, V., Limousin, P., and Foltynie, T. (2017). Subthalamic nucleus deep brain stimulation in Parkinson's disease: the effect of varying stimulation parameters. *J. Parkinsons Dis.* 7, 235–245. doi: 10.3233/JPD-171077

Dudman, J. T., and Krakauer, J. W. (2016). The basal ganglia: from motor commands to the control of vigor. *Curr. Opin. Neurobiol.* 37, 158–166. doi: 10.1016/j.conb.2016.02.005

Durieux, P. F., Schiffmann, S. N., and de Kerchove d'Exaerde, A. (2012). Differential regulation of motor control and response to dopaminergic drugs by D1R and D2R neurons in distinct dorsal striatum subregions. *EMBO J.* 31, 640–653. doi: 10.1038/emboj.2011.400

Emre, M. (2003). Dementia associated with Parkinson's disease. *Lancet Neurol.* 2, 229–237. doi: 10.1016/S1474-4422(03)00351-X

Evans, R. C., Twedell, E. L., Zhu, M., Ascencio, J., Zhang, R., and Khaliq, Z. M. (2020). Functional dissection of basal ganglia inhibitory inputs onto substantia nigra dopaminergic neurons. *Cell Rep.* 32:108156. doi: 10.1016/j.celrep.2020.108156

Evans, R. C., Zhu, M., and Khaliq, Z. M. (2017). Dopamine inhibition differentially controls excitability of substantia nigra dopamine neuron subpopulations through T-Type calcium channels. *J. Neurosci.* 37, 3704–3720. doi: 10.1523/JNEUROSCI.0117-17.2017

Fearnley, J. M., and Lees, A. J. (1991). Ageing and Parkinson's disease: substantia nigra regional selectivity. *Brain* 114 (Pt 5), 2283–2301. doi: 10.1093/brain/114.5.2283

Frim, D. M., Uhler, T. A., Galpern, W. R., Beal, M. F., Breakefield, X. O., and Isacson, O. (1994). Implanted fibroblasts genetically engineered to produce brain-derived neurotrophic factor prevent 1-methyl-4-phenylpyridinium toxicity to dopaminergic neurons in the rat. *Proc. Natl. Acad. Sci. U.S.A.* 91, 5104–5108. doi: 10.1073/pnas.91.11.5104

Galter, D., Buervenich, S., Carmine, A., Anvret, M., and Olson, L. (2003). ALDH1 mRNA: presence in human dopamine neurons and decreases in substantia nigra in Parkinson's disease and in the ventral tegmental area in schizophrenia. *Neurobiol. Dis.* 14, 637–647. doi: 10.1016/j.nbd.2003.09.001

Graves, S. M., Xie, Z., Stout, K. A., Zampese, E., Burbulla, L. F., Shih, J. C., et al. (2019). Dopamine metabolism by a monoamine oxidase mitochondrial shuttle activates the electron transport chain. *Nat. Neurosci.* 23, 15–20. doi: 10.1038/s41593-019-0556-3

Grunblatt, E., Ruder, J., Monoranu, C. M., Riederer, P., Youdim, M. B., and Mandel, S. A. (2017). Differential alterations in metabolism and proteolysis-related proteins in human Parkinson's disease substantia Nigra. *Neurotox Res.* doi: 10.1007/s12640-017-9843-5

Helie, S., Ell, S. W., and Ashby, F. G. (2015). Learning robust cortico-cortical associations with the basal ganglia: an integrative review. *Cortex* 64, 123–135. doi: 10.1016/j.cortex.2014.10.011

Heremans, E., Nackaerts, E., Vervoort, G., Broeder, S., Swinnen, S. P., and Nieuwboer, A. (2016). Impaired retention of motor learning of writing skills in patients with Parkinson's disease with freezing of gait. *PLoS One* 11:e0148933. doi: 10.1371/journal.pone.0148933

Hintiryan, H., Foster, N. N., Bowman, I., Bay, M., Song, M. Y., Gou, L., et al. (2016). The mouse cortico-striatal projectome. *Nat. Neurosci.* 19, 1100–1114. doi: 10.1038/nn.4332

Hook, P. W., McClymont, S. A., Cannon, G. H., Law, W. D., Morton, A. J., Goff, L. A., et al. (2018). Single-Cell RNA-Seq of mouse dopaminergic neurons informs candidate gene selection for sporadic Parkinson disease. *Am. J. Hum. Genet.* 102, 427–446. doi: 10.1016/j.ajhg.2018.02.001

Hutchison, M. A., Gu, X., Adrover, M. F., Lee, M. R., Hnasko, T. S., Alvarez, V. A., et al. (2018). Genetic inhibition of neurotransmission reveals role of glutamatergic input to dopamine neurons in high-effort behavior. *Mol. Psychiatry* 23, 1213–1225. doi: 10.1038/mp.2017.7

Jacobs, F. M., Smits, S. M., Noorlander, C. W., von Oerthel, L., van der Linden, A. J., Burbach, J. P., et al. (2007). Retinoic acid counteracts developmental defects in

the substantia nigra caused by Pitx3 deficiency. *Development* 134, 2673–2684. doi: 10.1242/dev.02865

Kantak, S. S., and Winstein, C. J. (2012). Learning-performance distinction and memory processes for motor skills: a focused review and perspective. *Behav. Brain Res.* 228, 219–231. doi: 10.1016/j.bbr.2011.11.028

Kim, J. I., Ganesan, S., Luo, S. X., Wu, Y. W., Park, E., Huang, E. J., et al. (2015). Aldehyde dehydrogenase 1a1 mediates a GABA synthesis pathway in midbrain dopaminergic neurons. *Science* 350, 102–106. doi: 10.1126/science.aac4690

Koppaka, V., Thompson, D. C., Chen, Y., Ellermann, M., Nicolaou, K. C., Juvonen, R. O., et al. (2012). Aldehyde dehydrogenase inhibitors: a comprehensive review of the pharmacology, mechanism of action, substrate specificity, and clinical application. *Pharmacol. Rev.* 64, 520–539. doi: 10.1124/pr.111.005538

Kordower, J. H., Olanow, C. W., Dodiya, H. B., Chu, Y., Beach, T. G., Adler, C. H., et al. (2013). Disease duration and the integrity of the nigrostriatal system in Parkinson's disease. *Brain* 136, 2419–2431. doi: 10.1093/brain/awt192

Kupferschmidt, D. A., Juczewski, K., Cui, G., Johnson, K. A., and Lovinger, D. M. (2017). Parallel, but dissociable, processing in discrete corticostriatal inputs encodes skill learning. *Neuron* 96, 476–489.e5. doi: 10.1016/j.neuron.2017.09.040

La Manno, G., Gyllborg, D., Codeluppi, S., Nishimura, K., Salto, C., Zeisel, A., et al. (2016). Molecular diversity of midbrain development in mouse, human, and stem cells. *Cell* 167, 566–580 e19. doi: 10.1016/j.cell.2016.09.027

Langston, J. W. (2017). The MPTP story. *J. Parkinsons Dis.* 7, S11–S19. doi: 10.3233/JPD-179006

Lawhorn, C., Smith, D. M., and Brown, L. L. (2009). Partial ablation of mu-opioid receptor rich striosomes produces deficits on a motor-skill learning task. *Neuroscience* 163, 109–119. doi: 10.1016/j.neuroscience.2009.05.021

Lerner, T. N., Shilyansky, C., Davidson, T. J., Evans, K. E., Beier, K. T., Zalocusky, K. A., et al. (2015). Intact-Brain analyses reveal distinct information carried by SNc dopamine subcircuits. *Cell* 162, 635–647. doi: 10.1016/j.cell.2015.07.014

Liu, G., Yu, J., Ding, J., Xie, C., Sun, L., Rudenko, I., et al. (2014). Aldehyde dehydrogenase 1 defines and protects a nigrostriatal dopaminergic neuron subpopulation. *J. Clin. Invest.* 124, 3032–3046. doi: 10.1172/JCI72176

Mandel, S. A., Fishman, T., and Youdim, M. B. (2007). Gene and protein signatures in sporadic Parkinson's disease and a novel genetic model of PD. *Parkinsonism Relat. Disord.* 13 (Suppl. 3), S242–S247. doi: 10.1016/S1353-8020(08)70009-9

Marchitti, S. A., Deitrich, R. A., and Vasiliou, V. (2007). Neurotoxicity and metabolism of the catecholamine-derived 3,4-dihydroxyphenylacetaldehyde and 3,4-dihydroxyphenylglycolaldehyde: the role of aldehyde dehydrogenase. *Pharmacol. Rev.* 59, 125–150. doi: 10.1124/pr.59.2.1

Mazzoni, P., Hristova, A., and Krakauer, J. W. (2007). Why don't we move faster? Parkinson's disease, movement vigor, and implicit motivation. *J. Neurosci.* 27, 7105–7116. doi: 10.1523/JNEUROSCI.0264-07.2007

McCaffery, P., and Drager, U. C. (1994). High levels of a retinoic acid-generating dehydrogenase in the meso-telencephalic dopamine system. *Proc. Natl. Acad. Sci. U.S.A.* 91, 7772–7776. doi: 10.1073/pnas.91.16.7772

McGregor, M. M., McKinsey, G. L., Girasole, A. E., Bair-Marshall, C. J., Rubenstein, J. L. R., and Nelson, A. B. (2019). Functionally distinct connectivity of developmentally targeted striosome neurons. *Cell Rep.* 29, 1419–1428.e5. doi: 10.1016/j.celrep.2019.09.076

Menegas, W., Bergan, J. F., Ogawa, S. K., Isogai, Y., Umadevi Venkataraju, K., Osten, P., et al. (2015). Dopamine neurons projecting to the posterior striatum form an anatomically distinct subclass. *Elife* 4:e10032. doi: 10.7554/eLife.10032.021

Pan, J., Yu, J., Sun, L., Xie, C., Chang, L., Wu, J., et al. (2019). ALDH1A1 regulates postsynaptic mu-opioid receptor expression in dorsal striatal projection neurons and mitigates dyskinesia through transsynaptic retinoic acid signaling. *Sci. Rep.* 9:3602. doi: 10.1038/s41598-019-40326-x

Patriarchi, T., Cho, J. R., Merten, K., Howe, M. W., Marley, A., Xiong, W. H., et al. (2018). Ultrafast neuronal imaging of dopamine dynamics with designed genetically encoded sensors. *Science* 360:eaat4422. doi: 10.1126/science.aat4422

Poulin, J. F., Caronia, G., Hofer, C., Cui, Q., Helm, B., Ramakrishnan, C., et al. (2018). Mapping projections of molecularly defined dopamine neuron subtypes using intersectional genetic approaches. *Nat. Neurosci.* 21, 1260–1271. doi: 10.1038/s41593-018-0203-4

Poulin, J. F., Zou, J., Drouin-Ouellet, J., Kim, K. Y., Cicchetti, F., and Awatramani, R. B. (2014). Defining midbrain dopaminergic neuron diversity by single-cell gene expression profiling. *Cell Rep.* 9, 930–943. doi: 10.1016/j.celrep.2014.10.008

Rees, J. N., Florang, V. R., Eckert, L. L., and Doorn, J. A. (2009). Protein reactivity of 3,4-dihydroxyphenylacetaldehyde, a toxic dopamine metabolite, is dependent on both the aldehyde and the catechol. *Chem. Res. Toxicol.* 22, 1256–1263. doi: 10.1021/tx9000557

Rochester, L., Baker, K., Hetherington, V., Jones, D., Willems, A. M., Kwakkel, G., et al. (2010). Evidence for motor learning in Parkinson's disease: acquisition, automaticity and retention of cued gait performance after training with external rhythmical cues. *Brain Res.* 1319, 103–111. doi: 10.1016/j.brainres.2010.01.001

Salinas, A. G., Davis, M. I., Lovinger, D. M., and Mateo, Y. (2016). Dopamine dynamics and cocaine sensitivity differ between striosome and matrix compartments of the striatum. *Neuropharmacology* 108, 275–283. doi: 10.1016/j.neuropharm.2016.03.049

Saunders, A., Macosko, E. Z., Wysoker, A., Goldman, M., Krienen, F. M., de Rivera, H., et al. (2018). Molecular diversity and specializations among the cells of the adult mouse brain. *Cell* 174, 1015–1030.e16. doi: 10.1016/j.cell.2018.07.028

Sgobio, C., Wu, J., Zheng, W., Chen, X., Pan, J., Salinas, A. G., et al. (2017). Aldehyde dehydrogenase 1-positive nigrostriatal dopaminergic fibers exhibit distinct projection pattern and dopamine release dynamics at mouse dorsal striatum. *Sci. Rep.* 7:5283. doi: 10.1038/s41598-017-05598-1

Sommer, W. H., Costa, R. M., and Hansson, A. C. (2014). Dopamine systems adaptation during acquisition and consolidation of a skill. *Front. Integr. Neurosci.* 8:87. doi: 10.3389/fnint.2014.00087

Sulzer, D., and Surmeier, D. J. (2013). Neuronal vulnerability, pathogenesis, and Parkinson's disease. *Mov. Disord.* 28, 41–50. doi: 10.1002/mds.25095

Sun, F., Zeng, J., Jing, M., Zhou, J., Feng, J., Owen, S. F., et al. (2018). Fluorescent sensor enables rapid and specific detection of dopamine in flies, fish, and mice. *Cell* 174, 481–496.e19. doi: 10.1016/j.cell.2018.06.042

Surmeier, D. J., and Schumacker, P. T. (2013). Calcium, bioenergetics, and neuronal vulnerability in Parkinson's disease. *J. Biol. Chem.* 288, 10736–10741. doi: 10.1074/jbc.R112.410530

Tasic, B. (2018). Single cell transcriptomics in neuroscience: cell classification and beyond. *Curr. Opin. Neurobiol.* 50, 242–249. doi: 10.1016/j.conb.2018.04.021

Tiklova, K., Bjorklund, A. K., Lahti, L., Fiorenzano, A., Nolbrant, S., Gillberg, L., et al. (2019). Single-cell RNA sequencing reveals midbrain dopamine neuron diversity emerging during mouse brain development. *Nat. Commun.* 10:581. doi: 10.1038/s41467-019-08453-1

Valentin, V. V., Maddox, W. T., and Ashby, F. G. (2016). Dopamine dependence in aggregate feedback learning: a computational cognitive neuroscience approach. *Brain Cogn.* 109, 1–18. doi: 10.1016/j.bandc.2016.06.002

Vogt Weisenhorn, D. M., Giesert, F., and Wurst, W. (2016). Diversity matters – heterogeneity of dopaminergic neurons in the ventral mesencephalon and its relation to Parkinson's Disease. *J. Neurochem.* 139 (Suppl. 1), 8–26. doi: 10.1111/jnc.13670

Watabe-Uchida, M., Zhu, L., Ogawa, S. K., Vamanrao, A., and Uchida, N. (2012). Whole-brain mapping of direct inputs to midbrain dopamine neurons. *Neuron* 74, 858–873. doi: 10.1016/j.neuron.2012.03.017

Werner, C. J., Heyny-von Haussen, R., Mall, G., and Wolf, S. (2008). Proteome analysis of human substantia nigra in Parkinson's disease. *Proteome Sci.* 6:8. doi: 10.1186/1477-5956-6-8

Wu, J., Kung, J., Dong, J., Chang, L., Xie, C., Habib, A., et al. (2019). Distinct connectivity and functionality of aldehyde dehydrogenase 1a1-positive nigrostriatal dopaminergic neurons in motor learning. *Cell Rep.* 28, 1167–1181 e7. doi: 10.1016/j.celrep.2019.06.095

Conflict of Interest: The authors declare that the research was conducted in the absence of any commercial or financial relationships that could be construed as a potential conflict of interest.

Copyright © 2021 Carmichael, Evans, Lopez, Sun, Kumar, Ding, Khaliq and Cai. This is an open-access article distributed under the terms of the Creative Commons Attribution License (CC BY). The use, distribution or reproduction in other forums is permitted, provided the original author(s) and the copyright owner(s) are credited and that the original publication in this journal is cited, in accordance with accepted academic practice. No use, distribution or reproduction is permitted which does not comply with these terms.

frontiers in Neural Circuits

REVIEW
published: 19 May 2021
doi: 10.3389/fncir.2021.665386

Dopamine Neurons That Cotransmit Glutamate, From Synapses to Circuits to Behavior

Daniel Eskenazi[1,2], Lauren Malave[1,2], Susana Mingote[1,2,3], Leora Yetnikoff[4,5], Samira Ztaou[1,2], Vlad Velicu[1,2], Stephen Rayport[1,2] and Nao Chuhma[1,2]**

[1] Department of Psychiatry, Columbia University, New York, NY, United States, [2] Department of Molecular Therapeutics, New York State Psychiatric Institute, New York, NY, United States, [3] Neuroscience Initiative, Advanced Science Research Center, Graduate Center of The City University of New York, New York, NY, United States, [4] Department of Psychology, College of Staten Island, City University of New York, Staten Island, NY, United States, [5] CUNY Neuroscience Collaborative, The Graduate Center, City University of New York, New York, NY, United States

Discovered just over 20 years ago, dopamine neurons have the ability to cotransmit both dopamine and glutamate. Yet, the functional roles of dopamine neuron glutamate cotransmission and their implications for therapeutic use are just emerging. This review article encompasses the current body of evidence investigating the functions of dopamine neurons of the ventral midbrain that cotransmit glutamate. Since its discovery in dopamine neuron cultures, further work *in vivo* confirmed dopamine neuron glutamate cotransmission across species. From there, growing interest has led to research related to neural functioning including roles in synaptic signaling, development, and behavior. Functional connectome mapping reveals robust connections in multiple forebrain regions to various cell types, most notably to cholinergic interneurons in both the medial shell of the nucleus accumbens and the lateral dorsal striatum. Glutamate markers in dopamine neurons reach peak levels during embryonic development and increase in response to various toxins, suggesting dopamine neuron glutamate cotransmission may serve neuroprotective roles. Findings from behavioral analyses reveal prominent roles for dopamine neuron glutamate cotransmission in responses to psychostimulants, in positive valence and cognitive systems and for subtle roles in negative valence systems. Insight into dopamine neuron glutamate cotransmission informs the pathophysiology of neuropsychiatric disorders such as addiction, schizophrenia and Parkinson Disease, with therapeutic implications.

Keywords: VGLUT2, VMAT2, glutaminase, schizophrenia, addiction, psychostimulant, Parkinson disease

OPEN ACCESS

Edited by:
Jean-Francois Poulin, McGill University, Canada

Reviewed by:
Åsa Wallén-Mackenzie, Uppsala University, Sweden
Louis-Eric Trudeau, Université de Montréal, Canada

***Correspondence:**
Stephen Rayport
Stephen.Rayport@nyspi.columbia.edu
Nao Chuhma
Nao.Chuma@nyspi.columbia.edu

Received: *08 February 2021*
Accepted: *16 April 2021*
Published: *19 May 2021*

Citation:
Eskenazi D, Malave L, Mingote S, Yetnikoff L, Ztaou S, Velicu V, Rayport S and Chuhma N (2021) Dopamine Neurons That Cotransmit Glutamate, From Synapses to Circuits to Behavior. Front. Neural Circuits 15:665386. doi: 10.3389/fncir.2021.665386

INTRODUCTION

Dopamine (DA) neurons were first identified by their monoamine content, and then by the expression of the DA synthetic enzyme tyrosine hydroxylase (TH) (for review see Iversen and Iversen, 2007). Heterogeneity of DA neurons was first recognized as mediolateral differences between ventral tegmental area (VTA) and substantia nigra (SN) DA neurons (for reviews on

this topic see Grace et al., 2007; Liss and Roeper, 2008). DA neurons, like most central nervous system neurons, use multiple neurotransmitters (Kupfermann, 1991), adding a further dimension of heterogeneity. Peptide cotransmission was recognized first, with evidence that DA neurons use cholecystokinin and neurotensin as cotransmitters (Hökfelt et al., 1980; Gonzalez-Reyes et al., 2012).

Cotransmission involving two small molecule neurotransmitters — especially with competing synaptic actions — was recognized more recently (for review see Hnasko and Edwards, 2012). DA neuron glutamate (GLU) cotransmission was first shown in single-cell microcultures of identified rat DA neurons (Sulzer et al., 1998). Electrical stimulation of genetically tagged DA neurons in quasi-horizontal mouse brain slices revealed DA neuron GLU cotransmission in the ventral striatum (Chuhma et al., 2004) and its frequency dependent modulation by concomitantly released DA (Chuhma et al., 2009). Optogenetic stimulation of DA neuron terminals showed that DA neurons make monosynaptic GLU connections to spiny projection neurons (SPNs) in the nucleus accumbens (NAc) (Stuber et al., 2010; Tecuapetla et al., 2010). DA neurons cotransmitting GLU (DA-GLU neurons) require both vesicular monoamine transporter 2 (VMAT2) for DA release (Fon et al., 1997) and vesicular glutamate transporter 2 (VGLUT2 for protein, *VGluT2* for gene and mRNA) for GLU release (Dal Bo et al., 2004; Hnasko et al., 2010; Stuber et al., 2010). DA neurons also use GABA as a small molecule cotransmitter (for reviews see Tritsch et al., 2012; Granger et al., 2017). DA neuron GLU cotransmission extends from fruit flies to humans (**Figure 1**), arguing for important physiological roles.

This review focuses on DA neuron GLU cotransmission and addresses the key questions: (1) Where do DA-GLU neurons project? (2) Are DA and GLU released together or separately? (3) What are the synaptic functions of DA neuron GLU cotransmission? (4) What are the developmental roles of DA neuron GLU cotransmission? (5) How are DA-GLU neurons affected by DA neuron toxins? (6) What are the behavioral roles of DA neuron GLU cotransmission? (7) Does DA neuron GLU cotransmission have a role in human disorders?

Abbreviations: 6-OHDA, 6-hydroxydopamine; BLA, basolateral amygdala; CeA, central nucleus of the amygdala; ChI, cholinergic interneuron; cHET, conditional heterozygous; CingC, cingulate cortex; cKO, conditional knockout; CLi, central linear nucleus; CS, conditioned stimulus; DA, dopamine; DAT, dopamine transporter; E#, embryonic day; EGFP, enhanced green fluorescent protein; EntC, entorhinal cortex; EPSC, excitatory postsynaptic current; flox, floxed allele; FSI, fast-spiking interneuron; GLU, glutamate; Gls1, glutaminase 1; Hippo, hippocampus; IF, interfascicular nucleus; iGluR, ionotropic glutamate receptor; IHC, immunohistochemistry; IRES, internal ribosome entry site; ISH, *in situ* hybridization; mGluR, metabotropic glutamate receptor; MPP^+, 1-methyl-4-phenyl pyridinium; MPTP, *N*-methyl-4-phenyl-1,2,3,6-tetrahydropyridine; m-shell, medial shell; nAChR, nicotinic acetylcholine receptor; NAc, nucleus accumbens; OT, olfactory tubercle; P#, postnatal day; PD, Parkinson disease; PBP, parabrachial pigmented nucleus; PFC, prefrontal cortex; PIF, parainterfascicular nucleus; PN, paranigral nucleus; RLi, rostral linear nucleus; sc RT-PCR, single cell reverse transcriptase polymerase chain reaction; SPN, spiny projection neuron; Shh, sonic hedgehog; SN, substantia nigra; SNc, substantia nigra pars compacta; SV, synaptic vesicle; TH, tyrosine hydroxylase; $TH^+/VGLUT^+$, TH and VGLUT2 double-labeling; US, unconditioned stimulus; VTA, ventral tegmental area; *VGluT2,* vesicular glutamate transporter 2 (rodent gene); *VGLUT2,* vesicular glutamate transporter 2 (human gene); VGLUT2, vesicular glutamate transporter 2 (protein); VMAT2, vesicular monoamine transporter 2; WT, wildtype.

WHERE DO DA-GLU NEURONS PROJECT?

DA-GLU Neurons in the Ventral Midbrain

Dopamine neurons in the ventral midbrain are divided between the VTA and SN. DA-GLU neurons show a medial preponderance, are mainly in the VTA, and project predominantly to the ventral striatum/NAc (Li et al., 2013; Morales and Root, 2014; Yamaguchi et al., 2015; Zhang et al., 2015; Root et al., 2016; Chuhma et al., 2018; Poulin et al., 2018; Mingote et al., 2019). DA-GLU neurons are identified by *TH* and *VGluT2* expression. Expression of *VGluT2* in DA neurons is necessary and sufficient to enable GLU cotransmission (Takamori et al., 2000). Indeed, DA-neuron-specific *VGluT2* cKO eliminated GLU-cotransmission synaptic responses (Stuber et al., 2010). Visualizing *VGluT2* expression in cell bodies requires *in situ* hybridization (ISH) or ectopic reporter expression driven by the *VGluT2* promoter, as VGLUT2 is rapidly exported to axon terminals. The number of DA-GLU (i.e., $TH^+/VGLUT2^+$) neurons varies across the lifespan, species, brain region and study (**Table 1**). In the VTA, DA-GLU neurons account for 10-30% of DA neurons, and are most abundant in the interfascicular nucleus (IF), the central linear nucleus (CLi), the rostral linear nucleus (RLi), and the parabrachial pigmented nucleus (PBP) (Kawano et al., 2006; Li et al., 2013). In the SN, DA-GLU neurons account for about 5–10%, and are most abundant in the dorsal SN pars compacta (SNc) and the pars lateralis in rodents, as well as primates including humans (Yamaguchi et al., 2013; Root et al., 2016; Steinkellner et al., 2018).

DA-GLU Projections

Combinatorial intersectional genetic strategies (Fenno et al., 2014, 2020) have enabled visualization of DA-GLU neurons and their projections (Poulin et al., 2018). This has confirmed that DA-GLU neurons comprise about 30% of VTA neurons (Poulin et al., 2018; Mingote et al., 2019) and send dense projections to the NAc medial shell (m-shell), discrete, dense, column-like projections to the olfactory tubercle (OT), and sparse projections to the prefrontal cortex (PFC), mostly to deeper layers of the infralimbic and prelimbic cortices (Poulin et al., 2018). Particularly in the dorsal portion of the m-shell, all TH^+ fibers are $VGLUT2^+$, indicating that DA neuron projections in this region are predominantly from DA-GLU neurons, consistent with recent retrograde tracer studies (Mongia et al., 2019). DA-GLU neurons in the lateral SNc project to the lateral dorsal striatum with denser projections to the caudal striatum, or tail (Poulin et al., 2018). SNc DA-GLU neurons also project to the central nucleus of the amygdala (CeA), the lateral part of the capsular division, and sparsely to the ventral-most lateral nucleus and the posterior nucleus, as well as to DA islands in the entorhinal cortex (EntC) (Poulin et al., 2018; Mingote et al., 2019).

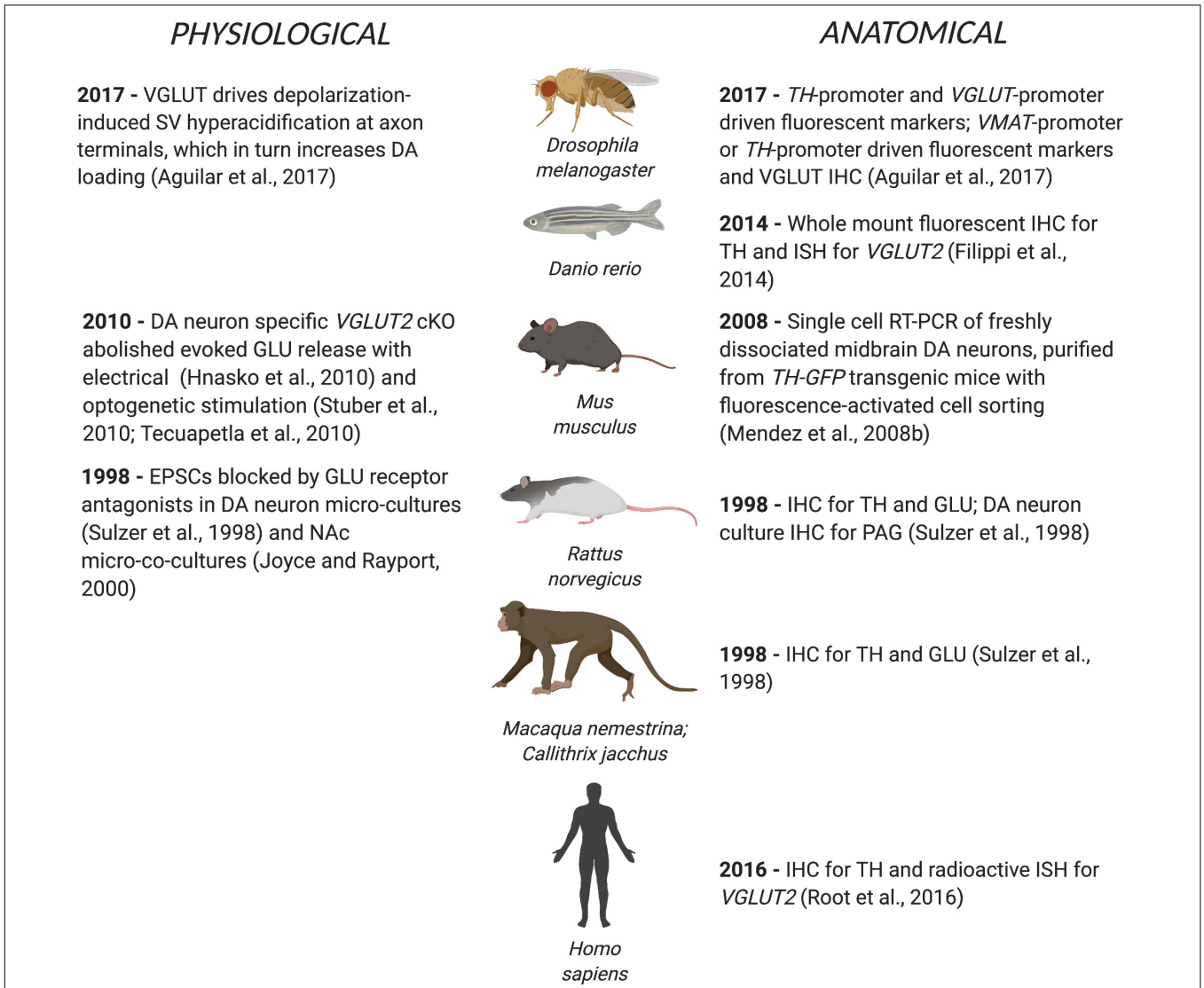

FIGURE 1 | DA neuron GLU cotransmission spans phylogeny from flies to humans. The first physiological or anatomical evidence for DA neuron GLU cotransmission is cited by species.

Thus, DA-GLU neurons have discrete, but widely distributed forebrain projections.

Physiological Connectivity of DA-GLU Neurons

Functional connectome mapping has addressed how the projections of DA-GLU neurons translate to their synaptic actions (Mingote et al., 2015a). *Functional connectome mapping* is the systematic recording of the strength and incidence of monosynaptic connections to identified postsynaptic neurons by optogenetic stimulation of genetically defined presynaptic neuron populations (Chuhma et al., 2011; Chuhma, 2015, 2021; Eskenazi et al., 2019). DA neurons make the most robust GLU connections in the ventral striatum, in the NAc core and shell, and the OT (Wieland et al., 2014), in accordance with the densest DA-GLU neuron projections (Poulin et al., 2018; Mingote et al., 2019; **Figure 2**). In the NAc m-shell, DA-GLU neurons elicit fast glutamatergic EPSCs mediated by inotropic GLU receptors (iGluR) in all SPNs, fast-spiking interneurons (FSIs) and cholinergic interneurons (ChIs), with the strongest in ChIs (Chuhma et al., 2014). In the lateral dorsal striatum, the strongest iGluR EPSCs are seen in striatonigral SPNs (Cai and Ford, 2018; Chuhma et al., 2018), and weaker EPSCs in ChIs. In addition, DA-GLU neurons elicit slower EPSCs mediated by metabotropic GLU receptors (mGluRs) in lateral dorsal striatum ChIs (Straub et al., 2014; Cai and Ford, 2018; Chuhma et al., 2018). Outside the striatum, EPSCs are seen occasionally in pyramidal neurons of layers II-III in cingulate cortex (CingC) (Mingote et al., 2015a), and in GABA interneurons in the PFC, contributing to disynaptic inhibition of pyramidal neurons (Kabanova et al., 2015; Pérez-López et al., 2018). DA-GLU

TABLE 1 | *TH* and *VGluT2* coexpression in midbrain DA neurons.

				$TH^+VGLUT2^+$/Total TH^+ %			
Age	**Species**	**Genotype**	**Method**	**Midbrain(Total)**	**Medial-only**	**Lateral-only**	**Citation**
E11	Mouse	WT	ISH		(>E14)		Dumas and Wallén-Mackenzie, 2019
E14	Mouse	WT	ISH		(<E11)		
E14	Mouse	*TH*^{EGFP}	sc RT-PCR	7			Fortin et al., 2012
E16				47			
E18				33			
E15, 16	Rat	WT	ISH	(High)			Dal Bo et al., 2008
E18, 21				(Low)			
P0	Mouse	*TH*^{EGFP}	dissociation, sc RT-PCR	25			Mendez et al., 2008b
P0	Mouse	*VGluT2*^{EGFP} bacterial artificial chromosome	IHC (TH, EGFP)	2			
P0-2	Mouse	*TH-EGFP*	sc RT-PCR	22	36	13	Fortin et al., 2012
P5	Rat	WT	ISH		3	<1	Dal Bo et al., 2008
P10	Mouse	*VGluT2*^{EGFP} bacterial artificial chromosome	IHC (TH, EGFP)	1			Mendez et al., 2008b
P10	Rat	WT	ISH		2	<1	Dal Bo et al., 2008
P14	Mouse	*TH*^{EGFP}	sc RT-PCR	14			Fortin et al., 2012
P14	Mouse	*TH*^{EGFP}	sc RT-PCR		18	14	Mendez et al., 2008b
P15	Rat	WT	ISH		2	<1	Dal Bo et al., 2008
P35	Mouse	*TH*^{EGFP}	sc RT-PCR	30			Fortin et al., 2012
P45	Mouse	*TH*^{EGFP}	dissociation, sc RT-PCR	14			Mendez et al., 2008b
P45	Mouse	*VGluT2*^{EGFP} bacterial artificial chromosome	IHC (TH, EGFP)	<1			
6–24 weeks	Mouse	WT	ISH (RNA Scope)		56	37	Yan et al., 2018
					Medial VTA	*Lateral VTA*	
P70	Mouse	*TH*^{EGFP}	sc RT-PCR	47	78	25	Fortin et al., 2012
P90	Rat	WT	ISH		2	<1	Bérubé-Carrière et al., 2009
8–12 weeks	Mouse	*DAT*$^{IRES-Cre}$; *VGluT2*$^{flox/+}$	ISH		15	20	Shen et al., 2018
Adult	Rat	WT	ISH		<1		Yamaguchi et al., 2007
Adult	Rat	WT	ISH		*PBP* 3 *IF* 22		Kawano et al., 2006
					PN 5 *CLi* 22		

(Continued)

TABLE 1 | Continued

Age	Species	Genotype	Method	$TH^+VGLUT2^+/Total\ TH^+$ %					Citation
				Midbrain(Total)		Medial-only		Lateral-only	
				A10	19	*RLi*	53		
Adult	Rat	WT	TH-IHC, *VGluT2*-ISH	*Medial PBP*	60	*IF*	10		Li et al., 2013
				medial PN	50	*RLi*	60		
			Laser micro-dissection, sc RT-PCR		*medial PBP*		42		
						RLi	42		
						IF	57		
Adult	Marmoset	WT	TH-IHC, *VGluT2*-ISH	*PBP*	23	*IF*	2	*Ventral SNc*	<1	Root et al., 2016
				PN	2	*CLi*	2	*Dorsal SNc*	<1	
				Caudal VTA	5	*RLi*	3	*Medial SNc*	<1	
				Rostral VTA	6	*PIF*	4	*Lateral SNc*	< 1	
				PBP	17	*VTA*	10	*Ventral SNc*	2	
Adult (55 years)	Human	WT	TH-IHC, *VGluT2*-ISH	*PN*	2	*RLi*	10	*Dorsal SNc*	3	
				VTA subdivision			10	*Medial SNc*	3	
								Lateral SNc	<1	

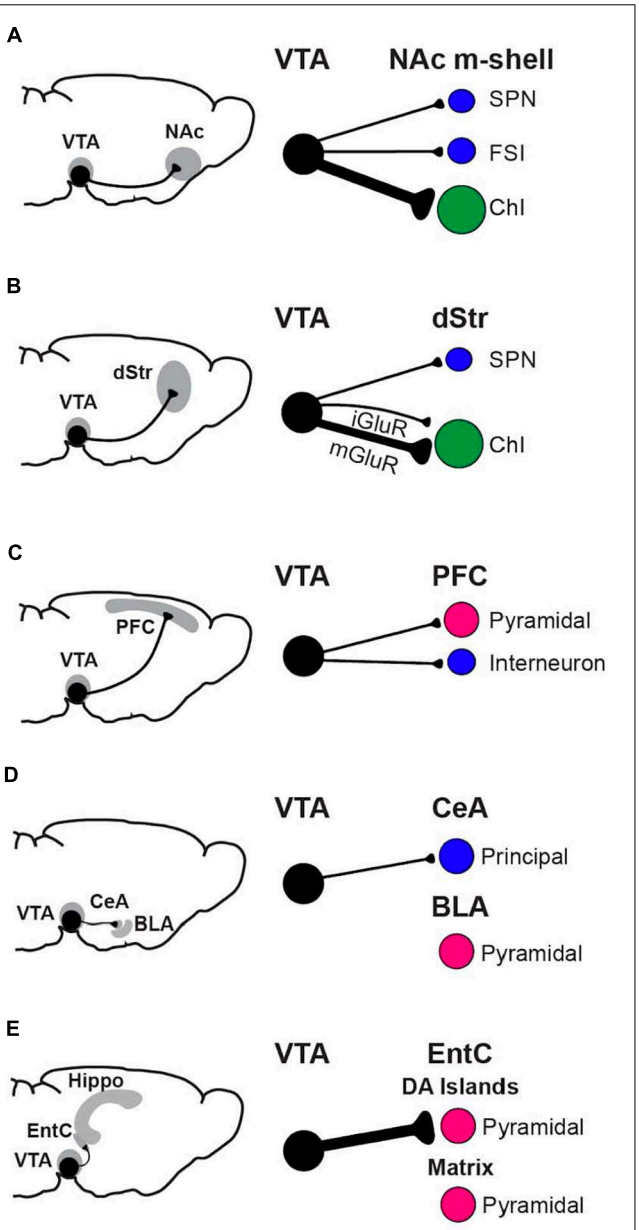

FIGURE 2 | Functional connectome analysis of VTA DA neuron GLU cotransmission. Regions with prominent connections, the NAc m-shell **(A)**, dorsal striatum **(B)**, prefrontal cortex **(C)**, amygdala **(D)**, and hippocampal formation **(E)** are shown, with the neurons principally targeted by DA-GLU neurons in each region. The strength of connections is indicated by the thickness of the axons (black lines). Postsynaptic neurons are GABAergic (blue), GLUergic (magenta), or cholinergic (green).

neurons projecting to the cortex are mainly located in the RLi, PBP, and rostral VTA (Gorelova et al., 2012). In the EntC, DA-GLU neurons elicit EPSCs in pyramidal neurons in DA islands, while they make no connections in the hippocampus (Mingote et al., 2015a). In line with higher levels of *VGluT2* expression in DA neurons projecting to the amygdala (Taylor et al., 2014; Poulin et al., 2018), DA-GLU neurons target the CeA

but not the basolateral amygdala (BLA) (Mingote et al., 2015a). Of note, most of these studies have been performed on brain slices from juvenile mice; thus, future studies on mice in early life or late adulthood may differ since the proportion of DA neurons expressing *VGluT2* may change with age (see below). In summary, DA-GLU neurons connect to different cell types in different target regions, with the highest incidence of connectivity in the NAc m-shell and lateral dorsal striatum and the largest EPSCs in the EntC.

ARE DA AND GLU RELEASED TOGETHER OR SEPARATELY?

Cotransmission can be viewed as a physiological/functional property that may arise from several anatomical/structural arrangements (**Figure 3**). Here we use the definitions of *cotransmission* as the release of multiple different neurotransmitters from the same neuron, and *corelease* as the release of different neurotransmitters from the same synaptic vesicle (SV) (Vaaga et al., 2014; Svensson et al., 2018). Furthermore, SVs with different neurotransmitters may colocalize within the same varicosity, or segregate to different varicosities of the same neuron (e.g., some at symmetric synapses, others at asymmetric synapses).

For corelease of DA and GLU, individual SVs must have both VMAT2 and VGLUT2. Co-immunoprecipitation with anti-VMAT2 and anti-VGLUT2 antibodies identified a population of striatal SVs consistent with corelease (Hnasko et al., 2010), although not in a subsequent study (Zhang et al., 2015). Uptake of GLU into a SV may potentiate the uptake and subsequent release of DA (Hnasko and Edwards, 2012; Aguilar et al., 2017), via vesicular synergy (Gras et al., 2008; Amilhon et al., 2010; El Mestikawy et al., 2011). *Vesicular synergy* refers to corelease where one neurotransmitter potentiates the uptake of another neurotransmitter in the same SV (El Mestikawy et al., 2011). VGLUT2 cotransports GLU with a single Cl^- into SVs in exchange for a single H^+, thereby increasing negative charge inside SVs (Maycox et al., 1988; Cidon and Sihra, 1989) (**Figure 4**). This negative charge drives vacuolar-type H^+-ATPase to increase inward flux of protons, causing SV acidification (Blakely and Edwards, 2012). In turn, DA enters SVs via VMAT2 in exchange for two H^+ (Johnson, 1988), resulting in increased intravesicular DA concentration, and increased vesicular DA upon release. Vesicular synergy in DA neuron SVs has been shown by changes in intravesicular pH in response to both DA and GLU gradients (Hnasko et al., 2010; Aguilar et al., 2017). In mouse striatal slices, VGLUT2-dependent SV acidification is associated with increased DA release (Aguilar et al., 2017). $DAT^{Cre};VGluT2^{flox/flox}$ cKO mice show less striatal DA release (Stuber et al., 2010; Alsiö et al., 2011) and injections of an AAV-*Cre* viral vector into the VTA of $VGluT2^{flox/flox}$ mice showed diminished SV acidification (Aguilar et al., 2017). These observations argue for corelease, as they require both VGLUT2 and VMAT2 in the same SV.

Anatomically, DA and GLU release sites appear to be segregated. In rats, anterograde tracing from the SN revealed two types of DA neuron synapses in the striatum (Hattori et al., 1991). Symmetric synapses were seen in TH^+ varicosities in *en passant* configuration, consistent with sites of DA release; asymmetric synapses were located in TH^- axon terminals, consistent with the release of a non-DA excitatory neurotransmitter. Immunostaining of microcultures of single DA neurons showed that DA neurons have partially overlapping populations of TH^+ and GLU^+ varicosities (Sulzer et al., 1998). Several subsequent ultrastructural studies have found sparse $TH^+/VGLUT2^+$ varicosities in rat (Bérubé-Carrière et al., 2009; Moss et al., 2011) and mouse striata (Bérubé-Carrière et al., 2012; Fortin et al., 2019). VMAT2 and VGLUT2 appear to be actively trafficked to different processes; VMAT2 overexpression does not reduce segregation, consistent with an active process that mediates spatial segregation (Zhang et al., 2015). DA neurons co-cultured with ventral striatal neurons demonstrated enhanced segregation of TH^+ and $VGLUT2^+$ varicosities, suggesting that target-dependent factors may influence *VGluT2* expression and/or VGLUT2 localization (Fortin et al., 2019).

Although DA transients and cotransmitted GLU EPSCs elicited by optogenetic stimulation share similar release properties (Adrover et al., 2014), more recent functional studies support segregation of DA and GLU release. DA and GLU release by optogenetic stimulation deplete with different kinetics, are coupled to different types of presynaptic Ca^{2+} channels, and are differentially coupled to active zone proteins (adaptor protein 3, synaptic vesicle protein 2 and piccolo) (Silm et al., 2019). These findings are consistent with spatial segregation of DA and GLU SVs. However, studies in *Drosophila* demonstrate that a single VGLUT protein is sufficient to fill a SV with GLU (Daniels et al., 2006); thus, *VGluT2* expression levels with a physiological impact may be below the detection threshold of some methods under certain conditions, e.g., immunohistochemistry (IHC) under electron microscopy. Ultimately, while low levels of VGLUT2 in VMAT2-containing SVs may mediate corelease, spatial segregation of DA and GLU release sites appears to be the predominant configuration in DA-GLU neurons.

WHAT ARE THE SYNAPTIC FUNCTIONS OF DA NEURON GLU COTRANSMISSION?

Excitatory Synaptic Transmission

DA volume transmission — where DA is released at non-synaptic sites and diffuses to extra-synaptic receptors — signals on a slower time frame than direct synaptic connections (Sulzer et al., 2016). In contrast, GLU cotransmission via direct synaptic connections operates on a faster time frame and conveys a discrete signal (though GLU can also act on a slower time scale at extrasynaptic sites via mGluRs). In NAc m-shell ChIs, optogenetic stimulation of DA neuron axons elicits a burst mediated by iGluRs, followed by a post-burst hyperpolarization mediated mainly by small conductance Ca^{2+}-dependent K^+ channels and partially by D2 receptors (Chuhma

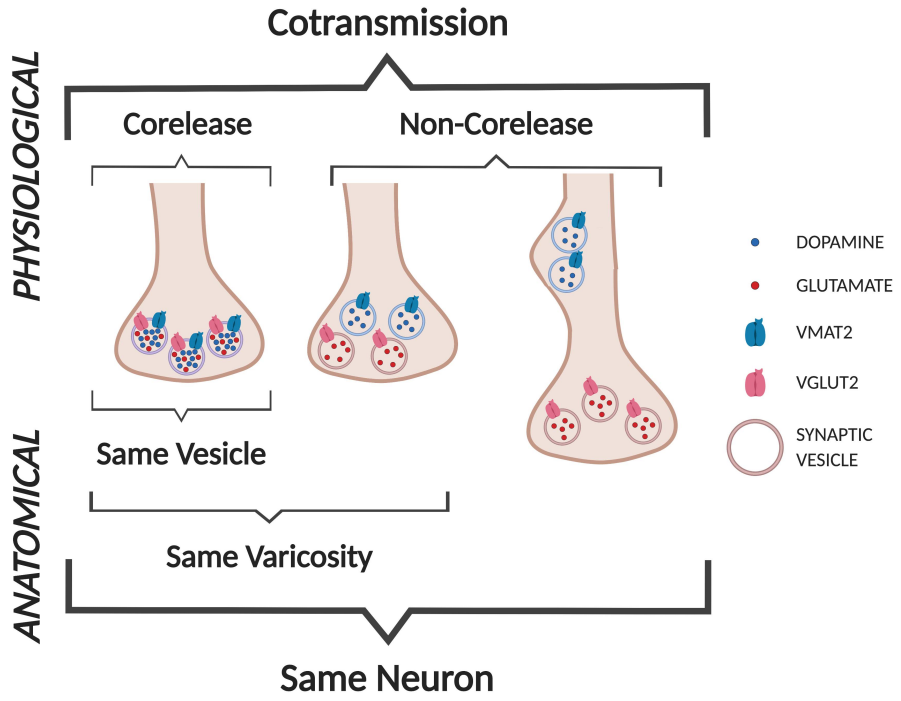

FIGURE 3 | Cotransmission configurations. We define DA neuron GLU *cotransmission* as the release of DA and GLU from the same neuron. Anatomically, DA and GLU could be released from the same vesicles (labeled as *corelease*), or from separate sites in the same varicosity, or more distant sites within the same axon (not shown).

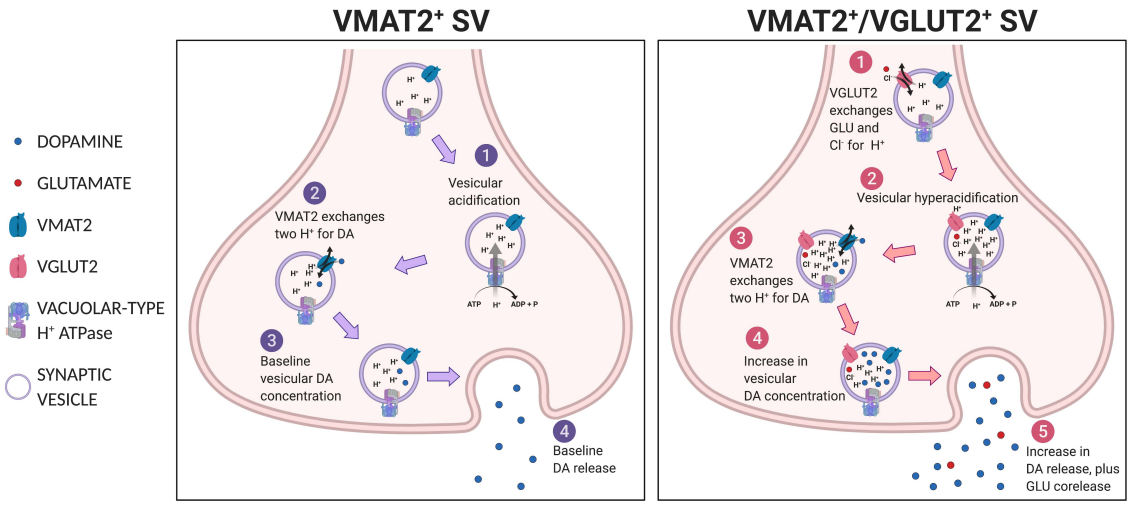

FIGURE 4 | Vesicular synergy. Shown in the left panel, a VMAT2$^+$ SV undergoes **(1)** vesicular acidification, then **(2)** VMAT2 exchanges two H^+s for DA to achieve **(3)** baseline vesicular DA concentration and subsequent **(4)** baseline DA release. Shown in the right panel, a VGLUT2$^+$/VMAT2$^+$ co-expressing SV, **(1)** VGLUT2 transports GLU and Cl^- into SV, which potentiates **(2)** vacuolar-type H^+ATPase to hyperacidify the SV, thus **(3)** more DA is drawn in via VMAT2 in exchange for protons, resulting in **(4)** greater intravesicular DA concentration and subsequent release **(5)**.

et al., 2014). In lateral dorsal striatum ChIs, the response is a pause mediated by D2 receptors followed by excitation mediated by mGluR1 and D1/5 receptors coupling to transient receptor potential channels 3 and 7 (Cai and Ford, 2018; Chuhma et al., 2018).

Dopamine neuron GLU EPSCs are subject to frequency-dependent DA modulation. In the NAc m-shell, DA causes counteracting D2-mediated presynaptic inhibition and D1-mediated postsynaptic facilitation through closure of K^+ channels on GLU cotransmission. At *tonic-firing* frequencies

D2-mediated presynaptic inhibition dominates and GLU responses are attenuated, while at *burst-firing* frequencies postsynaptic facilitation dominates and the GLU responses are enhanced (Chuhma et al., 2009). DA neuron GLU EPSPs are attenuated subsequent to low-dose amphetamine, whereas high-dose amphetamine attenuates fast DA transmission as well (Chuhma et al., 2014).

Circuit-Level Effects

In the striatum, DA neurons make GLU connections preferentially to ChIs in the NAc m-shell and lateral dorsal striatum (Chuhma et al., 2014, 2018; Cai and Ford, 2018). ChIs are distributed throughout the striatum with widespread axonal arborizations. Most striatal neurons express acetylcholine receptors, particularly on their presynaptic terminals (Lim et al., 2014; Ztaou and Amalric, 2019). This points to widespread effects of DA neuron GLU cotransmission on striatal circuits via modulation of ChI activity (Stocco, 2012; Zhang and Cragg, 2017; Assous and Tepper, 2019). DA neuron GLU cotransmission can also exert positive feedback on DA neuron transmission via presynaptic nicotinic acetylcholine receptors (nAChRs) (**Figure 5**). In the m-shell, DA neuron GLU cotransmission activates ChIs directly with short latency (Chuhma et al., 2014; Mingote et al., 2017), potentially inducing synchronized activation of ChIs (Mingote et al., 2019). Increased ChI activity may then activate nAChRs on DA neuron terminals resulting in an increase in DA release (Cachope et al., 2012; Threlfell et al., 2012), forming a positive feedback loop. Lack of DA neuron GLU cotransmission in $DAT^{Cre};VGluT2^{flox/flox}$ cKO mice disrupts this loop; it also reduces DA release in the striatum, in line with disrupted vesicular synergy (Stuber et al., 2010; Alsiö et al., 2011).

Dopamine neuron GLU cotransmission appears to regulate activity in multiple brain regions. $DAT^{Cre};VGluT2^{flox/flox}$ cKO mice have widespread alterations in immediate early genes *c-fos* and *Nur77* in striatal subregions (Alsiö et al., 2011). Circuit-level alterations are also shown by an increase in AMPA/NMDA ratio in D1-receptor expressing SPNs in the NAc in tamoxifen-inducible DA-neuron-specific *VGluT2* cKO ($DAT^{Cre-ERT2};VGluT2^{flox/flox}$) mice, in which *VGluT2* is conditionally excised from DA neurons in adulthood (Papathanou et al., 2018). In acute hippocampal slices, local field potential recordings revealed $TH^{IRES-Cre};VGluT2^{flox/flox}$ cKO mice had fewer kainate-induced gamma oscillations and more epileptic activity than controls (Nordenankar et al., 2015); suggesting network-wide effects that may alter excitation/inhibition balance involving multiple brain regions.

WHAT ARE THE DEVELOPMENTAL ROLES OF DA NEURON GLU COTRANSMISSION?

Embryonic Differentiation of DA Neurons and Development of VGluT2 Expression

During development most, if not all, DA neurons in the ventral midbrain express *VGluT2*, and a substantial portion continue to do so in adulthood (Wallén-Mackenzie et al., 2006; Dal Bo et al., 2008; Birgner et al., 2010; Fortin et al., 2012; Trudeau et al., 2014; Steinkellner et al., 2018; Bimpisidis and Wallén-Mackenzie, 2019; Dumas and Wallén-Mackenzie, 2019; Kouwenhoven et al., 2020; **Table 1**). Embryonic cell-fate labeling shows that >90% of DA neurons in the VTA and SN in adult mice expressed *VGluT2* during development (Steinkellner et al., 2018; Kouwenhoven et al., 2020; Fougère et al., 2021).

In the medial VTA, where most DA-GLU neurons are located, DA neuron differentiation is directed by zinc finger transcription factor Gli2 (Kabanova et al., 2015). Gli2 mediates sonic hedgehog (Shh)-induced formation of DA neuron progenitor cells around embryonic day (E) 9. Conditional knockout (cKO) of Gli2 during this period in $En1^{Cre/+};Gli2^{zfd/flox}$ (termed $Gli2^{\Delta Mb>E9.0}$) cKO mice reduced the number of TH^+ neurons by about 50% and $TH^+/VGLUT2^+$ neurons by about 70%, while the number of VGLUT2-only (i.e., $TH^-/VGLUT2^+$) neurons is unaffected (Kabanova et al., 2015). The decrease in $TH^+/VGLUT2^+$ DA neurons leads to a significant reduction of DA neuron GLU cotransmission to inhibitory interneurons in the PFC (Kabanova et al., 2015). Remarkably, Shh continues to provide trophic support to DA neurons in adulthood, as DA-neuron-specific Shh cKO ($Shh^{nLZC/C};DAT^{Cre}$) accelerates DA neuron degeneration via failure of reciprocal trophic support (Gonzalez-Reyes et al., 2012).

In addition to being the vesicular glutamate transporter subtype preferentially expressed in DA neurons, *VGluT2* is also the predominant subtype expressed in the embryonic brain (Boulland et al., 2004). *VGluT2* null mice ($VGluT2^{flox/flox;PCre}$) die shortly after birth due to the role of VGLUT2 in brainstem respiratory central pattern generators (Moechars et al., 2006; Wallén-Mackenzie et al., 2006). DA-neuron-specific *VGluT2* cKO, driven by either DAT^{Cre} or TH^{Cre} transgenes in $VGluT2^{flox/flox}$ mice, is not lethal. However, the *VGluT2* cKO affects DA neuron survival, maturation (including projections and formation of connections), and response to injury (Dal Bo et al., 2008; Bérubé-Carrière et al., 2009; Fortin et al., 2012; Shen et al., 2018; Steinkellner et al., 2018; Kouwenhoven et al., 2020). Since *VGluT2* expression in nascent DA neurons is detected around E10, prior to expression of DA neuron markers (Dumas and Wallén-Mackenzie, 2019), even $DAT^{Cre};VGluT2^{flox/flox}$ and $TH^{Cre};VGluT2^{flox/flox}$ cKO mice likely express *VGluT2* in DA neurons transiently. *DAT* expression starts at E14 and Cre-dependent recombination in DAT^{Cre} mice is clearly observed at E17 (Bäckman et al., 2006), indicating that Cre-dependent *VGluT2* excision occurs in late embryonic life. TH expression begins before this, as shown by $TH^+/VGLUT2^+$ neurons detected during E11.5–12.5 (Birgner et al., 2010; Nordenankar et al., 2015). Thus, it is important to note that findings from studies using $TH^{Cre};VGluT2^{flox/flox}$ cKO mice represent an earlier loss of VGLUT2 in DA neurons during embryonic development whereas $DAT^{Cre};VGluT2^{flox/flox}$ cKO mice reflect the loss of VGLUT2 function in DA neurons in the early postnatal period.

Regulation of Maturation and Growth

Dopamine neurons in $DAT^{Cre};VGluT2^{flox/flox}$ cKO mice have smaller soma size, shorter axonal lengths and reduced neurite

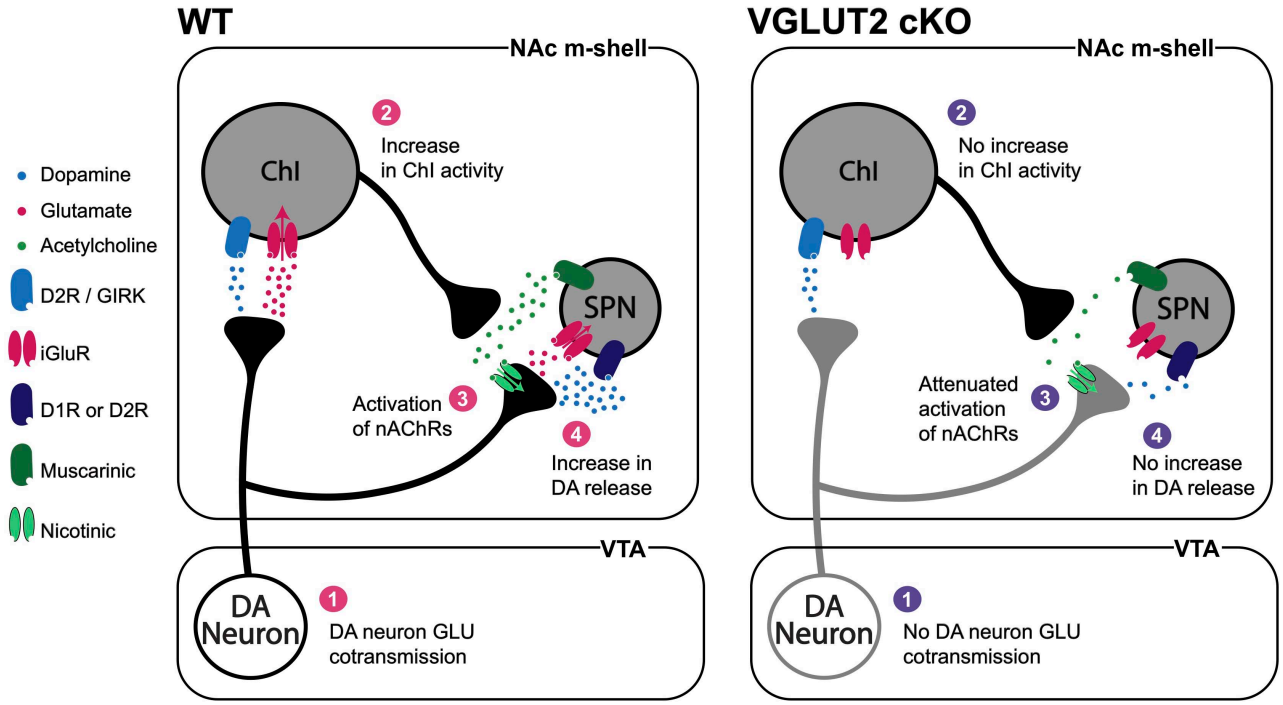

FIGURE 5 | DA neuron GLU cotransmission circuit effects. DA neuron GLU cotransmission **(1)** increases ChI activity **(2)** and acetylcholine release that activates nAChRs on DA neuron terminals **(3)** to increase DA release **(4)**. In DA-neuron-specific *VGluT2* cKO mice **(1)** there would be no increase in ChI activity, **(2)** attenuated activation of nAChRs **(3)** and reduced DA release **(4)**. Vesicular synergy is not shown in this figure.

complexity (Fortin et al., 2012). Although there were no apparent changes in the configuration of the medial forebrain bundle, the total number of TH^+ neurons are reduced by ∼25% in the VTA and ∼20% in the SNc (Fortin et al., 2012). There are significant reductions in TH^+ axon density and DA release, measured with cyclic voltammetry, in the NAc shell, but not in the NAc core (Fortin et al., 2012), consistent with the more prominent GLU cotransmission in the NAc shell. Expression of DA receptors was increased in both the dorsal and ventral striatum in $DAT^{Cre};VGluT2^{flox/flox}$ cKO mice, further suggesting a role for DA neuron GLU cotransmission in the establishment of meso-striatal projections (Alsiö et al., 2011).

In co-cultures of DA and GABA neurons, only ∼20% of TH^+ neurons coexpress *VGluT2*, whereas in pure DA neuron cultures ∼50% of TH^+ neurons coexpress *VGluT2* (Mendez et al., 2008b). GABA did *not* reduce $TH^+/VGLUT2^+$ co-labeling in DA neuron culture, suggesting that a contact-dependent mechanism is required for downregulation of *VGluT2* expression (Mendez et al., 2008b). Quinolinic acid lesions of the medial dorsal striatum led to increased *VGluT2* expression in midbrain DA neurons (Mendez et al., 2008b). This could be a consequence of lost neurotrophic support from postsynaptic targets, or lack of afferent inputs to midbrain DA neurons. A more recent study showed that co-culture of DA neurons with dorsal striatal neurons reduced *VGluT2* mRNA expression, whereas co-culture of DA neurons with ventral striatal neurons increased *VGluT2* expression (Fortin et al., 2019). These findings suggest further that striatal neurons exert trophic effects on *VGluT2* expression in midbrain DA neurons. Overall, both pre and postsynaptic mechanisms appear to be important for growth and survival of DA-GLU neurons.

HOW ARE DA-GLU NEURONS AFFECTED BY DA NEURON TOXINS?

DA-GLU neurons appear to be less vulnerable to the DA neuron toxins 6-hydroxydopamine (6-OHDA) and 1-methyl-4-phenyl-1,2,3,6-tetrahydropyridine (MPTP) (**Table 2**). Intraventricular 6-OHDA injections in juvenile and adult rats increase the proportion of $TH^+/VGLUT2^+$ neurons among TH^+ neurons in the VTA (Dal Bo et al., 2008; Bérubé-Carrière et al., 2009). 6-OHDA injections in the dorsal striatum increase the proportion of $TH^+/VGLUT2^+$ neurons in the SN (Steinkellner et al., 2018), and $TH^+/VGLUT2^+$ axon terminals in the NAc (Bérubé-Carrière et al., 2009). This increased ratio of $TH^+/VGLUT2^+$ neurons in ventral midbrain DA neurons after toxin exposure could be due to re-expression of *VGluT2* in the surviving $TH^+/VGLUT2^-$ neurons (i.e., 'neurotransmitter switching,' see Spitzer, 2015 for review), or reduced susceptibility of $TH^+/VGLUT2^+$ neurons. Thus, an increase of $TH^+/VGLUT2^+$ projections in the striatum could be due to new projections of VTA $TH^+/VGLUT2^+$ neurons compensating for the loss of SN $TH^+/VGLUT2^+$ neurons, or SN $TH^+/VGLUT2^-$ neurons switching to $TH^+/VGLUT2^+$, resulting in an increase in the

number of DA-GLU neurons. In mouse SN DA neuron culture, 1-methyl-4-phenylpyridinium (MPP+) exposure increases *VGluT2* copy number per cell, while TH copy number per cell is reduced (Kouwenhoven et al., 2020). This suggests that cellular stress drives neurotransmitter switching and similar mechanisms may be activated in surviving DA neurons after toxin exposure.

SN DA neurons in $DAT^{IRES-Cre/+};VGluT2^{flox/flox}$ cKO mice are more vulnerable to 6-OHDA and MPTP than those in $DAT^{IRES-Cre/+};VGluT2^{flox/+}$ conditional heterozygous (cHET) control mice (Shen et al., 2018; Steinkellner et al., 2018; Kouwenhoven et al., 2020). $DAT^{IRES-Cre/+};VGluT2^{flox/flox}$ cKO mice, compared to cHET mice, have reduced levels of brain derived neurotrophic factor and its receptor TrkB in VTA and SN DA neurons, and are more vulnerable to MPTP (Shen et al., 2018). Viral rescue of *VGluT2* expression with an AAV-DIO-*VGluT2* vector in DA neurons of $DAT^{IRES-Cre};VGluT2^{flox/flox}$ cKO mice recovered brain derived neurotrophic factor/TrkB expression and thereby attenuated MPTP-induced DA neuron toxicity. MPTP-induced expression of proapoptotic marker BAX in the midbrain is not different between $DAT^{IRES-Cre/+};VGluT2^{flox/flox}$ cKO mice and cHET control mice, suggesting that a neuroprotective function of VGLUT2 is not related to production of proapoptotic/antiapoptotic factors (Shen et al., 2018). Thus, *VGluT2* expression appears to be neuroprotective via neurotrophic signaling rather than an anti-apoptotic mechanism. However, VGLUT2 appears not to have a purely protective effect as overexpression of *VGluT2* is neurotoxic in both flies and mice, leading to upregulation of markers of apoptosis and inflammatory gliosis (Steinkellner et al., 2018).

WHAT ARE THE BEHAVIORAL ROLES OF DA NEURON GLU COTRANSMISSION?

In this section we have parsed pre-clinical behavioral findings from studies of DA neuron GLU cotransmission along the Research Domain Criteria delineated by the National Institute of Mental Health (**Table 3**–**7**). The Research Domain Criteria were constructed to provide a research framework for mental disorders based on multiple levels, from genomics to behaviors, organized around major divisions called *domains* and subdivisions called *constructs*, meant to encapsulate different aspects that model human functioning in areas related to emotion, cognition and behavior (Insel, 2014). Using this format facilitates comparisons across studies and species.

Positive Valence Systems

Within the Positive Valence Systems domain, DA neuron GLU cotransmission affects two constructs: reward-responsiveness (**Table 3**) and reward learning (**Table 4**). Disruption of DA neuron GLU cotransmission in $DAT^{Cre};VGluT2^{flox/flox}$ cKO mice blunts acute responses to psychostimulants (Birgner et al., 2010; Hnasko et al., 2010; Fortin et al., 2012; Steinkellner et al., 2018). Although $DAT^{Cre};VGluT2^{flox/flox}$ cKO mice were initially hyporesponsive to doses of cocaine, they still showed sensitization (Hnasko et al., 2010) — a measure of increasing reward-responsiveness to repeated exposures to the same dose, which models pathologic incentive motivation in addiction (Robinson and Berridge, 2008). Conversely, cHET of GLU recycling enzyme glutaminase (GLS1) in DA neurons did not affect acute responses to amphetamine, but did diminish sensitization and blunted responses to subsequent challenge doses (Mingote et al., 2017). Even when initial responses are intact, impaired DA neuron GLU cotransmission still disrupts reward responsiveness. Since reduced GLU cotransmission does not affect motor control or negative valence systems (see below), the blunted reward responsiveness is not secondary to motor or emotional impairment.

Cocaine-seeking induced by drug-paired cues and cocaine intravenous self-administration are enhanced in $DAT^{Cre};VGluT2^{flox/flox}$ in cKO mice (Alsiö et al., 2011). Operant conditioning for high-sucrose food is also enhanced in $DAT^{Cre};VGluT2^{flox/flox}$ cKO mice, showing that DA neuron GLU cotransmission modulates intensity of responses not only to psychostimulants, but also to natural rewards (Alsiö et al., 2011). $DAT^{IRES-Cre};VGluT2^{flox/flox}$ cKO mice showed reduced progressive intracranial optogenetic self-stimulation of VTA TH^+ neurons, supporting the hypothesis that DA neuron GLU cotransmission regulates the magnitude of operant behaviors (Wang et al., 2017). Although GLU released from DA neurons may not be critical for the acquisition of conditioned reinforcement, its loss nonetheless affects positive valence systems. For example, $VGluT2^{Cre};TH^{flox/flox}$ cKO mice, which have *TH* excised from $VGLUT2^+$ DA neurons (i.e., DA neurons with blunted DA transmission but intact GLU cotransmission), optogenetic stimulation of $VGluT2^{Cre/AAV-DIO-ChR2}$ VTA neurons was sufficient to reinforce behavior (Zell et al., 2020). Although this study did not discriminate contributions of GLU-only (non-DAergic) neurons and GLU cotransmission from DA-GLU neurons, GLU cotransmission from DA-GLU neurons presumably contributes to DA-independent positive reinforcement.

The only DA-neuron-specific *VGluT2* cKO study without an impaired response to acute psychostimulants used a $TH^{IRES-Cre}$ transgene instead of a DAT^{Cre} or $DAT^{IRES-Cre}$ transgene to establish the DA-neuron-specific *VGluT2* cKO (Nordenankar et al., 2015). Subsequent reviews have cautioned about comparisons between TH^{Cre} and DAT^{Cre} induced conditional gene expression (Pupe and Wallén-Mackenzie, 2015; Stuber et al., 2015; Lammel et al., 2015; Buck et al., 2020; Fischer et al., 2020). Briefly, TH^{Cre} mice cause more developmental effects than DAT^{Cre} mice, because *TH* expression begins earlier in development than *DAT* (see above), and is more widespread and ectopic (i.e., neurons that are positive for *TH* mRNA but not TH protein) (Di Porzio et al., 1990). Although, DAT^{Cre} mice also show off-target recombination in a subset of DAT-negative neurons in particular limbic areas (Papathanou et al., 2019). Also, because TH is part of the synthetic pathway of norepinephrine, norepinephrine neurons will be affected in TH^{Cre} mice as well. It should be noted that intensity of responses to psychostimulants can also be affected by background strain, e.g., *C57BL/6J* mice show greater responses than *129S2/SvHsd* mice (Chen et al., 2007). Although the background strain issue is partly mitigated

TABLE 2 | Effect of toxins on DA neuron GLU cotransmission.

Species and Age	Genotype	Method	Toxin	$TH^+VGLUT2^+$/Total TH^+%		Effect on DA neurons	Citation
				VTA	SN		
Rat P15	WT	ISH	**Vehicle**	7.1	0.7	In NAc% $TH^+/VGLUT2^+$ axon terminals higher in 6-OHDA group (37.4%) *vs.* vehicle (28.2%)	Dal Bo et al., 2008
			6-OHDA Intraventricular on P4 (perfusion 11d later)	26	0.0		
Mouse P52	WT	IHC	**Vehicle**	15	9.0	Increased loss of SN TH^+ neurons	Steinkellner et al., 2018
			6-OHDA Dorsal striatum on P42 (perfusion 10d later)	19	21		
	DAT$^{IRES-Cre/+}$; *VGluT2*$^{flox/+}$ or *DAT*$^{IRES-Cre/+}$; *VGluT2*$^{flox/flox}$	IHC	**6-OHDA** Dorsal striatum on P42 (perfusion 10d later)		–	Increased loss of SN TH^+ neurons, significantly more in cKO mice	
Mouse P8–12 weeks	*DAT*$^{IRES-Cre/+}$; *VGluT2*$^{flox/+}$ or *DAT*$^{IRES-Cre/+}$; *VGluT2*$^{flox/flox}$	IHC	**Acute MPTP** 15 mg/kg i.p. × 4 2 h apart, same day. (perfusion 7 h later)		–	Increased loss of midbrain TH^+ neurons in cKO mice	
			Chronic MPTP 30 mg/kg i.p. × 5 days (perfusion 21 days later)		–	Increased loss of midbrain TH^+ neurons in cKO mice	
Mouse P8–12 weeks	*DAT*$^{IRES-Cre/+}$; *VGluT2*$^{flox/+}$	IHC	**Vehicle**	15	20	Increased loss of VTA and SN TH^+ neurons in cKO mice. Reduced TH and DAT throughout striatum. Viral rescue of *VGluT2* in DA neurons slightly attenuated reduction	Shen et al., 2018
			Acute MPTP 18 mg/kg; i.p. × 4 2 h apart, same day. (perfusion 14 days later)	35	45		
	DAT$^{IRES-Cre/+}$; *VGluT2*$^{flox/flox}$		**Acute MPTP** 18 mg/kg; i.p. × 4 2 h apart, same day. (perfusion 14 days later)	–	–		
Mouse > P60	*DAT*$^{IRES-Cre/+}$; *VGluT2*$^{flox/flox}$		**Acute 6-OHDA** Dorsal striatum (perfusion 7 weeks later)	-	-	Impaired striatal re-innervation post-6-OHDA in cKO mice.	Kouwenhoven et al., 2020
Rat P90	WT	ISH	**Artificial cerebrospinal fluid**	2.4	0.3	In NAc% of $TH^+/VGLUT2^+$ axon terminals higher with 6-OHDA (0.05%) *vs.* vehicle (0%)	Bérubé-Carrière et al., 2009
			6-OHDA Intraventricular on P4 (perfusion 11 days later)	7.2	0.0		

TABLE 3 | Positive valence systems: reward responsiveness construct.

	Paradigm	Manipulation	Behavioral Result	Citation
Cocaine, acute response	20 mg/kg i.p.	*DAT^{Cre};VGluT2$^{flox/flox}$*	**Decreased** response	Hnasko et al., 2010
	10 mg/kg i.p.	*DAT^{Cre};VGluT2$^{flox/flox}$*	**Decreased** response	Fortin et al., 2012
	20 mg/kg i.p.	Heterologous *VGluT2* overexpression. Unilateral SNc *DAT^{Cre}*	**Decreased** response	Steinkellner et al., 2018
Cocaine sensitization	5 days of daily injections (20 mg/kg i.p) and re-test 72 h later	*DAT^{Cre};VGluT2$^{flox/flox}$*	**Intact** sensitization (cKO mice steadily increased responses over days 1–4, but at **lower** levels. By day 5 and on challenge cKO mice had similar responses.	Hnasko et al., 2010
	5 days of daily injections (20 mg/kg i.p.). No re-test	*DAT^{Cre};VGluT2$^{flox/flox}$; DRD1-EGFP*	Intact sensitization. However, on day 5, cKO mice had **less distance** traveled.	Papathanou et al., 2018
		DAT$^{Cre-ERT2}$; VGluT2$^{flox/flox}$; DRD1-EGFP Tamoxifen 2 mg i.p. daily × 5 days at P8–9 weeks.	Intact sensitization. Though, overall, **less distance** traveled in tamoxifen-treated group.	
Amphetamine, acute response	1.5, 3.0, and 5.0 mg/kg i.p.	*DAT^{Cre};VGluT2$^{flox/flox}$*	Overall activity of cKO **lower** than cHET, though total activity and rearing rose with increased doses.	Birgner et al., 2010
	0.75 mg/kg i.p.	*DAT^{Cre};VGluT2$^{flox/flox}$*	**Decreased** response.	Fortin et al., 2012
	1.5 mg/kg i.p.	*TH$^{IRES-Cre}$;VGluT2$^{flox/flox}$*	**Unaltered**.	Nordenankar et al., 2015
	3.0 and 5.0 mg/kg i.p.	*DAT$^{IRES-Cre}$;Gls1$^{flox/+}$*	**Unaltered**.	Mingote et al., 2017
	3.0 mg/kg i.p.	Heterologous *VGluT2* overexpression. Unilateral SNc *DAT^{Cre}*	**Decreased** response.	Steinkellner et al., 2018
Amphetamine sensitization	Five daily injections of 2.5 mg/kg i.p. Challenge to same dose 2 weeks later.	*DAT$^{IRES-Cre}$;Gls1$^{flox/+}$*	**No sensitization** over 5 days. Blunted response to challenge at 2 weeks.	Mingote et al., 2017
	Four daily injections of 3.0 mg/kg i.p. Challenge to same dose 2 weeks later	*DAT^{Cre};VGluT2$^{flox/flox}$*	**No sensitization** over 4 days. Blunted response to challenge at 2 weeks. Repeated protocol 1 week later with 2 challenges, no sensitization.	Papathanou et al., 2018
		DAT$^{Cre-ERT2}$;VGluT2$^{flox/flox}$; DRD1-EGFP Tamoxifen 2mg i.p. daily x 5d at P8-9w.	Both groups showed an increase in AMPH-induced locomotion, **no difference** between genotypes.	

by use of littermate controls, difference in background strains must be considered when comparing studies (Crawley et al., 1997; Bailey et al., 2006; Linder, 2006, 2001; Yoshiki and Moriwaki, 2006).

Behavioral studies using cKO mice with *DAT* or *TH* promoters to drive Cre recombinase to excise floxed *VGluT2* from DA neurons must be interpreted with caution, because effects seen in adulthood can be caused by developmental derangements *and/or* effects of diminished GLU cotransmission in adulthood. Both *DAT* and *TH* are expressed during embryogenesis (Di Porzio et al., 1990; Bäckman et al., 2006), thus, *DAT^{Cre};VGluT2$^{flox/flox}$* and *TH^{Cre};VGluT2$^{flox/flox}$* cKO mice lose VGLUT2 function in DA neurons in early life (see above). For example, *DAT^{Cre};VGluT2$^{flox/flox}$* cKO mice show impaired responses to psychostimulants, and have reduced TH$^+$ neuron numbers, thus the impaired responses to psychostimulants could be due to lack of DA neuron GLU cotransmission in adulthood and/or reduced TH$^+$ neurons (Birgner et al., 2010; Fortin et al., 2012). Of note, *DAT$^{IRES-Cre}$;Gls1$^{flox/+}$* cHET mice also have impaired responses to psychostimulants, *despite* unaffected DA neuron number or DA release (Mingote et al., 2017). To further circumvent issues related to developmental alterations, Papathanou and colleagues knocked out *VGluT2* from DA neurons in adulthood using tamoxifen-inducible DA-neuron-specific *VGluT2* cKO (*DAT$^{Cre-ERT2}$;VGluT2$^{flox/flox}$*) mice (Papathanou et al., 2018). Control *DAT^{Cre};VGluT2$^{flox/flox}$* cKO mice showed blunted sensitization to cocaine and amphetamine, in agreement with previous studies (Hnasko et al., 2010; Fortin et al., 2012; Mingote et al., 2017), whereas *DAT$^{Cre-ERT2}$;VGluT2$^{flox/flox}$* cKO mice given tamoxifen at 8–9 weeks of age did not show psychostimulant-induced hyperlocomotion (Papathanou et al., 2018), thus demonstrating that DA-neuron-specific *VGluT2* expression in adulthood is necessary for full psychostimulant responsivity. A potential confound is that all mice receiving tamoxifen showed blunted responses to psychostimulants –

TABLE 4 | Positive valence systems: reward learning construct.

Paradigm		Manipulation	Behavioral Result	Citation
Cocaine conditioned place preference	5 mg/kg s.c. for 3 days	*DAT^{Cre};VGluT2$^{flox/flox}$*	**Unaltered**	Hnasko et al., 2010
Cocaine IV Self-administration	0.0625, 0.125, and 1.0 mg/kg infusion	*DAT^{Cre};VGluT2$^{flox/flox}$*	**Enhanced** at low dose; **unaltered** at higher doses	Alsiö et al., 2011
Cocaine-seeking to drug-paired cues		*DAT^{Cre};VGluT2$^{flox/flox}$*	**Increased** by 76%	
Operant conditioning high-sucrose food		*DAT^{Cre};VGluT2$^{flox/flox}$*	**Enhanced**	
Intracranial self-optogenetic-stimulation VTA TH^{+} neurons		*DAT$^{IRES-Cre/+}$;VGluT2$^{flox/flox}$* Viral DIO-*ChR2* into VTA	**Slight impairment** with 32 mW/3 ms stimulation. **No difference** during 1st five sessions with 8 mW/1 ms stimulation.	Wang et al., 2017
Conditioned Place Preference to VTA TH^{+} neuron optogenetic-stimulation		*DAT$^{IRES-Cre/+}$;VGluT2$^{flox/flox}$* Viral DIO-*ChR2* into VTA	**No difference**.	
Intracranial self-stimulation of NAc m-shell		*VGluT2^{Cre};TH$^{flox/flox}$* Viral DIO-*ChR2* into VTA	**No difference**. Equivalent preference for nosepoke hole coupled to optogenetic stimulation.	Zell et al., 2020
Intracranial self-stimulation of VTA				
Real-time place preference of NAc m-shell			**No difference**. Loss of DA from VGLUT2^{+} neurons did not alter response (avoidance of 40 Hz optogenetic stimulation)	
Real-time place preference of VTA				
Intracranial self-stimulation of NAc m-shell		*VGluT2^{Cre}* Viral DIO-*ChR2* and Viral FLEX-SaCas9-sg*Th* into VTA	**No difference**. Equivalent preference for nosepoke hole coupled to optogenetic stimulation	
Intracranial self-stimulation of VTA				
Real-time place preference of NAc m-shell			**No difference**. Loss of DA from VGLUT2^{+} neurons did not alter response (avoidance of 40 Hz optogenetic stimulation)	
Real-time place preference of VTA				

TABLE 5 | Cognitive control systems.

Paradigm	Manipulation	Behavioral Result	Citation
Radial arm maze	*TH$^{IRES-Cre}$;VGluT2$^{flox/flox}$*	**Impaired:** cKO mice made more reference memory errors.	Nordenankar et al., 2015
Latent inhibition	*DAT$^{IRES-Cre}$;Gls1$^{flox/+}$*	**Potentiated:** sub-threshold pre-exposure to tone sufficient to induce latent inhibition in cHET mice.	Mingote et al., 2017

regardless of genotype (i.e., both *DAT$^{Cre-ERT2}$;VGluT2$^{flox/flox}$* cKO and *DAT$^{Cre-ERT2}$;VGluT2$^{flox/+}$* cHET). These blunted responses to psychostimulants could be due to tamoxifen itself, which impairs locomotor responses to amphetamine, even if tamoxifen is not given on the day of locomotor testing (Mikelman et al., 2018). Nonetheless, this suggests that DA neuron GLU cotransmission later in life still mediates psychostimulant responses, but perhaps less so than estimated from observations in *DAT^{Cre};VGluT2$^{flox/flox}$* and *TH^{Cre};VGluT2$^{flox/flox}$* cKO mice.

Cognitive Control

Roles for DA neuron GLU cotransmission in the cognitive control domain have been studied with latent inhibition and tests of spatial working memory (**Table 5**). Latent inhibition is a testable cognitive behavior with clinical relevance to schizophrenia, observed in both rodent models and in clinical studies (Gaisler-Salomon et al., 2009; Weiner and Arad, 2009). Latent inhibition assesses how pre-exposure to a conditioned stimulus (CS; typically, a tone) prevents formation of an association between that CS and an unconditioned stimulus (US; typically, a shock). In mice, testing for latent inhibition has three phases. First, *the CS-only pre-exposure phase*, all mice are placed in a chamber but only the experimental group is exposed several times to a tone, whereas the control group is not. Second, *the CS-US pairing phase*, both groups of mice are placed in the testing chamber and receive a footshock paired with the tone. Last, *the CS-only test phase*, all mice are exposed to the tone and freezing behaviors are measured. Sufficient pre-exposure to the tone reduces freezing during the CS-only test phase, despite the

TABLE 6 | Negative valence systems.

Paradigm	Manipulation	Behavioral Result	Citation
Construct: Acute threat ("Fear")			
Elevated plus maze	$DAT^{Cre};VGluT2^{flox/flox}$	**Increased** latency to start	Birgner et al., 2010
	$TH^{IRES-Cre};VGluT2^{flox/flox}$	**Normal**	Nordenankar et al., 2015
	$DAT^{IRES-Cre};Gls1^{flox/+}$	**Normal**	Mingote et al., 2017
	$DAT^{IRES-Cre};VGluT2^{flox/flox}$	**Increased** anxiety after MPTP administration	Shen et al., 2018
Fear conditioning	$DAT^{IRES-Cre};Gls1^{flox/+}$	**Normal**	Mingote et al., 2017
Open field test	$DAT^{Cre};VGluT2^{flox/flox}$	**Decreased** time in the central circle of the open field	Birgner et al., 2010
	$DAT^{IRES-Cre};Gls1^{flox/+}$	**Normal**	Mingote et al., 2017
		Construct: Sustained threat	
Forced swim test	$DAT^{Cre};VGluT2^{flox/flox}$	**Normal**	Birgner et al., 2010
	$DAT^{Cre};VGluT2^{flox/flox}$	**Normal** (though decreased latency to immobilization on Day 1)	Fortin et al., 2012
	$TH^{IRES-Cre};VGluT2^{flox/flox}$	**Normal**	Nordenankar et al., 2015

TABLE 7 | Motor control systems.

Paradigm	Manipulation	Behavioral Result	Citation
Locomotor activity	$DAT^{Cre};VGluT2^{flox/flox}$	**No difference** in novelty-associated locomotion over 4 h or total locomotion across 3 days	Hnasko et al., 2010
	$DAT^{Cre};VGluT2^{flox/flox}$	**No difference** in locomotion or rearing activity in novel environment; decreased horizontal activity	Fortin et al., 2012
	$TH^{IRES-Cre};VGluT2^{flox/flox}$	**Normal**	Nordenankar et al., 2015
	$DAT^{IRES-Cre};Gls1^{flox/+}$	**Normal**	Mingote et al., 2017
	Heterozygous *VGluT2* over-expression unilateral SNc DAT^{Cre}	**Significantly reduced** spontaneous locomotor activity	Steinkellner et al., 2018
	$DAT^{IRES-Cre};VGluT2^{flox/flox}$	MPTP induced a **significant reduction** in vertical activity. *Viral rescue of VGluT2 in DA neurons attenuated these reductions.*	Shen et al., 2018
Accelerating rotarod	$DAT^{Cre};VGluT2^{flox/flox}$	**Normal**	Birgner et al., 2010
	$DAT^{Cre};VGluT2^{flox/flox}$	**Normal** across 5 days	Hnasko et al., 2010
	$DAT^{Cre};VGluT2^{flox/flox}$	**Impaired** (significant decrease in distance day 1, speed/latency to fall both days)	Fortin et al., 2012
	$DAT^{IRES-Cre};Gls1^{flox/+}$	**Normal** across 3 days	Mingote et al., 2017
	$DAT^{IRES-Cre};VGluT2^{flox/flox}$	**No difference** in MPTP-induced deficits	Shen et al., 2018
Beam walk	$DAT^{Cre};VGluT2^{flox/flox}$	**Normal**	Birgner et al., 2010
Parallel rod floor	$DAT^{IRES-Cre};VGluT2^{flox/flox}$	MPTP-induced **deficits pronounced** in cKO mice. *Deficits were restored by viral rescue of VGluT2 expression in DA neurons.*	Shen et al., 2018

temporal delay between pre-exposure and test (*latent inhibition*). $DAT^{IRES-Cre};Gls1^{flox/+}$ cHET mice showed an enhanced latent inhibition, i.e., an enhanced ability to discriminate cue saliency (Mingote et al., 2017), suggesting that abrogated GLU release from DA neurons facilitates cognitive function.

$TH^{IRES-Cre};VGluT2^{flox/flox}$ cKO mice have impaired learning a radial arm maze, a task used to assess spatial working memory (Nordenankar et al., 2015). Although $TH^{IRES-Cre};VGluT2^{flox/flox}$ cKO mice were still able to learn the task, they took significantly longer and made more reference memory errors, but not working memory errors, than $TH^{IRES-Cre};VGluT2^{flox/+}$ cHET controls (Nordenankar et al., 2015). Reference memory errors are thought to reflect hippocampal deficits, whereas working memory errors reflect impairments in frontal cortical networks (Yoon et al., 2008). Lack of DA neuron GLU cotransmission appears to impair hippocampal reference memory, suggesting that intact cotransmission may facilitate spatial reasoning beyond simply improving attention. $Gli2^{\Delta\ Mb>E9.0}$ cKO also results in a substantial reduction in medial VTA $TH^+/VGLUT2^+$ neurons and increases perseverative behavior on the five-choice serial reaction time task, suggesting impaired visuospatial attention and motor impulsivity (Kabanova et al., 2015). However, the contribution of mesocortical GLU-only neurons, which are also reduced by *Gli2* cKO in DA neurons, cannot be excluded. Again, since reduced GLU cotransmission does not appear to affect motor control or negative valence systems (see below), the effects on cognitive control are not secondary to motor or emotional impairment.

Negative Valence Systems

Behaviors related to acute and sustained threats are largely unaffected by impaired DA neuron GLU cotransmission (Birgner et al., 2010; Fortin et al., 2012; Nordenankar et al., 2015; Mingote et al., 2017; **Table 6**). Standard tests

of anxiety, such as the elevated-plus maze and open field test, are mostly unaffected in $DAT^{Cre};VGluT2^{flox/flox}$ cKO mice and $TH^{IRES-Cre};VGluT2^{flox/flox}$ cKO mice (Birgner et al., 2010; Nordenankar et al., 2015); however, after MPTP administration, $DAT^{IRES-Cre};VGluT2^{flox/flox}$ showed increased anxiety on the elevated-plus maze (Shen et al., 2018). Similarly, freezing in a fear-conditioning paradigm did not differ in $DAT^{IRES-Cre};Gls1^{flox/+}$ cHET mice (Mingote et al., 2017). Performance on the forced-swim test, a measure of a depressive-like phenotype, is largely unchanged in $DAT^{Cre};VGluT2^{flox/flox}$ cKO mice and $TH^{IRES-Cre};VGluT2^{flox/flox}$ cKO mice (Birgner et al., 2010; Nordenankar et al., 2015), though one study showed a decreased latency to immobilization on day one but not on day two in $DAT^{Cre};VGluT2^{flox/flox}$ cKO mice (Fortin et al., 2012).

Motor Control

Loss or decrease of DA neuron GLU cotransmission, whether in $DAT^{Cre};VGluT2^{flox/flox}$ cKO mice, $TH^{IRES-Cre};VGluT2^{flox/flox}$ cKO mice or $DAT^{IRES-Cre};Gls1^{flox/+}$ cHET mice, does not alter basic motor and arousal function (Birgner et al., 2010; Hnasko et al., 2010; Fortin et al., 2012; Nordenankar et al., 2015; Mingote et al., 2017), with few exceptions in one study using $DAT^{IRES-Cre/+};VGluT2^{flox/flox}$ cKO mice (Steinkellner et al., 2018; **Table 7**). Gross locomotor function is normal in $DAT^{Cre};VGluT2^{flox/flox}$ cKO mice and $TH^{IRES-Cre};VGluT2^{flox/flox}$ cKO mice (Hnasko et al., 2010; Fortin et al., 2012; Nordenankar et al., 2015). Motor coordination tested with rotarod is normal in studies using both sexes of $DAT^{Cre};VGluT2^{flox/flox}$ cKO mice (Birgner et al., 2010; Hnasko et al., 2010), although one study using only $DAT^{Cre};VGluT2^{flox/flox}$ cKO male mice showed impairment (Fortin et al., 2012). It remains unresolved whether this reflects variation between studies or differential effects between males and females, as no female-only study has been performed. MPTP-induced motor impairments were more pronounced in $DAT^{IRES-Cre};VGluT2^{flox/flox}$ cKO mice, but restored by *VGluT2* viral rescue (Shen et al., 2018). The lack of change in motor control could be related to lesser DA neuron GLU cotransmission in the dorsal striatum, which is more associated with motor learning.

DOES DA NEURON GLU COTRANSMISSION HAVE A ROLE IN HUMAN DISORDERS?

Understanding behavioral roles of DA-GLU neurons offers potential insight into human neuropsychiatric disorders. Interactions between DA and GLU figure prominently in neuropsychiatric disorders, and DA neuron GLU cotransmission is one of the points where DA and GLU interact.

Substance Use Disorders/Addiction

In humans, post-mortem studies of cigarette smokers have demonstrated increased VTA *VGLUT2* (human gene) expression compared to healthy controls (Flatscher-Bader et al., 2008). Given that microarrays were performed specifically in the VTA, even though TH-VGLUT2 double-staining was not performed, it is likely some of the *VGLUT2* expressing neurons were DA neurons, suggesting that either increased cotransmission may be a risk factor for smoking or that smoking may alter *VGLUT2* expression in DA neurons. In mice, neonatal nicotine exposure increases numbers of DA-GLU neurons and nicotine preference in adulthood (Romoli et al., 2019). Selectively targeting DA neuron GLU cotransmission may thus serve as a potential treatment for addiction (Bimpisidis and Wallén-Mackenzie, 2019), especially psychostimulant use disorders perhaps by facilitating behavioral switching (Mingote et al., 2019). Further discussion about DA-GLU neurons and addiction is found in recent reviews (Trudeau et al., 2014; Steinkellner et al., 2018; Bimpisidis and Wallén-Mackenzie, 2019; Buck et al., 2020; Fischer et al., 2020).

Psychotic Disorders

Both DA and GLU are implicated in the patho-etiology of schizophrenia by findings ranging from psychopharmacology, post-mortem analyses and *in vivo* brain imaging (for review see Howes et al., 2015). DA neuron GLU cotransmission serves as one potential point of confluence of DA and GLU actions (Chuhma et al., 2017).

One specific role of DA-GLU cotransmission is perhaps best demonstrated in studies of latent inhibition, which models cognitive impairments in schizophrenia, as well as in animal models (Weiner and Arad, 2009). Humans at high-risk for developing psychosis demonstrate deficits in latent inhibition, suggesting it is a cognitive marker of psychotic propensity, rather than a secondary effect of medication or a consequence of chronic schizophrenia (Kraus et al., 2016). As mentioned above, potentiation of latent inhibition in DA neuron $DAT^{IRES-Cre};Gls1^{flox/+}$ cHET mice (Mingote et al., 2017) emphasizes the therapeutic potential of reducing DA neuron GLU cotransmission.

Parkinson Disease

The main motor symptoms of Parkinson Disease (PD) are primarily due to the loss of nigrostriatal DA neurons. A recent study found that following partial loss of DA inputs, DA-driven inhibition of cholinergic activity in the dorsomedial striatum is preserved due to reduced DA reuptake, while GLU co-release evoked excitation in the dorsolateral striatum is lost due to a downregulation of mGluR1 (Cai et al., 2021). Altered DA-acetylcholine interactions have been hypothesized to underpin some of the symptoms of PD (Ztaou and Amalric, 2019). Since DA neuron GLU cotransmission regulates ChI activity, elucidating mechanisms of this regulation may help delineate PD pathophysiology and therapeutics.

One of the most promising treatments for PD is stem cell implantation (Widner et al., 1992; Mendez et al., 2002, 2008a; Wijeyekoon and Barker, 2009). For successful implantation, it is crucial to choose DA neurons in the appropriate developmental stage to survive and form connections (Lindvall, 2012), which may benefit from appropriate *VGluT2* expression levels. For example, wildtype *VGluT2* expression appears to be neuroprotective to DA neurons in PD mouse models (Dal Bo et al., 2008; Bérubé-Carrière et al., 2009; Shen et al., 2018; Steinkellner et al., 2018; Kouwenhoven et al., 2020),

though *VGluT2* overexpression appears to be neurotoxic to DA neurons (Steinkellner et al., 2018). Thus, determining a specific range of appropriate *VGluT2* expression levels to optimize survival may be an important consideration in transplantation protocols to treat PD.

POTENTIAL DIRECTIONS FOR CIRCUIT-BASED PHARMACOTHERAPY

Given its involvement in circuitry underlying various neuropsychiatric disorders — ranging from schizophrenia, addiction, to PD — DA neuron GLU cotransmission is a considerable target of treatment for neuropsychiatric disorders. Refined molecular genetic manipulations can target discrete DA neuron subtypes, opening up new avenues for investigation and serving as proof-of-principle for future treatment of neuropsychiatric disorders.

One such approach is Genetic Pharmacotherapy, which is defined as the use of genetic interventions in mouse models to elucidate potential drug targets prior to the development of specific ligands (Gellman et al., 2011). This strategy enables the evaluation of therapeutic potential for target gene modification without costly and time-consuming development of specific ligands that may lack regional specificity and face issues regarding blood-brain barrier permeability. Genetic Pharmacotherapy achieves region-specific functional modulation by using molecular genetic techniques, such as conditional gene knockouts, to target neurons that express specific markers. This approach has already shown DA neuron GLU cotransmission as a viable target in schizophrenia treatment; DA neuron specific reduction of the GLU recycling enzyme GLS1 affects behaviors relevant to schizophrenia (Mingote et al., 2015b, 2017).

Furthermore, preclinical findings of neural function are applied to clinical trials using gene therapy with non-replicative, non-toxic viral vectors (for review see Lykken et al., 2018). Gene therapy requires characterization of specific circuits impacting a neuropsychiatric disorder, rather than pharmacologic targeting of specific, but widely distributed, cell-signaling receptors (Gordon, 2016). Additionally, because gene therapy can be brain-region specific, and even cell-type specific, it would presumably have less off-target effects compared to oral medications. DA neuron GLU cotransmission is an example of how a genetically distinct neuronal subpopulation affects phenotypes relevant to neuropsychiatric disorders, thus serving as a target for treatment development.

CONCLUSION

Dopamine neurons capable of GLU cotransmission serve as an example of how a specific subset of neurons within a diverse neuronal population can have distinct functions. As the gap between bench and bedside narrows and therapeutic options widen, e.g., non-pharmacological interventions such as gene therapy with intersectional control, DA neuron GLU cotransmission may be targeted for treatment of neuropsychiatric disorders.

AUTHOR CONTRIBUTIONS

DE, SR, and NC: concept, design, and writing. SR and NC: supervision. DE: literature research. DE, LM, SM, LY, SZ, VV, SR, and NC: analysis, interpretation, and critical review. All authors agreed to be accountable for the content of the work.

FUNDING

This work was supported by the National Institute on Drug Abuse R01 DA038966 and National Institute of Mental Health R01 MH117128 and T32 MH018870.

ACKNOWLEDGMENTS

Figures 1, **3**, **4** were created with BioRender.com.

REFERENCES

Adrover, M. F., Shin, J. H., and Alvarez, V. A. (2014). Glutamate and dopamine transmission from midbrain dopamine neurons share similar release properties but are differentially affected by cocaine. *J. Neurosci.* 34, 3183–3192. doi: 10.1523/JNEUROSCI.4958-13.2014

Aguilar, J. I., Dunn, M., Mingote, S., Karam, C. S., Farino, Z. J., Sonders, M. S., et al. (2017). Neuronal depolarization drives increased dopamine synaptic vesicle loading via VGLUT. *Neuron* 95, 1074–1088. doi: 10.1016/j.neuron.2017.07.038

Alsiö, J., Nordenankar, K., Arvidsson, E., Birgner, C., Mahmoudi, S., Halbout, B., et al. (2011). Enhanced sucrose and cocaine self-administration and cue-induced drug seeking after loss of VGLUT2 in midbrain dopamine neurons in mice. *J. Neurosci.* 31, 12593–12603. doi: 10.1523/JNEUROSCI.2397-11.2011

Amilhon, B., Lepicard, E., Renoir, T., Mongeau, R., Popa, D., Poirel, O., et al. (2010). VGLUT3 (vesicular glutamate transporter type 3) contribution to the regulation of serotonergic transmission and anxiety. *J. Neurosci.* 30, 2198–2210. doi: 10.1523/JNEUROSCI.5196-09.2010

Assous, M., and Tepper, J. M. (2019). Excitatory extrinsic afferents to striatal interneurons and interactions with striatal microcircuitry. *Eur. J. Neurosci.* 49, 593–603. doi: 10.1111/ejn.13881

Bäckman, C. M., Malik, N., Zhang, Y., Shan, L., Grinberg, A., Hoffer, B. J., et al. (2006). Characterization of a mouse strain expressing Cre recombinase from the 3' untranslated region of the dopamine transporter locus. *Genesis* 44, 383–390. doi: 10.1002/dvg.20228

Bailey, K. R., Rustay, N. R., and Crawley, J. N. (2006). Behavioral phenotyping of transgenic and knockout mice: practical concerns and potential pitfalls. *ILAR J.* 47, 124–131. doi: 10.1093/ilar.47.2.124

Bérubé-Carrière, N., Guay, G., Fortin, G. M., Kullander, K., Olson, L., Wallén-Mackenzie, Å, et al. (2012). Ultrastructural characterization of the mesostriatal dopamine innervation in mice, including two mouse lines of conditional VGLUT2 knockout in dopamine neurons. *Eur. J. Neurosci.* 35, 527–538. doi: 10.1111/j.1460-9568.2012.07992.x

Bérubé-Carrière, N., Riad, M., Dal Bo, G., Lévesque, D., Trudeau, L.-E., and Descarries, L. (2009). The dual dopamine-glutamate phenotype of growing mesencephalic neurons regresses in mature rat brain. *J. Comp. Neurol.* 517, 873–891. doi: 10.1002/cne.22194

Bimpisidis, Z., and Wallén-Mackenzie, Å (2019). Neurocircuitry of reward and addiction: potential impact of dopamine-glutamate co-release as future target in substance use disorder. *J. Clin. Med.* 8:1887. doi: 10.3390/jcm8111887

Birgner, C., Nordenankar, K., Lundblad, M., Mendez, J. A., Smith, C., le Grevès, M., et al. (2010). VGLUT2 in dopamine neurons is required for psychostimulant-induced behavioral activation. *Proc Natl Acad Sci USA* 107, 389–394. doi: 10.1073/pnas.0910986107

Blakely, R. D., and Edwards, R. H. (2012). Vesicular and plasma membrane transporters for neurotransmitters. *Cold Spring Harb. Perspect. Biol.* 4:a005595. doi: 10.1101/cshperspect.a005595

Boulland, J.-L., Qureshi, T., Seal, R. P., Rafiki, A., Gundersen, V., Bergersen, L. H., et al. (2004). Expression of the vesicular glutamate transporters during development indicates the widespread corelease of multiple neurotransmitters. *J. Comp. Neurol.* 480, 264–280. doi: 10.1002/cne.20354

Buck, S. A., Torregrossa, M. M., Logan, R. W., and Freyberg, Z. (2020). Roles of dopamine and glutamate co-release in the nucleus accumbens in mediating the actions of drugs of abuse. *FEBS J.* 288, 1462–1474. doi: 10.1111/febs.15496

Cachope, R., Mateo, Y., Mathur, B. N., Irving, J., Wang, H.-L., Morales, M., et al. (2012). Selective activation of cholinergic interneurons enhances accumbal phasic dopamine release: setting the tone for reward processing. *Cell Rep.* 2, 33–41. doi: 10.1016/j.celrep.2012.05.011

Cai, Y., and Ford, C. P. (2018). Dopamine cells differentially regulate striatal cholinergic transmission across regions through corelease of dopamine and glutamate. *Cell Rep.* 25, 3148–3157. doi: 10.1016/j.celrep.2018.11.053

Cai, Y., Nielsen, B. E., Boxer, E. E., Aoto, J., and Ford, C. P. (2021). Loss of nigral excitation of cholinergic interneurons contributes to parkinsonian motor impairments. *Neuron* 109, 1137–1149. doi: 10.1016/j.neuron.2021.01.028

Chen, R., Zhang, M., Park, S., and Gnegy, M. E. (2007). C57BL/6J mice show greater amphetamine-induced locomotor activation and dopamine efflux in the striatum than 129S2/SvHsd mice. *Pharmacol. Biochem. Behav.* 87, 158–163. doi: 10.1016/j.pbb.2007.04.012

Chuhma, N. (2015). "Optogenetic Analysis of Striatal Connections to Determine Functional Connectomes," in *Optogenetics*, eds H. Yawo, H. Kandori, and A. Koizumi (Tokyo: Springer), 265–277.

Chuhma, N. (2021). Functional connectome analysis of the striatum with optogenetics. *Adv. Exp. Med. Biol.* 1293, 417–428. doi: 10.1007/978-981-15-8763-4_27

Chuhma, N., Choi, W. Y., Mingote, S., and Rayport, S. (2009). Dopamine neuron glutamate cotransmission: frequency-dependent modulation in the mesoventromedial projection. *Neuroscience* 164, 1068–1083. doi: 10.1016/j.neuroscience.2009.08.057

Chuhma, N., Mingote, S., Kalmbach, A., Yetnikoff, L., and Rayport, S. (2017). Heterogeneity in dopamine neuron synaptic actions across the striatum and its relevance for schizophrenia. *Biol. Psychiatry* 81, 43–51. doi: 10.1016/j.biopsych.2016.07.002

Chuhma, N., Mingote, S., Moore, H., and Rayport, S. (2014). Dopamine neurons control striatal cholinergic neurons via regionally heterogeneous dopamine and glutamate signaling. *Neuron* 81, 901–912. doi: 10.1016/j.neuron.2013.12.027

Chuhma, N., Mingote, S., Yetnikoff, L., Kalmbach, A., Ma, T., Ztaou, S., et al. (2018). Dopamine neuron glutamate cotransmission evokes a delayed excitation in lateral dorsal striatal cholinergic interneurons. *elife* 7:e39786. doi: 10.7554/eLife.39786

Chuhma, N., Tanaka, K. F., Hen, R., and Rayport, S. (2011). Functional connectome of the striatal medium spiny neuron. *J. Neurosci.* 31, 1183–1192. doi: 10.1523/JNEUROSCI.3833-10.2011

Chuhma, N., Zhang, H., Masson, J., Zhuang, X., Sulzer, D., Hen, R., et al. (2004). Dopamine neurons mediate a fast excitatory signal via their glutamatergic synapses. *J. Neurosci.* 24, 972–981. doi: 10.1523/JNEUROSCI.4317-03.2004

Cidon, S., and Sihra, T. S. (1989). Characterization of a H+-ATPase in rat brain synaptic vesicles. Coupling to L-glutamate transport. *J. Biol. Chem.* 264, 8281–8288.

Crawley, J. N., Belknap, J. K., Collins, A., Crabbe, J. C., Frankel, W., Henderson, N., et al. (1997). Behavioral phenotypes of inbred mouse strains: implications and recommendations for molecular studies. *Psychopharmacology* 132, 107–124. doi: 10.1007/s002130050327

Dal Bo, G., Bérubé-Carrière, N., Mendez, J. A., Leo, D., Riad, M., Descarries, L., et al. (2008). Enhanced glutamatergic phenotype of mesencephalic dopamine neurons after neonatal 6-hydroxydopamine lesion. *Neuroscience* 156, 59–70. doi: 10.1016/j.neuroscience.2008.07.032

Dal Bo, G., St-Gelais, F., Danik, M., Williams, S., Cotton, M., and Trudeau, L.-E. (2004). Dopamine neurons in culture express VGLUT2 explaining their capacity to release glutamate at synapses in addition to dopamine. *J. Neurochem.* 88, 1398–1405. doi: 10.1046/j.1471-4159.2003.02277.x

Daniels, R. W., Collins, C. A., Chen, K., Gelfand, M. V., Featherstone, D. E., and DiAntonio, A. (2006). A single vesicular glutamate transporter is sufficient to fill a synaptic vesicle. *Neuron* 49, 11–16. doi: 10.1016/j.neuron.2005.11.032

Di Porzio, U., Zuddas, A., Cosenza-Murphy, D. B., and Barker, J. L. (1990). Early appearance of tyrosine hydroxylase immunoreactive cells in the mesencephalon of mouse embryos. *Int. J. Dev. Neurosci.* 8, 523–532. doi: 10.1016/0736-5748(90)90044-3

Dumas, S., and Wallén-Mackenzie, Å (2019). Developmental co-expression of Vglut2 and Nurr1 in a mes-di-encephalic continuum preceeds dopamine and glutamate neuron specification. *Front. Cell Dev. Biol.* 7:307. doi: 10.3389/fcell.2019.00307

El Mestikawy, S., Wallén-Mackenzie, A., Fortin, G. M., Descarries, L., and Trudeau, L.-E. (2011). From glutamate co-release to vesicular synergy: vesicular glutamate transporters. *Nat. Rev. Neurosci.* 12, 204–216. doi: 10.1038/nrn2969

Eskenazi, D., Chuhma, N., Mingote, S., Ztaou, S., and Rayport, S. (2019). "Functional Connectome Mapping," in *Compendium of In Vivo Monitoring in Real-Time Molecular Neuroscience. Volume 3: Probing Brain Function, Disease and Injury with Enhanced Optical and Electrochemical Sensors*, eds G. S. Wilson and A. C. Michael (Singapore: World Scientific Conpany), 49–71.

Fenno, L. E., Mattis, J., Ramakrishnan, C., Hyun, M., Lee, S. Y., He, M., et al. (2014). Targeting cells with single vectors using multiple-feature Boolean logic. *Nat. Methods* 11, 763–772. doi: 10.1038/nmeth.2996

Fenno, L. E., Ramakrishnan, C., Kim, Y. S., Evans, K. E., Lo, M., Vesuna, S., et al. (2020). Comprehensive dual- and triple-feature intersectional single-vector delivery of diverse functional payloads to cells of behaving mammals. *Neuron* 107, 836–853. doi: 10.1016/j.neuron.2020.06.003

Fischer, K. D., Knackstedt, L. A., and Rosenberg, P. A. (2020). Glutamate homeostasis and dopamine signaling: implications for psychostimulant addiction behavior. *Neurochem. Int.* 144:104896. doi: 10.1016/j.neuint.2020.104896

Flatscher-Bader, T., Zuvela, N., Landis, N., and Wilce, P. A. (2008). Smoking and alcoholism target genes associated with plasticity and glutamate transmission in the human ventral tegmental area. *Hum. Mol. Genet.* 17, 38–51. doi: 10.1093/hmg/ddm283

Fon, E. A., Pothos, E. N., Sun, B. C., Killeen, N., Sulzer, D., and Edwards, R. H. (1997). Vesicular transport regulates monoamine storage and release but is not essential for amphetamine action. *Neuron* 19, 1271–1283. doi: 10.1016/s0896-6273(00)80418-3

Fortin, G. M., Bourque, M.-J., Mendez, J. A., Leo, D., Nordenankar, K., Birgner, C., et al. (2012). Glutamate corelease promotes growth and survival of midbrain dopamine neurons. *J. Neurosci.* 32, 17477–17491. doi: 10.1523/JNEUROSCI.1939-12.2012

Fortin, G. M., Ducrot, C., Giguère, N., Kouwenhoven, W. M., Bourque, M.-J., Pacelli, C., et al. (2019). Segregation of dopamine and glutamate release sites in dopamine neuron axons: regulation by striatal target cells. *FASEB J.* 33, 400–417. doi: 10.1096/fj.201800713RR

Fougère, M., van der Zouwen, C. I., Boutin, J., and Ryczko, D. (2021). Heterogeneous expression of dopaminergic markers and Vglut2 in mouse mesodiencephalic dopaminergic nuclei A8-A13. *J. Comp. Neurol.* 529, 1273–1292. doi: 10.1002/cne.25020

Gaisler-Salomon, I., Miller, G. M., Chuhma, N., Lee, S., Zhang, H., Ghoddoussi, F., et al. (2009). Glutaminase-deficient mice display hippocampal hypoactivity, insensitivity to pro-psychotic drugs and potentiated latent inhibition: relevance to schizophrenia. *Neuropsychopharmacology* 34, 2305–2322. doi: 10.1038/npp.2009.58

Gellman, C., Mingote, S., Wang, Y., Gaisler-Salomon, I., and Rayport, S. (2011). "Genetic Pharmacotherapy," in *Drug Discovery and Development - Present and Future*, ed. I. M. Kapetanovic (Croatia: InTech), 125–150.

Gonzalez-Reyes, L. E., Verbitsky, M., Blesa, J., Jackson-Lewis, V., Paredes, D., Tillack, K., et al. (2012). Sonic hedgehog maintains cellular and neurochemical homeostasis in the adult nigrostriatal circuit. *Neuron* 75, 306–319. doi: 10.1016/j.neuron.2012.05.018

Gordon, J. A. (2016). On being a circuit psychiatrist. *Nat. Neurosci.* 19, 1385–1386. doi: 10.1038/nn.4419

Gorelova, N., Mulholland, P. J., Chandler, L. J., and Seamans, J. K. (2012). The glutamatergic component of the mesocortical pathway emanating from different subregions of the ventral midbrain. *Cereb. Cortex* 22, 327–336. doi: 10.1093/cercor/bhr107

Grace, A. A., Floresco, S. B., Goto, Y., and Lodge, D. J. (2007). Regulation of firing of dopaminergic neurons and control of goal-directed behaviors. *Trends Neurosci.* 30, 220–227. doi: 10.1016/j.tins.2007.03.003

Granger, A. J., Wallace, M. L., and Sabatini, B. L. (2017). Multi-transmitter neurons in the mammalian central nervous system. *Curr. Opin. Neurobiol.* 45, 85–91. doi: 10.1016/j.conb.2017.04.007

Gras, C., Amilhon, B., Lepicard, E. M., Poirel, O., Vinatier, J., Herbin, M., et al. (2008). The vesicular glutamate transporter VGLUT3 synergizes striatal acetylcholine tone. *Nat. Neurosci.* 11, 292–300. doi: 10.1038/nn2052

Hattori, T., Takada, M., Moriizumi, T., and Van der Kooy, D. (1991). Single dopaminergic nigrostriatal neurons form two chemically distinct synaptic types: possible transmitter segregation within neurons. *J. Comp. Neurol.* 309, 391–401. doi: 10.1002/cne.903090308

Hnasko, T. S., Chuhma, N., Zhang, H., Goh, G. Y., Sulzer, D., Palmiter, R. D., et al. (2010). Vesicular glutamate transport promotes dopamine storage and glutamate corelease in vivo. *Neuron* 65, 643–656. doi: 10.1016/j.neuron.2010.02.012

Hnasko, T. S., and Edwards, R. H. (2012). Neurotransmitter corelease: mechanism and physiological role. *Annu. Rev. Physiol.* 74, 225–243. doi: 10.1146/annurev-physiol-020911-153315

Hökfelt, T., Johansson, O., Ljungdahl, A., Lundberg, J. M., and Schultzberg, M. (1980). Peptidergic neurones. *Nature* 284, 515–521. doi: 10.1038/284515a0

Howes, O., McCutcheon, R., and Stone, J. (2015). Glutamate and dopamine in schizophrenia: an update for the 21st century. *J Psychopharmacol.* 29, 97–115. doi: 10.1177/0269881114563634

Insel, T. (2014). The NIMH research domain criteria (RDoC) project: precision medicine for psychiatry. *Am. J. Psychiatry* 171, 395–397. doi: 10.1176/appi.ajp.2014.14020138

Iversen, S. D., and Iversen, L. L. (2007). Dopamine: 50 years in perspective. *Trends Neurosci.* 30, 188–193. doi: 10.1016/j.tins.2007.03.002

Johnson, R. G. (1988). Accumulation of biological amines into chromaffin granules: a model for hormone and neurotransmitter transport. *Physiol. Rev.* 68, 232–307. doi: 10.1152/physrev.1988.68.1.232

Kabanova, A., Pabst, M., Lorkowski, M., Braganza, O., Boehlen, A., Nikbakht, N., et al. (2015). Function and developmental origin of a mesocortical inhibitory circuit. *Nat. Neurosci.* 18, 872–882. doi: 10.1038/nn.4020

Kawano, M., Kawasaki, A., Sakata-Haga, H., Fukui, Y., Kawano, H., Nogami, H., et al. (2006). Particular subpopulations of midbrain and hypothalamic dopamine neurons express vesicular glutamate transporter 2 in the rat brain. *J. Comp. Neurol.* 498, 581–592. doi: 10.1002/cne.21054

Kouwenhoven, W. M., Fortin, G., Penttinen, A.-M., Florence, C., Delignat-Lavaud, B., Bourque, M.-J., et al. (2020). Vglut2 expression in dopamine neurons contributes to postlesional striatal reinnervation. *J. Neurosci.* 40, 8262–8275. doi: 10.1523/JNEUROSCI.0823-20.2020

Kraus, M., Rapisarda, A., Lam, M., Thong, J. Y. J., Lee, J., Subramaniam, M., et al. (2016). Disrupted latent inhibition in individuals at ultra high-risk for developing psychosis. *Schizophr. Res. Cogn.* 6, 1–8. doi: 10.1016/j.scog.2016.07.003

Kupfermann, I. (1991). Functional studies of cotransmission. *Physiol. Rev.* 71, 683–732. doi: 10.1152/physrev.1991.71.3.683

Lammel, S., Steinberg, E. E., Földy, C., Wall, N. R., Beier, K., Luo, L., et al. (2015). Diversity of transgenic mouse models for selective targeting of midbrain dopamine neurons. *Neuron* 85, 429–438. doi: 10.1016/j.neuron.2014.12.036

Li, X., Qi, J., Yamaguchi, T., Wang, H.-L., and Morales, M. (2013). Heterogeneous composition of dopamine neurons of the rat A10 region: molecular evidence for diverse signaling properties. *Brain Struct. Funct.* 218, 1159–1176. doi: 10.1007/s00429-012-0452-z

Lim, S. A. O., Kang, U. J., and McGehee, D. S. (2014). Striatal cholinergic interneuron regulation and circuit effects. *Front. Synaptic Neurosci.* 6:22. doi: 10.3389/fnsyn.2014.00022

Linder, C. C. (2001). The influence of genetic background on spontaneous and genetically engineered mouse models of complex diseases. *Lab Anim.* 30, 34–39.

Linder, C. C. (2006). Genetic variables that influence phenotype. *ILAR J.* 47, 132–140. doi: 10.1093/ilar.47.2.132

Lindvall, O. (2012). Dopaminergic neurons for Parkinson's therapy. *Nat. Biotechnol.* 30, 56–58. doi: 10.1038/nbt.2077

Liss, B., and Roeper, J. (2008). Individual dopamine midbrain neurons: functional diversity and flexibility in health and disease. *Brain Res. Rev.* 58, 314–321. doi: 10.1016/j.brainresrev.2007.10.004

Lykken, E. A., Shyng, C., Edwards, R. J., Rozenberg, A., and Gray, S. J. (2018). Recent progress and considerations for AAV gene therapies targeting the central nervous system. *J. Neurodev. Disord.* 10:16. doi: 10.1186/s11689-018-9234-0

Maycox, P. R., Deckwerth, T., Hell, J. W., and Jahn, R. (1988). Glutamate uptake by brain synaptic vesicles. Energy dependence of transport and functional reconstitution in proteoliposomes. *J. Biol. Chem.* 263, 15423–15428. doi: 10.1016/S0021-9258(19)37605-7

Mendez, I., Dagher, A., Hong, M., Gaudet, P., Weerasinghe, S., McAlister, V., et al. (2002). Simultaneous intrastriatal and intranigral fetal dopaminergic grafts in patients with Parkinson disease: a pilot study. Report of three cases. *J. Neurosurg.* 96, 589–596. doi: 10.3171/jns.2002.96.3.0589

Mendez, I., Viñuela, A., Astradsson, A., Mukhida, K., Hallett, P., Robertson, H., et al. (2008a). Dopamine neurons implanted into people with Parkinson's disease survive without pathology for 14 years. *Nat. Med.* 14, 507–509. doi: 10.1038/nm1752

Mendez, J. A., Bourque, M.-J., Dal Bo, G., Bourdeau, M. L., Danik, M., Williams, S., et al. (2008b). Developmental and target-dependent regulation of vesicular glutamate transporter expression by dopamine neurons. *J. Neurosci.* 28, 6309–6318. doi: 10.1523/JNEUROSCI.1331-08.2008

Mikelman, S. R., Guptaroy, B., Schmitt, K. C., Jones, K. T., Zhen, J., Reith, M. E. A., et al. (2018). Tamoxifen directly interacts with the dopamine transporter. *J. Pharmacol. Exp. Ther.* 367, 119–128. doi: 10.1124/jpet.118.248179

Mingote, S., Amsellem, A., Kempf, A., Rayport, S., and Chuhma, N. (2019). Dopamine-glutamate neuron projections to the nucleus accumbens medial shell and behavioral switching. *Neurochem. Int.* 129:104482. doi: 10.1016/j.neuint.2019.104482

Mingote, S., Chuhma, N., Kalmbach, A., Thomsen, G. M., Wang, Y., Mihali, A., et al. (2017). Dopamine neuron dependent behaviors mediated by glutamate cotransmission. *elife* 6:e27566. doi: 10.7554/eLife.27566

Mingote, S., Chuhma, N., Kusnoor, S. V., Field, B., Deutch, A. Y., and Rayport, S. (2015a). Functional connectome analysis of dopamine neuron glutamatergic connections in forebrain regions. *J. Neurosci.* 35, 16259–16271. doi: 10.1523/JNEUROSCI.1674-15.2015

Mingote, S., Masson, J., Gellman, C., Thomsen, G. M., Lin, C.-S., Merker, R. J., et al. (2015b). Genetic pharmacotherapy as an early CNS drug development strategy: testing glutaminase inhibition for schizophrenia treatment in adult mice. *Front. Syst. Neurosci.* 9:165. doi: 10.3389/fnsys.2015.00165

Moechars, D., Weston, M. C., Leo, S., Callaerts-Vegh, Z., Goris, I., Daneels, G., et al. (2006). Vesicular glutamate transporter VGLUT2 expression levels control quantal size and neuropathic pain. *J. Neurosci.* 26, 12055–12066. doi: 10.1523/JNEUROSCI.2556-06.2006

Mongia, S., Yamaguchi, T., Liu, B., Zhang, S., Wang, H., and Morales, M. (2019). The ventral tegmental area has calbindin neurons with the capability to co-release glutamate and dopamine into the nucleus accumbens. *Eur. J. Neurosci.* 50, 3968–3984. doi: 10.1111/ejn.14493

Morales, M., and Root, D. H. (2014). Glutamate neurons within the midbrain dopamine regions. *Neuroscience* 282, 60–68. doi: 10.1016/j.neuroscience.2014.05.032

Moss, J., Ungless, M. A., and Bolam, J. P. (2011). Dopaminergic axons in different divisions of the adult rat striatal complex do not express vesicular glutamate transporters. *Eur. J. Neurosci.* 33, 1205–1211. doi: 10.1111/j.1460-9568.2011.07594.x

Nordenankar, K., Smith-Anttila, C. J. A., Schweizer, N., Viereckel, T., Birgner, C., Mejia-Toiber, J., et al. (2015). Increased hippocampal excitability and impaired spatial memory function in mice lacking VGLUT2 selectively in neurons defined by tyrosine hydroxylase promoter activity. *Brain Struct. Funct.* 220, 2171–2190. doi: 10.1007/s00429-014-0778-9

Papathanou, M., Creed, M., Dorst, M. C., Bimpisidis, Z., Dumas, S., Pettersson, H., et al. (2018). Targeting VGLUT2 in mature dopamine neurons decreases *Mesoaccumbal* glutamatergic transmission and identifies a role for glutamate co-release in synaptic plasticity by increasing baseline AMPA/NMDA Ratio. *Front. Neural. Circuits* 12:64. doi: 10.3389/fncir.2018.00064

Papathanou, M., Dumas, S., Pettersson, H., Olson, L., and Wallén-Mackenzie, Å (2019). Off-target effects in transgenic mice: characterization of dopamine transporter (DAT)-cre transgenic mouse lines exposes multiple non-dopaminergic neuronal clusters available for selective targeting within limbic neurocircuitry. *Eneuro* 6:ENEURO.198–ENEURO.119. doi: 10.1523/ENEURO.0198-19.2019

Pérez-López, J. L., Contreras-López, R., Ramírez-Jarquín, J. O., and Tecuapetla, F. (2018). Direct glutamatergic signaling from midbrain dopaminergic neurons onto pyramidal prefrontal cortex neurons. *Front. Neural Circuits* 12:70. doi: 10.3389/fncir.2018.00070

Poulin, J.-F., Caronia, G., Hofer, C., Cui, Q., Helm, B., Ramakrishnan, C., et al. (2018). Mapping projections of molecularly defined dopamine neuron subtypes using intersectional genetic approaches. *Nat. Neurosci.* 21, 1260–1271. doi: 10.1038/s41593-018-0203-4

Pupe, S., and Wallén-Mackenzie, Å (2015). Cre-driven optogenetics in the heterogeneous genetic panorama of the VTA. *Trends Neurosci.* 38, 375–386. doi: 10.1016/j.tins.2015.04.005

Robinson, T. E., and Berridge, K. C. (2008). Review. The incentive sensitization theory of addiction: some current issues. *Philos. Trans. R. Soc. Lond. B. Biol. Sci.* 363, 3137–3146. doi: 10.1098/rstb.2008.0093

Romoli, B., Lozada, A. F., Sandoval, I. M., Manfredsson, F. P., Hnasko, T. S., Berg, D. K., et al. (2019). Neonatal nicotine exposure primes midbrain neurons to a dopaminergic phenotype and increases adult drug consumption. *Biol. Psychiatry* 86, 344–355. doi: 10.1016/j.biopsych.2019.04.019

Root, D. H., Wang, H.-L., Liu, B., Barker, D. J., Mód, L., Szocsics, P., et al. (2016). Glutamate neurons are intermixed with midbrain dopamine neurons in nonhuman primates and humans. *Sci. Rep.* 6:30615. doi: 10.1038/srep30615

Shen, H., Marino, R. A. M., McDevitt, R. A., Bi, G.-H., Chen, K., Madeo, G., et al. (2018). Genetic deletion of vesicular glutamate transporter in dopamine neurons increases vulnerability to MPTP-induced neurotoxicity in mice. *Proc Natl Acad Sci USA* 115, E11532–E11541. doi: 10.1073/pnas.1800886115

Silm, K., Yang, J., Marcott, P. F., Asensio, C. S., Eriksen, J., Guthrie, D. A., et al. (2019). Synaptic vesicle recycling pathway determines neurotransmitter content and release properties. *Neuron* 102, 786–800. doi: 10.1016/j.neuron.2019.03.031

Spitzer, N. C. (2015). Neurotransmitter switching? no surprise. *Neuron* 86, 1131–1144. doi: 10.1016/j.neuron.2015.05.028

Steinkellner, T., Zell, V., Farino, Z. J., Sonders, M. S., Villeneuve, M., Freyberg, R. J., et al. (2018). Role for VGLUT2 in selective vulnerability of midbrain dopamine neurons. *J. Clin. Invest.* 128, 774–788. doi: 10.1172/JCI95795

Stocco, A. (2012). Acetylcholine-based entropy in response selection: a model of how striatal interneurons modulate exploration, exploitation, and response variability in decision-making. *Front. Neurosci.* 6:18. doi: 10.3389/fnins.2012.00018

Straub, C., Tritsch, N. X., Hagan, N. A., Gu, C., and Sabatini, B. L. (2014). Multiphasic modulation of cholinergic interneurons by nigrostriatal afferents. *J. Neurosci.* 34, 8557–8569. doi: 10.1523/JNEUROSCI.0589-14.2014

Stuber, G. D., Hnasko, T. S., Britt, J. P., Edwards, R. H., and Bonci, A. (2010). Dopaminergic terminals in the nucleus accumbens but not the dorsal striatum corelease glutamate. *J. Neurosci.* 30, 8229–8233. doi: 10.1523/JNEUROSCI.1754-10.2010

Stuber, G. D., Stamatakis, A. M., and Kantak, P. A. (2015). Considerations when using cre-driver rodent lines for studying ventral tegmental area circuitry. *Neuron* 85, 439–445. doi: 10.1016/j.neuron.2014.12.034

Sulzer, D., Cragg, S. J., and Rice, M. E. (2016). Striatal dopamine neurotransmission: regulation of release and uptake. *Basal Ganglia* 6, 123–148. doi: 10.1016/j.baga.2016.02.001

Sulzer, D., Joyce, M. P., Lin, L., Geldwert, D., Haber, S. N., Hattori, T., et al. (1998). Dopamine neurons make glutamatergic synapses in vitro. *J. Neurosci.* 18, 4588–4602.

Svensson, E., Apergis-Schoute, J., Burnstock, G., Nusbaum, M. P., Parker, D., and Schiöth, H. B. (2018). General principles of neuronal co-transmission: insights from multiple model systems. *Front. Neural Circuits* 12:117. doi: 10.3389/fncir.2018.00117

Takamori, S., Rhee, J. S., Rosenmund, C., and Jahn, R. (2000). Identification of a vesicular glutamate transporter that defines a glutamatergic phenotype in neurons. *Nature* 407, 189–194. doi: 10.1038/35025070

Taylor, S. R., Badurek, S., Dileone, R. J., Nashmi, R., Minichiello, L., and Picciotto, M. R. (2014). GABAergic and glutamatergic efferents of the mouse ventral tegmental area. *J. Comp. Neurol.* 522, 3308–3334. doi: 10.1002/cne.23603

Tecuapetla, F., Patel, J. C., Xenias, H., English, D., Tadros, I., Shah, F., et al. (2010). Glutamatergic signaling by mesolimbic dopamine neurons in the nucleus accumbens. *J. Neurosci.* 30, 7105–7110. doi: 10.1523/JNEUROSCI.0265-10.2010

Threlfell, S., Lalic, T., Platt, N. J., Jennings, K. A., Deisseroth, K., and Cragg, S. J. (2012). Striatal dopamine release is triggered by synchronized activity in cholinergic interneurons. *Neuron* 75, 58–64. doi: 10.1016/j.neuron.2012.04.038

Tritsch, N. X., Ding, J. B., and Sabatini, B. L. (2012). Dopaminergic neurons inhibit striatal output through non-canonical release of GABA. *Nature* 490, 262–266. doi: 10.1038/nature11466

Trudeau, L.-E., Hnasko, T. S., Wallén-Mackenzie, A., Morales, M., Rayport, S., and Sulzer, D. (2014). The multilingual nature of dopamine neurons. *Prog. Brain Res.* 211, 141–164. doi: 10.1016/B978-0-444-63425-2.00006-4

Vaaga, C. E., Borisovska, M., and Westbrook, G. L. (2014). Dual-transmitter neurons: functional implications of co-release and co-transmission. *Curr. Opin. Neurobiol.* 29, 25–32. doi: 10.1016/j.conb.2014.04.010

Wallén-Mackenzie, A., Gezelius, H., Thoby-Brisson, M., Nygård, A., Enjin, A., Fujiyama, F., et al. (2006). Vesicular glutamate transporter 2 is required for central respiratory rhythm generation but not for locomotor central pattern generation. *J. Neurosci.* 26, 12294–12307. doi: 10.1523/JNEUROSCI.3855-06.2006

Wang, D. V., Viereckel, T., Zell, V., Konradsson-Geuken, Å, Broker, C. J., Talishinsky, A., et al. (2017). Disrupting glutamate co-transmission does not affect acquisition of conditioned behavior reinforced by dopamine neuron activation. *Cell. Rep.* 18, 2584–2591. doi: 10.1016/j.celrep.2017.02.062

Weiner, I., and Arad, M. (2009). Using the pharmacology of latent inhibition to model domains of pathology in schizophrenia and their treatment. *Behav. Brain Res.* 204, 369–386. doi: 10.1016/j.bbr.2009.05.004

Widner, H., Tetrud, J., Rehncrona, S., Snow, B., Brundin, P., Gustavii, B., et al. (1992). Bilateral fetal mesencephalic grafting in two patients with parkinsonism induced by 1-methyl-4-phenyl-1,2,3,6-tetrahydropyridine (MPTP). *N. Engl. J. Med.* 327, 1556–1563. doi: 10.1056/NEJM199211263272203

Wieland, S., Du, D., Oswald, M. J., Parlato, R., Köhr, G., and Kelsch, W. (2014). Phasic dopaminergic activity exerts fast control of cholinergic interneuron firing via sequential NMDA, D2, and D1 receptor activation. *J. Neurosci.* 34, 11549–11559. doi: 10.1523/JNEUROSCI.1175-14.2014

Wijeyekoon, R., and Barker, R. A. (2009). Cell replacement therapy for Parkinson's disease. *Biochim. Biophys. Acta* 1792, 688–702. doi: 10.1016/j.bbadis.2008.10.007

Yamaguchi, T., Qi, J., Wang, H.-L., Zhang, S., and Morales, M. (2015). Glutamatergic and dopaminergic neurons in the mouse ventral tegmental area. *Eur. J. Neurosci.* 41, 760–772. doi: 10.1111/ejn.12818

Yamaguchi, T., Sheen, W., and Morales, M. (2007). Glutamatergic neurons are present in the rat ventral tegmental area. *Eur. J. Neurosci.* 25, 106–118. doi: 10.1111/j.1460-9568.2006.05263.x

Yamaguchi, T., Wang, H.-L., and Morales, M. (2013). Glutamate neurons in the substantia nigra compacta and retrorubral field. *Eur. J. Neurosci.* 38, 3602–3610. doi: 10.1111/ejn.12359

Yan, Y., Peng, C., Arvin, M. C., Jin, X.-T., Kim, V. J., Ramsey, M. D., et al. (2018). Nicotinic cholinergic receptors in VTA glutamate neurons modulate excitatory transmission. *Cell Rep.* 23, 2236–2244. doi: 10.1016/j.celrep.2018.04.062

Yoon, T., Okada, J., Jung, M. W., and Kim, J. J. (2008). Prefrontal cortex and hippocampus subserve different components of working memory in rats. *Learn. Mem.* 15, 97–105. doi: 10.1101/lm.850808

Yoshiki, A., and Moriwaki, K. (2006). Mouse phenome research: implications of genetic background. *ILAR J.* 47, 94–102. doi: 10.1093/ilar.47.2.94

Zell, V., Steinkellner, T., Hollon, N. G., Warlow, S. M., Souter, E., Faget, L., et al. (2020). VTA glutamate neuron activity drives positive reinforcement

absent dopamine co-release. *Neuron* 107, 864–873. doi: 10.1016/j.neuron.2020.06.011

Zhang, S., Qi, J., Li, X., Wang, H.-L., Britt, J. P., Hoffman, A. F., et al. (2015). Dopaminergic and glutamatergic microdomains in a subset of rodent mesoaccumbens axons. *Nat. Neurosci.* 18, 386–392. doi: 10.1038/nn.3945

Zhang, Y.-F., and Cragg, S. J. (2017). Pauses in striatal cholinergic interneurons: what is revealed by their common themes and variations? *Front. Syst. Neurosci.* 11:80. doi: 10.3389/fnsys.2017.00080

Ztaou, S., and Amalric, M. (2019). Contribution of cholinergic interneurons to striatal pathophysiology in Parkinson's disease. *Neurochem. Int.* 126, 1–10. doi: 10.1016/j.neuint.2019.02.019

Conflict of Interest: The authors declare that the research was conducted in the absence of any commercial or financial relationships that could be construed as a potential conflict of interest.

Copyright © 2021 Eskenazi, Malave, Mingote, Yetnikoff, Ztaou, Velicu, Rayport and Chuhma. This is an open-access article distributed under the terms of the Creative Commons Attribution License (CC BY). The use, distribution or reproduction in other forums is permitted, provided the original author(s) and the copyright owner(s) are credited and that the original publication in this journal is cited, in accordance with accepted academic practice. No use, distribution or reproduction is permitted which does not comply with these terms.

frontiers in Neural Circuits

REVIEW
published: 23 July 2021
doi: 10.3389/fncir.2021.700968

Dopaminergic Dysregulation in Syndromic Autism Spectrum Disorders: Insights From Genetic Mouse Models

Polina Kosillo[1] *and Helen S. Bateup*[1,2,3]*

[1] Department of Molecular and Cell Biology, University of California, Berkeley, Berkeley, CA, United States, [2] Helen Wills Neuroscience Institute, University of California, Berkeley, Berkeley, CA, United States, [3] Chan Zuckerberg Biohub, San Francisco, CA, United States

Autism spectrum disorder (ASD) is a neurodevelopmental disorder defined by altered social interaction and communication, and repetitive, restricted, inflexible behaviors. Approximately 1.5-2% of the general population meet the diagnostic criteria for ASD and several brain regions including the cortex, amygdala, cerebellum and basal ganglia have been implicated in ASD pathophysiology. The midbrain dopamine system is an important modulator of cellular and synaptic function in multiple ASD-implicated brain regions via anatomically and functionally distinct dopaminergic projections. The dopamine hypothesis of ASD postulates that dysregulation of dopaminergic projection pathways could contribute to the behavioral manifestations of ASD, including altered reward value of social stimuli, changes in sensorimotor processing, and motor stereotypies. In this review, we examine the support for the idea that cell-autonomous changes in dopaminergic function are a core component of ASD pathophysiology. We discuss the human literature supporting the involvement of altered dopamine signaling in ASD including genetic, brain imaging and pharmacologic studies. We then focus on genetic mouse models of syndromic neurodevelopmental disorders in which single gene mutations lead to increased risk for ASD. We highlight studies that have directly examined dopamine neuron number, morphology, physiology, or output in these models. Overall, we find considerable support for the idea that the dopamine system may be dysregulated in syndromic ASDs; however, there does not appear to be a consistent signature and some models show increased dopaminergic function, while others have deficient dopamine signaling. We conclude that dopamine dysregulation is common in syndromic forms of ASD but that the specific changes may be unique to each genetic disorder and may not account for the full spectrum of ASD-related manifestations.

Keywords: dopamine, autism spectrum disorder, Angelman syndrome, Fragile X syndrome, Rett syndrome, PTEN hamartoma tumor syndrome, Tuberous Sclerosis Complex, genetic mouse models

OPEN ACCESS

Edited by:
Talia Newcombe Lerner, Northwestern University, United States

Reviewed by:
Marc Vincent Fuccillo, University of Pennsylvania, United States
Wei Li, University of Alabama at Birmingham, United States

***Correspondence:**
Helen S. Bateup
bateup@berkeley.edu

Received: *27 April 2021*
Accepted: *21 June 2021*
Published: *23 July 2021*

Citation:
Kosillo P and Bateup HS (2021) Dopaminergic Dysregulation in Syndromic Autism Spectrum Disorders: Insights From Genetic Mouse Models. Front. Neural Circuits 15:700968. doi: 10.3389/fncir.2021.700968

INTRODUCTION

Autism spectrum disorder (ASD) is a neurodevelopmental disorder primarily characterized by deficits in social interactions, as well as repetitive, restricted, and inflexible behaviors (American Psychiatric Association, 2013). ASD is typically diagnosed early in life, although the clinical presentation and symptom severity can vary widely between individuals and across the lifespan. The latest CDC estimates suggest that 1 in 54 children are diagnosed with ASD by the age of 8, with ASD diagnosis being over four times more prevalent in boys than girls (Maenner et al., 2020).

The exact neurobiological basis of ASD remains unknown. This is in part due to a heterogenous behavioral presentation accompanied by widely divergent genetic, transcriptomic and epigenomic signatures found in individuals with ASD (De La Torre-Ubieta et al., 2016), although convergent molecular subtypes are being identified (Ramaswami et al., 2020). Studies in animal models and human subjects suggest that different brain regions and circuits contribute to distinct aspects of ASD symptomatology. Several brain regions implicated in ASD include the cortex (Donovan and Basson, 2017; Varghese et al., 2017), amygdala (Zalla and Sperduti, 2013; Donovan and Basson, 2017), cerebellum (Fatemi et al., 2012; Hampson and Blatt, 2015), and basal ganglia (Fuccillo, 2016; Subramanian et al., 2017). In particular, alterations in basal ganglia circuits may be a key driver of the restricted, repetitive behaviors in ASD (Fuccillo, 2016). Consistent with this, human neuroimaging studies have identified structural changes in the basal ganglia that correlate with repetitive behaviors (Asano et al., 2001). Increased striatal volume, the caudate nucleus in particular, has been identified in several studies (Hollander et al., 2005; Langen et al., 2009; Langen et al., 2014), while for other basal ganglia structures both volumetric decreases and increases have been reported (Estes et al., 2011; Schuetze et al., 2016). One study reported a decrease in ventral striatal volume in ASD subjects correlating with the severity of social deficits (Baribeau et al., 2019).

Dopaminergic projections originating from the midbrain exert wide-spread influence over multiple brain regions implicated in ASD pathophysiology including the basal ganglia, cortex and amygdala. Within these regions, dopamine (DA) serves as an important neuromodulator that fine-tunes cellular and synaptic function. Importantly, DA neurons and their projections are anatomically and functionally distinct. Dopaminergic input to the dorsal striatum originates primarily from the substantia nigra pars compacta (SNc; nigrostriatal pathway) and is fundamental to the context-appropriate, flexible selection of actions (Howard et al., 2017). In turn, ventral tegmental area (VTA) dopaminergic projections to the ventral striatum including the nucleus accumbens (mesolimbic pathway) are involved in reward processing (Watabe-Uchida et al., 2017), salience (De Jong et al., 2019), and motivation (Hamid et al., 2016; Mohebi et al., 2019). Cortical dopaminergic projections (mesocortical pathway) are sparser but provide important modulation of cognitive processes, including sensory gating and working memory (Ott and Nieder, 2019). Precisely controlled and appropriately timed release and clearance of DA at its targets is critical for adaptive behavior and learning. As discussed in other articles in this special issue, the dopaminergic system is highly heterogeneous. Recent gene profiling studies have identified several distinct sub-populations of DA neurons defined by their unique transcriptional signature (Poulin et al., 2014; La Manno et al., 2016; Hook et al., 2018; Kramer et al., 2018; Saunders et al., 2018; Tiklová et al., 2019; Poulin et al., 2020). Mouse models are being developed to allow intersectional genetic targeting of these newly defined dopaminergic populations to better understand their anatomical connectivity, functional properties and behavioral roles (Poulin et al., 2018; Kramer et al., 2021). Such approaches will enable a more fine-grained understanding of dopaminergic functions in both health and disease.

Given that DA is a key modulator of neuronal activity in several brain regions associated with ASD, there is compelling reason to ask whether dysfunctional DA signaling could impact brain activity across a range of ASD-implicated brain structures. The formally articulated dopamine hypothesis of ASD (Paval, 2017) postulates that functional dysregulation of DA projection pathways could contribute to the behavioral alterations that lead to ASD symptomology. For example, aberrant mesolimbic DA signaling could diminish the reward value assigned to social stimuli, eventually resulting in failure to acquire socioemotional reciprocity and/or communication skills. Alterations in mesocortical DA neurotransmission could translate to abnormal sensory processing and/or cognitive rigidity. Aberrant nigrostriatal DA signaling could promote stereotyped or repetitive motor movements and/or hyper-reliance on habitual behavioral control. Thus, the dopamine hypothesis of ASD as currently stated, predicts that either hyper- or hypo-dopaminergic signaling within target regions could lead to or exacerbate ASD-related behavioral changes (Paval, 2017). This is consistent with the idea of an "inverted U" shape to describe the optimal level of DA receptor signaling, wherein too much or too little DA are detrimental to cognitive functions (Arnsten, 1997; Cools and D'esposito, 2011). The DA hypothesis of ASD further predicts that aberrations at distinct projection targets could control discrete aspects of ASD symptomatology. Importantly, any changes in dopaminergic neurotransmission would likely lead to complex adaptations in downstream circuitry, involving pre- and post-synaptic alterations and plasticity.

In this review we will first summarize the evidence for dopaminergic involvement in ASD gleaned from human studies and then examine whether cell-autonomous changes in the DA system are commonly observed in animal models of ASD, with a focus on genetic mouse models. A particular question we aim to address is whether the wide diversity of genetic mouse models of ASD, with both constitutive (in which the mutation is present in all cells throughout development) and conditional mutations (in which the gene is altered in DA neurons only), show concordant changes in the function of midbrain DA neurons that may be causal for ASD-related behavioral changes. In other words, is there a consistent dopaminergic signature observable across different genetic causes of ASD?

For the purposes of this review, we will focus on the cell autonomous properties of DA neurons. Several important parameters determine the functionality of midbrain DA neurons at the level of the cell bodies, or somas, and axon terminals, typically examined within the striatum, which has the densest dopaminergic innervation. First, the number of DA neurons determines whether ASD-linked-mutations may cause DA neuron degeneration, or, in contrast, enhance the generation or survival of dopaminergic cells. Second, morphological properties such as cell size and dendritic architecture are examined to study structural aberrations that may impact the intrinsic excitability or connectivity of DA neurons. Third, changes in the firing properties of DA neurons can be assessed using electrophysiology or functional imaging techniques. Fourth, the levels of tyrosine hydroxylase (TH), the rate limiting enzyme in DA synthesis, determine overall DA production capacity and can be examined both in cell bodies and axon terminals by western blot or immunohistochemistry. DA production and storage determine the total tissue DA content in somas and axonal target regions, which is typically examined by high-performance liquid chromatography (HPLC). Finally, functional measures of basal (spontaneous) or evoked DA release by fast-scan cyclic voltammetry (sub-second timescale) or microdialysis (temporal resolution of minutes) are used to examine DA release and re-uptake in the midbrain somatodendritic region or axon terminal target regions.

Evidence for Dopaminergic Involvement in ASD

Brain Imaging and Pharmacological Interventions in Individuals With ASD

Neuroimaging studies in individuals with ASD support the potential involvement of altered DA signaling, especially in striatum and prefrontal cortex, in the behavioral manifestations of ASD. For example, PET imaging of fluorodopa accumulation revealed reduced presynaptic DA levels in the prefrontal cortex of children with ASD (Ernst et al., 1997). In turn, PET imaging of radioligand binding to the dopamine active transporter (DAT) showed increased binding in the orbitofrontal cortex of high-functioning adults with ASD (Nakamura et al., 2010); however, changes in dopaminergic function at rest have not been detected universally (Makkonen et al., 2008). During task performance, a reduction in phasic striatal DA events evoked by social stimuli in children and adolescents with ASD have been reported in several studies (Scott-Van Zeeland et al., 2010; Zürcher et al., 2020). Together, these data support the involvement of functional changes in dopaminergic signaling in ASD. Yet, differences in experimental methodology and the inherent heterogeneity among individuals with ASD, including differences between age groups, also lead to conflicting results across studies and warrant further investigation.

Pharmacological manipulations of DA neurotransmission are currently used to manage some of the symptoms of ASD. Roughly 80% of children with ASD suffer from irritability (Mayes et al., 2011). Several dopamine receptor D2 subtype antagonists, such as risperidone and aripiprazole, have been successfully used to improve irritability, aggression and tantrum behaviors in individuals with ASD (Mccracken et al., 2002; Owen et al., 2009; Aman et al., 2010). However, current guidelines recommend against long-term and wide-spread use of these medications due to significant side effects and modest evidence for clinical efficacy (Leclerc and Easley, 2015; Howes et al., 2018). Nonetheless, meta-analyses of placebo-controlled randomized clinical trials do find significant, albeit modest in size, improvement in irritability and aggression scores in children and adolescents with ASD following short-term (<6 months) risperidone or aripiprazole treatment (Sharma and Shaw, 2012; Hirsch and Pringsheim, 2016). Secondary outcome measures and *post hoc* analyses further show a significant decrease in stereotypy scores with aripiprazole in children with ASD (Aman et al., 2010; Marcus et al., 2011).

Together, functional neuroimaging and pharmacological interventions in human subjects support dopaminergic involvement in ASD. However, evidence from human studies for a role of DA in core autism symptoms of reduced sociability and restricted, repetitive behaviors is correlational. In contrast, rodent models in which manipulations of DA signaling are possible conclusively demonstrate causal DA involvement in sociability, stereotypies, and other ASD-relevant manifestations (Presti et al., 2003; Gunaydin et al., 2014; Lee et al., 2018).

Genetic Evidence for Dopaminergic Involvement in ASD

ASD is a complex polygenic disorder, with SFARI gene currently listing 1003 genes implicated in autism, with 418 genes classified as high confidence or strong candidate ASD risk genes ([1]database accessed 04/22/2021, version 2020 Q4). Strong candidate genes fall into two main categories based on the current SFARI classification. Those assigned 'score 1' are high confidence candidates and can be found on the SPARK gene list or on the list of genes reported by Satterstrom et al. (2020). These genes generally have at least three *de novo* likely gene-disrupting mutations reported in the literature. Genes assigned 'score 2' are strong candidates with two likely gene-disrupting mutations reported, implicated by GWAS replicated across different cohorts and supported by functional evidence. Both of these categories are therefore strongly supported by currently available published literature to play a causal role in ASD. However, the large majority of ASD-associated genes fall into the 'score 3' category based on a single reported mutation and either unreplicated association studies or rare inherited mutations. These 'score' metrics allow for consistent evaluation of the strength of evidence across different genes and have been widely adopted by researchers.

Polymorphisms and mutations in genes encoding proteins that directly control DA neurotransmission have been implicated in ASD (Nguyen et al., 2014). These include the genes encoding the dopamine active transporter ("DAT," *SLC6A3*) (Hamilton et al., 2013; Bowton et al., 2014; Campbell et al., 2019; Dicarlo et al., 2019), plasma membrane monoamine transporter (*SLC29A4*) (Adamsen et al., 2014), several dopamine receptors (*DRD1*, *DRD2, DRD3, DRD4*) (Hettinger et al., 2008; De Krom et al., 2009; Reiersen and Todorov, 2011; Staal et al.,

[1]https://gene.sfari.org

2011, 2018; Hettinger et al., 2012), and genes encoding proteins important for dopamine synthesis (*DDC*) (Toma et al., 2012) and catabolism (*MAO, COMT*) (Cohen et al., 2003; Yoo et al., 2009, 2013; Cohen et al., 2011; Verma et al., 2014; Wassink et al., 2014). Only *SLC6A3* is currently classified as a strong candidate 'score 2' gene, while others (*SLC29A4, DRD1, DRD2 DRD3, DDC, MAO*) fall into the 'score 3' category where causal involvement in ASD is supported only by suggestive evidence. Taken together, there is evidence that mutations in genes encoding key dopaminergic proteins may contribute to ASD risk, however, none of these currently rise to the top of the list of high confidence ASD-related genes.

Notably, there is overlap in the dopaminergic genes identified as altered in individuals with ASD with those found in individuals diagnosed with attention-deficit hyperactivity disorder, bipolar disorder, schizophrenia or obsessive-compulsive disorder (Khanzada et al., 2017). This suggests that while these disorders have distinct presentations, they may share some overlapping etiology, which could commonly involve aberrant DA signaling within basal ganglia and cortical circuits.

Dopaminergic Perturbations Can Cause ASD-Related Phenotypes in Mice

Several *SLC6A3* mutations identified in individuals with ASD have been modeled in mice. In a mouse model with a rare *Slc6a3* coding variant Val559, implicated in ASD in two unrelated male probands (Bowton et al., 2014), researchers observed increased basal striatal DA levels with *in vivo* microdialysis and a reduction in vertical motor behaviors such as rearing (Mergy et al., 2014). In a different model, with a threonine-to-methionine substitution at the 356 site in DAT (T356M) (Hamilton et al., 2013), researchers found reduced DA clearance rate concomitant with increased striatal DA metabolism and reduced DA synthesis (Dicarlo et al., 2019). Behaviorally, T356M mice showed hyperlocomotion, increased performance in the rotarod test and increased vertical rearing, resembling motor stereotypies. The mice also showed no preference for interacting with a novel mouse over a novel object, indicating reduced social approach behavior (Dicarlo et al., 2019). This study, in particular, demonstrates both construct and face validity of the *Slc6a3* T356M mouse for studying ASD-relevant changes in dopaminergic neurotransmission *in vivo*.

In general, pathogenic *SLC6A3* mutations, including those implicated in human ASD, are likely to increase the availability of extracellular DA due to reduced DAT function. This can happen either via impaired DA uptake and/or anomalous efflux leading to augmented DA signaling. In turn, increased DA signaling, either by reducing DAT expression in SNc neurons with siRNA or optogenetic stimulation of the nigrostriatal pathway, is sufficient to cause repetitive behaviors and sociability deficits in wild-type mice (Lee et al., 2018). Further, intra-striatal infusion of the D1 receptor antagonist SCH 23390 reduces naturally occurring motor stereotypies in a deer mouse model of ASD in the absence of general motor suppression (Presti et al., 2003). By contrast, in the ventral striatum, optogenetic suppression of the VTA-to-Nucleus Accumbens (NAc) (mesolimbic) pathway reduces sociability in mice, while activation increases social interactions via NAc D1 receptors (Gunaydin et al., 2014). Together, these studies suggest possible sub-region differences in DA dynamics contributing to distinct aspects of ASD-associated behaviors: hyperdopaminergia in the dorsal striatum could cause persistent and spontaneous stereotypies, while hypodopaminergia in the nucleus accumbens could lead to reduced sociability.

There are several unique features of the DA system that could support such distinct region-specific functional outcomes manifesting in ASD symptomatology. First, as a neuromodulator responsible for fine-tuning circuit function, either too much or too little DA signaling can cause aberrant information processing and behavior. The inverted U relationship between DA signaling and functional outcomes supports this interpretation (Cools and D'esposito, 2011). Second, the inherent heterogeneity of dopaminergic cell types based on projection targets, action potential properties and other parameters (Lammel et al., 2008), can support 'independent' functional outcomes within distinct brain regions through a combination of distinct cell intrinsic characteristics and local modulatory mechanisms (Sulzer et al., 2016). Third, the loop architecture of basal ganglia circuits could theoretically lend itself to either selective reinforcement or suppression of one dopaminergic domain by another (e.g., modulation of motor output by limbic domains) (Aoki et al., 2019; Lee et al., 2020). Finally, it should also be noted that compromised uptake or anomalous efflux of DA can augment dopaminergic catabolism thereby reducing DA recycling and increasing the burden of *de novo* DA synthesis, which over time could lead to reduced DA levels (Lee et al., 2018; Dicarlo et al., 2019). This, in turn, would compromise dopaminergic neurotransmission due to lack of neurotransmitter availability. Thus, an initial hyperdopaminergic state may over time evolve into deficient DA signaling. Consequently, it is possible that aberrations in DA neurotransmission in ASD are dynamic and evolve over time. In this respect, longitudinal studies conducted in humans with ASD and in mouse models would be helpful to our understanding of DA involvement in ASD pathophysiology across the lifespan.

Genetic Mouse Models of ASD

Without explicit biomarkers available for ASD and diagnostic criteria based on complex behaviors, ASD-related phenotypes in mouse models can only be approximated. Typically, studies assess ultrasonic vocalizations, social preference, social recognition and social interaction as a proxy for communication and sociability deficits, and motor learning and motor stereotypies as a proxy for repetitive, restrictive behaviors (Kazdoba et al., 2015). Tasks assessing cognitive performance, cognitive flexibility, sensory perception and learning have also been utilized. Yet, with these measurements of behavioral outcomes it is difficult to distinguish between mouse models of ASD and those modeling other neuropsychiatric conditions, which frequently present with overlapping behavioral phenotypes. Thus, while functional studies indeed provide evidence for ASD-related mutations in 'dopaminergic' genes causing changes in DA metabolism, release, re-uptake, or pre/post-synaptic signaling, the specificity of the reported behavioral phenotypes to ASD could be questioned. In other words, observing changes in the DA system with mutations

that directly affect DA neurotransmission is expected, but do other genetic causes of ASD also alter DA signaling?

To address whether there is a 'dopamine signature' in ASD, it can be useful to examine mouse models with mutations in high confidence ASD-risk genes. Several of these genes are associated with syndromic neurodevelopmental disorders, which also frequently present with epilepsy, intellectual disability and other medical and behavioral conditions. Angelman syndrome, Fragile X syndrome, Rett syndrome, PTEN hamartoma tumor syndrome, and Tuberous Sclerosis Complex are some examples of syndromic neurodevelopmental disorders associated with high rates of ASD. Genetic mouse models of these neurodevelopmental disorders are well-established and show some ASD-relevant behavioral phenotypes. These can include reduced social interaction, impaired cognitive performance, and perseverative or repetitive behaviors. Here we summarize studies that have directly examined dopaminergic function in these models. **Table 1** provides a summary of the mouse models discussed and the main findings related to DA neuron structure and function.

UBE3A, Angelman Syndrome and ASD

UBE3A encodes an E3-ubiquitin ligase, which is part of the ubiquitin proteasome pathway that adds ubiquitin molecules to proteins that are destined to be degraded. In neurons, *UBE3A* is expressed from the maternal allele due to imprinting (Rougeulle et al., 1997; Vu and Hoffman, 1997). Loss-of-function mutations in the maternal *UBE3A* copy or *de novo* deletions of chromosomal region 15q11-q13, in which *UBE3A* resides, cause the severe neurodevelopmental disorder Angelman syndrome (AS), characterized by abnormal motor development, lack of speech, seizures, and a happy demeanor (Kishino et al., 1997; Matsuura et al., 1997). In turn, duplications of *UBE3A* or the 15q11-q13 locus are strongly associated with ASD, although small deletions have also been reported in ASD probands (Nurmi et al., 2001; Glessner et al., 2009; Hogart et al., 2010). *UBE3A* is a high confidence 'score 1' autism gene with 22 possible genetic variants reported.

There are several indications that *UBE3A* mutations could cause perturbations to the dopaminergic system. First, *Ube3a* is highly expressed in midbrain DA neurons in mice (Gustin et al., 2010). Second, the ubiquitin-proteasome degradation pathway is critically important for DA neuron function with aberrations in this system linked to the pathogenesis of both familial and sporadic forms of Parkinson's disease (Olanow and Mcnaught, 2006). Third, patients with AS present with movement or balance disorders, usually ataxia of gait and/or tremulous movement of limbs, and frequently have rigidity and bradykinesia (Clayton-Smith and Laan, 2003). Reminiscent of Parkinson's disease, which is caused by the degeneration of DA neurons, case reports suggest that resting tremor and rigidity in AS patients can be alleviated with the drug levodopa, a precursor for DA (Harbord, 2001) (although see also Tan et al., 2017).

Multiple studies have examined the dopaminergic system in a mouse model of AS that lacks the maternal copy of *Ube3a* (*Ube3a*$^{m-/p+}$) (Jiang et al., 1998). An initial study reported that 7-8 month old male mice with loss of *Ube3a* had a reduced number of DA neurons in the SNc, but no change in striatal TH expression (Mulherkar and Jana, 2010). In contrast, using the same mouse model, another study in 3-4 month old male mice found no changes in midbrain DA neuron number or TH levels in dorsal or ventral striatum (Riday et al., 2012). Together, these data suggest a possible age-dependent decline in SNc DA neurons with loss-of-function of the maternal copy of *Ube3a*.

Electrophysiology recordings of VTA DA neurons in adult 2-3 month old *Ube3a*$^{m-/p+}$ mice showed no changes in their intrinsic excitability (Berrios et al., 2016); however, SNc neurons were not assessed. Several studies have measured DA release in *Ube3a*$^{m-/p+}$ mice, with mixed results. Using *in vivo* fast-scan cyclic voltammetry (FCV), researchers observed increased electrically evoked DA release in the ventral striatum, but decreased release in the dorsal striatum in 3-4 month old male animals (Riday et al., 2012). Based on these results, it is attractive to speculate that AS-associated phenotypes of motor difficulties and happy disposition are generally congruent with reduced DA release in dorsal striatum and enhanced DA release in ventral striatum reported for the *Ube3a*$^{m-/p+}$ mouse model (Riday et al., 2012). That said, a later study found no changes in optogenetically evoked DA release in the nucleus accumbens in 2-3 month-old *Ube3a*$^{m-/p+}$ mice or in mice with maternal deletion of *Ube3a* in TH+ neurons only (Berrios et al., 2016). Despite no changes in DA release, the authors did observe a large decrease in GABA co-release from TH+ VTA neurons with maternal deletion of *Ube3a*.

In terms of DA production, while the study by Riday et al. did not find any differences in DA levels in the striatum or NAc measured by HPLC, another study reported a different result. In this study the authors compared *Ube3a*$^{m-/p+}$ mice with mice harboring a 6.3 Mb duplication of the conserved linkage group on mouse chromosome 7, which is equivalent to human chromosome 15q11-q13 (Nakatani et al., 2009). Increased striatal DA levels were detected in animals with maternal deletion of *Ube3a*, and either paternal or maternal duplication of the 15q11-q13 locus (Farook et al., 2012). Further work will be needed to understand at a mechanistic level how both deletion and duplication of *Ube3a* could increase striatal DA tissue content.

The maximum rate of DA re-uptake back into the pre-synaptic terminal, which is a key factor that controls extracellular DA levels, is determined by DAT availability and its substrate affinity. Several lines of evidence suggest that *Ube3a* loss impacts DAT function. For example, superfusion experiments of synaptosomes showed significantly increased basal efflux of [^{3}H]MPP+ in *Ube3a*$^{m-/p+}$ mice compared to wild-type (Steinkellner et al., 2012). [^{3}H]MPP+ is taken up selectively by DAT, and hence enables assessment of DAT function. Increased basal efflux of [^{3}H]MPP+ suggests that with maternal *Ube3a* loss, extracellular DA levels could be increased, consistent with the findings of Farook et al. In the same synaptosomal preparation, researchers observed impaired [^{3}H]MPP+ efflux in response to amphetamine (Steinkellner et al., 2012), which augments extracellular DA by reverse transport. Together, these observations indicate that DAT function is altered in *Ube3a*$^{m-/p+}$ mice. This conclusion is further supported by the observation that *Ube3a*$^{m-/p+}$ mice have reduced behavioral

TABLE 1 | Summary of DA neuron phenotypes in mouse models of syndromic autism spectrum disorders.

Syndrome	Human gene	Mouse model	Gene manipulation	Type of mutation	Age at manipulation	Age at experiment	DA neuron number	DA neuron cell body morphology	DA neuron intrinsic excitability	DA neuron axonal morphology	DA release	TH expression	DA tissue content	DAT expression and function	References
Angelman	*UBE3A*	Ube3a m-/p+ and Ube3a flox/p+ x TH-Cre	deletion	constitutive and conditional	embryonic	P60-P90	–	–	Unchanged in VTA neurons	–	Unchanged evoked release in NAc (FCV, optogenetic stim)	–	–	–	Berrios et al., 2016
		Ube3a m-/p+	deletion	constitutive	embryonic	P210-240	Decreased SNc neuron number (IHC)	–	–	–	–	–	–	Increased striatal DAT expression (IHC)	Mulherkar and Jana, 2010
		Ube3a m-/p+	constitutive	deletion	embryonic	adult	–	–	–	–	–	–	–	Decreased DAT function (synaptosomal efflux)	Steinkellner et al., 2012
		Ube3a m-/p+	deletion	constitutive	embryonic	P90-120	No changes in SNc or VTA (IHC)	–	–	–	Decreased evoked release in dorsal striatum and increased in ventral striatum (*in vivo* FCV, MFB electrical stim)	No change in dorsal or ventral striatum (WB)	No change in dorsal or ventral striatum (HPLC)	–	Riday et al., 2012
		Ube3a m-/p+	constitutive	deletion	embryonic	P84-105	–	–	–	–	–	–	Increased in striatum and unchanged in midbrain (HPLC)	–	Farook et al., 2012
ASD	*15q11-q13*	7p duplication	duplication	constitutive	embryonic	P84-105	–	–	–	–	–	–	Increased in striatum and midbrain (HPLC)	–	Farook et al., 2012
Fragile X	*FMR1*	Fmr1 KO	deletion	constitutive	embryonic	adult	–	–	–	–	Increased evoked release in PFC and decreased in striatum (*in vivo* microdialysis, amphetamine stim)	–	–	–	Ventura et al., 2004
		deletion	Fmr1 KO	embryonic	constitutive	P28-42; P63-77	–	–	–	–	–	–	No change in young mice, increased striatal content in older mice (HPLC)	–	Sørensen et al., 2015
		Fmr1 KO	deletion	constitutive	embryonic	P28-31; P209-221	–	–	–	–	–	–	No change in striatum in young or old mice (HPLC)	–	Gruss and Braun, 2001, 2004
		Fmr1 KO	deletion	constitutive	embryonic	P70; P105-140	–	–	–	–	No change in evoked release in dorsal striatum in younger animals but decreased in older mice (FCV, electrical stim)	–	No change in striatum in young or old mice (HPLC)	No change in DAT function in young animals and reduced DAT function in older mice (FCV)	Fulks et al., 2010

(Continued)

TABLE 1 | Continued

Syndrome	Human gene	Mouse model	Gene manipulation	Type of mutation	Age at manipulation	Age at experiment	DA neuron number	DA neuron cell body morphology	DA neuron intrinsic excitability	DA neuron axonal morphology	DA release	TH expression	DA tissue content	DAT expression and function	References
		Fmr1 KO	deletion	constitutive	embryonic	P81-166	Decreased SNc and unchanged VTA neuron number (stereology)	–	–	–	–	No change in dorsal or ventral striatum (WB)	–	–	Fish et al., 2013
		Fmr1 KO	deletion	constitutive	embryonic	P56-112	–	–	–	Increased axonal complexity in striatum (IHC)	–	No change in midbrain (IHC), dorsal or ventral striatum (IHC, WB)	–	Decreased striatal DAT expression (WB)	Chao et al., 2020
Rett	*MECP2*	Mecp2-/y	deletion	constitutive	embryonic	P21; P56	–	–	–	–	–	–	No change in striatum or midbrain in juveniles or adults (HPLC)	–	Santos et al., 2010
		Mecp2-/y	constitutive	deletion	embryonic	P24; P35; P55	Decreased SNc cell number in adults (IHC)	Decreased SNc soma size in adults (IHC)	–	–	–	Decreased midbrain and striatal expression in adults (IHC)	No change in midbrain and decreased in striatum in adults (HPLC)	–	Panayotis et al., 2011a,b
		Mecp2-/y	deletion	constitutive	embryonic	adult	–	–	–	–	–	Decreased in midbrain (WB)	Decreased in striatum (HPLC)	–	Samaco et al., 2009
		Mecp2-/y	deletion	constitutive	embryonic	P28-35	–	–	–	–	–	–	Decreased in dorsal striatum, more in rostral than caudal striatum (HPLC)	–	Kao et al., 2013
		Mecp2fl/y x Dlx5/6-Cre	deletion	conditonal KO	embryonic	P28-35	–	–	–	–	–	No change in rostral striatum and midbrain, increased in caudal striatum (WB)	Decreased in rostral dorsal striatum, increased in caudal dorsal stratum, no change in middle striatum or midbrain (HPLC)	–	Su et al., 2015
		Mecp2-/y	deletion	constitutive	embryonic	P30-57; P101-105	–	–	Decreased membrane capacitance in SNc	–	–	–	–	–	Gantz et al., 2011

(Continued)

TABLE 1 | Continued

Syndrome	Human gene	Mouse model	Gene manipulation	Type of mutation	Age at manipulation	Age at experiment	DA neuron number	DA neuron cell body morphology	DA neuron intrinsic excitability	DA neuron axonal morphology	DA release	TH expression	DA tissue content	DAT expression and function	References
		Mecp2+/-	deletion	constitutive	embryonic	P16-30; P169-519	–	Decreased soma size and dendritic complexity in SNc (IHC)	Decreased membrane capacitance and increased resistance in SNc	–	Decreased evoked release in striatum of adult mice (FCV, electrical stim)	–	–	–	Gantz et al., 2011
PHTS	*PTEN*	Pten+/–	deletion	constitutive	embryonic	P56	–	–	–	–	–	Increased in striatum and PFC (IHC,WB)	–	–	He et al., 2015
		Ptenfl/fl x DAT-Cre	deletion	conditional KO	embryonic	adult	Increased SNc and VTA cell number (IHC)	Increased soma size in SNc (IHC)	–	Increased axon terminal size (IHC)	–	–	–	–	Inoue et al., 2013
		Ptenfl/fl x DAT-Cre	deletion	conditional KO	embryonic	P84-112	Increased SNc and VTA cell number (stereology)	Increased soma size in SNc and VTA and increased dendrites in SNc (IHC)	–	Increased axonal size in caudal striatum (IHC)	No changes in basal or evoked release in dorsal striatum (*in vivo* microdialysis)	Increased in midbrain and unchanged in striatum (IHC)	Increased in striatum and midbrain (HPLC)	No change in DA clearance rate (microdialysis)	Diaz-Ruiz et al., 2009
		Ptenfl/fl x DAT-Cre-ERT	deletion	conditional KO	8-10 weeks	P98-112	No changes in SNc (IHC)	Increased soma size in SNc and VTA (IHC)	–	Increased axon terminal density in striatum (IHC)	–	Increased in midbrain and striatum (WB)	Increased in striatum (HPLC)	Increased striatal DAT expression (IHC)	Domanskyi et al., 2011
TSC	*TSC1, TSC2*	Tsc1fl/fl x DAT-Cre	deletion	conditional KO	embryonic	P60-P112	No changes in SNc or VTA (IHC)	Increased soma size and dendritic branching in SNc and VTA (IHC)	Decreased excitability in SNc and VTA neurons	Hypertrohic axon terminals, greater enlargement in dorsal than ventral striatum (EM)	Strongly decreased evoked release, more pronouced in dorsal than ventral sitratum (FCV, electrical stim)	Increased in midbrain and striatum (IHC, WB)	Increased in dorsal and ventral striatum (HPLC)	Increased DAT function (FCV)	Kosillo et al., 2019

Cre-ERT, tamoxifen-dependent Cre-recombinase; DA, dopamine; DAT, dopamine active transporter; EM, electron microscopy; FCV, fast-scan cyclic voltammetry; HPLC, high performance liquid chromatography; KO, knock-out; MFB, medial forebrain bundle; NAc, nucleus accumbens; PFC, prefrontal cortex; SNc, substantia nigra pars compacta; TH, tyrosine hydroxylase; VTA, ventral tegmental Area; WB, western blot; IHC, immunohistochemistry.

sensitivity to cocaine (Riday et al., 2012), a drug that enhances extracellular DA availability by blocking DAT function.

Overall, research published to date suggests that maternal loss of *Ube3a* has a significant impact on several aspects of DA neuron function. Specifically, there is a possibility of an age-dependent decline in SNc DA neuron number, a reduction in evoked DA release in the dorsal striatum, altered striatal DA tissue content, and aberrant DAT function when *Ube3a* expression is disrupted. The augmented evoked DA release in the ventral striatum of $Ube3a^{m-/p+}$ mice may involve non-cell autonomous factors (Sulzer et al., 2016), as it was observed *in vivo* but was not replicated with cell type-specific optogenetic stimulation of DA release in slices. It would be interesting for future studies to assess whether restoration of dopaminergic function is sufficient to improve behavioral phenotypes in mice with altered *Ube3a* expression.

FMR1 and Fragile X Syndrome

Mutations in the X chromosome gene *FMR1*, which encodes the fragile X, which encodes the fragile X mental retardation protein (FMRP), cause Fragile X Syndrome (FXS), characterized by intellectual disability, physical features, and behavioral conditions. Up to ∼50% of male and ∼20% of female individuals with FXS are diagnosed with ASD (Bailey et al., 2008; Kaufmann et al., 2017). Currently, FXS is the leading monogenetic cause of ASD. FMRP has multiple functions but is most well known as an RNA binding protein that represses the translation of specific mRNAs (Darnell and Klann, 2013; Banerjee et al., 2018). The mRNAs bound by FMRP encode synaptic proteins as well as other proteins implicated in ASD risk (Darnell et al., 2011; Ascano et al., 2012). *FMR1* mutations include a trinucleotide CGG repeat expansion in the 5' untranslated region (UTR) (Farzin et al., 2006; Clifford et al., 2007; Tassone et al., 2012). The full mutation exceeding 200 repeats is thought to result in abnormal methylation, which effectively silences *FMR1* expression (Pieretti et al., 1991; Primerano et al., 2002), while the premutation range of 55-200 CGG repeats typically causes increased *FMR1* mRNA expression (Kenneson et al., 2001; Peprah et al., 2010). *FMR1* is a high confidence 'score 1' autism gene with 35 possible genetic variants associated with ASD.

In terms of dopaminergic signaling, FMRP has been shown to be critical for the ability of D1-type DA receptors to exercise their neuromodulatory function in the prefrontal cortex (Wang et al., 2008; Wang et al., 2010; Paul et al., 2013). FMRP also serves as a mediator of cocaine-induced behavioral and synaptic plasticity in the NAc (Smith et al., 2014). Further, there are several lines of evidence suggesting that FMRP directly controls DA neuron function. First, FMRP is highly expressed in SNc neurons (Zorio et al., 2017). Second, there are several reports documenting the occurrence of Fragile X-associated tremor/ataxia syndrome (FXTAS) in adults over 50, particularly men, who carry an expanded *FMR1* allele in the premutation range (55-200 CGG repeats) (Leehey et al., 2007; Hall et al., 2009; Hall et al., 2010). These individuals present with a progressive neurodegenerative disorder characterized by kinetic tremor, ataxia and parkinsonism, although they typically do not meet the diagnostic criteria for Parkinson's disease. Notably, a recent report showed that FMRP protein is lost in the SNc of Parkinson's disease patients, and is further down-regulated as a result of Parkinson's-linked α-synuclein overexpression in cultured DA neurons and mouse brain (Tan et al., 2019). Together, these studies indicate that changes in dopaminergic function may occur when *FMR1* expression is altered.

There are several animal models of FXS but the most widely used is the $Fmr1^{-/y}$ mouse, which has a disrupted coding sequence resulting in loss of FMRP protein expression (Bakker et al., 1994; Kazdoba et al., 2014). In 12-16-week-old adult male mice, researchers demonstrated a significant reduction in the number of DA neurons in the SNc but not the VTA of $Fmr1^{-/y}$ mice, with no overall change in TH levels in the dorsal or ventral striatum (Fish et al., 2013). The latter observation was replicated in a study showing normal TH expression in the striatum and midbrain in 8-16 week old $Fmr1^{-/y}$ mice (Chao et al., 2020). However, it was observed that TH-positive dopaminergic axons in the striatum appeared more branched (Chao et al., 2020). This may indicate a compensatory change, as experimentally induced death of SNc DA neurons leads to increased axonal sprouting of the remaining dopaminergic cells (Tanguay et al., 2021). Together, these studies indicate that nigrostriatal DA neurons are particularly sensitive to loss of FMRP, with the surviving SNc DA neurons undergoing dynamic remodeling to increase axonal arborization and potentially boost TH expression to augment dopaminergic signaling.

In terms of dopaminergic output, Ventura and colleagues showed using *in vivo* microdialysis that there were no differences in basal DA levels in $Fmr1^{-/y}$ mice in the prefrontal cortex but there was significantly reduced basal DA efflux within the striatum (Ventura et al., 2004). Reduced striatal DA transmission was also observed by FCV experiments in acute striatal slices, which showed that in $Fmr1^{-/y}$ mice, evoked DA release was significantly diminished at 15-20 weeks of age, but not at 10 weeks of age (Fulks et al., 2010). Together these studies suggest that nigrostriatal-projecting SNc neurons may have reduced output when FMRP expression is disrupted and that this change may be age-dependent.

Changes in DAT function have also been observed in mouse models of FXS. Functional assessment of striatal DA re-uptake by FCV revealed an age-dependent decrease in DAT activity in adult $Fmr1^{-/y}$ mice (Fulks et al., 2010). Another group verified decreased striatal expression of DAT in 8-12 week old $Fmr1^{-/y}$ mice with western blot (Chao et al., 2020). The observed changes in DA release and re-uptake are not likely due to altered DA availability as total striatal tissue DA content does not appear to be consistently altered either in juvenile (4-6 week old) or adult (10-30 week old) $Fmr1^{-/y}$ mice (Gruss and Braun, 2001, 2004; Fulks et al., 2010; Sørensen et al., 2015).

In summary, constitutive *Fmr1* deletion causes DA neuron loss that is specific to SNc neurons. The remaining DA neurons upregulate their TH expression such that there is no overall change in total striatal tissue DA content. Nonetheless, there is a significant age-dependent decrease in evoked DA release in the striatum, accompanied by reduced DA re-uptake due to a reduction in DAT expression. Both downregulation of DAT and increased axonal sprouting are likely compensatory changes,

which attempt to augment DA signaling by the remaining SNc DA neurons. Thus, loss of FMRP appears to reduce dopamine signaling within the striatum; however, dopaminergic cells projecting to other regions, such as the prefrontal cortex, may be differentially affected.

MECP2 and Rett Syndrome

Mutations in the MECP2 gene, located on the X chromosome, cause the severe neurodevelopmental disorder Rett syndrome (RTT) (Amir et al., 1999), which is characterized by progressive loss of motor and language functions, breathing problems, seizures, intellectual disability and autistic-like behaviors (Hagberg et al., 2002; Jeffrey et al., 2010). RTT affects 1/15,000 girls (Laurvick et al., 2006), although reports of male *MECP2* mutation carries have emerged recently (Reichow et al., 2015; Chahil et al., 2018; Pitzianti et al., 2019). MeCP2 protein has several proposed functions including in RNA splicing control and transcriptional regulation via binding to methylated DNA (Nan et al., 1997; Nan et al., 1998; Chahrour et al., 2008; Ip et al., 2018; Qiu, 2018). Importantly, *MECP2* mutations which both increase (e.g., duplication) and decrease (e.g., loss-of-function) its function are strongly implicated in neurodevelopmental disorders, including ASD and RTT (Carney et al., 2003; Samaco, 2004; Van Esch et al., 2005; Ramocki et al., 2010; Wang et al., 2016; Wen et al., 2017). There is significant variability in the clinical presentation of *MECP2* mutation carriers, with some types of mutations conferring milder phenotypes (Bebbington et al., 2008; Neul et al., 2008). Overall, *MECP2* mutations are strongly associated with ASD (Loat et al., 2008), and currently it is a high confidence 'score 1' autism gene with 180 possible genetic variants associated with ASD.

The importance of *MECP2* for dopaminergic function is supported by observations of low levels of monoaminergic metabolites and monoamine content in the cerebrospinal fluid of RTT patients (Roux and Villard, 2009; Samaco et al., 2009). In girls with RTT syndrome there are also reports of increased D2 receptor density in the brain (Chiron et al., 1993) and reduced DAT expression in the caudate-putamen (Wenk, 2007), both of which indicate reduced DA neurotransmission. Furthermore, regressive changes in fine motor control are associated with hyperkinetic features in young RTT patients, followed by bradykinesia and postural aberrations in RTT individuals in their late 20s (Fitzgerald et al., 1990; Temudo et al., 2008); both phenotypes are suggestive of dopaminergic alterations. In mice, *Mecp2* is expressed widely throughout the brain, including in the midbrain (Pelka et al., 2005). *Mecp2*$^{-/y}$ mice are a widely used mouse model with constitutive loss of *Mecp2* (Guy et al., 2001). Similar to human RTT patients, *Mecp2*$^{-/y}$ mice show deterioration of movement coordination between 4 and 9 weeks of age (Panayotis et al., 2011b; Kao et al., 2013; Liao, 2019). In turn, preservation of MeCP2 function selectively in TH-Cre-expressing catecholaminergic neurons is sufficient to prevent motor disturbances and other phenotypes (Lang et al., 2013).

Starting at 5 weeks of age, *Mecp2*$^{-/y}$ mice present with a significant reduction in the number of SNc DA neurons and have reduced SNc neuron soma size (Panayotis et al., 2011b). Reductions in SNc neuron soma size and dendritic arborization have also been reported in female *Mecp2*$^{+/-}$ mice and notably, these changes can be observed in the pre-symptomatic stage at 3-4 weeks of age (Gantz et al., 2011). Consistent with SNc cell loss, decreased TH expression in the midbrain and striatum of *Mecp2*$^{-/y}$ mice has been observed in several studies (Samaco et al., 2009; Kao et al., 2013). In the midbrain, a significant decrease in the activated form of TH, which is phosphorylated at Ser40 (pSer40-TH), is first detectable at 5 weeks of age, and levels decline further by 8 weeks (Panayotis et al., 2011b). These studies point to a significant reduction in the DA synthesis capacity of the remaining SNc neurons in *Mecp2*$^{-/y}$ mice. Consistent with this conclusion, several studies report a substantial reduction in total tissue DA content in the striatum (Panayotis et al., 2011a,b; Kao et al., 2013), with some also finding a significant reduction in total tissue DA content in the ventral midbrain (Kao et al., 2013). Given that these changes can be observed prior to symptom onset, this suggests that changes in nigrostriatal DA may be causal for the behavioral changes in *Mecp2*$^{-/y}$ mice, particularly related to motor function (Liao, 2019). Yet not all studies replicate the reduction in total striatal DA content in this model. One report documents no alterations in DA or its primary metabolite DOPAC at 3 or 8 weeks of age in striatum or cortical regions, yet finds substantial and progressive decline in cerebellar DA content (Santos et al., 2010). The latter finding suggests possible cerebellar contribution to the motor phenotypes in RTT.

On balance, the evidence for reduced DA synthesis and content in mouse models of RTT is strong, and consistent with the finding that evoked DA release from SNc axon terminals in the dorsal striatum is decreased to just under 50% of control levels in *Mecp2*$^{+/-}$ female mice (Gantz et al., 2011). Impaired dopaminergic transmission in *Mecp2*$^{+/-}$ animals is also supported by findings of decreased D2 autoreceptor current density in SNc cell bodies (Gantz et al., 2011). Since D2 autoreceptors normally constrain DA synthesis and release, a reduction in the D2R-generated current suggests a potential homeostatic alteration whereby the D2-mediated suppression of DA release is reduced in an attempt to boost DA signaling. Therefore, in *Mecp2*$^{+/-}$ mice, DA transmission is compromised both at the axon terminals in the striatum and within the somatodendritic compartment in the midbrain. Consistent with this, augmentation of DA signaling with combined administration of levodopa and a Dopa-decarboxylase inhibitor is able to improve motor phenotypes and increase the life-span of *Mecp2*$^{-/y}$ mice (Szczesna et al., 2014).

The reduction in total tissue DA content in *Mecp2*$^{+/-}$ mice appears more pronounced in the rostral than caudal striatum (Kao et al., 2013). Emerging evidence suggests that there are regional specializations of striatal function and discrete computational circuits across the rostro-caudal axis, which in turn differentially control behavior (Hintiryan et al., 2016; Liao, 2019; Miyamoto et al., 2019). The observation of a rostral-to-caudal gradient of compromised DA synthesis was also found in *Mecp2*-conditional KO mice (Su et al., 2015) in which *Mecp2* deletion was restricted to forebrain GABAergic neurons. In this mouse model, researchers found that the DA tissue content was reduced in rostral striatum and increased in caudal striatum, with a concurrent reduction in pSer40-TH in rostral

striatum and increase in caudal striatum (Su et al., 2015). Hence, GABAergic neurons lacking *Mecp2* appear to exert region-specific extrinsic control over local striatal DA production. Interestingly, conditional deletion of *Mecp2* from DA neurons using TH-Cre mice (Lindeberg et al., 2004) also leads to reduced TH expression and DA tissue content (Samaco et al., 2009). Therefore, multiple cell types may be involved in altered DA transmission in the context of *Mecp2* loss.

Overall, studies from mouse models show that disruption of *Mecp2* expression leads to a progressive loss of SNc DA neurons and a reduction in the soma size and dendritic branching of the remaining neurons, which is first observed in juvenile animals. The remaining SNc DA neurons have a diminished DA synthesis capacity and show a substantial reduction in dopaminergic transmission at striatal axon terminals and in the somatodendritic region. Furthermore, both cell autonomous and non-cell autonomous mechanisms result in compromised DA synthesis with *Mecp2* loss.

PTEN and *PTEN* Hamartoma Tumor Syndromes

PTEN encodes the phosphatidylinositol 3,4,5-trisphosphate 3-phosphatase and dual-specificity protein phosphatase PTEN (PTEN), which functions as a tumor suppressor by negatively regulating PI3K-AKT signaling (Maehama and Dixon, 1998; Stambolic et al., 1998). Loss-of-function mutations in *PTEN* cause a group of disorders known as PTEN hamartoma tumor syndrome (PHTS), which are characterized by benign tumors in peripheral organs and brain overgrowth (Hobert and Eng, 2009). *PTEN* mutations have been found in individuals with ASD and macrocephaly (head circumference >2 SD above the mean), with an estimated prevalence of 5-50% of *PTEN* mutation carriers meeting ASD diagnostic criteria (Butler et al., 2005; Buxbaum et al., 2007; Varga et al., 2009; Mcbride et al., 2010; Hansen-Kiss et al., 2017; Ciaccio et al., 2019). Several studies also find a strong association between *PTEN* mutations, including gene-disrupting *de novo* mutations, and ASD in individuals with typical brain/head growth (O'roak et al., 2012a,b; De Rubeis et al., 2014; Iossifov et al., 2015). Based on the evidence across multiple ASD patient cohorts, *PTEN* is classified as a high confidence 'score 1' autism gene with 129 possible genetic variants associated with ASD.

PTEN is involved in many processes relevant to brain development and neural circuit function via its regulation of PI3K-AKT and mechanistic target of rapamycin (mTOR) signaling (Van Diepen and Eickholt, 2008; Garcia-Junco-Clemente and Golshani, 2014; Skelton et al., 2019). By controlling cell cycle progression and cell migration/adhesion, PTEN is important for the proliferation and differentiation of neural progenitors (Groszer, 2001; Zhou and Parada, 2012; Tilot et al., 2015). In addition, PTEN controls neuronal size, dendritic morphology, and synaptic transmission (Fraser et al., 2008; Jurado et al., 2010; Sperow et al., 2012; Takeuchi et al., 2013). Specific to dopaminergic neurons, researchers have found elevated TH expression in the cortex and striatum of mice with a missense mutation in *Pten* (He et al., 2015). Additionally, cell type-specific deletion of *Pten* from DA neurons is sufficient to alter some aspects of social behavior (Clipperton-Allen and Page, 2014). Several studies demonstrated that loss of *Pten* protects dopaminergic cells from neurotoxic lesions and significantly enhances their survival (Diaz-Ruiz et al., 2009; Domanskyi et al., 2011). Furthermore, *Pten* suppression facilitates DA neuron integration in striatal grafts transplanted into a Parkinson's disease mouse model (Zhang et al., 2012). Therefore, concurrent increases in AKT and mTOR signaling caused by *Pten* deletion enable increased TH expression and enhanced DA neuron survival under conditions of cell stress.

To investigate how cell autonomous loss of *Pten* affects the DA system, several mouse lines have been generated with either embryonic deletion of *Pten* from DA neurons using DAT-IRES-Cre mice or postnatal deletion using tamoxifen-inducible DAT-Cre mice. *Pten* deletion beginning at 8-10 weeks of age (Domanskyi et al., 2011) or embryonic *Pten* loss (Diaz-Ruiz et al., 2009) both resulted in a substantial increase in the soma size of SNc and VTA DA neurons and increased *Th* mRNA levels in the midbrain. Furthermore, both embryonic and adult *Pten* deletion caused increased TH protein expression in midbrain and striatum, with a concurrent increase in striatal DA tissue content (Diaz-Ruiz et al., 2009; Domanskyi et al., 2011). However, increased TH expression and striatal DA content had no effect on basal or evoked DA release or the rate of DA clearance by DAT examined with microdialysis (Diaz-Ruiz et al., 2009).

Some differences in the consequences of adult versus embryonic loss of *Pten* from DA neurons have been observed. For example, adult, but not embryonic, *Pten* deletion results in increased density of striatal DA axon terminals (Domanskyi et al., 2011). Mice with embryonic *Pten* deletion on the other hand, have an increased number of TH+ neurons in the SNc and VTA (Diaz-Ruiz et al., 2009; Inoue et al., 2013). This suggests that depending on the developmental timing, *Pten* loss promotes dopaminergic function either via increasing the numbers of DA neurons or enhancing axonal branching of DA neurons.

In summary, deletion of *Pten* leads to a substantial increase in DA neuron soma size in both the SNc and VTA and causes significant upregulation of TH expression and DA tissue content in the midbrain and striatum. This increase in DA synthesis and tissue content, however, does not appear to affect basal or evoked striatal DA release. Adult *Pten* deletion causes an increase in striatal DA axon density 6 weeks later, while embryonic loss does not appear to alter axonal arbors but increases the total number of TH+ neurons in the midbrain. Together these studies demonstrate that loss of *Pten* impacts several aspects of DA neuron structure and function, generally leading to DA neuron hypertrophy.

TSC1/2 and Tuberous Sclerosis Complex

TSC1 and *TSC2* encode the proteins hamartin and tuberin, respectively. Hamartin and tuberin form a multimeric protein complex, which negatively regulates mTOR complex 1 (mTORC1) signaling (Tee et al., 2002; Huang and Manning, 2008). Loss-of-function mutations in either *TSC1* or *TSC2* cause Tuberous Sclerosis Complex (TSC), a neurodevelopmental disorder characterized by benign tumors in multiple organs, focal cortical malformations, epilepsy, and psychiatric and behavioral conditions (Krueger et al., 2013; De Vries et al.,

2015; Henske et al., 2016). Between 25 and 50% of individuals with TSC are diagnosed with ASD, with greater prevalence in males (Smalley, 1998; Numis et al., 2011; Curatolo et al., 2015; De Vries et al., 2020). Importantly, mutations in *TSC1* and *TSC2* have also been reported in individuals with ASD independent of TSC (Schaaf et al., 2011; Esteban et al., 2012; O'roak et al., 2012a; Iossifov et al., 2015; Kalsner et al., 2018). Thus, both *TSC1* and *TSC2* are high confidence 'score 1' genes with 34 and 82 possible genetic variants, respectively, associated with ASD.

Several lines of evidence support the importance of mTORC1 signaling for DA neuron function. DA neurons have high metabolic demands to support their extensive axonal processes (Matsuda et al., 2009) and mTORC1 is a central regulator of cellular metabolism via its control of protein and lipid synthesis, mitochondrial biogenesis and autophagy (Saxton and Sabatini, 2017). Related to this, stimulation of mTORC1 signaling by expression of a constitutively active form of Rheb (caRheb), the small GTP-ase that directly promotes mTORC1 activity, protects SNc DA neurons from neurotoxin lesions (Kim et al., 2012). In turn, both acute inhibition of mTORC1 signaling with rapamycin (Hernandez et al., 2012) or 2 week-long *mTOR* deletion in adult VTA neurons (Liu et al., 2018) reduce evoked DA release in the dorsal and ventral striatum, respectively.

To examine the impact of constitutive mTORC1 activation on the dopaminergic system in the context of TSC, our group generated a DA neuron-specific *Tsc1* KO mouse (*Tsc1*$^{fl/fl}$*; DAT-IRES-Cre*). Following embryonic loss of *Tsc1* and mTORC1 hyperactivation, no change in DA neuron cell number was observed (Kosillo et al., 2019). However, both SNc and VTA DA neurons had significantly increased soma size, as well as increased total length and number of dendritic arborizations (Kosillo et al., 2019). This morphological restructuring caused a significant reduction in DA neuron intrinsic excitability due to changes in passive membrane properties (Kosillo et al., 2019). TH protein expression in the striatum and midbrain and striatal DA tissue content were significantly increased (Kosillo et al., 2019). Despite increased DA synthesis and storage, evoked DA release assessed with FCV in striatal slices was severely compromised following *Tsc1* loss, with more profound deficits in the dorsal striatum compared to ventral regions (Kosillo et al., 2019). Electron microscopy analysis of striatal axon terminals showed significant enlargement of TH+ axon profiles, consistent with somatodendritic hypertrophy, which was most pronounced in the dorsal striatum (Kosillo et al., 2019). Axonal enlargement, in turn, was associated with greater vesicle distance from the plasma membrane and reduced vesicle clustering, which together likely reduces the efficiency of vesicle recruitment to release sites. Thus, the more pronounced axon terminal restructuring in the dorsal striatum is consistent with the larger DA release deficits in the dorsal versus ventral striatum. Notably, loss of Tsc1 from DA neurons did not impact motor or social behaviors but selectively impaired behavioral flexibility in a reversal learning task.

Importantly, some of the phenotypes observed in the Kosillo et al. study were also found in a postnatal model in which mTORC1 hyperactivation was caused by transduction of caRheb into SNc DA neurons at 8 weeks of age (Kim et al., 2012). 4 weeks post-injection, constitutive mTORC1 activation caused a significant increase in DA neuron soma size in the SNc and an increase in striatal TH expression, TH+ axon number, and DA tissue content (Kim et al., 2012), similar to postnatal loss of *Pten* (Domanskyi et al., 2011).

Overall, *Tsc1* loss leads to significant hypertrophy of SNc and VTA DA neurons at the level of soma, dendrites and axon terminals, while the total DA neuron number remains unchanged. Increased cell size, in turn, renders *Tsc1* KO dopaminergic cells hypoexcitable. *Tsc1* loss also results in significant upregulation of midbrain and striatal TH expression supporting elevated DA synthesis, with total striatal DA tissue content substantially increased. Despite this, evoked striatal DA release is compromised, at least in part due to aberrations in the architecture of axon terminals.

DISCUSSION

Across the five syndromic forms of ASD discussed here, there is clear evidence for alterations in the dopaminergic system that can include changes in DA neuron number, morphology, excitability, DA synthesis, and release. However, there is no consistent pattern of changes across different models. Soma size and DA synthesis capacity are impacted in all five syndromic ASD models, yet these can be changed in opposite ways. Alterations in cell number, axonal and dendritic architecture, membrane excitability and DA release were observed in some of the models; however, these properties were not universally assessed. Overall, findings from both syndromic and non-syndromic ASD mouse models support dopaminergic dysregulation being part of the molecular and cellular signature of autism in the brain (Robinson and Gradinaru, 2018). However, changes in DA function are not universal and are unlikely to be sufficient to drive all aspects of ASD.

The molecular processes controlled by UBE3A, FMRP, MECP2, PTEN and TSC1/TSC2 are important for maintaining balanced protein production and degradation and DA neurons may be particularly sensitive to aberrations in proteostasis. The studies discussed above show that alterations in protein degradation (*Ube3a*), gene expression (*Mecp2*), RNA regulation (*Fmr1*) or protein synthesis (*Pten, Tsc1*) can impact DA neuron structure and function. The overarching theme from these models is that interference with protein degradation or RNA processing leads to DA neuron death specifically in the SNc, coupled with progressive impairments in motor function. Specifically, gait, fine and gross motor coordination and motor learning are significantly compromised in both *Ube3a* and *Mecp2* mouse models (Jiang et al., 1998; Mulherkar and Jana, 2010; Panayotis et al., 2011b; Kao et al., 2013). Progressive motor decline is also seen in mice with *Fmr1* CGG expansion in the pre-mutation range (Van Dam et al., 2005). While not a core diagnostic feature of ASD, motor deficits are common in individuals with ASD (Fournier et al., 2010; Bhat et al., 2011;

Esposito et al., 2011), and may even contribute to difficulties with speech acquisition. In turn, chronic increases in cellular anabolic processes do not cause degeneration of DA neurons but are sufficient to impair cognitive flexibility (*Tsc1*) (Kosillo et al., 2019) or social approach (*Pten*) (Clipperton-Allen and Page, 2014), which are related to core ASD symptoms. Further, there are indications of reduced sociability (Chao et al., 2020) and social discrimination (Sørensen et al., 2015) in *Fmr1* mouse models, while mice overexpressing *Ube3a* in the VTA exhibit sociability deficits that are precipitated by seizures (Krishnan et al., 2017). Together, these studies suggest that mutations in ASD-risk genes can alter dopaminergic function in a variety of ways, but that dopaminergic changes are not sufficient to recapitulate all aspects of ASD in a given mouse model.

Studies published to date have examined aspects of DA neuron function using a variety of metrics and approaches, and different experimental designs. Factors such as whether the gene disruption occurs embryonically or in adulthood, or constitutively or in a cell type-specific manner, could all contribute to differing results. Consequently, heterogeneity in methodology and outcome measures, such as whether DA release is measured by FCV or microdialysis, makes it challenging to make comparisons across different ASD models and studies. To formally address whether there are convergent changes in dopaminergic function in ASD, the optimal starting point would be assessment of the DA system in mice with a constitutive mutation, similar to patients, that show a wide range of ASD-related behavior phenotypes. Subsequently, the same mutation could be introduced selectively in DA neurons to define which dopaminergic signatures and behavioral phenotypes can be recapitulated with DA-specific manipulations.

Many of the findings discussed in this review come from *in vitro* and *ex vivo* assays that have provided fundamental insights into the state of the DA system in syndromic ASD mouse models. Recent developments in DA monitoring, including $GRAB_{DA}$ and D-Light GPCR-based DA sensors (Labouesse et al., 2020; Patriarchi et al., 2020; Sun et al., 2020), coupled to spectral- and depth-resolved fiber photometry (Meng et al., 2018; Pisano et al., 2019), now grant unprecedented access to monitoring DA neurotransmission *in vivo*. The use of these newly developed tools to monitor DA dynamics in awake behaving animals, potentially across multiple brain regions simultaneously, will allow for comprehensive mapping of brain-wide DA neurotransmission dynamics and changes associated ASD. Furthermore, recently developed anatomical tools, which enable whole-brain pathway mapping via viral circuit tracing can be applied together with chemogenetic and optogenetic manipulations to aid in our understanding of ASD pathophysiology, as previously highlighted (Robinson and Gradinaru, 2018). Together, application of novel anatomical, circuit manipulating and DA monitoring tools will provide new insights into dopaminergic aberrations associated with ASD by connecting cellular and circuit-level aberrations with behavioral changes. This approach will facilitate the development of a data-driven theoretical frameworks on the role of DA in ASD pathogenesis.

In summary, as a neuromodulator, DA fulfills many distinct functions, and either too much or too little DA is likely to be disruptive to neural circuits with complex cascading effects. Some of these aspects may manifest early in development and over time exacerbate behavioral abnormalities culminating in ASD. In addition, dopaminergic changes associated with ASD are likely to be dynamic in nature, changing across the lifespan, and distinct between various brain regions and neural circuits. Consequently, further investigations are warranted to build a more complete picture of how DA dysregulation may contribute to ASD symptomology.

AUTHOR CONTRIBUTIONS

PK drafted the initial manuscript. HB contributed to the review and editing. Both authors devised the topic and scope of the review.

FUNDING

This work was supported by the SFARI Research Grant #514428 and NIH R01NS105634 (to HB). HB and PK were supported by the NARSAD Young Investigator Grants from the Brain & Behavior Research Foundation (#25073 to HB and #27458 to PK). HB is a Chan Zuckerberg Biohub Investigator.

REFERENCES

Adamsen, D., Ramaekers, V., Ho, H. T. B., Britschgi, C., Rüfenacht, V., Meili, D., et al. (2014). Autism spectrum disorder associated with low serotonin in CSF and mutations in the SLC29A4 plasma membrane monoamine transporter (PMAT) gene. *Mol. Autism* 5:43. doi: 10.1186/2040-2392-5-43

Aman, M. G., Kasper, W., Manos, G., Mathew, S., Marcus, R., Owen, R., et al. (2010). Line-Item Analysis of the Aberrant Behavior Checklist: Results from Two Studies of Aripiprazole in the Treatment of Irritability Associated with Autistic Disorder. *J. Child Adolesc. Psychopharmacol.* 20, 415–422. doi: 10.1089/cap.2009.0120

American Psychiatric Association (2013). *Diagnostic and statistical manual of mental disorders : DSM-5*, 5th Edn. Washington, DC: American Psychiatric Association.

Amir, R. E., Van Den Veyver, I. B., Wan, M., Tran, C. Q., Francke, U., and Zoghbi, H. Y. (1999). Rett syndrome is caused by mutations in X-linked MECP2, encoding methyl-CpG-binding protein 2. *Nat. Genet.* 23, 185–188.

Aoki, S., Smith, J. B., Li, H., Yan, X., Igarashi, M., Coulon, P., et al. (2019). An open cortico-basal ganglia loop allows limbic control over motor output via the nigrothalamic pathway. *eLife* 8:e49995

Arnsten, A. F. (1997). Catecholamine regulation of the prefrontal cortex. *J. Psychopharmacol.* 11, 151–162. doi: 10.1177/026988119701100208

Asano, E., Chugani, D. C., Muzik, O., Behen, M., Janisse, J., Rothermel, R., et al. (2001). Autism in tuberous sclerosis complex is related to both cortical and subcortical dysfunction. *Neurology* 57, 1269–1277. doi: 10.1212/wnl.57.7.1269

Ascano, M., Mukherjee, N., Bandaru, P., Miller, J. B., Nusbaum, J. D., Corcoran, D. L., et al. (2012). FMRP targets distinct mRNA sequence elements to regulate protein expression. *Nature* 492, 382–386. doi: 10.1038/nature11737

Bailey, D. B., Raspa, M., Olmsted, M., and Holiday, D. B. (2008). Co-occurring conditions associated withFMR1gene variations: Findings from a national

parent survey. *Am. J. Medical Genet. Part A* 146A, 2060–2069. doi: 10.1002/ajmg.a.32439

Bakker, C., Verheij, C., Willemsen, R., Vanderhelm, R., Oerlemans, F., Vermey, M., et al. (1994). Fmr1 knockout mice: a model to study fragile X mental retardation. The Dutch-Belgian Fragile X Consortium. *Cell* 78, 23–33.

Banerjee, A., Ifrim, M. F., Valdez, A. N., Raj, N., and Bassell, G. J. (2018). Aberrant RNA translation in fragile X syndrome: From FMRP mechanisms to emerging therapeutic strategies. *Brain Res.* 1693, 24–36. doi: 10.1016/j.brainres.2018.04.008

Baribeau, D. A., Dupuis, A., Paton, T. A., Hammill, C., Scherer, S. W., Schachar, R. J., et al. (2019). Structural neuroimaging correlates of social deficits are similar in autism spectrum disorder and attention-deficit/hyperactivity disorder: analysis from the POND Network. *Transl. Psychiatry* 9:72.

Bebbington, A., Anderson, A., Ravine, D., Fyfe, S., Pineda, M., De Klerk, N., et al. (2008). Investigating genotype-phenotype relationships in Rett syndrome using an international data set. *Neurology* 70, 868–875. doi: 10.1212/01.wnl.0000304752.50773.ec

Berrios, J., Stamatakis, A. M., Kantak, P. A., Mcelligott, Z. A., Judson, M. C., Aita, M., et al. (2016). Loss of UBE3A from TH-expressing neurons suppresses GABA co-release and enhances VTA-NAc optical self-stimulation. *Nat. Communicat.* 7:10702.

Bhat, A. N., Landa, R. J., and Galloway, J. C. (2011). Current perspectives on motor functioning in infants, children, and adults with autism spectrum disorders. *Phys. Ther.* 91, 1116–1129. doi: 10.2522/ptj.20100294

Bowton, E., Saunders, C., Reddy, I. A., Campbell, N. G., Hamilton, P. J., Henry, L. K., et al. (2014). SLC6A3 coding variant Ala559Val found in two autism probands alters dopamine transporter function and trafficking. *Translat. Psychiatry* 4, e464–e464.

Butler, M. G., Dasouki, M. J., Zhou, X. P., Talebizadeh, Z., Brown, M., Takahashi, T. N., et al. (2005). Subset of individuals with autism spectrum disorders and extreme macrocephaly associated with germline PTEN tumour suppressor gene mutations. *J. Med. Genet.* 42, 318–321. doi: 10.1136/jmg.2004.024646

Buxbaum, J. D., Cai, G., Chaste, P., Nygren, G., Goldsmith, J., Reichert, J., et al. (2007). Mutation screening of the PTEN gene in patients with autism spectrum disorders and macrocephaly. *Am. J. Med. Genet. B Neuropsychiatr. Genet.* 144B, 484–491.

Campbell, N. G., Shekar, A., Aguilar, J. I., Peng, D., Navratna, V., Yang, D., et al. (2019). Structural, functional, and behavioral insights of dopamine dysfunction revealed by a deletion in SLC6A3. *Proc. Natl. Acad. Sci.* 116, 3853–3862. doi: 10.1073/pnas.1816247116

Carney, R. M., Wolpert, C. M., Ravan, S. A., Shahbazian, M., Ashley-Koch, A., Cuccaro, M. L., et al. (2003). Identification of MeCP2 mutations in a series of females with autistic disorder. *Pediatr. Neurol.* 28, 205–211. doi: 10.1016/s0887-8994(02)00624-0

Chahil, G., Yelam, A., and Bollu, P. C. (2018). Rett Syndrome in Males: A Case Report and Review of Literature. *Cureus* 10:e3414.

Chahrour, M., Jung, S. Y., Shaw, C., Zhou, X., Wong, S. T., Qin, J., et al. (2008). MeCP2, a key contributor to neurological disease, activates and represses transcription. *Science* 320, 1224–1229. doi: 10.1126/science.1153252

Chao, O. Y., Pathak, S. S., Zhang, H., Dunaway, N., Li, J.-S., Mattern, C., et al. (2020). Altered dopaminergic pathways and therapeutic effects of intranasal dopamine in two distinct mouse models of autism. *Mol. Brain* 13:111.

Chiron, C., Bulteau, C., Loc'h, C., Raynaud, C., Garreau, B., Syrota, A., et al. (1993). Dopaminergic D2 receptor SPECT imaging in Rett syndrome: increase of specific binding in striatum. *J. Nucl. Med.* 34, 1717–1721.

Ciaccio, C., Saletti, V., D'arrigo, S., Esposito, S., Alfei, E., Moroni, I., et al. (2019). Clinical spectrum of PTEN mutation in pediatric patients. A bicenter experience. *Eur. J. Med. Genet.* 62:103596. doi: 10.1016/j.ejmg.2018.12.001

Clayton-Smith, J., and Laan, L. (2003). Angelman syndrome: a review of the clinical and genetic aspects. *J. Med. Genet.* 40, 87–95. doi: 10.1136/jmg.40.2.87

Clifford, S., Dissanayake, C., Bui, Q. M., Huggins, R., Taylor, A. K., and Loesch, D. Z. (2007). Autism spectrum phenotype in males and females with fragile X full mutation and premutation. *J. Autism Dev. Disord.* 37, 738–747. doi: 10.1007/s10803-006-0205-z

Clipperton-Allen, A. E., and Page, D. T. (2014). Pten haploinsufficient mice show broad brain overgrowth but selective impairments in autism-relevant behavioral tests. *Hum. Mol. Genet.* 23, 3490–3505. doi: 10.1093/hmg/ddu057

Cohen, I. L., Liu, X., Lewis, M. E. S., Chudley, A., Forster-Gibson, C., Gonzalez, M., et al. (2011). Autism severity is associated with child and maternal MAOA genotypes. *Clin. Genet.* 79, 355–362. doi: 10.1111/j.1399-0004.2010.01471.x

Cohen, I. L., Liu, X., Schutz, C., White, B. N., Jenkins, E. C., Brown, W. T., et al. (2003). Association of autism severity with a monoamine oxidase A functional polymorphism. *Clin. Genet.* 64, 190–197. doi: 10.1034/j.1399-0004.2003.00115.x

Cools, R., and D'esposito, M. (2011). Inverted-U–Shaped Dopamine Actions on Human Working Memory and Cognitive Control. *Biol. Psychiatr.* 69, e113–e125.

Curatolo, P., Moavero, R., and De Vries, P. J. (2015). Neurological and neuropsychiatric aspects of tuberous sclerosis complex. *Lancet Neurol.* 14, 733–745. doi: 10.1016/s1474-4422(15)00069-1

Darnell, J. C., and Klann, E. (2013). The translation of translational control by FMRP: therapeutic targets for FXS. *Nat. Neurosci.* 16, 1530–1536. doi: 10.1038/nn.3379

Darnell, J. C., Van Driesche, S. J., Zhang, C., Hung, K. Y., Mele, A., Fraser, C. E., et al. (2011). FMRP Stalls Ribosomal Translocation on mRNAs Linked to Synaptic Function and Autism. *Cell* 146, 247–261.

De Jong, J. W., Afjei, S. A., Pollak Dorocic, I., Peck, J. R., Liu, C., Kim, C. K., et al. (2019). A Neural Circuit Mechanism for Encoding Aversive Stimuli in the Mesolimbic Dopamine System. *Neuron* 101, 133–151e137.

De Krom, M., Staal, W. G., Ophoff, R. A., Hendriks, J., Buitelaar, J., Franke, B., et al. (2009). A Common Variant in DRD3 Receptor Is Associated with Autism Spectrum Disorder. *Biol. Psychiat.* 65, 625–630. doi: 10.1016/j.biopsych.2008.09.035

De La Torre-Ubieta, L., Won, H., Stein, J. L., and Geschwind, D. H. (2016). Advancing the understanding of autism disease mechanisms through genetics. *Nat. Med.* 22, 345–361. doi: 10.1038/nm.4071

De Rubeis, S., He, X., Goldberg, A. P., Poultney, C. S., Samocha, K., Cicek, A. E., et al. (2014). Synaptic, transcriptional and chromatin genes disrupted in autism. *Nature* 515, 209–215.

De Vries, P. J., Belousova, E., Benedik, M. P., Carter, T., Cottin, V., Curatolo, P., et al. (2020). Tuberous Sclerosis Complex-Associated Neuropsychiatric Disorders (TAND): New Findings on Age, Sex, and Genotype in Relation to Intellectual Phenotype. *Front. Neurol.* 11:603. doi: 10.3389/fneur.2020.00603

De Vries, P. J., Whittemore, V. H., Leclezio, L., Byars, A. W., Dunn, D., Ess, K. C., et al. (2015). Tuberous sclerosis associated neuropsychiatric disorders (TAND) and the TAND Checklist. *Pediatr. Neurol.* 52, 25–35.

Diaz-Ruiz, O., Zapata, A., Shan, L., Zhang, Y., Tomac, A. C., Malik, N., et al. (2009). Selective deletion of PTEN in dopamine neurons leads to trophic effects and adaptation of striatal medium spiny projecting neurons. *PLoS One* 4:e7027. doi: 10.1371/journal.pone.0007027

Dicarlo, G. E., Aguilar, J. I., Matthies, H. J. G., Harrison, F. E., Bundschuh, K. E., West, A., et al. (2019). Autism-linked dopamine transporter mutation alters striatal dopamine neurotransmission and dopamine-dependent behaviors. *J. Clin. Investigat.* 129, 3407–3419. doi: 10.1172/jci127411

Domanskyi, A., Geissler, C., Vinnikov, I. A., Alter, H., Schober, A., Vogt, M. A., et al. (2011). Pten ablation in adult dopaminergic neurons is neuroprotective in Parkinson's disease models. *FASEB J.* 25, 2898–2910. doi: 10.1096/fj.11-181958

Donovan, A. P., and Basson, M. A. (2017). The neuroanatomy of autism - a developmental perspective. *J. Anat.* 230, 4–15. doi: 10.1111/joa.12542

Ernst, M., Zametkin, A. J., Matochik, J. A., Pascualvaca, D., and Cohen, R. M. (1997). Low medial prefrontal dopaminergic activity in autistic children. *Lancet* 350:638. doi: 10.1016/s0140-6736(05)63326-0

Esposito, G., Venuti, P., Apicella, F., and Muratori, F. (2011). Analysis of unsupported gait in toddlers with autism. *Brain Dev.* 33, 367–373. doi: 10.1016/j.braindev.2010.07.006

Esteban, F. J., Kelleher, R. J. III, Geigenmüller, U., Hovhannisyan, H., Trautman, E., Pinard, R., et al. (2012). High-Throughput Sequencing of mGluR Signaling Pathway Genes Reveals Enrichment of Rare Variants in Autism. *PLoS One* 7:e35003. doi: 10.1371/journal.pone.0035003

Estes, A., Shaw, D. W., Sparks, B. F., Friedman, S., Giedd, J. N., Dawson, G., et al. (2011). Basal ganglia morphometry and repetitive behavior in young children with autism spectrum disorder. *Autism Res.* 4, 212–220. doi: 10.1002/aur.193

Farook, M. F., Decuypere, M., Hyland, K., Takumi, T., Ledoux, M. S., and Reiter, L. T. (2012). Altered Serotonin, Dopamine and Norepinepherine Levels in 15q Duplication and Angelman Syndrome Mouse Models. *PLoS One* 7:e43030. doi: 10.1371/journal.pone.0043030

Farzin, F., Perry, H., Hessl, D., Loesch, D., Cohen, J., Bacalman, S., et al. (2006). Autism spectrum disorders and attention-deficit/hyperactivity disorder in boys with the fragile X premutation. *J. Dev. Behav. Pediatr.* 27, S137–S144.

Fatemi, S. H., Aldinger, K. A., Ashwood, P., Bauman, M. L., Blaha, C. D., Blatt, G. J., et al. (2012). Consensus paper: pathological role of the cerebellum in autism. *Cerebellum* 11, 777–807. doi: 10.1007/s12311-012-0355-9

Fish, E. W., Krouse, M. C., Stringfield, S. J., Diberto, J. F., Robinson, J. E., and Malanga, C. J. (2013). Changes in sensitivity of reward and motor behavior to dopaminergic, glutamatergic, and cholinergic drugs in a mouse model of fragile X syndrome. *PLoS One* 8:e77896. doi: 10.1371/journal.pone.0077896

Fitzgerald, P. M., Jankovic, J., and Percy, A. K. (1990). Rett syndrome and associated movement disorders. *Movem. Disord.* 5, 195–202. doi: 10.1002/mds.870050303

Fournier, K. A., Hass, C. J., Naik, S. K., Lodha, N., and Cauraugh, J. H. (2010). Motor coordination in autism spectrum disorders: a synthesis and meta-analysis. *J. Autism Dev. Disord.* 40, 1227–1240. doi: 10.1007/s10803-010-0981-3

Fraser, M. M., Bayazitov, I. T., Zakharenko, S. S., and Baker, S. J. (2008). Phosphatase and tensin homolog, deleted on chromosome 10 deficiency in brain causes defects in synaptic structure, transmission and plasticity, and myelination abnormalities. *Neuroscience* 151, 476–488. doi: 10.1016/j.neuroscience.2007.10.048

Fuccillo, M. V. (2016). Striatal Circuits as a Common Node for Autism Pathophysiology. *Front. Neurosci.* 10:27. doi: 10.3389/fnins.2016.00027

Fulks, J. L., O'bryhim, B. E., Wenzel, S. K., Fowler, S. C., Vorontsova, E., Pinkston, J. W., et al. (2010). Dopamine Release and Uptake Impairments and Behavioral Alterations Observed in Mice that Model Fragile X Mental Retardation Syndrome. *ACS Chem. Neurosci.* 1, 679–690. doi: 10.1021/cn100032f

Gantz, S. C., Ford, C. P., Neve, K. A., and Williams, J. T. (2011). Loss of Mecp2 in substantia nigra dopamine neurons compromises the nigrostriatal pathway. *J. Neurosci.* 31, 12629–12637. doi: 10.1523/jneurosci.0684-11.2011

Garcia-Junco-Clemente, P., and Golshani, P. (2014). PTEN: A master regulator of neuronal structure, function, and plasticity. *Communicat. Integrat. Biol.* 7:e28358. doi: 10.4161/cib.28358

Glessner, J. T., Wang, K., Cai, G., Korvatska, O., Kim, C. E., Wood, S., et al. (2009). Autism genome-wide copy number variation reveals ubiquitin and neuronal genes. *Nature* 459, 569–573.

Groszer, M. (2001). Negative Regulation of Neural Stem/Progenitor Cell Proliferation by the Pten Tumor Suppressor Gene *in Vivo*. *Science* 294, 2186–2189. doi: 10.1126/science.1065518

Gruss, M., and Braun, K. (2001). Alterations of Amino Acids and Monoamine Metabolism in Male Fmr1 Knockout Mice: A Putative Animal Model of the Human Fragile X Mental Retardation Syndrome. *Neural Plasticity* 8, 285–298. doi: 10.1155/np.2001.285

Gruss, M., and Braun, K. (2004). Age- and region-specific imbalances of basal amino acids and monoamine metabolism in limbic regions of female Fmr1 knock-out mice. *Neurochem. Int.* 45, 81–88. doi: 10.1016/j.neuint.2003.12.001

Gunaydin, L. A., Grosenick, L., Finkelstein, J. C., Kauvar, I. V., Fenno, L. E., Adhikari, A., et al. (2014). Natural neural projection dynamics underlying social behavior. *Cell* 157, 1535–1551. doi: 10.1016/j.cell.2014.05.017

Gustin, R. M., Bichell, T. J., Bubser, M., Daily, J., Filonova, I., Mrelashvili, D., et al. (2010). Tissue-specific variation of Ube3a protein expression in rodents and in a mouse model of Angelman syndrome. *Neurobiol. Dis.* 39, 283–291. doi: 10.1016/j.nbd.2010.04.012

Guy, J., Hendrich, B., Holmes, M., Martin, J. E., and Bird, A. (2001). A mouse Mecp2-null mutation causes neurological symptoms that mimic Rett syndrome. *Nat. Genet.* 27, 322–326. doi: 10.1038/85899

Hagberg, B., Hanefeld, F., Percy, A., and Skjeldal, O. L. A. (2002). An update on clinically applicable diagnostic criteria in Rett syndrome. *Eur. J. Paediatr. Neurol.* 6, 293–297. doi: 10.1053/ejpn.2002.0612

Hall, D. A., Howard, K., Hagerman, R., and Leehey, M. A. (2009). Parkinsonism in FMR1 premutation carriers may be indistinguishable from Parkinson disease. *Parkinson. Related Disord.* 15, 156–159. doi: 10.1016/j.parkreldis.2008.04.037

Hall, D., Pickler, L., Riley, K., Tassone, F., and Hagerman, R. (2010). Parkinsonism and cognitive decline in a fragile X mosaic male. *Movem. Disord.* 25, 1523–1524. doi: 10.1002/mds.23150

Hamid, A. A., Pettibone, J. R., Mabrouk, O. S., Hetrick, V. L., Schmidt, R., Vander Weele, C. M., et al. (2016). Mesolimbic dopamine signals the value of work. *Nat. Neurosci.* 19, 117–126. doi: 10.1038/nn.4173

Hamilton, P. J., Campbell, N. G., Sharma, S., Erreger, K., Herborg Hansen, F., Saunders, C., et al. (2013). *De novo* mutation in the dopamine transporter gene associates dopamine dysfunction with autism spectrum disorder. *Mol. Psychiatry* 18, 1315–1323. doi: 10.1038/mp.2013.102

Hampson, D. R., and Blatt, G. J. (2015). Autism spectrum disorders and neuropathology of the cerebellum. *Front. Neurosci.* 9:420. doi: 10.3389/fnins.2015.00420

Hansen-Kiss, E., Beinkampen, S., Adler, B., Frazier, T., Prior, T., Erdman, S., et al. (2017). A retrospective chart review of the features of PTEN hamartoma tumour syndrome in children. *J. Med. Genet.* 54, 471–478. doi: 10.1136/jmedgenet-2016-104484

Harbord, M. (2001). Levodopa responsive Parkinsonism in adults with Angelman Syndrome. *J. Clin. Neurosci.* 8, 421–422. doi: 10.1054/jocn.2000.0753

He, X., Thacker, S., Romigh, T., Yu, Q., Frazier, T. W. Jr., and Eng, C. (2015). Cytoplasm-predominant Pten associates with increased region-specific brain tyrosine hydroxylase and dopamine D2 receptors in mouse model with autistic traits. *Mol. Autism* 6:63.

Henske, E. P., Jóźwiak, S., Kingswood, J. C., Sampson, J. R., and Thiele, E. A. (2016). Tuberous sclerosis complex. *Nat. Rev. Dis. Primers* 2:16035.

Hernandez, D., Torres, C. A., Setlik, W., Cebrián, C., Mosharov, E. V., Tang, G., et al. (2012). Regulation of Presynaptic Neurotransmission by Macroautophagy. *Neuron* 74, 277–284. doi: 10.1016/j.neuron.2012.02.020

Hettinger, J. A., Liu, X., Hudson, M. L., Lee, A., Cohen, I. L., Michaelis, R. C., et al. (2012). DRD2 and PPP1R1B (DARPP-32) polymorphisms independently confer increased risk for autism spectrum disorders and additively predict affected status in male-only affected sib-pair families. *Behav. Brain Funct.* 8:19. doi: 10.1186/1744-9081-8-19

Hettinger, J. A., Liu, X., Schwartz, C. E., Michaelis, R. C., and Holden, J. J. A. (2008). A DRD1 haplotype is associated with risk for autism spectrum disorders in male−only affected sib−pair families. *Am. J. Med. Genet. Part B Neuropsychiatr. Genet.* 147B, 628–636. doi: 10.1002/ajmg.b.30655

Hintiryan, H., Foster, N. N., Bowman, I., Bay, M., Song, M. Y., Gou, L., et al. (2016). The mouse cortico-striatal projectome. *Nat. Neurosci.* 19, 1100–1114. doi: 10.1038/nn.4332

Hirsch, L. E., and Pringsheim, T. (2016). Aripiprazole for autism spectrum disorders (ASD). *Cochrane Database Systemat. Rev.* 2016:CD009043.

Hobert, J. A., and Eng, C. (2009). PTEN hamartoma tumor syndrome: An overview. *Genet. Med.* 11, 687–694. doi: 10.1097/gim.0b013e3181ac9aea

Hogart, A., Wu, D., Lasalle, J. M., and Schanen, N. C. (2010). The comorbidity of autism with the genomic disorders of chromosome 15q11.2-q13. *Neurobiol. Dis.* 38, 181–191. doi: 10.1016/j.nbd.2008.08.011

Hollander, E., Anagnostou, E., Chaplin, W., Esposito, K., Haznedar, M. M., Licalzi, E., et al. (2005). Striatal volume on magnetic resonance imaging and repetitive behaviors in autism. *Biol. Psychiat.* 58, 226–232. doi: 10.1016/j.biopsych.2005.03.040

Hook, P. W., Mcclymont, S. A., Cannon, G. H., Law, W. D., Morton, A. J., Goff, L. A., et al. (2018). Single-Cell RNA-Seq of Mouse Dopaminergic Neurons Informs Candidate Gene Selection for Sporadic Parkinson Disease. *Am. J. Hum. Genet.* 102, 427–446. doi: 10.1016/j.ajhg.2018.02.001

Howard, C. D., Li, H., Geddes, C. E., and Jin, X. (2017). Dynamic Nigrostriatal Dopamine Biases Action Selection. *Neuron* 93, 1436–1450e1438.

Howes, O. D., Rogdaki, M., Findon, J. L., Wichers, R. H., Charman, T., King, B. H., et al. (2018). Autism spectrum disorder: Consensus guidelines on assessment, treatment and research from the British Association for Psychopharmacology. *J. Psychopharmacol.* 32, 3–29. doi: 10.1177/0269881117741766

Huang, J., and Manning, B. D. (2008). The TSC1-TSC2 complex: a molecular switchboard controlling cell growth. *Biochem. J.* 412, 179–190. doi: 10.1042/bj20080281

Inoue, K., Rispoli, J., Yang, L., Macleod, D., Beal, M. F., Klann, E., et al. (2013). Coordinate regulation of mature dopaminergic axon morphology by macroautophagy and the PTEN signaling pathway. *PLoS Genet.* 9:e1003845. doi: 10.1371/journal.pgen.1003845

Iossifov, I., Levy, D., Allen, J., Ye, K., Ronemus, M., Lee, Y. H., et al. (2015). Low load for disruptive mutations in autism genes and their biased transmission. *Proc. Natl. Acad. Sci. U S A.* 112, E5600–E5607.

Ip, J. P. K., Mellios, N., and Sur, M. (2018). Rett syndrome: insights into genetic, molecular and circuit mechanisms. *Nat. Rev. Neurosci.* 19, 368–382. doi: 10.1038/s41583-018-0006-3

Jeffrey, L. N., Kaufmann, W. E., Glaze, D. G., Christodoulou, J., Clarke, A. J., Bahi-Buisson, N., et al. (2010). Rett syndrome: Revised diagnostic criteria and nomenclature. *Ann. Neurol.* 68, 944–950. doi: 10.1002/ana.22124

Jiang, Y.-H., Armstrong, D., Albrecht, U., Atkins, C. M., Noebels, J. L., Eichele, G., et al. (1998). Mutation of the Angelman Ubiquitin Ligase in Mice Causes Increased Cytoplasmic p53 and Deficits of Contextual Learning and Long-Term Potentiation. *Neuron* 21, 799–811. doi: 10.1016/s0896-6273(00)80596-6

Jurado, S., Benoist, M., Lario, A., Knafo, S., Petrok, C. N., and Esteban, J. A. (2010). PTEN is recruited to the postsynaptic terminal for NMDA receptor-dependent long-term depression. *EMBO J.* 29, 2827–2840. doi: 10.1038/emboj.2010.160

Kalsner, L., Twachtman-Bassett, J., Tokarski, K., Stanley, C., Dumont-Mathieu, T., Cotney, J., et al. (2018). Genetic testing including targeted gene panel in a diverse clinical population of children with autism spectrum disorder: Findings and implications. *Mol. Genet. Genomic Med.* 6, 171–185. doi: 10.1002/mgg3.354

Kao, F.-C., Su, S.-H., Carlson, G. C., and Liao, W. (2013). MeCP2-mediated alterations of striatal features accompany psychomotor deficits in a mouse model of Rett syndrome. *Brain Struct. Funct.* 220, 419–434. doi: 10.1007/s00429-013-0664-x

Kaufmann, W. E., Kidd, S. A., Andrews, H. F., Budimirovic, D. B., Esler, A., Haas-Givler, B., et al. (2017). Autism Spectrum Disorder in Fragile X Syndrome: Cooccurring Conditions and Current Treatment. *Pediatrics* 139, S194–S206.

Kazdoba, T. M., Leach, P. T., and Crawley, J. N. (2015). Behavioral phenotypes of genetic mouse models of autism. *Genes Brain Behav.* 15, 7–26. doi: 10.1111/gbb.12256

Kazdoba, T. M., Leach, P. T., Silverman, J. L., and Crawley, J. N. (2014). Modeling fragile X syndrome in the Fmr1 knockout mouse. *Intractable Rare Dis. Res.* 3, 118–133. doi: 10.5582/irdr.2014.01024

Kenneson, A., Zhang, F., Hagedorn, C. H., and Warren, S. T. (2001). Reduced FMRP and increased FMR1 transcription is proportionally associated with CGG repeat number in intermediate-length and premutation carriers. *Hum. Mol. Genet.* 10, 1449–1454. doi: 10.1093/hmg/10.14.1449

Khanzada, N. S., Butler, M. G., and Manzardo, A. M. (2017). GeneAnalytics Pathway Analysis and Genetic Overlap among Autism Spectrum Disorder, Bipolar Disorder and Schizophrenia. *Int. J. Mol. Sci.* 18:527. doi: 10.3390/ijms18030527

Kim, S. R., Kareva, T., Yarygina, O., Kholodilov, N., and Burke, R. E. (2012). AAV transduction of dopamine neurons with constitutively active Rheb protects from neurodegeneration and mediates axon regrowth. *Mol. Ther.* 20, 275–286. doi: 10.1038/mt.2011.213

Kishino, T., Lalande, M., and Wagstaff, J. (1997). UBE3A/E6-AP mutations cause Angelman syndrome. *Nat. Genet.* 15, 70–73. doi: 10.1038/ng0197-70

Kosillo, P., Doig, N. M., Ahmed, K. M., Agopyan-Miu, A., Wong, C. D., Conyers, L., et al. (2019). Tsc1-mTORC1 signaling controls striatal dopamine release and cognitive flexibility. *Nat. Commun.* 10:5426.

Kramer, D. J., Aisenberg, E. E., Kosillo, P., Friedmann, D., Stafford, D. A., Lee, A. Y.-F., et al. (2021). Generation of a DAT-P2A-Flpo mouse line for intersectional genetic targeting of dopamine neuron subpopulations. *Cell Rep.* 35:109123. doi: 10.1016/j.celrep.2021.109123

Kramer, D. J., Risso, D., Kosillo, P., Ngai, J., and Bateup, H. S. (2018). Combinatorial Expression of Grp and Neurod6 Defines Dopamine Neuron Populations with Distinct Projection Patterns and Disease Vulnerability. *eNeuro* 5, ENEURO.152–ENEURO.118.

Krishnan, V., Stoppel, D. C., Nong, Y., Johnson, M. A., Nadler, M. J. S., Ozkaynak, E., et al. (2017). Autism gene Ube3a and seizures impair sociability by repressing VTA Cbln1. *Nature* 543, 507–512. doi: 10.1038/nature21678

Krueger, D. A., Northrup, H., International Tuberous, Sclerosis Complex, and Consensus, G. (2013). Tuberous sclerosis complex surveillance and management: recommendations of the 2012 International Tuberous Sclerosis Complex Consensus Conference. *Pediatr. Neurol.* 49, 255–265.

La Manno, G., Gyllborg, D., Codeluppi, S., Nishimura, K., Salto, C., Zeisel, A., et al. (2016). Molecular Diversity of Midbrain Development in Mouse, Human, and Stem Cells. *Cell* 167, 566.e–580.e.

Labouesse, M. A., Cola, R. B., and Patriarchi, T. (2020). GPCR-Based Dopamine Sensors—A Detailed Guide to Inform Sensor Choice for *In Vivo* Imaging. *Int. J. Mol. Sci.* 21:8048. doi: 10.3390/ijms21218048

Lammel, S., Hetzel, A., Häckel, O., Jones, I., Liss, B., and Roeper, J. (2008). Unique Properties of Mesoprefrontal Neurons within a Dual Mesocorticolimbic Dopamine System. *Neuron* 57, 760–773. doi: 10.1016/j.neuron.2008.01.022

Lang, M., Wither, R. G., Brotchie, J. M., Wu, C., Zhang, L., and Eubanks, J. H. (2013). Selective preservation of MeCP2 in catecholaminergic cells is sufficient to improve the behavioral phenotype of male and female Mecp2-deficient mice. *Hum. Mol. Genet.* 22, 358–371. doi: 10.1093/hmg/dds433

Langen, M., Bos, D., Noordermeer, S. D., Nederveen, H., Van Engeland, H., and Durston, S. (2014). Changes in the development of striatum are involved in repetitive behavior in autism. *Biol. Psychiatry* 76, 405–411. doi: 10.1016/j.biopsych.2013.08.013

Langen, M., Schnack, H. G., Nederveen, H., Bos, D., Lahuis, B. E., De Jonge, M. V., et al. (2009). Changes in the developmental trajectories of striatum in autism. *Biol. Psychiatry* 66, 327–333. doi: 10.1016/j.biopsych.2009.03.017

Laurvick, C. L., De Klerk, N., Bower, C., Christodoulou, J., Ravine, D., Ellaway, C., et al. (2006). Rett syndrome in Australia: a review of the epidemiology. *J. Pediatr.* 148, 347–352.

Leclerc, S., and Easley, D. (2015). Pharmacological therapies for autism spectrum disorder: a review. *P T* 40, 389–397.

Lee, J., Wang, W., and Sabatini, B. L. (2020). Anatomically segregated basal ganglia pathways allow parallel behavioral modulation. *Nat. Neurosci.* 23, 1388–1398. doi: 10.1038/s41593-020-00712-5

Lee, Y., Kim, H., Kim, J. E., Park, J. Y., Choi, J., Lee, J. E., et al. (2018). Excessive D1 Dopamine Receptor Activation in the Dorsal Striatum Promotes Autistic-Like Behaviors. *Mol. Neurobiol.* 55, 5658–5671. doi: 10.1007/s12035-017-0770-5

Leehey, M. A., Berry-Kravis, E., Goetz, C. G., Zhang, L., Hall, D. A., Li, L., et al. (2007). FMR1 CGG repeat length predicts motor dysfunction in premutation carriers. *Neurology* 70, 1397–1402. doi: 10.1212/01.wnl.0000281692.98200.f5

Liao, W. (2019). Psychomotor Dysfunction in Rett Syndrome: Insights into the Neurochemical and Circuit Roots. *Dev. Neurobiol.* 79, 51–59. doi: 10.1002/dneu.22651

Lindeberg, J., Usoskin, D., Bengtsson, H., Gustafsson, A., Kylberg, A., Söderström, S., et al. (2004). Transgenic expression of Cre recombinase from the tyrosine hydroxylase locus. *Genesis* 40, 67–73. doi: 10.1002/gene.20065

Liu, X., Li, Y., Yu, L., Vickstrom, C. R., and Liu, Q. S. (2018). VTA mTOR Signaling Regulates Dopamine Dynamics, Cocaine-Induced Synaptic Alterations, and Reward. *Neuropsychopharmacology* 43, 1066–1077. doi: 10.1038/npp.2017.247

Loat, C. S., Curran, S., Lewis, C. M., Duvall, J., Geschwind, D., Bolton, P., et al. (2008). Methyl-CpG-binding protein 2 polymorphisms and vulnerability to autism. *Genes Brain Behav.* 7, 754–760.

Maehama, T., and Dixon, J. E. (1998). The Tumor Suppressor, PTEN/MMAC1, Dephosphorylates the Lipid Second Messenger, Phosphatidylinositol 3,4,5-Trisphosphate. *J. Biol. Chem.* 273, 13375–13378. doi: 10.1074/jbc.273.22.13375

Maenner, M. J., Shaw, K. A., Baio, J., Washington, A., Patrick, M., Dirienzo, M., et al. (2020). Prevalence of Autism Spectrum Disorder Among Children Aged 8 Years — Autism and Developmental Disabilities Monitoring Network, 11 Sites, United States, 2016. *Surveill. Summar.* 69, 1–12. doi: 10.15585/mmwr.ss6802a1

Makkonen, I., Riikonen, R., Kokki, H., Airaksinen, M. M., and Kuikka, J. T. (2008). Serotonin and dopamine transporter binding in children with autism determined by SPECT. *Dev. Med. Child Neurol.* 50, 593–597. doi: 10.1111/j.1469-8749.2008.03027.x

Marcus, R. N., Owen, R., Manos, G., Mankoski, R., Kamen, L., Mcquade, R. D., et al. (2011). Safety and Tolerability of Aripiprazole for Irritability in Pediatric Patients With Autistic Disorder. *J. Clin. Psychiatry* 72, 1270–1276. doi: 10.4088/jcp.09m05933

Matsuda, W., Furuta, T., Nakamura, K. C., Hioki, H., Fujiyama, F., Arai, R., et al. (2009). Single nigrostriatal dopaminergic neurons form widely spread and highly dense axonal arborizations in the neostriatum. *J. Neurosci.* 29, 444–453. doi: 10.1523/jneurosci.4029-08.2009

Matsuura, T., Sutcliffe, J. S., Fang, P., Galjaard, R.-J., Jiang, Y.-H., Benton, C. S., et al. (1997). *De novo* truncating mutations in E6-AP ubiquitin-protein ligase gene (UBE3A) in Angelman syndrome. *Nat. Genet.* 15, 74–77. doi: 10.1038/ng0197-74

Mayes, S. D., Calhoun, S. L., Murray, M. J., Ahuja, M., and Smith, L. A. (2011). Anxiety, depression, and irritability in children with autism relative to other

neuropsychiatric disorders and typical development. *Res. Autism Spectr. Disord.* 5, 474–485. doi: 10.1016/j.rasd.2010.06.012

Mcbride, K. L., Varga, E. A., Pastore, M. T., Prior, T. W., Manickam, K., Atkin, J. F., et al. (2010). Confirmation study of PTEN mutations among individuals with autism or developmental delays/mental retardation and macrocephaly. *Autism Res.* 3, 137–141. doi: 10.1002/aur.132

Mccracken, J. T., Mcgough, J., Shah, B., Cronin, P., Hong, D., Aman, M. G., et al. (2002). Risperidone in children with autism and serious behavioral problems. *N. Engl. J. Med.* 347, 314–321.

Meng, C., Zhou, J., Papaneri, A., Peddada, T., Xu, K., and Cui, G. (2018). Spectrally Resolved Fiber Photometry for Multi-component Analysis of Brain Circuits. *Neuron* 98, 707.e–717.e.

Mergy, M. A., Gowrishankar, R., Gresch, P. J., Gantz, S. C., Williams, J., Davis, G. L., et al. (2014). The rare DAT coding variant Val559 perturbs DA neuron function, changes behavior, and alters *in vivo* responses to psychostimulants. *Proc. Natl. Acad. Sci. U S A.* 111, E4779–E4788.

Miyamoto, Y., Nagayoshi, I., Nishi, A., and Fukuda, T. (2019). Three divisions of the mouse caudal striatum differ in the proportions of dopamine D1 and D2 receptor-expressing cells, distribution of dopaminergic axons, and composition of cholinergic and GABAergic interneurons. *Brain Struct. Funct.* 224, 2703–2716. doi: 10.1007/s00429-019-01928-3

Mohebi, A., Pettibone, J. R., Hamid, A. A., Wong, J. T., Vinson, L. T., Patriarchi, T., et al. (2019). Dissociable dopamine dynamics for learning and motivation. *Nature* 570, 65–70. doi: 10.1038/s41586-019-1235-y

Mulherkar, S. A., and Jana, N. R. (2010). Loss of dopaminergic neurons and resulting behavioural deficits in mouse model of Angelman syndrome. *Neurobiol. Dis.* 40, 586–592. doi: 10.1016/j.nbd.2010.08.002

Nakamura, K., Sekine, Y., Ouchi, Y., Tsujii, M., Yoshikawa, E., Futatsubashi, M., et al. (2010). Brain Serotonin and Dopamine Transporter Bindings in Adults With High-Functioning Autism. *Archi. General Psychiat.* 67, 59–68. doi: 10.1001/archgenpsychiatry.2009.137

Nakatani, J., Tamada, K., Hatanaka, F., Ise, S., Ohta, H., Inoue, K., et al. (2009). Abnormal Behavior in a Chromosome- Engineered Mouse Model for Human 15q11-13 Duplication Seen in Autism. *Cell* 137, 1235–1246. doi: 10.1016/j.cell.2009.04.024

Nan, X., Campoy, F. J., and Bird, A. (1997). MeCP2 Is a Transcriptional Repressor with Abundant Binding Sites in Genomic Chromatin. *Cell* 88, 471–481. doi: 10.1016/s0092-8674(00)81887-5

Nan, X., Ng, H.-H., Johnson, C. A., Laherty, C. D., Turner, B. M., Eisenman, R. N., et al. (1998). Transcriptional repression by the methyl-CpG-binding protein MeCP2 involves a histone deacetylase complex. *Nature* 393, 386–389. doi: 10.1038/30764

Neul, J. L., Fang, P., Barrish, J., Lane, J., Caeg, E. B., Smith, E. O., et al. (2008). Specific mutations in Methyl-CpG-Binding Protein 2 confer different severity in Rett syndrome. *Neurology* 70, 1313–1321. doi: 10.1212/01.wnl.0000291011.54508.aa

Nguyen, M., Roth, A., Kyzar, E. J., Poudel, M. K., Wong, K., Stewart, A. M., et al. (2014). Decoding the contribution of dopaminergic genes and pathways to autism spectrum disorder (ASD). *Neurochem. Int.* 66, 15–26. doi: 10.1016/j.neuint.2014.01.002

Numis, A. L., Major, P., Montenegro, M. A., Muzykewicz, D. A., Pulsifer, M. B., and Thiele, E. A. (2011). Identification of risk factors for autism spectrum disorders in tuberous sclerosis complex. *Neurology* 76, 981–987. doi: 10.1212/wnl.0b013e3182104347

Nurmi, E. L., Bradford, Y., Chen, Y.-H., Hall, J., Arnone, B., Gardiner, M. B., et al. (2001). Linkage Disequilibrium at the Angelman Syndrome Gene UBE3A in Autism Families. *Genomics* 77, 105–113. doi: 10.1006/geno.2001.6617

Olanow, C. W., and Mcnaught, K. S. (2006). Ubiquitin-proteasome system and Parkinson's disease. *Mov. Disord.* 21, 1806–1823.

O'roak, B. J., Vives, L., Fu, W., Egertson, J. D., Stanaway, I. B., Phelps, I. G., et al. (2012a). Multiplex targeted sequencing identifies recurrently mutated genes in autism spectrum disorders. *Science* 338, 1619–1622. doi: 10.1126/science.1227764

O'roak, B. J., Vives, L., Girirajan, S., Karakoc, E., Krumm, N., Coe, B. P., et al. (2012b). Sporadic autism exomes reveal a highly interconnected protein network of *de novo* mutations. *Nature* 485, 246–250. doi: 10.1038/nature10989

Ott, T., and Nieder, A. (2019). Dopamine and Cognitive Control in Prefrontal Cortex. *Trends Cogn. Sci.* 23, 213–234. doi: 10.1016/j.tics.2018.12.006

Owen, R., Sikich, L., Marcus, R. N., Corey-Lisle, P., Manos, G., Mcquade, R. D., et al. (2009). Aripiprazole in the Treatment of Irritability in Children and Adolescents With Autistic Disorder. *Pediatrics* 124, 1533–1540. doi: 10.1542/peds.2008-3782

Panayotis, N., Ghata, A., Villard, L., and Roux, J.-C. (2011a). Biogenic amines and their metabolites are differentially affected in the Mecp2-deficient mouse brain. *BMC Neurosci.* 12:47. doi: 10.1186/1471-2202-12-47

Panayotis, N., Pratte, M., Borges-Correia, A., Ghata, A., Villard, L., and Roux, J.-C. (2011b). Morphological and functional alterations in the substantia nigra pars compacta of the Mecp2-null mouse. *Neurobiol. Dis.* 41, 385–397. doi: 10.1016/j.nbd.2010.10.006

Patriarchi, T., Mohebi, A., Sun, J., Marley, A., Liang, R., Dong, C., et al. (2020). An expanded palette of dopamine sensors for multiplex imaging *in vivo*. *Nat. Methods* 17, 1147–1155. doi: 10.1038/s41592-020-0936-3

Paul, K., Venkitaramani, D. V., and Cox, C. L. (2013). Dampened dopamine-mediated neuromodulation in prefrontal cortex of fragile X mice. *J. Physiol.* 591, 1133–1143. doi: 10.1113/jphysiol.2012.241067

Paval, D. (2017). A Dopamine Hypothesis of Autism Spectrum Disorder. *Dev. Neurosci.* 39, 355–360. doi: 10.1159/000478725

Pelka, G. J., Watson, C. M., Christodoulou, J., and Tam, P. P. L. (2005). Distinct expression profiles of Mecp2 transcripts with different lengths of 3'UTR in the brain and visceral organs during mouse development. *Genomics* 85, 441–452. doi: 10.1016/j.ygeno.2004.12.002

Peprah, E., He, W., Allen, E., Oliver, T., Boyne, A., and Sherman, S. L. (2010). Examination of FMR1 transcript and protein levels among 74 premutation carriers. *J. Hum. Genet.* 55, 66–68. doi: 10.1038/jhg.2009.121

Pieretti, M., Zhang, F., Fu, Y.-H., Warren, S. T., Oostra, B. A., Caskey, C. T., et al. (1991). Absence of expression of the FMR-1 gene in fragile X syndrome. *Cell* 66, 817–822. doi: 10.1016/0092-8674(91)90125-i

Pisano, F., Pisanello, M., Lee, S. J., Lee, J., Maglie, E., Balena, A., et al. (2019). Depth-resolved fiber photometry with a single tapered optical fiber implant. *Nat. Methods* 16, 1185–1192. doi: 10.1038/s41592-019-0581-x

Pitzianti, M. B., Santamaria Palombo, A., Esposito, S., and Pasini, A. (2019). Rett Syndrome in Males: The Different Clinical Course in Two Brothers with the Same Microduplication MECP2 Xq28. *Int. J. Environ. Res. Public Health* 16:3075. doi: 10.3390/ijerph16173075

Poulin, J. F., Caronia, G., Hofer, C., Cui, Q., Helm, B., Ramakrishnan, C., et al. (2018). Mapping projections of molecularly defined dopamine neuron subtypes using intersectional genetic approaches. *Nat. Neurosci.* 21, 1260–1271. doi: 10.1038/s41593-018-0203-4

Poulin, J.-F., Gaertner, Z., Moreno-Ramos, O. A., and Awatramani, R. (2020). Classification of Midbrain Dopamine Neurons Using Single-Cell Gene Expression Profiling Approaches. *Trends Neurosci.* 43, 155–169. doi: 10.1016/j.tins.2020.01.004

Poulin, J.-F., Zou, J., Drouin-Ouellet, J., Kim, K.-Y. A., Cicchetti, F., and Awatramani, R. B. (2014). Defining Midbrain Dopaminergic Neuron Diversity by Single-Cell Gene Expression Profiling. *Cell Rep.* 9, 930–943. doi: 10.1016/j.celrep.2014.10.008

Presti, M. F., Mikes, H. M., and Lewis, M. H. (2003). Selective blockade of spontaneous motor stereotypy via intrastriatal pharmacological manipulation. *Pharmacol. Biochem. Behav.* 74, 833–839. doi: 10.1016/s0091-3057(02)01081-x

Primerano, B., Tassone, F., Hagerman, R. J., Hagerman, P., Amaldi, F., and Bagni, C. (2002). Reduced FMR1 mRNA translation efficiency in fragile X patients with premutations. *RNA* 8, 1482–1488.

Qiu, Z. (2018). Deciphering MECP2 -associated disorders: disrupted circuits and the hope for repair. *Curr. Opin. Neurobiol.* 48, 30–36. doi: 10.1016/j.conb.2017.09.004

Ramaswami, G., Won, H., Gandal, M. J., Haney, J., Wang, J. C., Wong, C. C. Y., et al. (2020). Integrative genomics identifies a convergent molecular subtype that links epigenomic with transcriptomic differences in autism. *Nat. Commun.* 11:4873.

Ramocki, M. B., Tavyev, Y. J., and Peters, S. U. (2010). TheMECP2duplication syndrome. *Am. J. Med. Genet. Part A* 152A, 1079–1088. doi: 10.1002/ajmg.a.33184

Reichow, B., George-Puskar, A., Lutz, T., Smith, I. C., and Volkmar, F. R. (2015). Brief Report: Systematic Review of Rett Syndrome in Males. *J. Autism Dev. Disord.* 45, 3377–3383. doi: 10.1007/s10803-015-2519-1

Reiersen, A. M., and Todorov, A. A. (2011). Association between DRD4 genotype and Autistic Symptoms in DSM-IV ADHD. *J. Can. Acad. Child Adolesc. Psychiatry* 20, 15–21.

Riday, T. T., Dankoski, E. C., Krouse, M. C., Fish, E. W., Walsh, P. L., Han, J. E., et al. (2012). Pathway-specific dopaminergic deficits in a mouse model of Angelman syndrome. *J. Clin. Investigat.* 122, 4544–4554. doi: 10.1172/jci61888

Robinson, J. E., and Gradinaru, V. (2018). Dopaminergic dysfunction in neurodevelopmental disorders: recent advances and synergistic technologies to aid basic research. *Curr. Opin. Neurobiol.* 48, 17–29. doi: 10.1016/j.conb.2017.08.003

Rougeulle, C., Glatt, H., and Lalande, M. (1997). The Angelman syndrome candidate gene, UBE3A/E6-AP, is imprinted in brain. *Nat. Genet.* 17, 14–15. doi: 10.1038/ng0997-14

Roux, J.-C., and Villard, L. (2009). Biogenic Amines in Rett Syndrome: The Usual Suspects. *Behav. Genet.* 40, 59–75. doi: 10.1007/s10519-009-9303-y

Samaco, R. C. (2004). Multiple pathways regulate MeCP2 expression in normal brain development and exhibit defects in autism-spectrum disorders. *Hum. Mol. Genet.* 13, 629–639. doi: 10.1093/hmg/ddh063

Samaco, R. C., Mandel-Brehm, C., Chao, H. T., Ward, C. S., Fyffe-Maricich, S. L., Ren, J., et al. (2009). Loss of MeCP2 in aminergic neurons causes cell-autonomous defects in neurotransmitter synthesis and specific behavioral abnormalities. *Proc. Natl. Acad. Sci.* 106, 21966–21971. doi: 10.1073/pnas.0912257106

Santos, M., Summavielle, T., Teixeira-Castro, A., Silva-Fernandes, A., Duarte-Silva, S., Marques, F., et al. (2010). Monoamine deficits in the brain of methyl-CpG binding protein 2 null mice suggest the involvement of the cerebral cortex in early stages of Rett syndrome. *Neuroscience* 170, 453–467. doi: 10.1016/j.neuroscience.2010.07.010

Satterstrom, F. K., Kosmicki, J. A., Wang, J., Breen, M. S., De Rubeis, S., An, J.-Y., et al. (2020). Large-Scale Exome Sequencing Study Implicates Both Developmental and Functional Changes in the Neurobiology of Autism. *Cell* 180, 568.e–584.e.

Saunders, A., Macosko, E. Z., Wysoker, A., Goldman, M., Krienen, F. M., De Rivera, H., et al. (2018). Molecular Diversity and Specializations among the Cells of the Adult Mouse Brain. *Cell* 174, 1015.e–1030.e.

Saxton, R. A., and Sabatini, D. M. (2017). mTOR Signaling in Growth, Metabolism, and Disease. *Cell* 168, 960–976. doi: 10.1016/j.cell.2017.02.004

Schaaf, C. P., Sabo, A., Sakai, Y., Crosby, J., Muzny, D., Hawes, A., et al. (2011). Oligogenic heterozygosity in individuals with high-functioning autism spectrum disorders. *Hum. Mol. Genet.* 20, 3366–3375. doi: 10.1093/hmg/ddr243

Schuetze, M., Park, M. T., Cho, I. Y., Macmaster, F. P., Chakravarty, M. M., and Bray, S. L. (2016). Morphological Alterations in the Thalamus, Striatum, and Pallidum in Autism Spectrum Disorder. *Neuropsychopharmacology* 41, 2627–2637. doi: 10.1038/npp.2016.64

Scott-Van Zeeland, A. A., Dapretto, M., Ghahremani, D. G., Poldrack, R. A., and Bookheimer, S. Y. (2010). Reward processing in autism. *Autism Res.* 3, 53–67.

Sharma, A., and Shaw, S. R. (2012). Efficacy of Risperidone in Managing Maladaptive Behaviors for Children With Autistic Spectrum Disorder: A Meta-Analysis. *J. Pediatr. Health Care* 26, 291–299. doi: 10.1016/j.pedhc.2011.02.008

Skelton, P. D., Stan, R. V., and Luikart, B. W. (2019). The Role of PTEN in Neurodevelopment. *Mol. Neuropsychiat.* 5, 60–71. doi: 10.1159/000504782

Smalley, S. L. (1998). Autism and tuberous sclerosis. *J. Autism Dev. Disord.* 28, 407–414.

Smith, L. N., Jedynak, J. P., Fontenot, M. R., Hale, C. F., Dietz, K. C., Taniguchi, M., et al. (2014). Fragile X Mental Retardation Protein Regulates Synaptic and Behavioral Plasticity to Repeated Cocaine Administration. *Neuron* 82, 645–658. doi: 10.1016/j.neuron.2014.03.028

Sørensen, E. M., Bertelsen, F., Weikop, P., Skovborg, M. M., Banke, T., Drasbek, K. R., et al. (2015). Hyperactivity and lack of social discrimination in the adolescent Fmr1 knockout mouse. *Behav. Pharmacol.* 26, 733–740. doi: 10.1097/fbp.0000000000000152

Sperow, M., Berry, R. B., Bayazitov, I. T., Zhu, G., Baker, S. J., and Zakharenko, S. S. (2012). Phosphatase and tensin homologue (PTEN) regulates synaptic plasticity independently of its effect on neuronal morphology and migration. *J. Physiol.* 590, 777–792. doi: 10.1113/jphysiol.2011.220236

Staal, W. G., De Krom, M., and De Jonge, M. V. (2011). Brief Report: The Dopamine-3-Receptor Gene (DRD3) is Associated with Specific Repetitive Behavior in Autism Spectrum Disorder (ASD). *J. Autism Dev. Disord.* 42, 885–888. doi: 10.1007/s10803-011-1312-z

Staal, W. G., Langen, M., Van Dijk, S., Mensen, V. T., and Durston, S. (2018). DRD3 gene and striatum in autism spectrum disorder. *Br. J. Psychiatry* 206, 431–432. doi: 10.1192/bjp.bp.114.148973

Stambolic, V., Suzuki, A., De La Pompa, J. L., Brothers, G. M., Mirtsos, C., Sasaki, T., et al. (1998). Negative Regulation of PKB/Akt-Dependent Cell Survival by the Tumor Suppressor PTEN. *Cell* 95, 29–39. doi: 10.1016/s0092-8674(00)81780-8

Steinkellner, T., Yang, J.-W., Montgomery, T. R., Chen, W.-Q., Winkler, M.-T., Sucic, S., et al. (2012). Ca2+/Calmodulin-dependent Protein Kinase IIα (αCaMKII) Controls the Activity of the Dopamine Transporter. *J. Biol. Chem.* 287, 29627–29635.

Su, S.-H., Kao, F.-C., Huang, Y.-B., and Liao, W. (2015). MeCP2 in the Rostral Striatum Maintains Local Dopamine Content Critical for Psychomotor Control. *J. Neurosci.* 35, 6209–6220. doi: 10.1523/jneurosci.4624-14.2015

Subramanian, K., Brandenburg, C., Orsati, F., Soghomonian, J. J., Hussman, J. P., and Blatt, G. J. (2017). Basal ganglia and autism - a translational perspective. *Autism Res.* 10, 1751–1775. doi: 10.1002/aur.1837

Sulzer, D., Cragg, S. J., and Rice, M. E. (2016). Striatal dopamine neurotransmission: Regulation of release and uptake. *Basal Ganglia* 6, 123–148. doi: 10.1016/j.baga.2016.02.001

Sun, F., Zhou, J., Dai, B., Qian, T., Zeng, J., Li, X., et al. (2020). Next-generation GRAB sensors for monitoring dopaminergic activity *in vivo*. *Nat. Methods* 17, 1156–1166. doi: 10.1038/s41592-020-00981-9

Szczesna, K., De La Caridad, O., Petazzi, P., Soler, M., Roa, L., Saez, M. A., et al. (2014). Improvement of the Rett Syndrome Phenotype in a Mecp2 Mouse Model Upon Treatment with Levodopa and a Dopa-Decarboxylase Inhibitor. *Neuropsychopharmacology* 39, 2846–2856. doi: 10.1038/npp.2014.136

Takeuchi, K., Gertner, M. J., Zhou, J., Parada, L. F., Bennett, M. V. L., and Zukin, R. S. (2013). Dysregulation of synaptic plasticity precedes appearance of morphological defects in a Pten conditional knockout mouse model of autism. *Proc. Natl. Acad. Sci.* 110, 4738–4743. doi: 10.1073/pnas.1222803110

Tan, W. H., Bird, L. M., Sadhwani, A., Barbieri—Welge, R. L., Skinner, S. A., Horowitz, L. T., et al. (2017). A randomized controlled trial of levodopa in patients with Angelman syndrome. *Am. J. Med. Genet. Part A* 176, 1099–1107.

Tan, Y., Sgobio, C., Arzberger, T., Machleid, F., Tang, Q., Findeis, E., et al. (2019). Loss of fragile X mental retardation protein precedes Lewy pathology in Parkinson's disease. *Acta Neuropathol.* 139, 319–345. doi: 10.1007/s00401-019-02099-5

Tanguay, W., Ducrot, C., Giguère, N., Bourque, M.-J., and Trudeau, L.-E. (2021). Neonatal 6-OHDA lesion of the SNc induces striatal compensatory sprouting from surviving SNc dopaminergic neurons without VTA contribution. [Preprint].

Tassone, F., Choudhary, N. S., Tassone, F., Durbin-Johnson, B., Hansen, R., Hertz-Picciotto, I., et al. (2012). Identification of Expanded Alleles of the FMR1 Gene in the CHildhood Autism Risks from Genes and Environment (CHARGE) Study. *J. Autism Dev. Disord.* 43, 530–539. doi: 10.1007/s10803-012-1580-2

Tee, A. R., Fingar, D. C., Manning, B. D., Kwiatkowski, D. J., Cantley, L. C., and Blenis, J. (2002). Tuberous sclerosis complex-1 and -2 gene products function together to inhibit mammalian target of rapamycin (mTOR)-mediated downstream signaling. *Proc. Natl. Acad. Sci.* 99, 13571–13576. doi: 10.1073/pnas.202476899

Temudo, T., Ramos, E., Dias, K., Barbot, C., Vieira, J. P., Moreira, A., et al. (2008). Movement disorders in Rett syndrome: An analysis of 60 patients with detected MECP2 mutation and correlation with mutation type. *Mov. Disord.* 23, 1384–1390. doi: 10.1002/mds.22115

Tiklová, K., Björklund, ÅK., Lahti, L., Fiorenzano, A., Nolbrant, S., Gillberg, L., et al. (2019). Single-cell RNA sequencing reveals midbrain dopamine neuron diversity emerging during mouse brain development. *Nat. Commun.* 10:581.

Tilot, A. K., Frazier, T. W., and Eng, C. (2015). Balancing Proliferation and Connectivity in PTEN-associated Autism Spectrum Disorder. *Neurotherapeutics* 12, 609–619. doi: 10.1007/s13311-015-0356-8

Toma, C., Hervás, A., Balmaña, N., Salgado, M., Maristany, M., Vilella, E., et al. (2012). Neurotransmitter systems and neurotrophic factors in autism: association study of 37 genes suggests involvement of DDC. *World J. Biol. Psychiatry* 14, 516–527. doi: 10.3109/15622975.2011.602719

Van Dam, D., Errijgers, V., Kooy, R. F., Willemsen, R., Mientjes, E., Oostra, B. A., et al. (2005). Cognitive decline, neuromotor and behavioural disturbances in a mouse model for fragile-X-associated tremor/ataxia syndrome (FXTAS). *Behav. Brain Res.* 162, 233–239. doi: 10.1016/j.bbr.2005.03.007

Van Diepen, M. T., and Eickholt, B. J. (2008). Function of PTEN during the Formation and Maintenance of Neuronal Circuits in the Brain. *Dev. Neurosci.* 30, 59–64. doi: 10.1159/000109852

Van Esch, H., Bauters, M., Ignatius, J., Jansen, M., Raynaud, M., Hollanders, K., et al. (2005). Duplication of the MECP2 Region Is a Frequent Cause of Severe Mental Retardation and Progressive Neurological Symptoms in Males. *Am. J. Hum. Genet.* 77, 442–453. doi: 10.1086/444549

Varga, E. A., Pastore, M., Prior, T., Herman, G. E., and Mcbride, K. L. (2009). The prevalence of PTEN mutations in a clinical pediatric cohort with autism spectrum disorders, developmental delay, and macrocephaly. *Genet. Med.* 11, 111–117. doi: 10.1097/gim.0b013e31818fd762

Varghese, M., Keshav, N., Jacot-Descombes, S., Warda, T., Wicinski, B., Dickstein, D. L., et al. (2017). Autism spectrum disorder: neuropathology and animal models. *Acta Neuropathol.* 134, 537–566.

Ventura, R., Pascucci, T., Catania, M. V., Musumeci, S. A., and Puglisi-Allegra, S. (2004). Object recognition impairment in Fmr1 knockout mice is reversed by amphetamine: involvement of dopamine in the medial prefrontal cortex. *Behav. Pharmacol.* 15, 433–442. doi: 10.1097/00008877-200409000-00018

Verma, D., Chakraborti, B., Karmakar, A., Bandyopadhyay, T., Singh, A. S., Sinha, S., et al. (2014). Sexual dimorphic effect in the genetic association of monoamine oxidase A (MAOA) markers with autism spectrum disorder. *Prog. Neuropsychopharmacol. Biol. Psychiatry* 50, 11–20. doi: 10.1016/j.pnpbp.2013.11.010

Vu, T. H., and Hoffman, A. R. (1997). Imprinting of the Angelman syndrome gene, UBE3A, is restricted to brain. *Nat. Genet.* 17, 12–13. doi: 10.1038/ng0997-12

Wang, H., Kim, S. S., and Zhuo, M. (2010). Roles of Fragile X Mental Retardation Protein in Dopaminergic Stimulation-induced Synapse-associated Protein Synthesis and Subsequent α-Amino-3-hydroxyl-5-methyl-4-isoxazole-4-propionate (AMPA) Receptor Internalization. *J. Biol. Chem.* 285, 21888–21901. doi: 10.1074/jbc.m110.116293

Wang, H., Wu, L.-J., Kim, S. S., Lee, F. J. S., Gong, B., Toyoda, H., et al. (2008). FMRP Acts as a Key Messenger for Dopamine Modulation in the Forebrain. *Neuron* 59, 634–647. doi: 10.1016/j.neuron.2008.06.027

Wang, T., Guo, H., Xiong, B., Stessman, H. A., Wu, H., Coe, B. P., et al. (2016). *De novo* genic mutations among a Chinese autism spectrum disorder cohort. *Nat. Commun.* 7:13316.

Wassink, T. H., Hazlett, H. C., Davis, L. K., Reiss, A. L., and Piven, J. (2014). Testing for association of the monoamine oxidase A promoter polymorphism with brain structure volumes in both autism and the fragile X syndrome. *J. Neurodevelop. Disord.* 6:6.

Watabe-Uchida, M., Eshel, N., and Uchida, N. (2017). Neural Circuitry of Reward Prediction Error. *Annu. Rev. Neurosci.* 40, 373–394. doi: 10.1146/annurev-neuro-072116-031109

Wen, Z., Cheng, T.-L., Li, G.-Z., Sun, S.-B., Yu, S.-Y., Zhang, Y., et al. (2017). Identification of autism-related MECP2 mutations by whole-exome sequencing and functional validation. *Mol. Autism* 8:43.

Wenk, G. (2007). Alterations in Dopaminergic Function in Rett Syndrome. *Neuropediatrics* 26, 123–125. doi: 10.1055/s-2007-979741

Yoo, H. J., Cho, I. H., Park, M., Yang, S. Y., and Kim, S. A. (2013). Association of the catechol-o-methyltransferase gene polymorphisms with Korean autism spectrum disorders. *J. Korean Med. Sci.* 28, 1403–1406. doi: 10.3346/jkms.2013.28.9.1403

Yoo, H. J., Lee, S. K., Park, M., Cho, I. H., Hyun, S. H., Lee, J. C., et al. (2009). Family- and population-based association studies of monoamine oxidase A and autism spectrum disorders in Korean. *Neurosci. Res.* 63, 172–176. doi: 10.1016/j.neures.2008.11.007

Zalla, T., and Sperduti, M. (2013). The amygdala and the relevance detection theory of autism: an evolutionary perspective. *Front. Hum. Neurosci.* 7:894. doi: 10.3389/fnhum.2013.00894

Zhang, Y., Granholm, A. C., Huh, K., Shan, L., Diaz-Ruiz, O., Malik, N., et al. (2012). PTEN deletion enhances survival, neurite outgrowth and function of dopamine neuron grafts to MitoPark mice. *Brain* 135, 2736–2749. doi: 10.1093/brain/aws196

Zhou, J., and Parada, L. F. (2012). PTEN signaling in autism spectrum disorders. *Curr. Opin. Neurobiol.* 22, 873–879. doi: 10.1016/j.conb.2012.05.004

Zorio, D. A., Jackson, C. M., Liu, Y., Rubel, E. W., and Wang, Y. (2017). Cellular distribution of the fragile X mental retardation protein in the mouse brain. *J. Comp. Neurol.* 525, 818–849. doi: 10.1002/cne.24100

Zürcher, N. R., Walsh, E. C., Phillips, R. D., Cernasov, P. M., Tseng, C.-E. J., Dharanikota, A., et al. (2020). A Simultaneous [11C]Raclopride Positron Emission Tomography and Functional Magnetic Resonance Imaging Investigation of Striatal Dopamine Binding in Autism. *medRxiv*. [Preprint].

Conflict of Interest: The authors declare that the research was conducted in the absence of any commercial or financial relationships that could be construed as a potential conflict of interest.

Publisher's Note: All claims expressed in this article are solely those of the authors and do not necessarily represent those of their affiliated organizations, or those of the publisher, the editors and the reviewers. Any product that may be evaluated in this article, or claim that may be made by its manufacturer, is not guaranteed or endorsed by the publisher.

Copyright © 2021 Kosillo and Bateup. This is an open-access article distributed under the terms of the Creative Commons Attribution License (CC BY). The use, distribution or reproduction in other forums is permitted, provided the original author(s) and the copyright owner(s) are credited and that the original publication in this journal is cited, in accordance with accepted academic practice. No use, distribution or reproduction is permitted which does not comply with these terms.

frontiers in Neural Circuits

REVIEW
published: 08 September 2021
doi: 10.3389/fncir.2021.735625

Mesocorticolimbic Dopamine Pathways Across Adolescence: Diversity in Development

Lauren M. Reynolds[1,2]* *and Cecilia Flores*[3]*

[1]Plasticité du Cerveau CNRS UMR8249, École supérieure de physique et de chimie industrielles de la Ville de Paris (ESPCI Paris), Paris, France, [2]Neuroscience Paris Seine CNRS UMR 8246 INSERM U1130, Institut de Biologie Paris Seine, Sorbonne Université, Paris, France, [3]Department of Psychiatry and Department of Neurology and Neurosurgery, McGill University, Douglas Mental Health University Institute, Montréal, QC, Canada

Mesocorticolimbic dopamine circuity undergoes a protracted maturation during adolescent life. Stable adult levels of behavioral functioning in reward, motivational, and cognitive domains are established as these pathways are refined, however, their extended developmental window also leaves them vulnerable to perturbation by environmental factors. In this review, we highlight recent advances in understanding the mechanisms underlying dopamine pathway development in the adolescent brain, and how the environment influences these processes to establish or disrupt neurocircuit diversity. We further integrate these recent studies into the larger historical framework of anatomical and neurochemical changes occurring during adolescence in the mesocorticolimbic dopamine system. While dopamine neuron heterogeneity is increasingly appreciated at molecular, physiological, and anatomical levels, we suggest that a developmental facet may play a key role in establishing vulnerability or resilience to environmental stimuli and experience in distinct dopamine circuits, shifting the balance between healthy brain development and susceptibility to psychiatric disease.

Keywords: dopamine, adolescence, development, mesocorticolimbic dopamine system, microglia, guidance cues, miRNA, puberty

OPEN ACCESS

Edited by:
Mark Howe,
Boston University, United States

Reviewed by:
Anthony A. Grace,
University of Pittsburgh, United States
Bita Moghaddam,
University of Pittsburgh, United States

***Correspondence:**
Lauren M. Reynolds
lauren.reynolds@espci.fr
Cecilia Flores
cecilia.flores@mcgill.ca

Received: *02 July 2021*
Accepted: *17 August 2021*
Published: *08 September 2021*

Citation:
Reynolds LM and Flores C (2021) Mesocorticolimbic Dopamine Pathways Across Adolescence: Diversity in Development. Front. Neural Circuits 15:735625. doi: 10.3389/fncir.2021.735625

INTRODUCTION

Dopamine (DA) neurotransmission contributes to a multitude of behaviors, including motor control, reward learning, cognitive control, decision making, motivation, and salience attribution (Wise, 2004; Schultz, 2007; Bromberg-Martin et al., 2010; Cools and D'Esposito, 2011; Orsini et al., 2015; Coddington and Dudman, 2019). The ability of this modulatory neurotransmitter system to simultaneously direct different types of behavior may result from the heterogeneity of DA neurons originating in ventral midbrain nuclei and projecting to limbic or cortical regions. Limbic and cortical DA pathways have been shown to differ in their molecular markers, anatomical organization, and response to stimuli (Roeper, 2013; Lammel et al., 2014; Morales and Margolis, 2017; Poulin et al., 2018; Nguyen et al., 2021). However, less emphasis has been placed on the distinct developmental trajectories of dopamine projections. Mesocorticolimbic DA pathways continue to develop across postnatal life, throughout what is considered adolescence and, often, into early adulthood. Incorporating this knowledge in our understanding of DA diversity is

particularly important since the DA system is increasingly considered as a "plasticity system," whose development can be shaped by positive or negative experiences, allowing organisms to adapt to their surrounding environmental conditions (Barth et al., 2019; Reynolds and Flores, 2021).

Adolescence is a time when organisms undergo dramatic physical, hormonal, and behavioral changes as they transition from juveniles to adults. While in humans this period has been historically framed as ranging from 12–20 years of age, the boundaries of adolescence are increasingly recognized as difficult to define precisely, with modern definitions extending between 10 and 24 years of age (**Figure 1A**; Hollenstein and Lougheed, 2013; Sawyer et al., 2018). The brain undergoes exuberant development during this time, with cortical gray matter thickness, notably in the prefrontal cortex (PFC), decreasing before stabilizing at adult levels, and with white matter volume increasing until early adulthood (Blakemore, 2012; Paquola et al., 2019). These macroscale changes likely result from cellular, molecular, and connectivity neuroadaptations in adolescence, as postmortem studies show dramatic age-dependent changes in myelination, neuronal structure, and synapse density during this time (Petanjek et al., 2011; Miller et al., 2012; Catts et al., 2013).

A particular interest in the postnatal development of DAergic systems has emerged because of evidence showing that performance in DA-dependent cognitive tasks improves gradually across adolescence (Wahlstrom et al., 2010; Luciana et al., 2012; Galvan, 2017; Larsen and Luna, 2018). However, direct evidence of cellular and molecular maturational changes in the human DA system across adolescence remains scarce, and it is limited to post-mortem studies which suggest that DA signaling remains dynamic across postnatal life (Weickert et al., 2007; Rothmond et al., 2012). Studies in adult volunteers can estimate DA release in subcortical regions by measuring the binding of radioactive ligands to DA receptors using positron emission tomography (PET). However, because of its radioactive nature, PET is contraindicated for imaging in minors without medical necessity (Ernst and Luciana, 2015). To overcome this impasse, recent studies have introduced tissue iron concentration as a proxy measure for DA concentration, as it is easily distinguishable using non-invasive functional magnetic resonance imaging (fMRI), can be extracted from existing fMRI datasets (Peterson et al., 2019), and is correlated with radioligand binding for the vesicular monoamine transporter (VMAT2) in adult subjects (Larsen et al., 2020). Tissue iron levels in the human striatum increase throughout adolescence, before stabilizing in adulthood (Larsen and Luna, 2014; Larsen et al., 2020), and are associated with the ongoing maturation of DA-dependent behaviors (Parr et al., 2021). While changes in tissue iron levels have not yet been assessed in the developing PFC, these results suggest that striatal DA regions are undergoing dynamic maturation in adolescence, mirroring previous findings from preclinical studies.

Most of our knowledge about adolescent mesocorticolimbic DA development comes from preclinical research, and from rodent studies in particular. One practical advantage of using rodents in developmental research is their compressed lifespan since they are born after about 3 weeks of gestation and reach adulthood at 2 months of age. When considering the age range of adolescence in rodents, it is important to keep in mind that while puberty and adolescence necessarily coincide temporally, these terms are not interchangeable (Spear, 2000; Schneider, 2013). Puberty can be clearly defined by the onset of sexual maturity, while adolescence is a more diffuse period representing the gradual transition from a juvenile state to independence. While studies in rodents consider a range of PND 28–42 to be *peri-pubertal* in male animals, *adolescence* is instead suggested to extend from the age of weaning (PND 21) until adulthood (PND 60; Spear, 2000; Tirelli et al., 2003; Burke and Miczek, 2013; Schneider, 2013; **Figure 1B**). This timeline encompasses the entire post-weaning period when rodents exhibit distinct neurobiological and behavioral changes and are navigating their environment independently for the first time. This demarcation is more aligned with the modern, extended definition of human adolescence (Sawyer et al., 2018).

In this review, we provide an overview of preclinical findings regarding the adolescent development of mesocorticolimbic DA pathways, by both situating it within a historical context and by emphasizing novel advances in understanding its cellular and molecular underpinnings. While the majority of preclinical work on DA development has been performed exclusively in males, we highlight throughout the review studies that include both males and female subjects, since sex differences have been noted in adult DA circuitry architecture and function. We outline proposed mechanisms by which adolescent experiences interact with developmental programming to shape adult mesocorticolimbic DA connectivity and function. Finally, we identify important gaps in our knowledge which present promising avenues for future research.

MESOCORTICOLIMBIC DOPAMINE CIRCUIT ORGANIZATION

Since its initial characterization in the 1960s, the anatomical organization of the rodent DA circuitry has been comprehensively described and reviewed on several occasions (a non-exhaustive list of reviews: Björklund and Lindvall, 1984; Björklund and Dunnett, 2007; Sesack and Grace, 2010; Yetnikoff et al., 2014a; Morales and Margolis, 2017). This review focuses specifically on the mesocorticolimbic DA circuitry, which consists of cell bodies located in the ventral tegmental area (VTA) that send ascending fibers rostrally toward limbic and cortical regions through the tightly fasciculated medial forebrain bundle (**Figure 2A**; Nieuwenhuys et al., 1982). At the level of the nucleus accumbens (NAc) these fibers diverge to reach their terminal target, with the densest innervation comprising mesolimbic DA axons that remain in the NAc or that extend to more dorsal regions of the striatum (STR). Mesocortical DA fibers course along the medial forebrain bundle with mesolimbic DA axons, but split off toward the PFC by either passing through the NAc, STR, and external capsule; or by extending ventrally to bypass the NAc before curving dorsally, just caudal to the olfactory bulb (**Figure 2B**; Kalsbeek et al., 1988, 1992; Voorn et al., 1988; Kolk et al., 2009; Manitt et al., 2011; Brignani and Pasterkamp, 2017). Interestingly, despite the close proximity

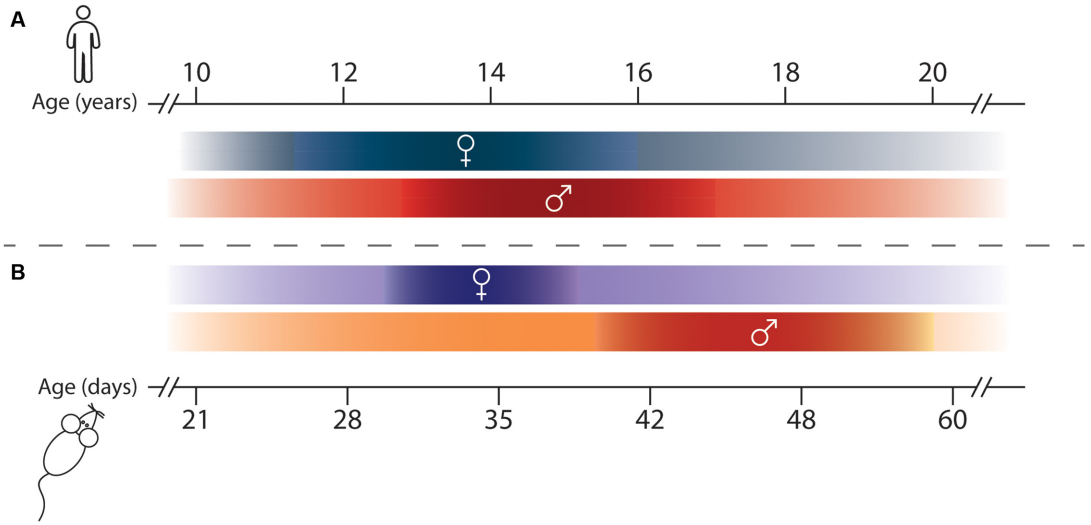

FIGURE 1 | Adolescence and Puberty timing in humans and rodents. **(A)** Timeline of adolescence (shaded lines) and puberty (darker portions of the lines) in girls (♀) and boys (♂), adapted from Hollenstein and Lougheed (2013), Sawyer et al. (2018), and Brix et al. (2019). **(B)** Adolescence (shaded lines) and puberty (darker portions of the lines) timing in female (♀) and male (♂) rodents, adapted from Vetter-O'Hagen and Spear (2012) and Schneider (2013).

of mesolimbic and mesocortical DA axons throughout their trajectory to forebrain regions, there is little or no overlap in the targets they innervate. Unlike other neuromodulatory systems, VTA DA neurons rarely send axon collaterals between different forebrain regions (Fallon, 1981; Fallon and Loughlin, 1982; Swanson, 1982; Lammel et al., 2008; Beier et al., 2015; Reynolds et al., 2018). Since mesocortical DA axons pass through the striatum *en route* to the PFC, the lack of mesocorticolimbic DA collaterals suggests that the striatum functions as a "choice point" (Stoeckli and Landmesser, 1998), where DA axons segregate into their cortical and limbic projections.

While these pathways begin to be established in embryonic or early postnatal development (see Riddle and Pollock, 2003; Prakash and Wurst, 2006; Heuvel and Pasterkamp, 2008; Money and Stanwood, 2013; Brignani and Pasterkamp, 2017 for detailed reviews), significant alterations in mesocorticolimbic DA wiring are increasingly observed in late postnatal development.

GROWTH AND ORGANIZATION OF THE MESOCORTICAL DOPAMINE PATHWAY IN ADOLESCENCE

Reports that the density of mesocortical DA innervation continues to increase during adolescence were first published in the 1980s, shortly after the introduction of antibodies against tyrosine hydroxylase (TH, the rate-limiting enzyme of dopamine synthesis), which allowed clear detection of DA axons in the PFC (Verney et al., 1982). The earliest studies used light microscopy and TH immunofluorescence to show that DA axons in the supragenual anterior cingulate and prelimbic cortices of rats already show their typical thin morphology with irregularly spaced varicosities by early-to-mid adolescence. The density of

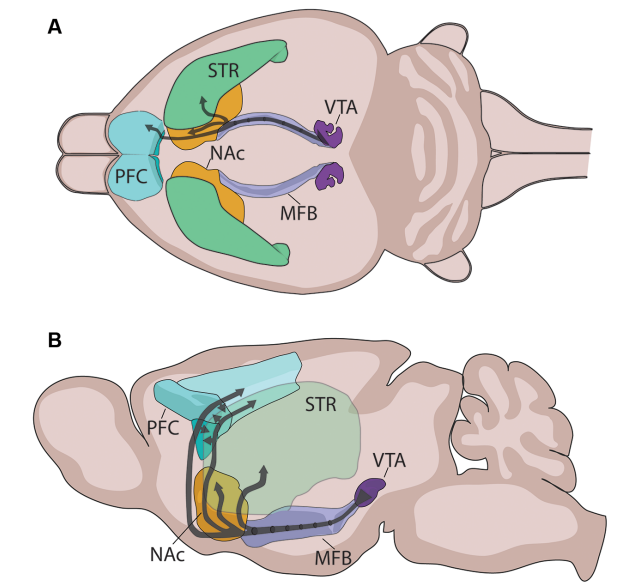

FIGURE 2 | Mesocorticolimbic dopamine system organization. **(A)** Two-dimensional rendering of the mesocorticolimbic DA pathway (black) and the major nuclei of interest in the horizontal plane. **(B)** Sagittal view of the mesocorticolimbic DA pathway (black) and the major nuclei, with the STR semi-transparent in the foreground. Two-dimensional representations were adapted from the three-dimensional regions of interest in the Allen brain atlas (Wang et al., 2020). PFC, prefrontal cortex; NAc, nucleus accumbens; STR, dorsal striatum; MFB, medial forebrain bundle; VTA, ventral tegmental area.

DA fibers in these regions, however, continues to increase until PND 60 (Berger et al., 1985; Kalsbeek et al., 1988), with no further changes between PND 60 and PND 90 (**Figure 3A**). This adolescent increase in PFC DA innervation density remains a

robust finding, as these initial qualitative descriptions have since been replicated (Benes et al., 1996) and extended by quantitative analysis in the PFC of rats and mice by several research teams (Manitt et al., 2011; Naneix et al., 2012; Willing et al., 2017; Hoops et al., 2018). Although the large majority of studies on mesocortical DA development have been performed only in male rodents, female rats have been shown to exhibit a similar pattern of innervation across postnatal ages (Willing et al., 2017).

The extended postnatal increase in PFC DA fiber density contrasts to other neuromodulatory systems, such as norepinephrine (NE) and serotonin, which reach adult PFC innervation density levels in rodents within the first 2–3 weeks of life (Levitt and Moore, 1979; Lidov et al., 1980). Distinguishing PFC DA axons from NE axons using immunolabeling for TH, which is required for the synthesis of both catecholamines, is often cited as a methodological concern for anatomical studies. Despite the fact that TH is also present in NE neurons, visually distinguishing DA and NE axons in the PFC is feasible. NE axons are thick, with regularly spaced rounded varicosities; while DA axons are thin and sinuous, with irregularly spaced varicosities (Berger et al., 1974; Miner et al., 2003). The two axonal populations differ further in their distribution, with DA fibers densely concentrated in the inner layers of the pregrenual and supragenual medial PFC, while NE fibers are spread across all layers (Berger et al., 1976; Levitt and Moore, 1979; Miner et al., 2003). Immunostaining for TH in the PFC labels PFC DA axons nearly exclusively because it only rarely overlaps with NE-specific markers, such as dopamine-β-hydroxylase (DBH) or the NE transporter (Pickel et al., 1975; Berger et al., 1983; Miner et al., 2003; Naneix et al., 2012). When compared directly within the same study, DA fiber density in the cingulate, prelimbic, and infralimbic subregions of the pregenual medial PFC has been shown to increase up to three-fold across adolescence, whereas DBH-stained NE fiber density remains stable across this time (Naneix et al., 2012). The seminal work of Rosenberg and Lewis shows that the same pattern of adolescent increase in PFC DA innervation is found in non-human primates, suggesting that this pattern is indeed conserved across mammalian species (Rosenberg and Lewis, 1994, 1995; Lewis, 1997).

For many years this increase in PFC DA fiber density across adolescence was thought to represent the progressive increase in the sprouting of new branches from DA axons already innervating the PFC early in life, as long-range axon growth was assumed to be complete before adolescence. However, studies using anterograde or retrograde labeling have challenged this notion by suggesting that axons are still growing during postnatal development to connect from PFC to the amygdala (Arruda-Carvalho et al., 2017), or from the forebrain to the VTA (Yetnikoff et al., 2014c). By harnessing an intersectional viral labeling technique (**Figure 4**), we were able to restrict fluorescent labeling only to DA neurons with axons present in the NAc at PND 21. When the mice reached adulthood, we found that a subset of these DA axons in fact grew through the NAc to reach the medial or orbital PFC during adolescence (**Figure 4A**; Hoops et al., 2018; Reynolds et al., 2018). When we performed these same intersectional viral injections in adult mice, we observed very few, if any, labeled DA axons in the PFC (**Figure 4B**), in line with the lack of collaterals observed in previous studies (Fallon, 1981; Fallon and Loughlin, 1982; Lammel et al., 2008; Beier et al., 2015). This discovery is the first proof of long-range growth of axons in adolescence and explains why the mesocorticolimbic DA system is particularly vulnerable to adolescent experiences.

The size of DAergic varicosities in the PFC increases from ∼1.2 μm at PND 20 to ∼2.4 μm by PND 60 (Benes et al., 1996), and PFC DA concentration increases significantly during this time (Nomura et al., 1976; Leslie et al., 1991; Naneix et al., 2012). Varicosities are sites of DA synthesis, release, and re-uptake, and in the PFC at least 93% of them form functional synaptic contacts with local neurons (Séguéla et al., 1988). DA axons form synapses onto PFC glutamatergic pyramidal neurons; which represent the primary projection neurons from the PFC to other regions of the brain (Goldman-Rakic and Brown, 1982; Goldman-Rakic et al., 1992; Krimer et al., 1997; Carr et al., 1999; Carr and Sesack, 2000; Lambe et al., 2000), a phenomenon that is conserved in humans, non-human primates, and rodents. GABAergic interneurons, and in particular those that express parvalbumin (e.g., fast-spiking interneurons), also receive inputs from DA axons and express high levels of DA receptors (Verney et al., 1990; Benes et al., 1993, 2000; Sesack et al., 1995, 1998; Le Moine and Gaspar, 1998; Seamans and Yang, 2004; Glausier et al., 2009; Tritsch and Sabatini, 2012). Both DAergic synapses onto PFC pyramidal neurons and GABAergic interneurons have been reported to increase during adolescence. A study in rats shows that the number of DA appositions onto PFC GABAergic interneurons increases in adolescence (Benes et al., 1996). A study in non-human primates shows that the number of DAergic, but not serotonergic, appositions onto pyramidal neurons proliferates during adolescence, however, no changes in the number of DA oppositions onto GABA neurons were detected in this study (Lambe et al., 2000). These results suggest that the release of DA in the PFC evolves during adolescence in parallel to the establishment of mature pre-synaptic connectivity. Indeed, disruption of PFC DA innervation in adolescence results in altered dendritic arborization and dendritic spine density of layer V pyramidal neurons, indicating that PFC DA development in adolescence drives the structural maturation of local PFC circuits (Manitt et al., 2011, 2013; Reynolds et al., 2018).

POSTSYNAPTIC CHANGES ACROSS ADOLESCENCE IN THE MESOCORTICAL DOPAMINE SYSTEM

Both pyramidal and GABAergic interneurons in the PFC express DA receptors of the D1 (D1 and D5) and D2 (D2, D3, D4) families (Gaspar et al., 1995; Vincent et al., 1995; Knable and Weinberger, 1997; Lu et al., 1997; Davidoff and Benes, 1998; Le Moine and Gaspar, 1998; Mitrano et al., 2014). DA receptors are seven transmembrane G-protein coupled receptors that initiate intracellular cascades by increasing cAMP (D1-type) or decreasing cAMP (D2-type; Seamans and Yang, 2004; Tritsch and Sabatini, 2012). DA receptors are localized to apical and basilar dendritic arbors of pyramidal neurons and to dendrites

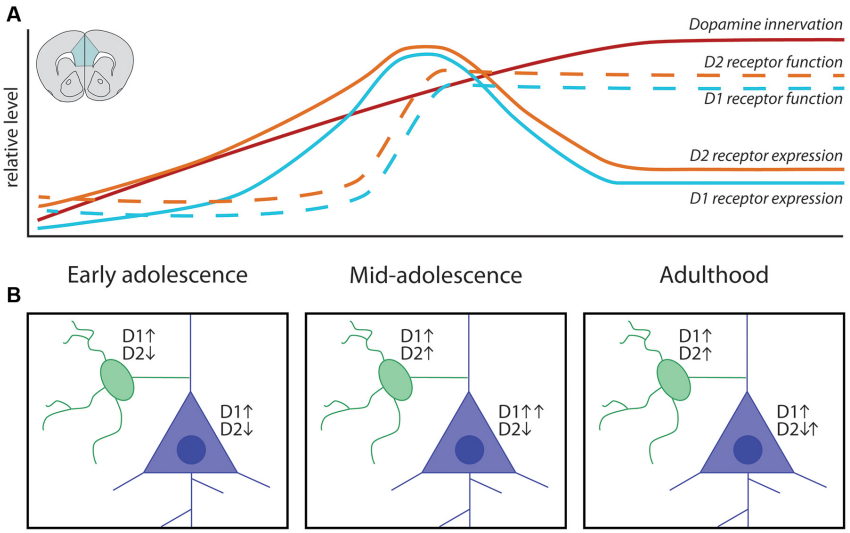

FIGURE 3 | Adolescent maturation of dopamine connectivity and function in the prefrontal cortex. **(A)** Summary of maturational changes in DA connectivity in the PFC across adolescence. **(B)** Early in adolescence DA signaling through D1 receptors is excitatory onto both classes of neurons, with DA signaling through D2 receptors inhibiting pyramidal neurons and weakly inhibiting GABAergic interneurons. In mid-adolescence DA signaling through D2 receptors becomes excitatory onto GABAergic interneurons. DA signaling through D1 receptors is now able to interact with glutamatergic NMDA receptors on pyramidal neurons, increasing the activating effect of DA. In adulthood D1 and D2 receptor populations attain their mature function.

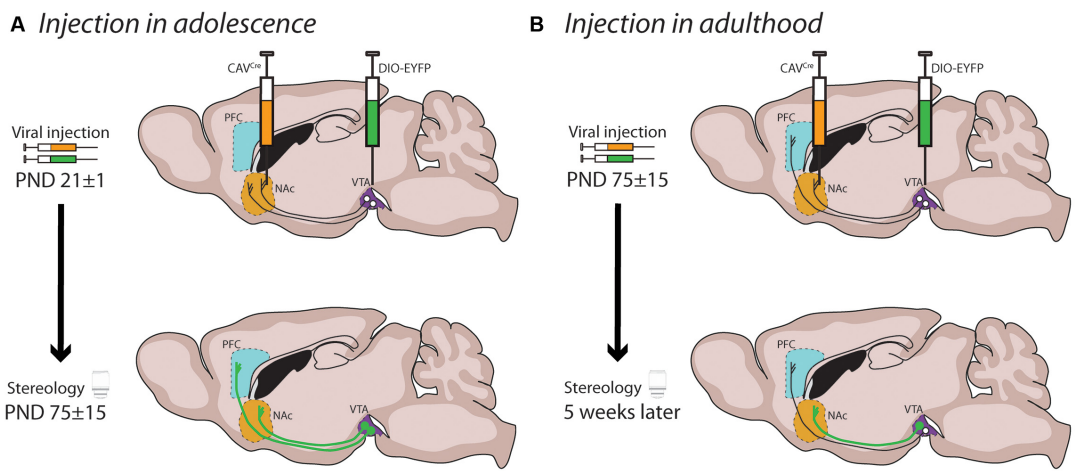

FIGURE 4 | Mesocortical axon growth in adolescence revealed by an intersectional viral labeling technique. **(A)** Spatiotemporally specific labeling of DA neurons with axons present in the NAc at PND21 reveals that DA axons continue to grow to the PFC in adolescence. **(B)** Labeled DA axons are not found in the PFC of mice when subjected to the same manipulation in adulthood, supporting previous findings that DA neurons do not commonly send collaterals between these regions.

and cell bodies of GABAergic interneurons that synapse onto pyramidal neurons. Signaling through PFC postsynaptic DA receptors thus directly and indirectly modulates PFC output (Gulledge and Jaffe, 2001; Seamans et al., 2001; Dong and White, 2003; Trantham-Davidson et al., 2004; Santana et al., 2009; Tritsch and Sabatini, 2012) and calibrates the balance of excitation/inhibition in the PFC, which also matures in adolescence (O'Donnell, 2011).

While the density of DA fibers in the PFC shows a linear increase across adolescence, the trajectory of postsynaptic DA receptor expression is more complex (**Figure 3A**). Autoradiography studies in rats using radio-labeled DA receptor ligands ([^{3}H]SCH-23390 for D1-like receptors, [^{3}H]nemonapride (YM-09151–2) or [^{3}H]-raclopride for D2-like receptors) show discrepant results regarding the patterns of receptor expression across postnatal life. While some studies indicate a steady increase in PFC D1-like receptor density until PND 60 in rats (Tarazi et al., 1999; Tarazi and Baldessarini, 2000), others show that D1-like expression in the PFC peaks in adolescence, before being pruned back in adulthood (Leslie

et al., 1991; Andersen et al., 2000; Brenhouse et al., 2008). These seemingly disparate findings may be reconciled by results from immunohistochemical tracing experiments showing that the adolescent peak in D1 receptor expression observed in adolescence occurs only in corticolimbic pyramidal projection neurons (Brenhouse et al., 2008; Brenhouse and Andersen, 2011), a level of nuance which may be difficult to capture with radioligand binding assays. Another consideration is that different subtypes of DA receptors may not follow the same developmental pattern of expression, but most radioligands do not differentiate between different receptors of the same family [e.g., [^{3}H]SCH-23390 will bind both D1 and D5 DA receptors, which are expressed in the rodent PFC (Lidow et al., 2003)]. Recent results from quantitative real-time PCR (qPCR) studies in rats bolster the idea that PFC D1 and D5 receptor subtypes show a peak in mRNA levels during adolescence (Naneix et al., 2012; Zbukvic et al., 2017).

Regarding D2-like receptors, early radioligand studies in rats also indicate that their expression in the PFC increases steadily in adolescence (Tarazi et al., 1998; Tarazi and Baldessarini, 2000), but later findings show peak expression in adolescence (Andersen et al., 2000; Brenhouse and Andersen, 2011). This inconsistency may also stem from the non-specific nature of radioligand binding, as Naneix et al. (2012) show an adolescent peak in mRNA expression for the long isoform of the D2 receptor and the D4 receptor, but not for the short isoform of the D2 receptor, in the PFC using qPCR. Another consideration when assessing apparent discrepancies in the literature is that radioligand binding assays indirectly determine receptor protein levels and/or functional capacity, whereas qPCR determines mRNA expression. Overall, evidence from studies in rats indicates that DA receptor expression in the PFC is dynamic in adolescence, most likely with a period of overexpression followed by pruning (**Figure 3A**). However, this adolescent peak is less apparent at least in C57BL6 mice, according to an autoradiography study (Pokinko et al., 2017), suggesting differences across species. It should be noted that the aforementioned receptor expression studies were performed exclusively in male rodents and whether sex differences exist in the trajectory of PFC DA receptor expression remains an open question.

In addition to the dynamic changes in DA receptor expression, postsynaptic responses to extracellular DA have also been shown to evolve in PFC pyramidal and GABAergic neurons during adolescence (**Figure 3B**; O'Donnell, 2010, 2011). Slice electrophysiology experiments have shown that both pyramidal and GABAergic PFC neurons respond to DA application (Seamans and Yang, 2004). Studies in adult rats show that DA signaling through D1 receptors in PFC pyramidal neurons interacts with glutamatergic NMDA receptor signaling, producing activity levels that resemble those observed *in vivo* during information processing. Notably, this process is absent before mid-adolescence (Tseng and O'Donnell, 2005), emerging only around PND 45, when D1 mRNA expression peaks in the rat PFC (Tseng and O'Donnell, 2005; Naneix et al., 2012). In fact, before PND 36, DA signaling through D1 receptors in GABAergic interneurons potentiates their firing, but signaling through D2 receptors has either a weak *inhibitory* effect or no effect (Gorelova et al., 2002; Tseng and O'Donnell, 2007). However, after adolescence an *excitatory* effect of D2 receptor stimulation emerges in PFC GABAergic interneurons, creating the inhibitory tone characteristic of the mature PFC and balancing the enhanced DA-driven excitation of pyramidal neurons (Tseng and O'Donnell, 2007; O'Donnell, 2011). The adolescent shift of DAergic regulation over excitatory and inhibitory transmission in the PFC is thought to be a critical step in the developmental calibration of cognitive control (Klune et al., 2021), and to be dysregulated in psychiatric disorders of adolescent onset (O'Donnell, 2011; Caballero et al., 2016; Caballero et al., 2021).

COMING OF AGE IN THE STRIATUM: MESOCORTICOLIMBIC DOPAMINE PATHWAY SEGREGATION AND FUNCTIONAL MATURATION

As our understanding of mesocorticolimbic DA system development progresses, it is clear that both mesolimbic and mesocortical pathways are still developing throughout the adolescent period. DA signaling in the striatum continues to mature across adolescence: both TH protein and DA content increase until adulthood (Pardo et al., 1977; Giorgi et al., 1987; Broaddus and Bennett, 1990; Rao et al., 1991; Naneix et al., 2012; Matthews et al., 2013; Lieberman et al., 2018), and are essential for the construction of postsynaptic circuits. Medium spiny neurons (MSNs) in the NAc and STR achieve their namesake spiny appearance during early adolescence, with marked increases in dendritic spine density occurring between PND 15 and 30 (Tepper and Trent, 1993; Tepper et al., 1998). The proportion of MSNs showing their characteristic DA-sensitive inward rectification potassium currents also continues to increase until early adulthood (Tepper et al., 1998; Zhao et al., 2016), and the effect of D2 receptor signaling of MSNs switches from inhibitory to facilitatory (Benoit-Marand and O'Donnell, 2008). During this same timeline, NAc DA varicosities shift their synaptic contacts from the soma of MSNs to their dendritic spines (Antonopoulos et al., 2002), and the intrinsic excitability of MSN changes from a juvenile hyper-excitable state to a reduced, mature level of responsivity. This process is triggered by the gradual increase in striatal DA concentration (Lieberman et al., 2018).

In contrast to the PFC, the changes in DA function in the striatum are not associated with changes in the density of DA innervation (**Figure 5**), as STR and NAc DA input achieves its adult density by PND 20 in rodents (Voorn et al., 1988; Kalsbeek et al., 1992), and the optical density of TH-positive DA fibers does not change during adolescence in these regions (Naneix et al., 2012). Nevertheless, these results should be interpreted with care, considering that the DA innervation to the STR and NAc is up to 40-fold denser than in the PFC. It is possible that the margin of error, even using precise stereological methods, masks potential anatomical differences between ages (Bérubé-Carrière et al., 2012; Manitt et al., 2013; Reynolds et al., 2015).

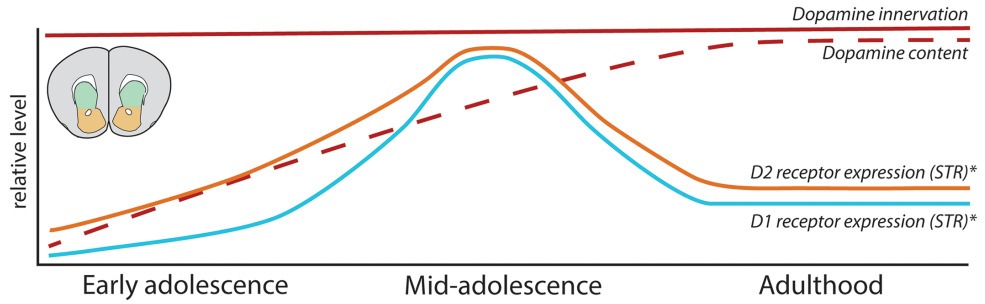

FIGURE 5 | Development of mesolimbic dopamine connectivity and function in the adolescent striatum. Summary of maturational changes in DA connectivity in the STR across adolescence. *Indicates that these findings are sex-dependent, with this pattern of receptor overexpression and pruning only seen in male rodents.

Our developmental studies using intersectional viral tracing techniques indeed demonstrate that the fine organization of mesolimbic DA connectivity is much more malleable than previously thought. The striatum represents a major choice point for DA axons: while the large majority of DA axons already innervating the striatum by early adolescence are destined to remain there, mesocortical axons must pass through this densely innervated DA region and continue to grow into the PFC during adolescence (Reynolds et al., 2018). Notably, the level of DA innervation in these two pathways is inversely correlated: the more DA axons that keep growing to the PFC in adolescence, the fewer that remain behind and form connections in the NAc. Mesolimbic DA axon targeting is not a passive process [i.e., they are actively undergoing target recognition processes within the NAc in adolescence (Reynolds et al., 2018; Cuesta et al., 2020)], and it profoundly influences the structural organization of postsynaptic MSN neurons.

DEVELOPMENTAL PATTERNS OF DOPAMINE RECEPTORS IN THE ADOLESCENT STRIATUM

In contrast to the high synaptic incidence of DA varicosities in the PFC (Séguéla et al., 1988), the majority of DA varicosities in the NAc and STR (60–70%) do not form direct synaptic contacts with postsynaptic neurons (Descarries et al., 1996; Descarries and Mechawar, 2000; Bérubé-Carrière et al., 2012). Recent reports further indicate that only ∼30% of DA varicosities in the STR contain the necessary active zone sites to release DA, and that many varicosities are in fact "silent" (Pereira et al., 2016; Liu et al., 2018, 2021; Liu and Kaeser, 2019). Up to 90% of local striatal neurons are GABAergic projection neurons, usually referred to as MSNs or as spiny projection neurons (Kreitzer, 2009; Collins and Saunders, 2020), and they can be segregated into two main populations based on their projection target. In rodents, striatonigral MSNs project mainly to the substantia nigra pars reticulata and entopeduncular nucleus, while striatopallidal MSNs instead project primarily to the globus pallidus (Smith et al., 1998). While striatonigral and striatopallidal MSNs are morphologically indistinguishable at the somatic level, they can be differentiated by a number of molecular markers, notably by prominent expression of D1 receptors in striatonigral MSNs and D2 receptors in striatopallidal MSNs (Ince et al., 1997; Smith et al., 1998; Kreitzer, 2009; Bamford et al., 2018). Unlike the PFC, where ∼25% of non-pyramidal neurons co-express D1 and D2 DA receptors (Vincent et al., 1995), D1 and D2 receptor expression is almost completely segregated between these two MSN populations (Hersch et al., 1995; Ince et al., 1997; Bertran-Gonzalez et al., 2010; Frederick et al., 2015). Interestingly, D1 and D2 colocalization in MSNs is apparent in embryos and neonates, but it decreases between E18 and PND 14 (Thibault et al., 2013; Biezonski et al., 2015). It remains to be determined whether the segregation of DA receptors in striatonigral and striatopallidal MSNs is dynamic at other postanal periods, as well as the age when the segregated pattern of MSN DA receptor expression is stabilized.

Rodent studies have shown that striatal DA receptor expression changes across adolescence, although their exact maturational pattern is controversial. Early autoradiography studies using the radioligand [^{3}H]SCH-23390 to assess D1 receptor binding in Sprague–Dawley rats found that striatal D1 receptors either increase until achieving stable adult levels before or during early adolescence (Murrin and Zeng, 1990; Leslie et al., 1991; Schambra et al., 1994) or exhibit no developmental changes (Broaddus and Bennett, 1990). Instead, more recent studies using the same radioligand and rat strain show that, similarly to the PFC, DA D1-like receptors are overexpressed during adolescence before being pruned back in adulthood in the NAc and STR (Gelbard et al., 1989; Teicher et al., 1995; Andersen et al., 1997; Tarazi et al., 1999; Tarazi and Baldessarini, 2000). Similar findings using autoradiography have been reported in C57BL/6 mice (Pokinko et al., 2017).

Striatal expression of D2 receptors has also been reported to change during adolescence. Early autoradiography studies showed increased D2 receptor expression across early postnatal life, reaching adult levels by early adolescence (Pardo et al., 1977; Hartley and Seeman, 1983; Murrin and Wanyun, 1986; Rao et al., 1991; Schambra et al., 1994). This evidence seems to be consistent despite the use of different radioligands and strains of rats, with changes in expression in the NAc showing a less pronounced peak than in the STR (Teicher et al., 1995; Andersen et al., 1997; Tarazi et al., 1998), and mRNA expression of D2 receptors peaks in the adolescent STR (Naneix et al., 2012). These D2 expression changes have not been detected in mice (Pokinko et al., 2017).

While the majority of these studies have been performed only in male rodents, evidence suggests that the adolescent overexpression and pruning of D1 receptors in striatal regions is not seen in female rats (Andersen et al., 1997). Similarly, the adolescent overexpression and subsequent pruning in striatal D2 receptors observed in male rats is absent in females (Andersen et al., 1997), with no apparent sex differences in D2 receptor expression levels in adulthood. Males and females may therefore have distinct developmental trajectories for DA receptors in striatal regions, which could lead to different sensitive periods of development.

MECHANISMS UNDERLYING MESOCORTICOLIMBIC DOPAMINE CIRCUIT ORGANIZATION IN ADOLESCENCE

DA circuitry is increasingly recognized as a "plasticity system" (Barth et al., 2019; Reynolds and Flores, 2021), where the environment can alter its development and induce long-term repercussions for adult behavioral functioning. The protracted maturational timeline of mesocortical DA circuitry, therefore, results in a prolonged period of vulnerability, when experiences such as exposure to stress or drugs of abuse can disrupt its development and induce susceptibility to psychiatric disease later in life (Meaney et al., 2002; Gulley and Juraska, 2013; Jordan and Andersen, 2017; Areal and Blakely, 2020). The studies discussed in the preceding sections provide a holistic understanding of the developmental changes occurring in the mesocorticolimbic DA circuitry during adolescence but only recently have the cellular and molecular mechanisms underlying these processes begun to be unraveled. Below, we outline three main mechanisms identified to date which orchestrate adolescent mesocorticolimbic DA development and show examples of how they can be impacted by ongoing experiences.

Role of Guidance Cues in Dopamine Axon Growth and Targeting

Guidance cues are secreted proteins, either diffusible or bound to cellular membranes, that act as a signal to direct growing axons to their appropriate targets (Battum et al., 2015). Their role in early DA development has long been appreciated, with a number of guidance cues shown to be implicated in the differentiation, migration, and early axonal pathfinding of DA neurons in embryonic and early postnatal life (see Heuvel and Pasterkamp, 2008; Bodea and Blaess, 2015; Brignani and Pasterkamp, 2017 for exhaustive reviews on the role of guidance cues in early DA development). The guidance cue Netrin-1 and its receptor DCC (deleted in colorectal cancer) have emerged as critical players in establishing mesocorticolimbic DA circuitry and are highly linked to psychiatric disorders of adolescent onset (Vosberg et al., 2019; Torres-Berrío et al., 2020a). Mice with *Dcc* haploinsufficiency show marked functional changes in DA systems, including blunted behavioral responses to amphetamine, methamphetamine, and cocaine (Flores et al., 2005; Grant et al., 2007; Flores, 2011; Kim et al., 2013; Reynolds et al., 2016); and blunted stimulant-induced DA release in the NAc (Grant et al., 2007). This protective *Dcc* haploinsufficient phenotype, which is also displayed by mice haploinsufficient for *Netrin-1*, is driven by increased DA innervation and content in the PFC, and by augmented stimulant drug-induced DA release in this region (Grant et al., 2007; Pokinko et al., 2015), indicating increased mesocortical inhibitory control over striatal DA function. Notably, these DAergic changes are only apparent in adult *Dcc* haploinsufficient mice, with no observable differences in mesocorticolimbic DA structure or function in juveniles, and occur in both males and females (Grant et al., 2009).

Netrin-1 and DCC are expressed across the lifetime in mesocorticolimbic DA circuits, and their spatiotemporal distribution is pathway-specific. DA neurons express high levels of DCC receptors across species, including humans (Osborne et al., 2005; Manitt et al., 2010; Reyes et al., 2013). Netrin-1 is expressed in forebrain terminal regions of DA axons, including the NAc, STR, and PFC (Shatzmiller et al., 2008; Manitt et al., 2011). In male rodents, the expression of DCC in the VTA and of Netrin-1 in the NAc is highest during embryonic and early postnatal development, waning gradually during adolescence, and stabilizing to low levels in adulthood (Manitt et al., 2010; Cuesta et al., 2018, 2020). While all mesolimbic DA axons are rich in DCC receptor levels, DA axons in the PFC only rarely express DCC (Manitt et al., 2011). The localization of DCC receptors in PFC DA axons is increased in adult *Dcc* haploinsufficent mice, suggesting that the greater PFC DA innervation and content results from ectopic growth of DCC-expressing mesolimbic DA fibers (Manitt et al., 2011). Conditional reduction of *Dcc* in DA neurons in adolescence recapitulates completely this ectopic DCC-positive DA axon phenotype in the PFC (Manitt et al., 2013).

Using the same intersectional viral labeling technique we used to demonstrate that mesocortical DA axons continue to grow to the PFC in adolescence, we also showed that the complementary action of Netrin-1 and DCC mediates the targeting of mesolimbic DA neurons at the NAc choice point. Reduced *Dcc* expression in DA axons innervating the NAc in adolescence, results in their ectopic growth in the PFC and a concomitant reduction in NAc DA varicosities (Reynolds et al., 2018). High levels of DCC in mesolimbic DA axons are necessary for them to recognize the NAc as their final target in adolescence. This phenotype is replicated when silencing Netrin-1 in the NAc (Cuesta et al., 2020).

Experience-induced regulation of Netrin-1 and/or DCC expression robustly shapes the adolescent brain. Social defeat stress in adolescence, but not in adulthood, downregulates *Dcc* expression in the VTA of male mice, disrupts PFC DA innervation, and leads to cognitive control deficits in adulthood (Vassilev et al., 2021). Mild traumatic brain injury in mid-adolescent male mice reduces Netrin-1 expression in the NAc and alters mesocorticolimbic DA organization (Kaukas et al., 2020). Both Netrin-1 and DCC levels expression can encode the effects of experience on DA circuitry. Notably, repeated exposure to amphetamine downregulates DCC in the VTA and Netrin-1 in the NAc, in early adolescence (Yetnikoff et al.,

2007, 2011, 2014b; Cuesta et al., 2018, 2019), overlapping with the period that mesolimbic DA axons are undergoing targeting events. Drug-induced DCC downregulation requires D2 receptor signaling (Cuesta et al., 2018), reinforcing the link between DCC function and mesolimbic DA axon targeting in adolescence, as mesocortical DA neurons lack D2 receptors (Lammel et al., 2008). Exposure to recreational-like doses of amphetamine in early adolescence, but not later in life, leads to a dramatic increase in the volume of PFC DA innervation, altered DA function, and long-term impairments in cognitive control in male mice (Reynolds et al., 2015, 2019; Hoops et al., 2018; Reynolds and Flores, 2019). These effects are not observed following exposure to therapeutic-like amphetamine doses, which instead increases DCC protein expression in the VTA and leads to the overall improvement in cognitive performance in adulthood (Cuesta et al., 2019), in line with reports in non-human primates (Soto et al., 2012). Studies of how experience regulates Netrin-1/DCC expression in female mice are ongoing, but their bidirectional regulation already observed in male mice indicates that the Netrin-1/DCC system can be viewed more as a molecular target of *plasticity* rather than a target of *vulnerability*. Experiences that upregulate DCC expression in adolescence may in fact promote healthy brain development.

Pruning of Connections in Adolescence: Microglia as Sculptors of Dopamine Circuitry

Neuro-immune interactions in adolescence are increasingly recognized as critical to the refinement of neural networks, and early immune challenges are a potential risk factor for DA-dependent neuropsychiatric disorders (Brenhouse and Schwarz, 2016). Microglia, in particular, have emerged as potent regulators of maturational processes, including activity-dependent synaptic pruning (Paolicelli et al., 2011; Schafer et al., 2012), the establishment of synaptic transmission and correlated brain activity (Zhan et al., 2014), and myelination in adolescence (Hughes and Appel, 2020). The neuroimmune system is tightly linked to the development of DA circuitry. Altered microglia function has been linked to DA system impairments, for example, DA damage in Parkinson's disease patients (Ouchi et al., 2005) and D1 receptor deficiency in the PFC of adult ADHD patients (Yokokura et al., 2020). Changes in the expression of complement cascade proteins, important markers for immune-mediated phagocytosis and elimination, have been observed in schizophrenia patients (Sekar et al., 2016; Rey et al., 2020). Functional studies suggest these complement cascade alterations result in exaggerated synapse pruning in the adolescent PFC by overactive microglia (Sellgren et al., 2019) and in impaired social behavior in adulthood (Comer et al., 2020; Yilmaz et al., 2021).

Preclinical studies have further elaborated the role of microglia in normative mesocorticolimbic DA adolescent development. In the PFC, microglia transiently prune dendritic spines of the densely DA-innervated layer V PFC neurons in mid-adolescence (Mallya et al., 2018) and microglial depletion in adolescence impairs the formation and elimination of synapses onto these pyramidal neurons (Parkhurst et al., 2013). In the NAc, microglia play an important role in the elimination of DA receptors as Kopec et al. show that the peak in DA D1 receptor levels observed in the NAc around PND 30 in male rats declines afterward due to microglia pruning. In agreement with earlier autoradiography results (Andersen et al., 1997), this event occurs only in males and aligns with a peak in their social behavior. Females show an earlier peak (∼PND20) in D1 receptor levels, which is followed by a microglia-*independent* decline in expression (Kopec et al., 2018). Indeed, a growing body of work shows that microglial processes are sex-dependent (Schwarz and Bilbo, 2012; VanRyzin et al., 2018, 2020; Bordt et al., 2020).

Several studies have linked experiences in adolescence to microglial changes within the mesocorticolimbic DA circuitry. Adolescent food restriction increases the ramification of microglia in the PFC of male and female rats (Ganguly et al., 2018), while social defeat stress decreases the number of PFC microglia in male mice and induced deficits in DA-dependent cognitive behavior (Reynolds et al., 2018; Zhang et al., 2019). Drugs of abuse in adolescence have been shown to induce noticeable changes in microglia expression in the NAc: nicotine exposure increases microglia ramification in the NAc of male and female mice in a DA D2 receptor-mediated process, leading to excessive synaptic pruning and increased cocaine self-administration in adulthood (Linker et al., 2020). Adolescent morphine exposure induces long-term changes in NAc microglial function in male rats, which are associated with increased conditioned place preference reinstatement to this drug in adulthood (Schwarz and Bilbo, 2013). Traumatic brain injury in adolescent, but not adult, mice increased microglia specifically in the NAc during early adulthood (Cannella et al., 2020), with a concomitant decrease in DA receptor expression. All of these findings poise microglial-mediated processes as a critical mechanism by which adolescent experiences shape mesocorticolimbic DA development.

Puberty as a Driver of Dopamine Circuitry Development

Sex differences have been described regarding the structure and function of adult pre- and postsynaptic components of DA circuitries, including differences in structural organization, DA content, and regulation of local DA release (Becker et al., 2001, 2012; Becker, 2009; Gillies et al., 2014; Walker et al., 2017; Becker and Chartoff, 2018; Kokane and Perrotti, 2020; Zachry et al., 2020). Ovarian hormones are key regulators of some of these observed sex differences, notably DA neuron firing rates (Zhang et al., 2008; Calipari et al., 2017) and striatal DA release (Xiao and Becker, 1994; Castner et al., 2005; Calipari et al., 2017; Yoest et al., 2019). A greater number of DA neurons have been shown to project to the PFC in adult female rats in comparison to adult males, with ∼50% of retrogradely labeled VTA neurons expressing TH in females compared to only ∼30% in males (Kritzer and Creutz, 2008).

Because gonadectomy in adult animals alters PFC DA fiber distribution (Kritzer and Kohama, 1998; Kritzer, 1998, 2003; Adler et al., 1999; Kritzer et al., 1999), the pubertal spike in

sex hormones has been long posited to drive sex differences in adult PFC DA innervation. However, contrary to the maturation of other PFC neurotransmitter systems (Drzewiecki et al., 2016, 2020; Piekarski et al., 2017; Delevich et al., 2020, 2021), evidence regarding a role for puberty in the development of mesocortical DA circuitry remains elusive. DA innervation to the PFC has been shown to increase along a similar timescale throughout adolescence in both male and female rats, with no apparent effect of puberty onset in this trajectory (Willing et al., 2017). However, puberty may drive subtle changes in PFC DA synthesis and release which would still profoundly impact the developing PFC, even without discernible alterations in DA axon architecture. For example, sex differences in PFC TH expression and in PFC neuronal organization emerge after puberty in mice with genetic reduction of the catechol-*o*-methyltransferase (COMT) enzyme (Sannino et al., 2017).

In the striatum, there are sex differences in the distribution of DA receptors, with female rats generally showing approximately 10% less D1 receptor density than males, and with D1 receptor density in females varying during the estrous cycle (Lévesque and Paolo, 1989, 1990; Lévesque et al., 1989). However, peripubertal sex hormones do not seem to play a role in establishing these sex-specific DA receptor patterns (Andersen et al., 2002). Sex differences in striatal DAergic structure and function have recently been suggested to be strain-dependent, with some of the sex-specific characteristics commonly seen in Sprague-Dawley rats not observable in Long-Evans rats (Rivera-Garcia et al., 2020), highlighting the need for the consideration not only of sex but also species and strain in experimental design. More evidence is needed to determine whether the sex differences observed in adult DA circuitry result from puberty-dependent or puberty-independent developmental processes. This issue will become clearer as SABV (sex as a biological variable) is increasingly included in study designs (Shansky and Murphy, 2021).

DISCUSSION

Aberrant mesocorticolimbic DA function is a prominent characteristic of psychiatric disorders that have an adolescent onset. Identification of the mechanisms underlying the normative maturation of this system during adolescence is essential to understand the developmental origins of mental health. The structure and function of pre- and postsynaptic components of mesocorticolimbic DA circuits differ significantly across terminal regions, between sexes, and as a function of experience. These differences include structural divergence, fluctuations in DA release, and/or variation in DA-induced modulation of postsynaptic neuron signaling pathways. Adolescence is a particularly sensitive time for the establishment of these properties; the discussion of DA projection heterogeneity is thus incomplete without considering the developmental programming of these systems.

While this review mainly focuses on advances in preclinical research, it is important to note that similar protracted developmental patterns in mesocorticolimbic DA circuitries have been observed in humans. As seen in rodents, post-mortem human brain studies have shown changes in DA receptor expression and DA content during adolescence, including a peak in DA D1 receptor expression in the PFC (Weickert et al., 2007; Rothmond et al., 2012), a marked decline in striatal DA receptors (Seeman et al., 1987), and a dramatic increase in striatal DA content (Haycock et al., 2003). A PET neuroimaging study in 18–32-year-old subjects shows that the decline in striatal D2/3 receptor expression also occurs in humans (Larsen et al., 2020), indicating that findings from preclinical studies on DA system development have strong translational implications.

Here, we integrate evidence regarding mechanistic processes underlying mesocorticolimbic DA development while situating them within the historical context. We chose to highlight three mechanisms involved in DA maturation: axon guidance and targeting, microglial-dependent pruning, and puberty. By no means do we intend to imply that these are the only ongoing processes involved in mesocorticolimbic DA development. For example, macroautophagy has been suggested to play a role in the synaptic pruning occurring in the adolescent striatum (Hernandez et al., 2012; Lieberman et al., 2020). DA neurons projecting to the PFC have been shown to have different molecular properties than those projecting to the NAc (Lammel et al., 2008), suggesting that intrinsic differences may also contribute to their divergent development. Inputs to the VTA are also still developing in adolescence (Yetnikoff et al., 2014c), which may influence the maturation of DA neurons themselves. Indeed, *in vivo* electrophysiology experiments indicate that DA neuron firing rates vary across adolescence in male rats (McCutcheon and Marinelli, 2009; McCutcheon et al., 2012). We propose that all these cellular and molecular processes converge and interact, and that experience may impact DA development through any one - or multiple - pathways (**Figure 6**). Indeed, mild traumatic brain injury in adolescent rats induces sex-specific

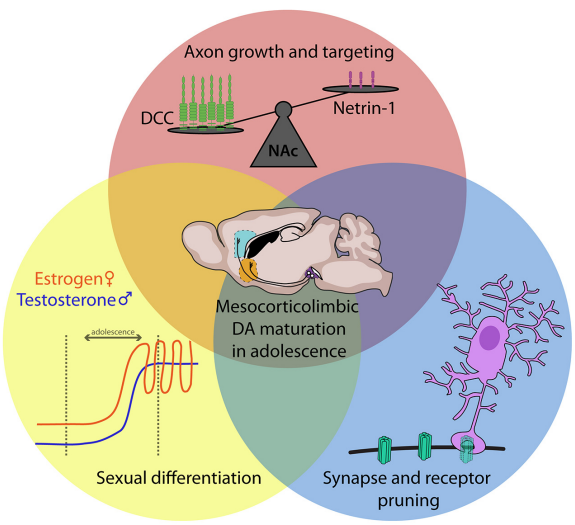

FIGURE 6 | Dopamine as a "plasticity system": convergent mechanistic processes shape adolescent mesocorticolimbic dopamine maturation in response to environmental cues. In this review, we identify three mechanistic processes that contribute to the adolescent establishment of DA pathways. We comment on how each of these processes may link experiential factors to alterations in DA development.

changes in Netrin-1 levels in the NAc (Kaukas et al., 2020), and also increases microglia-mediated pruning of DA receptors in this region (Cannella et al., 2020).

We are only at the beginning of understanding the complex interplay of genes and environmental factors that build DA circuitry in adolescence. Many interesting and important lines of inquiry remain to be addressed. The field will move forward by placing special emphasis on identifying molecular drivers of sex differences in mesocorticolimbic DA maturation and making the inclusion of male and female subjects obligatory in neurodevelopmental research. As work on these topics advances, a major focus should also be placed on unraveling epigenetic mechanisms linking adolescent experiences to changes in DA development, and on discovering non-invasive longitudinal biomarkers for evaluating the state of DA system development. This work would eventually allow for preventive and therapeutic interventions precisely targeted in time. MicroRNAs, for example, show promise to serve as such markers, as they regulate guidance cue genes in adolescence and are detectable in peripheral fluids (Torres-Berrío et al., 2020b; Morgunova and Flores, 2021). Finally, a critical question that remains open is whether and how "positive" experiences can promote healthy DA system development and improve mental health outcomes in emerging adults.

AUTHOR CONTRIBUTIONS

LMR and CF wrote the manuscript. All authors contributed to the article and approved the submitted version.

FUNDING

LMR was supported by a NIDA–Inserm Postdoctoral Drug Abuse Research Fellowship from the National Institute on Drug Abuse (NIDA, USA) and Institut national de la santé et de la recherche médicale (Inserm, France). CF was supported by the NIDA (R01DA037911) and the Canadian Institute for Health Research (MOP-74709; MOP-119543).

REFERENCES

Adler, A., Vescovo, P., Robinson, J. K., and Kritzer, M. F. (1999). Gonadectomy in adult life increases tyrosine hydroxylase immunoreactivity in the prefrontal cortex and decreases open field activity in male rats. *Neuroscience* 89, 939–954. doi: 10.1016/s0306-4522(98)00341-8

Andersen, S. L., Rutstein, M., Benzo, J. M., Hostetter, J. C., and Teicher, M. H. (1997). Sex differences in dopamine receptor overproduction and elimination. *Neuroreport* 8, 1495–1498. doi: 10.1097/00001756-199704140-00034

Andersen, S. L., Thompson, A. P., Krenzel, E., and Teicher, M. H. (2002). Pubertal changes in gonadal hormones do not underlie adolescent dopamine receptor overproduction. *Psychoneuroendocrinology* 27, 683–691. doi: 10.1016/s0306-4530(01)00069-5

Andersen, S. L., Thompson, A. T., Rutstein, M., Hostetter, J. C., and Teicher, M. H. (2000). Dopamine receptor pruning in prefrontal cortex during the periadolescent period in rats. *Synapse* 37, 167–169. doi: 10.1002/1098-2396(200008)37:2<167::AID-SYN11>3.0.CO;2-B

Antonopoulos, J., Dori, I., Dinopoulos, A., Chiotelli, M., and Parnavelas, J. G. (2002). Postnatal development of the dopaminergic system of the striatum in the rat. *Neuroscience* 110, 245–256. doi: 10.1016/s0306-4522(01)00575-9

Areal, L. B., and Blakely, R. D. (2020). Neurobehavioral changes arising from early life dopamine signaling perturbations. *Neurochem. Int.* 137:104747. doi: 10.1016/j.neuint.2020.104747

Arruda-Carvalho, M., Wu, W.-C., Cummings, K. A., and Clem, R. L. (2017). Optogenetic examination of prefrontal-amygdala synaptic development. *J. Neurosci.* 37, 2976–2985. doi: 10.1523/JNEUROSCI.3097-16.2017

Bamford, N. S., Wightman, R. M., and Sulzer, D. (2018). Dopamine's effects on corticostriatal synapses during reward-based behaviors. *Neuron* 97, 494–510. doi: 10.1016/j.neuron.2018.01.006

Barth, B., Portella, A. K., Dubé, L., Meaney, M. J., and Silveira, P. P. (2019). "The interplay between dopamine and environment as the biological basis for the early origins of mental health," in *Early Life Origins of Ageing and Longevity* (Cham: Springer), 121–140.

Battum, E. Y. V., Brignani, S., and Pasterkamp, R. J. (2015). Axon guidance proteins in neurological disorders. *Lancet Neurol.* 14, 532–546. doi: 10.1016/S1474-4422(14)70257-1

Becker, J. B. (2009). Sexual differentiation of motivation: a novel mechanism. *Horm. Behav.* 55, 646–654. doi: 10.1016/j.yhbeh.2009.03.014

Becker, J. B., and Chartoff, E. (2018). Sex differences in neural mechanisms mediating reward and addiction. *Neuropsychopharmacology* 44, 166–183. doi: 10.1038/s41386-018-0125-6

Becker, J. B., Molenda, H., and Hummer, D. L. (2001). Gender differences in the behavioral responses to cocaine and amphetamine. *Ann. N Y Acad. Sci.* 937, 172–187. doi: 10.1111/j.1749-6632.2001.tb03564.x

Becker, J. B., Perry, A. N., and Westenbroek, C. (2012). Sex differences in the neural mechanisms mediating addiction: a new synthesis and hypothesis. *Biol. Sex Differ.* 3:14. doi: 10.1186/2042-6410-3-14

Beier, K. T., Steinberg, E. E., DeLoach, K. E., Xie, S., Miyamichi, K., Schwarz, L., et al. (2015). Circuit architecture of VTA dopamine neurons revealed by systematic input-output mapping. *Cell* 162, 622–634. doi: 10.1016/j.cell.2015.07.015

Benes, F. M., Taylor, J. B., and Cunningham, M. C. (2000). Convergence and plasticity of monoaminergic systems in the medial prefrontal cortex during the postnatal period: implications for the development of psychopathology. *Cereb. Cortex* 10, 1014–1027. doi: 10.1093/cercor/10.10.1014

Benes, F. M., Vincent, S. L., and Molloy, R. (1993). Dopamnine-Immunoreactive axon varicosities form nonrandom contacts with GABA-immunoreactive neurons of rat medial prefrontal cortex. *Synapse* 15, 285–295. doi: 10.1002/syn.890150405

Benes, F. M., Vincent, S. L., Molloy, R., and Khan, Y. (1996). Increased interaction of dopamine-immunoreactive varicosities with GABA neurons of rat medial prefrontal cortex occurs during the postweanling period. *Synapse* 23, 237–245. doi: 10.1002/(SICI)1098-2396(199608)23:4<237::AID-SYN1>3.0.CO;2-8

Benoit-Marand, M., and O'Donnell, P. (2008). D2 dopamine modulation of corticoaccumbens synaptic responses changes during adolescence. *Eur. J. Neurosci.* 27, 1364–1372. doi: 10.1016/j.jinsphys.2021.104295

Berger, B., Tassin, J. P., Blanc, G., Moyne, M. A., and Thierry, A. M. (1974). Histochemical confirmation for dopaminergic innervation of the rat cerebral cortex after destruction of the noradrenergic ascending pathways. *Brain Res.* 81, 332–337. doi: 10.1016/0006-8993(74)90948-2

Berger, B., Thierry, A. M., Tassin, J. P., and Moyne, M. A. (1976). Dopaminergic innervation of the rat prefrontal cortex: a fluorescence histochemical study. *Brain Res.* 106, 133–145. doi: 10.1016/0006-8993(76)90078-0

Berger, B., Verney, C., Febvret, A., Vigny, A., and Helle, K. B. (1985). Postnatal ontogenesis of the dopaminergic innervation in the rat anterior cingulate cortex (Area 24). immunocytochemical and catecholamine fluorescence histochemical analysis. *Dev. Brain Res.* 21, 31–47. doi: 10.1016/0165-3806(85)90021-5

Berger, B., Verney, C., Gay, M., and Vigny, A. (1983). Immunocytochemical characterization of the dopaminergic and noradrenergic innervation of the rat neocortex during early ontogeny. *Prog. Brain Res.* 58, 263–267. doi: 10.1016/S0079-6123(08)60028-X

Bertran-Gonzalez, J., Hervé, D., Girault, J.-A., and Valjent, E. (2010). What is the degree of segregation between striatonigral and striatopallidal projections. *Front. Neuroanat.* 4:136. doi: 10.3389/fnana.2010.00136

Bérubé-Carrière, N., Guay, G., Fortin, G. M., Kullander, K., Olson, L., Wallén-Mackenzie, Å., et al. (2012). Ultrastructural characterization of the mesostriatal

dopamine innervation in mice, including two mouse lines of conditional VGLUT2 knockout in dopamine neurons. *Eur. J. Neurosci.* 35, 527–538. doi: 10.1111/j.1460-9568.2012.07992.x

Biezonski, D. K., Trifilieff, P., Meszaros, J., Javitch, J. A., and Kellendonk, C. (2015). Evidence for limited D1 and D2 receptor coexpression and colocalization within the dorsal striatum of the neonatal mouse. *J. Comp. Neurol.* 523, 1175–1189. doi: 10.1002/cne.23730

Björklund, A., and Dunnett, S. B. (2007). Dopamine neuron systems in the brain: an update. *Trends Neurosci.* 30, 194–202. doi: 10.1016/j.tins.2007.03.006

Björklund, A., and Lindvall, O. (1984). "Dopamine-containing system in the CNS," in *Handbook of Chemical Neuroanatomy*, eds A. Björklund, and T. Hökfelt (Amsterdam: Elsevier), 55–122.

Blakemore, S.-J. (2012). Imaging brain development: the adolescent brain. *NeuroImage* 61, 397–406. doi: 10.1016/j.neuroimage.2011.11.080

Bodea, G. O., and Blaess, S. (2015). Establishing diversity in the dopaminergic system. *FEBS Lett.* 589, 3773–3785. doi: 10.1016/j.febslet.2015.09.016

Bordt, E. A., Ceasrine, A. M., and Bilbo, S. D. (2020). Microglia and sexual differentiation of the developing brain: a focus on ontogeny and intrinsic factors. *Glia* 68, 1085–1099. doi: 10.1002/glia.23753

Brenhouse, H. C., and Andersen, S. L. (2011). Developmental trajectories during adolescence in males and females: a cross-species understanding of underlying brain changes. *Neurosci. Biobehav. Rev.* 35, 1687–1703. doi: 10.1016/j.neubiorev.2011.04.013

Brenhouse, H. C., and Schwarz, J. M. (2016). Immunoadolescence: neuroimmune development and adolescent behavior. *Neurosci. Biobehav. Rev.* 70, 288–299. doi: 10.1016/j.neubiorev.2016.05.035

Brenhouse, H. C., Sonntag, K. C., and Andersen, S. L. (2008). Transient D1 dopamine receptor expression on prefrontal cortex projection neurons: relationship to enhanced motivational salience of drug cues in adolescence. *J. Neurosci.* 28, 2375–2382. doi: 10.1523/JNEUROSCI.5064-07.2008

Brignani, S., and Pasterkamp, R. J. (2017). Neuronal subset-specific migration and axonal wiring mechanisms in the developing midbrain dopamine system. *Front. Neuroanat.* 11:55. doi: 10.3389/fnana.2017.00055

Brix, N., Ernst, A., Lauridsen, L. L. B., Parner, E., Støvring, H., Olsen, J., et al. (2019). Timing of puberty in boys and girls: a population-based study. *Paediatr. Perinat. Epidemiol.* 33, 70–78. doi: 10.1111/ppe.12507

Broaddus, W. C., and Bennett, J. P. (1990). Postnatal development of striatal dopamine function. I. an examination of D1 and D2 receptors, adenylate cyclase regulation and presynaptic dopamine markers. *Dev. Brain Res.* 52, 265–271. doi: 10.1016/0165-3806(90)90244-s

Bromberg-Martin, E. S., Matsumoto, M., and Hikosaka, O. (2010). Dopamine in motivational control: rewarding, aversive and alerting. *Neuron* 68, 815–834. doi: 10.1016/j.neuron.2010.11.022

Burke, A. R., and Miczek, K. A. (2013). Stress in adolescence and drugs of abuse in rodent models: role of dopamine, CRF and HPA axis. *Psychopharmacology (Berl)* 231, 1557–1580. doi: 10.1007/s00213-013-3369-1

Caballero, A., Granberg, R., and Tseng, K. Y. (2016). Mechanisms contributing to prefrontal cortex maturation during adolescence. *Neurosci. Biobehav. Rev.* 70, 4–12. doi: 10.1016/j.neubiorev.2016.05.013

Caballero, A., Orozco, A., and Tseng, K. Y. (2021). Developmental regulation of excitatory-inhibitory synaptic balance in the prefrontal cortex during adolescence. *Semin. Cell Dev. Biol.* S1084-9521(21)00032-X. doi: 10.1016/j.semcdb.2021.02.008

Calipari, E. S., Juarez, B., Morel, C., Walker, D. M., Cahill, M. E., Ribeiro, E., et al. (2017). Dopaminergic dynamics underlying sex-specific cocaine reward. *Nat. Commun.* 8:13877. doi: 10.1038/ncomms13877

Cannella, L. A., Andrews, A. M., Tran, F., Razmpour, R., McGary, H., Collie, C., et al. (2020). Experimental traumatic brain injury during adolescence enhances cocaine rewarding efficacy and dysregulates dopamine and neuroimmune systems in brain reward substrates. *J. Neurotrauma* 37, 27–42. doi: 10.1089/neu.2019.6472

Carr, D. B., O'Donnell, P., Card, J. P., and Sesack, S. R. (1999). Dopamine terminals in the rat prefrontal cortex synapse on pyramidal cells that project to the nucleus accumbens. *J. Neurosci.* 19, 11049–11060. doi: 10.1523/JNEUROSCI.19-24-11049.1999

Carr, D. B., and Sesack, S. R. (2000). Dopamine terminals synapse on callosal projection neurons in the rat prefrontal cortex. *J. Comp. Neurol.* 425, 275–283. doi: 10.1002/1096-9861(20000918)425:2<275::aid-cne9>3.0.co;2-z

Castner, S. A., Vosler, P. S., and Goldman-Rakic, P. S. (2005). Amphetamine sensitization impairs cognition and reduces dopamine turnover in primate prefrontal cortex. *Biol. Psychiatry.* 57, 743–751. doi: 10.1016/j.biopsych.2004.12.019

Catts, V. S., Fung, S. J., Long, L. E., Joshi, D., Vercammen, A., Allen, K. M., et al. (2013). Rethinking schizophrenia in the context of normal neurodevelopment. *Front. Cell Neurosci.* 7:60. doi: 10.3389/fncel.2013.00060

Coddington, L. T., and Dudman, J. T. (2019). Learning from action: reconsidering movement signaling in midbrain dopamine neuron activity. *Neuron* 104, 63–77. doi: 10.1016/j.neuron.2019.08.036

Collins, A. L., and Saunders, B. T. (2020). Heterogeneity in striatal dopamine circuits: form and function in dynamic reward seeking. *J. Neurosci. Res.* 98, 1046–1069. doi: 10.1002/jnr.24587

Comer, A. L., Jinadasa, T., Sriram, B., Phadke, R. A., Kretsge, L. N., Nguyen, T. P. H., et al. (2020). Increased expression of schizophrenia-associated gene C4 leads to hypoconnectivity of prefrontal cortex and reduced social interaction. *PLoS Biol.* 18:e3000604. doi: 10.1371/journal.pbio.3000604

Cools, R., and D'Esposito, M. (2011). Inverted-U-shaped dopamine actions on human working memory and cognitive control. *Biol. Psychiatry* 69, e113–e125. doi: 10.1016/j.biopsych.2011.03.028

Cuesta, S., Nouel, D., Reynolds, L. M., Morgunova, A., Torres-Berrío, A., White, A., et al. (2020). Dopamine axon targeting in the nucleus accumbens in adolescence requires netrin-1. *Front. Cell Dev. Biol.* 8:487. doi: 10.3389/fcell.2020.00487

Cuesta, S., Restrepo-Lozano, J. M., Popescu, C., He, S., Reynolds, L. M., Israel, S., et al. (2019). DCC-related developmental effects of abused- versus therapeutic-like amphetamine doses in adolescence. *Addict. Biol.* 25:e12791. doi: 10.1111/adb.12791

Cuesta, S., Restrepo-Lozano, J. M., Silvestrin, S., Nouel, D., Torres-Berrío, A., Reynolds, L. M., et al. (2018). Non-contingent exposure to amphetamine in adolescence recruits miR-218 to regulate Dcc expression in the VTA. *Neuropsychopharmacology* 43, 900–911. doi: 10.1038/npp.2017.284

Davidoff, S. A., and Benes, F. M. (1998). High-resolution Scatchard analysis shows D1 receptor binding on pyramidal and nonpyramidal neurons. *Synapse* 28, 83–90. doi: 10.1002/(SICI)1098-2396(199801)28:1<83::AID-SYN10>3.0.CO;2-Z

Delevich, K., Klinger, M., Okada, N. J., and Wilbrecht, L. (2021). Coming of age in the frontal cortex: the role of puberty in cortical maturation. *Semin. Cell Dev. Biol.*. S1084-9521(21)00094-X. doi: 10.1016/j.semcdb.2021.04.021

Delevich, K., Okada, N. J., Rahane, A., Zhang, Z., Hall, C. D., and Wilbrecht, L. (2020). Sex and pubertal status influence dendritic spine density on frontal corticostriatal projection neurons in mice. *Cereb. Cortex* 30, 3543–3557. doi: 10.1093/cercor/bhz325

Descarries, L., and Mechawar, N. (2000). Ultrastructural evidence for diffuse transmission by monoamine and acetylcholine neurons of the central nervous system. *Prog. Brain Res.* 125, 27–47. doi: 10.1016/S0079-6123(00)25005-X

Descarries, L., Watkins, K. C., Garcia, S., Bosler, O., and Doucet, G. (1996). Dual character, asynaptic and synaptic, of the dopamine innervation in adult rat neostriatum: a quantitative autoradiographic and immunocytochemical analysis. *J. Comp. Neurol.* 375, 167–186. doi: 10.1002/(SICI)1096-9861(19961111)375:2<167::AID-CNE1>3.0.CO;2-0

Dong, Y., and White, F. J. (2003). Dopamine D1-Class receptors selectively modulate a slowly inactivating potassium current in rat medial prefrontal cortex pyramidal neurons. *J. Neurosci.* 23, 2686–2695. doi: 10.1523/JNEUROSCI.23-07-02686.2003

Drzewiecki, C. M., Willing, J., and Juraska, J. M. (2016). Synaptic number changes in the medial prefrontal cortex across adolescence in male and female rats: a role for pubertal onset. *Synapse* 70, 361–368. doi: 10.1002/syn.21909

Drzewiecki, C. M., Willing, J., and Juraska, J. M. (2020). Influences of age and pubertal status on number and intensity of perineuronal nets in the rat medial prefrontal cortex. *Brain Struct. Funct.* 225, 2495–2507. doi: 10.1007/s00429-020-02137-z

Ernst, M., and Luciana, M. (2015). Neuroimaging of the dopamine/reward system in adolescent drug use. *CNS Spectr.* 20, 427–441. doi: 10.1017/S1092852915000395

Fallon, J. (1981). Collateralization of monoamine neurons: mesotelencephalic dopamine projections to caudate, septum and frontal cortex. *J. Neurosci.* 1, 1361–1368. doi: 10.1523/JNEUROSCI.01-12-01361.1981

Fallon, J. H., and Loughlin, S. E. (1982). Monoamine innervation of the forebrain: collateralization. *Brain Res. Bull.* 9, 295–307. doi: 10.1016/0361-9230(82)90143-5

Flores, C. (2011). Role of netrin-1 in the organization and function of the mesocorticolimbic dopamine system. *J. Psychiatry Neurosci.* 36, 296–310. doi: 10.1503/jpn.100171

Flores, C., Manitt, C., Rodaros, D., Thompson, K. M., Rajabi, H., Luk, K. C., et al. (2005). Netrin receptor deficient mice exhibit functional reorganization of dopaminergic systems and do not sensitize to amphetamine. *Mol. Psychiatry* 10, 606–612. doi: 10.1038/sj.mp.4001607

Frederick, A. L., Yano, H., Trifilieff, P., Vishwasrao, H. D., Biezonski, D., Mészáros, J., et al. (2015). Evidence against dopamine D1/D2 receptor heteromers. *Mol. Psychiatry* 20, 1373–1385. doi: 10.1038/mp.2014.166

Galvan, A. (2017). Adolescence, brain maturation and mental health. *Nat. Neurosci.* 20, 503–504. doi: 10.1038/nn.4530

Ganguly, P., Thompson, V., Gildawie, K., and Brenhouse, H. C. (2018). Adolescent food restriction in rats alters prefrontal cortex microglia in an experience-dependent manner. *Ann. N Y Acad. Sci.* 21, 162–168. doi: 10.1080/10253890.2017.1423054

Gaspar, P., Bloch, B., and Moine, C. (1995). D1 and D2 receptor gene expression in the rat frontal cortex: cellular localization in different classes of efferent neurons. *Eur. J. Neurosci.* 7, 1050–1063. doi: 10.1111/j.1460-9568.1995.tb01092.x

Gelbard, H. A., Teicher, M. H., Faedda, G., and Baldessarini, R. J. (1989). Postnatal development of dopamine D1 and D2 receptor sites in rat striatum. *Brain Res. Dev. Brain Res.* 49, 123–130. doi: 10.1016/0165-3806(89)90065-5

Gillies, G. E., Virdee, K., McArthur, S., and Dalley, J. W. (2014). Sex-dependent diversity in ventral tegmental dopaminergic neurons and developmental programing: a molecular, cellular and behavioral analysis. *Neuroscience* 282, 69–85. doi: 10.1016/j.neuroscience.2014.05.033

Giorgi, O., Montis, G. D., Porceddu, M. L., Mele, S., Calderini, G., Toffano, G., et al. (1987). Developmental and age-related changes in D1-dopamine receptors and dopamine content in the rat striatum. *Brain Res.* 35, 283–290. doi: 10.1016/0165-3806(87)90053-8

Glausier, J. R., Khan, Z. U., and Muly, E. C. (2009). Dopamine D1 and D5 receptors are localized to discrete populations of interneurons in primate prefrontal cortex. *Cereb. Cortex* 19, 1820–1834. doi: 10.1093/cercor/bhn212

Goldman-Rakic, P. S., and Brown, R. M. (1982). Postnatal development of monoamine content and synthesis in the cerebral cortex of rhesus monkeys. *Brain Res.* 256, 339–349. doi: 10.1016/0165-3806(82)90146-8

Goldman-Rakic, P. S., Lidow, M. S., Smiley, J. F., and Williams, M. S. (1992). The anatomy of dopamine in monkey and human prefrontal cortex. *J. Neural. Transm. Suppl.* 36, 163–177. doi: 10.1007/978-3-7091-9211-5_8

Gorelova, N., Seamans, J. K., and Yang, C. R. (2002). Mechanisms of dopamine activation of fast-spiking interneurons that exert inhibition in rat prefrontal cortex. *J. Neurophysiol.* 88, 3150–3166. doi: 10.1152/jn.00335.2002

Grant, A., Hoops, D., Labelle-Dumais, C., Prévost, M., Rajabi, H., Kolb, B., et al. (2007). Netrin-1 receptor-deficient mice show enhanced mesocortical dopamine transmission and blunted behavioural responses to amphetamine. *Eur. J. Neurosci.* 26, 3215–3228. doi: 10.1111/j.1460-9568.2007.05888.x

Grant, A., Speed, Z., Labelle-Dumais, C., and Flores, C. (2009). Post-pubertal emergence of a dopamine phenotype in netrin-1 receptor-deficient mice. *Eur. J. Neurosci.* 30, 1318–1328. doi: 10.1111/j.1460-9568.2009.06919.x

Gulledge, A. T., and Jaffe, D. B. (2001). Multiple effects of dopamine on layer V pyramidal cell excitability in rat prefrontal cortex. *J. Neurophysiol.* 86, 586–595. doi: 10.1152/jn.2001.86.2.586

Gulley, J. M., and Juraska, J. M. (2013). The effects of abused drugs on adolescent development of corticolimbic circuitry and behavior. *Neuroscience* 249, 3–20. doi: 10.1016/j.neuroscience.2013.05.026

Hartley, E. J., and Seeman, P. (1983). Development of receptors for dopamine and noradrenaline in rat brain. *Eur. J. Pharmacol.* 91, 391–397. doi: 10.1016/0014-2999(83)90163-2

Haycock, J. W., Becker, L., Ang, L., Furukawa, Y., Hornykiewicz, O., and Kish, S. J. (2003). Marked disparity between age-related changes in dopamine and other presynaptic dopaminergic markers in human striatum. *J. Neurochem.* 87, 574–585. doi: 10.1046/j.1471-4159.2003.02017.x

Hernandez, D., Torres, C. A., Setlik, W., Cebrián, C., Mosharov, E. V., Tang, G., et al. (2012). Regulation of presynaptic neurotransmission by macroautophagy. *Neuron* 74, 277–284. doi: 10.1016/j.neuron.2012.02.020

Hersch, S., Ciliax, B., Gutekunst, C., Rees, H., Heilman, C., Yung, K., et al. (1995). Electron microscopic analysis of D1 and D2 dopamine receptor proteins in the dorsal striatum and their synaptic relationships with motor corticostriatal afferents. *J. Neurosci.* 15, 5222–5237. doi: 10.1523/JNEUROSCI.15-07-05222.1995

Heuvel, D. M. A. V. D., and Pasterkamp, R. J. (2008). Getting connected in the dopamine system. *Prog. Neurobiol.* 85, 75–93. doi: 10.1016/j.pneurobio.2008.01.003

Hollenstein, T., and Lougheed, J. P. (2013). Beyond storm and stress. *Am. Psychol.* 68, 444–454. doi: 10.1037/a0033586

Hoops, D., Reynolds, L. M., Restrepo-Lozano, J. M., and Flores, C. (2018). Dopamine development in the mouse orbital prefrontal cortex is protracted and sensitive to amphetamine in adolescence. *eNeuro* 5:ENEURO.0372–17.2017. doi: 10.1523/ENEURO.0372-17.2017

Hughes, A. N., and Appel, B. (2020). Microglia phagocytose myelin sheaths to modify developmental myelination. *Nat. Neurosci.* 23, 1055–1066. doi: 10.1038/s41593-020-0654-2

Ince, E., Ciliax, B. J., and Levey, A. I. (1997). Differential expression of D1 and D2 dopamine and m4 muscarinic acetylcholine receptor proteins in identified striatonigral neurons. *Synapse* 27, 357–366. doi: 10.1002/(SICI)1098-2396(199712)27:4<357::AID-SYN9>3.0.CO;2-B

Jordan, C. J., and Andersen, S. L. (2017). Sensitive periods of substance abuse: early risk for the transition to dependence. *Dev. Cogn. Neurosci.* 25, 29–44. doi: 10.1016/j.dcn.2016.10.004

Kalsbeek, A., Voorn, P., and Buijs, R. M. (1992). "Development of dopamine - containing systems in the CNS," in *Handbook of Chemical Neuroanatomy, Vol: Ontogeny of Transmitters and Peptides in the Central Nervous System*, eds A. Björklund, T. Hökfelt and M. Tohyama (Amsterdam: Elsevier B.V.), 63–112. Available online at: https://pure.knaw.nl/portal/en/publications/development-of-dopamine-containing-systems-in-the-cns.

Kalsbeek, A., Voorn, P., Buijs, R. M., Pool, C. W., and Uylings, H. B. (1988). Development of the dopaminergic innervation in the prefrontal cortex of the rat. *J. Comp. Neurol.* 269, 58–72. doi: 10.1002/cne.902690105

Kaukas, L., Holmes, J. L., Rahimi, F., Collins-Praino, L., and Corrigan, F. (2020). Injury during adolescence leads to sex-specific executive function deficits in adulthood in a pre-clinical model of mild traumatic brain injury. *Behav. Brain Res.* 402:113067. doi: 10.1016/j.bbr.2020.113067

Kim, J. H., Lavan, D., Chen, N., Flores, C., Cooper, H., and Lawrence, A. J. (2013). Netrin-1 receptor-deficient mice show age-specific impairment in drug-induced locomotor hyperactivity but still self-administer methamphetamine. *Psychopharmacology* 230, 607–616. doi: 10.1007/s00213-013-3187-5

Klune, C. B., Jin, B., and DeNardo, L. A. (2021). Linking mPFC circuit maturation to the developmental regulation of emotional memory and cognitive flexibility. *eLife* 10:e64567. doi: 10.7554/eLife.64567

Knable, M. B., and Weinberger, D. R. (1997). Dopamine, the prefrontal cortex and schizophrenia. *J. Psychopharmacol.* 11, 123–131. doi: 10.1177/026988119701100205

Kokane, S. S., and Perrotti, L. I. (2020). Sex differences and the role of estradiol in mesolimbic reward circuits and vulnerability to cocaine and opiate addiction. *Front. Behav. Neurosci.* 14:74. doi: 10.3389/fnbeh.2020.00074

Kolk, S. M., Gunput, R.-A. F., Tran, T. S., Heuvel, D. M. A. V. D. H., Prasad, A. A., Hellemons, A. J. C. G. M., et al. (2009). Semaphorin 3F is a bifunctional guidance cue for dopaminergic axons and controls their fasciculation, channeling, rostral growth and intracortical targeting. *J. Neurosci.* 29, 12542–12557. doi: 10.1523/JNEUROSCI.2521-09.2009

Kopec, A. M., Smith, C. J., Ayre, N. R., Sweat, S. C., and Bilbo, S. D. (2018). Microglial dopamine receptor elimination defines sex-specific nucleus accumbens development and social behavior in adolescent rats. *Nat. Commun.* 9:3769. doi: 10.1038/s41467-018-06118-z

Kreitzer, A. C. (2009). Physiology and pharmacology of striatal neurons. *Annu. Rev. Neurosci.* 32, 127–147. doi: 10.1146/annurev.neuro.051508.135422

Krimer, L. S., Jakab, R. L., and Goldman-Rakic, P. S. (1997). Quantitative three-dimensional analysis of the catecholaminergic innervation of identified neurons in the macaque prefrontal cortex. *J. Neurosci.* 17, 7450–7461. doi: 10.1523/JNEUROSCI.17-19-07450.1997

Kritzer, M. F. (1998). Perinatal gonadectomy exerts regionally selective, lateralized effects on the density of axons immunoreactive for tyrosine hydroxylase in the cerebral cortex of adult male rats. *J. Neurosci.* 18, 10735–10748. doi: 10.1523/JNEUROSCI.18-24-10735.1998

Kritzer, M. F. (2003). Long-term gonadectomy affects the density of tyrosine hydroxylase- but not dopamine-β-hydroxylase-, choline acetyltransferase- or serotonin-immunoreactive axons in the medial prefrontal cortices of adult male rats. *Cereb. Cortex* 13, 282–296. doi: 10.1093/cercor/13.3.282

Kritzer, M. F., Adler, A., Marotta, J., and Smirlis, T. (1999). Regionally selective effects of gonadectomy on cortical catecholamine innervation in adult male rats are most disruptive to afferents in prefrontal cortex. *Cereb Cortex* 9, 507–518. doi: 10.1093/cercor/9.5.507

Kritzer, M. F., and Creutz, L. M. (2008). Region and sex differences in constituent dopamine neurons and immunoreactivity for intracellular estrogen androgen receptors in mesocortical projections in rats. *J. Neurosci.* 28, 9525–9535. doi: 10.1523/JNEUROSCI.2637-08.2008

Kritzer, M. F., and Kohama, S. G. (1998). Ovarian hormones influence the morphology, distribution and density of tyrosine hydroxylase immunoreactive axons in the dorsolateral prefrontal cortex of adult Rhesus monkeys. *J. Comp. Neurol.* 395, 1–17. doi: 10.1002/(sici)1096-9861(19980525)395:1<1::aid-cne1>3.0.co;2-4

Lambe, E. K., Krimer, L. S., and Goldman-Rakic, P. S. (2000). Differential postnatal development of catecholamine and serotonin inputs to identified neurons in prefrontal cortex of rhesus monkey. *J. Neurosci.* 20, 8780–8787. doi: 10.1523/JNEUROSCI.20-23-08780.2000

Lammel, S., Hetzel, A., Häckel, O., Jones, I., Liss, B., and Roeper, J. (2008). Unique properties of mesoprefrontal neurons within a dual mesocorticolimbic dopamine system. *Neuron* 57, 760–773. doi: 10.1016/j.neuron.2008.01.022

Lammel, S., Lim, B. K., and Malenka, R. C. (2014). Reward and aversion in a heterogeneous midbrain dopamine system. *Neuropharmacology* 76, 351–359. doi: 10.1016/j.neuropharm.2013.03.019

Larsen, B., and Luna, B. (2014). in vivo evidence of neurophysiological maturation of the human adolescent striatum. *Dev. Cogn. Neurosci.* 12, 74–85. doi: 10.1016/j.dcn.2014.12.003

Larsen, B., and Luna, B. (2018). Adolescence as a neurobiological critical period for the development of higher-order cognition. *Neurosci. Biobehav. Rev.* 94, 179–195. doi: 10.1016/j.neubiorev.2018.09.005

Larsen, B., Olafsson, V., Calabro, F., Laymon, C., Tervo-Clemmens, B., Campbell, E., et al. (2020). Maturation of the human striatal dopamine system revealed by PET and quantitative MRI. *Nat. Commun.* 11:846. doi: 10.1038/s41467-020-14693-3

Le Moine, C., and Gaspar, P. (1998). Subpopulations of cortical GABAergic interneurons differ by their expression of D1 and D2 dopamine receptor subtypes. *Mol. Brain Res.* 58, 231–236. doi: 10.1016/s0169-328x(98)00118-1

Leslie, C. A., Robertson, M. W., Cutler, A. J., and Bennett, J. P. (1991). Postnatal development of D 1 dopamine receptors in the medial prefrontal cortex, striatum and nucleus accumbens of normal and neonatal 6-hydroxydopamine treated rats: a quantitative autoradiographic analysis. *Brain Res. Dev. Brain Res.* 62, 109–114. doi: 10.1016/0165-3806(91)90195-o

Lévesque, D., Gagnon, S., and Paolo, T. D. (1989). Striatal D1 dopamine receptor density fluctuates during the rat estrous cycle. *Neurosci. Lett.* 98, 345–350. doi: 10.1016/0304-3940(89)90426-6

Lévesque, D., and Paolo, T. D. (1989). Chronic estradiol treatment increases ovariectomized rat striatal D-1 dopamine receptors. *Life Sci.* 45, 1813–1820. doi: 10.1016/0024-3205(89)90522-5

Lévesque, D., and Paolo, T. D. (1990). Effect of the rat estrous cycle at ovariectomy on striatal D-1 dopamine receptors. *Brain Res. Bull.* 24, 281–284. doi: 10.1016/0361-9230(90)90216-m

Levitt, P., and Moore, R. Y. (1979). Development of the noradrenergic innervation of neocortex. *Brain Res.* 162, 243–259. doi: 10.1016/0006-8993(79)90287-7

Lewis, D. A. (1997). Development of the prefrontal cortex during adolescence: insights into vulnerable neural circuits in schizophrenia. *Neuropsychopharmacology* 16, 385–398. doi: 10.1016/S0893-133X(96)00277-1

Lidov, H. G. W., Grzanna, R., and Molliver, M. E. (1980). The serotonin innervation of the cerebral cortex in the rat—an immunohistochemical analysis. *Neuroscience* 5, 207–227. doi: 10.1016/0306-4522(80)90099-8

Lidow, M. S., Koh, P.-O., and Arnsten, A. F. T. (2003). D1 dopamine receptors in the mouse prefrontal cortex: immunocytochemical and cognitive neuropharmacological analyses. *Synapse* 47, 101–108. doi: 10.1002/syn.10143

Lieberman, O. J., Cartocci, V., Pigulevskiy, I., Molinari, M., Carbonell, J., Broseta, M. B., et al. (2020). mTOR suppresses macroautophagy during striatal postnatal development and is hyperactive in mouse models of autism spectrum disorders. *Front. Cell. Neurosci.* 14:70. doi: 10.3389/fncel.2020.00070

Lieberman, O. J., McGuirt, A. F., Mosharov, E. V., Pigulevskiy, I., Hobson, B. D., Choi, S., et al. (2018). Dopamine triggers the maturation of striatal spiny projection neuron excitability during a critical period. *Neuron* 99, 540–554.e4. doi: 10.1016/j.neuron.2018.06.044

Linker, K. E., Gad, M., Tawadrous, P., Cano, M., Green, K. N., Wood, M. A., et al. (2020). Microglial activation increases cocaine self-administration following adolescent nicotine exposure. *Nat. Commun.* 11:306. doi: 10.1038/s41467-019-14173-3

Liu, C., Goel, P., and Kaeser, P. S. (2021). Spatial and temporal scales of dopamine transmission. *Nat. Rev. Neurosci.* 22, 345–358. doi: 10.1038/s41583-021-00455-7

Liu, C., and Kaeser, P. S. (2019). Mechanisms and regulation of dopamine release. *Curr. Opin. Neurobiol.* 57, 46–53. doi: 10.1016/j.conb.2019.01.001

Liu, C., Kershberg, L., Wang, J., Schneeberger, S., and Kaeser, P. S. (2018). Dopamine secretion is mediated by sparse active zone-like release sites. *Cell* 172, 706–718.e15. doi: 10.1016/j.cell.2018.01.008

Lu, X., Churchill, L., and Kalivas, P. W. (1997). Expression of D1 receptor mRNA in projections from the forebrain to the ventral tegmental area. *Synapse* 25, 205–214. doi: 10.1002/(SICI)1098-2396(199702)25:2<205::AID-SYN11>3.0.CO;2-X

Luciana, M., Wahlstrom, D., Porter, J. N., and Collins, P. F. (2012). Dopaminergic modulation of incentive motivation in adolescence: age-related changes in signaling, individual differences, and implications for the development of self-regulation. *Dev. Psychol.* 48, 844–861. doi: 10.1037/a0027432

Mallya, A. P., Wang, H.-D., Lee, H. N. R., and Deutch, A. Y. (2018). Microglial pruning of synapses in the prefrontal cortex during adolescence. *Cereb. Cortex* 29, 1634–1643. doi: 10.1093/cercor/bhy061

Manitt, C., Eng, C., Pokinko, M., Ryan, R. T., Torres-Berrío, A., Lopez, J. P., et al. (2013). dcc orchestrates the development of the prefrontal cortex during adolescence and is altered in psychiatric patients. *Transl. Psychiatry* 3:e338. doi: 10.1038/tp.2013.105

Manitt, C., Labelle-Dumais, C., Eng, C., Grant, A., Mimee, A., Stroh, T., et al. (2010). Peri-pubertal emergence of UNC-5 homologue expression by dopamine neurons in rodents. *PLoS One* 5:e11463. doi: 10.1371/journal.pone.0011463

Manitt, C., Mimee, A., Eng, C., Pokinko, M., Stroh, T., Cooper, H. M., et al. (2011). The netrin receptor DCC is required in the pubertal organization of mesocortical dopamine circuitry. *J. Neurosci.* 31, 8381–8394. doi: 10.1523/JNEUROSCI.0606-11.2011

Matthews, M., Bondi, C., Torres, G., and Moghaddam, B. (2013). Reduced presynaptic dopamine activity in adolescent dorsal striatum. *Neuropsychopharmacology* 38, 1344–1351. doi: 10.1038/npp.2013.32

McCutcheon, J. E., Conrad, K. L., Carr, S. B., Ford, K. A., McGehee, D. S., and Marinelli, M. (2012). Dopamine neurons in the ventral tegmental area fire faster in adolescent rats than in adults. *J. Neurophysiol.* 108, 1620–1630. doi: 10.1152/jn.00077.2012

McCutcheon, J. E., and Marinelli, M. (2009). Age matters. *Eur. J. Neurosci.* 29, 997–1014. doi: 10.1111/j.1460-9568.2009.06648.x

Meaney, M. J., Brake, W., and Gratton, A. (2002). Environmental regulation of the development of mesolimbic dopamine systems: a neurobiological mechanism for vulnerability to drug abuse? *Psychoneuroendocrino* 27, 127–138. doi: 10.1016/s0306-4530(01)00040-3

Miller, D. J., Duka, T., Stimpson, C. D., Schapiro, S. J., Baze, W. B., McArthur, M. J., et al. (2012). Prolonged myelination in human neocortical evolution. *Proc. Natl. Acad. Sci. U S A* 109, 16480–16485. doi: 10.1073/pnas.1117943109

Miner, L. H., Schroeter, S., Blakely, R. D., and Sesack, S. R. (2003). Ultrastructural localization of the norepinephrine transporter in superficial and deep layers of the rat prelimbic prefrontal cortex and its spatial relationship to probable dopamine terminals. *J. Comp. Neurol.* 466, 478–494. doi: 10.1002/cne.10898

Mitrano, D. A., Pare, J.-F., Smith, Y., and Weinshenker, D. (2014). D1-dopamine and α1-adrenergic receptors co-localize in dendrites of the rat prefrontal cortex. *Neuroscience* 258, 90–100. doi: 10.1016/j.neuroscience.2013.11.002

Money, K. M., and Stanwood, G. D. (2013). Developmental origins of brain disorders: roles for dopamine. *Front. Cell. Neurosci.* 7:260. doi: 10.3389/fncel.2013.00260

Morales, M., and Margolis, E. B. (2017). Ventral tegmental area: cellular heterogeneity, connectivity and behaviour. *Nat. Rev. Neurosci.* 18, 73–85. doi: 10.1038/nrn.2016.165

Morgunova, A., and Flores, C. (2021). MicroRNA regulation of prefrontal cortex development and psychiatric risk in adolescence. *Semin. Cell Dev. Biol.* doi: 10.1016/j.semcdb.2021.04.011. [Epub ahead of print].

Murrin, L. C., and Wanyun, Z. (1986). Postnatal ontogeny of dopamine D2 receptors in rat striatum. *Biochem. Pharmacol.* 35, 1159–1162. doi: 10.1016/0006-2952(86)90154-1

Murrin, L. C., and Zeng, W. (1990). Ontogeny of dopamine D1 receptors in rat forebrain: a quantitative autoradiographic study. *Dev. Brain Res.* 57, 7–13. doi: 10.1016/0165-3806(90)90178-2

Naneix, F., Marchand, A. R., Scala, G. D., Pape, J.-R., and Coutureau, E. (2012). Parallel maturation of goal-directed behavior and dopaminergic systems during adolescence. *J. Neurosci.* 32, 16223–16232. doi: 10.1523/JNEUROSCI.3080-12.2012

Nguyen, C., Mondoloni, S., Borgne, T. L., Centeno, I., Come, M., Jehl, J., et al. (2021). Nicotine inhibits the VTA-to-amygdala dopamine pathway to promote anxiety. *Neuron* 109, 2604.e9–2615.e9. doi: 10.1016/j.neuron.2021.06.013

Nieuwenhuys, R., Geeraedts, L. M., and Veening, J. G. (1982). The medial forebrain bundle of the rat. I. General introduction. *J. Comp. Neurol.* 206, 49–81. doi: 10.1002/cne.902060106

Nomura, Y., Naitoh, F., and Segawa, T. (1976). Regional changes in monoamine content and uptake of the rat brain during postnatal development. *Brain Res.* 101, 305–315. doi: 10.1016/0006-8993(76)90271-7

O'Donnell, P. (2010). Adolescent maturation of cortical dopamine. *Neurotox. Res.* 18, 306–312. doi: 10.1007/s12640-010-9157

O'Donnell, P. (2011). Adolescent onset of cortical disinhibition in schizophrenia: insights from animal models. *Schizophr. Bull.* 37, 484–492. doi: 10.1093/schbul/sbr028

Orsini, C. A., Moorman, D. E., Young, J. W., Setlow, B., and Floresco, S. B. (2015). Neural mechanisms regulating different forms of risk-related decision-making: insights from animal models. *Neurosci. Biobehav. Rev.* 58, 147–167. doi: 10.1016/j.neubiorev.2015.04.009

Osborne, P. B., Halliday, G. M., Cooper, H. M., and Keast, J. R. (2005). Localization of immunoreactivity for deleted in colorectal cancer (DCC), the receptor for the guidance factor netrin-1, in ventral tier dopamine projection pathways in adult rodents. *Neuroscience* 131, 671–681. doi: 10.1016/j.neuroscience.2004.11.043

Ouchi, Y., Yoshikawa, E., Sekine, Y., Futatsubashi, M., Kanno, T., Ogusu, T., et al. (2005). Microglial activation and dopamine terminal loss in early Parkinson's disease. *Ann. Neurol.* 57, 168–175. doi: 10.1002/ana.20338

Paolicelli, R. C., Bolasco, G., Pagani, F., Maggi, L., Scianni, M., Panzanelli, P., et al. (2011). Synaptic pruning by microglia is necessary for normal brain development. *Science* 333, 1456–1458. doi: 10.1126/science.1202529

Paquola, C., Bethlehem, R. A., Seidlitz, J., Wagstyl, K., Romero-Garcia, R., Whitaker, K. J., et al. (2019). Shifts in myeloarchitecture characterise adolescent development of cortical gradients. *eLife* 8:e50482. doi: 10.7554/eLife.50482

Pardo, J. V., Creese, I., Burt, D. R., and Snyder, S. H. (1977). Ontogenesis of dopamine receptor binding in the corpus striatum of the rat. *Brain Res.* 125, 376–382. doi: 10.1016/0006-8993(77)90633-3

Parkhurst, C. N., Yang, G., Ninan, I., Savas, J. N., Yates, J. R., Lafaille, J. J., et al. (2013). Microglia promote learning-dependent synapse formation through brain-derived neurotrophic factor. *Cell* 155, 1596–1609. doi: 10.1016/j.cell.2013.11.030

Parr, A. C., Calabro, F., Larsen, B., Tervo-Clemmens, B., Elliot, S., Foran, W., et al. (2021). Dopamine-related striatal neurophysiology is associated with specialization of frontostriatal reward circuitry through adolescence. *Prog. Neurobiol.* 201:101997. doi: 10.1016/j.pneurobio.2021.101997

Pereira, D. B., Schmitz, Y., Mészáros, J., Merchant, P., Hu, G., Li, S., et al. (2016). Fluorescent false neurotransmitter reveals functionally silent dopamine vesicle clusters in the striatum. *Nat. Neurosci.* 19, 578–586. doi: 10.1038/nn.4252

Petanjek, Z., Judaš, M., Simic, G., Rasin, M. R., Uylings, H. B. M., Rakic, P., et al. (2011). Extraordinary neoteny of synaptic spines in the human prefrontal cortex. *Proc. Natl. Acad. Sci. U S A* 108, 13281–13286. doi: 10.1073/pnas.1105108108

Peterson, E. T., Kwon, D., Luna, B., Larsen, B., Prouty, D., Bellis, M. D. D., et al. (2019). Distribution of brain iron accrual in adolescence: evidence from cross-sectional and longitudinal analysis. *Hum. Brain Mapp.* 40, 1480–1495. doi: 10.1002/hbm.24461

Pickel, V. M., Joh, T. H., Field, P. M., Becker, C. G., and Reis, D. J. (1975). Cellular localization of tyrosine hydroxylase by immunohistochemistry. *J. Histochem. Cytochem.* 23, 1–12. doi: 10.1177/23.1.234988

Piekarski, D. J., Boivin, J. R., and Wilbrecht, L. (2017). Ovarian hormones organize the maturation of inhibitory neurotransmission in the frontal cortex at puberty onset in female mice. *Curr. Biol.* 27, 1735–1745.e3. doi: 10.1016/j.cub.2017.05.027

Pokinko, M., Grant, A., Shahabi, F., Dumont, Y., Manitt, C., and Flores, C. (2017). Dcc haploinsufficiency regulates dopamine receptor expression across postnatal lifespan. *Neuroscience* 346, 182–189. doi: 10.1016/j.neuroscience.2017.01.009

Pokinko, M., Moquin, L., Torres-Berrío, A., Gratton, A., and Flores, C. (2015). Resilience to amphetamine in mouse models of netrin-1 haploinsufficiency: role of mesocortical dopamine. *Psychopharmacology* 232, 182–189. doi: 10.1007/s00213-015-4032-9

Poulin, J.-F., Caronia, G., Hofer, C., Cui, Q., Helm, B., Ramakrishnan, C., et al. (2018). Mapping projections of molecularly defined dopamine neuron subtypes using intersectional genetic approaches. *Nat. Neurosci.* 21, 1260–1271. doi: 10.1038/s41593-018-0203-4

Prakash, N., and Wurst, W. (2006). Development of dopaminergic neurons in the mammalian brain. *Cell. Mol. Life Sci.* 63, 187–206. doi: 10.1007/s00018-005-5387-6

Rao, P. A., Molinoff, P. B., and Joyce, J. N. (1991). Ontogeny of dopamine D1 and D2 receptor subtypes in rat basal ganglia: a quantitative autoradiographic study. *Dev. Brain Res.* 60, 161–177. doi: 10.1016/0165-3806(91)90045-k

Rey, R., Suaud-Chagny, M.-F., Bohec, A.-L., Dorey, J.-M., d'Amato, T., Tamouza, R., et al. (2020). Overexpression of complement component C4 in the dorsolateral prefrontal cortex, parietal cortex, superior temporal gyrus and associative striatum of patients with schizophrenia. *Brain Behav. Immun.* 90, 216–225. doi: 10.1016/j.bbi.2020.08.019

Reyes, S., Fu, Y., Double, K. L., Cottam, V., Thompson, L. H., Kirik, D., et al. (2013). Trophic factors differentiate dopamine neurons vulnerable to Parkinson's disease. *Neurobiol. Aging* 34, 873–886. doi: 10.1016/j.neurobiolaging.2012.07.019

Reynolds, L. M., and Flores, C. (2019). Guidance cues: linking drug use in adolescence with psychiatric disorders. *Neuropsychopharmacology* 44, 225–226. doi: 10.1038/s41386-018-0221-7

Reynolds, L. M., and Flores, C. (2021). "Adolescent dopamine development: connecting experience with vulnerability or resilience to psychiatric disease," in *Diagnosis, Management and Modeling of Neurodevelopmental Disorders*, eds C. R. Martin, V. R. Preedy and R. Rajendram (Cambridge, MA: Academic Press).

Reynolds, L. M., Gifuni, A. J., McCrea, E. T., Shizgal, P., and Flores, C. (2016). dcc haploinsufficiency results in blunted sensitivity to cocaine enhancement of reward seeking. *Behav. Brain Res.* 298, 27–31. doi: 10.1016/j.bbr.2015.05.020

Reynolds, L. M., Makowski, C. S., Yogendran, S. V., Kiessling, S., Cermakian, N., and Flores, C. (2015). Amphetamine in adolescence disrupts the development of medial prefrontal cortex dopamine connectivity in a dcc-dependent manner. *Neuropsychopharmacology* 40, 1101–1112. doi: 10.1038/npp.2014.287

Reynolds, L. M., Pokinko, M., Torres-Berrío, A., Cuesta, S., Lambert, L. C., Pellitero, E. D. C., et al. (2018). DCC receptors drive prefrontal cortex maturation by determining dopamine axon targeting in adolescence. *Biol. Psychiatry* 83, 181–192. doi: 10.1016/j.biopsych.2017.06.009

Reynolds, L. M., Yetnikoff, L., Pokinko, M., Wodzinski, M., Epelbaum, J. G., Lambert, L. C., et al. (2019). Early adolescence is a critical period for the maturation of inhibitory behavior. *Cereb. Cortex* 29, 3676–3686. doi: 10.1093/cercor/bhy247

Riddle, R., and Pollock, J. D. (2003). Making connections: the development of mesencephalic dopaminergic neurons. *Dev. Brain Res.* 147, 3–21. doi: 10.1016/j.devbrainres.2003.09.010

Rivera-Garcia, M. T., McCane, A. M., Chowdhury, T. G., Wallin-Miller, K. G., and Moghaddam, B. (2020). Sex and strain differences in dynamic and static

properties of the mesolimbic dopamine system. *Neuropsychopharmacology* 45, 2079–2086. doi: 10.1038/s41386-020-0765-1

Roeper, J. (2013). Dissecting the diversity of midbrain dopamine neurons. *Trends Neurosci.* 36, 336–342. doi: 10.1016/j.tins.2013.03.003

Rosenberg, D. R., and Lewis, D. A. (1994). Changes in the dopaminergic innervation of monkey prefrontal cortex during late postnatal development: a tyrosine hydroxylase immunohistochemical study. *Biol. Psychiatry* 36, 272–277. doi: 10.1016/0006-3223(94)90610-6

Rosenberg, D. R., and Lewis, D. A. (1995). Postnatal maturation of the dopaminergic innervation of monkey prefrontal and motor cortices: a tyrosine hydroxylase immunohistochemical analysis. *J. Comp. Neurol.* 358, 383–400. doi: 10.1002/cne.903580306

Rothmond, D. A., Weickert, C. S., and Webster, M. J. (2012). Developmental changes in human dopamine neurotransmission: cortical receptors and terminators. *BMC Neurosci.* 13:18. doi: 10.1186/1471-2202-13-18

Sannino, S., Padula, M. C., Manago, F., Schaer, M., Schneider, M., Armando, M., et al. (2017). Adolescence is the starting point of sex-dichotomous COMT genetic effects. *Transl. Psychiatry* 7:e1141. doi: 10.1038/tp.2017.109

Santana, N., Mengod, G., and Artigas, F. (2009). Quantitative analysis of the expression of dopamine D1 and D2 receptors in pyramidal and GABAergic neurons of the rat prefrontal cortex. *Cereb. Cortex* 19, 849–860. doi: 10.1093/cercor/bhn134

Sawyer, S. M., Azzopardi, P. S., Wickremarathne, D., and Patton, G. C. (2018). The age of adolescence. *Lancet Child Adolesc. Health* 2, 223–228. doi: 10.1016/S2352-4642(18)30022-1

Schafer, D. P., Lehrman, E. K., Kautzman, A. G., Koyama, R., Mardinly, A. R., Yamasaki, R., et al. (2012). Microglia sculpt postnatal neural circuits in an activity and complement-dependent manner. *Neuron* 74, 691–705. doi: 10.1016/j.neuron.2012.03.026

Schambra, U. B., Duncan, G. E., Breese, G. R., Fornaretto, M. G., Caron, M. G., and Fremeau, R. T. (1994). Ontogeny of D1a and D2 dopamine receptor subtypes in rat brain using in situ hybridization and receptor binding. *Neuroscience* 62, 65–85. doi: 10.1016/0306-4522(94)90315-8

Schneider, M. (2013). Adolescence as a vulnerable period to alter rodent behavior. *Cell Tissue Res.* 354, 99–106. doi: 10.1007/s00441-013-1581-2

Schultz, W. (2007). Behavioral dopamine signals. *Trends Neurosci.* 30, 203–210. doi: 10.1016/j.tins.2007.03.007

Schwarz, J. M., and Bilbo, S. D. (2012). Sex, glia, and development: interactions in health and disease. *Horm. Behav.* 62, 243–253. doi: 10.1016/j.yhbeh.2012.02.018

Schwarz, J. M., and Bilbo, S. D. (2013). Adolescent morphine exposure affects long-term microglial function and later-life relapse liability in a model of addiction. *J. Neurosci.* 33, 961–971. doi: 10.1523/JNEUROSCI.2516-12.2013

Seamans, J. K., Gorelova, N., Durstewitz, D., and Yang, C. R. (2001). Bidirectional dopamine modulation of GABAergic inhibition in prefrontal cortical pyramidal neurons. *J. Neurosci.* 21, 3628–3638. doi: 10.1523/JNEUROSCI.21-10-03628.2001

Seamans, J. K., and Yang, C. R. (2004). The principal features and mechanisms of dopamine modulation in the prefrontal cortex. *Prog. Neurobiol.* 74, 1–58. doi: 10.1016/j.pneurobio.2004.05.006

Seeman, P., Bzowej, N. H., Guan, H. -C., Bergeron, C., Becker, L. E., Reynolds, G. P., et al. (1987). Human brain dopamine receptors in children and aging adults. *Synapse* 1, 399–404. doi: 10.1002/syn.890010503

Séguéla, P., Watkins, K. C., and Descarries, L. (1988). Ultrastructural features of dopamine axon terminals in the anteromedial and the suprarhinal cortex of adult rat. *Brain Res.* 442, 11–22. doi: 10.1016/0006-8993(88)91427-8

Sekar, A., Bialas, A. R., de Rivera, H., Davis, A., Hammond, T. R., Kamitaki, N., et al. (2016). Schizophrenia risk from complex variation of complement component 4. *Nature* 530, 177–183. doi: 10.1038/nature16549

Sellgren, C. M., Gracias, J., Watmuff, B., Biag, J. D., Thanos, J. M., Whittredge, P. B., et al. (2019). Increased synapse elimination by microglia in schizophrenia patient-derived models of synaptic pruning. *Nat. Neurosci.* 22, 374–385. doi: 10.1038/s41593-018-0334-7

Sesack, S. R., and Grace, A. A. (2010). Cortico-Basal Ganglia reward network: microcircuitry. *Neuropsychopharmacology* 35, 27–47. doi: 10.1038/npp.2009.93

Sesack, S. R., Hawrylak, V. A., Melchitzky, D. S., and Lewis, D. A. (1998). Dopamine innervation of a subclass of local circuit neurons in monkey prefrontal cortex: ultrastructural analysis of tyrosine hydroxylase and parvalbumin immunoreactive structures. *Cereb. Cortex* 8, 614–622. doi: 10.1093/cercor/8.7.614

Sesack, S. R., Snyder, C. L., and Lewis, D. A. (1995). Axon terminals immunolabeled for dopamine or tyrosine hydroxylase synapse on GABA-immunoreactive dendrites in rat and monkey cortex. *J. Comp. Neurol.* 363, 264–280. doi: 10.1002/cne.903630208

Shansky, R. M., and Murphy, A. Z. (2021). Considering sex as a biological variable will require a global shift in science culture. *Nat. Neurosci.* 24, 457–464.doi: 10.1038/s41593-021-00806-8

Shatzmiller, R. A., Goldman, J. S., Simard-Emond, L., Rymar, V., Manitt, C., Sadikot, A. F., et al. (2008). Graded expression of netrin-1 by specific neuronal subtypes in the adult mammalian striatum. *Neuroscience* 157, 621–636. doi: 10.1016/j.neuroscience.2008.09.031

Smith, Y., Bevan, M. D., Shink, E., and Bolam, J. P. (1998). Microcircuitry of the direct and indirect pathways of the basal ganglia. *Neuroscience* 86, 353–387. doi: 10.1016/s0306-4522(98)00004-9

Soto, P. L., Wilcox, K. M., Zhou, Y., Ator, N. A., Riddle, M. A., Wong, D. F., et al. (2012). Long-term exposure to oral methylphenidate or dl-amphetamine mixture in peri-adolescent rhesus monkeys: effects on physiology, behavior, and dopamine system development. *Neuropsychopharmacology* 37, 2566–2579. doi: 10.1038/npp.2012.119

Spear, L. P. (2000). The adolescent brain and age-related behavioral manifestations. *Neurosci. Biobehav. Rev.* 24, 417–463. doi: 10.1016/s0149-7634(00)00014-2

Stoeckli, E. T., and Landmesser, L. T. (1998). Axon guidance at choice points. *Curr. Opin. Neurobiol.* 8, 73–79. doi: 10.1016/s0959-4388(98)80010-x

Swanson, L. W. (1982). The projections of the ventral tegmental area and adjacent regions: a combined fluorescent retrograde tracer and immunofluorescence study in the rat. *Brain Res. Bull.* 9, 321–353. doi: 10.1016/0361-9230(82)90145-9

Tarazi, F. I., and Baldessarini, R. J. (2000). Comparative postnatal development of dopamine D1, D2 and D4 receptors in rat forebrain. *Int. J. Dev. Neurosci.* 18, 29–37. doi: 10.1016/s0736-5748(99)00108-2

Tarazi, F. I., Tomasini, E. C., and Baldessarini, R. (1999). Postnatal development of dopamine D_1-like receptors in rat cortical and striatolimbic brain regions: an autoradiographic study. *Dev. Neurosci.* 21, 43–49. doi: 10.1159/000017365

Tarazi, F. I., Tomasini, E. C., and Baldessarini, R. J. (1998). Postnatal development of dopamine D4-like receptors in rat forebrain regions: comparison with D2-like receptors. *Dev. Brain Res.* 110, 227–233. doi: 10.1016/s0165-3806(98)00111-4

Teicher, M. H., Andersen, S. L., and Hostetter, J. C. Jr. (1995). Evidence for dopamine receptor pruning between adolescence and adulthood in striatum but not nucleus accumbens. *Dev. Brain Res.* 89, 167–172. doi: 10.1016/0165-3806(95)00109-q

Tepper, J. M., Sharpe, N. A., Koós, T. Z., and Trent, F. (1998). Postnatal development of the rat neostriatum: electrophysiological, light- and electron-microscopic studies. *Dev. Neurosci.* 20, 125–145. doi: 10.1159/000017308

Tepper, J. M., and Trent, F. (1993). Chapter 3 in vivo studies of the postnatal development of rat neostriatal neurons. *Prog. Brain Res.* 99, 35–50. doi: 10.1016/s0079-6123(08)61337-0

Thibault, D., Loustalot, F., Fortin, G. M., Bourque, M.-J., and Trudeau, L.-É. (2013). Evaluation of D1 and D2 dopamine receptor segregation in the developing striatum using BAC transgenic mice. *PLoS One* 8:e67219. doi: 10.1371/journal.pone.0067219

Tirelli, E., Laviola, G., and Adriani, W. (2003). Ontogenesis of behavioral sensitization and conditioned place preference induced by psychostimulants in laboratory rodents. *Neurosci. Biobehav. Rev.* 27, 163–178. doi: 10.1016/s0149-7634(03)00018-6

Torres-Berrío, A., Hernandez, G., Nestler, E. J., and Flores, C. (2020a). The Netrin-1/DCC guidance cue pathway as a molecular target in depression: translational evidence. *Biol. Psychiatry* 88, 611–624. doi: 10.1016/j.biopsych.2020.04.025

Torres-Berrío, A., Morgunova, A., Giroux, M., Cuesta, S., Nestler, E. J., and Flores, C. (2020b). miR-218 in adolescence predicts and mediates vulnerability to stress. *Biol. Psychiatry* 89, 911–919. doi: 10.1016/j.biopsych.2020.10.015

Trantham-Davidson, H., Neely, L. C., Lavin, A., and Seamans, J. K. (2004). Mechanisms underlying differential D1 versus D2 dopamine receptor regulation of inhibition in prefrontal cortex. *J. Neurosci.* 24, 10652–10659. doi: 10.1523/JNEUROSCI.3179-04.2004

Tritsch, N. X., and Sabatini, B. L. (2012). Dopaminergic modulation of synaptic transmission in cortex and striatum. *Neuron* 76, 33–50. doi: 10.1016/j.neuron.2012.09.023

Tseng, K. Y., and O'Donnell, P. (2005). Post-pubertal emergence of prefrontal cortical up states induced by D1-NMDA co-activation. *Cereb. Cortex* 15, 49–57. doi: 10.1093/cercor/bhh107

Tseng, K.-Y., and O'Donnell, P. (2007). Dopamine modulation of prefrontal cortical interneurons changes during adolescence. *Cereb. Cortex* 17, 1235–1240. doi: 10.1093/cercor/bhl034

VanRyzin, J. W., Marquardt, A. E., Pickett, L. A., and McCarthy, M. M. (2020). Microglia and sexual differentiation of the developing brain: a focus on extrinsic factors. *Glia* 68, 1100–1113. doi: 10.1002/glia.23740

VanRyzin, J. W., Pickett, L. A., and McCarthy, M. M. (2018). Microglia: driving critical periods and sexual differentiation of the brain. *Dev. Neurobiol.* 78, 580–592. doi: 10.1002/dneu.22569

Vassilev, P., Pantoja-Urban, A. H., Giroux, M., Nouel, D., Hernandez, G., Orsini, T., et al. (2021). Unique effects of social defeat stress in adolescent male mice on the Netrin-1/DCC pathway, prefrontal cortex dopamine and cognition (Social stress in adolescent vs. adult male mice). *eNeuro* 2:ENEURO.0045–21.2021. doi: 10.1523/ENEURO.0045-21.2021

Verney, C., Alvarez, C., Geffard, M., and Berger, B. (1990). Ultrastructural double-labelling study of dopamine terminals and GABA-containing neurons in rat anteromedial cerebral cortex. *Eur. J. Neurosci.* 2, 960–972. doi: 10.1111/j.1460-9568.1990.tb00008.x

Verney, C., Berger, B., Adrien, J., Vigny, A., and Gay, M. (1982). Development of the dopaminergic innervation of the rat cerebral cortex. A light microscopic immunocytochemical study using anti-tyrosine hydroxylase antibodies. *Dev. Brain Res.* 5, 41–52. doi: 10.1016/0165-3806(82)90111-0

Vetter-O'Hagen, C. S., and Spear, L. P. (2012). Hormonal and physical markers of puberty and their relationship to adolescent-typical novelty-directed behavior. *Dev. Psychobiol.* 54, 523–535. doi: 10.1007/s00248-021-01809-5

Vincent, S. L., Khan, Y., and Benes, F. M. (1995). Cellular colocalization of dopamine D1 and D2 receptors in rat medial prefrontal cortex. *Synapse* 19, 112–120. doi: 10.1002/syn.890190207

Voorn, P., Kalsbeek, A., Jorritsma-Byham, B., and Groenewegen, H. J. (1988). The pre- and postnatal development of the dopaminergic cell groups in the ventral mesencephalon and the dopaminergic innervation of the striatum of the rat. *Neuroscience* 25, 857–887. doi: 10.1016/0306-4522(88)90041-3

Vosberg, D. E., Leyton, M., and Flores, C. (2019). The Netrin-1/DCC guidance system: dopamine pathway maturation and psychiatric disorders emerging in adolescence. *Mol. Psychiatry* 25, 297–307. doi: 10.1038/s41380-019-0561-7

Wahlstrom, D., Collins, P., White, T., and Luciana, M. (2010). Developmental changes in dopamine neurotransmission in adolescence: behavioral implications and issues in assessment. *Brain Cogn.* 72, 146–159. doi: 10.1016/j.bandc.2009.10.013

Walker, D. M., Bell, M. R., Flores, C., Gulley, J. M., Willing, J., and Paul, M. J. (2017). Adolescence and reward: making sense of neural and behavioral changes amid the chaos. *J. Neurosci.* 37, 10855–10866. doi: 10.1523/JNEUROSCI.1834-17.2017

Wang, Q., Ding, S.-L., Li, Y., Royall, J., Feng, D., Lesnar, P., et al. (2020). The allen mouse brain common coordinate framework: a 3D reference atlas. *Cell* 181, 936–953.e20. doi: 10.1016/j.cell.2020.04.007

Weickert, C. S., Webster, M. J., Gondipalli, P., Rothmond, D., Fatula, R. J., Herman, M. M., et al. (2007). Postnatal alterations in dopaminergic markers in the human prefrontal cortex. *Neuroscience* 144, 1109–1119. doi: 10.1016/j.neuroscience.2006.10.009

Willing, J., Cortes, L. R., Brodsky, J. M., Kim, T., and Juraska, J. M. (2017). Innervation of the medial prefrontal cortex by tyrosine hydroxylase immunoreactive fibers during adolescence in male and female rats. *Dev. Psychobiol.* 59, 583–589. doi: 10.1002/dev.21525

Wise, R. A. (2004). Dopamine, learning and motivation. *Nat. Rev. Neurosci.* 5, 483–494. doi: 10.1038/nrn1406

Xiao, L., and Becker, J. B. (1994). Quantitative microdialysis determination of extracellular striatal dopamine concentration in male and female rats: effects of estrous cycle and gonadectomy. *Neurosci. Lett.* 180, 155–158. doi: 10.1016/0304-3940(94)90510-x

Yetnikoff, L., Almey, A., Arvanitogiannis, A., and Flores, C. (2011). Abolition of the behavioral phenotype of adult netrin-1 receptor deficient mice by exposure to amphetamine during the juvenile period. *Psychopharmacology* 217, 505–514. doi: 10.1007/s00213-011-2312-6

Yetnikoff, L., Labelle-Dumais, C., and Flores, C. (2007). Regulation of netrin-1 receptors by amphetamine in the adult brain. *Neuroscience* 150, 764–773. doi: 10.1016/j.neuroscience.2007.09.069

Yetnikoff, L., Lavezzi, H. N., Reichard, R. A., and Zahm, D. S. (2014a). An update on the connections of the ventral mesencephalic dopaminergic complex. *Neuroscience* 282, 23–48. doi: 10.1016/j.neuroscience.2014.04.010

Yetnikoff, L., Pokinko, M., Arvanitogiannis, A., and Flores, C. (2014b). Adolescence: a time of transition for the phenotype of dcc heterozygous mice. *Psychopharmacology* 231, 1705–1714. doi: 10.1007/s00213-013-3083-z

Yetnikoff, L., Reichard, R. A., Schwartz, Z. M., Parsely, K. P., and Zahm, D. S. (2014c). Protracted maturation of forebrain afferent connections of the ventral tegmental area in the rat. *J. Comp. Neurol.* 522, 1031–1047. doi: 10.1002/cne.23459

Yilmaz, M., Yalcin, E., Presumey, J., Aw, E., Ma, M., Whelan, C. W., et al. (2021). Overexpression of schizophrenia susceptibility factor human complement C4A promotes excessive synaptic loss and behavioral changes in mice. *Nat. Neurosci.* 24, 214–224. doi: 10.1038/s41593-020-00763-8

Yoest, K. E., Cummings, J. A., and Becker, J. B. (2019). Oestradiol influences on dopamine release from the nucleus accumbens shell: sex differences and the role of selective oestradiol receptor subtypes. *Br. J. Pharmacol.* 176, 4136–4148. doi: 10.1111/bph.14531

Yokokura, M., Takebasashi, K., Takao, A., Nakaizumi, K., Yoshikawa, E., Futatsubashi, M., et al. (2020). in vivo imaging of dopamine D1 receptor and activated microglia in attention-deficit/hyperactivity disorder: a positron emission tomography study. *Mol. Psychiatry* doi: 10.1038/s41380-020-0784-7. [Epub ahead of print].

Zachry, J. E., Nolan, S. O., Brady, L. J., Kelly, S. J., Siciliano, C. A., and Calipari, E. S. (2020). Sex differences in dopamine release regulation in the striatum. *Neuropsychopharmacology* 46, 491–499. doi: 10.1038/s41386-020-00915-1

Zbukvic, I. C., Park, C. H. J., Ganella, D. E., Lawrence, A. J., and Kim, J. H. (2017). Prefrontal dopaminergic mechanisms of extinction in adolescence compared to adulthood in rats. *Front. Behav. Neurosci.* 11:32. doi: 10.3389/fnbeh.2017.00032

Zhan, Y., Paolicelli, R. C., Sforazzini, F., Weinhard, L., Bolasco, G., Pagani, F., et al. (2014). Deficient neuron-microglia signaling results in impaired functional brain connectivity and social behavior. *Nat. Neurosci.* 17, 400–406. doi: 10.1038/nn.3641

Zhang, D., Yang, S., Yang, C., Jin, G., and Zhen, X. (2008). Estrogen regulates responses of dopamine neurons in the ventral tegmental area to cocaine. *Psychopharmacology* 199, 625–635. doi: 10.1007/s00213-008-1188-6

Zhang, Y., Xu, H., Zhang, F., Shao, F., Ellenbroek, B., Wang, J., et al. (2019). Deficiency of microglia and TNFα in the mPFC-mediated cognitive inflexibility induced by social stress during adolescence. *Brain Behav. Immun.* 79, 256–266. doi: 10.1016/j.bbi.2019.02.010

Zhao, B., Zhu, J., Dai, D., Xing, J., He, J., Fu, Z., et al. (2016). Differential dopaminergic regulation of inwardly rectifying potassium channel mediated subthreshold dynamics in striatal medium spiny neurons. *Neuropharmacology* 107, 396–410. doi: 10.1016/j.neuropharm.2016.03.037

Conflict of Interest: The authors declare that the research was conducted in the absence of any commercial or financial relationships that could be construed as a potential conflict of interest.

Publisher's Note: All claims expressed in this article are solely those of the authors and do not necessarily represent those of their affiliated organizations, or those of the publisher, the editors and the reviewers. Any product that may be evaluated in this article, or claim that may be made by its manufacturer, is not guaranteed or endorsed by the publisher.

Copyright © 2021 Reynolds and Flores. This is an open-access article distributed under the terms of the Creative Commons Attribution License (CC BY). The use, distribution or reproduction in other forums is permitted, provided the original author(s) and the copyright owner(s) are credited and that the original publication in this journal is cited, in accordance with accepted academic practice. No use, distribution or reproduction is permitted which does not comply with these terms.

frontiers in Neural Circuits

REVIEW
published: 12 October 2021
doi: 10.3389/fncir.2021.746582

The Development of the Mesoprefrontal Dopaminergic System in Health and Disease

K. Ushna S. Islam[1†], Norisa Meli[1,2†] and Sandra Blaess[1]*

[1] Neurodevelopmental Genetics, Institute of Reconstructive Neurobiology, Medical Faculty, University of Bonn, Bonn, Germany, [2] Institute of Neuropathology, Section for Translational Epilepsy Research, Medical Faculty, University of Bonn, Bonn, Germany

Midbrain dopaminergic neurons located in the substantia nigra and the ventral tegmental area are the main source of dopamine in the brain. They send out projections to a variety of forebrain structures, including dorsal striatum, nucleus accumbens, and prefrontal cortex (PFC), establishing the nigrostriatal, mesolimbic, and mesoprefrontal pathways, respectively. The dopaminergic input to the PFC is essential for the performance of higher cognitive functions such as working memory, attention, planning, and decision making. The gradual maturation of these cognitive skills during postnatal development correlates with the maturation of PFC local circuits, which undergo a lengthy functional remodeling process during the neonatal and adolescence stage. During this period, the mesoprefrontal dopaminergic innervation also matures: the fibers are rather sparse at prenatal stages and slowly increase in density during postnatal development to finally reach a stable pattern in early adulthood. Despite the prominent role of dopamine in the regulation of PFC function, relatively little is known about how the dopaminergic innervation is established in the PFC, whether and how it influences the maturation of local circuits and how exactly it facilitates cognitive functions in the PFC. In this review, we provide an overview of the development of the mesoprefrontal dopaminergic system in rodents and primates and discuss the role of altered dopaminergic signaling in neuropsychiatric and neurodevelopmental disorders.

Keywords: prefrontal cortex, innervation, dopamine receptors, neuropsychiatric diseases, ventral midbrain

OPEN ACCESS

Edited by:
Jean-Francois Poulin, McGill University, Canada

Reviewed by:
Leora Yetnikoff, College of Staten Island, United States
Raj Awatramani, Northwestern University, United States

***Correspondence:**
Sandra Blaess
sblaess@uni-bonn.de

[†] These authors have contributed equally to this work

Received: *24 July 2021*
Accepted: *10 September 2021*
Published: *12 October 2021*

Citation:
Islam KUS, Meli N and Blaess S (2021) The Development of the Mesoprefrontal Dopaminergic System in Health and Disease. Front. Neural Circuits 15:746582. doi: 10.3389/fncir.2021.746582

MESOPREFRONTAL DOPAMINERGIC NEURONS

Midbrain dopaminergic (mDA) neurons modulate many brain functions including voluntary movement, reward behavior, and cognitive processes (Iversen et al., 2009). Degeneration of a subset of mDA neurons underlies the motor deficits in Parkinson's disease, while altered dopamine (DA) transmission is implicated in neuropsychiatric disorders including depression, schizophrenia, autism, ADHD, and substance abuse (Del Campo et al., 2011; Volkow and Morales, 2015; Grace, 2016; Surmeier et al., 2017; Marotta et al., 2020; Sonnenschein et al., 2020). mDA neurons are located in the ventral midbrain where they form the A8, A9, and A10 group. The A10 neurons are located in the ventral tegmental area (VTA) and linear nucleus (LiN), the A9 neurons in the substantia nigra pars compacta (SNpc) and substantia nigra pars lateralis (SNl), while the A8 group is found in the retrorubral field (RRF). mDA neuronal projections run through the medial forebrain bundle (MFB) and then diverge into the various forebrain target areas, including dorsal striatum, amygdala, nucleus accumbens, olfactory tubercle, and prefrontal cortex (PFC)

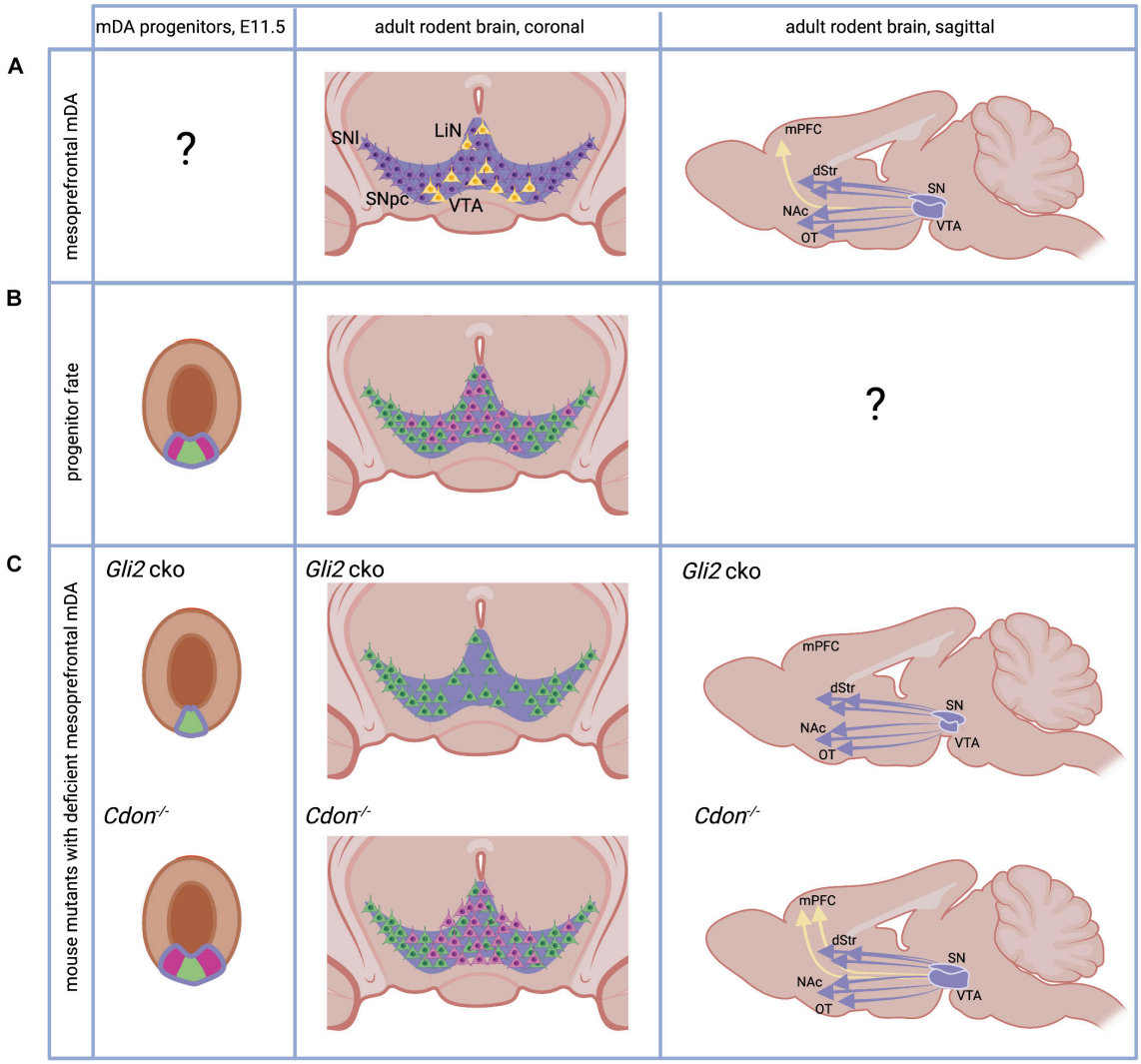

FIGURE 1 | The adult and developing mesoprefrontal DA system in rodents**. (A)** Localization of mesoprefrontal mDA neurons (yellow) in the adult ventral midbrain (coronal view) and their projections (yellow arrow) to the adult medial PFC (mPFC, sagittal view). Non-mesoprefrontal mDA neurons and projections are in purple. Note that it is unknown whether there are specific mesoprefrontal mDA progenitors (indicated by "?"). **(B)** The mDA progenitor domain (purple outline) is divided in a medial (green) and lateral (pink) domain based on gene expression. Progenitors from these two domains give rise to mDA neurons with different anatomical location in the adult brain (pink and green neurons in coronal view). Note that it has not been examined whether mDA progenitors from these two domains form specific subcircuits in the DA system (indicated by "?"). **(C)** Mice with alterations in the SHH signaling pathway have an altered mesoprefrontal DA system. Conditional inactivation of GLI2 (*Gli2* cko) results in loss of the lateral progenitor domain, a reduced number of VTA neurons and loss of mesoprefrontal DA projections. Inactivation of CDON (*Cdon*$^{-/-}$) results in increased proliferation of mDA progenitors, an increased number of VTA neurons and increased DA release in the mPFC. See main text for details. dStr, dorsal striatum, NAc, nucleus accumbens, OT, olfactory tubercle. Created with BioRender.com.

(Iversen et al., 2009; **Figure 1A**). In recent years, molecularly distinct mDA subpopulations as well as anatomically and physiologically discrete DA circuits and their effects on various aspects of behavior have been studied in increasing detail, driven by rapid advances in single-cell gene expression profiling, viral tracing systems, DA sensors, and opto- and chemogenetic techniques (e.g., Lammel et al., 2011; Beier et al., 2015; Menegas et al., 2018; Poulin et al., 2018, 2020; Saunders et al., 2018; Engelhard et al., 2019; Lee et al., 2021). Based on these and numerous other studies, it is now evident that the DA system is composed of diverse populations of mDA neurons and that this diversity is critical for the various functional performances of the DA system. In this review, we focus specifically on the mesoprefrontal DA system, which is formed by mDA neurons that project to the PFC.

In the adult rodent brain, mesoprefrontal mDA neurons are primarily localized in the medial and ventral VTA region and LiN (Lammel et al., 2011; Yamaguchi et al., 2011; **Figure 1A**). These mesoprefrontal mDA neurons differ in their molecular profile (e.g., express low levels of dopamine transporter) and in their electrophysiological properties from other mDA neurons, indicating that they form a distinct subclass of mDA neurons

(Lammel et al., 2011). This is supported by tracing studies in rodents that show that mesoprefrontal mDA neurons do not send extensive collaterals to other forebrain areas (Aransay et al., 2015; Beier et al., 2019). On a functional level, it has been demonstrated that aversion is encoded by mesoprefrontal mDA neurons while mDA neurons projecting to the nucleus accumbens encode reward. These distinct functions are associated with distinct inputs: aversion-encoding mesoprefrontal mDA neurons receive inputs from the lateral habenula, while the reward-encoding mDA neurons are activated by inputs from the lateral-dorsal tegmentum (Lammel et al., 2012). It is important to note that a substantial fraction of these mesoprefrontal mDA neurons co-express *Slc17a6* (the gene encoding the vesicular glutamate transporter 2, vGLUT2) indicating that they have the ability to co-release the neurotransmitter glutamate (Yamaguchi et al., 2011; Poulin et al., 2018). In the primate brain, the results of a recent viral tracing study in macaques suggest that mDA neurons in the medial VTA may be the main source of DA innervation to the PFC, whereas lateral VTA or medial SNpc mDA neurons are more likely to send projections to motor and somatosensory cortices (Zubair et al., 2021). An analysis of *SLC17A6* expression in marmosets and humans demonstrates that mDA neurons in the lateral VTA and LiN co-express vGLUT2 also in primates, but whether these co-expressing cells are part of the mesoprefrontal DA system is unknown (Root et al., 2016).

At the functional level, decades of research have shown that the mesoprefrontal DA system exerts a profound modulatory function on the PFC and strongly influences PFC-mediated executive functions (i.e., working memory, decision making, behavioral flexibility) and PFC-regulated behaviors (goal-directed behavior, approach-avoidance behavior, response to stress or pain). Since the focus of this review is the development of the mesoprefrontal system, we refer the interested reader to some recent reviews covering the functional aspects of the mesoprefrontal DA system (Weele et al., 2018; Pastor and Medina, 2021; Starkweather and Uchida, 2021).

PREFRONTAL CORTEX IN RODENTS AND PRIMATES

Before discussing the organization of the mesoprefrontal system and its development in more detail, we will briefly describe how we define the terms PFC and medial PFC (mPFC) in rodents and primates in the context of this review. There is still no consensus on what constitutes the PFC, especially since there is disagreement regarding the subdivisions of prefrontal cortical areas in different species. Functionally, the human PFC is subdivided into dorsolateral, dorsomedial, ventrolateral, ventromedial, and orbital prefrontal cortex. These areas are mostly granular, showing a six-layered laminar organization with a distinct granular layer IV. However, some parts of the primate PFC consist of dysgranular cortex with an indistinct layer IV or agranular cortex in which layer IV is completely absent, such as the anterior cingulate cortex. In contrast, all frontal cortical areas are agranular in rodents, thus lacking the subdivision into granular and dysgranular cortices (Carlén, 2017; Laubach et al., 2018). Nevertheless, functional data suggest that the prelimbic, infralimbic, and anterior cingulate cortices of rodent frontal cortex have functions that are attributed to the dorsolateral PFC and anterior cingulate cortices in primates (Uylings et al., 2003; Seamans et al., 2008). These regions are classified as prefrontal in rodents. Because these areas are located in the medial frontal cortex in both rodents and primates, they are referred to as the mPFC (Laubach et al., 2018). We therefore use the term mPFC to describe the prelimbic, infralimbic, and anterior cingulate cortex in rodents. The cingulate cortex that extends from the genu of corpus callosum caudally, the anatomical region immediately posterior to the mPFC, is referred to as caudal cingulate cortex in our review. For studies in primates and rodents in which the prefrontal subregions are not specified in terms of the above definitions, we followed the terminologies used in the original publications.

DEVELOPMENT OF THE PREFRONTAL CORTEX

The cerebral cortex exhibits an orderly laminar organization that is established during embryonic development. While the PFC is the last cortical area to fully mature in terms of inputs and local microcircuits, there is no clear evidence that the timing of early cortical development (neurogenesis, layer formation) is markedly different from other cortical areas. Two recent reviews have discussed in detail the development of the PFC in anatomical and functional terms (Schubert et al., 2015; Chini and Hanganu-Opatz, 2020). The basic steps of corticogenesis are summarized in **Supplementary Figure 1**.

In the next paragraphs, we will focus on the development of the mesoprefrontal DA system in rodents and primates. For a detailed account of the general development of the rodent DA system see the following reviews (Blaess and Ang, 2015; Brignani and Pasterkamp, 2017; Ásgrímsdóttir and Arenas, 2020).

THE DOPAMINERGIC PROGENITOR DOMAIN – SPECIFIC PROGENITORS FOR MESOPREFRONTAL DOPAMINERGIC NEURONS?

Midbrain dopaminergic neurons develop from progenitors in the floor plate of the ventral midbrain. The floor plate, located in the ventral midline of the neural tube, is different from the surrounding neuroepithelia tissue in the neural tube since: (1) its lineage diverges from the neuroepithelia fate quite early, and (2) it serves as one of the organizing centers in the development of the midbrain, by secreting the ventralizing factor Sonic Hedgehog (SHH) (Bodea and Blaess, 2015). The expression of *Shh* in the midbrain floor plate is dynamic (Joksimovic et al., 2009; Blaess et al., 2011; Hayes et al., 2011). Initially, around E8.0 in mice, *Shh* is expressed only in the notochord, a mesodermal structure underlying the ventral neural tube. Cells in the midline of the forming neural tube respond to SHH signaling. This response can be visualized by the presence of *Gli1,* a transcription

factor in the SHH signaling pathway only expressed in cells that receive high levels of SHH signaling. SHH-responding cells are specified into floor plate cells, characterized by the expression of the transcription factor FOXA2 (Forkhead box A2). The FOXA2-positive floor plate cells stop responding to SHH signaling but start to secret SHH themselves and induce floor plate fate in neighboring cells. This process continues until E10.5, when the middle third of the ventral midbrain has been transformed into FOXA2-expressing cells. Within the floor plate domain, the medial area expresses the transcription factor LMX1A (LIM homeobox transcription factor 1 alpha) and this is the region that eventually gives rise to mDA neurons (Andersson et al., 2006; **Figure 1B**). This LMX1A-expressing domain can be further subdivided into a medial and lateral domain based on gene expression. For example, it has been shown that OTX2 (Orthodenticle Homeobox 2) and NOLZ1 (also known as ZNF503) are restricted to the lateral domain, while SOX6 (sex determining region Y (SRY)-box 6) is expressed in medial progenitors (Panman et al., 2014; **Figure 1B**). Fate-mapping studies of medial and lateral domain progenitors come to conflicting results about their contribution to different anatomical domains of the DA system in the adult brain (Poulin et al., 2020), but several lines of evidence suggest that the medial progenitor domain is biased to give rise to neurons of the SNpc and the lateral VTA while the lateral progenitor domain gives rise to the medial VTA (Blaess et al., 2011; Hayes et al., 2011; Panman et al., 2014; **Figure 1B**). SHH signaling is essential for the induction of the mDA progenitor domain, but SHH signaling is required longer for induction of the lateral progenitor domain than for induction of the medial domain. This is evident from *Gli1* expression, the above-mentioned readout for high-level SHH signaling, which is downregulated first in the medial and then in the lateral domain. Thus, conditional inactivation of the transcription factor GLI2 downstream of the SHH pathway in the midbrain around E8.5 (*Gli2* conditional ko mice) essentially abolishes SHH signaling activity in the ventral midbrain. Since the medial domain no longer requires SHH for its induction at this time point, it is formed, albeit at a smaller size. In contrast, the lateral mDA progenitor domain is almost completely absent. In the brain of adult *Gli2* conditional ko mice, the number of mDA neurons in the medial VTA is severely reduced and projections to the mPFC are absent, while projections to other VTA or SNpc target areas are not overtly reduced (Kabanova et al., 2015; **Figure 1C**). Interestingly, inactivation of the gene encoding CDON (Cell adhesion molecule-related/downregulated by oncogenes), a co-receptor of the SHH receptor Patched 1 that modulates SHH pathway activity and is expressed in mDA progenitors, leads to the opposite result: the number of proliferating mDA progenitors is increased and so is the number of mDA neurons in the VTA in the adult brain. The number of mDA neurons in the SN is not significantly altered. The increase in VTA-mDA neurons goes along with increased DA release and a higher number of DA presynaptic sites in the mPFC, an effect that is not observed in other target areas of the VTA (Verwey et al., 2016; **Figure 1C**). Importantly, the function of SHH signaling in cell fate specification in the ventral midbrain can be largely pinpointed to its role in mDA progenitors. GLI transcription factors, which are essential for SHH downstream signaling, are not expressed in differentiated mDA neurons and accordingly *Gli1,* the readout for the activated pathway, is not detected in differentiated mDA neurons (Mesman et al., 2014). In summary, these studies suggest that SHH signaling is required after E8.5 in the developing mouse brain to induce the lateral mDA progenitor domain and that this domain contains the progenitors that give rise to mesoprefrontal mDA neurons.

DIFFERENTIATION ONSET OF MIDBRAIN DOPAMINERGIC NEURONS - LATE BIRTH DATE OF MESOPREFRONTAL DOPAMINERGIC NEURONS?

In mouse, cell cycle exit of mDA neurons starts at around E10 and continues until about E14.5 (Bayer et al., 1995; Bye et al., 2012). Expression of tyrosine hydroxylase (TH), the rate limiting enzyme of the DA synthesis pathway is first observed between E10 and E10.5 (Dumas and Wallén-Mackenzie, 2019). Besides the evidence for spatial distinct progenitor domains described in the previous paragraph, there is also evidence that specific mDA subpopulations differ in their birth date (i.e., differentiation onset). In mice, the peak of cell cycle exit occurs earlier for mDA neurons of the SNpc (around E10.5) than for the ones forming the VTA (around E11.5). This peak is shifted to an even later time point (E13.5) for the interfascicular nucleus in the ventromedial VTA (Bayer et al., 1995; Bye et al., 2012). A similar temporal sequence in mDA differentiation onset has been described in rat: SNpc neurons are born between E12.5 and E15.5, with a peak at E12.5; mDA neurons of the lateral VTA are born in the same period but with a peak at E13.5; and those of the medial VTA are generated between E13.5 and E16.5 with a peak around E15.5 (Altman and Bayer, 1981). Since mesoprefrontal mDA neurons are mostly located in the medial and ventral VTA in rodents (Yamaguchi et al., 2011), this could suggest that these neurons are born later than other mDA neurons. In primates, the development of the catecholaminergic system starts early in embryonic development and the onset of SNpc neuron generation is also earlier than the one for VTA neurons. In rhesus monkey, mDA neurons are detected during the first quarter of gestation [5–6 gestational weeks (gw)]. mDA neurons in the SNpc are generated first, between E36-E43, followed by mDA neurons in the VTA (E38-E43) (Levitt and Rakic, 1982). In humans, distinct TH-expressing cell populations can be detected along the rostrocaudal axis of the brain already at 6 gw (Freeman et al., 1991; Verney et al., 1991; Zecevic and Verney, 1995). At this stage, prominent regions with dense clusters of TH-expressing cells are found in the mesencephalon probably representing the anlage of the three different midbrain mDA groups: A8 caudally, A9 laterally, and A10 medially (**Figure 2**). Generally, the sequence of these early events in the developing DA system in rodents and primates are remarkably similar. However, the timing of these events is not synchronized across these species, considering their respective gestational lengths.

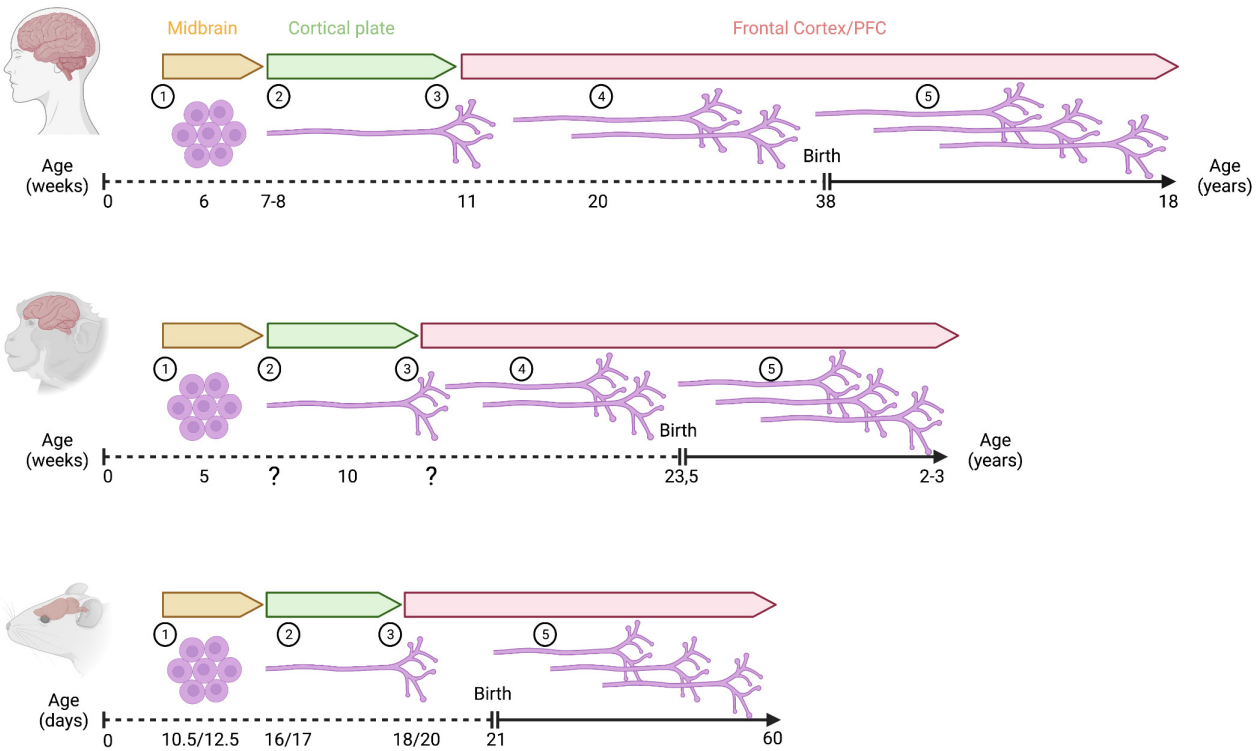

FIGURE 2 | Development of mesoprefrontal DA projections in primates and rodents. Critical developmental stages of the mesoprefrontal DA system are shown as follows: (1) onset of differentiation of dopaminergic neurons, (2) dopaminergic axons reach the cortical region, but do not yet enter into the developing cortical plate (3) dopaminergic axons innervate the cortical plate, (4) density of innervation increases during embryonic development (indicated by multiple axons), (5) density of innervation increases further during postnatal development (indicated by multiple axons). Note that the increase in innervation density occurs essentially only during the postnatal period in rodents. In primates, the timeline of prenatal development is shown in weeks, and the postnatal period is shown in years. In rodents, prenatal and postnatal stages are indicated in days (mouse/rat). Created with BioRender.com.

Based on a study that equates neurodevelopmental stages across mammalian species (Clancy et al., 2001), 6 gw in humans and 5 gw in macaques are considered earlier gestational timepoints than E10.5 in mice and E12.5 in rats (**Supplementary Figure 1**). Thus, the first appearance of TH-expressing neurons seems to occur earlier in primates than in rodents.

While these rodent and primate data indicate that mDA neurons in SNpc, lateral, and medial VTA differ in their onset of differentiation, there is as yet no clear evidence that birth date also correlates with mDA subpopulations with specific projection targets (e.g., in mice, are all mesoprefrontal mDA neurons born after E13.5, or all mDA neurons projecting to the nucleus accumbens born before E13.5?). Moreover, it is not known whether mesoprefrontal mDA neurons (and other mDA subpopulations defined by their projection targets) can be characterized by a particular gene expression profile (Poulin et al., 2020). *Slc17a6*, the gene encoding vGLUT2, is expressed in a subset of mesoprefrontal mDA neurons in the adult rodent brain but is not in itself a marker for this subset, as it is also expressed in a subpopulation of nucleus accumbens-projecting VTA-mDA neurons and in SNl-mDA neurons projecting to the tail of the striatum (Yamaguchi et al., 2011; Poulin et al., 2018). Interestingly, *Slc17a6* is broadly expressed in mDA neurons during development and only gets restricted to the above-mentioned mDA subtypes in the postnatal brain (Steinkellner et al., 2018; Dumas and Wallén-Mackenzie, 2019; Kouwenhoven et al., 2020). The expression of *Slc17a6* in mesoprefrontal mDA neurons in the adult mouse brain is consistent with data showing that a subset of these mDA neurons co-release glutamate in the PFC. This glutamate release primarily leads to the excitation of cortical interneurons (Kabanova et al., 2015; Mingote et al., 2015; Pérez-López et al., 2018; Zhong et al., 2020).

This restricted effect of mDA-mediated glutamate release on GABAergic interneurons, and in particular on a subset of fast-spiking interneurons, could contribute to the refinement of local PFC circuit function. One important component of the protracted functional remodeling process of the PFC during postnatal development is the maturation of these local circuits. This is thought to be largely driven by the maturation of GABAergic interneurons. These changes ultimately lead to the fine-tuning of the excitatory–inhibitory balance in the PFC, which is essential for its normal function (Caballero and Tseng, 2016). Rapid activation of GABAergic interneurons by mDA-mediated glutamate release could lead to the rapid inhibition of projection neurons in the PFC and regulate the sparseness and precision of their activation, thus acutely modulating the excitatory–inhibitory balance in PFC neuronal networks. In

contrast, the long-term processing dynamics of local circuits in the PFC could be modified by the long-lasting effect of DA. This target specificity of the glutamate effect is consistent with the results of a study in which it was shown that electrical stimulation in the VTA leads to glutamate-dependent feed-forward activation of interneurons in the PFC, whereas a form of DA-induced potentiation occurs over a much longer period (Lavin et al., 2005).

DEVELOPMENT OF THE MESOPREFRONTAL DOPAMINERGIC PROJECTIONS IN RODENTS

Several studies in rodents have followed the development of mDA projections and innervation of their forebrain targets by means of antibody labeling, directed either against DA or TH. Before we start to describe the development of mDA fibers in the PFC, it is necessary to briefly discuss the expression of DA and TH, the primary markers that have been used for this analysis. TH is the rate-limiting enzyme in DA synthesis and thus a marker for mDA neurons. Since DA is the direct precursor of noradrenaline, TH and DA are also present in noradrenergic (NA) neurons. Thus, TH and DA are markers for both DA and NA neurons. Since mDA neurons and NA neurons from the locus coeruleus send projections to the PFC (Levitt and Moore, 1979), TH or DA staining in the PFC should in principle detect both DA and NA axons. However, double immunohistochemistry for TH and Dopamine beta-hydroxylase (DBH, a specific marker for NA axons) in the prefrontal areas of adult human brain shows that approximately 15% of DBH-positive axons are also co-labeled with TH. In fetal brains, the overlap is even lower (ca. 5%) (Gaspar et al., 1989; Verney et al., 1993). These data suggest that, at least in humans, both during development and in the adult brain, TH immunoreactivity in axonal fibers is largely restricted to projections from mDA neurons. Nevertheless, when drawing conclusions from studies using TH or DA as markers for mDA projections in the PFC, it should be kept in mind that NA fibers may also be labeled to a certain extent.

In the adult rodent mPFC, there is a dense input of TH-positive fibers to the deep layers, while innervation of TH-expressing fibers is much sparser in the superficial layers of the mPFC, except for the caudal cingulate cortex, which also has dense TH-positive innervation in layers I-III (Kalsbeek et al., 1988; Naneix et al., 2012).

In the developing rodent brain, TH immunoreactivity reveals that mDA neurons in the ventral midbrain of rodents start to extend axonal processes between E11 and E12. In mice, axons initially grow slightly dorsally, but by E13, almost all axons follow a rostral course and by E13.5 form a TH-positive axon tract within the MFB, which is directed toward forebrain targets (Nakamura et al., 2000; Kolk et al., 2009). One day later in development, the TH-positive fiber tract reaches a region ventral to the ganglionic eminences (Kolk et al., 2009). Analysis of DA-positive fiber bundles in rats showed that they reach this region also around E14 (Kalsbeek et al., 1988; Voorn et al., 1988). In mice, while most of the TH-positive axons from the MFB begin to move dorsally to innervate the maturing striatum, a small number of fibers follows a rostrodorsal trajectory towards the frontal cortex. These TH-positive axons follow two paths to reach the mPFC. The larger TH bundle bends just before the olfactory bulb and extends toward the cortical subplate, while the smaller subset of TH axons passes through the striatum to the developing mPFC. The TH-positive fibers arrive in the subplate and marginal zone around E15 and continue to grow for about 2 days without entering the cortical plate, which develops and enlarges in the meantime. At E18.5, the first TH-positive axons are detected in the cortical plate (**Figure 2**). Tracing experiments with the lipophilic fluorescent dye DiI show that after microinjection of DiI into the mPFC at E16.5 and postnatal day (P)0, the dye is eventually detected in the rostral VTA. Conversely, after DiI microinjection into the rostromedial VTA, DiI-stained, TH-positive axons are found in the subplate at E16 and in the cortical plate at E18.5. However, no DiI-stained fibers are found in the marginal zone of the PFC in the latter experiment. Together, these data suggest that one subset of mesoprefrontal projections in mice originates in the rostral medial VTA, while a second subset originates from mDA neurons in another ventral midbrain region (Kolk et al., 2009). In rats, the TH-positive axons within the MFB also arrive in the mPFC in two separate bundles. At E18, one of the axonal bundles is observed above the subplate while the other axonal trail can be detected within the marginal zone. The DA fibers in the future mPFC adopt a coiled structure and start innervating the thickening cortical plate from E20 onwards (Kalsbeek et al., 1988; Kolk et al., 2009; Garcia et al., 2019).

Shortly after birth, DA-positive fibers in rats are primarily located in the developing layer VI of mPFC, orbital cortex, and caudal cingulate cortex (defined as supragenual mPFC in the original study by Kalsbeek and colleagues). At P2, the fiber density in layer VI increases substantially. Between P2 and P4, the DA axons change their morphology from thick, straight fibers to thin fibers with irregularly shaped varicosities. This marks the beginning of postnatal maturation of DA-positive fibers in the mPFC, which continues into early adulthood. By the end of the first postnatal week, the infralimbic subdomain of the mPFC shows already an adult-like pattern of DA innervation, with DA-positive fibers reaching up to the pial surface. In other areas of the mPFC, only a few DA-positive fibers in layer I are detectable at this developmental stage. The density of DA fibers in the deeper layers continues to increase in the second postnatal week. At P20, DA-positive projections reach the upper cortical layers II and I in the prelimbic cortex. At this stage, the DA-positive fibers in layer I of the anterior cingulate cortex of mPFC fade away, but the projections in the caudal cingulate cortex are found in layers II and III. The morphological characteristics of DA-positive fibers in the mPFC, with thin axons and multiple varicosities, do not change significantly after P35, but the density of fibers continues to increase until adulthood, with the deeper layers becoming more densely innervated than the upper layers (Kalsbeek et al., 1988). TH immunostaining in rat mPFC shows that the increase in TH-positive fibers is relatively rapid during adolescence, whereas the density of DBH-expressing NA fibers in mPFC remains constant from early adolescence to adulthood (Naneix et al., 2012; Willing et al., 2017) (**Figure 2**). The delayed

developmental trajectory of prefrontal TH-positive axons from early adolescence to adulthood is similar in male and female rats, even though pubertal onset is approximately 10 days earlier in female than in male rats. These data indicate that sex or pubertal onset do not affect the maturation profile of mesoprefrontal innervation (Willing et al., 2017).

In addition to the innervation density, the formation of varicosities on DA fibers and thus potential release sites is likely another important indicator of functional maturation of DA fibers. DA immunoreactive varicosities have been found to form appositions with both pyramidal and nonpyramidal somata in the mPFC. This is especially noticeable in layer VI, where the density of DA varicosities is higher and GABA-positive cell bodies are frequently found to be in close contact with DA varicosities (Benes et al., 1993). The number of close appositions formed by GABA-positive cell bodies with DA varicosities shows a steady increase from P5 to P60, while the number of varicosities closely interacting with each GABA-positive neuron increases more rapidly during the postweaning period (P25–P59) to reach young adult levels (P60) (Benes et al., 1996).

In mice, the change in TH/DA fiber density in the mPFC during the juvenile and adolescent periods has not yet been studied in detail. To gain insight into potential mechanisms underlying protracted DA innervation of the mPFC, Reynolds and colleagues used an elegant virus-based approach to axon labeling. In this study, retrogradely transported canine adenovirus (CAV) expressing Cre recombinase was injected into the nucleus accumbens of mice during early adolescence (P21), whereas a virus expressing a fluorescent protein after Cre-mediated recombination was injected into the VTA. CAV-Cre is taken up by axon terminals in the nucleus accumbens, so that only VTA neurons whose axons have reached the nucleus accumbens around P21 are fluorescently labeled. The authors then showed that fluorescently labeled fibers are present in the mPFC of adult mice. These results indicate that the late maturation of DA fibers in the mPFC may be due to at least some of the fibers initially innervating the nucleus accumbens and only projecting into the mPFC during later stages of adolescence (Reynolds et al., 2018).

Directing the extending DA axons to their proper targets requires precise coordination of extracellular axon guidance cues, receptor complexes, cell adhesion molecules, neurotrophic and growth factors (Hoops and Flores, 2017; Vosberg et al., 2020). Several guidance cue pathways involved in regulating the axonal pathfinding of mesoprefrontal DA axons have been identified. This includes Ephrins, Slits, Semaphorins, Netrins and their receptors. During early stages of mDA development, Semaphorin 3F acts via its receptor Neuropilin-2 to repel mDA axons away from the midbrain, while it changes its role into a chemoattractant to guide the DA axons towards the cortical plate of the mPFC at the prenatal stage (Kolk et al., 2009). The extracellular protein Netrin-1 and its receptor, DCC (deleted in colorectal cancer) also play a key role in mesoprefrontal/mesolimbic axon growth and the fine-tuning of their expression levels during adolescence is critical to help DA axons find their final target (Reynolds et al., 2018). We will not discuss these molecular mechanisms further here, as they have been extensively addressed in two recent reviews (Brignani and Pasterkamp, 2017; Hoops and Flores, 2017).

DEVELOPMENT OF THE MESOPREFRONTAL DOPAMINERGIC PROJECTIONS IN PRIMATES

In the adult primate brain, the densest TH-positive innervation is observed in primary motor cortex rather than in PFC areas (Gaspar et al., 1989; Raghanti et al., 2008). While primary motor cortex (area 4) shows even distribution of TH-positive fibers across all layers in the human brain, the PFC shows a bilaminar distribution with highest innervation density in layer I and V–VI (area 9 and 32) (Gaspar et al., 1989; Raghanti et al., 2008). Such bilaminar innervation was not detected in adult non-human primate PFC (Lewis and Harris, 1991; Rosenberg and Lewis, 1995; Raghanti et al., 2008). On an ultrastructural level, electron microscopy of DA axonal boutons (marked with antibodies against DA and TH) in the PFC of rhesus monkey shows that they form symmetric synaptic connections with dendritic spines of pyramidal cells (Goldman-Rakic et al., 1989). In addition, DA afferents also contact dendrites of nonpyramidal inhibitory interneurons in rhesus monkey PFC (Smiley and Goldman-Rakic, 1993).

How does this innervation pattern develop? Similar to rodents, primate mesoprefrontal DA fibers undergo a protracted development that may involve reorganization of innervation density until the functionally mature innervation pattern of the adult brain is established (Gaspar et al., 1989; Raghanti et al., 2008). In rhesus monkey, TH-expressing axons are observed in the cortical anlage during the 10th gw (Verney, 1999). In neonatal rhesus monkeys, the TH positive innervation is bilaminar in the PFC (area 9), similar to the pattern in the adult human brain. TH positive axons in the rhesus monkey PFC are reorganized from birth till adulthood, resulting in the relatively uniform distribution of TH positive innervation across layers in the adult PFC (Lewis and Harris, 1991; Rosenberg and Lewis, 1995). Accordingly, it is the innervation of intermediated cortical layers (especially layer III) that increases with age and reaches its peak in 2-3-year-old adolescent rhesus monkeys (Rosenberg and Lewis, 1995). Based on the observation that the direct effect of DA on the spontaneous activity of PFC neurons is mostly inhibitory, the increased TH positive innervation in layer III of adolescent PFC might indicate an increase in a DA-mediated inhibitory effect onto the pyramidal neurons in these layers (Rosenberg and Lewis, 1995; **Figure 2**).

In humans, TH-expressing neurons are detected as early as 6 gw and already extend processes that eventually give rise to the mesencephalic tract. This tract, along with the dorsal tegmental bundle, forms the MFB (Zecevic and Verney, 1995; Verney, 1999). TH-positive fibers enter the telencephalic wall at 7-8 gw but remain below the cortical plate (intermediate and subplate area) for 4 weeks before they enter the cortex (Zecevic and Verney, 1995). At 20-24 gw, DA innervation is observed in the frontal cortex with a higher density of TH positive innervation in the anterior cingulate and motor area compared

to the rostral prefrontal cortical anlage (Verney et al., 1993). It is interesting that this area-specific distribution and density of TH-expressing fibers at this stage is similar to what has been reported in the adult cortex (Gaspar et al., 1989; Verney et al., 1993; Verney, 1999), suggesting that the DA innervation pattern is in principle established already during fetal development in the human brain and subsequently only increases in density. Eventually, the adult PFC acquires its distinctive bilaminar innervation pattern (Gaspar et al., 1989; Raghanti et al., 2008; **Figure 2**).

Similar to the timing of differentiation onset of mDA neurons in rodents and primates, the outgrowth of TH-positive fibers and frontal cortex innervation also seems to occur earlier in humans than in rodents as 11 gw in humans is considered a much earlier gestational timepoint than E18 or E20 in mice and rats, respectively (Clancy et al., 2001; **Figure 2** and **Supplementary Figure 1**).

DOPAMINE RELEASE AND DOPAMINE RECEPTORS IN THE DEVELOPING PREFRONTAL CORTEX

While the location and density of DA projections gives some indication about when and where mesoprefrontal mDA neurons may modulate PFC function, the functional relevance of these projections can only be fully assessed by insights into actual DA release, DA receptor (DRD) expression, and the response of receiving cells to the DA release. In addition, as discussed previously, the release of neurotransmitters other than DA (most prominently glutamate) is likely to contribute to the functional output of the mesoprefrontal mDA neurons.

Dopamine Release

Analysis of DA and its metabolites in rat mPFC by high throughput liquid chromatography (HPLC) showed that DA concentrations were significantly lower in juvenile and adolescent rats than in adults. DA concentration rose steadily between the juvenile (P25) and late adolescent stages (P45) and increased particularly sharply between the end of adolescence and adulthood. In parallel, a decrease in DA turnover ratios was observed with increasing age, an effect that could contribute to the overall increase in DA availability in the mPFC (Naneix et al., 2012). Analysis of DA tissue concentrations in rhesus monkey PFC showed that DA levels fluctuated between 2, 5, 8 and 15-18 months old animals and significantly increased in 2–3 years old animals (Goldman-Rakic and Brown, 1982). These data suggest that both in rats and rhesus monkey, the overall DA concentration coincides with the increase in DA fiber innervation of the PFC. However, whether this increase in concentration correlates with active DA release has not been investigated in the developing PFC. The recent development of genetically encoded DA sensors that allow the monitoring of DA release in the behaving animal, offer the opportunity to correlate behavior, PFC function and DA release in real-time in adolescent and adult animals (Labouesse et al., 2020).

Dopamine Receptors and Downstream Signaling

Once released from the axonal varicosities of DA axons, DA binds to DA receptors (DRDs) of the D1-like or D2-like subfamily of G-protein coupled receptors. DRD1 and DRD5 belong to the D1-like subfamily, while DRD2, DRD3, and DRD4 are subtypes of the D2-like subfamily. Unlike *Drd1* and *Drd5*, the D2-like subfamily receptor genes contain introns that allow differential splicing of the transcripts, generating additional isoforms. *Drd2* comes in two alternatively spliced variants, Drd2s (short form) and Drd2l (long form), and isoforms of *Drd3* and *Drd4* have also been identified (Missale et al., 1998). D1-like receptors signal by coupling to G proteins G_{as} and G_{aolf}, which stimulate adenylyl cyclase and lead to activation of protein kinase A (PKA). D2-like receptors stimulate G_{ai} and G_{ao} proteins, blocking adenylyl cyclase and consequently inhibiting PKA activity (Missale et al., 1998; Tritsch and Sabatini, 2012). Furthermore, DRDs can activate a signaling cascade by interacting with ß-arrestin (Beaulieu et al., 2005) or induce phospholipase C-mediated increase of intracellular calcium levels (Lee et al., 2004), although the signal transduction pathway of this modulation remains to be resolved (Chun et al., 2013). The striatum and the nucleus accumbens receive dense projections from mDA neurons and have high expression levels of DRDs. In the PFC, the expression levels of the DRDs are considerably lower, correlating with relatively sparse innervation by DA fibers.

Dopamine Receptor Expression in Rodent Prefrontal Cortex

The distribution and expression of DRDs and their transcripts in rodent PFC have been studied using multiple histological methods, real-time quantitative PCR and in recent years, genetic tools and single-cell transcriptome analysis (**Table 1**). Early studies include autoradiographic experiments employing radiolabeled agonist or antagonist of DRDs (Boyson et al., 1986; Noisin and Thomas, 1988), immunohistochemical and immunoblotting approach targeting the receptor protein (Levey et al., 1993; Sesack et al., 1994) and in-situ hybridization technique detecting *Drd* transcripts (Gaspar et al., 1995). Some of the radioligands used in binding assays were later found to lack selectivity for specific subtypes of DRD (Landwehrmeyer et al., 1993) and similar doubts have been expressed for commercially available antibodies for the receptors (Bodei et al., 2009). RNA in situ hybridization methods have characterized the distribution of certain *Drd* mRNAs within the subregions of the PFC (Santana and Artigas, 2017) and RT-qPCR approaches were used to quantify the relative gene expression of the *Drd* subtypes in the PFC (Araki et al., 2007). Whether the transcript levels reliably correspond to the expression levels of DRD protein is not known.

Taking into account these methodological limitations, studies on DRD proteins and their transcripts indicate that of the five DRD subtypes, DRD1 and its mRNA are most highly expressed in the adult rodent PFC, followed by DRD2/*Drd2*. In comparison, DRD3, 4 and 5 show limited expression (Tarazi and Baldessarini,

TABLE 1 | Laminar distribution of *Drds*/DRDs in the PFC of rodent, rhesus monkey and human.

	Receptor/ Gene	Rodent						Human / Non-human Primate								
		L2/3	L5	L6	Species	Method	References	L1	L2	L3	L4	L5	L6	Species	Method	References
D1-like Family	DRD1 / *Drd1*	++	++	+++	Rats	*In situ*	Santana and Artigas, 2017	(+)	+++	++	++	+++	+++	Humans	*In situ*	Weickert et al., 2007
		++	+++	+++	Rats	Receptor binding	Vincent et al., 1993									
		++	++	+++	Mice	Genetic labeling	Wei et al., 2018	+++	+++	+++	++	+++	+++	Rhesus Monkeys	Receptor Autoradiography	Lidow and Rakic, 1992
	DRD5 / *Drd5*	++	++	++	Mice	Immunohistochemistry	Lidow et al., 2003									
		+++	++	++	Rats	Immunohistochemistry	Ciliax et al., 2000									
D2-like Family	DRD2 / *Drd2*	+	+++	++	Rats	*In situ*	Santana and Artigas, 2017	(+)	++	+	+	+++	+++	Humans	*In situ*	Weickert et al., 2007
		++	+++	+++	Rats	Receptor binding	Vincent et al., 1993									
		+	+++	++	Rats	Genetic labeling	Yu et al., 2019	++	++	++	++	+++	++	Rhesus Monkeys	Receptor Autoradiography	Lidow and Rakic, 1992
		+++	++	++	Mice	Genetic labeling	Wei et al., 2018									
	DRD3 / *Drd3*	?	?	++	Mice	Genetic labeling	Li and Kuzhikandathil, 2012									
	DRD4 / *Drd4*	?	++	++	Mice	Genetic labeling	Noaín et al., 2006	(+)	++	+	++	+++	+++	Humans	*In situ*	Weickert et al., 2007

L, cortical layer; +++ highest expression; ++ intermediate expression; + low expression; (+) absent/very low expression.

2000; Lidow et al., 2003; Araki et al., 2007; Rajput et al., 2009; Santana et al., 2009). DRD1 and DRD2 are expressed in both pyramidal neurons and interneurons of rodent PFC but are rarely colocalized (Santana et al., 2009; Zhang et al., 2010). RNA in situ hybridization studies in adult rats show that cells expressing *Drd1* mRNA are most prominent in layer VI, extending into layer V, with an additional thin band of positive cells in layer II. *Drd2*-expressing cells are mainly localized in layer V and VI, with few positive cells in layer II and III (Gaspar et al., 1995; Santana and Artigas, 2017). This laminar distribution pattern of DRD1 and DRD2 in rat mPFC was also observed in an earlier receptor binding study using fluorescently coupled receptor antagonists (Vincent et al., 1993). More recently, genetic labeling has emerged as an additional tool to monitor *Drd1*- and *Drd2*-expressing neurons in rodents. Genetic labeling studies involve transgenic mice that accommodate a BAC (bacterial artificial chromosome) construct containing *Drd1* or *Drd2* regulatory regions directing expression of Cre recombinase (*Drd1-Cre* or *Drd2-Cre* mice) (Gong et al., 2007). These Cre mice are crossed with reporter mice that express fluorescent proteins upon Cre-mediated recombination (such as *Ai14* or *Ai6* mice) allowing the identification of cells that express *Drd1* or *Drd2* (Madisen et al., 2010; Wei et al., 2018). In rats, *Drd2-Cre* knock-in animals have been generated and crossed with a fluorescent rat reporter line (*Ai9)* (Madisen et al., 2010; Yu et al., 2019). An important aspect to keep in mind with these Cre reporter systems is that recombination of the reporter allele is permanent, meaning that if the *Drd1* or *Drd2* promoter is transiently active in certain cell populations during embryonic or postnatal development, these cells will be recombined and continue to express the fluorescent protein in the adult brain even when these neuronal populations may no longer express *Drd1* or *Drd2* in the adult. Furthermore, in this system, the expression level of the fluorescent protein does not correspond to the level of endogenous gene or protein expression. Despite these caveats, in *Drd2-Cre, Ai9* reporter rats, the distribution of recombined cells (expressing fluorescent reporter protein) is largely in agreement with previous findings on *Drd2* expression in the mPFC (Santana and Artigas, 2017). Analysis of recombined cells in the anterior cingulate cortex show them mostly to be putative pyramidal neurons of upper and deep layers. Only a small number of inhibitory interneurons exhibit fluorescent labeling in this region (Yu et al., 2019). Similarly, in *Drd1-Cre, Ai6 or Drd1-Cre, Ai14* reporter mice, fluorescently labeled cells show a laminar distribution comparable to what has been reported for *Drd1* transcript expression in mPFC, with a higher overall density of *Drd1* expression in deep layers. In *Drd2-Cre Ai6/Ai14* mice, however, distribution of fluorescently labeled cells in mPFC is strikingly distinct from the one reported in *Drd2-Cre, Ai9* reporter rats or the expression patterns observed in RNA in situ hybridization studies, showing high expression of *Drd2* in superficial layers rather than in deep layers (Wei et al., 2018). Whether this is due to the different approaches used to generate the Cre-lines (BAC transgenic mice versus knock-in rats) or reflects a transient expression of *Drd2* in superficial layers of the mPFC during development in the mouse is unclear (Beil et al., 2012; Yu et al., 2019). BAC transgenic mice expressing enhanced green fluorescent protein (EGFP) under the transcriptional regulation of *Drd3* (*Drd3-Egfp* mice) or *Drd4* (*Drd4-Egfp* mice) locus have also been used to study the expression of *Drd3* and *Drd4* in different regions of the brain (Gong et al., 2003). In the *Drd3-Egfp* mouse model, the fluorescent cells in the caudal cingulate cortex are mainly located in layer VI (Li and Kuzhikandathil, 2012). Analysis of *Drd4-Egfp* mice showed strongly labeled EGFP-expressing neurons in layer V and VI of prelimbic and cingulate cortices (Noaín et al., 2006). DRD5 immunoreactivity has been detected in layer II to layer VI of prelimbic and cingulate cortices, with more labeled cells in layer II and III. In mice, DRD5 is more uniformly distributed across the cortical layers of the mPFC (Ciliax et al., 2000; Lidow et al., 2003; **Table 1**).

The developmental time course of DRD expression in rodent PFC is not well characterized and appears to vary considerably between rats and mice. RT-qPCR analysis in the murine cingulate cortex (both at rostral and caudal levels) at P0, P21, and P60 reveals that other than *Drd4*, which has the highest expression at birth followed by a rapid postnatal decrease in expression, transcript levels of the *Drd* subtypes do not show any significant developmental change between P0 and P60 (Araki et al., 2007). In the frontal cortex of rats, in situ hybridization signals for *Drd1* or *Drd2* transcripts have been detected around E14 or E18, respectively (Schambra et al., 1994). According to the same study, expression levels for both *Drd1* and *Drd2* appear to reach maximal levels between P14 and P30, although the change in signal intensity has not been quantified. Another study, however, shows that *Drd1, Drd5, Drd4, Drd2l* (but not *Drd2s*) expression in the mPFC of rats reaches peak expression only at P45 and then decreases between P45 and P70 (Naneix et al., 2012). At the protein level, there is a marked decline of DRD1 and DRD2 density in PFC of rats between adolescence (P40) and adulthood (P120) (Andersen et al., 2000). An earlier study using quantitative autoradiography in rats has described a similar pattern for DRD1 in mPFC, but with peak receptor binding density at P14 and P21, and a decrease in binding between P21-P42 (Leslie et al., 1991). A certain population of mPFC pyramidal neurons projecting to the nucleus accumbens also shows differential expression of DRD1 across postnatal development. In retrogradely traced prelimbic pyramidal neurons projecting to the nucleus accumbens core, the number of DRD1 immunoreactive cells was significantly higher in adolescents (P44) than in juveniles (P27) or adults (P105) (Brenhouse et al., 2008). Tarazi and Baldessarini, however, report a different temporal expression pattern in frontal cortex of rats. In their investigation, binding of radioligands to DRD1, DRD2 and DRD4 receptors gradually rises from P7 to maximal levels at P60 (Tarazi and Baldessarini, 2000). Overall, the data from various published studies do not deliver a conclusive picture on the time course and distribution of DRD/*Drd* expression in the developing mPFC (**Table 2**).

An additional potent tool to investigate the distribution of *Drd* transcripts is single-cell mRNA sequencing (scRNA seq). DropViz is an extensive collection of scRNA seq data, assembled from analysis of RNA expression of thousands of individual cells across different regions of mouse brain (P60–P70) (Macosko et al., 2015; Saunders et al., 2018). Based on

TABLE 2 | Relative changes in expression of *Drds*/DRDs in PFC throughout postnatal development.

	Receptor/ Gene	Rodent								Human / Non-human Primate									
		0W	1W	3W	6W	9W	Species	Method	References	S1	S2	S3	S4	S5	S6	S7	Species	Method	References
D1 – like Family	DRD1 / *Drd1*	+		↔		↔	Rats	RT-qPCR	Araki et al., 2007	+	↓			↑	↔	↓	Humans	*In situ*	Weickert et al., 2007
				+	↑	↓*	Rats	*In situ*	Naneix et al., 2012	+	↑	↑	↑	↔	↓	↓	Humans	RT-qPCR + Microarray	Rothmond et al., 2012
			+	↑*	↑	↑	Rats	Receptor Autoradiography	Tarazi and Baldessarini, 2000	+	↑	↑	↔	↑	↑*	↔	Humans	Western Blot	Rothmond et al., 2012
			+	↑	↓		Rats	Receptor Autoradiography	Leslie et al., 1991	+	↔	↑*	↓	↓	↔	↔	Rhesus Monkeys	Receptor Autoradiography	Lidow and Rakic, 1992
	DRD5 / *Drd5*	+		↔		↔	Rats	RT-qPCR	Araki et al., 2007	+	↔	↔	↔	↔	↔	↔	Humans	RT-qPCR + Microarray	Rothmond et al., 2012
				+	↑	↓*	Rats	RT-qPCR	Naneix et al., 2012										
D2 – like Family	DRD2 / *Drd2*	+		↔		↔	Rats	RT-qPCR	Araki et al., 2007	+	↓*			↑	↓	↑	Humans	*In situ*	Weickert et al., 2007
	Drd2l			+	↑	↓*	Rats	RT-qPCR	Naneix et al., 2012	+	↓	↑	↓	↓	↔	↔	Humans	RT-qPCR	Rothmond et al., 2012
	Drd2s			+	↔	↔	Rats	RT-qPCR	Naneix et al., 2012	+	↓	↔	↓*	↔	↔	↔	Humans	RT-qPCR	Rothmond et al., 2012
			+	↑*	↑	↑	Rats	Receptor Autoradiography	Tarazi and Baldessarini, 2000	+	↔	↑*	↓	↔	↔	↔	Rhesus Monkeys	Receptor Autoradiography	Lidow and Rakic, 1992
	DRD3 / *Drd3*	+		↔		↔	Rats	RT-qPCR	Araki et al., 2007										
	DRD4 / *Drd4*	+		↓*		↔	Rats	RT-qPCR	Araki et al., 2007	+	↔			↔	↔	↔	Humans	*In situ*	Weickert et al., 2007
				+	↑	↓*	Rats	RT-qPCR	Naneix et al., 2012	+	↔	↔	↔	↔	↔	↔	Humans	RT-qPCR	Rothmond et al., 2012
			+	↑*	↑	↑	Rats	Receptor Autoradiography	Tarazi and Baldessarini, 2000										

*+ first postnatal stage analyzed & expression detected. ↑ increase; ↓ decrease; ↔ no change in expression compared to previous timepoint; * indicates increase or decrease in expression compared to previous timepoint that were statistically significant; empty cells: no data available.* ***W:*** *Week* ***S:*** *Stage;* ***S1****: neonate in humans, 0 month in rhesus monkeys;* ***S2****: infant in humans, 1 month in rhesus monkeys;* ***S3****: toddler in humans, 2 months in rhesus monkeys;* ***S4****: school age in humans, 8 months in rhesus monkeys;* ***S5****: adolescent in humans, 12 months in rhesus monkeys;* ***S6****: young adult in humans, 36 months in rhesus monkeys;* ***S7****: adult in humans, 60 months in rhesus monkeys.*

gene expression profiles in the frontal cortex (including the mPFC, orbital cortices, frontal association cortex, anterior parts of primary and secondary motor cortices, insular cortex and somatosensory cortex), *Drd1* and *Drd5* expression is highest in deep layer pyramidal neurons and *Drd4* is mostly expressed in pyramidal cells of layer II/III. *Drd2* transcript levels are notably low and are predominantly found in interneurons rather than in projection neurons. Additionally, a rather remarkable observation is that the highest level of *Drd1* and *Drd2* expression is found in microglia. *Drd3* expression is not included in this transcriptional analysis of the frontal cortex, possibly because of low expression levels. The transcriptional dynamics of the *Drds* in the frontal cortex during development has not yet been investigated. However, dynamic regulation of *Drd1* has been demonstrated in the context of mouse models of drug abuse. Bhattacherjee and colleagues have shown that chronic cocaine addiction induces cell type-specific transcriptional changes in the murine mPFC. The effect of cocaine addiction on gene expression changes was particularly striking during the withdrawal period, with excitatory neurons in the deeper layers being more affected. While the most significantly affected excitatory clusters expressed *Drd1*, the analysis also detected *Drd1* expressing excitatory clusters that did not respond robustly to cocaine. Although the functional role of each subtype remains to be investigated, this suggests that certain *Drd1*-expressing neuronal subtypes in the PFC may be more involved in the process of cocaine addiction than others (Bhattacherjee et al., 2019). Further analysis on dataset of cocaine-addicted mice revealed that *Drd1* and *Drd2* genes are both upregulated in cocaine addiction and are almost solely expressed in excitatory neurons, with *Drd1* also being found at lower levels in inhibitory neurons, oligodendrocyte and endothelial cells in the mPFC (Bhattacherjee et al., 2019; Navandar et al., 2021).

In addition to DRD expression patterns, maturation of receptor function could also contribute to changing impact of the mesoprefrontal system over time. Investigations into DRD function have shown that DRD1-mediated modulation of NMDA receptor transmission prompt recurrent depolarizing plateaus in pyramidal neurons of mPFC slices, an effect that develops only after P45 (Tseng and O'Donnell, 2005). Furthermore, DRD2-mediated increase in excitability of fast-spiking interneurons in PFC slices appears only after P50 (Tseng and O'Donnell, 2007). Thus, while the changes in postnatal expression levels of DRD/*Drd* are still unclear, there is indeed a change in activity of DRDs in the post-pubertal stage, hinting towards the role of DA in the remodeling of PFC microcircuits during the transition from adolescence to adulthood.

Another gap in our understanding of DRD receptor expression and function in the developing and adult mPFC is that we know little about the subcellular localization of receptors in DRD-expressing neurons. Because existing antibodies against DRDs have limited utility for detecting DRDs in brain tissue (Bodei et al., 2009), alternative approaches should be considered for investigating this question. Vincent and colleagues analyzed cellular localization of D1- and D2-like family of receptors in the mPFC using receptor antagonists coupled to fluoroprobes and observed that around 25% of all fluoroprobe-labeled cells displayed both D1 and D2-like subfamily receptor binding fluorescence along the outer edge of the soma. Further analysis on cell size distribution suggested that the cells in which colocalization could be detected were non-pyramidal (Vincent et al., 1995). A recent promising technique to examine subcellular localization of DRDs may be the application of CRISPR/Cas9 based genome editing tools to introduce fluorescent tags to endogenous receptor proteins. A recent study used a modified CRISPR/Cas9 knock-in strategy with two guide RNAs to knock-in a fluorescent protein to α-amino-3-hydroxy-5-methyl-4-isoxazolepropionic acid (AMPA) and N-methyl D-aspartic acid (NMDA) receptor subunits in primary mouse cortical cultures (Fang et al., 2021). The application of these epitope tags in vivo is also possible. Using the so-called ORANGE (Open Resource for the Application of Neuronal Genome Editing) toolbox, adeno-associated virus plasmids containing fluorescent tag knock-in constructs for PSD95 and AMPA receptor subunit (GLUA1) were injected into the hippocampus of Cas9-P2A-GFP transgenic mice resulting in robust labeling of both proteins (Willems et al., 2020). Applying these methods for the fluorescent tagging of DRDs has the potential to aid in determining the subcellular localization of DRDs in fixed tissue as well as monitoring dynamics of receptor localization in dissociated cell cultures in vitro or in acute slices.

The distribution of DRDs in the rodent mPFC correlates largely with the innervation pattern of DA fibers, suggesting that DRD expression might be influenced by DA release in the mPFC. In this context, DA might play a role during the phase when projections are established (as in a critical developmental period) and/or influence DRD expression levels in the adult brain. Indeed, there is evidence from the striatum that ablating DA innervation during early postnatal development (using 6-OHDA-mediated lesion of the nigrostriatal and mesolimbic pathway at neonatal stages) results in reduced binding of radioligand to DRD1 in the caudate putamen and nucleus accumbens of the adult (P90) rat. Radioligand binding to DRD2 is not affected (Thomas et al., 1998). In the adult brain, the loss of striatal DA input in Parkinson's disease patients or in animal models of the disease leads to compensatory upregulation of DRDs, while drug-induced DA increase in the nucleus accumbens leads to reduced expression of DRDs to adjust for elevated DA in the system (Hisahara and Shimohama, 2011; Volkow and Morales, 2015). In the mPFC, the influence of DA on DRD expression has not been studied in detail. One study has examined the effect of depletion of DA projections in the postnatal rat by intracisternal injection of 6-OHDA 5 days after birth and found that DRD1 receptor binding remains unaltered (Leslie et al., 1991). Mouse models interfering with the development of mesoprefrontal projections, such as the *Dcc* and *Netrin-1* haploinsufficient mice that elevate DA transmission in the mPFC (Vosberg et al., 2020) or mouse models that lack mesoprefrontal innervation (Kabanova et al., 2015) may offer a suitable approach to determine the role of DA innervation in the developmental trajectory of DRD expression in the mPFC.

Dopamine Receptor Expression in Primate Prefrontal Cortex

In the adult PFC of rhesus monkeys, autoradiographic receptor binding assays showed that DRD1 is most densely present in layers I, II, IIIa, V, and VI, while DRD2 shows the highest expression density in layer V of adult PFC (Lidow and Rakic, 1992) (**Table 1**). Immunohistochemistry for DRD1 and DRD5 in rhesus monkey PFC (area 9) demonstrated that these receptors widely colocalize on spines of pyramidal neurons and axon terminals (Bordelon-Glausier et al., 2008). In the adult human PFC, DRD1, DRD2 and DRD4 are highly expressed in deeper layers (layer V and VI) and layer II (Weickert et al., 2007; **Table 1**). These studies did not report on the expression of DRD3.

DRDs appear to be dynamically expressed in the developing PFC in primates. In the adult rhesus monkey PFC (5–6 years old), DRD1 and DRD2 density (examined by autoradiographic receptor binding assays) was found to be significantly lower compared to 2 months of age (Lidow and Rakic, 1992). Another study, using [^{11}C] FLB 457 (high-affinity radioligand for DRD2/3) in positron emission tomography (PET) on human subjects (age range 19–74 years), detected a significant decline in DRD2/3 expression with age in the frontal cortex area (Kaasinen et al., 2000). An immunohistochemistry study was not performed for these receptors. At the transcriptional level, a cohort study of human post-mortem PFC tissue revealed that *DRD1* mRNA is expressed at neonatal stages. Expression levels decline within the first year of life, are highest during adolescence and young adults, and gradually decline again in adult and aged cohorts (Weickert et al., 2007). However, in a similar cohort study of the human dorsolateral PFC, *DRD1* mRNA expression was reported to increase steadily until adolescence but to decrease slightly thereafter. Western blot analysis of DRD1 expression indicated that protein levels also increase gradually with age, but the highest expression was found in the young adult and adult groups (Rothmond et al., 2012). Moreover, a similar layer-specific pattern was observed across all studied ages: *DRD1* transcript levels were not detected in layer I of the human dorsolateral PFC, were present at an intermediate level in layers III and IV and highest expression was found in layers II, V, and VI (Weickert et al., 2007). Unlike *DRD1, DRD2* expression levels peak at neonatal age, followed by a significant decrease in infants. At all later developmental time points examined, expression levels remain below neonatal levels. Similarly, mRNA levels of the short (*DRD2S*) and long (*DRD2L*) *DRD2* isoform are highest at the neonatal stage and decrease with age in the dorsolateral PFC. A layer-specific pattern was observed also for *DRD2* with highest expressions in layers II, V, and VI. *DRD1* and *DRD2* mRNA was found in both pyramidal and non-pyramidal neurons in adult brain (Weickert et al., 2007). *DRD4* mRNA expression was detected in presumed non-pyramidal neurons and glia but was barely present in pyramidal cells (Weickert et al., 2007). Generally, *DRD4* did not show any age-specific changes in expression and highest signal intensity was detected in layer V (Weickert et al., 2007; Rothmond et al., 2012). *DRD5* expression levels did not show any significant differences between age groups (Rothmond et al., 2012). To the best of our knowledge, the distribution of *DRD3* expression in the developing primate PFC has not yet been reported (**Table 2**).

Similar to what we have highlighted above for the investigation of *Drd* expression in the rodent brain, high-throughput techniques for transcriptome analysis, such as scRNAseq, give now the opportunity to explore the cell-type specific expression of *DRD* transcripts in the developing and adult human PFC in further detail (Allen Institute for Brain Science, 2010; Fan et al., 2018, 2020; Zhong et al., 2018; Polioudakis et al., 2019; Tanaka et al., 2020; Maynard et al., 2021). This will be instrumental in defining temporal dynamics and cell type-specific responsiveness to DA.

Finally, neither DA release nor receptor expression may offer a full reflection of how DA impacts on cortical neurons in the PFC. As discussed above, DRDs act on DA-receiving cells by modulating PKA activity. Thus, monitoring PKA activity may offer additional insight into the effects of DA on cortical neuronal function. A recent study used a PKA activity sensor to monitor the effect of DA release on *Drd1*- versus *Drd2*-expressing medium spiny neurons in the nucleus accumbens during learning in real-time (Lee et al., 2021). However, given that DA innervation and release is much sparser in the mPFC than in the nucleus accumbens and other modulatory neurotransmitters released in the mPFC (e.g., NA, Serotonin) act also via G-protein coupled receptors and modulation of PKA activity, further studies would be needed to determine whether a similar approach could be applied in the PFC.

In summary, a better understanding of the developmental time course of DA release; the laminar distribution, neuronal subtype expression, and subcellular localization of DRD receptors as well as downstream signaling events would greatly contribute to our knowledge of the functional role of DA in the developing and adult PFC.

THE DEVELOPING MESOPREFRONTAL SYSTEM IN NEUROPSYCHIATRIC DISEASES

As discussed above, the PFC is the region of the brain that is particularly important for executive functions and the control of goal-directed and self-regulatory behaviors. Dysregulation of local micronetworks in the PFC has been associated with impaired social, affective, and cognitive functions typically seen in neurodevelopmental disorders such as schizophrenia, autism spectrum disorder and attention deficit/hyperactivity disorder as well as in depression and substance abuse disorders. An open question is to what extent deficits in the mesoprefrontal DA system, and thus DA-influenced neuromodulation of local PFC networks, contribute to the pathophysiology of these neuropsychiatric disorders. In particular, it is unclear whether these changes occur secondary to alterations in the PFC (and other cortical areas) or can also be attributed to developmental deficits in the mesoprefrontal DA system. Many of the mutations associated with schizophrenia or autism spectrum disorder are found in genes encoding synaptic proteins. While loss of function of these genes has been shown to lead to deficits in

synaptic transmission in cortical regions and particularly in the PFC, it is not known whether this also directly affects the function of mesoprefrontal DA neurons (Yan and Rein, 2021). Another point that should be considered in this context, is that mesoprefrontal DA neurons (at least in rodents) can co-release glutamate (Kabanova et al., 2015; Mingote et al., 2015; Pérez-López et al., 2018; Zhong et al., 2020). Thus, any developmental deficits or alterations in the mesoprefrontal system could have consequences for both DA and glutamate release in the PFC. In the following, we will focus on the possible dysfunction of the mesoprefrontal system in three neuropsychiatric diseases with a clear developmental etiology: schizophrenia, autism spectrum disorder, and attention deficit/hyperactivity disorder. In the context of these diseases, we will briefly discuss a few studies that have examined potential alterations in the developing DA system.

Schizophrenia

Schizophrenia is a neuropsychiatric disorder with severe symptoms that usually become manifest in full during adolescence or early adulthood. These include the so-called positive symptoms (psychosis), negative symptoms (deficits in emotional responses and thought processes), and cognitive dysfunction (e.g., deficits in working memory, long-term memory, semantic processing, learning) (Marder and Cannon, 2019). According to the so-called DA hypothesis of schizophrenia, alterations in DA signaling are a major factor in these disease symptoms: DA hyperactivity in the striatum promotes psychosis, while DA hypoactivity in other brain areas, including the PFC, contributes to the negative symptoms and cognitive dysfunction. There is ample evidence from human studies to support this hypothesis. To name a few: (1) DA agonists and stimulants such as cocaine or amphetamine can induce psychosis in healthy individuals and exacerbate psychosis in patients with schizophrenia; (2) antipsychotic drugs act on the DA system via DRD2 receptors (e.g., haloperidol); (3) postmortem studies have demonstrated increased levels of DRDs, DA, and DA metabolites in the striatum of patients with schizophrenia; (4) imaging studies in patients with schizophrenia show that stimulant-induced presynaptic DA release is decreased in most brain regions, except for the striatum, where it is increased. For further details, we refer the interested reader to a collection of reviews on the DA hypothesis of schizophrenia (Biol Psychiat, 2017).

With respect to the mesoprefrontal DA system, its hypoactivity is most likely associated with the cognitive dysfunctions in schizophrenia. The cause of the overall DA imbalance may be caused by deficits in local cortical or hippocampal networks that in turn lead to changes in the inputs to the VTA from these regions and ultimately to DA hypoactivity in VTA targets. Alternatively, or in addition, defects in the regulation of DA release in target regions (including the PFC) or in the developmental of the mesoprefrontal system could contribute to the DA hypoactivity (Rice et al., 2016; Abi-Dargham, 2017; Chuhma et al., 2017; Grace, 2017; Walker et al., 2017; Sonnenschein et al., 2020; Braun et al., 2021). Whether the development of the mesoprefrontal DA system (or other parts of the DA system) is altered in patients with schizophrenia has not yet been studied in detail.

Autism Spectrum Disorders

Autism spectrum disorder (ASD) encompasses a group of severe neurodevelopmental disorders that exhibit core symptoms of social and communication deficits and stereotyped, repetitive behaviors (Association, 2013; Fein et al., 2021). Many studies highlight similar behavioral and cognitive impairments between ASD and schizophrenia such as social and language deficits and there is a high co-occurrence of both neurodevelopmental disorders (Spek and Wouters, 2010; King and Lord, 2011; Chisholm et al., 2015; Crescenzo et al., 2019). Based on this, it has been speculated that dysfunction in the DA system may also contribute to the cognitive disorders in ASD and, similar to schizophrenia, a DA hypothesis has been proposed for ASD. According to this hypothesis, aberrant mesocorticolimbic and nigrostriatal DA circuitry may contribute to reward deficits and goal-directed motor impairments manifested in ASD children (Pavăl, 2017; Pavăl and Micluția, 2021). Initial evidence for impairments in the DA system in ASD came from a study that found elevated levels of DA metabolites, such as homovanillic acid, in the cerebrospinal fluid of autistic children (age 1- 16 years old) (Gillberg and Svennerholm, 1987). Further evidence supporting this hypothesis comes from (1) the discovery that de novo genetic variants of the gene encoding the dopamine transporter (*DAT)* (Neale et al., 2012; Hamilton et al., 2013; Bowton et al., 2014; Cartier et al., 2015) and gene polymorphisms in *DRD3* and *DRD4* (Gadow et al., 2010; Staal, 2014; Staal et al., 2015) are associated with ASD; (2) the therapeutic efficacy of DRD blockers (risperidone and aripiprazole) in alleviating stereotypic and/or abnormal social behaviors in children with autism (McCracken et al., 2002; McDougle et al., 2005; Ghaeli et al., 2014) and (3) studies showing that the reward circuitry is hypoactivated in autistic patients in response to social and monetary rewards (Zeeland et al., 2010; Dichter et al., 2012; Kohls et al., 2012). According to the DA hypothesis in ASD, this diminished ability to register rewards for social cues could lead to the decreased pursuit of social interaction and ultimately to the deficits in social and communication skills observed in ASD patients (Pavăl, 2017). Regarding the mesoprefrontal system, an early PET scanning study for fluorine-18-labeled fluorodopa (F-DOPA) revealed significantly decreased F-DOPA ratio in the anterior mPFC of autistic children compared to healthy subjects, indicating decreased DA activity in the mPFC in autistic patients (Ernst et al., 1997). ASD patients underperform in working memory tasks involving planning, cognitive flexibility, and high working memory load compared to control subjects, which could be due to, or at least influenced by, a dysfunctional mesoprefrontal DA system (Kercood et al., 2014). Moreover, computational models predict that decreasing DA modulation in the PFC could lead to executive dysfunctions such as decreased cognitive flexibility, as occurs in ASD (Kriete and Noelle, 2015). Nevertheless, it remains largely unclear whether impairments of the mesoprefrontal DA system contribute to cognitive deficits in ASD patients and whether the development of mesoprefrontal mDA neurons is altered in ASD. The phenotypic heterogeneity

of ASD and largely unknown disease mechanisms complicate the investigations of these potential deficits.

To uncover the potential role of altered development of the DA system and in particular the mesoprefrontal DA neurons in ASD etiology and associated social and executive dysfunctions, further DA system-focused studies in patients and ASD mouse models are needed. Evidence from mouse models for the involvement of the DA system in ASD is discussed in detail in a recent review (Kosillo and Bateup, 2021), thus we will only discuss two examples here. Mutations in the gene encoding SH3 and multiple ankyrin repeat domains 3 (SHANK3), a postsynaptic scaffolding protein, have been discovered in ASD patients, making it a prominent autism gene candidate (Gauthier et al., 2009; Phelan and McDermid, 2012; Boccuto et al., 2013). Studies on the *Shank3* haploinsufficient mouse model show that impaired preference for social interactions is due to decreased DA activity in the VTA (Bariselli et al., 2016, 2018). Whether this hypoactivity results in decreased DA release in the nucleus accumbens and/or the mPFC has not yet been addressed. A potential link between autistic-like phenotypes and aberrant development of the DA system emerges from animal models for Mucopolysaccharidosis (MPS). MPS are hereditary lysosomal storage diseases, in which dysfunctions in lysosomal hydrolases lead to the accumulation of undegraded glycosaminoglycans in lysosomes and eventually to disturbances in cellular metabolism. In MPS IIIa, in which the gene coding for the lysosomal hydrolase sulfamidase is mutated, the metabolic cellular deficits result in neurodegeneration and dementia in children. Dementia is preceded by severe autistic-like behaviors (Valstar et al., 2010; Rumsey et al., 2014). In a mouse model of MPS IIIa, inactivation of the gene coding for sulfamidase, results in severely impaired behavior that that can be considered autism-like. These behavioral deficits are associated with increased DA release in the dorsal and ventral striatum and can be ameliorated with a DRD1 antagonist. This hyperdopaminergic state in MPS IIIa mice appears to be caused by developmental changes in the DA system: increased proliferation of mDA progenitors results in an increased number of mDA neurons in the SNpc and the VTA in the adult brain. Moreover, the same study shows that autistic-like behaviors and increased DA cell number are also present in a mouse model for a different type of MPS (MPS-II) (Risi et al., 2021). While this study suggests that altered development of the mDA system may be one of the causes of autism-like behaviors, it has not been investigated whether the increase in VTA neurons in these animal models leads also to alterations in the mesoprefrontal DA system. Further investigation of existing and potentially novel ASD candidate genes in animal models will be necessary to uncover developmental, structural, and/or functional impairments of the mesoprefrontal DA system in association with ASD.

Attention Deficit Hyperactivity Disorder

Attention deficit/hyperactivity disorder (ADHD) is a highly heritable, early-onset neurodevelopmental disorder, characterized by symptoms of hyperactivity, short attention span, and impulsivity. The PFC is a key region afflicted in this disorder. Studies report thinning of PFC areas, reduced density of the dorsolateral PFC, and decreased PFC activity in ADHD patients compared to controls (Arnsten and Pliszka, 2011; Cortese, 2012; Klein et al., 2019). Shaw and colleagues reported that the PFC in children with ADHD takes significantly longer to reach peak cortical thickness compared to the PFC in typically developing individuals, suggesting a delay in PFC maturation (Shaw et al., 2007a). The typical ADHD symptoms also reflect impaired executive functioning of PFC, which in turn is related to dysregulated NA and DA signaling in the PFC (Arnsten and Pliszka, 2011). There are several points of evidence that suggest that alterations in the DA system may contribute to ADHD symptoms. An F-DOPA PET study showed low DOPA-decarboxylase activity in the PFC of adult ADHD patients compared to healthy controls, an effect that could however not be replicated in adolescents with ADHD (Del Campo et al., 2011). Methylphenidate and amphetamine, which are used in the treatment of ADHD, act by inhibiting DA and NA reuptake and consequently by increasing DA and NA transmission in the PFC. Low doses of methylphenidate have been shown to improve PFC function in rats and monkeys, which can be counteracted by blocking DRD1 receptor. Moreover, mice heterozygous for the gene encoding dopamine transporter (DAT hypofunction mice), show behavior typical for ADHD such as hyperactivity, inattention, and impulsivity. Inattentive and impulsive behavior in these mice can be rescued by amphetamine. In humans, using radiolabeled altropane, a high-affinity selective probe for DAT, neuroimaging studies point towards evidence of increased DAT activity in striatum of children and adults with ADHD. However, due to its limited expression, it has been challenging to analyze DAT levels in the cortex using PET imaging techniques and it is still poorly characterized in the PFC of ADHD patients (Spencer et al., 2005; Prince, 2008). In addition, there is a significant association between ADHD and polymorphism in the genes that encode DRD4, DRD5, and DAT. *DRD4* has a high number of polymorphisms in its nucleotide sequence. Comprehensive meta-analyses showed that the so-called *DRD4* 7-repeat allele (*DRD4* 7R; a 7-repeat form of the 48–base pair (bp) variable number tandem repeat) elevates the risk of ADHD (Wu et al., 2012). Shaw and colleagues showed that presence of *DRD4* 7R was linked to cortical thinning in orbitofrontal and inferior prefrontal cortex that was augmented in ADHD patients (Shaw et al., 2007b). Another study suggests a considerable reduction in gyrification of inferior frontal gyrus in children with ADHD, who were *DRD4* 7R allele carrier. The authors hypothesize that this *DRD4* polymorphism could affect early stages of cortical development in children who later develop ADHD (Palaniyappan et al., 2019). Additionally, a 148-bp and a 136-bp dinucleotide repeat allele from the *DRD5* gene have also received considerable attention while the most extensively studied *DAT* polymorphism involves the 40 bp 9-repeat and 10-repeat alleles (Gizer et al., 2009; Wu et al., 2012).

An evolutionary perspective on ADHD argues for an adaptive role of the mesoprefrontal system in the disorder. Symptoms associated with ADHD, such as hyperactivity or limited sustained attention, could help animals to detect threats more rapidly and hence serve as beneficial features in endangered situations (Jensen et al., 1997; Lee and Goto, 2015). When

delayed PFC maturation puts animals at a disadvantage in an adverse environment, ADHD symptoms arising from reduced mesoprefrontal DA could emerge as a compensative mechanism to make animals less vulnerable to the environmental threats. While such an adaptive response may have aided ancestral humans in stressful conditions, it does not translate well to modern social settings (Lee and Goto, 2015).

In summary, these data indicate that changes in DA signaling, in particular in the PFC may play a critical role in the pathophysiology of ADHD. However, it remains challenging to separate the impact of altered DA versus NA signaling on PFC dysfunction in ADHD. It also should be taken into consideration, that similar to schizophrenia and ASD, alterations in DA signaling could be secondary to functional changes in cortical areas (Arnsten and Dudley, 2005; Gamo et al., 2010; Arnsten and Pliszka, 2011; Mereu et al., 2017). The etiology of ADHD is multifaceted, having a strong genetic background but also contributions from environmental risk factors. Beside PFC, other brain regions having reciprocal connection to PFC, such as caudate and cerebellum are affected and there is an intricate interplay of neurotransmitters distinctive to each region (Arnsten and Pliszka, 2011; Cortese, 2012). Our understanding of the role of reduced mesoprefrontal signaling among these complex interactions is still evolving (Stanford and Heal, 2019) and requires further studies to better understand both, its specific function, and its complementary role along with DA signaling in the subcortical brain regions, in the pathophysiology of ADHD.

CONCLUSION

Research over the past decade has vastly increased our knowledge of the development of mDA neurons and their molecular and functional diversity. Despite these advances, fundamental questions about the development and function of the mesoprefrontal DA system remain unresolved. For example, it is still unclear whether mesoprefrontal mDA neurons arise from a specific mDA progenitor population during development and whether these neurons can be defined at the molecular level as a specific mDA subset. Findings on the developmental history and molecular profile of these neurons would facilitate specific manipulation of the mesoprefrontal DA system by genetic methods (e.g., optogenetics, chemogenetics). This would allow to examine the consequences of functional changes in mesoprefrontal DA release on PFC development and PFC-regulated behavior. A possibility to specifically study the mesoprefrontal system during development and in the adult brain would most likely also provide further insights into a potential causative role of mesoprefrontal dysfunction in neurodevelopmental and neuropsychiatric disorders. Finally, how the mesoprefrontal system affects the activity of micronetworks in the PFC is still an open question, as it is still not fully understood at which stages, in which cell types and cortical layers DRDs are expressed in PFC and how DA release is coordinated with co-release of glutamate.

AUTHOR CONTRIBUTIONS

KI, NM, and SB: writing—original draft and review and editing. All authors contributed to the article and approved the submitted version.

FUNDING

This work was supported by the German Research Foundation [BL 767/5-1 (Project number: 417960915) to SB], the German Research Foundation SFB 1089 (to KI and SB) and the BONFOR program of the Medical Faculty, University of Bonn (O-154.0120, to NM and SB).

SUPPLEMENTARY MATERIAL

The Supplementary Material for this article can be found online at: https://www.frontiersin.org/articles/10.3389/fncir.2021.746582/full#supplementary-material

REFERENCES

Abi-Dargham, A. (2017). A dual hit model for dopamine in schizophrenia. *Biol. Psychiat.* 81, 2–4. doi: 10.1016/j.biopsych.2016.10.008

Allen Institute for Brain Science (2010). *BrainSpan Atlas of the Developing Human Brain*. Washington, DC: Allen Institute for Brain Science

Altman, J., and Bayer, S. A. (1981). Development of the brain stem in the rat. V. Thymidine−radiographic study of the time of origin of neurons in the midbrain tegmentum. *J. Comp. Neurol.* 198, 677–716. doi: 10.1002/cne.901980409

Andersen, S. L., Thompson, A. T., Rutstein, M., Hostetter, J. C., and Teicher, M. H. (2000). Dopamine receptor pruning in prefrontal cortex during the periadolescent period in rats. *Synapse* 37, 167–169.

Andersson, E., Tryggvason, U., Deng, Q., Friling, S., Alekseenko, Z., Robert, B., et al. (2006). Identifica-tion of intrinsic determinants of midbrain dopamine neurons. *Cell* 124, 393–405. doi: 10.1016/j.cell.2005.10.037

Araki, K. Y., Sims, J. R., and Bhide, P. G. (2007). Dopamine receptor mRNA and protein expression in the mouse corpus striatum and cerebral cortex during pre- and postnatal development. *Brain Res.* 1156, 31–45. doi: 10.1016/j.brainres.2007.04.043

Aransay, A., Rodríguez-López, C., García-Amado, M., Clascá, F., and Prensa, L. (2015). Long-range pro-jection neurons of the mouse ventral tegmental area: a single-cell axon tracing analysis. *Front. Neuroanat.* 9:59. doi: 10.3389/fnana.2015.00059

Arnsten, A. F. T., and Pliszka, S. R. (2011). Catecholamine influences on prefrontal cortical function: Rel-evance to treatment of attention deficit/hyperactivity disorder and related disorders. *Pharmacol. Biochem. Behav.* 99, 211–216. doi: 10.1016/j.pbb.2011.01.020

Arnsten, A. F., and Dudley, A. G. (2005). Methylphenidate improves prefrontal cortical cognitive function through alpha2 adrenoceptor and dopamine D1 receptor actions: Relevance to therapeutic effects in Attention Deficit Hyperactivity Disorder. *Behav. Brain Funct. BBF* 1:2. doi: 10.1186/1744-9081-1-2

Ásgrímsdóttir, E. S., and Arenas, E. (2020). Midbrain dopaminergic neuron development at the single cell level: in vivo and in stem cells. *Front. Cell Dev. Biol.* 8:463. doi: 10.3389/fcell.2020.00463

Association, A. P. (2013). *Diagnostic and Statistical Manual of Mental Disorders (DSM- 5), Fifth Edition*, 5th Edn. Washington, DC: American Psychiatric Association Publishing

Bariselli, S., Contestabile, A., Tzanoulinou, S., Musardo, S., and Bellone, C. (2018). SHANK3 downregu-lation in the ventral tegmental area accelerates

the extinction of contextual associations induced by juvenile non-familiar conspecific interaction. *Front. Mol. Neurosci.* 11:360. doi: 10.3389/fnmol.2018.00360

Bariselli, S., Tzanoulinou, S., Glangetas, C., Prévost-Solié, C., Pucci, L., Viguié, J., et al. (2016). SHANK3 controls maturation of social reward circuits in the VTA. *Nat. Neurosci.* 19, 926–934. doi: 10.1038/nn.4319

Bayer, S. A., Wills, K. V., Triarhou, L. C., and Ghetti, B. (1995). Time of neuron origin and gradients of neurogenesis in midbrain dopaminergic neurons in the mouse. *Exp. Brain Res.* 105, 191–199. doi: 10.1007/bf00240955

Beaulieu, J.-M., Sotnikova, T. D., Marion, S., Lefkowitz, R. J., Gainetdinov, R. R., and Caron, M. G. (2005). An Akt/β-Arrestin 2/PP2A signaling complex mediates dopaminergic neurotransmission and behavior. *Cell* 122, 261–273. doi: 10.1016/j.cell.2005.05.012

Beier, K. T., Gao, X. J., Xie, S., DeLoach, K. E., Malenka, R. C., and Luo, L. (2019). Topological organi-zation of ventral tegmental area connectivity revealed by viral-genetic dissection of input-output relations. *Cell Rep.* 26, 159–167.e6. doi: 10.1016/j.celrep.2018.12.040

Beier, K. T., Steinberg, E. E., DeLoach, K. E., Xie, S., Miyamichi, K., Schwarz, L., et al. (2015). Circuit architecture of VTA dopamine neurons revealed by systematic input-output mapping. *Cell* 162, 622–634. doi: 10.1016/j.cell.2015.07.015

Beil, J., Fairbairn, L., Pelczar, P., and Buch, T. (2012). Is BAC transgenesis obsolete? State of the art in the era of designer nucleases. *J. Biomed. Biotechnol.* 2012:308414. doi: 10.1155/2012/308414

Benes, F. M., Vincent, S. L., and Molloy, R. (1993). Dopamine-Immunoreactive axon varicosities form nonrandom contacts with GABA-immunoreactive neurons of rat medial prefrontal cortex. *Synapse* 14, 285–295. doi: 10.1002/syn.890150405

Benes, F. M., Vincent, S. L., Molloy, R., and Khan, Y. (1996). Increased interaction of dopamine- immu-noreactive varicosities with GABA neurons of rat medial prefontal cortex occurs during the post-weanling period. *Synapse* 23, 237–245.

Bhattacherjee, A., Djekidel, M. N., Chen, R., Chen, W., Tuesta, L. M., and Zhang, Y. (2019). Cell type-specific transcriptional programs in mouse prefrontal cortex during adolescence and addiction. *Nat. Commun.* 10:4169. doi: 10.1038/s41467-019-12054-3

Biol Psychiat (2017). Special issue: the dopamine hypothesis of schizophrenia. *Biol. Psychiat.* 81:1. doi: 10.1016/j.biopsych.2016.11.002

Blaess, S., and Ang, S. (2015). Genetic control of midbrain dopaminergic neuron development. *Wiley Interdiscip. Rev. Dev. Biol.* 4, 113–134. doi: 10.1002/wdev.169

Blaess, S., Bodea, G. O., Kabanova, A., Chanet, S., Mugniery, E., Derouiche, A., et al. (2011). Temporal-spatial changes in Sonic Hedgehog expression and signaling reveal different potentials of ventral mesencephalic progenitors to populate distinct ventral midbrain nuclei. *Neural Dev.* 6:29. doi: 10.1186/1749-8104-6-29

Boccuto, L., Lauri, M., Sarasua, S. M., Skinner, C. D., Buccella, D., Dwivedi, A., et al. (2013). Prevalence of SHANK3 variants in patients with different subtypes of autism spectrum disorders. *Eur. J. Hum. Genet.* 21, 310–316. doi: 10.1038/ejhg.2012.175

Bodea, G. O., and Blaess, S. (2015). Establishing diversity in the dopaminergic system. *FEBS Lett.* 589, 3773–3785. doi: 10.1016/j.febslet.2015.09.016

Bodei, S., Arrighi, N., Spano, P., and Sigala, S. (2009). Should we be cautious on the use of commercially available antibodies to dopamine receptors? *Naunyn Schmiedebergs Arch. Pharmacol.* 379, 413–415. doi: 10.1007/s00210-008-0384-6

Bordelon-Glausier, J. R., Khan, Z. U., and Muly, E. C. (2008). Quantification of D1 and D5 dopamine re-ceptor localization in layers I, III, and V of *Macaca mulatta* prefrontal cortical area 9: Coexpression in dendritic spines and axon terminals. *J. Comp. Neurol.* 508, 893–905. doi: 10.1002/cne.21710

Bowton, E., Saunders, C., Reddy, I. A., Campbell, N. G., Hamilton, P. J., Henry, L. K., et al. (2014). SLC6A3 coding variant Ala559Val found in two autism probands alters dopamine transporter function and trafficking. *Transl. Psychiatry* 4:e00464-64. doi: 10.1038/tp.2014.90

Boyson, S., McGonigle, P., and Molinoff, P. (1986). Quantitative autoradiographic localization of the D1 and D2 subtypes of dopamine receptors in rat brain. *J. Neurosci.* 6, 3177–3188. doi: 10.1523/jneurosci.06-11-03177.1986

Braun, U., Harneit, A., Pergola, G., Menara, T., Schäfer, A., Betzel, R. F., et al. (2021). Brain network dy-namics during working memory are modulated by dopamine and diminished in schizophrenia. *Nat. Commun.* 12:3478. doi: 10.1038/s41467-021-23694-9

Brenhouse, H. C., Sonntag, K. C., and Andersen, S. L. (2008). Transient D1 dopamine receptor expres-sion on prefrontal cortex projection neurons: relationship to enhanced motivational salience of drug cues in adolescence. *J. Neurosci.* 28, 2375–2382. doi: 10.1523/jneurosci.5064-07.2008

Brignani, S., and Pasterkamp, R. J. (2017). Neuronal subset-specific migration and axonal wiring mech-anisms in the developing midbrain dopamine system. *Front. Neuroanat.* 11:55. doi: 10.3389/fnana.2017.00055

Bye, C. R., Thompson, L. H., and Parish, C. L. (2012). Birth dating of midbrain dopamine neurons identi-fies A9 enriched tissue for transplantation into Parkinsonian mice. *Exp. Neurol.* 236, 58–68. doi: 10.1016/j.expneurol.2012.04.002

Caballero, A., and Tseng, K. Y. (2016). GABAergic function as a limiting factor for prefrontal maturation during adolescence. *Trends Neurosci.* 39, 441–448. doi: 10.1016/j.tins.2016.04.010

Carlén, M. (2017). What constitutes the prefrontal cortex? *Science* 358, 478–482. doi: 10.1126/science.aan8868

Cartier, E., Hamilton, P. J., Belovich, A. N., Shekar, A., Campbell, N. G., Saunders, C., et al. (2015). Rare autism-associated variants implicate syntaxin 1 (STX1 R26Q) phosphorylation and the dopamine transporter (hDAT R51W) in dopamine neurotransmission and behaviors. *Ebiomedicine* 2, 135–146. doi: 10.1016/j.ebiom.2015.01.007

Chini, M., and Hanganu-Opatz, I. L. (2020). Prefrontal cortex development in health and disease: les-sons from rodents and humans. *Trends Neurosci.* 44, 227–240. doi: 10.1016/j.tins.2020.10.017

Chisholm, K., Lin, A., Abu-Akel, A., and Wood, S. J. (2015). The association between autism and schizo-phrenia spectrum disorders: A review of eight alternate models of co-occurrence. *Neurosci. Biobehav. Rev.* 55, 173–183. doi: 10.1016/j.neubiorev.2015.04.012

Chuhma, N., Mingote, S., Kalmbach, A., Yetnikoff, L., and Rayport, S. (2017). Heterogeneity in dopamine neuron synaptic actions across the striatum and its relevance for schizophrenia. *Biol. Psychiatry* 81, 43–51. doi: 10.1016/j.biopsych.2016.07.002

Chun, L. S., Free, R. B., Doyle, T. B., Huang, X.-P., Rankin, M. L., and Sibley, D. R. (2013). D1-D2 do-pamine receptor synergy promotes calcium signaling via multiple mechanisms. *Mol. Pharmacol.* 84, 190–200. doi: 10.1124/mol.113.085175

Ciliax, B. J., Nash, N., Heilman, C., Sunahara, R., Hartney, A., Tiberi, M., et al. (2000). Dopamine D5 re-ceptor immunolocalization in rat and monkey brain. *Synapse* 37, 125–145.

Clancy, B., Darlington, R. B., and Finlay, B. L. (2001). Translating developmental time across mammalian species. *Neuroscience* 105, 7–17. doi: 10.1016/s0306-4522(01)00171-3

Cortese, S. (2012). The neurobiology and genetics of Attention-Deficit/Hyperactivity Disorder (ADHD): What every clinician should know. *Eur. J. Paediatr Neurol.* 16, 422–433. doi: 10.1016/j.ejpn.2012.01.009

Crescenzo, F. D., Postorino, V., Siracusano, M., Riccioni, A., Armando, M., Curatolo, P., et al. (2019). Autistic symptoms in schizophrenia spectrum disorders: a systematic review and meta-analysis. *Front. Psychiatry* 10:78. doi: 10.3389/fpsyt.2019.00078

Del Campo, N., Chamberlain, S. R., Sahakian, B. J., and Robbins, T. W. (2011). The roles of dopamine and noradrenaline in the pathophysiology and treatment of attention-deficit/hyperactivity disorder. *Biol. Psychiatry* 69:e00145-57. doi: 10.1016/j.biopsych.2011.02.036

Dichter, G. S., Richey, J. A., Rittenberg, A. M., Sabatino, A., and Bodfish, J. W. (2012). Reward circuitry function in autism during face anticipation and outcomes. *J. Autism Dev. Disord.* 42, 147–160. doi: 10.1007/s10803-011-1221-1

Dumas, S., and Wallén-Mackenzie, Å (2019). Developmental co-expression of Vglut2 and Nurr1 in a mes-di-encephalic continuum preceeds dopamine and glutamate neuron specification. *Front. Cell Dev. Biol.* 7:307. doi: 10.3389/fcell.2019.00307

Engelhard, B., Finkelstein, J., Cox, J., Fleming, W., Jang, H. J., Ornelas, S., et al. (2019). Specialized coding of sensory, motor and cognitive variables in VTA dopamine neurons. *Nature* 570, 509–513. doi: 10.1038/s41586-019-1261-9

Ernst, M., Zametkin, A., Matochik, J., Pascualvaca, D., and Cohen, R. (1997). Low medial prefrontal do-paminergic activity in autistic children. *Lancet* 350:638. doi: 10.1016/s0140-6736(05)63326-0

Fan, X., Dong, J., Zhong, S., Wei, Y., Wu, Q., Yan, L., et al. (2018). Spatial transcriptomic survey of hu-man embryonic cerebral cortex by single-cell RNA-seq analysis. *Cell Res.* 28, 730–745. doi: 10.1038/s41422-018-0053-3

Fan, X., Fu, Y., Zhou, X., Sun, L., Yang, M., Wang, M., et al. (2020). Single-cell transcriptome analysis reveals cell lineage specification in temporal-spatial patterns in human cortical development. *Sci. Adv.* 6:eaaz2978. doi: 10.1126/sciadv.aaz2978

Fang, H., Bygrave, A. M., Roth, R. H., Johnson, R. C., and Huganir, R. L. (2021). An optimized CRISPR/Cas9 approach for precise genome editing in neurons. *Elife* 10:e65202. doi: 10.7554/elife.65202

Fein, R. H., Venta, A., Meinert, A. C., Mire, S. S., and Bergez, K. (2021). "Autism spectrum disorder," in *Developmental Psychopathology*, eds A. Venta, C. Sharp, J. M. Fletcher, and P. Fonagy (Hoboken, NJ: John Wiley & Sons, Inc), 119–156. doi: 10.1002/9781118686089.ch6

Franco, S. J., and Müller, U. (2013). Shaping our minds: stem and progenitor cell diversity in the mam-malian neocortex. *Neuron* 77, 19–34. doi: 10.1016/j.neuron.2012.12.022

Freeman, T. B., Spence, M. S., Boss, B. D., Spector, D. H., Strecker, R. E., Olanow, C. W., et al. (1991). Development of dopaminergic neurons in the human substantia nigra. *Exp. Neurol.* 113, 344–353. doi: 10.1016/0014-4886(91)90025-8

Gadow, K. D., DeVincent, C. J., Olvet, D. M., Pisarevskaya, V., and Hatchwell, E. (2010). Association of DRD4 polymorphism with severity of oppositional defiant disorder, separation anxiety disorder and repetitive behaviors in children with autism spectrum disorder. *Eur. J. Neurosci.* 32, 1058–1065. doi: 10.1111/j.1460-9568.2010.07382.x

Gamo, N. J., Wang, M., and Arnsten, A. F. T. (2010). Methylphenidate and atomoxetine enhance prefron-tal function through α2-adrenergic and dopamine D1 receptors. *J. Am. Acad. Child Adolesc. Psychiatry* 49, 1011–1023. doi: 10.1016/j.jaac.2010.06.015

Garcia, L. P., Witteveen, J. S., Middelman, A., van Hulten, J. A., Martens, G. J. M., Homberg, J. R., et al. (2019). Perturbed developmental serotonin signaling affects prefrontal catecholaminergic innerva-tion and cortical integrity. *Mol. Neurobiol.* 56, 1405–1420. doi: 10.1007/s12035-018-1105-x

Gaspar, P., Berger, B., Febvret, A., Vigny, A., and Henry, J. (1989). Catecholamine innervation the hu-man cerebral cortex as revealed comparative immunohistochemistry tyrosine hydroxylase and do-pamine-Beta-H ydroxylase. *J. Comp. Neurol.* 279, 249–271. doi: 10.1002/cne.902790208

Gaspar, P., Bloch, B., and Moine, C. (1995). D1 and D2 receptor gene expression in the rat frontal cortex: cellular localization in different classes of efferent neurons. *Eur. J. Neurosci.* 7, 1050–1063. doi: 10.1111/j.1460-9568.1995.tb01092.x

Gauthier, J., Spiegelman, D., Piton, A., Lafrenière, R. G., Laurent, S., St−Onge, J., et al. (2009). Novel de novo SHANK3 mutation in autistic patients. *Am. J. Med. Genet. Part B Neuropsychiatr. Genet.* 150B, 421–424. doi: 10.1002/ajmg.b.30822

Ghaeli, P., Nikvarz, N., Alaghband-Rad, J., Alimadadi, A., and Tehrani-Doost, M. (2014). Effects of risperidone on core symptoms of autistic disorder based on childhood autism rating scale: an open label study. *Indian J. Psychol. Med.* 36, 66–70. doi: 10.4103/0253-7176.127254

Gillberg, C., and Svennerholm, L. (1987). CSF monoamines in autistic syndromes and other pervasive developmental disorders of early childhood. *Br. J. Psychiatry* 151, 89–94. doi: 10.1192/bjp.151.1.89

Gizer, I. R., Ficks, C., and Waldman, I. D. (2009). Candidate gene studies of ADHD: a meta-analytic re-view. *Hum. Genet.* 126, 51–90. doi: 10.1007/s00439-009-0694-x

Goldman-Rakic, P. S., and Brown, R. M. (1982). Postnatal development of monoamine content and syn-thesis in the cerebral cortex of rhesus monkeys. *Dev. Brain Res.* 4, 339–349. doi: 10.1016/0165-3806(82)90146-8

Goldman-Rakic, P. S., Leranth, C., Williams, S. M., Mons, N., and Geffard, M. (1989). Dopamine synaptic complex with pyramidal neurons in primate cerebral cortex. *Proc. Natl. Acad. Sci. U.S.A.* 86, 9015–9019. doi: 10.1073/pnas.86.22.9015

Gong, S., Doughty, M., Harbaugh, C. R., Cummins, A., Hatten, M. E., Heintz, N., et al. (2007). Targeting cre recombinase to specific neuron populations with bacterial artificial chromosome constructs. *J. Neurosci.* 27, 9817–9823. doi: 10.1523/jneurosci.2707-07.2007

Gong, S., Zheng, C., Doughty, M. L., Losos, K., Didkovsky, N., Schambra, U. B., et al. (2003). A gene expression atlas of the central nervous system based on bacterial artificial chromosomes. *Nature* 425, 917–925. doi: 10.1038/nature02033

Grace, A. A. (2016). Dysregulation of the dopamine system in the pathophysiology of schizophrenia and depression. *Nat. Rev. Neurosci.* 17, 524–532. doi: 10.1038/nrn.2016.57

Grace, A. A. (2017). Dopamine system dysregulation and the pathophysiology of schizophrenia: insights from the methylazoxymethanol acetate model. *Biol. Psychiatry* 81, 5–8. doi: 10.1016/j.biopsych.2015.11.007

Hamilton, P. J., Campbell, N. G., Sharma, S., Erreger, K., Hansen, F. H., Saunders, C., et al. (2013). De novo mutation in the dopamine transporter gene associates dopamine dysfunction with autism spec-trum disorder. *Mol. Psychiatry* 18, 1315–1323. doi: 10.1038/mp.2013.102

Hayes, L., Zhang, Z., Albert, P., Zervas, M., and Ahn, S. (2011). Timing of Sonic hedgehog and Gli1 ex-pression segregates midbrain dopamine neurons. *J. Comp. Neurol.* 519, 3001–3018. doi: 10.1002/cne.22711

Hisahara, S., and Shimohama, S. (2011). Dopamine receptors and Parkinson's disease. *Int. J. Med. Chem.* 2011, 1–16. doi: 10.1155/2011/403039

Hoops, D., and Flores, C. (2017). Making dopamine connections in adolescence. *Trends Neurosci.* 40, 709–719. doi: 10.1016/j.tins.2017.09.004

Iversen, L., Iversen, S., Dunnett, S., and Björklund, A. eds (2009). *Dopamine Handbook*. Oxford: Oxford University Press, doi: 10.1093/acprof:oso/9780195373035.001.0001

Jensen, P. S., Mrazek, D., Knapp, P. K., Steinberg, L., Pfeffer, C., Schowalter, J., et al. (1997). Evolution and revolution in child psychiatry. *J. Am. Acad. Child Adolesc. Psychiatry* 36, 1672–1681. doi: 10.1097/00004583-199712000-00015

Joksimovic, M., Anderegg, A., Roy, A., Campochiaro, L., Yun, B., Kittappa, R., et al. (2009). Spatiotemporally separable Shh domains in the midbrain define distinct dopaminergic progenitor pools. *Proc. Natl. Acad. Sci. U.S.A.* 106, 19185–19190. doi: 10.1073/pnas.0904285106

Kaasinen, V., Vilkman, H., Hietala, J., Någren, K., Helenius, H., Olsson, H., et al. (2000). Age-related do-pamine D2/D3 receptor loss in extrastriatal regions of the human brain. *Neurobiol. Aging* 21, 683–688. doi: 10.1016/s0197-4580(00)00149-4

Kabanova, A., Pabst, M., Lorkowski, M., Braganza, O., Boehlen, A., Nikbakht, N., et al. (2015). Function and developmental origin of a mesocortical inhibitory circuit. *Nat. Neurosci.* 18, 872–882. doi: 10.1038/nn.4020

Kalsbeek, A., Voorn, P., Buijs, R. M., Pool, C. W., and Uylings, H. B. M. (1988). Development of the do-paminergic innervation in the prefrontal cortex of the rat. *J. Comp. Neurol.* 269, 58–72. doi: 10.1002/cne.902690105

Kercood, S., Grskovic, J. A., Banda, D., and Begeske, J. (2014). Working memory and autism: a review of literature. *Res. Autism Spect. Dis.* 8, 1316–1332. doi: 10.1016/j.rasd.2014.06.011

Kim, J.-Y., and Paredes, M. F. (2021). Implications of extended inhibitory neuron development. *Int. J. Mol. Sci.* 22:5113. doi: 10.3390/ijms22105113

King, B. H., and Lord, C. (2011). Is schizophrenia on the autism spectrum? *Brain Res.* 1380, 34–41. doi: 10.1016/j.brainres.2010.11.031

Klein, M. O., Battagello, D. S., Cardoso, A. R., Hauser, D. N., Bittencourt, J. C., and Correa, R. G. (2019). Dopamine: functions, signaling, and association with neurological diseases. *Cell. Mol. Neurobiol.* 39, 31–59. doi: 10.1007/s10571-018-0632-3

Kohls, G., Schulte-Rüther, M., Nehrkorn, B., Müller, K., Fink, G. R., Kamp-Becker, I., et al. (2012). Reward system dysfunction in autism spectrum disorders. *Soc. Cogn. Affect. Neurosci.* 8, 565–572. doi: 10.1093/scan/nss033

Kolk, S. M., Gunput, R.-A. F., Tran, T. S., van den Heuvel, D. M. A., Prasad, A. A., Hellemons, A. J. C. G. M., et al. (2009). Semaphorin 3F is a bifunctional guidance cue for dopaminergic axons and con-trols their fasciculation, channeling, rostral growth, and intracortical targeting. *J. Neurosci.* 29, 12542–12557. doi: 10.1523/jneurosci.2521-09.2009

Kosillo, P., and Bateup, H. S. (2021). Dopaminergic dysregulation in syndromic autism spectrum disor-ders: insights from genetic mouse models. *Front. Neural Circuits* 15:68. doi: 10.3389/fncir.2021.700968

Kouwenhoven, W., Fortin, G., Penttinen, A., Florence, C., Delignat-Lavaud, B., Bourque, M., et al. (2020). VGluT2 expression in dopamine neurons contributes to postlesional striatal reinnervation. *J. Neurosci.* 40, 8262–8275. doi: 10.1523/JNEUROSCI.0823-20.2020

Kriete, T., and Noelle, D. C. (2015). Dopamine and the development of executive dysfunction in autism spectrum disorders. *PLoS One* 10:e0121605. doi: 10.1371/journal.pone.0121605

Labouesse, M. A., Cola, R. B., and Patriarchi, T. (2020). GPCR-Based dopamine sensors—a detailed guide to inform sensor choice for in vivo imaging. *Int. J. Mol. Sci.* 21:8048. doi: 10.3390/ijms21218048

Lammel, S., Ion, D. I., Roeper, J., and Malenka, R. C. (2011). Projection-Specific modulation of dopamine neuron synapses by aversive and rewarding stimuli. *Neuron* 70, 855–862. doi: 10.1016/j.neuron.2011.03.025

Lammel, S., Lim, B. K., Ran, C., Huang, K. W., Betley, M. J., Tye, K. M., et al. (2012). Input-specific con-trol of reward and aversion in the ventral tegmental area. *Nature* 491, 212–217. doi: 10.1038/nature11527

Landwehrmeyer, B., Mengod, G., and Palacios, J. M. (1993). Differential visualization of dopamine D2 and D3 receptor sites in rat brain. a comparative study using in situ hybridization histochemistry and ligand binding autoradiography. *Eur. J. Neurosci.* 5, 145–153. doi: 10.1111/j.1460-9568.1993.tb00480.x

Laubach, M., Amarante, L. M., Swanson, T. K., and White, S. R. (2018). What, if anything, is rodent pre-frontal cortex? *Eneuro* 5:ENEURO.0315-18.2018. doi: 10.1523/eneuro.0315-18.2018

Lavin, A., Nogueira, L., Lapish, C. C., Wightman, R. M., Phillips, P. E. M., and Seamans, J. K. (2005). Mesocortical dopamine neurons operate in distinct temporal domains using multimodal signaling. *J. Neurosci.* 25, 5013–5023. doi: 10.1523/jneurosci.0557-05.2005

Lee, S. J., Lodder, B., Chen, Y., Patriarchi, T., Tian, L., and Sabatini, B. L. (2021). Cell-type-specific asynchronous modulation of PKA by dopamine in learning. *Nature* 590, 451–456. doi: 10.1038/s41586-020-03050-5

Lee, S. P., So, C. H., Rashid, A. J., Varghese, G., Cheng, R., Lança, A. J., et al. (2004). Dopamine D1 and D2 receptor co-activation generates a novel phospholipase c-mediated calcium signal*. *J. Biol. Chem.* 279, 35671–35678. doi: 10.1074/jbc.m401923200

Lee, Y.-A., and Goto, Y. (2015). Prefrontal cortical dopamine from an evolutionary perspective. *Neurosci. Bull.* 31, 164–174. doi: 10.1007/s12264-014-1499-z

Leslie, C. A., Robertson, M. W., Cutler, A. J., and Bennett, J. P. (1991). Postnatal development of D 1 dopamine receptors in the medial prefrontal cortex, striatum and nucleus accumbens of normal and neonatal 6-hydroxydopamine treated rats: a quantitative autoradiographic analysis. *Dev. Brain Res.* 62, 109–114. doi: 10.1016/0165-3806(91)90195-o

Levey, A. I., Hersch, S. M., Rye, D. B., Sunahara, R. K., Niznik, H. B., Kitt, C. A., et al. (1993). Localiza-tion of D1 and D2 dopamine receptors in brain with subtype-specific antibodies. *Proc. Natl. Acad. Sci. U.S.A.* 90, 8861–8865. doi: 10.1073/pnas.90.19.8861

Levitt, P., and Moore, R. (1979). Development of the noradrenergic innervation of neocortex. *Brain Res.* 162, 243–259. doi: 10.1016/0006-8993(79)90287-7

Levitt, P., and Rakic, P. (1982). The time of genesis, embryonic origin and differentiation of the brain stem monoamine neurons in the rhesus monkey. *Dev. Brain Res.* 4, 35–57. doi: 10.1016/0165-3806(82)90095-5

Lewis, D. A., and Harris, H. W. (1991). Differential laminar distribution of tyrosine hydroxylase-immunoreactive axons in infant and adult monkey prefrontal cortex. *Neurosci. Lett.* 125, 151–154. doi: 10.1016/0304-3940(91)90014-k

Lewitus, E., Kelava, I., Kalinka, A. T., Tomancak, P., and Huttner, W. B. (2014). An adaptive threshold in mammalian neocortical evolution. *PLoS Biol.* 12:e1002000. doi: 10.1371/journal.pbio.1002000

Li, Y., and Kuzhikandathil, E. V. (2012). Molecular characterization of individual D3 dopamine receptor-expressing cells isolated from multiple brain regions of a novel mouse model. *Brain Struct. Funct.* 217, 809–833. doi: 10.1007/s00429-012-0383-8

Lidow, M. S., and Rakic, P. (1992). Scheduling of monoaminergic neurotransmitter receptor expression in the primate neocortex during postnatal development. *Cereb. Cortex* 2, 401–416. doi: 10.1093/cercor/2.5.401

Lidow, M. S., Koh, P., and Arnsten, A. F. T. (2003). D1 dopamine receptors in the mouse prefrontal cor-tex: Immunocytochemical and cognitive neuropharmacological analyses. *Synapse* 47, 101–108. doi: 10.1002/syn.10143

Lim, L., Mi, D., Llorca, A., and Marín, O. (2018). Development and functional diversification of cortical interneurons. *Neuron* 100, 294–313. doi: 10.1016/j.neuron.2018.10.009

Lui, J. H., Hansen, D. V., and Kriegstein, A. R. (2011). Development and evolution of the human neocor-tex. *Cell* 146, 18–36. doi: 10.1016/j.cell.2011.06.030

Macosko, E. Z., Basu, A., Satija, R., Nemesh, J., Shekhar, K., Goldman, M., et al. (2015). Highly parallel genome-wide expression profiling of individual cells using nanoliter droplets. *Cell* 161, 1202–1214. doi: 10.1016/j.cell.2015.05.002

Madisen, L., Zwingman, T. A., Sunkin, S. M., Oh, S. W., Zariwala, H. A., Gu, H., et al. (2010). A robust and high-throughput Cre reporting and characterization system for the whole mouse brain. *Nat. Neurosci.* 13, 133–140. doi: 10.1038/nn.2467

Marder, S. R., and Cannon, T. D. (2019). Schizophrenia. *N. Engl. J. Med.* 381, 1753–1761. doi: 10.1056/nejmra1808803

Marotta, R., Risoleo, M. C., Messina, G., Parisi, L., Carotenuto, M., Vetri, L., et al. (2020). The neuro-chemistry of autism. *Brain Sci.* 10:163. doi: 10.3390/brainsci10030163

Maynard, K. R., Collado-Torres, L., Weber, L. M., Uytingco, C., Barry, B. K., Williams, S. R., et al. (2021). Transcriptome-scale spatial gene expression in the human dorsolateral prefrontal cortex. *Nat. Neurosci.* 24, 425–436. doi: 10.1038/s41593-020-00787-0

McCracken, J. T., McGough, J., Shah, B., Cronin, P., Hong, D., Aman, M. G., et al. (2002). Risperidone in children with autism and serious behavioral problems. *N. Engl. J. Med.* 347, 314–321. doi: 10.1056/nejmoa013171

McDougle, C. J., Scahill, L., Aman, M. G., McCracken, J. T., Tierney, E., Davies, M., et al. (2005). Risper-idone for the core symptom domains of autism: results from the study by the autism network of the research units on pediatric psychopharmacology. *Am. J. Psychiatry* 162, 1142–1148. doi: 10.1176/appi.ajp.162.6.1142

Menegas, W., Akiti, K., Amo, R., Uchida, N., and Watabe-Uchida, M. (2018). Dopamine neurons project-ing to the posterior striatum reinforce avoidance of threatening stimuli. *Nat. Neurosci.* 21, 1421–1430. doi: 10.1038/s41593-018-0222-1

Mereu, M., Contarini, G., Buonaguro, E. F., Latte, G., Managò, F., Iasevoli, F., et al. (2017). Dopamine transporter (DAT) genetic hypofunction in mice produces alterations consistent with ADHD but not schizophrenia or bipolar disorder. *Neuropharmacology* 121, 179–194. doi: 10.1016/j.neuropharm.2017.04.037

Mesman, S., von Oerthel, L., and Smidt, M. P. (2014). Mesodiencephalic dopaminergic neuronal differ-entiation does not involve GLI2A-Mediated SHH-signaling and is under the direct influence of ca-nonical WNT signaling. *PLoS One* 9:e97926. doi: 10.1371/journal.pone.0097926

Mingote, S., Chuhma, N., Kusnoor, S. V., Field, B., Deutch, A. Y., and Rayport, S. (2015). Functional connectome analysis of dopamine neuron glutamatergic connections in forebrain regions. *J. Neurosci.* 35, 16259–16271. doi: 10.1523/jneurosci.1674-15.2015

Miškiæ, T., Kostoviæ, I., Rašin, M.-R., and Krsnik, Ž (2021). Adult upper cortical layer specific transcrip-tion factor CUX2 is expressed in transient subplate and marginal zone neurons of the developing human brain. *Cells* 10:415. doi: 10.3390/cells10020415

Missale, C., Nash, S. R., Robinson, S. W., Jaber, M., and Caron, M. G. (1998). Dopamine receptors: from structure to function. *Physiol. Rev.* 78, 189–225. doi: 10.1152/physrev.1998.78.1.189

Mukhtar, T., and Taylor, V. (2018). Untangling cortical complexity during development. *J. Exp. Neurosci.* 12:1179069518759332. doi: 10.1177/1179069518759332

Nakamura, S., Ito, Y., Shirasaki, R., and Murakami, F. (2000). Local directional cues control growth po-larity of dopaminergic axons along the rostrocaudal axis. *J. Neurosci.* 20, 4112–4119. doi: 10.1523/jneurosci.20-11-04112.2000

Naneix, F., Marchand, A. R., Scala, G. D., Pape, J.-R., and Coutureau, E. (2012). Parallel maturation of goal-directed behavior and dopaminergic systems during adolescence. *J. Neurosci.* 32, 16223–16232. doi: 10.1523/jneurosci.3080-12.2012

Navandar, M., Martín-García, E., Maldonado, R., Lutz, B., Gerber, S., and de Azua, I. R. (2021). Tran-scriptional signatures in prefrontal cortex confer vulnerability versus resilience to food and cocaine addiction-like behavior. *Sci. Rep.* 11:9076. doi: 10.1038/s41598-021-88363-9

Neale, B. M., Kou, Y., Liu, L., Ma'ayan, A., Samocha, K. E., Sabo, A., et al. (2012). Patterns and rates of exonic de novo mutations in autism spectrum disorders. *Nature* 485, 242–245. doi: 10.1038/nature11011

Noaín, D., Avale, M. E., Wedemeyer, C., Calvo, D., Peper, M., and Rubinstein, M. (2006). Identification of brain neurons expressing the dopamine D4 receptor gene using BAC transgenic mice. *Eur. J. Neurosci.* 24, 2429–2438. doi: 10.1111/j.1460-9568.2006.05148.x

Noisin, E. L., and Thomas, W. E. (1988). Ontogeny of dopaminergic function in the rat midbrain tegmen-tum, corpus striatum and frontal cortex. *Dev. Brain Res.* 41, 241–252. doi: 10.1016/0165-3806(88)90186-1

Palaniyappan, L., Batty, M. J., Liddle, P. F., Liddle, E. B., Groom, M. J., Hollis, C., et al. (2019). Reduced prefrontal gyrification in carriers of the dopamine D4 receptor 7-Repeat allele with attention deficit/hyperactivity disorder: a preliminary report. *Front. Psychiatry* 10:235. doi: 10.3389/fpsyt.2019.00235

Panman, L., Papathanou, M., Laguna, A., Oosterveen, T., Volakakis, N., Acampora, D., et al. (2014). Sox6 and Otx2 control the specification of substantia nigra and ventral tegmental area dopamine neurons. *Cell Rep.* 8, 1018–1025. doi: 10.1016/j.celrep.2014.07.016

Paredes, M. F., James, D., Gil-Perotin, S., Kim, H., Cotter, J. A., Ng, C., et al. (2016). Extensive migration of young neurons into the infant human frontal lobe. *Science* 354:aaf7073. doi: 10.1126/science.aaf7073

Pastor, V., and Medina, J. H. (2021). Medial prefrontal cortical control of reward—and aversion—based behavioral output: Bottom—up modulation. *Eur. J. Neurosci.* 53, 3039–3062. doi: 10.1111/ejn.15168

Pavăl, D. (2017). A dopamine hypothesis of autism spectrum disorder. *Dev. Neurosci.* 39, 355–360. doi: 10.1159/000478725

Pavăl, D., and Micluția, I. V. (2021). The dopamine hypothesis of autism spectrum disorder revisited: current status and future prospects. *Dev. Neurosci.* 43, 73–83. doi: 10.1159/000515751

Pérez-López, J. L., Contreras-López, R., Ramírez-Jarquín, J. O., and Tecuapetla, F. (2018). Direct glu-tamatergic signaling from midbrain dopaminergic neurons onto pyramidal prefrontal cortex neu-rons. *Front. Neural Circuit* 12:70. doi: 10.3389/fncir.2018.00070

Phelan, K., and McDermid, H. E. (2012). The 22q13.3 deletion syndrome (Phelan-McDermid Syndrome). *Mol. Syndromol.* 2, 186–201. doi: 10.1159/000334260

Polioudakis, D., de la Torre-Ubieta, L., Langerman, J., Elkins, A. G., Shi, X., Stein, J. L., et al. (2019). A single-cell transcriptomic atlas of human neocortical development during mid-gestation. *Neuron* 103, 785–801.e8. doi: 10.1016/j.neuron.2019.06.011

Poulin, J.-F., Caronia, G., Hofer, C., Cui, Q., Helm, B., Ramakrishnan, C., et al. (2018). Mapping projec-tions of molecularly defined dopamine neuron subtypes using intersectional genetic approaches. *Nat. Neurosci.* 21, 1260–1271. doi: 10.1038/s41593-018-0203-4

Poulin, J.-F., Gaertner, Z., Moreno-Ramos, O. A., and Awatramani, R. (2020). Classification of midbrain dopamine neurons using single-cell gene expression profiling approaches. *Trends Neurosci.* 43, 155–169. doi: 10.1016/j.tins.2020.01.004

Prince, J. (2008). Catecholamine dysfunction in attention-deficit/hyperactivity disorder: an update. *J. Clin. Psychopharm.* 28, S39–S45. doi: 10.1097/jcp.0b013e318174f92a

Raghanti, M. A., Stimpson, C. D., Marcinkiewicz, J. L., Erwin, J. M., Hof, P. R., and Sherwood, C. C. (2008). Cortical dopaminergic innervation among humans, chimpanzees, and macaque monkeys: A comparative study. *Neuroscience* 155, 203–220. doi: 10.1016/j.neuroscience.2008.05.008

Rajput, P. S., Kharmate, G., Somvanshi, R. K., and Kumar, U. (2009). Colocalization of dopamine recep-tor subtypes with dopamine and cAMP-regulated phosphoprotein (DARPP-32) in rat brain. *Neurosci. Res.* 65, 53–63. doi: 10.1016/j.neures.2009.05.005

Reynolds, L. M., Pokinko, M., Torres-Berrío, A., Cuesta, S., Lambert, L. C., Pellitero, E. D. C., et al. (2018). DCC receptors drive prefrontal cortex maturation by determining dopamine axon targeting in adolescence. *Biol. Psychiatry* 83, 181–192. doi: 10.1016/j.biopsych.2017.06.009

Rice, M. W., Roberts, R. C., Melendez-Ferro, M., and Perez-Costas, E. (2016). Mapping dopaminergic deficiencies in the substantia nigra/ventral tegmental area in schizophrenia. *Brain Struct. Funct.* 221, 185–201. doi: 10.1007/s00429-014-0901-y

Risi, M. D., Tufano, M., Alvino, F. G., Ferraro, M. G., Torromino, G., Gigante, Y., et al. (2021). Altered heparan sulfate metabolism during development triggers dopamine-dependent autistic-behaviours in models of lysosomal storage disorders. *Nat. Commun.* 12:3495. doi: 10.1038/s41467-021-23903-5

Root, D. H., Wang, H.-L., Liu, B., Barker, D. J., Mód, L., Szocsics, P., et al. (2016). Glutamate neurons are intermixed with midbrain dopamine neurons in nonhuman primates and humans. *Sci. Rep.* 6:30615. doi: 10.1038/srep30615

Rosenberg, D. R., and Lewis, D. A. (1995). Postnatal maturation of the dopaminergic innervation of mon-key prefrontal and motor cortices: A tyrosine hydroxylase immunohistochemical analysis. *J. Comp. Neurol.* 358, 383–400. doi: 10.1002/cne.903580306

Rothmond, D. A., Weickert, C. S., and Webster, M. J. (2012). Developmental changes in human dopa-mine neurotransmission: cortical receptors and terminators. *BMC Neurosci.* 13:18. doi: 10.1186/1471-2202-13-18

Rumsey, R. K., Rudser, K., Delaney, K., Potegal, M., Whitley, C. B., and Shapiro, E. (2014). Acquired autistic behaviors in children with mucopolysaccharidosis type IIIA. *J. Pediatrics* 164:1147–1151.e1. doi: 10.1016/j.jpeds.2014.01.007

Santana, N., and Artigas, F. (2017). Laminar and cellular distribution of monoamine receptors in rat medial prefrontal cortex. *Front. Neuroanat.* 11:87. doi: 10.3389/fnana.2017.00087

Santana, N., Mengod, G., and Artigas, F. (2009). Quantitative analysis of the expression of dopamine D1 and D2 receptors in pyramidal and GABAergic neurons of the rat prefrontal cortex. *Cereb. Cortex* 19, 849–860. doi: 10.1093/cercor/bhn134

Saunders, B. T., Richard, J. M., Margolis, E. B., and Janak, P. H. (2018). Dopamine neurons create Pav-lovian conditioned stimuli with circuit-defined motivational properties. *Nat. Neurosci.* 21, 1072–1083. doi: 10.1038/s41593-018-0191-4

Schambra, U. B., Duncan, G. E., Breese, G. R., Fornaretto, M. G., Caron, M. G., and Fremeau, R. T. (1994). Ontogeny of D1a and D2 dopamine receptor subtypes in rat brain using in situ hybridization and receptor binding. *Neuroscience* 62, 65–85. doi: 10.1016/0306-4522(94)90315-8

Schubert, D., Martens, G. J. M., and Kolk, S. M. (2015). Molecular underpinnings of prefrontal cortex development in rodents provide insights into the etiology of neurodevelopmental disorders. *Mol. Psychiatry* 20, 795–809. doi: 10.1038/mp.2014.147

Seamans, J. K., Lapish, C. C., and Durstewitz, D. (2008). Comparing the prefrontal cortex of rats and primates: Insights from electrophysiology. *Neurotox. Res.* 14, 249–262. doi: 10.1007/bf03033814

Sesack, S., Aoki, C., and Pickel, V. (1994). Ultrastructural localization of D2 receptor-like immunoreactivi-ty in midbrain dopamine neurons and their striatal targets. *J. Neurosci.* 14, 88–106. doi: 10.1523/jneurosci.14-01-00088.1994

Shaw, P., Eckstrand, K., Sharp, W., Blumenthal, J., Lerch, J. P., Greenstein, D., et al. (2007a). Attention-deficit/hyperactivity disorder is characterized by a delay in cortical maturation. *Proc. Natl. Acad. Sci. U.S.A.* 104, 19649–19654. doi: 10.1073/pnas.0707741104

Shaw, P., Gornick, M., Lerch, J., Addington, A., Seal, J., Greenstein, D., et al. (2007b). Polymorphisms of the dopamine D4 receptor, clinical outcome, and cortical structure in attention-deficit/hyperactivity disorder. *Arch. Gen. Psychiatry* 64, 921–931. doi: 10.1001/archpsyc.64.8.921

Smiley, J. F., and Goldman-Rakic, P. S. (1993). Heterogeneous targets of dopamine synapses in mon-key prefrontal cortex demonstrated by serial section electron microscopy: a laminar analysis using the silver-enhanced diaminobenzidine sulfide (SEDS) immunolabeling technique. *Cereb. Cortex* 3, 223–238. doi: 10.1093/cercor/3.3.223

Sonnenschein, S. F., Gomes, F. V., and Grace, A. A. (2020). Dysregulation of midbrain dopamine sys-tem and the pathophysiology of schizophrenia. *Front. Psychiatry* 11:613. doi: 10.3389/fpsyt.2020.00613

Spek, A. A., and Wouters, S. G. M. (2010). Autism and schizophrenia in high functioning adults: Behav-ioral differences and overlap. *Res. Autism Spect. Dis.* 4, 709–717. doi: 10.1016/j.rasd.2010.01.009

Spencer, T. J., Biederman, J., Madras, B. K., Faraone, S. V., Dougherty, D. D., Bonab, A. A., et al. (2005). In vivo neuroreceptor imaging in attention-deficit/hyperactivity disorder: a focus on the do-pamine transporter. *Biol. Psychiatry* 57, 1293–1300. doi: 10.1016/j.biopsych.2005.03.036

Staal, W. G. (2014). Autism, DRD3 and repetitive and stereotyped behavior, an overview of the current knowledge. *Eur. Neuropsychopharmacol. J. Eur. Coll. Neuropsychopharmacol.* 25, 1421–1426. doi: 10.1016/j.euroneuro.2014.08.011

Staal, W. G., Langen, M., van Dijk, S., Mensen, V. T., and Durston, S. (2015). DRD3 gene and striatum in autism spectrum disorder. *Br. J. Psychiatry* 206, 431–432. doi: 10.1192/bjp.bp.114.148973

Stanford, S. C., and Heal, D. J. (2019). Catecholamines: Knowledge and understanding in the 1960s, now, and in the future. *Brain Neurosci. Adv.* 3:2398212818810682. doi: 10.1177/2398212818810682

Starkweather, C. K., and Uchida, N. (2021). Dopamine signals as temporal difference errors: recent ad-vances. *Curr. Opin. Neurobiol.* 67, 95–105. doi: 10.1016/j.conb.2020.08.014

Steinkellner, T., Zell, V., Farino, Z. J., Sonders, M. S., Villeneuve, M., Freyberg, R. J., et al. (2018). Role for VGLUT2 in selective vulnerability of midbrain dopamine neurons. *J. Clin. Invest.* 128, 774–788. doi: 10.1172/jci95795

Surmeier, D. J., Obeso, J. A., and Halliday, G. M. (2017). Selective neuronal vulnerability in Parkinson disease. *Nat. Rev. Neurosci.* 18, 101–113. doi: 10.1038/nrn.2016.178

Tanaka, Y., Cakir, B., Xiang, Y., Sullivan, G. J., and Park, I.-H. (2020). Synthetic analyses of single-cell transcriptomes from multiple brain organoids and fetal brain. *Cell Rep.* 30, 1682–1689.e3. doi: 10.1016/j.celrep.2020.01.038

Tarazi, F. I., and Baldessarini, R. J. (2000). Comparative postnatal development of dopamine D1, D2 and D4 receptors in rat forebrain. *Int. J. Dev. Neurosci.* 18, 29–37. doi: 10.1016/s0736-5748(99)00108-2

Thomas, W. S., Neal-Beliveau, B. S., and Joyce, J. N. (1998). There is a limited critical period for dopa-mine's effects on D1 receptor expression in the developing rat neostriatum. *Dev. Brain Res.* 111, 99–106. doi: 10.1016/s0165-3806(98)00126-6

Tritsch, N. X., and Sabatini, B. L. (2012). Dopaminergic modulation of synaptic transmission in cortex and striatum. *Neuron* 76, 33–50. doi: 10.1016/j.neuron.2012.09.023

Tseng, K. Y., and O'Donnell, P. (2005). Post-pubertal emergence of prefrontal cortical up states in-duced by D1–NMDA co-activation. *Cereb. Cortex* 15, 49–57. doi: 10.1093/cercor/bhh107

Tseng, K.-Y., and O'Donnell, P. (2007). Dopamine modulation of prefrontal cortical interneurons chang-es during adolescence. *Cereb. Cortex* 17, 1235–1240. doi: 10.1093/cercor/bhl034

Uylings, H. B. M., Groenewegen, H. J., and Kolb, B. (2003). Do rats have a prefrontal cortex? *Behav. Brain Res.* 146, 3–17. doi: 10.1016/j.bbr.2003.09.028

Valstar, M. J., Neijs, S., Bruggenwirth, H. T., Olmer, R., Ruijter, G. J. G., Wevers, R. A., et al. (2010). Mu-copolysaccharidosis type IIIA: Clinical spectrum and genotype-phenotype correlations. *Ann. Neurol.* 68, 876–887. doi: 10.1002/ana.22092

Verney, C. (1999). Distribution of the catecholaminergic neurons in the central nervous system of human embryos and fetuses. *Microsc. Res. Tech.* 46, 24–47.

Verney, C., Milosevic, A., Alvarez, C., and Berger, B. (1993). Immunocytochemical evidence of well−developed dopaminergic and noradrenergic innervations in the frontal cerebral cortex of human fetus-es at midgestation. *J. Comp. Neurol.* 336, 331–344. doi: 10.1002/cne.903360303

Verney, C., Zecevic, N., Nikolic, B., Alvarez, C., and Berger, B. (1991). Early evidence of catecholaminer-gic cell groups in 5- and 6-week-old human embryos using tyrosine hydroxylase and dopamine-β-hydroxylase immunocytochemistry. *Neurosci. Lett.* 131, 121–124. doi: 10.1016/0304-3940(91)90351-s

Verwey, M., Grant, A., Meti, N., Adye-White, L., Torres-Berrío, A., Rioux, V., et al. (2016). Mesocortical dopamine phenotypes in mice lacking the sonic hedgehog receptor Cdon. *Eneuro* 3:ENEU-RO.0009-16.2016. doi: 10.1523/eneuro.0009-16.2016

Vincent, S. L., Khan, Y., and Benes, F. M. (1993). Cellular distribution of dopamine D, and D, receptors in rat medial prefrontal cortex. *J. Neurosci.* 13, 2251–2564. doi: 10.1523/JNEUROSCI.13-06-02551.1993

Vincent, S. L., Khan, Y., and Benes, F. M. (1995). Cellular colocalization of dopamine D1 and D2 recep-tors in rat medial prefrontal cortex. *Synapse* 19, 112–120. doi: 10.1002/syn.890190207

Volkow, N. D., and Morales, M. (2015). The brain on drugs: from reward to addiction. *Cell* 162, 712–725. doi: 10.1016/j.cell.2015.07.046

Voorn, P., Kalsbeek, A., Jorritsma-Byham, B., and Groenewegen, H. (1988). The pre- and postnatal de-velopment of the dopaminergic cell groups in the ventral mesencephalon and the dopaminergic inner-vation of the striatum of the rat. *Neuroscience* 25, 857–887. doi: 10.1016/0306-4522(88)90041-3

Vosberg, D. E., Leyton, M., and Flores, C. (2020). The Netrin-1/DCC guidance system: dopamine path-way maturation and psychiatric disorders emerging in adolescence. *Mol. Psychiatry* 25, 297–307. doi: 10.1038/s41380-019-0561-7

Walker, A. E., Spring, J. D., and Travis, M. J. (2017). Addressing cognitive deficits in schizophrenia: toward a neurobiologically informed approach. *Biol. Psychiatry* 81, e1–e3. doi: 10.1016/j.biopsych.2016.10.023

Wamsley, B., and Fishell, G. (2017). Genetic and activity-dependent mechanisms underlying interneuron diversity. *Nat. Rev. Neurosci.* 18, 299–309. doi: 10.1038/nrn.2017.30

Weele, C. M. V., Siciliano, C. A., and Tye, K. M. (2018). Dopamine tunes prefrontal outputs to orchestrate aversive processing. *Brain Res.* 1713, 16–31. doi: 10.1016/j.brainres.2018.11.044

Wei, X., Ma, T., Cheng, Y., Huang, C. C. Y., Wang, X., Lu, J., et al. (2018). Dopamine D1 or D2 receptor−expressing neurons in the central nervous system. *Addict. Biol.* 23, 569–584. doi: 10.1111/adb.12512 s

Weickert, C. S., Webster, M. J., Gondipalli, P., Rothmond, D., Fatula, R. J., Herman, M. M., et al. (2007). Postnatal alterations in dopaminergic markers in the human prefrontal cortex. *Neuroscience* 144, 1109–1119. doi: 10.1016/j.neuroscience.2006.10.009

Willems, J., de Jong, A. P. H., Scheefhals, N., Mertens, E., Catsburg, L. A. E., Poorthuis, R. B., et al. (2020). ORANGE: a CRISPR/Cas9-based genome editing toolbox for epitope tagging of endogenous proteins in neurons. *PLoS Biol.* 18:e3000665. doi: 10.1371/journal.pbio.3000665

Willing, J., Cortes, L. R., Brodsky, J. M., Kim, T., and Juraska, J. M. (2017). Innervation of the medial prefrontal cortex by tyrosine hydroxylase immunoreactive fibers during adolescence in male and female rats. *Dev. Psychobiol.* 59, 583–589. doi: 10.1002/dev.21525

Wu, J., Xiao, H., Sun, H., Zou, L., and Zhu, L.-Q. (2012). Role of dopamine receptors in ADHD: a sys-tematic meta-analysis. *Mol. Neurobiol.* 45, 605–620. doi: 10.1007/s12035-012-8278-5

Yamaguchi, T., Wang, H.-L., Li, X., Ng, T. H., and Morales, M. (2011). Mesocorticolimbic glutamatergic pathway. *J. Neurosci.* 31, 8476–8490. doi: 10.1523/jneurosci.1598-11.2011

Yan, Z., and Rein, B. (2021). Mechanisms of synaptic transmission dysregulation in the prefrontal cortex: pathophysiological implications. *Mol. Psychiatry.* doi: 10.1038/s41380-021-01092-3 [Online ahead of print].

Yu, Q., Liu, Y.-Z., Zhu, Y.-B., Wang, Y.-Y., Li, Q., and Yin, D.-M. (2019). Genetic labeling reveals tem-poral and spatial expression pattern of D2 dopamine receptor in rat forebrain. *Brain Struct. Funct.* 224, 1035–1049. doi: 10.1007/s00429-018-01824-2

Zecevic, N., and Verney, C. (1995). Development of the catecholamine neurons in human embryos and fetuses, with special emphasis on the innervation of the cerebral cortex. *J. Comp. Neurol.* 351, 509–535. doi: 10.1002/cne.903510404

Zeeland, A. A. S.-V., Dapretto, M., Ghahremani, D. G., Poldrack, R. A., and Bookheimer, S. Y. (2010). Reward processing in autism. *Autism Res. Official J. Int. Soc. Autism Res.* 3, 53–67. doi: 10.1002/aur.122

Zhang, Z.-W., Burke, M. W., Calakos, N., Beaulieu, J.-M., and Vaucher, E. (2010). Confocal analysis of cholinergic and dopaminergic inputs onto pyramidal cells in the prefrontal cortex of rodents. *Front. Neuroanat.* 4:21. doi: 10.3389/fnana.2010.00021

Zhong, P., Qin, L., and Yan, Z. (2020). Dopamine differentially regulates response dynamics of pre-frontal cortical principal neurons and interneurons to optogenetic stimulation of inputs from ventral tegmental area. *Cereb. Cortex* 30, 4402–4409. doi: 10.1093/cercor/bhaa027

Zhong, S., Zhang, S., Fan, X., Wu, Q., Yan, L., Dong, J., et al. (2018). A single-cell RNA-seq survey of the developmental landscape of the human prefrontal cortex. *Nature* 555, 524–528. doi: 10.1038/nature25980

Zubair, M., Murris, S. R., Isa, K., Onoe, H., Koshimizu, Y., Kobayashi, K., et al. (2021). Divergent whole brain projections from the ventral midbrain in macaques. *Cereb. Cortex* 31, 2913–2931. doi: 10.1093/cercor/bhaa399

Conflict of Interest: The authors declare that the research was conducted in the absence of any commercial or financial relationships that could be construed as a potential conflict of interest.

Publisher's Note: All claims expressed in this article are solely those of the authors and do not necessarily represent those of their affiliated organizations, or those of the publisher, the editors and the reviewers. Any product that may be evaluated in this article, or claim that may be made by its manufacturer, is not guaranteed or endorsed by the publisher.

Copyright © 2021 Islam, Meli and Blaess. This is an open-access article distributed under the terms of the Creative Commons Attribution License (CC BY). The use, distribution or reproduction in other forums is permitted, provided the original author(s) and the copyright owner(s) are credited and that the original publication in this journal is cited, in accordance with accepted academic practice. No use, distribution or reproduction is permitted which does not comply with these terms.

frontiers in Neural Circuits

REVIEW
published: 09 November 2021
doi: 10.3389/fncir.2021.752420

Dopamine Circuit Mechanisms of Addiction-Like Behaviors

Carli L. Poisson[1,2,3], *Liv Engel*[1,2] *and Benjamin T. Saunders*[1,2,3]*

[1] Department of Neuroscience, University of Minnesota, Minneapolis, MN, United States, [2] Medical Discovery Team on Addiction, University of Minnesota, Minneapolis, MN, United States, [3] Graduate Program in Neuroscience, University of Minnesota, Minneapolis, MN, United States

Addiction is a complex disease that impacts millions of people around the world. Clinically, addiction is formalized as substance use disorder (SUD), with three primary symptom categories: exaggerated substance use, social or lifestyle impairment, and risky substance use. Considerable efforts have been made to model features of these criteria in non-human animal research subjects, for insight into the underlying neurobiological mechanisms. Here we review evidence from rodent models of SUD-inspired criteria, focusing on the role of the striatal dopamine system. We identify distinct mesostriatal and nigrostriatal dopamine circuit functions in behavioral outcomes that are relevant to addictions and SUDs. This work suggests that striatal dopamine is essential for not only positive symptom features of SUDs, such as elevated intake and craving, but also for impairments in decision making that underlie compulsive behavior, reduced sociality, and risk taking. Understanding the functional heterogeneity of the dopamine system and related networks can offer insight into this complex symptomatology and may lead to more targeted treatments.

Keywords: dopamine, striatum, addiction, substance use disorder, animal model, nigrostriatal, mesostriatal

OPEN ACCESS

Edited by:
Talia Newcombe Lerner, Northwestern University, United States

Reviewed by:
Marco Venniro, University of Maryland, Baltimore, United States
Barbara Juarez, University of Washington, United States
Donna J. Calu, University of Maryland, Baltimore, United States
Susan Ferguson, University of Washington, United States

***Correspondence:**
Benjamin T. Saunders
bts@umn.edu

Received: *03 August 2021*
Accepted: *08 October 2021*
Published: *09 November 2021*

Citation:
Poisson CL, Engel L and Saunders BT (2021) Dopamine Circuit Mechanisms of Addiction-Like Behaviors. Front. Neural Circuits 15:752420. doi: 10.3389/fncir.2021.752420

INTRODUCTION

Addiction is characterized by a transition from recreational drug use to compulsive, disordered use, punctuated by cycles of abstinence, withdrawal, craving, and relapse. Features of human drug use are complicated by social and political factors, including stigmatization, criminalization, and barriers to treatment access. Over the past 30 years, the prevailing scientific consensus has identified addiction as a chronic disease, codified as substance use disorder (SUD). SUDs are characterized by pharmacological effects of tolerance and withdrawal, as well as a core set of behavioral features defined by the Diagnostic and Statistical Manual of Mental Disorders (DSM-5). These can be grouped into three major categories: I. Impaired control of substance use; II. Social impairment; and III. Risky use of substance (**Figure 1**, top). Significant research efforts have been made to characterize the neurobiological and psychological underpinnings of these behavioral symptoms. The hope is that understanding the basic science behind these behaviors will lead to more effective treatments for SUD, and other psychiatric illnesses with comorbid symptoms (such as compulsive gambling, ADHD, and schizophrenia).

Research making use of non-human animals is essential to this effort. Leveraging convergent biology of reward learning and decision-making systems across species, addiction scientists have established a variety of animal models to investigate drug-related behaviors (**Figure 1**). While considerable debate exists surrounding the translational efficacy of individual models to the complexity of human addiction (for recent review, see Venniro et al., 2020), they

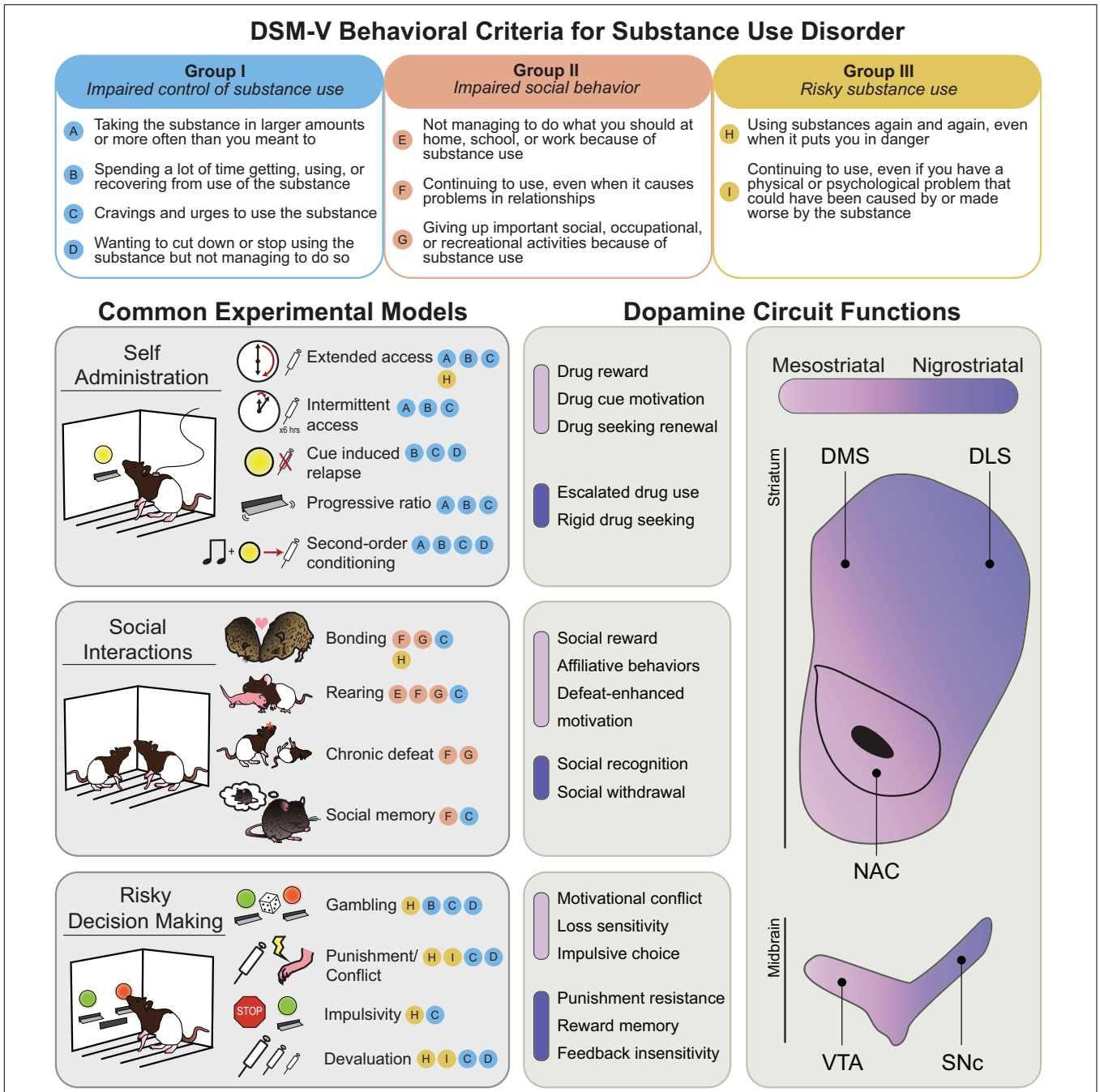

FIGURE 1 | Behavioral models used to classify phenotypes of substance use disorder. **(Top)** The behavioral criteria of SUDs (circled letters) can be sorted into three main categories: impaired control of substance use (Group I), impaired social behavior (Group II), and risky substance use (Group III). **(Left)** Common rodent experimental models and the SUD criteria they are thought to best approximate. Note that most models capture multiple SUD features. **(Right)** Mesostriatal circuits (light purple), including dopamine projections from the ventral tegmental area (VTA) to the nucleus accumbens (NAC), and nigrostriatal circuits (dark purple), including dopamine projections to the dorsomedial (DMS) and dorsolateral striatum (DLS), have generally dissociable roles in different components of major SUD models. In the middle panels, the most clearly defined roles for these two systems in each SUD category are listed.

nonetheless offer powerful experimental insight into neurobehavioral mechanisms that govern core features of drug use.

Among brain systems, dopamine (DA) circuits are a key modulator of behaviors associated with SUDs. *Via* several mechanisms, including direct excitation of DA neurons (nicotine, alcohol), blockade of terminal DA reuptake (amphetamine, cocaine), and DA neuron disinhibition (opioids and cannabinoids), nearly all drugs used by humans acutely increase signaling of DA within the striatum, and blocking

DA receptors decreases the reinforcing effects of many drugs (Wise and Bozarth, 1987; Johnson and North, 1992; Nutt et al., 2015; Volkow et al., 2017; Nestler and Lüscher, 2019; Solinas et al., 2019; Wise and Robble, 2020). The connection between DA and drug use is further supported by *in vivo* measurements of drug-evoked DA release in human and non-human animal studies (Hernandez et al., 1987; Chiara and Imperato, 1988; Robinson et al., 1988; Pontieri et al., 1995; Ito et al., 2002; Porrino et al., 2004; Volkow et al., 2006; Belin and Everitt, 2008; Willuhn et al., 2012, 2014). Humans with a history of drug use, including those meeting DSM criteria for SUDs, have altered DA system transmission and function (Stewart, 2008; Volkow et al., 2009; Diana, 2011; Leyton and Vezina, 2014; Ikemoto et al., 2015; Leyton, 2017). As such, popular theories of addiction and compulsive behavior are built on the notion of altered activity in the DA system (Robinson and Berridge, 1993; Everitt and Robbins, 2005; Wise, 2009; Keiflin and Janak, 2015; Nestler and Lüscher, 2019). Advances in neuroscience research technology and theory surrounding addiction-like behaviors in animal models of reward seeking have afforded the opportunity to characterize the role of precisely defined brain circuits and regions in behavior. In this review, we will discuss current evidence for regional and circuit-specific functions within the DA system in different aspects of addiction-like behavior, in the context of animal studies derived from DSM criteria for the behavioral features of SUDs.

DOPAMINE CIRCUITS

Most of the brain's neurons are in two midbrain regions (**Figure 1**): the ventral tegmental area (VTA) and substantia nigra pars compacta (SNc). DA neurons in the VTA largely project to the ventral striatum, in particular, the nucleus accumbens (NAc) core and shell, comprising the mesostriatal pathway, and to other frontal targets in the pallidum, amygdala, and prefrontal cortex (Swanson, 1982; Ikemoto, 2007). Intermingled with DA neurons in the VTA are a substantial fraction of GABAergic and glutamatergic neurons (Olson and Nestler, 2007; Nair-Roberts et al., 2008; Bouarab et al., 2019). The SNc, in contrast, contains DA neurons that project almost exclusively to the dorsomedial (DMS) and dorsolateral (DLS) striatum, comprising the nigrostriatal pathway (Beckstead et al., 1979; Swanson, 1982; Fields et al., 2007; Ikemoto, 2007; Britt et al., 2012). At their targets in the striatum, DA neurons primarily contact GABAergic medium spiny neurons (MSNs) that contain excitatory type 1 (D1-MSNs), or inhibitory type 2 (D2-MSNs) DA receptors (Gerfen, 1984; Kupchik et al., 2015). Dopamine's modulatory influence on striatal activity *via* these outputs is a predominant mechanism of behavioral control in reward learning and motivation. Notably, many drugs act in the striatum to increase DA release locally, *via* regionally specific terminal mechanisms (Collins and Saunders, 2020), which plays a key role in heterogeneous mechanisms of drug use, craving, and relapse behaviors that underlie features of SUDs (Koob and Bloom, 1988; Ahmed and Koob, 1998; Lobo et al., 2010; Thompson et al., 2010; Oliver et al., 2019).

Dopamine neurons across VTA and SNc circuits exhibit considerable heterogeneity with respect to behavioral function (**Figure 1**; Björklund and Dunnett, 2007; Lammel et al., 2014; Morales and Margolis, 2017; Cox and Witten, 2019; Collins and Saunders, 2020). In the classic framework, mesostriatal DA neurons contribute to learning and execution of goal-directed behaviors, while nigrostriatal DA, especially in the DLS, is involved in movement control and the execution of rigid, habitual actions (Haber et al., 2000; Hassani et al., 2001; Everitt, 2014; Burton et al., 2015; Saunders et al., 2018; Cox and Witten, 2019). From an extensive literature, deficits in VTA and SNc DA signaling typically impair learning and reward-directed behaviors, or movement planning, execution and vigor, respectively. Exaggerated VTA and SNc DA signaling, conversely, underlies compulsive motivation and behavioral inflexibility (Robinson and Berridge, 1993; Cardinal et al., 2002; Everitt and Robbins, 2005; Wise, 2005). In the context of Pavlovian learning, sensory cues associated with increased VTA DA neuron activity evoke approach behavior and acquire value that supports second-order conditioning of instrumental actions, which is critical for persistent and adaptive reward pursuit (Berridge, 2007; Flagel et al., 2011; Saunders and Robinson, 2012; Saunders et al., 2018). Nigrostriatal DA neurons, especially those projecting to the DMS, are important for linking instrumental actions with outcomes they produce (Yin et al., 2005). Further, activation of SNc DA neurons evokes movement, and their activity encodes movement initiation (Dodson et al., 2016; Coddington and Dudman, 2018; da Silva et al., 2018), suggesting they contribute more generally to movement invigoration. VTA DA neuron activity and release in the NAc is in contrast engaged when animals emit cue- or goal-directed movements (Carelli, 2004; Burton et al., 2015; Howe and Dombeck, 2016; Mohebi et al., 2019). As such, mesostriatal DA can be conceptualized as generating a motivational "pull" to cues and the rewards they predict, while nigrostriatal DA provides a "push" that underlies general behavioral invigoration or arousal (Bolles, 1967; Ostlund, 2019). Thus, while dissociable, normal activity in these parallel circuits is necessary for successful reward seeking and reward-based decision making (Arias-Carrión and Pöppel, 2007; Aarts et al., 2011; Hsu et al., 2018; Le Heron et al., 2018, 2020; Cox and Witten, 2019; Collins and Saunders, 2020).

Via its roles in signaling expectation, value, and action invigoration, DA has strong influence on both goal-directed and habitual actions that result from reward learning. These fundamental behavioral classifications are each maladapted in addiction (Tiffany, 1990; Singer et al., 2018; Ostlund, 2019; Hogarth, 2020; Vandaele and Ahmed, 2021). Given that drugs impinge heavily on DA circuitry, functional, circuit-level differences within the DA system have important implications for the understanding of SUDs. In the following, we will review some of the ways in which mesostriatal and nigrostriatal DA pathways regulate behaviors associated with major SUD criteria. Notably, emerging work highlights that striatal DA is essential not only for features of SUDs characterized by exaggerated behavior, such as drug use and craving, but also for behavioral deficits, including impairments in decision

making that underlie compulsive behavior, reduced sociality, and risk taking.

CATEGORY I – IMPAIRED CONTROL OF SUBSTANCE USE

A hallmark of SUDs is a progression to impaired control over drug use, associated with increased drug intake, craving, and relapse vulnerability. As such, a major DSM criterion includes behavioral features such as "taking the substance in larger amounts or more often," "spending a lot of time getting, using, or recovering from use of the substance," and "cravings and urges to use the substance." Animal studies of these SUD features are among the most common, leveraging the power of drug self administration models. The self administration models that align best with Category I SUD criteria are shown in **Figure 1**. Rodents, like humans, will readily self administer most commonly used drugs, such as; opioids, alcohol, cocaine, amphetamine, nicotine, and cannabinoids. In widely used paradigms, rats and mice are trained to engage in behaviors (typically, lever presses, or nose port responses) to receive drug doses delivered intravenously, orally, or *via* inhalation. Drug-associated cues and contexts, as well as small "priming" drug doses, stress and pain play a central role in promoting and maintaining drug use and relapse (Stewart, 1984; Balster and Lukas, 1985; Goeders and Guerin, 1994; Shaham et al., 2003; Chaudhri et al., 2008; Spanagel, 2017). In relapse models, the resumption of drug seeking following abstinence can be used as a behavioral index of drug "craving". Notably, drug craving assessed in animal models undergoes "incubation" in the weeks to months following abstinence from many drug types. That is, the longer it has been since the last drug exposure, the greater the probability and intensity of relapse (Grimm et al., 2001; Venniro et al., 2016). This sensitization of the relapse-inducing power of drug cues in particular results in a persistent threat of a return to drug use, a feature of SUDs that is especially difficult to treat.

A major development in rodent addiction models came when it was discovered that giving rats extended access to drugs promotes an escalation of intake, where more drug is taken in a shorter time period, mimicking a central tenet of human SUDs. This has been observed with many drugs, including cocaine, heroin, methamphetamine, alcohol, and nicotine (Ahmed and Koob, 1998; Ahmed et al., 2000; Roberts et al., 2000; Kitamura et al., 2006; O'Dell et al., 2007). Escalation of drug intake following extended access is associated with other addiction-like features, including increased motivation for drug, drug seeking in the face of high effort cost, and seeking despite negative consequences. This approach has since informed a large portion of preclinical addiction research, including attempts to create a DSM-inspired composite addiction phenotype that can be applied to rodents (Deroche-Gamonet et al., 2004; Robinson, 2004; Vanderschuren and Everitt, 2004; O'Neal et al., 2020). More recently, intermittent access drug self administration models have gained attention (Zimmer et al., 2012; Kawa et al., 2019a). In these paradigms, brief periods of drug availability are interspersed with longer drug unavailability periods. This intermittency promotes rapid, binge-like drug intake that may better approximate some human drug use patterns. Intermittent self administration of cocaine, alcohol, and opioids, despite resulting in much less total drug intake compared to extended access models, promotes escalation of intake and elevated drug craving (Simms et al., 2008; Zimmer et al., 2012; Calipari et al., 2013; Kawa et al., 2016; O'Neal et al., 2020; Fragale et al., 2021; Samaha et al., 2021). Binge-like self administration can also develop in rats given extended, continuous access to cocaine, and individual differences in binge patterns early in self administration training predict the intensity of future use (Tornatzky and Miczek, 2000; Belin et al., 2009). Finally, some rodent models have also incorporated a behavioral economics framework to quantify drugs as commodities, to examine choice elasticity and demand (Oleson and Roberts, 2009; Bentzley et al., 2013; Mohammadkhani et al., 2019). This approach is useful for standardization of core behavioral indices related to decision making and motivation, which could facilitate quantitative comparisons across different tasks and reward modalities.

Mesostriatal

Drugs act on DA circuits to promote synaptic plasticity that amplifies VTA activity and DA signaling in the NAc, even following a single exposure (Ungless et al., 2001; Mameli et al., 2009; Pascoli et al., 2012; Ungless and Grace, 2012; Ji et al., 2017; Morel et al., 2019; Thompson et al., 2021). Within the mesostriatal pathway, DA release evoked by drugs occurs *via* multiple mechanisms that impinge on VTA cells and their axon terminals (Ritz et al., 1987; Thomas et al., 2008; Volkow et al., 2009; Mark et al., 2011; Ford, 2014; Lammel et al., 2014). Given the central role that mesostriatal DA plays in reward learning and behavioral reinforcement (Fouriezos and Wise, 1976; Corbett and Wise, 1980; Witten et al., 2011; Steinberg et al., 2014), this system is key in the control of drug seeking, drug cue-evoked motivation, and craving. Manipulation of VTA DA neuron activity can regulate drug self administration in animal models. One way this has been studied is through manipulation of DA D2 autoreceptors. Activation of these receptors decreases activity of DA neurons and phasic DA release through a negative feedback loop (Schmitz et al., 2003), leading to changes in drug-taking behavior. Dopamine binding on VTA D2 receptors is negatively correlated with cocaine and amphetamine seeking and consumption (Buckholtz et al., 2010; Bello et al., 2011). Further, elevating VTA DA neuron activity *via* D2 knockdown increases cocaine self administration (Chen et al., 2018) and blocking the negative feedback activity of these receptors increases cocaine self administration (McCall et al., 2017). Additionally, rats with knockdown D2Rs will also work harder for sucrose and cocaine (de Jong et al., 2015). In line with this, reducing DA signaling in VTA neurons blunts cocaine self administration motivation, as measured by impaired behavior on a progressive ratio task (Ranaldi and Wise, 2001). These studies illustrate some ways that alterations in normal signaling with the mesostriatal pathway can alter motivation for drugs. Elevating VTA DA neuron activity can also promote impulsive choice behavior, for example, where rats prefer small, immediate rewards over larger rewards that require a longer waiting period (Bernosky-Smith et al., 2018), another

component of impaired control over reward seeking behavior that is common in SUDs (de Wit, 2009; Dalley and Ersche, 2019).

Mesostriatal DA signaling is important for the escalation of drug intake. Repeated drug exposure, *via* passive administration or self administration, generally increases DA signaling in the NAc and produces exaggerated drug seeking motivation (Robinson and Berridge, 2001). Recent work, however, highlights how the pattern of drug intake can produce starkly different effects on mesostriatal DA circuits (reviewed in Samaha et al., 2021). Extended or long access to drug self administration, which produces escalation of drug intake, craving, and other addiction-like behaviors across a variety of drug types (Ahmed and Koob, 1998; Vanderschuren and Ahmed, 2013; Ahmed, 2018), is also associated with blunted drug-evoked NAc DA signaling, especially in cocaine use models (Mateo et al., 2005; Calipari et al., 2014; Willuhn et al., 2014; Siciliano et al., 2015). Intermittent, binge-like cocaine use, in contrast, sensitizes mesostriatal DA signals, relative to animals with a history of extended or continuous access, despite also producing strong escalation of intake and craving after much less total drug exposure (Kawa et al., 2019a). Intermittent drug exposure also selectively potentiates cocaine's actions to inhibit DA transporter function, to facilitate elevated NAc DA signaling, relative to continuous or extended access (Calipari et al., 2013).

The distinction between the impact of extended versus intermittent access self administration on NAc DA signaling illustrates how DA circuits are sensitive to a number of features of drug experience, and careful consideration of the details of animal behavior models are critical for interpreting reported brain mechanism outcomes. For example, extended drug access may produce blunted NAc DA responses during well predicted and well learned drug-taking actions, an acute "hypodopaminergic" state that could promote greater drug taking to make up the reward deficit (Blum et al., 2000, 2015; Leyton and Vezina, 2014). Simultaneously, DA responses to drug-paired cues and unpredicted drug exposure can become sensitized, which underlies exaggerated cue-evoked drug seeking motivation, especially after a period of abstinence (Robinson and Berridge, 2001; Bradberry, 2007; Kawa et al., 2019b). Thus, it is possible for DA to be both down and upregulated in the context of SUD models, depending on specific DA circuits, task features, and when the signals are measured. Notably, humans use drugs in a variety of patterns, depending on the reason for use, the drug's pharmacology and route of administration, and various other social and cultural factors (Gardner, 2011; Allain et al., 2015), so animal models featuring extended, continuous, and intermittent exposure are all likely important for capturing different features of addiction that reflect complex adaptations in the DA system.

Drug seeking responses maintained by the conditioned reinforcing value of cocaine-paired cues rely on VTA activity (McFarland and Kalivas, 2001; Shaham et al., 2003; Ciano and Everitt, 2004; Yun et al., 2004; Kufahl et al., 2009; Lüscher and Malenka, 2011; Mahler and Aston-Jones, 2012). This feature of mesostriatal control of addiction-like behavior is clear in models of relapse, which is often precipitated by exposure to a cue or location that was previously paired with drug delivery. VTA DA neurons mediate drug-cue induced relapse behaviors, and drug cues elicit VTA DA activity and DA release in the NAc with cocaine, alcohol, and other drugs (Ito et al., 2000; Phillips et al., 2003; Aragona et al., 2009; Ostlund et al., 2014; Wolf, 2016; Liu et al., 2020). Under periods of abstinence, VTA activity and NAC DA release facilitates relapse to cocaine, heroin, and alcohol in the presence of these cues (Shaham et al., 2003; Saunders et al., 2013; Corre et al., 2018; Mahler et al., 2019). Conversely, drug seeking is reduced by inactivation of the mesolimbic pathway (McFarland and Kalivas, 2001; Chaudhri et al., 2009; Saunders et al., 2013; Corre et al., 2018; Mahler et al., 2019; Valyear et al., 2020). These data fit within the framework of mesostriatal DA primarily controlling cue-guided or goal-directed drug seeking motivation.

Nigrostriatal

A crucial part of SUDs is that drug taking is no longer recreational, but can become habitual, characterized by inflexible drug-taking actions that are insensitive to feedback and changing contingencies. A central feature of the organization of dopamine-striatum circuitry is the transition from ventromedial signaling early in reward learning, when behaviors are primarily goal directed, to later signaling in dorsolateral striatum that accompanies the development of habit-like behaviors (Haber et al., 2000; Joel et al., 2002; Ikemoto, 2007; Burton et al., 2015). This transition is readily demonstrated across drug classes in animal models (Zapata et al., 2010; Clemens et al., 2014; Hodebourg et al., 2019; Zhou et al., 2019), where habit-like behaviors are associated with nigrostriatal activity. Notably, the nigrostriatal DA pathway is less directly activated by acute drug exposure in animals with limited drug use history, compared to the mesostriatal pathway (Mereu et al., 1987; Ito et al., 2002; Keath et al., 2007; Belin and Everitt, 2008; Murray et al., 2012; Willuhn et al., 2012, 2014). Drug use is thought to accelerate the transition to addiction-like behaviors *via* progressive engagement of the dorsolateral striatum. Evidence from rodent self-administration models supports this notion. Dopamine signaling in response to cocaine and cocaine-associated cues is initially strongest in the NAc as rats learn to self administer the drug. Over time, the DA response to cocaine delivery in the NAc weakens, and DLS DA signaling emerges (Ito et al., 2002; Willuhn et al., 2012, 2014). Further, the emergence of robust DLS DA signaling predicts the degree of escalation of drug use, and DA signaling and activity in the DLS is necessary for robust cocaine and alcohol self administration only after extended drug use (Belin and Everitt, 2008; Corbit et al., 2012; Murray et al., 2012; Willuhn et al., 2012, 2014). In line with this, DLS D1-MSN activity is associated with escalated methamphetamine self-administration (Oliver et al., 2019). Extended nicotine self administration is associated with exaggerated neural activity in the SNc and DLS (Clemens et al., 2014). DLS DA signaling is necessary for cocaine self administration maintained on second-order reinforcement schedules (Vanderschuren et al., 2005), which is thought to reflect the development of stimulus-response associations that are resistant to extinction. Further, within the DLS, well learned alcohol seeking actions are preferentially encoded over drug receipt (Fanelli et al., 2013), which is consistent with the notion of this system in mediating habitual or ritualistic features of drug taking (Everitt and Robbins, 2005). Together these results

suggest that the nigrostriatal DA pathway is recruited to promote the escalation of drug use and rigid drug-intake patterns, which underlies the development of addiction-like states in SUDs.

An inability to change behavior in response to changing outcome value is proposed to be a key reason behind drug craving and the draw of drug-associated cues. Interestingly, SNc DA neurons have been shown to encode reward values over the long term, even when these rewards are no longer expected (Kim et al., 2015). This could suggest that even if tolerance to some of the pharmacological features of a drug is developed, SNc DA retains the drug taking "habit" *via* an inflexible memory of the reward when first experienced. Disordered memory could also impact relapse susceptibility. For example, inflating rewarding memories of drug use, or decreasing memories of negative experience, could make one more likely to use a drug even after a period of abstinence. Supporting this general notion, in one study where rat SNc DA neurons were chemically lesioned, lesioned rats performed worse on a task that delivered negative feedback for poor performance (Da Cunha et al., 2001). Exaggerated or otherwise altered nigrostriatal activity that accompanies drug exposure may produce a state of feedback insensitivity that promotes exaggerated behaviors in SUDs.

CATEGORY II – IMPAIRED SOCIAL BEHAVIOR

The social and lifestyle consequences of SUDs are perhaps the most difficult to study in non-human animals, as this category includes behavioral features such as "continuing to use, even when it causes problems in relationships" and "giving up important social, occupational, or recreational activities because of substance use". Common models of social behavior that align with SUD diagnostic criteria are shown in **Figure 1**. Recent modeling efforts have focused on elements of sociality that are readily measured in species like rodents, including social interaction and affiliative and rearing behaviors, and the effects of social experience on decision making. Importantly, the interaction between social experience and drug-related behaviors is bidirectional. Conspecific-based stressors, including disrupted parental care, social isolation, and social defeat or subordinate status, generally increase future self administration of amphetamine, cocaine, alcohol, and heroin (Schenk et al., 1987; Bardo et al., 2013). In contrast, positively valenced or rewarding social interactions can be protective against cocaine and heroin self administration, craving, and other addiction-like behaviors, even in rats with extensive drug-taking experience (Banks and Negus, 2017; Venniro et al., 2018, 2019). Social play is highly rewarding in most mammals and relies on normal function in striatal DA systems (Vanderschuren et al., 1997; Manduca et al., 2016). As such, social behavior can be disrupted with prenatal or adolescent drug exposure (Trezza et al., 2014; Achterberg et al., 2019). Further, isolation from social play, particularly during adolescence, can promote future drug use and decision-making deficits associated with addiction (McCutcheon and Marinelli, 2009; Lesscher et al., 2015). Like social exposure, other forms of environmental enrichment and access to other non-food rewards, such as an exercise wheel, can have protective effects against escalation of cocaine self administration (Zlebnik and Carroll, 2015). While much remains to identify neural mechanisms of these effects, this work potentially underscores the importance of prosocial, lifestyle, and community-based SUD treatments for humans (Higgins et al., 2003; Meyers et al., 2011; Stitzer et al., 2011).

Mesostriatal

Given its core role in reward processes, the mesostriatal pathway has a central role in social behavior. Social interaction increases mesostriatal DA signaling and NAc neurons are active during approach to both novel conspecifics and pair-bonded partners (Robinson et al., 2002; Gunaydin et al., 2014; Scribner et al., 2020). Mesostriatal DA neurons projecting to the NAc are necessary for normal social interaction behavior (Gunaydin et al., 2014). Inhibition of mesostriatal DA neurons can disrupt exploration of novel conspecifics (Bariselli et al., 2018) and stimulating these neurons can enhance social preference (Bariselli et al., 2016). Drug-evoked changes in VTA DA signaling and physiology can impact these social behaviors. For example, neonatal exposure to amphetamine increases VTA DA activity and decreases social behavior in adulthood (Fukushiro et al., 2015). This may be due to a D1-specific mechanism in the NAc, as blocking D1-like DA receptors in this region rescues impaired social bonding behavior in amphetamine-treated male prairie voles (Liu et al., 2010). Further, following repeated exposure to amphetamine, female prairie voles show decreased social bonding behavior, accompanied by decreased DA D2 receptor immunoreactivity and increased DA levels in the NAc. Notably, administering oxytocin can restore social bonding and NAc DA levels, suggesting an interaction between oxytocin and DA systems in social behavior and drug use (Young et al., 2014).

In addition to drugs affecting mesostriatal DA signaling and social behavior, social interactions can in turn alter drug taking and signaling as well. Social defeat stress has been shown to enhance the long-term potentiation of glutamatergic signaling in the VTA as well as potentiate cocaine conditioned place preference (Stelly et al., 2016). Further, increased cocaine use following social defeat stress can be mimicked by directly infusing corticotropin releasing factor into the VTA, which modulates DA neurons (Leonard et al., 2017). Maternal separation can also disrupt reward seeking and DA signaling in the mesostriatal pathway. For example, female, but not male mice subjected to maternal separation and social isolation show a decreased conditioned place preference for a palatable reward and a decreased level of D1 receptor mRNA in the NAc (Sasagawa et al., 2017). Social isolation can also reduce the total dendritic length of MSNs in the NAc (Wang et al., 2012), while increasing DA signaling (Hall et al., 1999; Yorgason et al., 2016). The ability to produce aberrant or exaggerated mesostriatal DA signaling is thus one mechanism by which social stressors can produce addiction vulnerability.

Nigrostriatal

Given its role in movement control, the function of nigrostriatal DA in the context of Parkinson's disease (PD) models has

driven most research investigations. Notably, while severe PD is primarily characterized by motor impairments, patients also experience cognitive and emotional deficits that affect social behavior. As such, some (Tadaiesky et al., 2008; Matheus et al., 2016) suggest this pathway could be critical for social impairments seen in people with SUD's. Supporting this, in rats, nigrostriatal damage can increase depression-like symptoms and cognitive impairments in a social recognition test, as well as promote social withdrawal (Tadaiesky et al., 2008; Matheus et al., 2016). Interestingly, these effects were observed after an initial anhedonic response which mapped onto changes in dorsal striatal D1 and D2 receptor activity. Specifically, DA lesions increased the density of D1 and D2 receptors in the DLS after 7 days, which returned to control levels at 21 days when the anhedonic-like effects were no longer present and social withdrawal emerged. Cholinergic interneurons (ChIs) in the dorsal striatum, which can regulate DA release locally *via* terminal mechanisms (Collins and Saunders, 2020), may also play a role in regulating social behaviors in mild nigrostriatal lesioned mice. For example, inhibiting striatal ChIs reverses social memory impairments caused by DA depletion (Ztaou et al., 2018). While the connection between nigrostriatal DA and socially-based behavioral changes in the context of SUDs has not been characterized in animal models, this system is engaged by social experiences (Robinson et al., 2002). Lesions of the substantia nigra in general seem to reduce some social behaviors, including mate investigation and social grooming (Eison et al., 1977). Other studies have shown that rats with SNc lesions exhibit no difference on a social interaction test (Loiodice et al., 2019), however, so the connection between nigrostriatal DA signaling and normal social behaviors, independent of non-specific motor effects, requires more consideration.

Rearing conditions also affect the nigrostriatal dopaminergic pathway. Social enrichment can reverse the behavioral effects of nigrostriatal lesions in mice. Specifically, it slows the progressive nature of lesioning damage as well as reverses motor impairments (Goldberg et al., 2012). Social isolation increases DA release and uptake in the dorsal striatum in rats, *via* alterations in DA transporter function, which results in greater psychostimulant potency (Yorgason et al., 2016). Together these studies show that disruptions to the nigrostriatal dopaminergic pathway produce social and cognitive deficits and different social conditions can affect this pathway and in turn, drug reactivity.

CATEGORY III – RISKY SUBSTANCE USE

The DSM criteria for risky use of substances includes "using substances again and again, even when it puts you in danger" and "continuing to use, even when you know you have a physical or psychological problem that could have been caused or made worse by the substance". Common decision-making tasks thought to capture these SUD criteria are shown in **Figure 1**. Recently, animal models of behaviors related to this SUD criterion have become more common, including "risky" choice assessment, conflict procedures, and punishment-resistant intake models (Venniro et al., 2020).

Risky substance use is associated with compulsivity, which in animal models is typically operationalized as a continuation of behavior despite negative consequences. This is measured in a few ways. For example, rodent tasks that approximate human gambling conditions can assess cost-benefit decision making, sensitivity to loss or punishment, and performance under conditions of uncertainty as metrics of risk taking (Orsini et al., 2015; Winstanley and Clark, 2016; Lüscher et al., 2020). Approach-avoidance paradigms impose a situation of motivational conflict on the research subject, between the urge to seek out a reward and avoid an aversive or costly stimulus (Oleson and Cheer, 2013). In related punishment-based models, reward seeking actions also result in the delivery of noxious or otherwise aversive stimulus, such as footshock, or a bitter taste. A history of escalated use of several drugs, including cocaine, alcohol, and opiates promotes punishment resistance (Vanderschuren and Everitt, 2004; Pelloux et al., 2007; Marchant et al., 2013; Hopf and Lesscher, 2014; Blackwood et al., 2020; Monroe and Radke, 2021; Domi et al., 2021). Notably, these tasks are particularly useful for assessing individual differences in addiction-like behavior, as only a subset of animal subjects will persist in drug seeking in the face of high cost (Shaham et al., 2003; Everitt and Robbins, 2005; Cooper et al., 2007; Vanderschuren et al., 2017; Giuliano et al., 2018).

Mesostriatal

Ventral tegmental area DA neuron stimulation, in the absence of other reward-related stimuli, can lead to compulsive-like behavior. When given the option to self stimulate VTA DA neurons in the face of a punishing footshock, a subset of mice will perseverate, enduring high shock levels (Pascoli et al., 2015). Mesostriatal DA signaling is also important for conflict-based behaviors. In rats, phasic DA signaling in the NAc encodes motivational conflict: cues signaling threats evoke greater DA release compared to neutral cues, and this signal correlates with successful behavioral avoidance (Oleson et al., 2012; Gentry et al., 2016). Further, blocking NAc DA abolishes, and increasing NAc DA potentiates, drug-seeking behavior in a task where rats were required to cross an electrified barrier to receive infusions of cocaine (Saunders et al., 2013). Notably, this effect was strongest in the subset of rats who were willing to experience the highest shock levels, suggesting a link between mesostriatal DA and individual differences in motivation in the face of adverse consequences.

Disruptions to the mesostriatal pathway modulate so-called risk-based decisions that incorporate cost-benefit probabilities (Orsini et al., 2015). For example, DA signaling within the NAc encodes risky decisions in gambling-inspired tasks (Sugam et al., 2012). Notably, subsets of VTA DA neurons have different roles in risky decision making (Verharen et al., 2018). Activation of the mesostriatal pathway reduces sensitivity to loss and punishment, while activating the VTA-PFC pathway promotes risky decisions when there is no loss present. Further, stimulating the VTA after a non-rewarded risky choice, which overrides the phasic dip in DA release that would normally occur, biases rats to choose a risky reward in the future and reduces sensitivity to reward omissions (Stopper et al., 2014).

Hyperdopaminergic states, such as those evoked by drugs, can lead to disordered decision making that favors risk taking, feedback insensitivity, and behavioral inflexibility (Stalnaker et al., 2009; Izquierdo et al., 2010; Groman et al., 2018). Drug exposure can affect future risk-based decisions, *via* alterations in mesostriatal DA. For example, adolescent alcohol exposure in rats reduces overall mesostriatal DA tone, but potentiates phasic DA release, an effect that positively correlates with risk preference, and is reversed when the DA signal is normalized (Schindler et al., 2016). Adolescent drug exposure selectively disrupts NAc DA encoding of costs (Nasrallah et al., 2011), suggesting that feedback insensitivity associated with addiction-like behavior relies on specific drug-induced mesostriatal adaptations. Interestingly, the role of mesostriatal DA in risky decision making may be somewhat sex dependent, as males exhibit decreased cue-induced risky choice behavior following VTA inhibition while females exhibit increased risky choice (Hynes et al., 2021). These results suggest that altering VTA DA activity leads to an impairment of decision making that is facilitated by, and could contribute to, risky drug use.

Outside of the striatum, VTA projections to the prefrontal cortex also play a major role in reward seeking in risky situations. During reward-seeking actions, risk of punishment diminishes synchrony between the VTA and PFC (Park and Moghaddam, 2017). Further, during learning, phasic activity in the PFC of rats encodes risky seeking actions but not safe taking actions or reward delivery, suggesting that the PFC is preferentially involved in the learning of punishment probability. This effect was also sex specific, with females exhibiting greater sensitivity to probabilistic punishment than males (Jacobs and Moghaddam, 2020). However, this effect may not be mediated by VTA-PFC DA projections *per se*, given some studies showing that these neurons do not exhibit differential activity under threat of punishment (Verharen et al., 2020).

Nigrostriatal

The role of nigrostriatal DA in habit-like actions underlies its connection to compulsive behaviors that contribute to risky drug use (Everitt and Robbins, 2005). One characteristic of habit-like behavior is an encoding of a stable reward value despite changes to the reward itself. Notably, a subset of DA neurons in the lateral SNC demonstrate a "sustain-type" firing pattern that is insensitive to changes in expected reward after extended learning (Kim et al., 2015). Further, DLS DA axon terminals don't exhibit a clear decrease in activity when the actual reward is smaller than predicted, unlike terminals in dorsomedial and ventral striatum (Tsutsui-Kimura et al., 2020). This lack of feedback within the nigrostriatal pathway in learning could result in drug-taking behavior despite a negative consequence or in risky situations.

In an approach-avoidance decision making task, dopamine's actions within the DMS have opposing effects on behavior, with D1-MSN activation facilitating approach and D2-MSN receptors suppress approach. In contrast, DLS DA manipulations don't as clearly affect approach-avoidance behavior (Nguyen et al., 2019). However, after extended access to cocaine self administration, DLS inactivation selectively reduces self administration in the face of punishment, compared to unpunished use (Jonkman et al., 2012). Further, individual differences in the extent to which alcohol seeking engages activity in the DLS predicts susceptibility to punishment resistance (Giuliano et al., 2019), suggesting a specific role in compulsivity and threat-based feedback. DMS inactivation increases risky choice on a probabilistic discounting task in rats, suggesting that it in contrast can facilitate flexibility in reward prediction (Schumacher et al., 2021). Taken together, these results are consistent with the notion that SNc-DLS DA projections contribute to inflexible behavior, the SNc-DMS projections promote flexibility in goal-directed behavior, both of which are engaged during risk-reward decisions (Lerner et al., 2015; Vandaele and Ahmed, 2021). Recent evidence suggests that unlike other DA neurons, projections to the caudal "tail" portion of the dorsal striatum preferentially encode threatening stimuli and threat avoidance, relative to positively valenced stimuli (Menegas et al., 2018). This suggests they could have a critical role in risk-based decisions and compulsivity. Notably, the effect of a history of drug exposure on nigrostriatal and striatal tail function in conflict or avoidance tasks remains relatively unexplored. Nevertheless, the above data suggest that in SUD patients, dysregulation or imbalance of DA signaling across SNC output targets could promote risk insensitivity to underlie dangerous substance use.

Further insight into the connection between altered nigrostriatal DA signaling and compulsive behavior comes from PD patients receiving DA replacement therapy, which can result in impulse control disorders that lead to risky decision making. Levodopa treatment, for example, can be effective at restoring motor function associated with nigrostriatal DA degeneration in Parkinson's, but a subset of patients experience an increase in addiction-like behaviors, including compulsive use of levodopa itself (Lawrence et al., 2003; Evans et al., 2006). These effects are partially mediated by the emergence of D1-receptor supersensitivity that results from nigrostriatal DA neuron degeneration (Gerfen, 2003). Notably, and consistent with the human PD phenomenon, a subset of parkinsonian rats display high sensitivity to DA replacement drugs, after a history of drug self administration (Engeln et al., 2013). More work on the link between Parkinson's states and the behavioral effects of DA replacement in animal models will be useful in understanding nigrostriatal DA's role in risky and disordered drug use (Cenci et al., 2015; Napier et al., 2020).

OTHER CONSIDERATIONS FOR ANIMAL MODELS OF SUBSTANCE USE DISORDER

Drug Type and Route of Administration

Given historical patterns in addiction research, much of the current conceptualization of SUD is based on behavioral modeling in a relatively narrow range of compounds, compared to the broad scope of drug types and routes of administration used by humans. Much of the work discussed here, for example, made use of stimulant drugs (primarily cocaine), although application of SUD animal models to non-stimulant drugs is becoming more common. This is an important consideration for future research, given that the majority of

drug use in contemporary humans is of non-stimulant drugs, including opioids, cannabis, and alcohol (Substance Abuse and Mental Health Services Administration, 2019). More SUD-model research on a broader set of drugs is critical because not all drugs engage the same learning mechanisms to produce patterns of addiction-like behaviors. Nicotine, for example, is relatively weak as a primary reinforcer of drug self administration, compared to other drugs (Pontieri et al., 1996). Instead, nicotine may augment reward seeking to promote addiction-like behavior by potentiating the motivational value of other stimuli and actions *via* non-associative mechanisms (Donny et al., 2003; Chaudhri et al., 2006). This heterogeneity is underscored by the fact that while most self administered drugs increase DA release and act on striatal circuits, they do so to different degrees, and through different mechanisms that may produce unique signaling patterns with specific behavioral relevance (Wise and Bozarth, 1987; Johnson and North, 1992; Nutt et al., 2015; Volkow et al., 2017; Nestler and Lüscher, 2019; Solinas et al., 2019; Wise and Robble, 2020). Further complications come from the fact that some drugs used by humans, such as some hallucinogens, do not as reliably increase DA signaling, and are not readily self administered by rodents, making the application of SUD behavioral models described here difficult (Griffiths et al., 1979; Fantegrossi et al., 2008; Serra et al., 2015).

Drugs are taken by humans through different routes of administration, including most commonly *via* oral consumption, intravenous or subcutaneous injection, or inhalation. The route of delivery affects the pharmacological impact that drugs have on the brain and peripheral physiology, producing unique neurobiological changes and vulnerabilities to addiction-like behaviors (Jones, 1990; Gossop et al., 1992; Cone, 1998; Allain et al., 2015). Intravenous injection and smoking produce the fastest rise and highest drug concentration in the blood, which is associated with greater DA signaling and neural activity in reward circuits (Samaha et al., 2021). Notably, the large majority of drug self administration animal models have relied on intravenous or oral consumption drug delivery, which may obscure unique neurobiological and behavioral adaptations produced by other delivery routes. Smoked cannabis and nicotine are among the most consumed drugs by humans, for example, underscoring the need for SUD models that are amenable to inhalation exposure. Recent work has progressed on this front, with technology for vapor-based delivery of cannabis, cannabinoids, nicotine, and other drugs in rodents (Nguyen et al., 2016; Marusich et al., 2019; Freels et al., 2020).

Co-substance/Poly-Drug Use Models

Simultaneous or serial use of multiple drug types is a common feature of human behavior and is reflected in many SUD patients. Alcohol, nicotine, and cannabis are commonly used alongside drugs like cocaine and heroin, for example, and poly-use SUD patients experience worse treatment outcomes, compared to patients who primarily use a single drug (Leri et al., 2003; Mccabe et al., 2006; Substance Abuse and Mental Health Services Administration, 2019; Crummy et al., 2020; Compton et al., 2021). Despite this, animal models of SUDs have nearly exclusively made use of single-drug procedures, studying drug effects in isolation. Given the unique adaptations in the DA system produced by different drug types, this single-drug focus likely prevents understanding of unique brain changes associated with poly-drug use. From a treatment perspective, a given individual's specific drug combination history could produce individualized SUD vulnerabilities that are not captured in classic models. Recently, more emphasis has gone to modeling poly-drug use in rodents (reviewed in Crummy et al., 2020). For example, rats will readily self administer some drug cocktails, including cocaine and heroin (Crombag and Shaham, 2002). This produces DA responses in the NAc that are greater than those evoked by either drug alone (Hemby et al., 1999). In line with this, exposure to both methamphetamine and morphine results in greater locomotor activity than either drug in isolation (Trujillo et al., 2011), and sequential self administration of alcohol and cocaine produces unique neuroadaptations in the NAc compared to cocaine alone (Stennett et al., 2020). Thus, some single-drug studies may actually produce below threshold neurobiological changes, resulting in failure to detect SUD-like features that are more common in poly-use humans. Other work has been done on drug combinations that are popular among humans, such as alcohol and nicotine. Access to both of these can have synergistic effects on reward-related behaviors in rodents, although individual preferences for one drug or the other may drive co-self administration competition (DeBaker et al., 2020; Angelyn et al., 2021). Poly-drug studies can also offer insight into unique, drug-specific pathways to addiction-like behavior and treatment. For example, social defeat stress more reliably produces escalation of speedball self administration, compared to heroin self administration (Cruz et al., 2011). Further, methadone treatment, commonly used in human opioid use patients, is effective at reducing both cocaine and heroin relapse in rat models (Leri et al., 2003). Notably, little is known about unique adaptations in nigrostriatal DA circuits associated with poly-drug use. If some drug combinations evoke greater DA release in the NAc compared to others, they may also produce exaggerated SNc DA activity, facilitating a more rapid transition to habit-like drug related behaviors.

Individual Differences in Substance Use Disorder Vulnerability

Variability in drug use profiles is highlighted by the fact that among all recreational drug users, only ∼20% progress to meet some DSM diagnostic criteria of SUD (Substance Abuse and Mental Health Services Administration, 2019). Furthermore, in the current framework, a SUD diagnosis requires the presence of only two or more criteria (**Figure 1**). While more severe cases of SUD typically involve several common criteria (American Psychiatric Association, 2013), mild to moderate cases can present with relatively divergent behavioral features. This creates challenges for treatment, as there is no singular "addiction phenotype": the SUD of one person can look quite different from another person. Animal studies have underscored this by demonstrating that only a small fraction of rodents, when given access to drugs, will progress to develop multiple addiction-like behavioral criteria (Deroche-Gamonet et al., 2004; Robinson, 2004; Vanderschuren and Everitt, 2004; O'Neal et al., 2020). Further, and perhaps more striking, when given the choice

between a drug reward and a non-drug reward, such as food or a mate, only a small fraction of rats choose the drug option (Lenoir et al., 2007; Cantin et al., 2010). This non-drug preference persists even in rats with a history of extended drug self administration (Caprioli et al., 2015), but can be overcome with high drug doses and in tasks that equate the rate of reinforcement for drug and non-drug rewards, at least for cocaine (Thomsen et al., 2013; Beckmann et al., 2019). This suggests that individual differences in drug metabolism may intersect with and impact decision making in the context of drug use, contributing to individual vulnerabilities to SUD. This represents a challenge for animal models, where the comparatively limited genetic diversity of research subjects may elide some variability factors. Recent work has made use of "heterogeneous stock" rodents – the product of multiple strain crossings - to increase genetic diversity and investigate individual differences in addiction-like behavior and reward learning in the context of drug use (Hughson et al., 2019; de Guglielmo et al., 2021; King et al., 2021; Sedighim et al., 2021). One such study identified a relationship between gut bacterial content and behavioral features of impulsivity and attention (Peterson et al., 2020). Thus, individualized peripheral systems such as the microbiome can impinge on central brain systems, including DA circuits, in ways that could produce unique SUD vulnerabilities (Lucerne et al., 2021).

Humans exhibit considerable individual differences in SUD characteristics as a function of sex, gender, age, and social and environmental demographics (Brady and Randall, 1999; Degenhardt et al., 2017; Substance Abuse and Mental Health Services Administration, 2019). The factors that promote exaggerated drug use in only a fraction of people are likely myriad, but individual differences in DA system activity and function play a key role (Piray et al., 2010; Saunders et al., 2013). For example, humans with genetic polymorphisms that result in elevated DA system activity show greater reward cue-evoked striatal activity and craving that could denote a predisposition toward exaggerated drug use (Wittmann et al., 2013; Ray et al., 2014). Consistent with this, in animal models, variability in DA signaling and expression of striatal DA receptors is associated with higher drug cue responsivity and relapse (Flagel et al., 2007; Verheij and Cools, 2008; Piray et al., 2010; Saunders et al., 2013; Klanker et al., 2015; Ferguson et al., 2020). Furthermore, at certain stages of the estrus cycle, female rodents have larger NAc DA signals in response to cocaine and cocaine-associated cues, which is thought to underlie their generally higher propensity for addiction-like behaviors (Becker and Cha, 1989; Becker, 1999; Calipari et al., 2017; Johnson et al., 2019).

Given the circuit-specific DA functions in reward learning and addiction-like behavior, some of which we have outlined here, a detailed appreciation of the anatomical locus of variability within DA systems in humans will be essential to forming a link to unique SUD-related vulnerabilities. This will require a better understanding of the DA system across multiple levels of analysis, from genetic and developmental trajectories to *in vivo* circuit connectivity and activity patterns. Critically, much work remains to better understand how the larger mesocorticostriatal network changes over time as both an antecedent and consequence of drug taking. A functional circuit diagram, coupled with computational approaches for modeling preclinical individual and sex-based differences in decision making strategies (Groman et al., 2019; Chen et al., 2021), will be important for determining the neurobehavioral mechanisms underlying unique vulnerabilities for different types of SUD.

CONCLUSION

Here we have reviewed evidence for overlapping, but distinct mesostriatal and nigrostriatal DA circuit functions in behavioral outcomes that are relevant to addictions and SUDs (summarized in **Figure 1**). Dopamine innervation to the striatum contributes to multiple, parallel functions in the context of addiction-like behavior, with the mesostriatal pathway providing a "pull" toward drug seeking by signaling drug and drug-associated stimulus value, especially early in the use cycle. The nigrostriatal pathway, and particularly DLS projecting DA neurons, in contrast are more important for generating the "push" toward exaggerated drug use by controlling rigid, feedback insensitive drug-seeking actions. Notably, as highlighted above, striatal DA is important not only for these positive symptom features of SUDs, including exaggerated seeking and craving, but also for impairments in decision making that underlie compulsive behavior, reduced sociality, and risk taking. Through the use of animal models, greater understanding of the functional heterogeneity of the DA system and related networks can offer insight into this complex symptomatology and may lead to more targeted treatments.

AUTHOR CONTRIBUTIONS

CP and LE conceptualized and wrote the original manuscript draft, in consultation with BS. CP and BS generated **Figure 1**. All authors contributed to writing and editing the final manuscript and approved its submission.

FUNDING

This work was supported by National Institute on Drug Abuse grants T32 DA007234 (CP) and R00 DA042895 (BS).

REFERENCES

Aarts, E., van Holstein, M., and Cools, R. (2011). Striatal dopamine and the interface between motivation and cognition. *Front. Psychol.* 2:163. doi: 10.3389/fpsyg.2011.00163

Achterberg, E. J. M., van Swieten, M. M. H., Houwing, D. J., Trezza, V., and Vanderschuren, L. J. M. J. (2019). Opioid modulation of social play reward in juvenile rats. *Neuropharmacology* 159:107332. doi: 10.1016/j.neuropharm.2018.09.007

Ahmed, S. H. (2018). Trying to make sense of rodents' drug choice behavior. *Prog. Neuropsychopharmacol. Biol. Psychiatry* 87, 3–10.

Ahmed, S. H., and Koob, G. F. (1998). Transition from moderate to excessive drug intake: change in hedonic set point. *Science* 282, 298–300. doi: 10.1126/science.282.5387.298

Ahmed, S. H., Walker, J. R., and Koob, G. F. (2000). Persistent increase in the motivation to take heroin in rats with a history of drug escalation. *Neuropsychopharmacology* 22, 413–421. doi: 10.1016/S0893-133X(99)00133-5

Allain, F., Minogianis, E.-A., Roberts, D. C. S., and Samaha, A.-N. (2015). How fast and how often: the pharmacokinetics of drug use are decisive in addiction. *Neurosci. Biobehav. Rev.* 56, 166–179. doi: 10.1016/j.neubiorev.2015.06.012

American Psychiatric Association (2013). *Diagnostic and Statistical Manual of Mental Disorders*, 5th Edn. American Psychiatric Association. doi: 10.1176/appi.books.9780890425596

Angelyn, H., Loney, G. C., and Meyer, P. J. (2021). Nicotine enhances goal-tracking in ethanol and food Pavlovian conditioned approach paradigms. *Front. Neurosci.* 15:561766. doi: 10.3389/fnins.2021.561766

Aragona, B. J., Day, J. J., Roitman, M. F., Cleaveland, N. A., Wightman, R. M., and Carelli, R. M. (2009). Regional specificity in the real-time development of phasic dopamine transmission patterns during acquisition of a cue–cocaine association in rats. *Eur. J. Neurosci.* 30, 1889–1899. doi: 10.1111/j.1460-9568.2009.07027.x

Arias-Carrión, O., and Pöppel, E. (2007). Dopamine, learning, and reward-seeking behavior. *Acta Neurobiol. Exp*. 67, 481–488.

Balster, R. L., and Lukas, S. E. (1985). Review of self-administration. *Drug Alcohol Depend.* 14, 249–261. doi: 10.1016/0376-8716(85)90060-2

Banks, M. L., and Negus, S. S. (2017). Insights from preclinical choice models on treating drug addiction. *Trends Pharmacol. Sci.* 38, 181–194. doi: 10.1016/j.tips.2016.11.002

Bardo, M. T., Neisewander, J. L., and Kelly, T. H. (2013). Individual differences and social influences on the neurobehavioral pharmacology of abused drugs. *Pharmacol. Rev.* 65, 255–290. doi: 10.1124/pr.111.005124

Bariselli, S., Hörnberg, H., Prévost-Solié, C., Musardo, S., Hatstatt-Burklé, L., Scheiffele, P., et al. (2018). Role of VTA dopamine neurons and neuroligin 3 in sociability traits related to nonfamiliar conspecific interaction. *Nat. Commun.* 9:3173. doi: 10.1038/s41467-018-05382-3

Bariselli, S., Tzanoulinou, S., Glangetas, C., Prévost-Solié, C., Pucci, L., Viguié, J., et al. (2016). SHANK3 controls maturation of social reward circuits in the VTA. *Nat. Neurosci.* 19, 926–934. doi: 10.1038/nn.4319

Becker, J. B. (1999). Gender differences in dopaminergic function in striatum and nucleus accumbens. *Pharmacol. Biochem. Behav.* 64, 803–812. doi: 10.1016/s0091-3057(99)00168-9

Becker, J. B., and Cha, J.-H. (1989). Estrous cycle-dependent variation in amphetamine-induced behaviors and striatal dopamine release assessed with microdialysis. *Behav. Brain Res.* 35, 117–125. doi: 10.1016/S0166-4328(89)80112-3

Beckmann, J. S., Chow, J. J., and Hutsell, B. A. (2019). Cocaine-associated decision-making: toward isolating preference. *Neuropharmacology* 153, 142–152. doi: 10.1016/j.neuropharm.2019.03.025

Beckstead, R. M., Domesick, V. B., and Nauta, W. J. H. (1979). Efferent connections of the substantia nigra and ventral tegmental area in the rat. *Brain Res.* 175, 191–217. doi: 10.1016/0006-8993(79)91001-1

Belin, D., Balado, E., Piazza, P. V., and Deroche-Gamonet, V. (2009). Pattern of intake and drug craving predict the development of cocaine addiction-like behavior in rats. *Biol. Psychiatry* 65, 863–868. doi: 10.1016/j.biopsych.2008.05.031

Belin, D., and Everitt, B. J. (2008). Cocaine seeking habits depend upon dopamine-dependent serial connectivity linking the ventral with the dorsal striatum. *Neuron* 57, 432–441. doi: 10.1016/j.neuron.2007.12.019

Bello, E. P., Mateo, Y., Gelman, D. M., Noaín, D., Shin, J. H., Low, M. J., et al. (2011). Cocaine supersensitivity and enhanced motivation for reward in mice lacking dopamine D2 autoreceptors. *Nat. Neurosci.* 14, 1033–1038. doi: 10.1038/nn.2862

Bentzley, B. S., Fender, K. M., and Aston-Jones, G. (2013). The behavioral economics of drug self-administration: a review and new analytical approach for within-session procedures. *Psychopharmacology* 226, 113–125. doi: 10.1007/s00213-012-2899-2

Bernosky-Smith, K. A., Qiu, Y.-Y., Feja, M., Lee, Y. B., Loughlin, B., Li, J.-X., et al. (2018). Ventral tegmental area D2 receptor knockdown enhances choice impulsivity in a delay-discounting task in rats. *Behav. Brain Res.* 341, 129–134. doi: 10.1016/j.bbr.2017.12.029

Berridge, K. C. (2007). The debate over dopamine's role in reward: the case for incentive salience. *Psychopharmacology* 191, 391–431. doi: 10.1007/s00213-006-0578-x

Björklund, A., and Dunnett, S. B. (2007). Dopamine neuron systems in the brain: an update. *Trends Neurosci.* 30, 194–202. doi: 10.1016/j.tins.2007.03.006

Blackwood, C. A., McCoy, M. T., Ladenheim, B., and Cadet, J. L. (2020). Escalated oxycodone self-administration and punishment: differential expression of opioid receptors and immediate early genes in the rat dorsal striatum and prefrontal cortex. *Front. Neurosci.* 13:1392. doi: 10.3389/fnins.2019.01392

Blum, K., Braverman, E. R., Holder, J. M., Lubar, J. F., Monastra, V. J., Miller, D., et al. (2000). Reward deficiency syndrome: a biogenetic model for the diagnosis and treatment of impulsive, addictive, and compulsive behaviors. *J. Psychoactive Drugs* 32(Suppl., i–iv), 1–112. doi: 10.1080/02791072.2000.10736099

Blum, K., Thanos, P. K., Oscar-Berman, M., Febo, M., Baron, D., Badgaiyan, R. D., et al. (2015). Dopamine in the brain: hypothesizing surfeit or deficit links to reward and addiction. *J. Reward Defic. Syndr.* 1, 95–104. doi: 10.17756/jrds.2015-016

Bolles, R. C. (1967). *Theory of Motivation*. New York, NY: Harper & Row.

Bouarab, C., Thompson, B., and Polter, A. M. (2019). VTA GABA neurons at the interface of stress and reward. *Front. Neural Circuits* 13:78. doi: 10.3389/fncir.2019.00078

Bradberry, C. W. (2007). Cocaine sensitization and dopamine mediation of cue effects in rodents, monkeys, and humans: areas of agreement, disagreement, and implications for addiction. *Psychopharmacology* 191, 705–717. doi: 10.1007/s00213-006-0561-6

Brady, K. T., and Randall, C. L. (1999). Gender differences in substance use disorders. *Psychiatr. Clin. North Am.* 22, 241–252. doi: 10.1016/S0193-953X(05)70074-5

Britt, J. P., Benaliouad, F., McDevitt, R. A., Stuber, G. D., Wise, R. A., and Bonci, A. (2012). Synaptic and behavioral profile of multiple glutamatergic inputs to the nucleus accumbens. *Neuron* 76, 790–803. doi: 10.1016/j.neuron.2012.09.040

Buckholtz, J. W., Treadway, M. T., Cowan, R. L., Woodward, N. D., Li, R., Ansari, M. S., et al. (2010). Dopaminergic network differences in human impulsivity. *Science* 329:532. doi: 10.1126/science.1185778

Burton, A. C., Nakamura, K., and Roesch, M. R. (2015). From ventral-medial to dorsal-lateral striatum: neural correlates of reward-guided decision-making. *Neurobiol. Learn. Mem.* 117, 51–59. doi: 10.1016/j.nlm.2014.05.003

Calipari, E. S., Ferris, M. J., and Jones, S. R. (2014). Extended access of cocaine self-administration results in tolerance to the dopamine-elevating and locomotor-stimulating effects of cocaine. *J. Neurochem.* 128, 224–232. doi: 10.1111/jnc.12452

Calipari, E. S., Ferris, M. J., Zimmer, B. A., Roberts, D. C., and Jones, S. R. (2013). Temporal pattern of cocaine intake determines tolerance vs sensitization of cocaine effects at the dopamine transporter. *Neuropsychopharmacology* 38, 2385–2392. doi: 10.1038/npp.2013.136

Calipari, E. S., Juarez, B., Morel, C., Walker, D. M., Cahill, M. E., Ribeiro, E., et al. (2017). Dopaminergic dynamics underlying sex-specific cocaine reward. *Nat. Commun.* 8:13877. doi: 10.1038/ncomms13877

Cantin, L., Lenoir, M., Augier, E., Vanhille, N., Dubreucq, S., Serre, F., et al. (2010). Cocaine is low on the value ladder of rats: possible evidence for resilience to addiction. *PLoS One* 5:e11592. doi: 10.1371/journal.pone.0011592

Caprioli, D., Zeric, T., Thorndike, E. B., and Venniro, M. (2015). Persistent palatable food preference in rats with a history of limited and extended access to methamphetamine self-administration. *Addict. Biol.* 20, 913–926. doi: 10.1111/adb.12220

Cardinal, R. N., Parkinson, J. A., Hall, J., and Everitt, B. J. (2002). Emotion and motivation: the role of the amygdala, ventral striatum, and prefrontal cortex. *Neurosci. Biobehav. Rev.* 26, 321–352. doi: 10.1016/S0149-7634(02)00007-6

Carelli, R. M. (2004). Nucleus accumbens cell firing and rapid dopamine signaling during goal-directed behaviors in rats. *Neuropharmacology* 47(Suppl. 1), 180–189. doi: 10.1016/j.neuropharm.2004.07.017

Cenci, M. A., Francardo, V., O'Sullivan, S. S., and Lindgren, H. S. (2015). Rodent models of impulsive–compulsive behaviors in Parkinson's disease: How far have we reached? *Neurobiol. Dis.* 82, 561–573. doi: 10.1016/j.nbd.2015.08.026

Chaudhri, N., Caggiula, A. R., Donny, E. C., Palmatier, M. I., Liu, X., and Sved, A. F. (2006). Complex interactions between nicotine and nonpharmacological stimuli reveal multiple roles for nicotine in reinforcement. *Psychopharmacology* 184, 353–366. doi: 10.1007/s00213-005-0178-1

Chaudhri, N., Sahuque, L. L., and Janak, P. H. (2008). Context-induced relapse of conditioned behavioral responding to ethanol cues in rats. *Biol. Psychiatry* 64, 203–210. doi: 10.1016/j.biopsych.2008.03.007

Chaudhri, N., Sahuque, L. L., and Janak, P. H. (2009). Ethanol seeking triggered by environmental context is attenuated by blocking dopamine D1 receptors in the nucleus accumbens core and shell in rats. *Psychopharmacology* 207, 303–314. doi: 10.1007/s00213-009-1657-6

Chen, C. S., Ebitz, R. B., Bindas, S. R., Redish, A. D., Hayden, B. Y., and Grissom, N. M. (2021). Divergent strategies for learning in males and females. *Curr. Biol.* 31, 39–50.e4. doi: 10.1016/j.cub.2020.09.075

Chen, R., McIntosh, S., Hemby, S., Sun, H., Sexton, T., Thomas, M., et al. (2018). High and low doses of cocaine intake are differentially regulated by dopamine D2 receptors in the ventral tegmental area and the nucleus accumbens. *Neurosci. Lett.* 671, 133–139. doi: 10.1016/j.neulet.2018.02.026

Chiara, G. D., and Imperato, A. (1988). Drugs abused by humans preferentially increase synaptic dopamine concentrations in the mesolimbic system of freely moving rats. *Proc. Natl. Acad. Sci. U.S.A.* 85, 5274–5278. doi: 10.1073/pnas.85.14.5274

Ciano, P. D., and Everitt, B. J. (2004). Contribution of the ventral tegmental area to cocaine-seeking maintained by a drug-paired conditioned stimulus in rats. *Eur. J. Neurosci.* 19, 1661–1667. doi: 10.1111/j.1460-9568.2004.03232.x

Clemens, K. J., Castino, M. R., Cornish, J. L., Goodchild, A. K., and Holmes, N. M. (2014). Behavioral and neural substrates of habit formation in rats intravenously self-administering nicotine. *Neuropsychopharmacology* 39, 2584–2593. doi: 10.1038/npp.2014.111

Coddington, L. T., and Dudman, J. T. (2018). The timing of action determines reward prediction signals in identified midbrain dopamine neurons. *Nat. Neurosci.* 21, 1563–1573. doi: 10.1038/s41593-018-0245-7

Collins, A. L., and Saunders, B. T. (2020). Heterogeneity in striatal dopamine circuits: form and function in dynamic reward seeking. *J. Neurosci. Res.* 98, 1046–1069. doi: 10.1002/jnr.24587

Compton, W. M., Valentino, R. J., and DuPont, R. L. (2021). Polysubstance use in the U.S. opioid crisis. *Mol. Psychiatry* 26, 41–50. doi: 10.1038/s41380-020-00949-3

Cone, E. J. (1998). Recent discoveries in pharmacokinetics of drugs of abuse. *Toxicol. Lett.* 10, 97–101. doi: 10.1016/S0378-4274(98)00292-6

Cooper, A., Barnea-Ygael, N., Levy, D., Shaham, Y., and Zangen, A. (2007). A conflict rat model of cue-induced relapse to cocaine seeking. *Psychopharmacology* 194, 117–125. doi: 10.1007/s00213-007-0827-7

Corbett, D., and Wise, R. A. (1980). Intracranial self-stimulation in relation to the ascending dopaminergic systems of the midbrain: a moveable electrode mapping study. *Brain Res.* 185, 1–15. doi: 10.1016/0006-8993(80)90666-6

Corbit, L. H., Nie, H., and Janak, P. H. (2012). Habitual alcohol seeking: time course and the contribution of subregions of the dorsal striatum. *Biol. Psychiatry* 72, 389–395. doi: 10.1016/j.biopsych.2012.02.024

Corre, J., van Zessen, R., Loureiro, M., Patriarchi, T., Tian, L., Pascoli, V., et al. (2018). Dopamine neurons projecting to medial shell of the nucleus accumbens drive heroin reinforcement. *eLife* 7:e39945. doi: 10.7554/eLife.39945

Cox, J., and Witten, I. B. (2019). Striatal circuits for reward learning and decision-making. *Nat. Rev. Neurosci.* 20, 482–494. doi: 10.1038/s41583-019-0189-2

Crombag, H. S., and Shaham, Y. (2002). Renewal of drug seeking by contextual cues after prolonged extinction in rats. *Behav. Neurosci.* 116, 169–173. doi: 10.1037//0735-7044.116.1.169

Crummy, E. A., O'Neal, T. J., Baskin, B. M., and Ferguson, S. M. (2020). One is not enough: understanding and modeling polysubstance use. *Front. Neurosci.* 14:569. doi: 10.3389/fnins.2020.00569

Cruz, F. C., Quadros, I. M., Hogenelst, K., Planeta, C. S., and Miczek, K. A. (2011). Social defeat stress in rats: escalation of cocaine and "speedball" binge self-administration, but not heroin. *Psychopharmacology* 215, 165–175. doi: 10.1007/s00213-010-2139-6

Da Cunha, C., Gevaerd, M. S., Vital, M. A., Miyoshi, E., Andreatini, R., Silveira, R., et al. (2001). Memory disruption in rats with nigral lesions induced by MPTP: a model for early Parkinson's disease amnesia. *Behav. Brain Res.* 124, 9–18. doi: 10.1016/s0166-4328(01)00211-x

da Silva, J. A., Tecuapetla, F., Paixão, V., and Costa, R. M. (2018). Dopamine neuron activity before action initiation gates and invigorates future movements. *Nature* 554, 244–248. doi: 10.1038/nature25457

Dalley, J. W., and Ersche, K. D. (2019). Neural circuitry and mechanisms of waiting impulsivity: relevance to addiction. *Philos. Trans. R. Soc. Lond. B Biol. Sci.* 374:20180145 doi: 10.1098/rstb.2018.0145

de Guglielmo, G., Carrette, L. L., Kallupi, M., Brennan, M., Boomhower, B., Maturin, L., et al. (2021). Characterization of cocaine addiction-like behavior in heterogeneous stock rats. *bioRxiv* [Preprint]. doi: 10.1101/2021.07.22.453410

de Jong, J. W., Roelofs, T. J. M., Mol, F. M. U., Hillen, A. E. J., Meijboom, K. E., Luijendijk, M. C. M., et al. (2015). Reducing ventral tegmental dopamine D2 receptor expression selectively boosts incentive motivation. *Neuropsychopharmacology* 40, 2085–2095. doi: 10.1038/npp.2015.60

de Wit, H. (2009). Impulsivity as a determinant and consequence of drug use: a review of underlying processes. *Addict. Biol.* 14, 22–31. doi: 10.1111/j.1369-1600.2008.00129.x

DeBaker, M. C., Robinson, J. M., Moen, J. K., Wickman, K., and Lee, A. M. (2020). Differential patterns of alcohol and nicotine intake: combined alcohol and nicotine binge consumption behaviors in mice. *Alcohol* 85, 57–64. doi: 10.1016/j.alcohol.2019.09.006

Degenhardt, L., Peacock, A., Colledge, S., Leung, J., Grebely, J., Vickerman, P., et al. (2017). Global prevalence of injecting drug use and sociodemographic characteristics and prevalence of HIV, HBV, and HCV in people who inject drugs: a multistage systematic review. *Lancet Glob. Health* 5, e1192–e1207. doi: 10.1016/S2214-109X(17)30375-3

Deroche-Gamonet, V., Belin, D., and Piazza, P. V. (2004). Evidence for addiction-like behavior in the rat. *Science* 305, 1014–1017. doi: 10.1126/science.1099020

Diana, M. (2011). The dopamine hypothesis of drug addiction and its potential therapeutic value. *Front. Psychiatry* 2:64. doi: 10.3389/fpsyt.2011.00064

Dodson, P. D., Dreyer, J. K., Jennings, K. A., Syed, E. C. J., Wade-Martins, R., Cragg, S. J., et al. (2016). Representation of spontaneous movement by dopaminergic neurons is cell-type selective and disrupted in parkinsonism. *Proc. Natl. Acad. Sci. U.S.A.* 113, E2180–E2188. doi: 10.1073/pnas.1515941113

Domi, E., Xu, L., Toivainen, S., Nordeman, A., Gobbo, F., Venniro, M. E., et al. (2021). A neural substrate of compulsive alcohol use. *Sci. Adv.* 7:eabg9045. doi: 10.1126/sciadv.abg9045

Donny, E. C., Chaudhri, N., Caggiula, A. R., Evans-Martin, F. F., Booth, S., Gharib, M. A., et al. (2003). Operant responding for a visual reinforcer in rats is enhanced by noncontingent nicotine: implications for nicotine self-administration and reinforcement. *Psychopharmacology* 169, 68–76. doi: 10.1007/s00213-003-1473-3

Eison, M. S., Stark, A. D., and Ellison, G. (1977). Opposed effects of locus coeruleus and substantia Nigra lesions on social behavior in rat colonies. *Pharmacol. Biochem. Behav.* 7, 87–90. doi: 10.1016/0091-3057(77)90016-8

Engeln, M., Ahmed, S. H., Vouillac, C., Tison, F., Bezard, E., and Fernagut, P.-O. (2013). Reinforcing properties of Pramipexole in normal and parkinsonian rats. *Neurobiol. Dis.* 49, 79–86. doi: 10.1016/j.nbd.2012.08.005

Evans, A. H., Pavese, N., Lawrence, A. D., Tai, Y. F., Appel, S., Doder, M., et al. (2006). Compulsive drug use linked to sensitized ventral striatal dopamine transmission. *Ann. Neurol.* 59, 852–858. doi: 10.1002/ana.20822

Everitt, B. J. (2014). Neural and psychological mechanisms underlying compulsive drug seeking habits and drug memories – indications for novel treatments of addiction. *Eur. J. Neurosci.* 40, 2163–2182. doi: 10.1111/ejn.12644

Everitt, B. J., and Robbins, T. W. (2005). Neural systems of reinforcement for drug addiction: from actions to habits to compulsion. *Nat. Neurosci.* 8, 1481–1489. doi: 10.1038/nn1579

Fanelli, R. R., Klein, J. T., Reese, R. M., and Robinson, D. L. (2013). Dorsomedial and dorsolateral striatum exhibit distinct phasic neuronal activity during alcohol self-administration in rats. *Eur. J. Neurosci.* 38, 2637–2648. doi: 10.1111/ejn.12271

Fantegrossi, W. E., Murnane, K. S., and Reissig, C. J. (2008). The behavioral pharmacology of hallucinogens. *Biochem. Pharmacol.* 75, 17–33. doi: 10.1016/j.bcp.2007.07.018

Ferguson, L. M., Ahrens, A. M., Longyear, L. G., and Aldridge, J. W. (2020). Neurons of the ventral tegmental area encode individual differences in motivational "wanting" for reward cues. *J. Neurosci.* 40, 8951–8963. doi: 10.1523/JNEUROSCI.2947-19.2020

Fields, H. L., Hjelmstad, G. O., Margolis, E. B., and Nicola, S. M. (2007). Ventral tegmental area neurons in learned appetitive behavior and positive reinforcement. *Annu. Rev. Neurosci.* 30, 289–316. doi: 10.1146/annurev.neuro.30.051606.094341

Flagel, S. B., Clark, J. J., Robinson, T. E., Mayo, L., Czuj, A., Willuhn, I., et al. (2011). A selective role for dopamine in reward learning. *Nature* 469, 53–57. doi: 10.1038/nature09588

Flagel, S. B., Watson, S. J., Robinson, T. E., and Akil, H. (2007). Individual differences in the propensity to approach signals vs goals promote different adaptations in the dopamine system of rats. *Psychopharmacology* 191, 599–607. doi: 10.1007/s00213-006-0535-8

Ford, C. P. (2014). The role of D2-autoreceptors in regulating dopamine neuron activity and transmission. *Neuroscience* 282, 13–22. doi: 10.1016/j.neuroscience.2014.01.025

Fouriezos, G., and Wise, R. A. (1976). Pimozide-induced extinction of intracranial self-stimulation: response patterns rule out motor or performance deficits. *Brain Res.* 103, 377–380. doi: 10.1016/0006-8993(76)90809-x

Fragale, J. E., James, M. H., and Aston-Jones, G. (2021). Intermittent self-administration of fentanyl induces a multifaceted addiction state associated with persistent changes in the orexin system. *Addict. Biol.* 26:e12946. doi: 10.1111/adb.12946

Freels, T. G., Baxter-Potter, L. N., Lugo, J. M., Glodosky, N. C., Wright, H. R., Baglot, S. L., et al. (2020). Vaporized cannabis extracts have reinforcing properties and support conditioned drug-seeking behavior in rats. *J. Neurosci.* 40, 1897–1908. doi: 10.1523/JNEUROSCI.2416-19.2020

Fukushiro, D. F., Olivera, A., Liu, Y., and Wang, Z. (2015). Neonatal exposure to amphetamine alters social affiliation and central dopamine activity in adult male prairie voles. *Neuroscience* 307, 109–116. doi: 10.1016/j.neuroscience.2015.08.051

Gardner, E. L. (2011). Addiction and brain reward and antireward pathways. *Adv. Psychosom. Med.* 30, 22–60. doi: 10.1159/000324065

Gentry, R. N., Lee, B., and Roesch, M. R. (2016). Phasic dopamine release in the rat nucleus accumbens predicts approach and avoidance performance. *Nat. Commun.* 7:13154. doi: 10.1038/ncomms13154

Gerfen, C. R. (1984). The neostriatal mosaic: compartmentalization of corticostriatal input and striatonigral output systems. *Nature* 311, 461–464. doi: 10.1038/311461a0

Gerfen, C. R. (2003). D1 dopamine receptor supersensitivity in the dopamine-depleted striatum animal model of Parkinson's disease. *Neuroscientist* 9, 455–462. doi: 10.1177/1073858403255839

Giuliano, C., Belin, D., and Everitt, B. J. (2019). Compulsive alcohol seeking results from a failure to disengage dorsolateral striatal control over behavior. *J. Neurosci.* 39, 1744–1754. doi: 10.1523/JNEUROSCI.2615-18.2018

Giuliano, C., Peña-Oliver, Y., Goodlett, C. R., Cardinal, R. N., Robbins, T. W., Bullmore, E. T., et al. (2018). Evidence for a long-lasting compulsive alcohol seeking phenotype in rats. *Neuropsychopharmacology* 43, 728–738. doi: 10.1038/npp.2017.105

Goeders, N. E., and Guerin, G. F. (1994). Non-contingent electric footshock facilitates the acquisition of intravenous cocaine self-administration in rats. *Psychopharmacology* 114, 63–70. doi: 10.1007/BF02245445

Goldberg, N. R. S., Fields, V., Pflibsen, L., Salvatore, M. F., and Meshul, C. K. (2012). Social enrichment attenuates nigrostriatal lesioning and reverses motor impairment in a progressive 1-methyl-2-phenyl-1,2,3,6-tetrahydropyridine (MPTP) mouse model of Parkinson's disease. *Neurobiol. Dis.* 45, 1051–1067. doi: 10.1016/j.nbd.2011.12.024

Gossop, M., Griffiths, P., Powis, B., and Strang, J. (1992). Severity of dependence and route of administration of heroin, cocaine and amphetamines. *Br. J. Addict.* 87, 1527–1536. doi: 10.1111/j.1360-0443.1992.tb02660.x

Griffiths, R. R., Brady, J. V., and Bradford, L. D. (1979). "Predicting the abuse liability of drugs with animal drug self-administration procedures: psychomotor stimulants and hallucinogens," in *Advances in Behavioral Pharmacology*, Vol. 2, eds T. Thompson and P. B. Dews (Amsterdam: Elsevier), 163–208. doi: 10.1016/B978-0-12-004702-4.50010-2

Grimm, J. W., Hope, B. T., Wise, R. A., and Shaham, Y. (2001). Incubation of cocaine craving after withdrawal. *Nature* 412, 141–142. doi: 10.1038/35084134

Groman, S. M., Massi, B., Mathias, S. R., Lee, D., and Taylor, J. R. (2019). Model-free and model-based influences in addiction-related behaviors. *Biol. Psychiatry* 85, 936–945. doi: 10.1016/j.biopsych.2018.12.017

Groman, S. M., Rich, K. M., Smith, N. J., Lee, D., and Taylor, J. R. (2018). Chronic exposure to methamphetamine disrupts reinforcement-based decision making in rats. *Neuropsychopharmacology* 43, 770–780. doi: 10.1038/npp.2017.159

Gunaydin, L. A., Grosenick, L., Finkelstein, J. C., Kauvar, I. V., Fenno, L. E., Adhikari, A., et al. (2014). Natural neural projection dynamics underlying social behavior. *Cell* 157, 1535–1551. doi: 10.1016/j.cell.2014.05.017

Haber, S. N., Fudge, J. L., and McFarland, N. R. (2000). Striatonigrostriatal pathways in primates form an ascending spiral from the shell to the dorsolateral striatum. *J. Neurosci.* 20, 2369–2382. doi: 10.1523/JNEUROSCI.20-06-02369.2000

Hall, F. S., Wilkinson, L. S., Humby, T., and Robbins, T. W. (1999). Maternal deprivation of neonatal rats produces enduring changes in dopamine function. *Synapse* 32, 37–43.

Hassani, O. K., Cromwell, H. C., and Schultz, W. (2001). Influence of expectation of different rewards on behavior-related neuronal activity in the striatum. *J. Neurophysiol.* 85, 2477–2489. doi: 10.1152/jn.2001.85.6.2477

Hemby, S. E., Co, C., Dworkin, S. I., and Smith, J. E. (1999). Synergistic elevations in nucleus accumbens extracellular dopamine concentrations during self-administration of cocaine/heroin combinations (speedball) in rats. *J. Pharmacol. Exp. Ther.* 288, 274–280.

Hernandez, L., Lee, F., and Hoebel, B. G. (1987). Simultaneous microdialysis and amphetamine infusion in the nucleus accumbens and striatum of freely moving rats: increase in extracellular dopamine and serotonin. *Brain Res. Bull.* 19, 623–628. doi: 10.1016/0361-9230(87)90047-5

Higgins, S. T., Sigmon, S. C., Wong, C. J., Heil, S. H., Badger, G. J., Donham, R., et al. (2003). Community reinforcement therapy for cocaine-dependent outpatients. *Arch. Gen. Psychiatry* 60, 1043–1052. doi: 10.1001/archpsyc.60.9.1043

Hodebourg, R., Murray, J. E., Fouyssac, M., Puaud, M., Everitt, B. J., and Belin, D. (2019). Heroin seeking becomes dependent on dorsal striatal dopaminergic mechanisms and can be decreased by N-acetylcysteine. *Eur. J. Neurosci.* 50, 2036–2044. doi: 10.1111/ejn.13894

Hogarth, L. (2020). Addiction is driven by excessive goal-directed drug choice under negative affect: translational critique of habit and compulsion theory. *Neuropsychopharmacology* 45, 720–735. doi: 10.1038/s41386-020-0600-8

Hopf, F. W., and Lesscher, H. M. B. (2014). Rodent models for compulsive alcohol intake. *Alcohol* 48, 253–264. doi: 10.1016/j.alcohol.2014.03.001

Howe, M. W., and Dombeck, D. A. (2016). Rapid signalling in distinct dopaminergic axons during locomotion and reward. *Nature* 535, 505–510. doi: 10.1038/nature18942

Hsu, T. M., McCutcheon, J. E., and Roitman, M. F. (2018). Parallels and overlap: the integration of homeostatic signals by mesolimbic dopamine neurons. *Front. Psychiatry* 9:410. doi: 10.3389/fpsyt.2018.00410

Hughson, A. R., Horvath, A. P., Holl, K., Palmer, A. A., Solberg Woods, L. C., Robinson, T. E., et al. (2019). Incentive salience attribution, "sensation-seeking" and "novelty-seeking" are independent traits in a large sample of male and female heterogeneous stock rats. *Sci. Rep.* 9:2351. doi: 10.1038/s41598-019-39519-1

Hynes, T. J., Hrelja, K. M., Hathaway, B. A., Hounjet, C. D., Chernoff, C. S., Ebsary, S. A., et al. (2021). Dopamine neurons gate the intersection of cocaine use, decision making, and impulsivity. *Addict. Biol.* 26:e13022. doi: 10.1111/adb.13022

Ikemoto, S. (2007). Dopamine reward circuitry: two projection systems from the ventral midbrain to the nucleus accumbens-olfactory tubercle complex. *Brain Res. Rev.* 56, 27–78. doi: 10.1016/j.brainresrev.2007.05.004

Ikemoto, S., Yang, C., and Tan, A. (2015). Basal ganglia circuit loops, dopamine and motivation: a review and enquiry. *Behav. Brain Res.* 290, 17–31. doi: 10.1016/j.bbr.2015.04.018

Ito, R., Dalley, J. W., Howes, S. R., Robbins, T. W., and Everitt, B. J. (2000). Dissociation in conditioned dopamine release in the nucleus accumbens core and shell in response to cocaine cues and during cocaine-seeking behavior in rats. *J. Neurosci.* 20, 7489–7495. doi: 10.1523/JNEUROSCI.20-19-07489.2000

Ito, R., Dalley, J. W., Robbins, T. W., and Everitt, B. J. (2002). Dopamine release in the dorsal striatum during cocaine-seeking behavior under the control of a drug-associated cue. *J. Neurosci.* 22, 6247–6253. doi: 10.1523/JNEUROSCI.22-14-06247.2002

Izquierdo, A., Belcher, A. M., Scott, L., Cazares, V. A., Chen, J., O'Dell, S. J., et al. (2010). Reversal-specific learning impairments after a binge regimen of methamphetamine in rats: possible involvement of striatal dopamine. *Neuropsychopharmacology* 35, 505–514. doi: 10.1038/npp.2009.155

Jacobs, D. S., and Moghaddam, B. (2020). Prefrontal Cortex Representation of Learning of Punishment Probability During Reward-Motivated Actions. *J. Neurosci.* 40, 5063–5077. doi: 10.1523/JNEUROSCI.0310-20.2020

Ji, X., Saha, S., Kolpakova, J., Guildford, M., Tapper, A. R., and Martin, G. E. (2017). Dopamine receptors differentially control binge alcohol drinking-mediated synaptic plasticity of the core nucleus accumbens direct and indirect pathways. *J. Neurosci.* 37, 5463–5474. doi: 10.1523/JNEUROSCI.3845-16.2017

Joel, D., Niv, Y., and Ruppin, E. (2002). Actor-critic models of the basal ganglia: new anatomical and computational perspectives. *Neural Netw.* 15, 535–547. doi: 10.1016/s0893-6080(02)00047-3

Johnson, A. R., Thibeault, K. C., Lopez, A. J., Peck, E. G., Sands, L. P., Sanders, C. M., et al. (2019). Cues play a critical role in estrous cycle-dependent enhancement of cocaine reinforcement. *Neuropsychopharmacology* 44, 1189–1197. doi: 10.1038/s41386-019-0320-0

Johnson, S. W., and North, R. A. (1992). Opioids excite dopamine neurons by hyperpolarization of local interneurons. *J. Neurosci.* 12, 483–488.

Jones, R. T. (1990). The pharmacology of cocaine smoking in humans. *NIDA Res. Monogr.* 99, 30–41.

Jonkman, S., Pelloux, Y., and Everitt, B. J. (2012). Differential Roles of the Dorsolateral and Midlateral Striatum in Punished Cocaine Seeking. *J. Neurosci.* 32, 4645–4650. doi: 10.1523/JNEUROSCI.0348-12.2012

Kawa, A. B., Allain, F., Robinson, T. E., and Samaha, A.-N. (2019a). The transition to cocaine addiction: the importance of pharmacokinetics for preclinical models. *Psychopharmacology* 236, 1145–1157. doi: 10.1007/s00213-019-5164-0

Kawa, A. B., Valenta, A. C., Kennedy, R. T., and Robinson, T. E. (2019b). Incentive and dopamine sensitization produced by intermittent but not long access cocaine self-administration. *Eur. J. Neurosci.* 50, 2663–2682. doi: 10.1111/ejn.14418

Kawa, A. B., Bentzley, B. S., and Robinson, T. E. (2016). Less is more: prolonged intermittent access cocaine self-administration produces incentive-sensitization and addiction-like behavior. *Psychopharmacology* 233, 3587–3602. doi: 10.1007/s00213-016-4393-8

Keath, J. R., Iacoviello, M. P., Barrett, L. E., Mansvelder, H. D., and McGehee, D. S. (2007). Differential modulation by nicotine of substantia nigra versus ventral tegmental area dopamine neurons. *J. Neurophysiol.* 98, 3388–3396. doi: 10.1152/jn.00760.2007

Keiflin, R., and Janak, P. H. (2015). Dopamine prediction errors in reward learning and addiction: from theory to neural circuitry. *Neuron* 88, 247–263. doi: 10.1016/j.neuron.2015.08.037

Kim, H. F., Ghazizadeh, A., and Hikosaka, O. (2015). Dopamine neurons encoding long-term memory of object value for habitual behavior. *Cell* 163, 1165–1175. doi: 10.1016/j.cell.2015.10.063

King, C. P., Tripi, J. A., Hughson, A. R., Horvath, A. P., Lamparelli, A. C., Holl, K. L., et al. (2021). Sensitivity to food and cocaine cues are independent traits in a large sample of heterogeneous stock rats. *Sci. Rep.* 11:2223. doi: 10.1038/s41598-020-80798-w

Kitamura, O., Wee, S., Specio, S. E., Koob, G. F., and Pulvirenti, L. (2006). Escalation of methamphetamine self-administration in rats: a dose-effect function. *Psychopharmacology* 186, 48–53. doi: 10.1007/s00213-006-0353-z

Klanker, M., Sandberg, T., Joosten, R., Willuhn, I., Feenstra, M., and Denys, D. (2015). Phasic dopamine release induced by positive feedback predicts individual differences in reversal learning. *Neurobiol. Learn. Mem.* 125, 135–145. doi: 10.1016/j.nlm.2015.08.011

Koob, G. F., and Bloom, F. E. (1988). Cellular and molecular mechanisms of drug dependence. *Science* 242, 715–723. doi: 10.1126/science.2903550

Kufahl, P. R., Zavala, A. R., Singh, A., Thiel, K. J., Dickey, E. D., Joyce, J. N., et al. (2009). C-Fos expression associated with reinstatement of cocaine-seeking behavior by response-contingent conditioned cues. *Synapse* 63, 823–835. doi: 10.1002/syn.20666

Kupchik, Y. M., Brown, R. M., Heinsbroek, J. A., Lobo, M. K., Schwartz, D. J., and Kalivas, P. W. (2015). Coding the direct/indirect pathways by D1 and D2 receptors is not valid for accumbens projections. *Nat. Neurosci.* 18, 1230–1232. doi: 10.1038/nn.4068

Lammel, S., Lim, B. K., and Malenka, R. C. (2014). Reward and aversion in a heterogeneous midbrain dopamine system. *Neuropharmacology* 76, 351–359. doi: 10.1016/j.neuropharm.2013.03.019

Lawrence, A. D., Evans, A. H., and Lees, A. J. (2003). Compulsive use of dopamine replacement therapy in Parkinson's disease: reward systems gone awry? *Lancet Neurol.* 2, 595–604. doi: 10.1016/s1474-4422(03)00529-5

Le Heron, C., Kolling, N., Plant, O., Kienast, A., Janska, R., Ang, Y.-S., et al. (2020). Dopamine modulates dynamic decision-making during foraging. *J. Neurosci.* 40, 5273–5282. doi: 10.1523/JNEUROSCI.2586-19.2020

Le Heron, C., Plant, O., Manohar, S., Ang, Y.-S., Jackson, M., Lennox, G., et al. (2018). Distinct effects of apathy and dopamine on effort-based decision-making in Parkinson's disease. *Brain* 141, 1455–1469. doi: 10.1093/brain/awy110

Lenoir, M., Serre, F., Cantin, L., and Ahmed, S. H. (2007). Intense sweetness surpasses cocaine reward. *PLoS One* 2:e698. doi: 10.1371/journal.pone.0000698

Leonard, M. Z., DeBold, J. F., and Miczek, K. A. (2017). Escalated cocaine "binges" in rats: enduring effects of social defeat stress or intra-VTA CRF. *Psychopharmacology* 234, 2823–2836. doi: 10.1007/s00213-017-4677-7

Leri, F., Bruneau, J., and Stewart, J. (2003). Understanding polydrug use: review of heroin and cocaine co-use. *Addiction* 98, 7–22. doi: 10.1046/j.1360-0443.2003.00236.x

Lerner, T. N., Shilyansky, C., Davidson, T. J., Evans, K. E., Beier, K. T., Zalocusky, K. A., et al. (2015). Intact-brain analyses reveal distinct information carried by SNc dopamine subcircuits. *Cell* 162, 635–647. doi: 10.1016/j.cell.2015.07.014

Lesscher, H. M. B., Spoelder, M., Rotte, M. D., Janssen, M. J., Hesseling, P., Lozeman-van't Klooster, J. G., et al. (2015). Early social isolation augments alcohol consumption in rats. *Behav. Pharmacol.* 26, 673–680. doi: 10.1097/FBP.0000000000000165

Leyton, M. (2017). Altered dopamine transmission as a familial risk trait for addictions. *Curr. Opin. Behav. Sci.* 13, 130–138. doi: 10.1016/j.cobeha.2016.11.011

Leyton, M., and Vezina, P. (2014). Dopamine ups and downs in vulnerability to addictions: a neurodevelopmental model. *Trends Pharmacol. Sci.* 35, 268–276. doi: 10.1016/j.tips.2014.04.002

Liu, Y., Aragona, B. J., Young, K. A., Dietz, D. M., Kabbaj, M., Mazei-Robison, M., et al. (2010). Nucleus accumbens dopamine mediates amphetamine-induced impairment of social bonding in a monogamous rodent species. *Proc. Natl. Acad. Sci. U.S.A.* 107, 1217–1222. doi: 10.1073/pnas.0911998107

Liu, Y., Jean-Richard-Dit-Bressel, P., Yau, J. O.-Y., Willing, A., Prasad, A. A., Power, J. M., et al. (2020). The mesolimbic dopamine activity signatures of relapse to alcohol-seeking. *J. Neurosci.* 40, 6409–6427. doi: 10.1523/JNEUROSCI.0724-20.2020

Lobo, M. K., Covington, H. E., Chaudhury, D., Friedman, A. K., Sun, H., Damez-Werno, D., et al. (2010). Cell type-specific loss of BDNF signaling mimics optogenetic control of cocaine reward. *Science* 330, 385–390. doi: 10.1126/science.1188472

Loiodice, S., Wing Young, H., Rion, B., Méot, B., Montagne, P., Denibaud, A.-S., et al. (2019). Implication of nigral dopaminergic lesion and repeated L-dopa exposure in neuropsychiatric symptoms of Parkinson's disease. *Behav. Brain Res.* 360, 120–127. doi: 10.1016/j.bbr.2018.12.007

Lucerne, K. E., Osman, A., Meckel, K. R., and Kiraly, D. D. (2021). Contributions of neuroimmune and gut-brain signaling to vulnerability of developing substance use disorders. *Neuropharmacology* 192:108598. doi: 10.1016/j.neuropharm.2021.108598

Lüscher, C., and Malenka, R. C. (2011). Drug-evoked synaptic plasticity in addiction: from molecular changes to circuit remodeling. *Neuron* 69, 650–663. doi: 10.1016/j.neuron.2011.01.017

Lüscher, C., Robbins, T. W., and Everitt, B. J. (2020). The transition to compulsion in addiction. *Nat. Rev. Neurosci.* 21, 247–263. doi: 10.1038/s41583-020-0289-z

Mahler, S. V., and Aston-Jones, G. S. (2012). Fos activation of selective afferents to ventral tegmental area during cue-induced reinstatement of cocaine seeking in rats. *J. Neurosci.* 32, 13309–13325. doi: 10.1523/JNEUROSCI.2277-12.2012

Mahler, S. V., Brodnik, Z. D., Cox, B. M., Buchta, W. C., Bentzley, B. S., Quintanilla, J., et al. (2019). Chemogenetic manipulations of ventral tegmental area dopamine neurons reveal multifaceted roles in cocaine abuse. *J. Neurosci.* 39, 503–518. doi: 10.1523/JNEUROSCI.0537-18.2018

Mameli, M., Halbout, B., Creton, C., Engblom, D., Parkitna, J. R., Spanagel, R., et al. (2009). Cocaine-evoked synaptic plasticity: persistence in the VTA triggers adaptations in the NAc. *Nat. Neurosci.* 12, 1036–1041. doi: 10.1038/nn.2367

Manduca, A., Servadio, M., Damsteegt, R., Campolongo, P., Vanderschuren, L. J., and Trezza, V. (2016). Dopaminergic Neurotransmission in the Nucleus

Accumbens Modulates Social Play Behavior in Rats. *Neuropsychopharmacology* 41, 2215–2223. doi: 10.1038/npp.2016.22

Marchant, N. J., Khuc, T. N., Pickens, C. L., Bonci, A., and Shaham, Y. (2013). Context-induced relapse to alcohol seeking after punishment in a rat model. *Biol. Psychiatry* 73, 256–262. doi: 10.1016/j.biopsych.2012.07.007

Mark, G. P., Shabani, S., Dobbs, L. K., and Hansen, S. T. (2011). Cholinergic modulation of mesolimbic dopamine function and reward. *Physiol. Behav.* 104, 76–81. doi: 10.1016/j.physbeh.2011.04.052

Marusich, J. A., Wiley, J. L., Silinski, M. A. R., Thomas, B. F., Meredith, S. E., Gahl, R. F., et al. (2019). Comparison of cigarette, little cigar, and waterpipe tobacco smoke condensate and e-cigarette aerosol condensate in a self-administration model. *Behav. Brain Res.* 372:112061. doi: 10.1016/j.bbr.2019.112061

Mateo, Y., Lack, C. M., Morgan, D., Roberts, D. C. S., and Jones, S. R. (2005). Reduced dopamine terminal function and insensitivity to cocaine following cocaine binge self-administration and deprivation. *Neuropsychopharmacology* 30, 1455–1463. doi: 10.1038/sj.npp.1300687

Matheus, F. C., Rial, D., Real, J. I., Lemos, C., Takahashi, R. N., Bertoglio, L. J., et al. (2016). Temporal dissociation of striatum and prefrontal cortex uncouples Anhedonia and defense behaviors relevant to depression in 6-OHDA-lesioned rats. *Mol. Neurobiol.* 53, 3891–3899. doi: 10.1007/s12035-015-9330-z

Mccabe, S. E., Cranford, J. A., Morales, M., and Young, A. (2006). Simultaneous and concurrent polydrug use of alcohol and prescription drugs: prevalence, correlates, and consequences. *J. Stud. Alcohol* 67, 529–537. doi: 10.15288/jsa.2006.67.529

McCall, N. M., Kotecki, L., Dominguez-Lopez, S., Marron Fernandez de Velasco, E., Carlblom, N., Sharpe, A. L., et al. (2017). Selective ablation of GIRK channels in dopamine neurons alters behavioral effects of cocaine in mice. *Neuropsychopharmacology* 42, 707–715. doi: 10.1038/npp.2016.138

McCutcheon, J. E., and Marinelli, M. (2009). Age matters. *Eur. J. Neurosci.* 29, 997–1014. doi: 10.1111/j.1460-9568.2009.06648.x

McFarland, K., and Kalivas, P. W. (2001). The circuitry mediating cocaine-induced reinstatement of drug-seeking behavior. *J. Neurosci.* 21, 8655–8663. doi: 10.1523/JNEUROSCI.21-21-08655.2001

Menegas, W., Akiti, K., Amo, R., Uchida, N., and Watabe-Uchida, M. (2018). Dopamine neurons projecting to the posterior striatum reinforce avoidance of threatening stimuli. *Nat. Neurosci.* 21, 1421–1430. doi: 10.1038/s41593-018-0222-1

Mereu, G., Yoon, K. W., Boi, V., Gessa, G. L., Naes, L., and Westfall, T. C. (1987). Preferential stimulation of ventral tegmental area dopaminergic neurons by nicotine. *Eur. J. Pharmacol.* 141, 395–399. doi: 10.1016/0014-2999(87)90556-5

Meyers, R. J., Roozen, H. G., and Smith, J. E. (2011). The community reinforcement approach. *Alcohol Res. Health* 33, 380–388.

Mohammadkhani, A., Fragale, J. E., Pantazis, C. B., Bowrey, H. E., James, M. H., and Aston-Jones, G. (2019). Orexin-1 receptor signaling in ventral pallidum regulates motivation for the opioid remifentanil. *J. Neurosci.* 39, 9831–9840. doi: 10.1523/JNEUROSCI.0255-19.2019

Mohebi, A., Pettibone, J. R., Hamid, A. A., Wong, J.-M. T., Vinson, L. T., Patriarchi, T., et al. (2019). Dissociable dopamine dynamics for learning and motivation. *Nature* 570, 65–70. doi: 10.1038/s41586-019-1235-y

Monroe, S. C., and Radke, A. K. (2021). Aversion-resistant fentanyl self-administration in mice. *Psychopharmacology* 238, 699–710. doi: 10.1007/s00213-020-05722-6

Morales, M., and Margolis, E. B. (2017). Ventral tegmental area: cellular heterogeneity, connectivity and behaviour. *Nat. Rev. Neurosci.* 18, 73–85. doi: 10.1038/nrn.2016.165

Morel, C., Montgomery, S., and Han, M.-H. (2019). Nicotine and alcohol: the role of midbrain dopaminergic neurons in drug reinforcement. *Eur. J. Neurosci.* 50, 2180–2200. doi: 10.1111/ejn.14160

Murray, J. E., Belin, D., and Everitt, B. J. (2012). Double dissociation of the dorsomedial and dorsolateral striatal control over the acquisition and performance of cocaine seeking. *Neuropsychopharmacology* 37, 2456–2466. doi: 10.1038/npp.2012.104

Nair-Roberts, R. G., Chatelain-Badie, S. D., Benson, E., White-Cooper, H., Bolam, J. P., and Ungless, M. A. (2008). Stereological estimates of dopaminergic, GABAergic and glutamatergic neurons in the ventral tegmental area, substantia nigra and retrorubral field in the rat. *Neuroscience* 152, 1024–1031. doi: 10.1016/j.neuroscience.2008.01.046

Napier, T. C., Kirby, A., and Persons, A. L. (2020). The role of dopamine pharmacotherapy and addiction-like behaviors in Parkinson's disease. *Prog. Neuropsychopharmacol. Biol. Psychiatry* 102:109942. doi: 10.1016/j.pnpbp.2020.109942

Nasrallah, N. A., Clark, J. J., Collins, A. L., Akers, C. A., Phillips, P. E., and Bernstein, I. L. (2011). Risk preference following adolescent alcohol use is associated with corrupted encoding of costs but not rewards by mesolimbic dopamine. *Proc. Natl. Acad. Sci. U.S.A.* 108, 5466–5471. doi: 10.1073/pnas.1017732108

Nestler, E. J., and Lüscher, C. (2019). The molecular basis of drug addiction: linking epigenetic to synaptic and circuit mechanisms. *Neuron* 102, 48–59. doi: 10.1016/j.neuron.2019.01.016

Nguyen, D., Alushaj, E., Erb, S., and Ito, R. (2019). Dissociative effects of dorsomedial striatum D1 and D2 receptor antagonism in the regulation of anxiety and learned approach-avoidance conflict decision-making. *Neuropharmacology* 146, 222–230. doi: 10.1016/j.neuropharm.2018.11.040

Nguyen, J. D., Aarde, S. M., Vandewater, S. A., Grant, Y., Stouffer, D. G., Parsons, L. H., et al. (2016). Inhaled delivery of Δ9-tetrahydrocannabinol (THC) to rats by e-cigarette vapor technology. *Neuropharmacology* 109, 112–120. doi: 10.1016/j.neuropharm.2016.05.021

Nutt, D. J., Lingford-Hughes, A., Erritzoe, D., and Stokes, P. R. A. (2015). The dopamine theory of addiction: 40 years of highs and lows. *Nat. Rev. Neurosci.* 16, 305–312. doi: 10.1038/nrn3939

O'Dell, L. E., Chen, S. A., Smith, R. T., Specio, S. E., Balster, R. L., Paterson, N. E., et al. (2007). Extended access to nicotine self-administration leads to dependence: circadian measures, withdrawal measures, and extinction behavior in rats. *J. Pharmacol. Exp. Ther.* 320, 180–193. doi: 10.1124/jpet.106.105270

Oleson, E. B., and Cheer, J. F. (2013). On the role of subsecond dopamine release in conditioned avoidance. *Front. Neurosci.* 7:96. doi: 10.3389/fnins.2013.00096

Oleson, E. B., Gentry, R. N., Chioma, V. C., and Cheer, J. F. (2012). Subsecond dopamine release in the nucleus accumbens predicts conditioned punishment and its successful avoidance. *J. Neurosci.* 32, 14804–14808. doi: 10.1523/JNEUROSCI.3087-12.2012

Oleson, E. B., and Roberts, D. C. (2009). Behavioral economic assessment of price and cocaine consumption following self-administration histories that produce escalation of either final ratios or intake. *Neuropsychopharmacology* 34, 796–804. doi: 10.1038/npp.2008.195

Oliver, R. J., Purohit, D. C., Kharidia, K. M., and Mandyam, C. D. (2019). Transient Chemogenetic inhibition of D1-MSNs in the dorsal striatum enhances methamphetamine self-administration. *Brain Sci.* 9:330. doi: 10.3390/brainsci9110330

Olson, V. G., and Nestler, E. J. (2007). Topographical organization of GABAergic neurons within the ventral tegmental area of the rat. *Synapse* 61, 87–95. doi: 10.1002/syn.20345

O'Neal, T. J., Nooney, M. N., Thien, K., and Ferguson, S. M. (2020). Chemogenetic modulation of accumbens direct or indirect pathways bidirectionally alters reinstatement of heroin-seeking in high- but not low-risk rats. *Neuropsychopharmacology* 45, 1251–1262. doi: 10.1038/s41386-019-0571-9

Orsini, C. A., Moorman, D. E., Young, J. W., Setlow, B., and Floresco, S. B. (2015). Neural mechanisms regulating different forms of risk-related decision-making: insights from animal models. *Neurosci. Biobehav. Rev.* 58, 147–167. doi: 10.1016/j.neubiorev.2015.04.009

Ostlund, S. B. (2019). The push and pull of dopamine in cue-reward learning. *Learn. Behav.* 47, 273–274. doi: 10.3758/s13420-018-0370-x

Ostlund, S. B., LeBlanc, K. H., Kosheleff, A. R., Wassum, K. M., and Maidment, N. T. (2014). Phasic mesolimbic dopamine signaling encodes the facilitation of incentive motivation produced by repeated cocaine exposure. *Neuropsychopharmacology* 39, 2441–2449. doi: 10.1038/npp.2014.96

Park, J., and Moghaddam, B. (2017). Risk of punishment influences discrete and coordinated encoding of reward-guided actions by prefrontal cortex and VTA neurons. *eLife* 6:e30056. doi: 10.7554/eLife.30056

Pascoli, V., Terrier, J., Hiver, A., and Lüscher, C. (2015). Sufficiency of mesolimbic dopamine neuron stimulation for the progression to addiction. *Neuron* 88, 1054–1066. doi: 10.1016/j.neuron.2015.10.017

Pascoli, V., Turiault, M., and Lüscher, C. (2012). Reversal of cocaine-evoked synaptic potentiation resets drug-induced adaptive behaviour. *Nature* 481, 71–75. doi: 10.1038/nature10709

Pelloux, Y., Everitt, B. J., and Dickinson, A. (2007). Compulsive drug seeking by rats under punishment: effects of drug taking history. *Psychopharmacology* 194, 127–137. doi: 10.1007/s00213-007-0805-0

Peterson, V. L., Richards, J. B., Meyer, P. J., Cabrera-Rubio, R., Tripi, J. A., King, C. P., et al. (2020). Sex-dependent associations between addiction-related behaviors and the microbiome in outbred rats. *EBioMedicine* 55:102769. doi: 10.1016/j.ebiom.2020.102769

Phillips, P. E. M., Stuber, G. D., Heien, M. L. A. V., Wightman, R. M., and Carelli, R. M. (2003). Subsecond dopamine release promotes cocaine seeking. *Nature* 422, 614–618. doi: 10.1038/nature01476

Piray, P., Keramati, M. M., Dezfouli, A., Lucas, C., and Mokri, A. (2010). Individual differences in nucleus accumbens dopamine receptors predict development of addiction-like behavior: a computational approach. *Neural Comput.* 22, 2334–2368. doi: 10.1162/NECO_a_00009

Pontieri, F. E., Tanda, G., and Chiara, G. D. (1995). Intravenous cocaine, morphine, and amphetamine preferentially increase extracellular dopamine in the "shell" as compared with the "core" of the rat nucleus accumbens. *Proc. Natl. Acad. Sci. U.S.A.* 92, 12304–12308. doi: 10.1073/pnas.92.26.12304

Pontieri, F. E., Tanda, G., Orzi, F., and Chiara, G. D. (1996). Effects of nicotine on the nucleus accumbens and similarity to those of addictive drugs. *Nature* 382, 255–257. doi: 10.1038/382255a0

Porrino, L. J., Lyons, D., Smith, H. R., Daunais, J. B., and Nader, M. A. (2004). Cocaine self-administration produces a progressive involvement of limbic, association, and sensorimotor striatal domains. *J. Neurosci.* 24, 3554–3562. doi: 10.1523/JNEUROSCI.5578-03.2004

Ranaldi, R., and Wise, R. A. (2001). Blockade of D1 dopamine receptors in the ventral tegmental area decreases cocaine reward: possible role for dendritically released dopamine. *J. Neurosci.* 21, 5841–5846. doi: 10.1523/JNEUROSCI.21-15-05841.2001

Ray, L. A., Courtney, K. E., Hutchison, K. E., MacKillop, J., Galvan, A., and Ghahremani, D. G. (2014). Initial evidence that Oprm1 genotype moderates ventral and dorsal striatum functional connectivity during alcohol cues. *Alcohol. Clin. Exp. Res.* 38, 78–89. doi: 10.1111/acer.12136

Ritz, M. C., Lamb, R. J., Goldberg, S. R., and Kuhar, M. J. (1987). Cocaine receptors on dopamine transporters are related to self-administration of cocaine. *Science* 237, 1219–1223. doi: 10.1126/science.2820058

Roberts, A. J., Heyser, C. J., Cole, M., Griffin, P., and Koob, G. F. (2000). Excessive ethanol drinking following a history of dependence: animal model of allostasis. *Neuropsychopharmacology* 22, 581–594. doi: 10.1016/S0893-133X(99)00167-0

Robinson, D. L., Heien, M. L. A. V., and Wightman, R. M. (2002). Frequency of dopamine concentration transients increases in dorsal and ventral striatum of male rats during introduction of conspecifics. *J. Neurosci.* 22, 10477–10486. doi: 10.1523/JNEUROSCI.22-23-10477.2002

Robinson, T. E. (2004). Addicted rats. *Science* 305, 951–953. doi: 10.1126/science.1102496

Robinson, T. E., and Berridge, K. C. (1993). The neural basis of drug craving: an incentive-sensitization theory of addiction. *Brain Res. Brain Res. Rev.* 18, 247–291. doi: 10.1016/0165-0173(93)90013-p

Robinson, T. E., and Berridge, K. C. (2001). Incentive-sensitization and addiction. *Addiction* 96, 103–114. doi: 10.1046/j.1360-0443.2001.9611038.x

Robinson, T. E., Jurson, P. A., Bennett, J. A., and Bentgen, K. M. (1988). Persistent sensitization of dopamine neurotransmission in ventral striatum (nucleus accumbens) produced by prior experience with (+)-amphetamine: a microdialysis study in freely moving rats. *Brain Res.* 462, 211–222. doi: 10.1016/0006-8993(88)90549-5

Samaha, A.-N., Khoo, S. Y.-S., Ferrario, C. R., and Robinson, T. E. (2021). Dopamine "ups and downs" in addiction revisited. *Trends Neurosci.* 44, 516–526. doi: 10.1016/j.tins.2021.03.003

Sasagawa, T., Horii-Hayashi, N., Okuda, A., Hashimoto, T., Azuma, C., and Nishi, M. (2017). Long-term effects of maternal separation coupled with social isolation on reward seeking and changes in dopamine D1 receptor expression in the nucleus accumbens *via* DNA methylation in mice. *Neurosci. Lett.* 641, 33–39. doi: 10.1016/j.neulet.2017.01.025

Saunders, B. T., Richard, J. M., Margolis, E. B., and Janak, P. H. (2018). Dopamine neurons create Pavlovian conditioned stimuli with circuit-defined motivational properties. *Nat. Neurosci.* 21, 1072–1083. doi: 10.1038/s41593-018-0191-4

Saunders, B. T., and Robinson, T. E. (2012). The role of dopamine in the accumbens core in the expression of Pavlovian conditioned responses. *Eur. J. Neurosci.* 36, 2521–2532. doi: 10.1111/j.1460-9568.2012.08217.x

Saunders, B. T., Yager, L. M., and Robinson, T. E. (2013). Cue-evoked cocaine "craving": role of dopamine in the accumbens core. *J. Neurosci.* 33, 13989–14000. doi: 10.1523/JNEUROSCI.0450-13.2013

Schenk, S., Lacelle, G., Gorman, K., and Amit, Z. (1987). Cocaine self-administration in rats influenced by environmental conditions: Implications for the etiology of drug abuse. *Neurosci. Lett.* 81, 227–231. doi: 10.1016/0304-3940(87)91003-2

Schindler, A. G., Soden, M. E., Zweifel, L. S., and Clark, J. J. (2016). Reversal of alcohol-induced dysregulation in dopamine network dynamics may rescue maladaptive decision-making. *J. Neurosci.* 36, 3698–3708. doi: 10.1523/JNEUROSCI.4394-15.2016

Schmitz, Y., Benoit-Marand, M., Gonon, F., and Sulzer, D. (2003). Presynaptic regulation of dopaminergic neurotransmission. *J. Neurochem.* 87, 273–289. doi: 10.1046/j.1471-4159.2003.02050.x

Schumacher, J. D., van Holstein, M., Bagrodia, V., Le Bouder, H. B., and Floresco, S. B. (2021). Dorsomedial striatal contributions to different forms of risk/reward decision making. *Neurobiol. Learn. Mem.* 178:107369. doi: 10.1016/j.nlm.2020.107369

Scribner, J. L., Vance, E. A., Protter, D. S. W., Sheeran, W. M., Saslow, E., Cameron, R. T., et al. (2020). A neuronal signature for monogamous reunion. *Proc. Natl. Acad. Sci. U.S.A.* 117, 11076–11084. doi: 10.1073/pnas.1917287117

Sedighim, S., Carrette, L. L., Venniro, M., Shaham, Y., de Guglielmo, G., and George, O. (2021). Individual differences in addiction-like behaviors and choice between cocaine versus food in Heterogeneous Stock rats. *Psychopharmacology.* doi: 10.1007/s00213-021-05961-1 [Epub ahead of print].

Serra, V., Fattore, L., Scherma, M., Collu, R., Spano, M. S., Fratta, W., et al. (2015). Behavioural and neurochemical assessment of salvinorin A abuse potential in the rat. *Psychopharmacology* 232, 91–100. doi: 10.1007/s00213-014-3641-z

Shaham, Y., Shalev, U., Lu, L., de Wit, H., and Stewart, J. (2003). The reinstatement model of drug relapse: history, methodology and major findings. *Psychopharmacology* 168, 3–20. doi: 10.1007/s00213-002-1224-x

Siciliano, C. A., Ferris, M. J., and Jones, S. R. (2015). Cocaine self-administration disrupts mesolimbic dopamine circuit function and attenuates dopaminergic responsiveness to cocaine. *Eur. J. Neurosci.* 42, 2091–2096. doi: 10.1111/ejn.12970

Simms, J. A., Steensland, P., Medina, B., Abernathy, K. E., Chandler, L. J., Wise, R., et al. (2008). Intermittent access to 20% ethanol induces high ethanol consumption in Long-Evans and Wistar rats. *Alcohol. Clin. Exp. Res.* 32, 1816–1823. doi: 10.1111/j.1530-0277.2008.00753.x

Singer, B. F., Fadanelli, M., Kawa, A. B., and Robinson, T. E. (2018). Are cocaine-seeking "Habits" necessary for the development of addiction-like behavior in rats? *J. Neurosci.* 38, 60–73. doi: 10.1523/JNEUROSCI.2458-17.2017

Solinas, M., Belujon, P., Fernagut, P. O., Jaber, M., and Thiriet, N. (2019). Dopamine and addiction: what have we learned from 40 years of research. *J. Neural Transm.* 126, 481–516. doi: 10.1007/s00702-018-1957-2

Spanagel, R. (2017). Animal models of addiction. *Dialogues Clin. Neurosci.* 19, 247–258.

Stalnaker, T. A., Takahashi, Y., Roesch, M. R., and Schoenbaum, G. (2009). Neural substrates of cognitive inflexibility after chronic cocaine exposure. *Neuropharmacology* 56, 63–72. doi: 10.1016/j.neuropharm.2008.07.019

Steinberg, E. E., Boivin, J. R., Saunders, B. T., Witten, I. B., Deisseroth, K., and Janak, P. H. (2014). Positive reinforcement mediated by midbrain dopamine neurons requires D1 and D2 receptor activation in the nucleus accumbens. *PLoS One* 9:e94771. doi: 10.1371/journal.pone.0094771

Stelly, C. E., Pomrenze, M. B., Cook, J. B., and Morikawa, H. (2016). Repeated social defeat stress enhances glutamatergic synaptic plasticity in the VTA and cocaine place conditioning. *eLife* 5:e15448. doi: 10.7554/eLife.15448

Stennett, B. A., Padovan-Hernandez, Y., and Knackstedt, L. A. (2020). Sequential cocaine-alcohol self-administration produces adaptations in rat nucleus accumbens core glutamate homeostasis that are distinct from those produced by cocaine self-administration alone. *Neuropsychopharmacology* 45, 441–450. doi: 10.1038/s41386-019-0452-2

Stewart, J. (1984). Reinstatement of heroin and cocaine self-administration behavior in the rat by intracerebral application of morphine in the ventral

tegmental area. *Pharmacol. Biochem. Behav.* 20, 917–923. doi: 10.1016/0091-3057(84)90017-0

Stewart, J. (2008). Psychological and neural mechanisms of relapse. *Philos. Trans. R. Soc. Lond. B Biol. Sci.* 363, 3147–3158. doi: 10.1098/rstb.2008.0084

Stitzer, M. L., Jones, H. E., Tuten, M., and Wong, C. (2011). "Community reinforcement approach and contingency management interventions for substance abuse," in *Handbook of Motivational Counseling: Goal-Based Approaches to Assessment and Intervention with Addiction and other Problems*, 2nd Edn, eds M. Cox and E. Klinger (Hoboken, NJ: Wiley Blackwell), 549–569. doi: 10.1002/9780470979952.ch23

Stopper, C. M., Tse, M. T. L., Montes, D. R., Wiedman, C. R., and Floresco, S. B. (2014). Overriding phasic dopamine signals redirects action selection during risk/reward decision making. *Neuron* 84, 177–189. doi: 10.1016/j.neuron.2014.08.033

Substance Abuse and Mental Health Services Administration (2019). *Key substance use and Mental Health Indicators in the United States: Results from the 2018 National Survey on Drug Use and Health*. Rockville, MD: Substance Abuse and Mental Health Services Administration.

Sugam, J. A., Day, J. J., Wightman, R. M., and Carelli, R. M. (2012). Phasic nucleus accumbens dopamine encodes risk-based decision-making behavior. *Biol. Psychiatry* 71, 199–205. doi: 10.1016/j.biopsych.2011.09.029

Swanson, L. W. (1982). The projections of the ventral tegmental area and adjacent regions: a combined fluorescent retrograde tracer and immunofluorescence study in the rat. *Brain Res. Bull.* 9, 321–353. doi: 10.1016/0361-9230(82)90145-9

Tadaiesky, M. T., Dombrowski, P. A., Figueiredo, C. P., Cargnin-Ferreira, E., Da Cunha, C., and Takahashi, R. N. (2008). Emotional, cognitive and neurochemical alterations in a premotor stage model of Parkinson's disease. *Neuroscience* 156, 830–840. doi: 10.1016/j.neuroscience.2008.08.035

Thomas, M. J., Kalivas, P. W., and Shaham, Y. (2008). Neuroplasticity in the mesolimbic dopamine system and cocaine addiction. *Br. J. Pharmacol.* 154, 327–342. doi: 10.1038/bjp.2008.77

Thompson, B. L., Oscar-Berman, M., and Kaplan, G. B. (2021). Opioid-induced structural and functional plasticity of medium-spiny neurons in the nucleus accumbens. *Neurosci. Biobehav. Rev.* 120, 417–430. doi: 10.1016/j.neubiorev.2020.10.015

Thompson, D., Martini, L., and Whistler, J. L. (2010). Altered ratio of D1 and D2 dopamine receptors in mouse striatum is associated with behavioral sensitization to cocaine. *PLoS One* 5:e11038. doi: 10.1371/journal.pone.0011038

Thomsen, M., Barrett, A. C., Negus, S. S., and Caine, S. B. (2013). Cocaine versus food choice procedure in rats: environmental manipulations and effects of amphetamine. *J. Exp. Anal. Behav.* 99, 211–233. doi: 10.1002/jeab.15

Tiffany, S. T. (1990). A cognitive model of drug urges and drug-use behavior: role of automatic and nonautomatic processes. *Psychol. Rev.* 97, 147–168. doi: 10.1037/0033-295x.97.2.147

Tornatzky, W., and Miczek, K. A. (2000). Cocaine self-administration "binges": transition from behavioral and autonomic regulation toward homeostatic dysregulation in rats. *Psychopharmacology* 148, 289–298. doi: 10.1007/s002130050053

Trezza, V., Baarendse, P. J. J., and Vanderschuren, L. J. M. J. (2014). On the interaction between drugs of abuse and adolescent social behavior. *Psychopharmacology* 231, 1715–1729. doi: 10.1007/s00213-014-3471-z

Trujillo, K. A., Smith, M. L., and Guaderrama, M. M. (2011). Powerful behavioral interactions between methamphetamine and morphine. *Pharmacol. Biochem. Behav.* 99, 451–458. doi: 10.1016/j.pbb.2011.04.014

Tsutsui-Kimura, I., Matsumoto, H., Akiti, K., Yamada, M. M., Uchida, N., and Watabe-Uchida, M. (2020). Distinct temporal difference error signals in dopamine axons in three regions of the striatum in a decision-making task. *eLife* 9:e62390. doi: 10.7554/eLife.62390

Ungless, M. A., and Grace, A. A. (2012). Are you or aren't you? Challenges associated with physiologically identifying dopamine neurons. *Trends Neurosci.* 35, 422–430. doi: 10.1016/j.tins.2012.02.003

Ungless, M. A., Whistler, J. L., Malenka, R. C., and Bonci, A. (2001). Single cocaine exposure *in vivo* induces long-term potentiation in dopamine neurons. *Nature* 411, 583–587. doi: 10.1038/35079077

Valyear, M. D., Glovaci, I., Zaari, A., Lahlou, S., Trujillo-Pisanty, I., Andrew Chapman, C., et al. (2020). Dissociable mesolimbic dopamine circuits control responding triggered by alcohol-predictive discrete cues and contexts. *Nat. Commun.* 11:3764. doi: 10.1038/s41467-020-17543-4

Vandaele, Y., and Ahmed, S. H. (2021). Habit, choice, and addiction. *Neuropsychopharmacology* 46, 689–698. doi: 10.1038/s41386-020-00899-y

Vanderschuren, L. J., Minnaard, A. M., Smeets, J. A., and Lesscher, H. M. (2017). Punishment models of addictive behavior. *Curr. Opin. Behav. Sci.* 13, 77–84. doi: 10.1016/j.cobeha.2016.10.007

Vanderschuren, L. J. M. J., and Ahmed, S. H. (2013). Animal studies of addictive behavior. *Cold Spring Harb. Perspect. Med.* 3:a011932. doi: 10.1101/cshperspect.a011932

Vanderschuren, L. J. M. J., Ciano, P. D., and Everitt, B. J. (2005). Involvement of the dorsal striatum in cue-controlled cocaine seeking. *J. Neurosci.* 25, 8665–8670. doi: 10.1523/JNEUROSCI.0925-05.2005

Vanderschuren, L. J. M. J., and Everitt, B. J. (2004). Drug seeking becomes compulsive after prolonged cocaine self-administration. *Science* 305, 1017–1019. doi: 10.1126/science.1098975

Vanderschuren, L. J. M. J., Niesink, R. J. M., and Van Pee, J. M. (1997). The neurobiology of social play behavior in rats. *Neurosci. Biobehav. Rev.* 21, 309–326. doi: 10.1016/S0149-7634(96)00020-6

Venniro, M., Banks, M. L., Heilig, M., Epstein, D. H., and Shaham, Y. (2020). Improving translation of animal models of addiction and relapse by reverse translation. *Nat. Rev. Neurosci.* 21, 625–643. doi: 10.1038/s41583-020-0378-z

Venniro, M., Caprioli, D., and Shaham, Y. (2016). Animal models of drug relapse and craving: from drug priming-induced reinstatement to incubation of craving after voluntary abstinence. *Prog. Brain Res.* 224, 25–52. doi: 10.1016/bs.pbr.2015.08.004

Venniro, M., Russell, T. I., Zhang, M., and Shaham, Y. (2019). Operant social reward decreases incubation of heroin craving in male and female rats. *Biol. Psychiatry* 86, 848–856. doi: 10.1016/j.biopsych.2019.05.018

Venniro, M., Zhang, M., Caprioli, D., Hoots, J. K., Golden, S. A., Heins, C., et al. (2018). Volitional social interaction prevents drug addiction in rat models. *Nat. Neurosci.* 21, 1520–1529. doi: 10.1038/s41593-018-0246-6

Verharen, J. P. H., de Jong, J. W., Roelofs, T. J. M., Huffels, C. F. M., van Zessen, R., Luijendijk, M. C. M., et al. (2018). A neuronal mechanism underlying decision-making deficits during hyperdopaminergic states. *Nat. Commun.* 9:731. doi: 10.1038/s41467-018-03087-1

Verharen, J. P. H., Luijendijk, M. C. M., Vanderschuren, L. J. M. J., and Adan, R. A. H. (2020). Dopaminergic contributions to behavioral control under threat of punishment in rats. *Psychopharmacology* 237, 1769–1782. doi: 10.1007/s00213-020-05497-w

Verheij, M. M. M., and Cools, A. R. (2008). Twenty years of dopamine research: individual differences in the response of accumbal dopamine to environmental and pharmacological challenges. *Eur. J. Pharmacol.* 585, 228–244. doi: 10.1016/j.ejphar.2008.02.084

Volkow, N. D., Fowler, J. S., Wang, G. J., Baler, R., and Telang, F. (2009). Imaging dopamine's role in drug abuse and addiction. *Neuropharmacology* 56(Suppl. 1), 3–8. doi: 10.1016/j.neuropharm.2008.05.022

Volkow, N. D., Wang, G.-J., Telang, F., Fowler, J. S., Logan, J., Childress, A.-R., et al. (2006). Cocaine cues and dopamine in dorsal striatum: mechanism of craving in cocaine addiction. *J. Neurosci.* 26, 6583–6588. doi: 10.1523/JNEUROSCI.1544-06.2006

Volkow, N. D., Wise, R. A., and Baler, R. (2017). The dopamine motive system: implications for drug and food addiction. *Nat. Rev. Neurosci.* 18, 741–752. doi: 10.1038/nrn.2017.130

Wang, Y.-C., Ho, U.-C., Ko, M.-C., Liao, C.-C., and Lee, L.-J. (2012). Differential neuronal changes in medial prefrontal cortex, basolateral amygdala and nucleus accumbens after postweaning social isolation. *Brain Struct. Funct.* 217, 337–351. doi: 10.1007/s00429-011-0355-4

Willuhn, I., Burgeno, L. M., Everitt, B. J., and Phillips, P. E. M. (2012). Hierarchical recruitment of phasic dopamine signaling in the striatum during the progression of cocaine use. *Proc. Natl. Acad. Sci. U.S.A.* 109, 20703–20708. doi: 10.1073/pnas.1213460109

Willuhn, I., Burgeno, L. M., Groblewski, P. A., and Phillips, P. E. M. (2014). Excessive cocaine use results from decreased phasic dopamine signaling in the striatum. *Nat. Neurosci.* 17, 704–709. doi: 10.1038/nn.3694

Winstanley, C. A., and Clark, L. (2016). Translational models of gambling-related decision-making. *Curr. Top. Behav. Neurosci.* 28, 93–120. doi: 10.1007/7854_2015_5014

Wise, R. A. (2005). Forebrain substrates of reward and motivation. *J. Comp. Neurol.* 493, 115–121. doi: 10.1002/cne.20689

Wise, R. A. (2009). Roles for nigrostriatal—Not just mesocorticolimbic—Dopamine in reward and addiction. *Trends Neurosci.* 32, 517–524. doi: 10.1016/j.tins.2009.06.004

Wise, R. A., and Bozarth, M. A. (1987). A psychomotor stimulant theory of addiction. *Psychol. Rev.* 94, 469–492.

Wise, R. A., and Robble, M. A. (2020). Dopamine and addiction. *Annu. Rev. Psychol.* 71, 79–106. doi: 10.1146/annurev-psych-010418-103337

Witten, I. B., Steinberg, E. E., Lee, S. Y., Davidson, T. J., Zalocusky, K. A., Brodsky, M., et al. (2011). Recombinase-driver rat lines: tools, techniques, and optogenetic application to dopamine-mediated reinforcement. *Neuron* 72, 721–733. doi: 10.1016/j.neuron.2011.10.028

Wittmann, B. C., Tan, G. C., Lisman, J. E., Dolan, R. J., and Düzel, E. (2013). DAT genotype modulates striatal processing and long-term memory for items associated with reward and punishment. *Neuropsychologia* 51, 2184–2193. doi: 10.1016/j.neuropsychologia.2013.07.018

Wolf, M. E. (2016). Synaptic mechanisms underlying persistent cocaine craving. *Nat. Rev. Neurosci.* 17, 351–365. doi: 10.1038/nrn.2016.39

Yin, H. H., Ostlund, S. B., Knowlton, B. J., and Balleine, B. W. (2005). The role of the dorsomedial striatum in instrumental conditioning. *Eur. J. Neurosci.* 22, 513–523. doi: 10.1111/j.1460-9568.2005.04218.x

Yorgason, J. T., Calipari, E. S., Ferris, M. J., Karkhanis, A. N., Fordahl, S. C., Weiner, J. L., et al. (2016). Social isolation rearing increases dopamine uptake and psychostimulant potency in the striatum. *Neuropharmacology* 101, 471–479. doi: 10.1016/j.neuropharm.2015.10.025

Young, K. A., Liu, Y., Gobrogge, K. L., Wang, H., and Wang, Z. (2014). Oxytocin reverses amphetamine-induced deficits in social bonding: Evidence for an interaction with nucleus accumbens dopamine. *J. Neurosci.* 34, 8499–8506. doi: 10.1523/JNEUROSCI.4275-13.2014

Yun, I. A., Wakabayashi, K. T., Fields, H. L., and Nicola, S. M. (2004). The ventral tegmental area is required for the behavioral and nucleus accumbens neuronal firing responses to incentive cues. *J. Neurosci.* 24, 2923–2933. doi: 10.1523/JNEUROSCI.5282-03.2004

Zapata, A., Minney, V. L., and Shippenberg, T. S. (2010). Shift from goal-directed to habitual cocaine seeking after prolonged experience in rats. *J. Neurosci.* 30, 15457–15463. doi: 10.1523/JNEUROSCI.4072-10.2010

Zhou, Z., Liu, X., Chen, S., Zhang, Z., Liu, Y., Montardy, Q., et al. (2019). A VTA GABAergic neural circuit mediates visually evoked innate defensive responses. *Neuron* 103, 473–488.e6. doi: 10.1016/j.neuron.2019.05.027

Zimmer, B. A., Oleson, E. B., and Roberts, D. C. (2012). The motivation to self-administer is increased after a history of spiking brain levels of cocaine. *Neuropsychopharmacology* 37, 1901–1910. doi: 10.1038/npp.2012.37

Zlebnik, N. E., and Carroll, M. E. (2015). Prevention of the incubation of cocaine seeking by aerobic exercise in female rats. *Psychopharmacology* 232, 3507–3513. doi: 10.1007/s00213-015-3999-6

Ztaou, S., Lhost, J., Watabe, I., Torromino, G., and Amalric, M. (2018). Striatal cholinergic interneurons regulate cognitive and affective dysfunction in partially dopamine-depleted mice. *Eur. J. Neurosci.* 48, 2988–3004.

Conflict of Interest: The authors declare that the research was conducted in the absence of any commercial or financial relationships that could be construed as a potential conflict of interest.

Publisher's Note: All claims expressed in this article are solely those of the authors and do not necessarily represent those of their affiliated organizations, or those of the publisher, the editors and the reviewers. Any product that may be evaluated in this article, or claim that may be made by its manufacturer, is not guaranteed or endorsed by the publisher.

Copyright © 2021 Poisson, Engel and Saunders. This is an open-access article distributed under the terms of the Creative Commons Attribution License (CC BY). The use, distribution or reproduction in other forums is permitted, provided the original author(s) and the copyright owner(s) are credited and that the original publication in this journal is cited, in accordance with accepted academic practice. No use, distribution or reproduction is permitted which does not comply with these terms.

frontiers in Neural Circuits

ORIGINAL RESEARCH
published: 11 November 2021
doi: 10.3389/fncir.2021.726893

Midbrain Dopamine Neurons Defined by TrpV1 Modulate Psychomotor Behavior

*Gian Pietro Serra[1], Adriane Guillaumin[1], Sylvie Dumas[2], Bianca Vlcek[1] and Åsa Wallén-Mackenzie[1]**

[1] Unit of Comparative Physiology, Department of Organism Biology, Uppsala University, Uppsala, Sweden,
[2] Oramacell, Paris, France

Dopamine (DA) neurons of the ventral tegmental area (VTA) continue to gain attention as far more heterogeneous than previously realized. Within the medial aspect of the VTA, the unexpected presence of TrpV1 mRNA has been identified. TrpV1 encodes the Transient Receptor Potential cation channel subfamily V member 1, TRPV1, also known as the capsaicin receptor, well recognized for its role in heat and pain processing by peripheral neurons. In contrast, the brain distribution of TrpV1 has been debated. Here, we hypothesized that the TrpV1$^+$ identity defines a distinct subpopulation of VTA DA neurons. To explore these brain TrpV1$^+$ neurons, histological analyses and Cre-driven mouse genetics were employed. TrpV1 mRNA was most strongly detected at the perinatal stage forming a band of scattered neurons throughout the medial VTA, reaching into the posterior hypothalamus. Within the VTA, the majority of TrpV1 co-localized with both Tyrosine hydroxylase (Th) and Vesicular monoamine transporter 2 (Vmat2), confirming a DA phenotype. However, TrpV1 also co-localized substantially with Vesicular glutamate transporter 2 (Vglut2), representing the capacity for glutamate (GLU) release. These TrpV1$^+$/Th$^+$/Vglut2$^+$/Vmat2$^+$ neurons thus constitute a molecularly and anatomically distinct subpopulation of DA-GLU co-releasing neurons. To assess behavioral impact, a *TrpV1^{Cre}*-driven strategy targeting the *Vmat2* gene in mice was implemented. This manipulation was sufficient to alter psychomotor behavior induced by amphetamine. The acute effect of the drug was accentuated above control levels, suggesting super-sensitivity in the drug-naïve state resembling a "pre-sensitized" phenotype. However, no progressive increase with repeated injections was observed. This study identifies a distinct TrpV1$^+$ VTA subpopulation as a critical modulatory component in responsiveness to amphetamine. Moreover, expression of the gene encoding TRPV1 in selected VTA neurons opens up for new possibilities in pharmacological intervention of this heterogeneous, but clinically important, brain area.

Keywords: glutamate, VGLUT2, VMAT2, co-release, transient receptor vanilloid, amphetamine, sensitization, psychostimulant

OPEN ACCESS

Edited by:
Jean-Francois Poulin, McGill University, Canada

Reviewed by:
Nao Chuhma, New York State Psychiatric Institute (NYSPI), United States
Helen S. Bateup, Harvard Medical School, United States

***Correspondence:**
Åsa Wallén-Mackenzie
asa.mackenzie@ebc.uu.se

Received: *17 June 2021*
Accepted: *28 September 2021*
Published: *11 November 2021*

Citation:
Serra GP, Guillaumin A, Dumas S, Vlcek B and Wallén-Mackenzie Å (2021) Midbrain Dopamine Neurons Defined by TrpV1 Modulate Psychomotor Behavior. Front. Neural Circuits 15:726893. doi: 10.3389/fncir.2021.726893

INTRODUCTION

Dopamine (DA) neurons of the ventral tegmental area (VTA) are critical to limbic and cognitive functions, and, hence, exert a major impact on behavioral regulation. Consequently, their dysfunction is correlated with the severe neuropsychiatric disorder, including addiction, attention deficit/hyperactivity disorder (ADHD), schizophrenia, and the affective/cognitive non-motor domain of Parkinson's disease (PD) (Björklund and Dunnett, 2007). Major efforts are, therefore, aimed at elucidating the neurobiological underpinnings of the VTA in order to advance prediction, prevention, and treatment prospects of brain dysfunction implicating this brain area.

The VTA was long considered a homogeneous DA structure. However, it is today well recognized that VTA DA neurons coexist with glutamate (GLU)- and GABA-signaling neurons, and that DA, GLU, and GABA neurons show regional distribution within the VTA, also reflected in their projections (Lammel et al., 2011; Hnasko et al., 2012; Watabe-Uchida et al., 2012; Beier et al., 2015; Menegas et al., 2015). In addition, several layers of heterogeneity have been reported within the VTA DA system, including electrophysiological properties, afferent/efferent projections, responsiveness to positive and negative reinforcers, the ability for neurotransmitter co-release, gene expression, and vulnerability to disease (Roeper, 2013; Brichta and Greengard, 2014; Pupe and Wallén-Mackenzie, 2015; Morales and Margolis, 2017; Poulin et al., 2020). The VTA can be further subdivided into anatomically distinct subnuclei based on the distribution of DA neurons. For example, medial VTA subnuclei consist of the interfascicular nucleus (IF) and rostral linear nucleus (RLi), whereas more lateral VTA subnuclei include the paranigral (PN) and parabrachial pigmented (PBP) nuclei. In addition, the caudal linear nucleus (CLi) is sometimes, but not always, grouped with the VTA, and there is also a medial-lateral distribution within each VTA subnucleus. VTA DA neurons send extensive forebrain projections, primarily to the nucleus accumbens and cerebral cortex. The *Th* and *Slc18a2* genes encoding the Tyrosine hydroxylase (TH) and Vesicular monoamine transporter 2 (VMAT2) proteins that are essential to DA production (TH) and vesicular packaging (VMAT2), respectively, are, by necessity, expressed in all neurons defined as dopaminergic, while other genes important to DA cell function may vary more. For example, the *Slc6a3 (Dat)* gene, encoding the dopamine transporter (DAT), which mediates DA reuptake after vesicular release, shows a medial^{low}-lateral^{high} expression pattern in the VTA (Lammel et al., 2008; Papathanou et al., 2018). Furthermore, the density of DA neurons differs across VTA subnuclei (Morales and Margolis, 2017).

The medial VTA is of particular interest for several reasons. The mesoaccumbal DA projection, which is strongly associated with reward processing, motivation, and behavioral reinforcement, shows a topographical projection pattern. Medial VTA DA neurons innervate the medial aspect of the nucleus accumbens shell (mAcbSh), and lateral VTA DA neurons target the lateral shell and core areas within the nucleus accumbens (Ikemoto, 2007; Poulin et al., 2018). DA release in the mAcbSh is associated with the reinforcing effects of both natural and drug rewards, and drugs of abuse increase DA levels more efficiently in the mAcbSh than lateral shell and core (Di Chiara and Imperato, 1988; Pontieri et al., 1995; Lüscher, 2016). Furthermore, medial VTA DA neurons show higher expression of the *Vglut2* gene than DA neurons of the lateral VTA (Kawano et al., 2006; Li et al., 2013; Papathanou et al., 2018). The presence of the VGLUT2 protein allows GLU packaging into presynaptic vesicles for fast excitatory neurotransmission (Hnasko and Edwards, 2012). Within the VTA, the *Vglut2* gene is expressed in GLU neurons and DA-GLU co-releasing neurons, the latter primarily, but not uniquely, located in medial subareas (reviewed in Trudeau et al., 2014; Trudeau and El Mestikawy, 2018; Eskenazi et al., 2021). DA-GLU neurons project within the nucleus accumbens to mAcbSh, where they primarily target cholinergic interneurons and medium spiny neurons (Kawano et al., 2006; Li et al., 2013; Chuhma et al., 2014; Mingote et al., 2015; Poulin et al., 2018). Conditional knockout (cKO) of *Vglut2* in DA neurons in mice ($Vglut2^{lx/lx}$; $Slc6a3^{Cre/wt}$) results in modest deficits in emotional behavior and vigor (Birgner et al., 2010; Fortin et al., 2012; Wang et al., 2017) but strongly alters the behavioral response to psychostimulants (Birgner et al., 2010; Hnasko et al., 2010; Alsiö et al., 2011; Fortin et al., 2012; Papathanou et al., 2018). Together, the results of several cKO studies converge in a model where GLU co-release plays an intricate role in reward responsiveness and behavioral reinforcement mediated by DA (Eskenazi et al., 2021). However, knowledge is still sparse, and improved resolution in dissecting out the role of this complex neurotransmitter phenotype should be useful to increase current understanding of the VTA.

In addition to the mixture of different neurotransmitter phenotypes in the VTA, also molecularly defined subtypes of DA neurons have recently been identified. These provide yet another level of heterogeneity and complexity but also render distinct DA neurons taggable and distinguishable from each other. These molecular fingerprints have been derived from gene expression studies using microarray (Chung et al., 2005; Greene et al., 2005; Viereckel et al., 2016) and, more recently, transcriptomics methodology (Poulin et al., 2014; La Manno et al., 2016; Tiklová et al., 2019; Phillips et al., 2021). These studies are often based around the quest to identify molecular properties that distinguish VTA DA neurons from those in substantia nigra *pars compacta* (SNc), and that might help explain their different vulnerability to PD. However, genes that might provide information of VTA DA neurons in other conditions, such as neuropsychiatric disorder, have also been identified. One such example is *NeuroD6*, which has consistently been reported to show higher expression levels in the VTA compared to the SNc in most microarray and transcriptomics-based studies. Anatomical mapping has revealed NeuroD6 to define a modest DA subtype regionally distributed in the VTA (Khan et al., 2017; Kramer et al., 2018; Bimpisidis et al., 2019). Functional assays showed that NeuroD6 is critical to DA cell survival and vulnerability to PD (Khan et al., 2017; Kramer et al., 2018) while recent behavior analysis has identified a role for NeuroD6-positive VTA DA neurons in approach behavior and psychostimulant response (Bimpisidis et al., 2019).

Another gene, which has been identified in a microarray approach as higher expressed in the VTA than SNc, is *TrpV1* (Viereckel et al., 2016). This gene encodes the transient receptor potential cation channel subfamily V member 1 (TRPV1; also known as the capsaicin receptor) (Caterina et al., 1997), a nonselective cation channel highly expressed in certain sensory neurons, but for which the brain distribution has been elusive and, hence, the topic of debate (Cavanaugh et al., 2011; Ramírez-Barrantes et al., 2016). However, using reporter gene expression driven by a $TrpV1^{Cre/+}$ mouse transgene to allow detection with high sensitivity and precision, *TrpV1* expression could be distinctly detected in a contiguous band of neurons reaching from the caudal hypothalamus through to the VTA, including the medially located subnucleus IF (Cavanaugh et al., 2011). While described already 10 years ago, this finding has remained largely unexplored. However, a subsequent report not only identified TrpV1 mRNA within the medial VTA but also showed that TrpV1$^+$ VTA neurons were positive for both Th and Vglut2, suggesting a DA-GLU neurotransmitter phenotype. The same study demonstrated GLU release in the AcbSh upon optogenetic stimulation in $TrpV1^{Cre/wt}$ mice, thus identifying a mesoaccumbal projection of combined TrpV1/GLU identity (Viereckel et al., 2016).

Given the recent demonstration of the medial distribution of TrpV1 mRNA within the VTA, its co-expression with both DA and GLU markers, and GLU release in the $TrpV1^{Cre}$ mesoaccumbal projection, we hypothesized that TrpV1 is a molecular marker for a distinct subpopulation of VTA neurons of DA-GLU identity. This was tested by addressing the distribution pattern and molecular fingerprint of TrpV1$^+$ neurons in mice. Furthermore, to determine if TrpV1$^+$ VTA neurons contribute to behavioral regulation, a new cKO mouse line was generated in which the prerequisite for vesicular DA packaging, VMAT2, was abrogated in $TrpV1^{Cre}$ neurons. Control and cKO mice were analyzed in behavioral paradigms relevant to the VTA, including psychomotor response upon amphetamine challenge.

RESULTS

TrpV1-Positive Cells Are Primarily Present in the Medial VTA and Excluded From SNc

Based on the original report identifying TrpV1-positive (TrpV1$^+$) neurons primarily in the border area connecting the ventro-medial midbrain and caudal hypothalamus, with the strongest expression in the IF subnucleus (Cavanaugh et al., 2011), it was of interest to study *TrpV1* gene expression in this brain region in more detail. Colorimetric *in situ* hybridization (CISH) was performed on serial sections from newborn mice of postnatal day 3 (P3). TrpV1 mRNA (**Figures 1A1–A9**) was analyzed with Th (**Figures 1B1–B9**) and Vglut2 (**Figures 1C1–C9**) mRNAs as references for DA and GLU neurons throughout this brain region. The P3 stage was selected based on our previous microarray analysis, which identified elevated *TrpV1* gene expression levels in VTA compared to SNc at this postnatal stage (Viereckel et al., 2016). Here, scattered, but distinct, TrpV1$^+$ cells were detected in a continuum stretching rostrally from the posterior hypothalamic nucleus (PHA) and retromammillary nucleus (RM) of the caudal hypothalamus through to, and including, all VTA subnuclei (IF, RLi, CLi, PN, and PBP), as well as the A8 DA area of the caudal midbrain (**Figures 1A1-A9** and **Supplementary Figure 1**). The density of TrpV1$^+$ neurons in the VTA was visibly higher in medial (IF, RLi, CLi, and medial PN) than lateral (lateral PN, PBP) VTA subnuclei (**Figures 1A1–A9**). Furthermore, the lateral DA cell group of the SNc was devoid of TrpV1 mRNA (**Figures 1A6,A7**).

TrpV1$^+$ VTA Neurons Are Mainly of Mixed DA-GLU Identity (TrpV1$^+$/Th$^+$/Vglut2$^+$)

To define neurotransmitter identity and molecular properties of the neuronal population in the VTA identified as positive for TrpV1 mRNA, a battery of histological analyses was performed. Using fluorescent *in situ* hybridization (FISH), the neurotransmitter identity of TrpV1$^+$ neurons was first addressed (**Figure 2**). Co-localization analysis at P3 was performed assessing Th, Vglut2, and the vesicular inhibitory amino acid transporter (Viaat) mRNAs to enable detection of DA, GLU, and GABA neurons, respectively. Similar to CISH, FISH analysis detected TrpV1 mRNA in the VTA, primarily in the IF, followed by RLi, CLi, PN, and PBP (**Figure 2A1**). Counting of cells positive for TrpV1 mRNA showed that 49% were located in the IF subnucleus, while the corresponding percentage in other VTA subnuclei was lower (18% in RLi; 15% CLi; 11% PN; and 7% PBP) (**Figure 2A1**).

TrpV1 co-localized substantially with Th mRNA. More than 90% of TrpV1$^+$ cells were positive for Th in the IF, PN, and PBP (**Figure 2A2** and **Table 1**). These are all VTA subnuclei defined by a strong DA (Th$^+$) phenotype. In contrast, RLi contains fewer DA (Th$^+$) neurons, and, here, less TrpV1/Th co-labeling was observed (less than 5%). NoTrpV1/Th co-localization was observed in the PHA and RM, an expected finding as these hypothalamic areas are largely devoid of Th mRNA and, instead, are glutamatergic (**Supplementary Figure 1**).

Addressing a GLU neurotransmitter phenotype, TrpV1/Vglut2 co-labeling analysis showed that the far majority of TrpV1$^+$ cells throughout the VTA-hypothalamus (PHA, RM) continuum were positive for Vglut2 (**Figure 2A3**, **Table 1**, and **Supplementary Figure 1**). However, a substantially lower degree of overlap was observed between TrpV1 and Vglut2 in the CLi (33%) than in the RLi (100%) and IF (89%). This was due to the variable amount of both TrpV1 and Vglut2 mRNAs in different VTA subnuclei (**Table 1**). In contrast to the substantial TrpV1/Vglut2 co-labeling throughout the VTA and hypothalamus, few, if any, TrpV1$^+$ cells were positive for Viaat mRNA, indicating a lack of a GABA phenotype. TrpV1 co-labeling with Viaat was only observed in the RLi, the area with low co-labeling with Th (**Supplementary Figure 1** and **Table 1**).

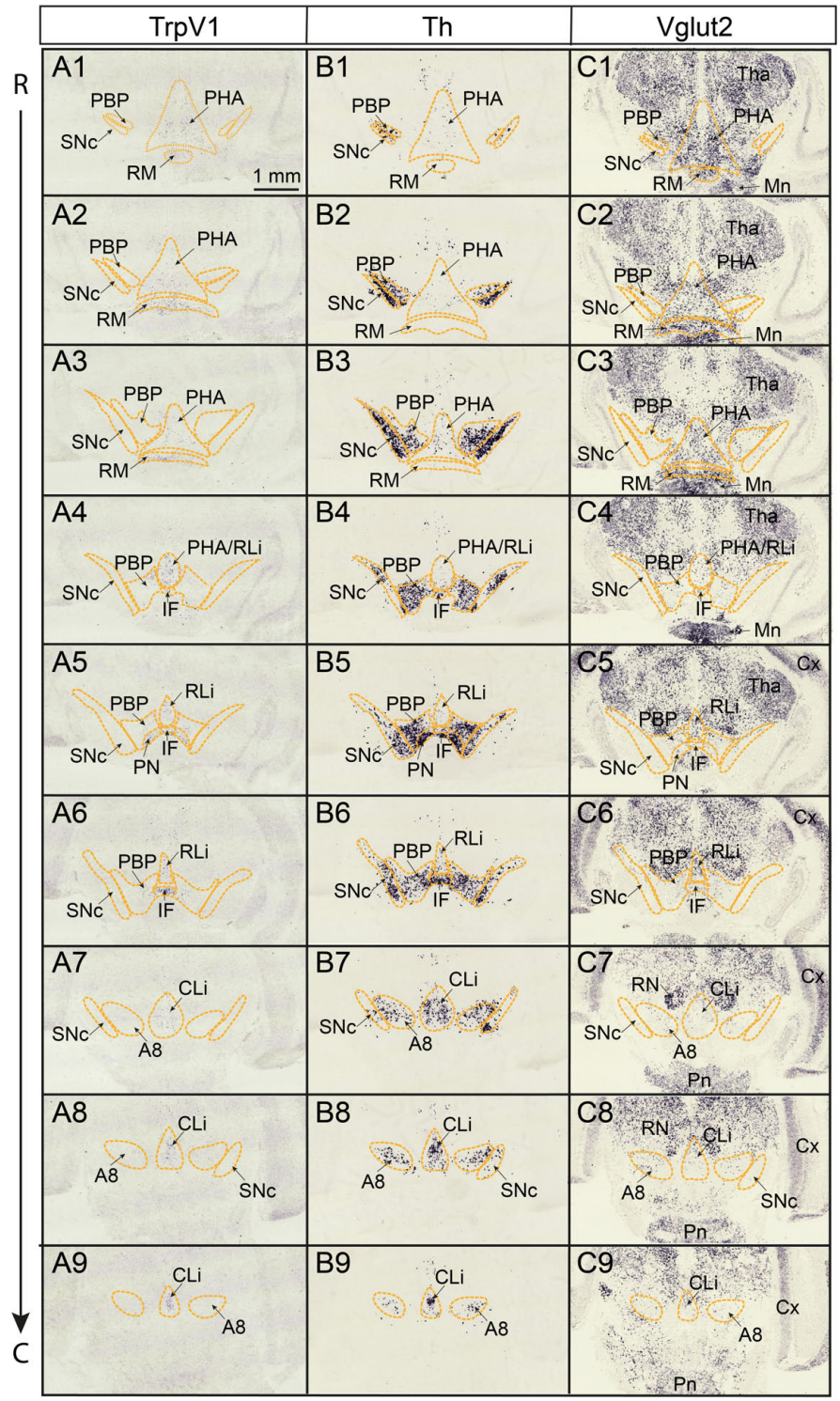

FIGURE 1 | TrpV1 mRNA is detected in scattered medial cells in a continuous manner reaching from the posterior hypothalamus rostrally throughout the VTA caudally. TrpV1, Th, Vglut2 mRNAs analyzed by colorimetric *in situ* hybridization (CISH) in serial coronal brain sections at postnatal day (P) 3. The rostral end of series at the levels of PHA, RM, and PBP; the caudal end of series at the level of CLi, A8. **(A1–A9)** TrpV1; **(B1–B9)** Th; **(C1–C9)** Vglut2. Scale bar; 1 mm. A8, A8 dopamine area; CLi, caudal linear nucleus; Cx, cerebral cortex; IF, interfascicular nucleus; Mn, mammillary nucleus; PBP parabrachial pigmented nucleus; PHA posterior hypothalamic nucleus; RLi, rostral linear nucleus; Pn, pontine nucleus; PN, paranigral nucleus; RM, retromammillary nucleus; RN, red nucleus; SNc, substantia nigra *pars compacta*; VTA, ventral tegmental area; Tha, thalamus; R, rostral; C, caudal.

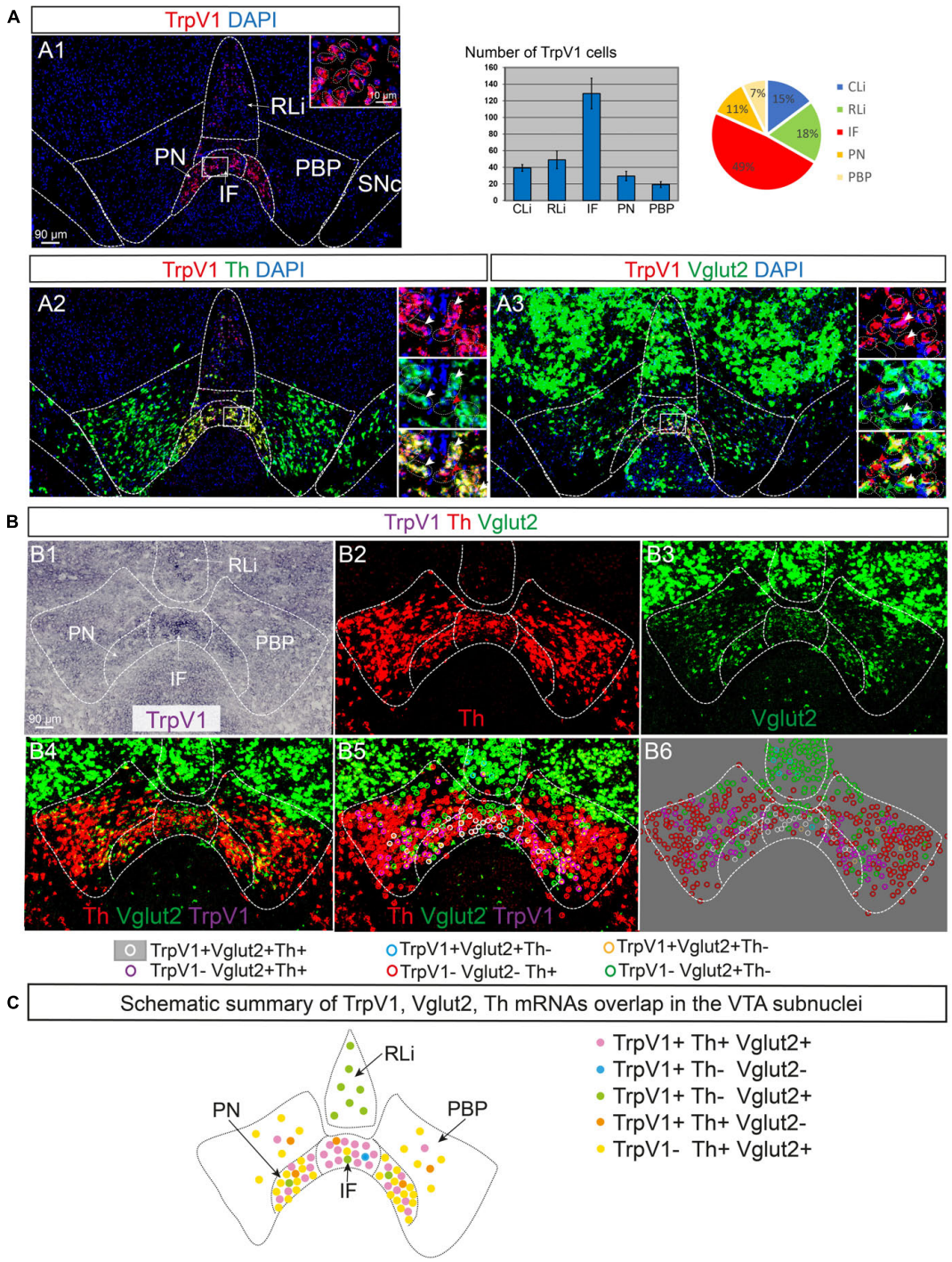

FIGURE 2 | TrpV1 mRNA primarily in medial VTA subnuclei co-localizes strongly with Th and Vglut2 mRNAs. TrpV1, Th, and Vglut2 mRNAs were analyzed by fluorescent and colorimetric *in situ* hybridization (FISH and CISH) in serial coronal brain sections at postnatal day (P) 3. DAPI is used for the detection of cell nuclei. **(A1–A3)** FISH: TrpV1 (**A1**; a table and a pie chart show result of counting of TrpV1-positive cells per VTA subnucleus, *N* = 3 mice, serial sections throughout the VTA, allowing for analysis of adjacent sections); TrpV1/Th **(A2)**; TrpV1/Vglut2 **(A3)**; closeup's in insets; cells indicated by dotted lines. The yellow color indicates colocalization of red and green fluorophores. FISH-positive cells are indicated in insets by arrowheads; white arrows indicate co-labeling of red and green fluorophores. **(B)** Triple labeling by combined CISH/FISH visualized in separate channels **(B1–B3)** and merged **(B4)**: TrpV1 (**B1**, CISH), Th (**B2**, FISH), Vglut2 (**B3**, FISH), merged TrpV1/Th/Vglut2 **(B4)**; colored circles indicate double and triple mRNA labeling (**B5** histological section; **B6**-colored circles indicating positive cells in B5 superimposed on gray background for clarity; **B5,B6** legends indicate mRNA detected per colored circle). **(C)** A schematic summary of results in **(A,B)**, an illustrated map of TrpV1/Vglut2/Th overlap in VTA subnuclei. Scale bars, 90 µm; 10 µm (insets). See **Table 1** for cell counting. IF, interfasicular nucleus; PN, paranigral nucleus; PBP, parabrachial pigmented nucleus; RLi, rostral linear nucleus; VTA, ventral tegmental area.

TABLE 1 | TrpV1mRNA and its extent of co-localization with a range of neurotransmitter and neuronal subtype markers.

Characterisation of Trpv1 mRNA-positive phenotype in VTA subnuclei					
	IF	**PN**	**PBP**	**RLi**	**CLi**
%Trpv1 **Th$^+$**	95%	92%	95%	3%	73%
%Trpv1 **Vmat2$^+$**	75%	77%	90%	2%	80%
%Trpv1 **Vglut2$^+$**	89%	82%	60%	100%	33%
%Trpv1 **Viaat$^+$**	3%	0	0	31%	9%
%Trpv1 **Dat$^+$**	0	14%	40%	0	0
%Trpv1 **NeuroD6$^+$**	6%	8%	20%	0	5%
%Trpv1 **Grp$^+$**	14%	34%	23%	0	0
%Trpv1 **(Th$^+$ Vglut2$^-$)**	9%	18%	38%	0%	68%
%Trpv1 **(Vglut2$^+$ Th$^-$)**	5%	3%	3%	97%	27%
%Trpv1 **(Vglut2$^-$ Th$^-$)**	1%	0%	0%	0%	0%
%Trpv1 **(Vglut2$^+$ Th$^+$)**	85%	79%	59%	3%	5%
% (Vglut2 Th) **Trpv1$^+$**	85%	30%	15%	almost no Th/Vglut2 coloc	

Result of counting of double- or triple-positive cells obtained in in situ hybridization analysis at postnatal day 3 (P3). N = 3 mice per detection, serial sections throughout the VTA. Percentage of co-labeling between TrpV1 and one or two other mRNAs (in bold). Example, 95% of TrpV1-positive cells in IF are positive for Th mRNA.

Triple-detection, achieved by combining CISH (TrpV1) and FISH (Th and Vglut2) detection methods, was performed to allow assessment of single and dual neurotransmitter phenotypes (DA *vs.* GLU *vs.* DA-GLU) (**Figures 2B1–B6** and **Table 1**). This analysis revealed that very few TrpV1$^+$ neurons in the VTA were positive for either Th or Vglut2 mRNAs (**Figures 2B4–B6,C** and **Table 1**). TrpV1$^+$/Th$^+$/Vglut2$^-$ (DA) neurons were primarily present in PBP while TrpV1$^+$/Th$^-$/Vglut2$^+$ (GLU) neurons represented the most common TrpV1$^+$ phenotype in RLi, in a continuum with PHA and RM (**Supplementary Figure 1**). However, the far majority of TrpV1$^+$ neurons were positive for both Th and Vglut2 mRNAs (TrpV1$^+$/Th$^+$/Vglut2$^+$), thus demonstrating the histological properties of a DA-GLU phenotype (**Figures 2B4–B6,C** and **Table 1**). For example, in the IF, where most TrpV1$^+$ neurons reside, 85% of TrpV1$^+$ cells were positive for both Th and Vglut2 (TrpV1$^+$/Th$^+$/Vglut2$^+$) (**Table 1**).

While the majority of TrpV1$^+$ neurons showed a DA-GLU identity, not all DA-GLU neurons were positive for TrpV1 (**Table 1**). In the IF subarea, containing the largest proportion of TrpV1$^+$ cells, 85% of Th$^+$/Vglut2$^+$ (DA-GLU) neurons were positive for TrpV1 (TrpV1$^+$/Th$^+$/Vglut2$^+$). More modest numbers were obtained for the other VTA subnuclei (PN, 30%; PBP, 15%; barely at all in RLi and CLi) (**Table 1**). The results suggest that TrpV1 defines a subpopulation of DA-GLU VTA neurons, which show a medial^{high}–lateral^{low} distribution within VTA subnuclei IF, PN, and PBP (**Figure 2C**).

To pinpoint the temporal expression of *TrpV1*, serial brain sections derived from embryonic day 14.5 (E14.5), P12, and adult (9 weeks) mice were prepared to complement the analysis at P3. Also, here, TrpV1, Th, and Vglut2 mRNAs were analyzed on adjacent sections. TrpV1 mRNA was detected within the developing VTA at E14.5 but was very low at P12 and in adulthood (**Supplementary Figure 2**). A similar profile was evident for the hypothalamic nuclei (**Supplementary Figure 2**). Taken together, histological analyses identify a perinatal peak of TrpV1 mRNA in the medial aspect of the VTA/PHA/RM region between E14.5 and P3, and its subsequent downregulation.

TrpV1 Co-localizes Substantially With Vmat2 but Not With Dat mRNA or Dopamine Neuron Subtype Markers NeuroD6 and Grp

As the substantial co-localization of TrpV1 with Th and Vglut2 points to a strong DA-GLU identity at P3, this was further assessed by analysis of additional components essential to the DA machinery. Dat and Vmat2 mRNAs, encoding the proteins required for DA reuptake (DAT) and vesicular DA transport (VMAT2), were assessed for co-localization with TrpV1 mRNA using FISH in serial sections at P3. In accordance with the reported lateral^{high}–medial^{low} distribution pattern of VTA neurons positive for Dat mRNA (Lammel et al., 2008; Papathanou et al., 2018) and the herein described opposite pattern for TrpV1 mRNA (medial^{high} – lateral^{low}); very few cells showed TrpV1/Dat co-labeling (**Figures 3A1–A3** and **Table 1**). In contrast, in accordance with the broader distribution of Vmat2 than Dat mRNA in the VTA, a clear TrpV1/Vmat2 overlap was identified in all VTA subnuclei positive for TrpV1, except in the RLi (**Figures 3A4–A6**, **Supplementary Figure 3**, and **Table 1**). In IF and PN subnuclei, over 70% of TrpV1$^+$ cells were Vmat2$^+$. In PBP, containing substantially fewer TrpV1$^+$ neurons, over 90% colocalization TrpV1/Vmat2 was observed, in accordance with the strong DA phenotype in this VTA subnucleus (**Table 1**).

Next, based on the strong TrpV1/Th/Vglut2 and TrpV1/Vmat2 overlap, the extent of Vmat2/Vglut2 overlap was assessed. Confirming data above, TrpV1 and Vglut2 mRNAs highly co-localized in the VTA, primarily in the medial aspect (**Figures 3A7–A9**). A similar pattern of medial co-labeling was observed between Vglut2 and Vmat2 mRNAs, albeit in a larger proportion of cells than TrpV1 and Vglut2 (**Figures 3A10–A12**). This is in accordance with the observation of a higher abundance of Vmat2 and Vglut2 mRNAs than TrpV1 mRNA in the medial VTA. Furthermore, Vmat2 mRNA was far less abundant than Vglut2 in RLi, in accordance with the low levels of Th mRNA in this medial subnucleus (**Figures 3A10–A12**). Instead, most Vglut2/Vmat2 co-localization was detected in the IF and medial PN (**Figures 3A10–A12**); the subnuclei that are most positive for TrpV1 mRNA.

Having identified that the majority of TrpV1$^+$ VTA neurons are positive for the two mRNAs that encode the vesicular transporters essential for the DA-GLU phenotype (VMAT2 and VGLUT2), the hypothesized DA-GLU identity was histologically confirmed. Next, to further define the molecular fingerprint of TrpV1$^+$ VTA neurons, additional markers were addressed using CISH and FISH analysis at P3. NeuroD6 and Grp have been identified as molecular markers for medially distributed DA neurons (Chung et al., 2005; Greene et al., 2005; Viereckel et al., 2016; Khan et al., 2017; Kramer et al., 2018; Bimpisidis et al., 2019). Here, it was of interest to find out if TrpV1$^+$ VTA neurons form a subgroup within any of these recently described subtypes, or if TrpV1$^+$ VTA neurons form a distinct subpopulation.

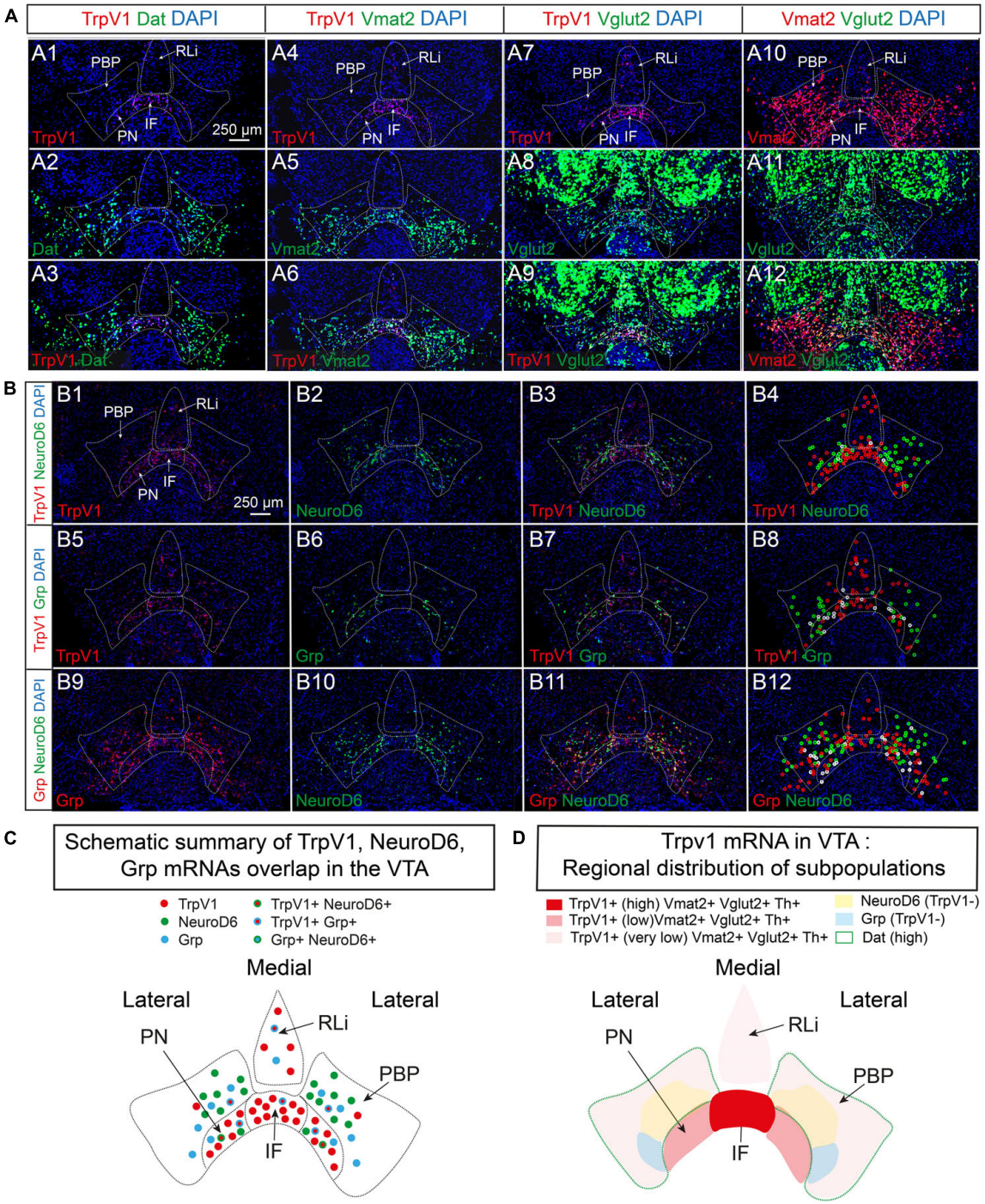

FIGURE 3 | TrpV1 mRNA forms a unique distribution pattern in the medial VTA and co-localizes strongly with Vmat2 but not with Dat, NeuroD6, or Grp mRNAs. **(A,B)** Fluorescent *in situ* hybridization (FISH) was analyzed in coronal VTA sections at postnatal day 3 (P3). DAPI is used for the detection of cell nuclei. **(A)** Left panel: TrpV1 **(A1)**, Dat **(A2)**, TrpV1/Dat **(A3)**. A left-middle panel: TrpV1 **(A4)**, Vmat2 **(A5)**, and TrpV1/Vmat2 **(A6)**. A right-middle panel: TrpV1 **(A7)**, Vglut2 **(A8)**, and TrpV1/Vglut2 **(A9)**. A right panel: Vmat2 **(A10)**, Vglut2 **(A11)**, and Vmat2/Vglut2 **(A12)**. **(B)** A top panel: TrpV1 **(B1)**, NeuroD6 **(B2)**, TrpV1/NeuroD6 **(B3)**, TrpV1/NeuroD6 (**B4**, positive cells encircled). A middle panel: TrpV1 **(B5)**, Grp **(B6)**, TrpV1/Grp **(B7)**, TrpV1/Grp (**B8**, positive cells encircled). A bottom panel: Grp **(B9)**, NeuroD6 **(B10)**, Grp/NeuroD6 **(B11)**, and Grp/NeuroD6 (**B12**, positive cells encircled). Red circles label the red fluorophore, green circles label the green fluorophore, white circles label co-labeling both fluorophores. **(C)** A schematic summary of results obtained in **(B)** outlining TrpV1-positive cells and co-labeling (or its absence) TrpV1, Grp, and NeuroD6 mRNAs in the VTA. **(D)** A schematic summary of results obtained in **(A,B)**, and **Figure 1**, outlining the main distribution of areas positive for TrpV1 mRNA and co-labeling (or its absence) with Th, Vmat2, Vglut2, Dat, NeuroD6, and Grp mRNAs in the VTA. Scale bars, 250 µm. See **Table 1** for cell counting. IF, interfascicular nucleus; PN, paranigral nucleus; PBP, parabrachial pigmented nucleus; RLi, rostral linear nucleus; VTA, ventral tegmental area.

First, using CISH analysis in serial sections throughout the mesencephalic-hypothalamic area, the pattern of TrpV1 was compared to that of NeuroD6 and Grp mRNAs, using Th as reference for the VTA area (**Supplementary Figure 4**). NeuroD6 mRNA was most prominent in the PN and PBP subareas and was also found in the RM, but not more than in sparse cells, in the PHA, or the other VTA subareas (IF, RLi, and CLi). Grp mRNA was detected in the IF and PN primarily and was also detected in the lateral PBP and CLi. Grp was also detected in sparse cells in PHA and RM. Some Grp^+ cells were detected in the SNc (**Supplementary Figure 4**).

Given this distribution pattern within the VTA, it was of interest to discern if there was any co-localization between TrpV1, NeuroD6, and Grp mRNAs. With the above-shown low NeuroD6 mRNAs levels in VTA subnuclei most positive for TrpV1 mRNA, FISH analysis confirmed a low level of TrpV1/NeuroD6 co-labeling (**Figures 3B1–B4** and **Table 1**). PBP contained some TrpV1/NeuroD6 double-positive cells, corresponding to 20% of TrpV1 cells in this area. The IF and PN, both largely devoid of NeuroD6, showed less than 10% TrpV1/NeuroD6 co-labeling. Furthermore, despite the seemingly similar distribution of TrpV1 and Grp in IF and PN using CISH, analysis using FISH to enable co-localization analysis showed rather modest TrpV1/Grp co-labeling (**Figures 3B5–B8** and **Table 1**). No, or very little, co-labeling of TrpV1 with either NeuroD6 or Grp was observed in either the RLi and CLi, areas where TrpV1 did also not co-localize with Dat (**Table 1**). Furthermore, NeuroD6 and Grp were not abundantly co-detected but co-localized to some degree in the PN and PBP (**Figures 3B9–B12**). This co-labeling analysis found that TrpV1, NeuroD6, and Grp mRNAs, that, in gross single-channel CISH observation, showed a similar scattered distribution within the VTA, actually represent largely different VTA neurons, with each mRNA displayed in a unique distribution pattern (**Figures 3B1–B12**, illustrated in **3C**).

To summarize these observations of the P3 mouse brain, TrpV1 mRNA is primarily detected in the IF of the medial VTA, followed by RLi, CLi, PN, and PBP. The molecular identity of $TrpV1^+$ VTA neurons includes both DA markers Th and Vmat2 and GLU marker Vglut2, thus defining a $TrpV1^+/Th^+/Vglut2^+/Vmat2^+$ subpopulation of DA-GLU neurons. Furthermore, sparse PBP neurons show a $TrpV1^+/Th^+/Vglut2^-/Vmat2^+$ (DA) phenotype, while RLi contains ample $TrpV1^+/Th^-/Vglut2^+/Vmat2^-$ (GLU) neurons. $TrpV1^+$ neurons are generally low in Dat mRNA and are largely distinct from those positive for NeuroD6 and Grp (**Figure 3D**).

TrpV1$^+$ Neurons of the VTA and Hypothalamus Project Primarily to Limbic Brain Areas

A $TrpV1^{tm1(cre)Bbm}$ (abbreviated $TrpV1^{Cre/wt}$) transgenic mouse line drives expression of floxed alleles in the hypothalamic-mesencephalic area as demonstrated by analysis of several Cre-driven floxed reporters (Cavanaugh et al., 2011). Here, we took advantage of this validated transgene to address the projection pattern of the identified $TrpV1^+$ neuronal population. Placed into a stereotactic frame, adult $TrpV1^{Cre/wt}$ mice were unilaterally injected into the PHA/rostral VTA with an adeno-associated virus (AAV) to enable Cre-driven expression of a floxed construct, encoding the enhanced yellow fluorescent protein (eYFP) (rAAV2/EF1a-DIO-eYFP) (**Figure 4A**). To validate the injection strategy, brain sections throughout the PHA-VTA area that originated from such injected mice (here referred to as *TrpV1: EF1a-DIO-eYFP* mice) were analyzed for cellular YFP immunofluorescence. YFP^+ cell bodies were distinct, but sparse, throughout the PHA-VTA area (**Figures 4A,B**). In accordance with the histological mapping above, the densest YFP^+ cellular population was observed in the medial location, encompassing the PHA and RM of the caudal hypothalamus, and the IF and medial PN of the VTA (**Figures 4A,B**). Sparsely distributed YFP^+ cells were observed in the RLi, PBP, and lateral aspects of the PN (**Figures 4A,B**). YFP^+ cells were detected as a string-of-pearl-like band across the PHA-VTA area, similar as described in the original publication showing reporter expression driven by the same $TrpV1^{Cre/wt}$ transgene (Cavanaugh et al., 2011).

Next, YFP^+ projections and target areas were addressed throughout the brain. Multiple positive sites were identified, primarily areas associated with limbic functions. YFP^+ projections were detected within the median forebrain bundle. Several known target structures of the PHA/RM and VTA were identified as positive for YFP^+ fibers. These included mAcbSh; septal, amygdalohippocampal, and preoptic areas; fimbria, CA3, and CA1 fields of the hippocampus; endopiriform nucleus (dorsal); bed nucleus of stria terminalis (dorsolateral) (**Figures 4C1–C6',D**). Within the septal area, the medial and lateral septa, the nucleus of the vertical limb of the diagonal band, and the septal hypothalamic nucleus were identified as positive for YFP fibers. Within the preoptic areas, the medial, median, and lateral preoptic areas were identified as positive (**Figures 4C1–C6',D**). While target areas reflect projections originating from $TrpV1^+$ cells in both VTA and PHA/RM, projections to mAcbSh are likely to originate from the medial VTA, as are sparse YFP-positive projections in the infralimbic and orbital cortices (**Figures 4C1–C6',D**).

In summary, by using a *TrpV1: EF1a-DIO-eYFP* strategy with viral injection into the PHA/VTA, scattered YFP^+ cell bodies were confirmed in the IF, PN, PBP, and RLi of the VTA as well as in the PHA and RM of the caudal hypothalamus. Furthermore, projections from YFP^+ cells were identified reaching several limbic forebrain areas.

$TrpV1^{Cre}$-Driven Targeted Deletion of Vmat2 Causes Its Selective Abrogation in TrpV1$^+$ DA and TrpV1$^+$ DA-GLU Neurons

To assess if $TrpV1^+$ DA-GLU and DA neurons (defined by $TrpV1^+/Th^+/Vglut2^+/Vmat2^+$ and $TrpV1^+/Th^+/Vglut2^-/Vmat2^+$) contribute to behaviors associated with VTA DA neurons, *Vmat2* gene expression was selectively abrogated in $TrpV1^+$ neurons by the generation of a new cKO mouse line (referred to as the $TrpV1^{Cre}$; $Vmat2^{flox/flox}$ cKO mouse line). Since the VMAT2 protein is essential for packaging monoamines (including DA) into presynaptic vesicles, *Vmat2* gene-targeting will disable neurons from this mechanism, causing a disruption of DA signaling. This has previously been

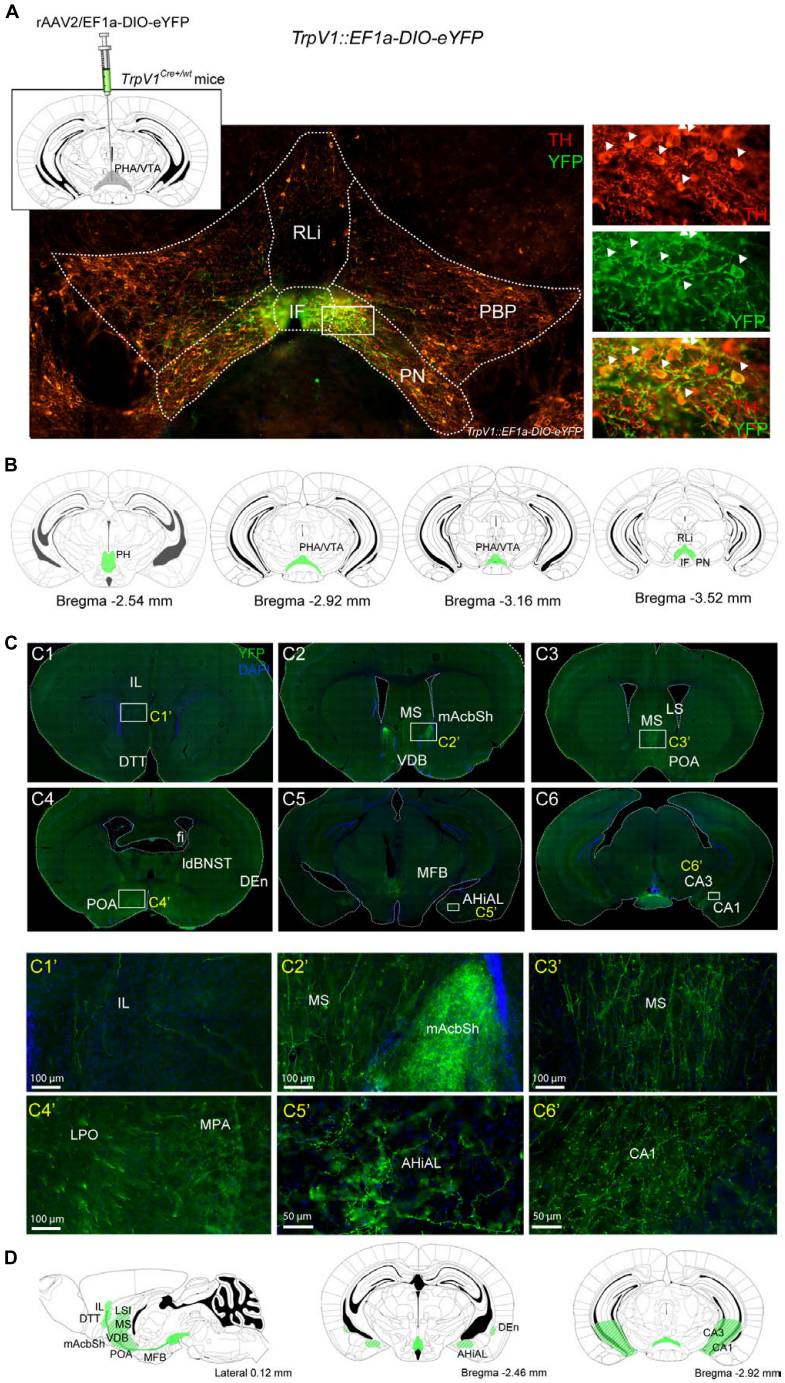

FIGURE 4 | Projections from TrpV1^{+} cells reach multiple forebrain target areas, including nucleus accumbens. **(A)** Top, left: Illustration of virus injection. *TrpV1*$^{Cre+/wt}$ mice were unilaterally injected with the AAV-EF1a-DIO-eYFP virus to reach the TrpV1-positive area in the posterior hypothalamic nucleus (PHA) and ventral tegmental area (VTA). Bottom: Verification of injection in *TrpV1::EF1a-DIO-eYFP* mice (age postinjection, 13–18 weeks). YFP (green) and TH (red) immunofluorescence in coronal vibratome slice, double-positive cells detected primarily in IF and medial PN of the VTA, close-up in the right-side panel. **(B)** Illustration of coronal sections visualizing sites identified as positive for YFP-positive cell bodies (green fields) along the rostro-caudal axis. **(C)** YFP immunofluorescence in projections reaching various target areas, representative examples are shown. **(C1'–C6')** Close up of areas shown in white squares in **(C1–C6)**. **(D)** Illustration-visualizing sites identified as positive for YFP-positive projections (green/white stripes in fields). Scale bars 100; 50 µm. AHiAL, a lateral part of the amygdalohippocampal area; CA1, field C1 of the hippocampus; CA3, field C3 of the hippocampus; DEn, dorsal endopirifom claustrum; DTT, dorsal tenia tegmental; fi, fimbria of the hippocampus; IF, interfascicular nucleus; ldBNST, a lateral dorsal part of the bed nucleus of the stria terminalis; LPO, lateral preoptic area; LS, lateral septum; MFB, medial forebrain bundle; mNAcSh, nucleus accumbens medial shell; MPA, medial preoptic area; MS, medial septum; PHA, posterior hypothalamic nucleus; PH, posterior hypothalamus; PN, paranigral nucleus of the ventral tegmental area; POA, preoptic areas; RLi, rostral linear nucleus; VDB, the nucleus of the vertical limb of the diagonal band.

demonstrated using transgenic mice in which Cre recombinase is under control of promoters directing the *Vmat2*-gene-targeting event either to distinct monoamine systems [DA *via* Dat-Cre, 5′HT *via* Sert-Cre, noradrenaline *via* Net-Cre (Narboux-Nême et al., 2011; Isingrini et al., 2016, 2017)] or to distinct VTA subpopulations [NeuroD6 *via* NeuroD6(NEX)-Cre, Calbindin2/Calretinin/Calb2 *via* Calb2-Cre (Bimpisidis et al., 2019; König et al., 2020)]. As the majority of VTA TrpV1$^+$ neurons are Vmat2$^+$ and show a dopaminergic phenotype (either as DA-GLU, defined by TrpV1$^+$/Th$^+$/Vglut2$^+$/Vmat2$^+$, or DA but not GLU, defined by TrpV1$^+$/Th$^+$/Vglut2$^-$/Vmat2$^+$), the knockout of the *Vmat2* gene selectively in TrpV1$^+$ neurons will allow assessment of behaviors disturbed by this perturbation of dopaminergic function. Notably, TrpV1-negative Vmat2$^+$ monoamine neurons throughout the brain should remain unaffected, as should Vmat2-negative TrpV1$^+$ GLU neurons (TrpV1$^+$/Th$^-$/Vglut2$^+$/Vmat2$^-$).

By breeding *TrpV1*$^{Cre/wt}$ mice with *Vmat2*$^{flox/flox}$ mice in which *exon 2* of the *Vmat2* gene is surrounded by *LoxP* sites (Narboux-Nême et al., 2011), *TrpV1*$^{Cre+/wt}$*; Vmat2*$^{flox/flox}$ (cKO) mice and *TrpV1*$^{Cre-/wt}$*; Vmat2*$^{flox/flox}$ (control) mice were generated as littermates in the *TrpV1*^{Cre}*; Vmat2*$^{flox/flox}$ cKO mouse line. All mice were genotyped by PCR. To confirm the *Vmat2*-targeting event, a two-probe strategy was implemented to allow the distinction of Vmat2 full-length mRNA from that of truncated Vmat2 mRNA due to the conditional gene targeting (**Figure 5A**). Using this strategy, wild-type Vmat2 mRNA (full length) should be detected by binding of two probes (Probe 2 binding to mRNA derived from *Vmat2 gene exon 2*, Probe 6-15 binding to mRNA derived from *Vmat2 gene exons 6-15*). In contrast, Vmat2 cKO mRNA, containing a truncated mRNA due to the targeted deletion of *Vmat2 exon 2*, should fail to bind Probe 2 and, instead, only bind Probe 6-15. In CISH/FISH analysis, binding of both probes will result in a purple/green color precipitate (Vmat2 wild-type mRNA) while binding of only Probe 6-15 will display as fluorescent green color (Vmat2 cKO mRNA) (**Figure 5A**). Green-only cells thus define the Vmat2 cKO phenotype, and purple/green cells define Vmat2 undisturbed by the targeting event, i.e., wild-type Vmat2 mRNA.

Upon implementing the two-probe strategy in brain sections from adult mice genotyped as control and cKO mice, control mice showed the expected normal distribution of wild-type Vmat2 mRNA labeling (co-localization of both Vmat2 probes) in all monoaminergic brain areas, including VTA and SNc (**Figures 5B1–B3** and **Supplementary Figure 5**).

When addressing cKO mice, it was clear that all monoaminergic systems (including raphe nuclei and noradrenergic, as well as adrenergic cells) outside the VTA and adjacent A8 area were positive for both Vmat2 probes, showing a Vmat2 wild-type phenotype (**Supplementary Table 1**). However, distributed within VTA subnuclei was a clear density of cells positive only for Vmat2 Probe 6-15, thereby identifying Vmat2 cKO cells (**Figures 5B4–B6**).

Analysis of serial sections throughout the midbrain showed that the distribution of Vmat2 cKO cells was similar to the described distribution of TrpV1 mRNA with a higher density medially. In the IF, 92% of all Vmat2 mRNA was represented by binding the Vmat2 Probe 6-15 only, thus representing cKO cells, while the remaining 8% were detected by both Vmat2 probes. The Vmat2 cKO phenotype is thereby nearly complete in the IF subnucleus of the VTA. Furthermore, 46% of all Vmat2 cKO cells were found in the IF (**Figure 5C** and **Supplementary Table 1**). Thus, in accordance with the highest abundance of TrpV1$^+$ neurons of the dopaminergic phenotype (Th, Vmat2) in the IF subnucleus, most Vmat2 cKO cells were found here. Other subnuclei showed a variable density of Vmat2 cKO cells, in accordance with the level of TrpV1, Vmat2, and their co-localization. For example, PBP, which is strongly positive for Vmat2 but sparse for TrpV1, contained 7% Vmat2 cKO cells, while PN, which is positive for both Vmat2 and TrpV1 (but to a lesser degree than IF), contained 43% cKO cells. About 16% of all Vmat2 cKO cells were found in the PN. The linear nuclei (RLi and CLi) represented a smaller proportion of cKO cells, in accordance with the lower abundance of co-localization of Vmat2 and TrpV1 (**Figure 5C** and **Supplementary Table 1**).

Following through with triple-probe FISH analysis using the Vmat2 Probe 2 and Vmat2 Probe 6-15 in combination with the Th probe, most VTA Vmat2 neurons (both wild-type and cKO neurons in the cKO mice) were positive for Th mRNA, supporting a dopaminergic phenotype of *Vmat2*-gene-targeted cells (**Supplementary Figure 5**). Furthermore, to find out more about the timing of the onset of TrpV1^{Cre}-driven *Vmat2* gene targeting, E15.5 control, and cKO embryos were addressed. Sparse but distinct Vmat2 cKO cells were detected at E15.5 (**Supplementary Figure 5**), demonstrating the onset of *Vmat2* gene targeting during embryogenesis.

Finally, TH immunoreactivity was assessed in adult mice to validate the histological integrity of the midbrain DA system in the absence of normal levels of Vmat2 mRNA from development onwards in TrpV1$^+$ VTA neurons. No difference between control and cKO mice could be detected either within the VTA or any of the projection target areas of VTA neurons. Furthermore, no difference between genotypes was observed in the SNc or any other monoaminergic (VMAT2$^+$) system as detected by TH immunoreactivity, including the locus coeruleus and dorsal raphe. Thus, the gross anatomy of the DA system as detected histologically by TH immunohistochemistry remained intact despite the abrogation of *Vmat2* gene expression in TrpV1$^+$ VTA neurons (**Figure 6**).

In summary, by generating a new cKO mouse line in which the *Vmat2* gene is conditionally targeted in *TrpV1*^{Cre}-positive neurons, all VTA subnuclei contain a certain proportion of Th$^+$ neurons that lack normal *Vmat2* gene expression levels. By far, the highest proportion of these cKO cells is medially located and primarily distributed within the IF. Next, behavioral assessments were carried out to determine if this genetic manipulation caused any measurable deficits in behavioral capacity.

TrpV1$^{Cre+/wt}$*; Vmat2*$^{flox/flox}$ Conditional Knockout Mice Show No or Modest Behavioral Alteration in the Open Field and Elevated Plus Maze Paradigms

By observation of the mice in their home-cage environment, there was no apparent difference between *TrpV1*$^{Cre-/wt}$*; Vmat2*$^{flox/flox}$ control and *TrpV1*$^{Cre+/wt}$*;Vmat2*$^{flox/flox}$ cKO mice

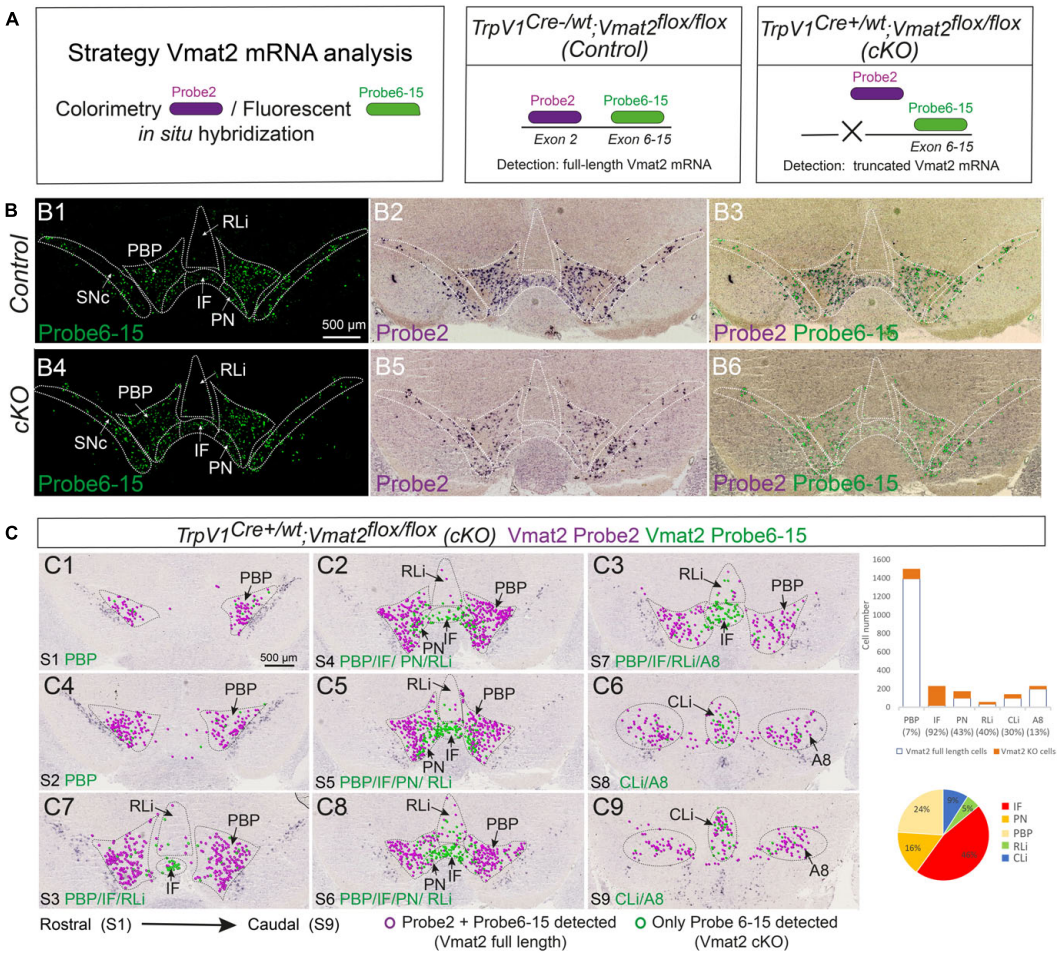

FIGURE 5 | *TrpV1*$^{Cre+/wt}$;*Vmat2*$^{flox/flox}$ cKO mice show substantial deletion of full-length Vmat2 mRNA in the medial VTA. Analysis of age-matched *TrpV1*$^{Cre-/wt}$;*Vmat2*$^{flox/flox}$ control and *TrpV1*$^{Cre+/wt}$;*Vmat2*$^{flox/flox}$ cKO adult mice (12 weeks old). **(A)** Schematic illustration of the Vmat2-two-probe approach used to distinguish the full-length wild-type Vmat2 mRNA (binding Probe 2 and Probe 6–15) from the abrogated Vmat2 mRNA (binding only Probe 6–15) generated in *TrpV1*$^{Cre+/wt}$;*Vmat2*$^{flox/flox}$ cKO mice. **(B)** Vmat2-two-probe approach implemented on VTA brain sections from *TrpV1*$^{Cre-/wt}$;*Vmat2*$^{flox/flox}$ control (Control, a top panel) and *TrpV1*$^{Cre+/wt}$;*Vmat2*$^{flox/flox}$ (cKO, a bottom panel) mice: Vmat2 Probe 2 **(B1,B4)**; Vmat2 Probe 2 combined with Probe 6–15 **(B2,B5)**; same image with colored circles indicating labeled cells **(B3,B6)**. **(C)** Serial sections throughout the VTA area [**C1–C9**, rostral (Section Level 1, S1)] to caudal (Section Level 9, S9) of representative cKO mouse brain for a full assessment of cells positive for wild-type Vmat2 (Probe 2 and Probe 6–15) mRNA and cKOVmat2 mRNA (Probe 6–15 only) as detected by the Vmat2 two-probe approach; the result of cell counting shown in a bar graph (% cells positive for Vmat2 Probe 6–15 in each VTA subnucleus indicated in legend) and a pie chart (distribution of Vmat2cKO cells throughout VTA subnuclei). *N* = 3 mice per genotype and detection, serial sections throughout the brain. Green circles, Vmat2 cKO cells; purple circles, Vmat2 wild-type cells. Scale bars, 500 µm. See **Supplementary Figure 5** and **Supplementary Table 1** for more details. A8, A8 dopamine area; cKO, conditional knockout; IF, interfascicular nucleus; PBP, parabrachial pigmented nucleus; PN, paranigral nucleus; RLi, rostral linear nucleus; SNc, substantia nigra *pars compacta*; VTA, ventral tegmental area.

in the way they moved around, interacted, or fed. Thus, caretaker inspection revealed no difference between control and cKO mice. Throughout subsequent analyses, age-matched control and cKO mice of two age groups [Young adult (YA) mice, 8 weeks of age, and mature adult (MA) mice, 18 weeks of age, at the start of behavioral analyses] were assessed to determine if any age-related progression in the behavioral display could be detected (**Supplementary File 1**; statistical details of all behavior analyses). First, regular weight measures confirmed that control and cKO mice increased their body weight at a similar rate throughout their first weeks (**Supplementary Figure 6**). At 8 and 18 weeks of age (when behavior experiments started), there was no difference in weights between genotypes of either age group (**Figures 7A,B**).

To ascertain basal locomotor and exploratory activities, mice were analyzed in the open field test. Multiple parameters relevant to vertical and horizontal movement, exploratory visits to different areas in the open field chamber, and bodily arrangements, such as self-grooming, contraction, and sniffing, were analyzed (**Figures 7C,E,G,I** and **Supplementary Figure 7**). No major difference in either of these behaviors was detected in either YA (**Figures 7C–F** and **Supplementary Figure 7**) or MA (**Figures 7D,F,H,J** and **Supplementary Figure 7**) cKO mice compared with control mice. However, while locomotor

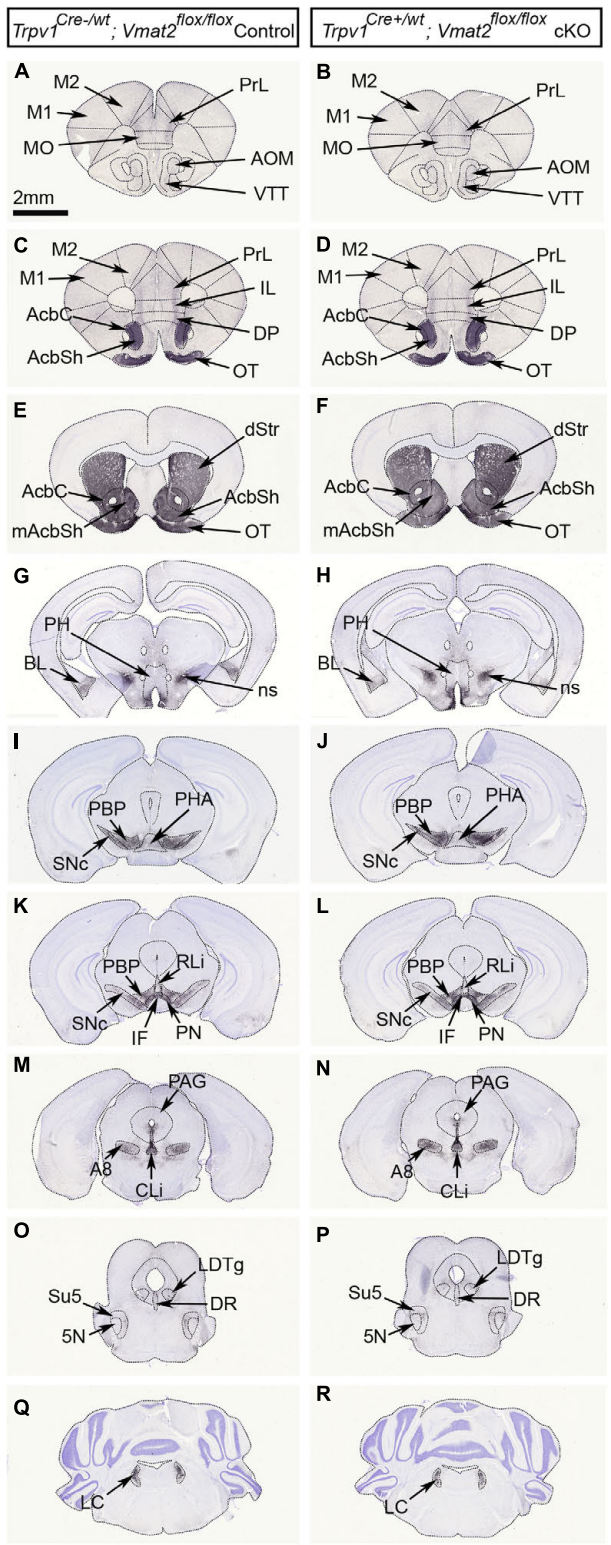

FIGURE 6 | Gross anatomical evaluation reveals intact monoaminergic neurons in *TrpV1*$^{Cre+/wt}$;*Vmat2*$^{flox/flox}$ *cKO mice.* Analysis of age-matched *TrpV1*$^{Cre-/wt}$;*Vmat2*$^{flox/flox}$ control and *TrpV1*$^{Cre+/wt}$;*Vmat2*$^{flox/flox}$ cKO adult mice (24 weeks). Coronal serial brain sections showing the distribution of *(Continued)*

FIGURE 6 | (Continued)
tyrosine hydroxylase (TH) immunoreactivity in the midbrain dopamine system; midbrain (VTA subnuclei and SNc) and its target areas in *TrpV1*$^{Cre-/wt}$;*Vmat2*$^{flox/flox}$ control **(A,C,E,G,I,K,M,O,Q)** and *TrpV1*$^{Cre+/wt}$;*Vmat2*$^{flox/flox}$ cKO **(B,D,F,H,J,L,N,P,R)** mice. Also shown are additional monoamine populations, including the LC and DR. 5N, motor trigeminal nucleus; A8, A8 dopamine cells of the retrorubral field; AcbC, nucleus accumbens core; AcbSh, nucleus accumbens shell; AOM, anterior olfactory area medial part; BL, basolateral amygdaloid nucleus; CLi, caudal linear nucleus; DP, dorsal peduncular cortex; DR, dorsal raphe nucleus; dStr, dorsal striatum; IF, interfascicular nucleus; IL, infralimbic cortex; LC, locus coeruleus; LDTg, laterodorsal tegmental nucleus; M1, primary motor cortex; M2, secondary motor cortex; mAcbSh, medial accumbens shell; MO, medial orbital cortex; ns, nigrostriatal tract; OT, olfactory tubercle; PAG, periaqueductal gray; PBP, parabrachial pigmented nucleus; PH, posterior hypothalamus; PHA, posterior hypothalamus nucleus; PN, paranigral nucleus; PrL, prelimbic cortex; RLi, rostral linear nucleus; SNc, substantia nigra *pars compacta*; Su5, supratrigeminal nucleus; VTA, ventral tegmental area; VTT, ventral tenia tecta.

parameters (distance moved and rearing) were similar between cKO and control mice of both age groups (**Figures 7C–F**), there was a difference in the time spent in the center of the arena in the MA, but not YA, age group (**Figures 7G,H**). MA cKO mice spent significantly less time in the center than their corresponding control group, showing a profile that more looked like YA control and cKO mice than MA control mice. Also sniffing was different between the genotype groups, but only in the MA age group (**Figures 7I,J**). Overall, MA control mice showed increased time in the center and decreased their sniffing compared with MA cKO mice, but this difference was not shown in the YA group (**Figures 7G,J**).

To ascertain if these observations were correlated with anxiety, mice were analyzed in the elevated plus maze (EPM). This maze consists of four arms elevated from the floor, two arms sheltered (closed), and two arms open. Generally, mice explore the whole maze but prefer the sheltered areas and avoid the open arms. An anxious phenotype is defined by a heightened stay in the closed arms due to avoidance of the open arms, while an anxiolytic phenotype shows an increased preference for the open arms and increased number of visits around the arena. Comparing cKO and control mice, no difference in their behavior in the EPM was observed (**Figures 7K–N** and **Supplementary Figure 7**). All mice spent significantly more time in the closed than open arms (**Figures 7K,L**). There was no difference between cKO and control mice at any age. Mice also moved around the maze at a similar amount, with no significant differences in visits to any arena between genotype groups at any age (**Figures 7M,N**). Thus, no genotype-dependent display of anxiety (avoidance or preference phenotype) was confirmed in the EPM. Instead, among ample parameters analyzed, increased sniffing and reduced explorations manifested by mature cKO mice in the open field were the only differences detected between cKO and control mice.

In summary, quantified behavioral data in the open field and EPM paradigms along with caretakers observations demonstrate that *TrpV1*$^{Cre+/wt}$;*Vmat2*$^{flox/flox}$ cKO mice are largely indistinguishable from control mice, regardless of age.

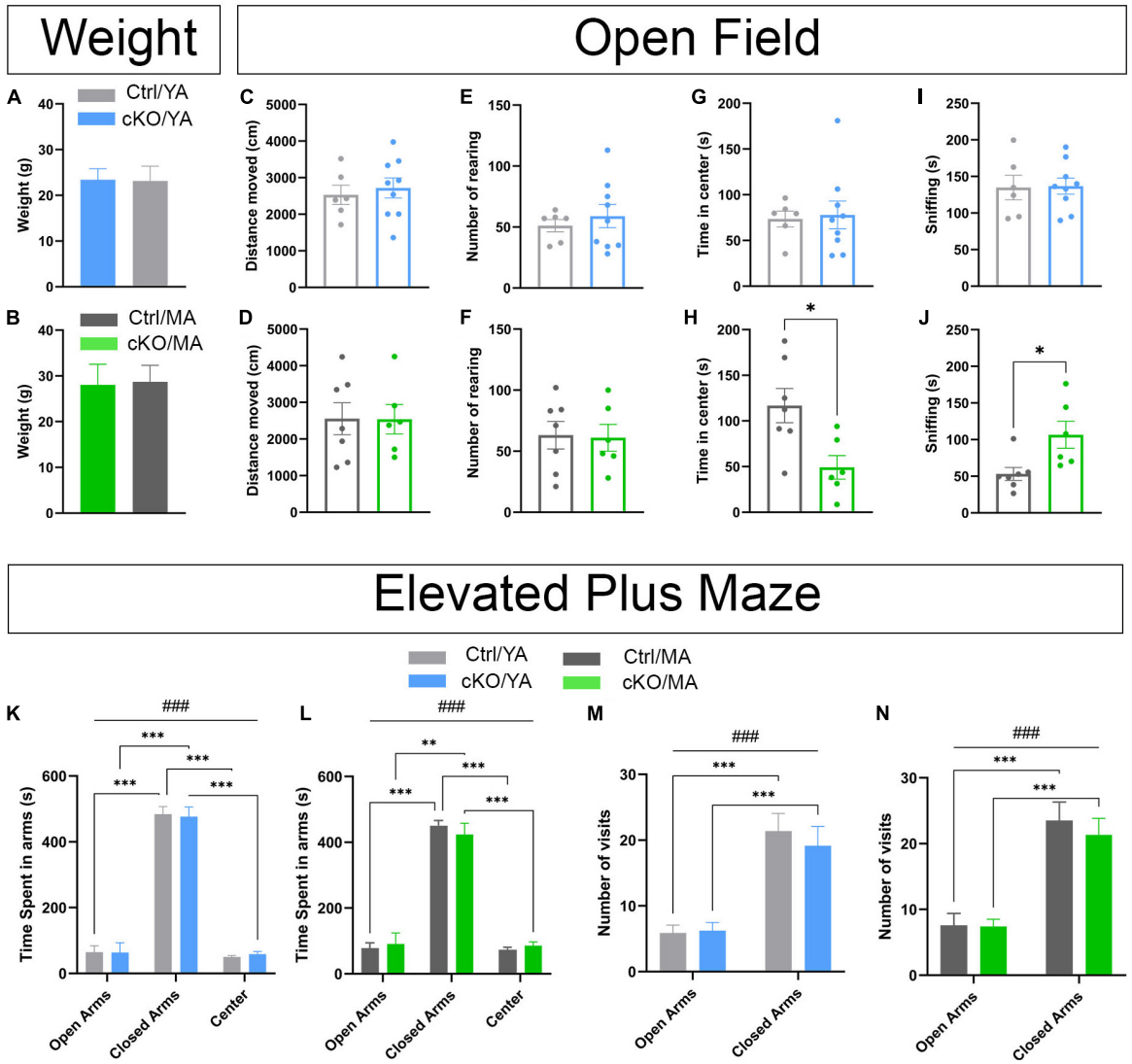

FIGURE 7 | No or modest genotype-dependent alterations in basal behavior were displayed by *TrpV1*$^{Cre+/wt}$;*Vmat2*$^{flox/flox}$ cKO mice. Analysis and comparison of age-matched *TrpV1*$^{Cre-/wt}$;*Vmat2*$^{flox/flox}$ *control (Ctrl)* and *TrpV1*$^{Cre+/wt}$;*Vmat2*$^{flox/flox}$ conditional knockout (cKO) mice at young adult (YA; 8 weeks old) and mature adult (MA; 18 weeks old) age. **(A,B)** Weight at the beginning of an amphetamine sensitization paradigm (**A**, YA; **B**, MA). **(C–J)** An open field test. Ctrl/YA (N = 6) and cKO/YA (N = 9), Ctrl/MA (N = 7), and cKO/MA (N = 6) data are expressed as mean ± SEM. **(C)** distance-moved YA. **(D)** distance-moved MA. **(E)** Number of rearing YA. **(F)** Number of rearing MA. **(G)** Time spent in center YA. **(H)** Time spent in center MA (*p = .0154, Ctrl/MA vs. cKO/MA). **(I)** sniffing YA. **(J)** sniffing MA (*p = 0.0193, Ctrl/MA vs. cKO/MA). **(K–N)** Elevated plus maze (EPM). Ctrl/YA (N = 8) and cKO/YA (N = 13), Ctrl/MA (N = 11) and cKO/MA (N = 12), data are expressed as mean ± SEM. **(K)** time spent in arms YA (###p < 0.001, arms effect; ***p < 0.001, Closed Arms vs. Open Arms and Center). **(L)** Time spent in arms MA (###p < 0.001, arms effect; ***p < 0.001, Closed Arms vs. Open Arms and Center; **p = 0.001, Closed Arms vs. Open Arms). **(M)** Number of visits in arms YA (###p < 0.001, arms effect; ***p < 0.001, Closed Arms vs. Open Arms). **(N)** Number of visits in arms MA (###p < 0.001, arms effect; ***p < 0.001, Closed Arms vs. Open Arms).

An Amphetamine Sensitization Paradigm Reveals a "Pre-sensitized" Phenotype of *TrpV1*$^{Cre+/wt}$;*Vmat2*$^{flox/flox}$ Conditional Knockout Mice

VTA DA neurons have long been associated with many different aspects of reward processing correlated with DA release in limbic and cognitive forebrain target areas (Berridge and Robinson, 1998; Di Chiara, 1998; Salamone and Correa, 2012; Schultz, 2016). For example, DA release is a critical aspect of psychostimulant response and can be detected as increased locomotion, often referred to as psychomotor behavior. The concept of behavioral sensitization refers to a progressively greater and enduring behavioral response (including locomotion) that occurs following repeated stimulant administration. This phenomenon has been hypothesized to underlie aspects of human stimulant addiction, as well as several psychiatric conditions (Robinson and Becker, 1986; Robinson, 1993).

Lately, also the DA-GLU phenotype of VTA neurons has been associated with psychostimulant-induced responses, with similar implications for addiction and psychiatric conditions (reviewed in Mingote et al., 2017; Morales and Margolis, 2017; Bimpisidis and Wallén-Mackenzie, 2019; Eskenazi et al., 2021). To determine if targeted deletion of VMAT2 selectively in TrpV1^{+} VTA neurons had any consequence for a psychostimulant response, drug-induced locomotor effects were analyzed using an amphetamine sensitization paradigm.

The sensitization protocol lasted 17 days, during which a saline injection was given on Day1, followed by one injection per day of 3-mg/kg amphetamine during 4 days (Days 2, 3, 4, and 5), and a challenging day in which the mice received a last amphetamine injection (Day 17) (**Figure 8A**). Baseline locomotion was measured on Day 1, prior to the saline injection. No difference between cKO and control mice was observed in either young adult (YA) or mature adult (MA) groups (**Figures 8B,C**). Furthermore, no sex differences were observed (**Supplementary File 1**). For all analyses, mice were, therefore, pooled according to genotype (control and cKO) and age (YA and MA).

Upon administration of amphetamine, mice commonly show significantly heightened locomotion (hyperlocomotion) above baseline levels that last for 60–90 min, with a peak around 30–40 min. Such hyperlocomotion was observed. All control mice responded with hyperlocomotion (**Figures 8D,E**). In both YA and MA control mice, this hyperlocomotion increased progressively and was significantly stronger on each subsequent injection day, an index of sensitization toward the psychostimulant (**Figures 8D,E**). Curiously, *TrpV1*$^{Cre+/wt}$;*Vmat2*$^{flox/flox}$ cKO mice showed a different response profile to the drug (**Figures 8F,G**). Both YA and MA cKO mice did, indeed, show strong hyperlocomotion on Day 2, the first day of amphetamine injection (**Figures 8F,G**). However, they failed to progressively increase their locomotor response across sessions. This led to a lack of significant difference between Day 2 and Day 5, and also between Day 2 and Day 17, despite repeated exposure to the stimulus. This difference was observed in both the YA and MA cKO groups, demonstrating an absence of the normally observed behavioral sensitization.

When comparing responses between genotype groups (control *vs* cKO), significant differences were evident when amphetamine, but not saline, was administered (**Figures 8H,I**). Saline injection (Day 1) induced no differences in locomotion between cKO and control mice in any age group. In response to amphetamine, MA cKO mice increased their locomotion above control mice on both Day 2 and Day 3. On Day 2, a tendency for a higher effect on cKO compared with control mice was observed also in the YA group. Thus, cKO mice showed accentuated hyperlocomotion above the level of control mice. For this reason, further analysis was motivated. The locomotor response was assessed by dividing each amphetamine session into 10-min periods (**Figures 8J–M** and **Supplementary Figures 8A–F**). The statistical analysis supported the observation of heightened hyperlocomotor response in the cKO groups by showing a genotype effect on Day 2 for both the YA and MA groups (**Figures 8J,K**). On Day 3, a difference was observed only in MA mice (**Figures 8L,M**). Upon subsequent injections (Days 4, 5, and 17), both YA and MA cKO mice still achieved hyperlocomotion in response to amphetamine, but the response was similar to that observed in control mice (**Figures 8H,I** and **Supplementary Figures 8A–F**).

The accentuated hyperlocomotion displayed by the two cKO groups was thereby observed in the initial (acute) phase of the sensitization paradigm but did not progress further. This initially strong amphetamine-induced behavioral response suggests a "pre-sensitized" phenotype caused by the absence of normal *Vmat2* gene expression levels in selected VTA neurons. cKO mice thus show immediately enhanced hyperlocomotion that control mice reach only after repeated stimuli. The strong initial increase upon a first injection followed by a blunted response curve demonstrates a lack of regular sensitization to amphetamine but suggests an enhanced sensitivity to the drug. Finally, the effect was more pronounced in mature than young cKO mice, suggesting a progression in a phenotype with age.

DISCUSSION

Major attention has been directed at the role of the TRPV1 channel in the sensory processing of heat, pain, and body temperature, as well as its responsivity to various ligands, such as capsaicin and cannabinoids (Caterina et al., 1997; Szallasi et al., 2007). However, the presence of TRPV1 in the brain has been debated due to the difficulty in pinpointing its detection (Cavanaugh et al., 2011; Ramírez-Barrantes et al., 2016). Here, we present a series of findings that allow us to classify a distinct VTA neuron subtype according to its expression of the *TrpV1* gene. Furthermore, by abrogation of vesicular DA packaging *via* selective targeting of VMAT2 in TrpV1^{+} neurons, we identify a role in mediating the behavioral response to the psychostimulant amphetamine, a substance often clinically prescribed to alleviate symptoms in ADHD but which is also used/misused and can cause addiction.

The VTA is a heterogeneous brain area in which subtypes/subpopulations of neurons today can be distinguished by molecular fingerprints. This advancement is based on recent efforts using microarray and transcriptomics-based methodology which allows for dissociation of neurons beyond neurotransmitter identity (reviewed in Poulin et al., 2020). Here, we demonstrate that expression of the *TrpV1* gene, which we previously detected as elevated in the VTA over SNc in the newborn mouse (Viereckel et al., 2016), represents a distinct marker for certain VTA subpopulations, primarily one that defines DA-GLU neurons positioned close to the midline. Histological mapping across the rostro-caudal axis of the VTA in newborn mice allowed the identification of three classes of neurons that, based on the presence of TrpV1 mRNA, can be defined according to: 1) One main *DA-GLU subpopulation* distinguished by a TrpV1^{+}/Th^{+}/Vglut2^{+}/Vmat2^{+} phenotype, strongly located to the medial VTA (e.g., 49% of TrpV1^{+} VTA cells are in the IF); 2) one small *DA subpopulation* defined by a TrpV1^{+}/Th^{+}/Vglut2^{-}/Vmat2^{+} phenotype present primarily

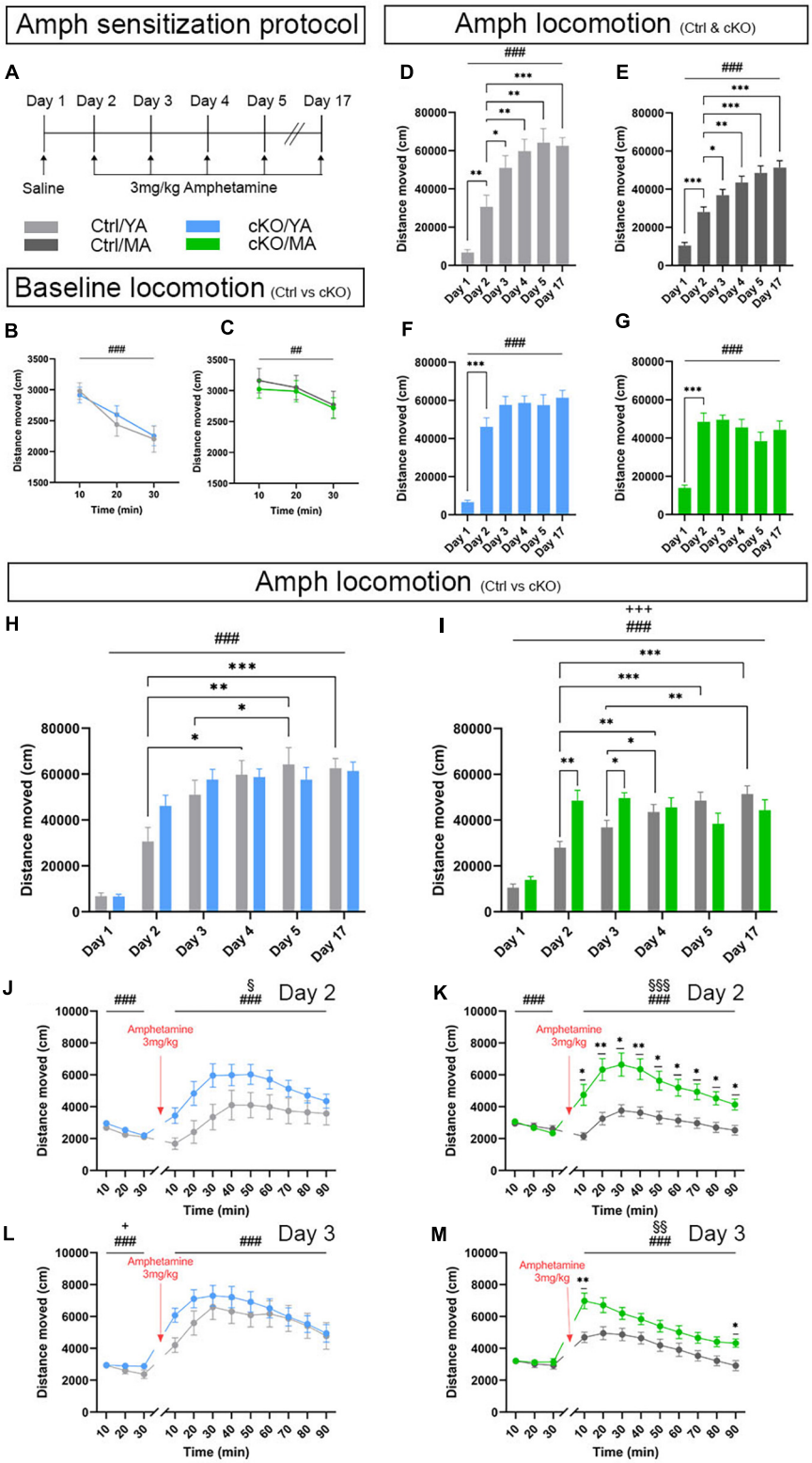

FIGURE 8 | An amphetamine sensitization paradigm identifies altered locomotor response displayed by *TrpV1*$^{Cre+/wt}$;*Vmat2*$^{flox/flox}$cKO mice. Analysis and comparison of age-matched *TrpV1*$^{Cre-/wt}$;*Vmat2*$^{flox/flox}$control (Ctrl) and *TrpV1*$^{Cre+/wt}$;*Vmat2*$^{flox/flox}$ conditional knockout (cKO) mice at young adult (YA; 8 weeks old) and mature adult (MA; 18 weeks old) age. **(A)** Amphetamine sensitization protocol. **(B,C)** Locomotor activity during 30 min that preceded saline injection. **(B)** Ctrl/YA (N = 14) and cKO/YA (N = 22). Data expressed as mean ± SEM (###p < 0.001, time effect). **(C)** Ctrl/MA (N = 18) and cKO/MA (N = 18). Data expressed

(Continued)

FIGURE 8 | (Continued)
as mean ± SEM (##p = 0.02, time effect). **(D–M)** Amphetamine-induced locomotion, 90 min following amphetamine injection; Ctrl/YA (N = 22) and cKO/YA mice (N = 22). Ctrl/MA (N = 18) and cKO/MA mice (N = 18). **(D)** Distance moved presented as mean ± SEM for each session Ctrl/YA (###p < 0.001, day effect; **p = 0.003, Day 2 vs. Day 1; *p = 0.047, Day 2 vs. Day 3; **p = 0.008, Day 2 vs. Day 4; **p = 0.002, Day 2 vs. Day 5; ***p < 0.001, Day 2 vs. Day 17). **(E)** Distance moved presented as mean ± SEM for each session Ctrl/MA (###p < 0.001, day effect; ***p < 0.001, Day 2 vs. Day 1; *p = 0.028, Day 2 vs. Day 3; **p = 0.002, Day 2 vs. Day 4; ***p < 0.001, Day 2 vs. Day 5; ***p < 0.001, Day 2 vs. Day 17). **(F)** Distance moved presented as mean ± SEM for each session cKO/YA (###p < 0.001, day effect; ***p < 0.001, Day 2 vs. Day 1). **(G)** Distance moved presented as mean ± SEM for each session cKO/MA (###p < 0.001, day effect; ***p < 0.001, Day 2 vs. Day 1). **(H)** Distance moved presented as mean ± SEM for each session, Ctrl/YA vs. cKO/YA (###p < 0.001, day effect; *p = 0.027, Ctrl/YA Day 2 vs. Day 4; **p = 0.006, Ctrl/YA Day 2 vs. Day 5; **p = 0.016, Ctrl/YA Day 3 vs. Day 5; ***p < 0.001, Ctrl/YA Day 2 vs. Day 17). **(I)** Distance moved presented as mean ± SEM for each session, Ctrl/MA vs. cKO/MA (###p < 0.001, day effect; +++p < 0.001, day × genotype effect; **p = 0.003, Day 2 Ctrl/MA vs. cKO/MA; *p = 0.017, Day 3 Ctrl/MA vs. cKO/MA; **p = 0.007, Ctrl/MA Day 2 vs. Day 4; ***p < 0.001, Ctrl/MA Day 2 vs. Day 5; ***p < 0.001, Ctrl/MA Day 2 vs. Day 17; *p = .03, Ctrl/MA Day 3 vs. Day 4; **p = 0.001, Ctrl/MA Day 3 vs. Day 4). **(J)** Amphetamine-induced locomotion on Day 2, YA. Distance moved presented as mean ± SEM for each 10-min period (###p < 0.001, time effect; §p = 0.049, genotype effect). **(K)** Amphetamine-induced locomotion on Day 2, MA. Distance moved presented as mean ± SEM for each 10-min period (###p < 0.001, time effect; §§§p < 0.001, genotype effect; *p < 0.05, Ctrl/MA vs. cKO/MA; **p < 0.01, Ctrl/MA vs. cKO/MA). **(L)** Amphetamine-induced locomotion on Day 3, YA. Distance moved presented as mean ± SEM for each 10-min period (###p < 0.001, time effect). **(M)** Amphetamine-induced locomotion on Day 3, MA. Distance moved presented as mean ± SEM for each 10-min period (###p < 0.001, time effect; §§p = 0.002, genotype effect; *p < 0.05, Ctrl/MA vs. cKO/MA; **p < 0.01, Ctrl/MA vs. cKO/MA).

in the PBP; and 3) one small *GLU subpopulation* defined by a TrpV1$^+$/Th$^-$/Vglut2$^+$/Vmat2$^-$phenotype present in the RLi at the border to, and continuing into, the PHA and RM. DA-GLU neurons located in the IF are largely positive for TrpV1 mRNA (85%), while other more rarely occurring DA-GLU neurons, for example, in the laterally positioned SNc, are TrpV1-negative. Thus, TrpV1 mRNA distinguishes a medial subpopulation of DA-GLU neurons.

Further defining the molecular properties of the TrpV1$^+$ phenotype, we can conclude that it is largely distinct from VTA DA subpopulations defined by NeuroD6 or Grp, described in several recent reports (Viereckel et al., 2016; Khan et al., 2017; Kramer et al., 2018; Bimpisidis et al., 2019). Both NeuroD6 and Grp mRNAs show a similar level of scattered distribution within the VTA as TrpV1. However, by implementing fluorescent co-localization analysis throughout the VTA, a non-overlapping distribution could be revealed. The medial position of TrpV1$^+$ VTA neurons is further emphasized by their low level of Dat mRNA, a property primarily of lateral midbrain DA neurons, as well as by the altered locomotor response to amphetamine of mice gene targeted for *Vmat2* in TrpV1$^+$ VTA neurons (further discussed below).

Parallel to the specific spatial distribution and molecular identity of TrpV1$^+$ neurons, a striking temporal regulation of TrpV1 is revealed in the mouse brain. TrpV1 mRNA is detected at E14.5 and P3, while almost no TrpV1 mRNA can be detected 9 days later (P12), yet alone in adulthood. A previous study showed its absence at E11.5 and earlier, the time point when DA neurons start differentiating and express both *Th* and *Vglut2* genes (Dumas and Wallén-Mackenzie, 2019). Together, these results demonstrate a temporal curve, with a TrpV1 peak in the developing VTA around E14.5-P3. Lower TrpV1 mRNA levels in adolescent and adult mice than in perinatal mice likely are correlated with the reported difficulties with detection in adult rodents, as discussed in several studies (see references in Cavanaugh et al., 2011; Ramírez-Barrantes et al., 2016). Furthermore, low detection levels in adult mice might contribute to an underestimate of the presence of TrpV1 mRNA in the mouse brain. Temporal regulation of gene expression is a common feature, not unique to *TrpV1*. It follows that histological features defined by addressing multiple gene expression patterns in the brain of newborn mice might not show the same co-localization patterns at any other age but represent snap shots of the given time point. However, the temporal regulation is of particular interest from a functional point of view, tentatively supporting the idea of a role for TRPV1 in the perinatal function of the midbrain-forebrain area that should be of interest to future study. While not addressing any such role for the TRPV1 protein here, pharmacological studies have already shown that neuronal excitability across the brain, including in DA neurons, is affected upon treatment with TRPV1 ligands, arguing for its presence and function in the brain (Marinelli et al., 2003, 2005, 2007). With the current identification of *TrpV1* gene expression in a restricted set of VTA neurons, functional approaches should be of particular interest to pursue, not least considering the abundance of pharmacological substances available to manipulate the TRPV1 channel.

Despite temporal regulation of the *TrpV1* gene and any reported difficulties with detection of its transcribed and translated products in adulthood, adult *TrpV1*$^{Cre/wt}$ transgenic mice can be used to study the mature brain. This was shown already in the original publication (Cavanaugh et al., 2011) and reinforced here. By implementing viral-genetic mapping of projection patterns, a series of limbic structures could be reliably identified as targets of *TrpV1*$^{Cre/wt}$ VTA/PHA neurons, including septal, hippocampal, and accumbal structures. These likely reflect the sum of projections originating from *TrpV1*$^{Cre/wt}$-positive neurons of both the VTA and posterior hypothalamus, thus neurons of DA, GLU, and DA-GLU neurotransmitter phenotype. Using this same strain of *TrpV1*$^{Cre/wt}$mice, direct focus on TrpV1$^+$ VTA neurons of the dopaminergic phenotype (DA and DA-GLU) was purposefully enabled by taking advantage of a Vmat2 cKO approach. A new mouse line produced, *TrpV1*$^{Cre+/wt}$;*Vmat2*$^{flox/flox}$ cKO mice showed a distinct lack of full-length Vmat2 mRNA in TrpV1$^+$/Vmat2$^+$neurons of the VTA, primarily in the IF. However, general behavior was undisturbed by this manipulation. The only differences noted between control and cKO mice in the drug-naïve state were decreased exploration and increased sniffing in mature, but not

young, adult cKO mice compared with age-matched control mice. However, these were not confirmed by altered behavior in the elevated plus maze, and a relevant interpretation is, therefore, challenging.

The most striking behavioral finding was, instead, the altered response curve in an amphetamine sensitization paradigm. This experiment was motivated by the association of VTA DA and DA-GLU neurons with amphetamine response. Considering the main neurotransmitter phenotype of TrpV1$^+$ VTA neurons identified as DA-GLU (TrpV1$^+$/Th$^+$/Vglut2$^+$/Vmat2$^+$), amphetamine was selected to challenge these neurons. The current correlation between DA-GLU neurons and amphetamine-induced locomotion is primarily based on cKO studies of the GLU aspect of the DA-GLU phenotype, either *via* cKO of the *Vglut2* gene (Birgner et al., 2010; Hnasko et al., 2010; Fortin et al., 2012) or the glutamate recycling enzyme glutaminase (gene *Gls1*) (Mingote et al., 2017) in DA neurons. Summarizing several studies targeting *Vglut2* in DAT$^+$ neurons (*Vglut2*$^{lx/lx}$;*Slc6a3*$^{Cre/wt}$), this kind of manipulation has been shown to cause reduced GLU release and reduced glutamatergic postsynaptic currents accompanied by secondary effects on striatal DA release as well as significant alteration of psychomotor response upon psychostimulant (amphetamine, cocaine) administration (Birgner et al., 2010; Hnasko et al., 2010; Alsiö et al., 2011; Fortin et al., 2012).

Despite these studies, a detailed understanding of how DA-GLU neurons contribute to behavioral regulation is still limited (recently reviewed in Eskenazi et al., 2021). With our identification of a subpopulation of DA-GLU neurons as positive for TrpV1, a new opportunity to further the understanding of this complex neuronal phenotype has been provided. Here, instead of targeting the GLU aspect of the DA-GLU phenotype, we abrogated their DA identity by producing the *TrpV1*$^{Cre+/wt}$;*Vmat2*$^{flox/flox}$ cKO mice. This was important as both sensory TrpV1$^+$ neurons (Lagerström et al., 2010; Scherrer et al., 2010), and those TrpV1$^+$ neurons we describe in the hypothalamus, are of glutamatergic identity (Vglut2). Thus, specificity for VTA DA-GLU neurons could never be achieved by using a similar Vglut2 cKO approach (even with *TrpV1*$^{Cre/wt}$ as a driver) as used in previous studies of DA-GLU neurons. Instead, the current *TrpV1*^{Cre};*Vmat2*$^{flox/flox}$ cKO approach achieved high specificity for gene targeting of *Vmat2* selectively in TrpV1$^+$ neurons of the VTA, as validated by detailed histological analysis throughout the brain. Thus, using the present Vmat2-based approach, in addition to targeting VMAT2 rather than VGLUT2 in DA-GLU neurons, a new level of selectivity for a subgroup of DA-GLU neurons is reached. Building onto the revelation of a TrpV1$^+$/Th$^+$/Vglut2$^+$/Vmat2$^+$ phenotype in the medial VTA, and the established association of medial VTA DA and DA-GLU neurons with the psychostimulant response, the current results reveal a role for the TrpV1$^+$ subpopulation of DA-GLU neurons in amphetamine response. Heightened locomotion above control levels upon amphetamine injection was observed in both young and mature (YA and MA) *TrpV1*$^{Cre+/wt}$;*Vmat2*$^{flox/flox}$cKO mice during the first 1–2 injection days. The effect was stronger in MA cKO mice than in YA cKO mice, suggesting an enhancement of the cKO phenotype with age. Furthermore, all cKO mice, independent of age, show a lack of progressive sensitization upon repeated amphetamine administration.

We reason that the initial robust response to amphetamine might be due to a compensatory postsynaptic effect induced by the inability of TrpV1$^+$ neurons to synthesize the VMAT2 protein. With the onset of *Vmat2* gene targeting in TrpV1-Cre-positive cells during embryonic development of the VTA, functional compensations effects likely occur as a consequence of the disrupted VMAT2 function. While not observed as altered levels of TH in the mesolimbic or other monoaminergic systems, a more refined methodology might have identified neurocircuitry alterations. Responses caused by altered VMAT2 levels have been amply reported in the literature. For example, heterozygous VMAT2 KO mice show increased horizontal locomotor activity compared with wild-type littermates in response to acute administration of the drug (Wang et al., 1997). Also, hypomorphic *Vmat2* transgenic mice display "behavioral supersensitivity" to amphetamine (Mooslehner et al., 2001). Knocking out the *Vmat2* gene may induce a redistribution of DA from the vesicles to the cytoplasm, where, under physiological conditions, it is metabolized to DOPAC (3,4-dihydroxyphenylacetic acid) by cytosolic monoamine oxidase, MAO. In addition, VMAT2 has been shown to provide a protective effect from oxidative stress-related damage in neurons (Guillot and Miller, 2009; Lohr et al., 2016). This condition of decreased release of DA in response to action potential could probably induce plastic changes at the postsynaptic level that result in supersensitization toward DA.

Furthermore, based on the knowledge that chronic treatment with reserpine leads to upregulation and sensitization of D1 and D2 receptors (Rubinstein et al., 1990; Neisewander et al., 1991), it has been proposed that the same mechanism underlies amphetamine-induced hyperlocomotion observed in different VMAT2 cKO mice, targeting distinct monoaminergic populations (Isingrini et al., 2016). Thus, similar findings as reported here have been observed in other mouse strains that lack normal VMAT2 levels in the monoamine systems. It is evident that mice lacking normal levels of VMAT2 show an initial heightened response to amphetamine above control levels. This has been shown with both acute injections and with sensitization paradigms. Importantly, it is only the initial responses that are accentuated in such a sensitization paradigm (that is, the acute effect).

By affecting VMAT2 levels (rather than VGLUT2), the impact on response to amphetamine is direct. Amphetamine binds to the VMAT2 protein, reducing the ability of this transporter to refill the vesicles with neurotransmitters and, in turn, increasing cytosolic DA (Sulzer and Rayport, 1990; Sulzer et al., 1995). The level of VMAT2 is crucial both for exocytotic and carrier-mediated release of DA because it regulates the size of the vesicular pool and the concentration of DA in the cytosol (Patel et al., 2003). In addition to VMAT2, amphetamine affects DA levels by inhibiting MAO, thus preventing the metabolism of DA, leading to accumulation of DA in the cytosol (Miller et al., 1980; Brown et al., 2001; Fleckenstein et al., 2007) and by a carrier-reversal release mechanism through the

DAT molecule (Giros et al., 1996). Based on this previous knowledge, and the lack of progressive increase in response observed here, it may seem as if the amphetamine effect were blunted in VMAT2 cKO mice. However, in non-physiological conditions (such as upon cKO of VMAT2), when less DA is stored in vesicles, the availability of DA in the cytosol, which can be released through a DAT-mediated modality, may become significant. In addition, the capacity of amphetamine to inhibit MAO (Miller et al., 1980) can momentarily increase the intracellular concentration of DA, which can be released by reverse transport of DAT. Thus, the behavioral augmentation observed in $TrpV1^{Cre+/wt}$;$Vmat2^{flox/flox}$cKO mice upon acute amphetamine administration (initial doses) can be seen as the combined result of a momentarily increased release of DA and the postsynaptic supersensitization due to the absence of VMAT2 protein from prenatal development.

Mice lacking normal VMAT2 levels thus seem to display a "pre-sensitized," or "super-sensitized" state, which is reflected in their enhanced psychomotor behavior to initial (acute) amphetamine injections. The behavioral phenotype of the cKO mice presented here shows that $TrpV1^{+}$ VTA neurons contribute to this response. Similar to any study implementing knockout methodology induced during brain development, compensatory neurocircuitry mechanisms might contribute to the observed phenotype. All the same, given that alterations in response to amphetamine sensitization are an indicator of dysfunction, the "pre-sensitized phenotype" of mice lacking VMAT2 in the TrpV1 subpopulation of VTA DA and DA-GLU neurons may be of critical importance to addiction and other psychiatric conditions.

To summarize this study, TrpV1 defines a subset of medial VTA neurons which can be associated with behavioral response to the psychostimulant amphetamine. Future studies should be important to fully uncover how the TrpV1 identity contributes to VTA function in normal and pathological conditions.

METHODS SECTION

Mice

Transgenics, Housing, and Ethical Permits

Mice were housed at the animal facility of Uppsala University (UU) where they had access to food and water *ad libitum* in standard humidity and temperature conditions and lived under a 12-h dark/light cycle. All animal experimental procedures performed at UU (generation and maintenance of mice, viral-genetic tracing, immunohistochemistry, behavior analyses) followed Swedish (Animal Welfare Act SFS 1998:56) and European Union Legislation (Convention ETS 123 and Directive 2010/63/EU) and were approved by the local Uppsala Ethical Committee. Experimental procedures performed at Oramacell, Paris (*in situ* hybridization on tissue derived from UU, maintenance of wild-type mice) were approved by the Regional Ethics Committee No. 3 of Ile-de-France region on Animal Experiments, and followed the guidelines of the European Communities Council Directive (86/809/EEC) and the Ministère de l'Agriculture et de la Forêt, Service Vétérinaire de la Santé et de la Protection Animale (permit No. A 94-028- 21).

A colony of transgenic mice for the study was generated from initial breeding of two $TrpV1^{tm1(cre)Bbm}$ (here abbreviated $TrpV1^{Cre/wt}$) transgenic male mice purchased from The Jackson Laboratory (stock #017769) and maintained by breeding to female wild type [C57BL/6N (abbreviated Bl6) Taconic]. $TrpV1^{Cre/wt}$mice were originally produced by, and donated to, The Jackson Laboratory by Dr. Allan Basbaum, University of California, United States. The $TrpV1^{Cre/+}$mice containing a myc-tagged IRES-cre sequence inserted downstream of the TrpV1 stop codon. The endogenous TrpV1-coding sequence is not disrupted. When bred with a mouse strain containing a *lox*-flanked sequence, Cre-mediated recombination will occur, as previously validated (Cavanaugh et al., 2011). $Vmat2^{flox/flox}$ mice, in which exon 2 of the *Vmat2* gene is flanked by *LoxP* sites, were originally donated by Dr. Bruno Giros, McGill University, Canada (Narboux-Nême et al., 2011). A new cKO mouse line ($TrpV1^{Cre}$;$Vmat2^{flox/flox}$) was produced for this study by breeding male $TrpV1^{Cre/wt}$ mice with female $Vmat2^{flox/flox}$ mice, first generating heterozygous mice of which male mice were bred with female $Vmat2^{flox/flox}$ mice to generate $TrpV1^{Cre+/wt}$;$Vmat2^{flox/flox}$ cKO and $TrpV1^{Cre-/wt}$;$Vmat2^{flox/flox}$ control mice in the same litter. Littermate mice of both male and female sex were used throughout the analyses.

Genotyping

PCR analyses were performed to confirm the genotype of transgenic mice using DNA extracted from ear biopsies.

TrpV1-Cre forward primer: 5′GCGGTCTGGCAGTAAAAA CTATC;TrpV1-Cre reverse primer: 5′GTGAAACAGCATTG CTGTCACTT; Vmat2-Lox forward primer: 5′GACTCAGG GCAGCACAAATCTCC; Vmat2-Lox reverse primer: 5′GAA ACATGAAGGACAACTGGGACCC.

In situ Hybridization Histochemistry

Brain Section Preparation

Wild-type Bl6, $TrpV1^{Cre+/wt}$;$Vmat2^{flox/flox}$ cKO, and $TrpV1^{Cre-/wt}$;$Vmat2^{flox/flox}$ control mice were euthanized, brains dissected, and snap frozen in cold isopentane (2-Methylbutane, (−30°/−35°C). Sections were cut on a cryostat at the 16-μm thickness and kept at −80°C until their use. For a generation of mouse embryos, mice were mated and females checked for a vaginal plug in the morning. The morning of vaginal plus was determined as the embryonal day (E) 0.5. Embryos were collected at E14.5 and E15.5. Females were euthanized and embryos removed and rapidly frozen in cold isopentane (2-Methylbutane, −20°/−25°C) before sectioning. Brains were cryo-sectioned in series [P3, series of eight sections; P12 and adult (8–12 weeks), series of 10 sections; embryos (E14.5, E15.5), series of five sections; N = 2–4 mice per stage/genotype/detection].

Colorimetric *in situ* Hybridization and Fluorescent *in situ* Hybridization

Riboprobes

Detection of TrpV1, Th, Vglut2, Viaat, Dat, NeuroD6, Grp mRNA, and Vmat2 [Probe 2 (*Vmat2 exon 2*) and Probe 6-15 (*Vmat2 exon 6-15*)] mRNA in brain tissue using Colorimetric

In situ Hybridization (CISH) and/or Fluorescent ISH (FISH) was performed using a previously published protocol (Bimpisidis et al., 2019). Riboprobes detecting the following sequences were prepared: TrpV1: NM_001001445.2; bases 426-1239. Th: NM_009377.1; bases 456-1453. Dat: NM_012694.2; bases 1015-1938. Vglut2: NM_080853.3; bases 2315-3244; Viaat: NM_009508.2; bases 649-1488; NeuroD6: NM_009717.2; bases 632-1420. Grp: NM_175012.4; bases 127-851. Vmat2 Probe 6-15: Vmat2: NM_0130331.1; bases 701-1439 (corresponds to exon 6-15 of mouse sequence NM_172523.3). Vmat2 Probe 2: NM_172523.3; bases 142-274 covering the whole *exon 2* of the *Vmat2* gene. Digoxigenin, fluorescein, and DNP-labeled RNA probes were made by a transcriptional reaction with the incorporation of digoxigenin or fluorescein-labeled nucleotides. The specificity of probes was verified using NCBI blast.

Hybridization and Detection

For the hybridization step, coronal cryosections were air-dried, fixed in 4% paraformaldehyde, and acetylated in.25% acetic anhydride/100-mM triethanolamine (pH 8), followed by hybridization for 18 h at 65°C in 100 μl of formamide-buffer containing a 1-μg/ml digoxigenin (DIG)-labeled probe for colorimetric detection or 1-μg/ml DIG-labeled and 1-μg/ml fluorescein-labeled probes for fluorescent detection. Sections were washed at 65°C with SSC buffers of decreasing strength and blocked with 20% FBS and 1% blocking solution. For colorimetric detection, DIG epitopes were detected with alkaline phosphatase-coupled anti-DIG fab fragments at 1/1,000 and a signal developed with NBT/BCIP (*p*-nitroblue tetrazolium chloride/5-bromo-4-chloro-3-indolyl phosphate; 1/100). For fluorescent detection, sections were incubated with horseradish peroxidase (HRP)-conjugated anti-fluorescein antibody (1/5,000). Signals were revealed using Cy2-tyramide (1/250). HRP-activity was stopped by incubation of sections in.1-M glycine, followed by a 3% H_2O_2 treatment. DIG epitopes were detected with HRP anti-DIG Fab fragments (1/2,000) and revealed using Cy3 tyramide (1/100). DNP epitopes were detected with HRP anti-DNP Fab fragments (1/2,000) and revealed using Cy3 tyramide (1/100). Nuclear staining was performed with 4' 6-diamidino-2-phenylindole (DAPI). All slides were scanned on a NanoZoomer 2.0-HT (Hamamatsu Photonics, Hamamatsu City, Japan) at 20x resolution. Laser intensity and time of acquisition were set separately for each riboprobe. Images were analyzed using the NDP.view2 software (Hamamatsu Photonics). Published atlases (Franklin and Paxinos, 2013) were used to outline anatomical borders.

Definition of Positive Cells and Counting

For a cell to be considered as TrpV1-positive ($TrpV1^+$), fluorescent TrpV1 mRNA labeling was defined as a cluster of fluorescent dots (minimum six dots) on the cell surface in agreement with the cellular colorimetric TrpV1 labeling. The background was defined by a single dot, with no clustering. The fluorescent stain 4′,6-diamidino-2-phenylindole (DAPI) was used to define cell nuclei. Since TrpV1 mRNA labeling was generally weak (defined as weaker than labeling for Th and Vglut2 in the same area), criteria for cell counting were based on three requirements: Size of cells strongly positive for TrpV1; the size of Th and Vglut2 positive cells in regions where TrpV1 is strongly expressed; one cell nucleus present. Based on these criteria, a circle of diameter of 11 μm was generated for each such defined $TrpV1^+$ cell. Manual counting of $TrpV1^+$ cells was performed in CISH and FISH detections. Counting were made in all regions in which Trpv1 mRNA was detected: VTA (subnuclei IF, PN, PBP, RLi, and CLi), PHA, and paraventricular nucleus, spanning Bregma −2.18 to Bregma −4.16 (Franklin and Paxinos, 2013). To define an area, outlines defined by CISH detection were used (see **Supplementary Figure 1** as an example of outlines defined in a CISH detection). Counting was performed in both CISH and FISH detections (N = 3 mice per detection and probe combination, serial sections). Similar results obtained using both detections validated the method.

Co-fluorescent in situ Hybridization Analysis

The percentage of $TrpV1^+$ cells co-labeled with each marker (TrpV1/Th, TrpV1/Vmat2, Trpv1/Vglut2, TrpV1/Dat, Trpv1/Viaat, Trpv1/Grp, and TrpV1/NeuroD6) was established in each VTA subnucleus using CISH detection to define outlines as described above.

Vmat2 Wild Type and Conditional Knockout Cells

$TrpV1^{Cre+/wt};Vmat2^{flox/flox}$ $TrpV1^{Cre-/wt};Vmat2^{flox/flox}$ mice at E15.5 and adult stages (N = 3 mice per genotype and stage; serial sections per probe combination) were analyzed using a probe mixture of Vmat2 Probe 2 and Vmat2 Probe 6–15. The occurrence of cells positive for both probes (representing *Vmat2* wild-type cells) and cells positive for Probe 6-15 only (*Vmat2*cKO cells) was quantified by manual counting, using detection of Vmat2 Probe 6–15 and the Thprobe as references for anatomical boundaries and outline of distinct cell soma.

Stereotaxic Virus Injection

Stereotaxic injections were performed on anesthetized $TrpV1^{Cre+/wt}$ mice (9–12 weeks of age; N = 11 male and female mice) maintained at 1.4–1.8% isoflurane-air mix v/v (0.5–2 L/min). Prior to surgery and, also, 24-h post-surgery, mice received a subcutaneous injection of analgesics (Carprofen; 5-mg/kg, Norocarp). A topical analgesic (Marcain; 1.5 mg/kg, AstraZeneca) was locally injected on the site of the incision. After exposing the skull, drill holes were prepared. The mice were unilaterally injected in the PHA/VTA region with an adeno-associated (AAV) virus containing a floxed DNA construct carrying the gene encoding the yellow fluorescent protein, eYFP (rAAV2/EF1a-DIO-eYFP). Virus concentration was 4.6×10^{12} virus molecules/ml delivered at the following mouse brain coordinate (Franklin and Paxinos, 2013): anteroposterior (AP) = −2.80 mm, mediolateral (ML) = −0.60 mm from the midline with an 8° angle in the frontal plan to avoid the sagittal vein, dorsoventral level (DV) = −4.40 mm from the dura matter. About 300 nL of virus solution was injected with a NanoFil syringe (World Precision Instruments, Sarasota, FL, United States) at the speed of 100 nL per minute. The rAAV2/EF1a-DIO-eYFP was purchased from UNC Vector Core, Chapel Hill, NC, USA, in accordance with

Material Transfer Agreement. Injected mice are referred to as *TrpV1::EF1a-DIO-eYFP* mice.

Immunohistochemistry Analysis

Fluorescent Immunohistochemistry

TrpV1::EF1a-DIO-eYFP mice (13–18-week old mice: 4–6 weeks after injection at 9–12 weeks of age) were deeply anesthetized and perfused trans-cardially with phosphate-buffer-saline (PBS), followed by ice-cold 4% formaldehyde. Brains were extracted and 60-μm vibratome-cut sections were freshly prepared. Fluorescent immunohistochemistry was performed to detect TH and enhance the YFP signal. After rinsing in PBS, sections were incubated for 90 min in PBS.3% X-100 Triton, containing 5% blocking solution (normal donkey serum), followed by incubation with a primary antibody (Rabbit anti-TH, ab152, Millipore, 1/1,000; chicken anti-GFP 1/1,000, cat. No. ab13970, Abcam), diluted in 1% normal donkey serum in PBS, overnight at 4°C. The next day, sections were rinsed in PBS plus.1% Tween-20 solution and incubated for 90 min with a secondary antibody diluted in PBS (A488 donkey anti-chicken 1/1,000, cat. No. 703-545-155, Jackson ImmunoResearch). After rinsing in PBS containing.1% Tween-20, sections were incubated for 30 min with DAPI diluted in distilled water (1/5,000). Sections were mounted with a Fluoromount aqueous mounting medium (Sigma, United States) and cover-slipped. Sections were digitally imaged with the NanoZoomer 2-0-HT.0 scanner (Hamamatsu) and visualized with NDPView2 software (Hamamatsu). YFP-positive cell bodies, fibers, and projections were analyzed and evaluated upon comparison with TH (visualizing brain monoamine systems) and DAPI staining.

Chromogenic Immunohistochemistry

$Trpv1^{Cre-/wt};Vmat2^{flox/flox}$ control (N = 4; three males, one female) and $Trpv1^{Cre+/wt};Vmat2^{flox/flox}$cKO ($N$ = 4; three males, one female) mice (24 weeks of age) were perfused trans-cardially with PBS, followed by ice-cold 4% formaldehyde. Brains were extracted, cryoprotected in 30% sucrose solution, and stored at −80°C until sectioning at 60-μm sections with a cryostat. Sections were washed with 1% H_2O_2 in PBS with.1% Triton-X for endogenous peroxidase activity inhibition and incubated for 90 min with a blocking solution containing 5% goat serum. Sections were then incubated with primary TH antibody (Rabbit anti-TH, ab152, Millipore, 1/4,000) overnight at 4°C, followed by 90-min incubation with a biotinylated anti-rabbit antibody and subsequent 90-min incubation with ABC solution (Vectastain ABC kit). Sections were washed with.1-M a Tris-HCl buffer (pH 7.4) and exposed to DAB solution (a DAB peroxidase substrate kit, Vector Laboratories) until a signal appeared. The chromogenic reaction was then blocked with Tris buffer. Sections were counterstained with cresyl violet followed by dehydration with increasing ethanol concentrations (75, 90, and 100%) and histological clearing using Histoclear (Histolab). Sections were mounted on slides using a DPX mounting medium (Sigma) and cover-slipped. Sections were digitally imaged with the NanoZoomer 2-0-HT.0 (Hamamatsu) scanner and visualized with NDPView2 software (Hamamatsu). TH-positive cell bodies, fibers, and projections were analyzed and evaluated by comparison between genotypes.

Behavior Analysis

$TrpV1^{Cre+/wt};Vmat2^{flox/flox}$cKO and $TrpV1^{Cre-/wt};Vmat2^{flox/flox}$ control (Ctrl) littermate mice were analyzed in behavior experiments. Throughout the process, mice had access to food and water *ad libitum* in standard humidity and temperature conditions and with a 12-h dark/light cycle. Behavioral tests were performed during the light cycle between 9:00 a.m. and 4:00 p.m. All mice were handled for 4 days prior to behavioral testing and habituated to the experimental room for 30 min before handling and testing. Young adult (YA) mice were 8 weeks old, and mature adult (MA) mice were 18 weeks old at the start of the behavioral testing. Each mouse performed either the open field test or the elevated plus maze (both of which consist of a 1-day test) 24 h prior to starting the amphetamine sensitization protocol. Mice (males and females mixed) were analyzed in the following behavioral tests according to the procedure described below:

Open Field Test

Mice (Ctrl/YA N = 6, two males, four females; cKO/YA N = 9, five males, four females; Ctrl/MAN = 7, three males, four females; cKO/MAN = 6, three males, three females) were individually placed in the central zone of the open field arena and allowed to freely explore it for 10 min. The open-field chamber consisted of a 50-cm, squared, transparent, plastic arena with a white floor that has been divided into a central zone (center, 25% of the total area) and a peripheral zone (borders). Total distance moved, time spent, and frequency in crossing to the center, time spent in the corners, time spent not moving, and body elongation were automatically documented. Rearing, self-grooming, and sniffing behaviors were manually recorded by an experimenter blind to the experimental groups using the EthoVision XT tracking software (Noldus Information Technology, Netherlands).

Elevated Plus Maze

The elevated plus maze apparatus consists of two open arms (35-cm length) and two closed arms (35-cm length) in which walls (15-cm high) provide shelter; the open and closed arms cross in the middle to create a center platform. The maze is elevated 50 cm from the floor. Mice (Ctrl/YAN = 8, two males, six females; cKO/YA N = 13, six males, seven females; Ctrl/MA N = 11, six males, five females; cKO/MA N = 12, five males, seven females) were placed individually in the center of the maze facing one of the open arms and allowed to freely explore the apparatus for 10 min. The results of the test were recorded with a camera placed above the EPM arena. Time spent in arms, number of entries in arms, number of head dips, distance moved, time spent moving and body elongation were automatically scored by the EthovisionXT software (Noldus Information Technology, The Netherlands).

Baseline Locomotion

Spontaneous locomotion was monitored for 30 min upon placing the mice (Ctrl/YA N = 14, 4 males, 10 females; cKO/YA N = 22, 11 males, 11 females; Ctrl/MA N = 18, nine males, nine females; cKO/MAN = 18, 8 males, 10 females) in Makrolon polycarbonate boxes covered with a transparent Plexiglas lid, containing 1.5-cm bedding. Locomotion was recorded by the EthovisionXT software (Noldus Information Technology, Netherlands).

Amphetamine Sensitization

Mice (Ctrl/YA N = 14, 4 males, 10 females; cKO/YA N = 22, 11 males, 11 females; Ctrl/MA N = 18, nine males, nine females; cKO/MAN = 18, 8 males, 10 females) received a saline injection (Day 1), followed by four consecutive days of amphetamine injection (Days 2–5, 3 mg/kg, i.p.), followed by a last injection on Day 17 (3 mg/kg, i.p.). Locomotion was recorded 30 min before (baseline) and 90 min after injection using the EthovisionXT software (Noldus Information Technology, Netherlands). The software allowed the calculation for the entire period (90 min) as well as measures of different sub-periods (10 min). Distance moved across 90 min represents the sum of 10-min sub-periods.

Statistical Analysis

All mice used for the behavioral studies were included in the analysis.

Repeated measures (RM) two-way ANOVA with Greenhouse–Geisser corrections were used to compare the mean of the weight of control and cKO mice. *Post-hoc* comparisons were performed by Sidak's multiple comparison test.

Unpaired *t*-tests were used to compare the mean scores of control and cKO mice in the open field test.

Repeated measures two-way ANOVA was used to compare the mean of scores for time spent and the number of visits in arms for the EPM. *Post hoc* comparisons were performed by Sidak's multiple comparison test. Unpaired *t*-tests were used to compare mean scores of control and cKO mice for other parameters of the elevated plus maze.

Repeated measures two-way ANOVA was used to compare the mean of baseline locomotion. *Post hoc* comparisons were performed by Sidak's multiple comparison test.

Repeated measures one-way ANOVA with Greenhouse–Geisser corrections were used to compare mean scores of amphetamine-induced locomotion across a session for every single group. *Post hoc* comparisons were performed by Dunnett's multiple comparison tests to compare Day 2 with other sessions.

Repeated measures two-way ANOVA with Greenhouse–Geisser corrections were used to compare mean scores of amphetamine-induced locomotion. *Post hoc* comparisons were performed by Sidak's multiple comparison test.

Data are presented as mean ± SEM. Data analysis was performed with Prism (GraphPad Prism version 9.00 for Windows, GraphPad Software, La Jolla, CA, United States).

Details from the statistical analysis are available in **Supplementary File 1**.

SIGNIFICANCE STATEMENT

Teasing out the impact of distinct brain neurons on behavioral regulation is critical in neuroscience. TRPV1 is well known for its role in heat and pain processing *via* peripheral sensory neurons. However, the distribution of this receptor in the brain has remained elusive. This study identifies a peak of TrpV1 mRNA in the ventral tegmental area (VTA) of the mouse midbrain at the perinatal stage, allowing for its careful histological characterization. TrpV1 is primarily detected in medial VTA subnuclei but is absent from the substantia nigra *pars compacta* (SNc). The far majority of TrpV1 mRNA co-localizes with markers of dopamine (Th, Vmat2) and glutamate (Vglut2) neurons. This $TrpV1^{+}/Th^{+}/Vglut2^{+}/Vmat2^{+}$ molecular signature thus defines a distinct subpopulation within the dopamine-glutamate (DA-GLU) co-releasing neuronal population present within the VTA. In accordance with a role for such DA-GLU neurons in psychostimulant response, selective manipulation of dopamine release by this $TrpV1^{+}$ subpopulation was sufficient to modulate amphetamine-induced psychomotor behavior. This study highlights the behavioral role of a distinct group of VTA neurons.

DATA AVAILABILITY STATEMENT

The raw data supporting the conclusions of this article will be made available by the authors, without undue reservation.

ETHICS STATEMENT

The animal study outline was reviewed and approved by Uppsala Local Committee.

AUTHOR CONTRIBUTIONS

GS: behavior experiments, data analysis, figure preparation, and manuscript text (original and revision). AG: tracing and immunohistochemistry, data analysis, manuscript revision, and figure preparation. SD: *in situ* hybridization, data analysis, figure preparation, and manuscript revision. BV: tracing and immunohistochemistry, data analysis, figure preparation, and manuscript revision. ÅW-M: project design and funding, data analysis, figure preparation, and manuscript text writing (original draft, editing, and revision).

FUNDING

This work was supported by Uppsala University and by grants to ÅW-M from the Swedish Research Council (Vetenskapsrådet 2017-02039), the Swedish Brain Foundation (Hjärnfonden), Parkinsonfonden, Bertil Hållsten Research Foundation, Zoologiska stiftelsen and Åhlénstiftelsen, and by a grant from OE & Edla Johansson Foundation to GS.

ACKNOWLEDGMENTS

The authors thank Bruno Giros, McGill University, Canada, for generously providing the *Vmat2*$^{flox/flox}$ mouse line, and Allan Basbaum, University of California, United States, for donating the *TrpV1*$^{tm1(cre)Bbm}$ mouse line for access at the Jackson Laboratory. Marie-Laure Niepon at the image platform at Institute de la Vision, Paris, France is thanked for slide scanning. Uppsala University Behavior Facility (UUBF) is acknowledged for providing localities for virus safety and behavior analyses.

SUPPLEMENTARY MATERIAL

The Supplementary Material for this article can be found online at: https://www.frontiersin.org/articles/10.3389/fncir.2021.726893/full#supplementary-material

Supplementary Figure 1 | Colorimetric and fluorescent in situ hybridization (CISH and FISH) of coronal mouse brain sections at postnatal day (P) **3. (A,B)** The area encompassing the posterior hypothalamus (including PHA, RM) displayed. DAPI is used for the detection of cell nuclei. Top panel, CISH: TrpV1 **(A1)**, Th **(A2)**, Vglut2 **(A3)**. Bottom panel, FISH: TrpV1/Th **(B1)**, TrpV1/Vglut2 **(B2)**, TrpV1/Viaat **(B3)**; positive cells indicated in insets by arrows; white arrows indicate co-labeling of red and green fluorophores. **(C)** Bottom: TrpV1/Viaat **(C)**, the same section level as shown in **Figure 1A**. Scale bars, 500 μm **(A)**; 120 μm (**B**, insets 20 μm); 100 μm (**C**, insets 10, μm). IF, interfascicular nucleus; PBP parabrachial pigmented nucleus; PHA, posterior hypothalamic nucleus; PN, paranigral nucleus; RM, retromammillary nucleus; RLi, rostral linear nucleus; SNc, substantia nigra *pars compacta*; VTA, ventral tegmental area.

Supplementary Figure 2 | Colorimetricribo probe in situ hybridization of serial sections at mouse embryonic Day (E) 14.5, postnatal day (P) P12, and adult (9 weeks). The area encompassing the posterior hypothalamus (including PHA and RM) and midbrain (including VTA and SNc) was displayed. Detection of TrpV1, Th, Vglut2 mRNAs in **(A)** sagittal and horizontal sections at E14.5 [a line in **A1,A3,A5** indicates section level (S1) shown in **A2,A4,A6**]; **(B)** coronal sections at P12; **(C)** coronal sections of the adult mouse brain. Scale bars, 500 μm. ms, mesencephalic flexure; RLi, rostral linear nucleus; IF, interfascicular nucleus; PBP, parabrachial pigmented nucleus; PHA, posterior hypothalamic nucleus; PN, paranigral nucleus; RM, retromammillary nucleus; SNc, substantia nigra *pars compacta*; VTA, ventral tegmental area.

Supplementary Figure 3 | Double-labeling riboprobe fluorescent in situ hybridization (FISH) of serial brain sections at postnatal day (P) 3 identifying TrpV1 co-localization with Vmat2 in VTA subnuclei. Left panel, TrpV1 (red), Vmat2 (green); sections encompassing the posterior hypothalamus through the VTA toward, and including, the CLi and A8. Yellow indicates co-localization TrpV1/Vmat2. DAPI is used for the detection of cell nuclei. Right-side panels show close-ups of cells in areas indicated by a square in the left panel. Positive cells are indicated in insets by arrowheads; white arrows indicate co-labeling of red and green fluorophores. Scale bars, 500 μm (12 μm in insets where each dotted line indicates a discrete cell). RLi, rostral linear nucleus; IF, interfascicular nucleus; PN, paranigral nucleus; PBP, parabrachial pigmented nucleus; PHA, posterior hypothalamic nucleus; RM, retromammillary nucleus; PBP, parabrachial pigmented nucleus; SNc, substantia nigra *pars compacta*; CLi, caudal linear nucleus; A8, A8 dopamine area; VTA, ventral tegmental area.

Supplementary Figure 4 | Colorimetric riboprobe in situ hybridization (CISH) of serial brain sections at postnatal day (P) 3. TrpV1, Th, NeuroD6, Grp mRNAs analyzed in coronal sections encompassing the posterior hypothalamus through the VTA toward, and including, the CLi and A8. TrpV1 **(A1,A5,A9,A13)**; Th **(A2,A6,A10,A14)**; NeuroD6 **(A3,A7,A11,A15)**; Grp **(A4,A8,A12,A16)**. Scale bars, 500 μm. A8, A8 dopaminearea; CLi, caudal linear nucleus; IF, interfascicular nucleus; PN, paranigral nucleus; PBP, parabrachial pigmented nucleus; PHA, posterior hypothalamic nucleus; RM, retromammillary nucleus; RLi, rostral linear nucleus; SNc, substantia nigra *pars compacta*; VTA, ventral tegmental area; R, rostral; C, caudal.

Supplementary Figure 5 | Vmat2 riboprobe in situ hybridization. Serial sections throughout the VTA area in *TrpV1*$^{Cre+/wt}$*;Vmat2*$^{flox/flox}$ conditional knockout (cKO) mice (12 weeks old). DAPI is used for the detection of cell nuclei. **(A)** Triple fluorescent *in situ* hybridization (FISH) co-assessing Th mRNA with Vmat2 Probe 2 and Vmat2 Probe 6–15 using the two-probe approach illustrated in **Figure 5** combined with the Th probe. Scale bar, 500 μm. **(B)** Mid-sagittal brain sections of a mouse embryo at E15.5 (covering the area around the mesencephalic flexure where midbrain dopamine neurons are born), showing labeling of Vmat2 Probe 2 (purple) and Probe 6–15 (green). A square in top panels indicates an area selected for a closeup in bottom panels. Only few cells show the presence of only Probe 6–15 (an indicator of the cKO phenotype); most cells are positive for both Vmat2 probes at this stage. Scale bar, 300 μm. CLi, caudal linear nucleus; IF, interfascicular nucleus; PN, paranigral nucleus; PBP, parabrachial pigmented nucleus; RLi, rostral linear nucleus; SNc, substantia *nigra pars compacta*; VTA, ventral tegmental area.

Supplementary Figure 6 | Weight analysis. Analysis and comparison of *TrpV1*$^{Cre-/wt}$*;Vmat2*$^{flox/flox}$ control (Ctrl) and *TrpV1*$^{Cre+/wt}$*;Vmat2*$^{flox/flox}$ conditional knockout (cKO) mice. **(A)** A weight curve for Ctrl (N = 31) and cKO (N = 25) mice. Weight is expressed in grams for each week ± SEM (###$p < 0.001$, age effect).

Supplementary Figure 7 | Open-field and elevated-plus maze paradigms. Analysis and comparison of *TrpV1*$^{Cre-/wt}$*;Vmat2*$^{flox/flox}$ control (Ctrl) and *TrpV1*$^{Cre+/wt}$*;Vmat2*$^{flox/flox}$ conditional knockout (cKO) mice at young adult (YA; 8 weeks old) and mature adult (MA; 18 weeks old) age in the open field and plus-maze paradigms. Open field test (OFT), Ctrl/YA (N = 6) and cKO/YA (N = 9), Ctrl/MA (N = 7) and cKO/MA (N = 6) data are expressed as mean ± SEM. **(A)** Time spent not moving YA. **(B)** Self-grooming YA. **(C)** Visits to the center YA. **(D)** Time spent in corners YA. **(E)** Time spent contracted YA. **(F)** Time spent not moving MA. **(G)** Self-grooming MA. **(H)** Visits to the center MA. **(I)** Time spent in corners MA. **(J)** Time spent contracted MA. Elevated plus maze (EPM), Ctrl/YA (N = 8) and cKO/YA (N = 13), Ctrl/MA (N = 11) and cKO/MA (N = 12), data are expressed as mean ± SEM. **(K)** Distance moved YA. **(L)** Time spent moving YA. **(M)** Number of head dips YA. **(N)** Time spent stretched YA. **(O)** Distance moved MA. **(P)** Time spent moving MA. **(Q)** Number of head dips MA. **(R)** Time spent stretched MA.

Supplementary Figure 8 | Amphetamine-induced locomotion. Analysis and comparison of *TrpV1*$^{Cre-/wt}$*;Vmat2*$^{flox/flox}$ control (Ctrl) and *TrpV1*$^{Cre+/wt}$*;Vmat2*$^{flox/flox}$ conditional knockout (cKO) mice at young adult (YA; 8 weeks old) and mature adult (MA; 18 weeks old) age in the amphetamine sensitization paradigm. Amphetamine-induced locomotion, 90 min following amphetamine injection (YA); Ctrl/YA (N = 22) and cKO/YA mice (N = 22). **(A)** Amphetamine-induced locomotion on Day 4. Distance moved presented as mean ± SEM for each 10-min period (###$p < 0.001$, time effect; +$p = 0.023$, time × genotype interaction). **(B)** Amphetamine-induced locomotion on Day 5. Distance moved presented as mean ± SEM for each 10-min period (###$p < 0.001$, time effect). **(C)** Amphetamine-induced locomotion on Day 17. Distance moved presented as mean ± SEM for each 10-min period (###$p < .001$, time effect; +$p = 0.039$, time × genotype interaction). Amphetamine-induced locomotion, 90 min following amphetamine injection (MA); Ctrl/MA (N = 18) and cKO/MA mice (N = 18). **(D)** Amphetamine-induced locomotion on Day 4. Distance moved presented as mean ± SEM for each 10-min period (###$p < 0.001$, time effect). **(E)** Amphetamine-induced locomotion on Day 5. Distance moved presented as mean ± SEM for each 10-min period [###$p < 0.001$, time effect; +$p = 0.02$, time × genotype interaction)]. **(F)** Amphetamine-induced locomotion on Day 17. Distance moved presented as mean ± SEM for each 10-min period (###$p < 0.001$, time effect; ++$p = 0.008$, time × genotype interaction).

Supplementary Table 1 | The extent of cells detected as positive for targeted (cKO) Vmat2 mRNA. The table shows the percentage of Vmat2 cKO cells in several brain areas as indicated by the terminology (including the hypothalamus, mammillary nuclei, and monoaminergic neuronal populations of the VTA, SNc, raphe, and medulla) and distribution of Vmat2 cKO cells within the VTA. Analysis performed in adult mice (12 weeks old). N = 3 mice, serial sections per detection. RLi, rostral linear nucleus; IF, interfascicular nucleus; PIF, parainterfascicular nucleus; PN, paranigral nucleus; PHA, posterior hypothalamic nucleus; RM, retromammillary nucleus; PBP, parabrachial pigmented nucleus; SNc, substantia

nigra *pars compacta*; CLi, caudal linear nucleus; A8, A8 dopamine area (aka RRF, retrorubral field); VTA, ventral tegmental area; LC, locus coeruleus; C1–C3, adrenergic C1–C3 cell groups; Arc, arcuate nucleus; LH, lateral hypothalamus; DR, dorsal raphe; A11, A11 dopamine area; AH, anterior hypothalamus nucleus; PMV, premammillary nucleus ventral part; MnR, median raphe nucleus; DRI, dorsal raphe interfascicular part; RMg, raphe magnus nucleus; RIP, raphe interpositus nucleus; R0b, raphe obscurus nucleus; LPGi, lateral paragigantocellular nucleus.

Supplementary File 1 | Statistical analysis of results obtained in behavior analysis. *TrpV1*$^{Cre-/wt}$;*Vmat2*$^{flox/flox}$ control (Ctrl) and *TrpV1*$^{Cre+/wt}$;*Vmat2*$^{flox/flox}$ conditional knockout (cKO) mice at young adult (YA; 8 weeks old) and mature adult (MA; 18 weeks old) age were analyzed in behavioral paradigms. The file shows the detailed statistical analysis and results obtained from these experiments, including the number of animals and sex for each test, with reference to the figure where data are displayed.

REFERENCES

Alsiö, J., Nordenankar, K., Arvidsson, E., Birgner, C., Mahmoudi, S., Halbout, B., et al. (2011). Enhanced sucrose and cocaine self-administration and cue-induced drug seeking after loss of VGLUT2 in midbrain dopamine neurons in mice. *J. Neurosci.* 31, 12593–12603. doi: 10.1523/JNEUROSCI.2397-11.2011

Beier, K. T., Steinberg, E. E., DeLoach, K. E., Xie, S., Miyamichi, K., Schwarz, L., et al. (2015). Circuit architecture of VTA dopamine neurons revealed by systematic input-output mapping. *Cell* 162, 622–634. doi: 10.1016/j.cell.2015.07.015

Berridge, K. C., and Robinson, T. E. (1998). What is the role of dopamine in reward: hedonic impact, reward learning, or incentive salience? *Brain Res. Rev.* 28, 309–369. doi: 10.1016/S0165-0173(98)00019-8

Bimpisidis, Z., König, N., Stagkourakis, S., Zell, V., Vlcek, B., Dumas, S., et al. (2019). The neurod6 subtype of VTA neurons contributes to psychostimulant sensitization and behavioral reinforcement. *Eneuro* 6:ENEURO.0066-19.2019. doi: 10.1523/ENEURO.0066-19.2019

Bimpisidis, Z., and Wallén-Mackenzie, Å (2019). Neurocircuitry of reward and addiction: potential impact of dopamine–glutamate co-release as future target in substance use disorder. *J. Clin. Med.* 8:1887. doi: 10.3390/jcm8111887

Birgner, C., Nordenankar, K., Lundblad, M., Mendez, J. A., Smith, C., Grevès, M. l., et al. (2010). VGLUT2 in dopamine neurons is required for psychostimulant-induced behavioral activation. *Proc. Natl. Acad. Sci. U.S.A.* 107, 389–394. doi: 10.1073/pnas.0910986107

Björklund, A., and Dunnett, S. B. (2007). Dopamine neuron systems in the brain: an update. *Trends Neurosci.* 30, 194–202.

Brichta, L., and Greengard, P. (2014). Molecular determinants of selective dopaminergic vulnerability in parkinson's disease: an update. *Front. Neuroanatomy* 8:152. doi: 10.3389/fnana.2014.00152

Brown, J. M., Hanson, G. R., and Fleckenstein, A. E. (2001). Regulation of the vesicular monoamine transporter-2: a novel mechanism for cocaine and other psychostimulants. *J. Pharmacol. Exp. Ther.* 296:762.

Caterina, M. J., Schumacher, M. A., Tominaga, M., Rosen, T. A., Levine, J. D., and Julius, D. (1997). The capsaicin receptor: a heat-activated ion channel in the pain pathway. *Nature* 389, 816–824. doi: 10.1038/39807

Cavanaugh, D. J., Chesler, A. T., Jackson, A. C., Sigal, Y. M., Yamanaka, H., Grant, R., et al. (2011). Trpv1 reporter mice reveal highly restricted brain distribution and functional expression in arteriolar smooth muscle cells. *J. Neurosci.* 31, 5067–5077. doi: 10.1523/JNEUROSCI.6451-10.2011

Chuhma, N., Mingote, S., Moore, H., and Rayport, S. (2014). Dopamine neurons control striatal cholinergic neurons via regionally heterogeneous dopamine and glutamate signaling. *Neuron* 81, 901–912. doi: 10.1016/j.neuron.2013.12.027

Chung, C. Y., Seo, H., Sonntag, K. C., Brooks, A., Lin, L., and Isacson, O. (2005). Cell type-specific gene expression of midbrain dopaminergic neurons reveals molecules involved in their vulnerability and protection. *Human Mol. Genet.* 14, 1709–1725. doi: 10.1093/hmg/ddi178

Di Chiara, G. (1998). A motivational learning hypothesis of the role of mesolimbic dopamine in compulsive drug use. *J. Psychopharmacol.* 12, 54–67. doi: 10.1177/026988119801200108

Di Chiara, G., and Imperato, A. (1988). Drugs abused by humans preferentially increase synaptic dopamine concentrations in the mesolimbic system of freely moving rats. *Proc. Natl. Acad. Sci. U.S.A.* 85, 5274–5278. doi: 10.1073/pnas.85.14.5274

Dumas, S., and Wallén-Mackenzie, Å (2019). Developmental co-expression of Vglut2 and Nurr1 in a mes-di-encephalic continuum preceeds dopamine and glutamate neuron specification. *Front. Cell Dev. Biol.* 7:307. doi: 10.3389/fcell.2019.00307

Eskenazi, D., Malave, L., Mingote, S., Yetnikoff, L., Ztaou, S., Velicu, V., et al. (2021). Dopamine neurons that cotransmit glutamate, from synapses to circuits to behavior. *Front. Neural Circ.* 15:665386. doi: 10.3389/fncir.2021.665386

Fleckenstein, A. E., Volz, T. J., Riddle, E. L., Gibb, J. W., and Hanson, G. R. (2007). New insights into the mechanism of action of amphetamines. *Ann. Rev. Pharmacol. Toxicol.* 47, 681–698. doi: 10.1146/annurev.pharmtox.47.120505.105140

Fortin, G. M., Bourque, M. J., Mendez, J. A., Leo, D., Nordenankar, K., Birgner, C., et al. (2012). Glutamate corelease promotes growth and survival of midbrain dopamine neurons. *J. Neurosci.* 32, 17477–17491. doi: 10.1523/JNEUROSCI.1939-12.2012

Franklin, K. B. J., and Paxinos, G. (2013). *Paxinos and Franklin's The Mouse Brain in Stereotaxic Coordinates*. Amsterdam: Academic Press, an imprint of Elsevier.

Giros, B., Jaber, M., Jones, S. R., Wightman, R. M., and Caron, M. G. (1996). Hyperlocomotion and indifference to cocaine and amphetamine in mice lacking the dopamine transporter. *Nature* 379, 606–612. doi: 10.1038/379606a0

Greene, J. G., Dingledine, R., and Greenamyre, J. T. (2005). Gene expression profiling of rat midbrain dopamine neurons: implications for selective vulnerability in parkinsonism. *Neurobiol. Dis.* 18, 19–31. doi: 10.1016/j.nbd.2004.10.003

Guillot, T. S., and Miller, G. W. (2009). Protective actions of the vesicular monoamine transporter 2 (VMAT2) in monoaminergic neurons. *Mol. Neurobiol.* 39, 149–170. doi: 10.1007/s12035-009-8059-y

Hnasko, T. S., Chuhma, N., Zhang, H., Goh, G. Y., Sulzer, D., Palmiter, R. D., et al. (2010). Vesicular glutamate transport promotes dopamine storage and glutamate corelease in vivo. *Neuron* 65, 643–656. doi: 10.1016/j.neuron.2010.02.012

Hnasko, T. S., and Edwards, R. H. (2012). Neurotransmitter corelease: mechanism and physiological role. *Ann. Rev. Physiol.* 74, 225–243. doi: 10.1146/annurev-physiol-020911-153315

Hnasko, T. S., Hjelmstad, G. O., Fields, H. L., and Edwards, R. H. (2012). Ventral tegmental area glutamate neurons: electrophysiological properties and projections. *J. Neurosci.* 32, 15076. doi: 10.1523/JNEUROSCI.3128-12.2012

Ikemoto, S. (2007). Dopamine reward circuitry: two projection systems from the ventral midbrain to the nucleus accumbens–olfactory tubercle complex. *Brain Res. Rev.* 56, 27–78. doi: 10.1016/j.brainresrev.2007.05.004

Isingrini, E., Guinaudie, C., Perret, L. C., Rainer, Q., Moquin, L., Gratton, A., et al. (2017). Genetic elimination of dopamine vesicular stocks in the nigrostriatal pathway replicates parkinson's disease motor symptoms without neuronal degeneration in adult mice. *Sci. Rep.* 7:12432. doi: 10.1038/s41598-017-12810-9

Isingrini, E., Perret, L., Rainer, Q., Sagueby, S., Moquin, L., Gratton, A., et al. (2016). Selective genetic disruption of dopaminergic, serotonergic and noradrenergic neurotransmission: insights into motor, emotional and addictive behaviour. *J. Psychiatry Neurosci.* 41, 169–181. doi: 10.1503/jpn.150028

Kawano, M., Kawasaki, A., Sakata-Haga, H., Fukui, Y., Kawano, H., Nogami, H., et al. (2006). Particular subpopulations of midbrain and hypothalamic dopamine neurons express Vesicular glutamate transporter 2 in the rat brain. *J. Comparat. Neurol.* 498, 581–592. doi: 10.1002/cne.21054

Khan, S., Stott, S. R. W., Chabrat, A., Truckenbrodt, A. M., Spencer-Dene, B., Nave, K. A., et al. (2017). Survival of a novel subset of midbrain dopaminergic neurons projecting to the lateral septum is dependent on neurod proteins. *J. Neurosci.* 37:2305. doi: 10.1523/JNEUROSCI.2414-16.2016

König, N., Bimpisidis, Z., Dumas, S., and Wallén-Mackenzie, Å (2020). Selective knockout of the Vesicular monoamine transporter 2 (Vmat2) gene in Calbindin2/Calretinin-positive neurons results in profound changes in behavior and response to drugs of abuse. *Front. Behav. Neurosci.* 14:578443. doi: 10.3389/fnbeh.2020.578443

Kramer, D. J., Risso, D., Kosillo, P., Ngai, J., and Bateup, H. S. (2018). Combinatorial expression of Grp and NeuroD6 defines dopamine neuron

populations with distinct projection patterns and disease vulnerability. *Eneuro* 5:ENEURO.0152-18.2018. doi: 10.1523/ENEURO.0152-18.2018

La Manno, G., Gyllborg, D., Codeluppi, S., Nishimura, K., Salto, C., Zeisel, A., et al. (2016). Molecular diversity of midbrain development in mouse, human, and stem cells. *Cell* 167, 566–580.e19. doi: 10.1016/j.cell.2016.09.027

Lagerström, M. C., Rogoz, K., Abrahamsen, B., Persson, E., Reinius, B., Nordenankar, K., et al. (2010). VGLUT2-dependent sensory neurons in the TrpV1 population regulate pain and itch. *Neuron* 68, 529–542. doi: 10.1016/j.neuron.2010.09.016

Lammel, S., Hetzel, A., Häckel, O., Jones, I., Liss, B., and Roeper, J. (2008). Unique properties of mesoprefrontal neurons within a dual mesocorticolimbic dopamine system. *Neuron* 57, 760–773. doi: 10.1016/j.neuron.2008.01.022

Lammel, S., Ion, D. I., Roeper, J., and Malenka, R. C. (2011). Projection-specific modulation of dopamine neuron synapses by aversive and rewarding stimuli. *Neuron* 70, 855–862. doi: 10.1016/j.neuron.2011.03.025

Li, X., Qi, J., Yamaguchi, T., Wang, H. L., and Morales, M. (2013). Heterogeneous composition of dopamine neurons of the rat A10 region: molecular evidence for diverse signaling properties. *Brain Struct. Funct.* 218, 1159–1176.

Lohr, K. M., Chen, M., Hoffman, C. A., McDaniel, M. J., Stout, K. A., Dunn, A. R., et al. (2016). Vesicular monoamine transporter 2 (VMAT2) level regulates MPTP vulnerability and clearance of excess dopamine in mouse striatal terminals. *Toxicol. Sci.* 153, 79–88. doi: 10.1093/toxsci/kfw106

Lüscher, C. (2016). The emergence of a circuit model for addiction. *Ann. Rev. Neurosci.* 39, 257–276.

Marinelli, S., Di Marzo, V., Berretta, N., Matias, I., Maccarrone, M., Bernardi, G., et al. (2003). Presynaptic facilitation of glutamatergic synapses to dopaminergic neurons of the rat substantia nigra by endogenous stimulation of vanilloid receptors. *J. Neurosci.* 23, 3136–3144. doi: 10.1523/JNEUROSCI.23-08-03136.2003

Marinelli, S., Di Marzo, V., Florenzano, F., Fezza, F., Viscomi, M. T., van der Stelt, M., et al. (2007). N-arachidonoyl-dopamine tunes synaptic transmission onto dopaminergic neurons by activating both cannabinoid and vanilloid receptors. *Neuropsychopharmacology* 32, 298–308. doi: 10.1038/sj.npp.1301118

Marinelli, S., Pascucci, T., Bernardi, G., Puglisi-Allegra, S., and Mercuri, N. B. (2005). Activation of TRPV1 in the VTA excites dopaminergic neurons and increases chemical- and noxious-induced dopamine release in the nucleus accumbens. *Neuropsychopharmacology* 30, 864–870. doi: 10.1038/sj.npp.1300615

Menegas, W., Bergan, J. F., Ogawa, S. K., Isogai, Y., Venkataraju, K. U., Osten, P., et al. (2015). Dopamine neurons projecting to the posterior striatum form an anatomically distinct subclass. *ELife* 4:e10032. doi: 10.7554/eLife.10032

Miller, H. H., Shore, P. A., and Clarke, D. E. (1980). In vivo monoamine oxidase inhibition by D-amphetamine. *Biochem. Pharmacol.* 29, 1347–1354. doi: 10.1016/0006-2952(80)90429-3

Mingote, S., Chuhma, N., Kalmbach, A., Thomsen, G. M., Wang, Y., Mihali, A., et al. (2017). Dopamine neuron dependent behaviors mediated by glutamate cotransmission. *ELife* 6:e27566. doi: 10.7554/eLife.27566

Mingote, S., Chuhma, N., Kusnoor, S. V., Field, B., Deutch, A. Y., and Rayport, S. (2015). Functional connectome analysis of dopamine neuron glutamatergic connections in forebrain regions. *J. Neurosci.* 35, 16259–16271. doi: 10.1523/JNEUROSCI.1674-15.2015

Mooslehner, K. A., Chan, P. M., Xu, W., Liu, L., Smadja, C., Humby, T., et al. (2001). Mice with very low expression of the vesicular monoamine transporter 2 gene survive into adulthood: potential mouse model for parkinsonism. *Mol. Cell. Biol.* 21, 5321–5331. doi: 10.1128/MCB.21.16.5321-5331.2001

Morales, M., and Margolis, E. B. (2017). Ventral tegmental area: cellular heterogeneity, connectivity and behaviour. *Nat. Rev. Neurosci.* 18:73.

Narboux-Nême, N., Sagné, C., Doly, S., Diaz, S. L., Martin, C. B. P., Angenard, G., et al. (2011). Severe serotonin depletion after conditional deletion of the vesicular monoamine transporter 2 gene in serotonin neurons: neural and behavioral consequences. *Neuropsychopharmacology* 36, 2538–2550. doi: 10.1038/npp.2011.142

Neisewander, J. L., Lucki, I., and McGonigle, P. (1991). Behavioral and neurochemical effects of chronic administration of reserpine and skf-38393 in rats. *J. Pharmacol. Exp. Therapeutics* 257:850.

Papathanou, M., Creed, M., Dorst, M. C., Bimpisidis, Z., Dumas, S., Pettersson, H., et al. (2018). Targeting VGLUT2 in mature dopamine neurons decreases mesoaccumbal glutamatergic transmission and identifies a role for glutamate co-release in synaptic plasticity by increasing baseline AMPA/NMDA Ratio. *Front. Neural Circ.* 12:64. doi: 10.3389/fncir.2018.00064

Patel, J., Mooslehner, K. A., Chan, P. M., Emson, P. C., and Stamford, J. A. (2003). Presynaptic control of striatal dopamine neurotransmission in adult vesicular monoamine transporter 2 (VMAT2) mutant mice: dopamine neurotransmission in VMAT2 mutant mice. *J. Neurochem.* 85, 898–910. doi: 10.1046/j.1471-4159.2003.01732.x

Phillips, R. A., Tuscher, J. J., Black, S. L., Ianov, L., and Day, J. J. (2021). An atlas of transcriptionally defined cell populations in the rat ventral tegmental area. *Neuroscience* [Preprint]. doi: 10.1101/2021.06.02.446737

Pontieri, F. E., Tanda, G., and Di Chiara, G. (1995). Intravenous cocaine, morphine, and amphetamine preferentially increase extracellular dopamine in the 'shell' as compared with the 'core' of the rat nucleus accumbens. *Proc. Natl. Acad. Sci. U.S.A.* 92, 12304–12308. doi: 10.1073/pnas.92.26.12304

Poulin, J. F., Caronia, G., Hofer, C., Cui, Q., Helm, B., Ramakrishnan, C., et al. (2018). Mapping projections of molecularly defined dopamine neuron subtypes using intersectional genetic approaches. *Nat. Neurosci.* 21:1260. doi: 10.1038/s41593-018-0203-4

Poulin, J. F., Gaertner, Z., Moreno-Ramos, O. A., and Awatramani, R. (2020). Classification of midbrain dopamine neurons using single-cell gene expression profiling approaches. *Trends Neurosci.* 43, 155–169. doi: 10.1016/j.tins.2020.01.004

Poulin, J. F., Zou, J., Drouin-Ouellet, J., Kim, K. Y. A., Cicchetti, F., and Awatramani, R. B. (2014). Defining midbrain dopaminergic neuron diversity by single-cell gene expression profiling. *Cell Rep.* 9, 930–943. doi: 10.1016/j.celrep.2014.10.008

Pupe, S., and Wallén-Mackenzie, Å (2015). Cre-driven optogenetics in the heterogeneous genetic panorama of the VTA. *Trends Neurosci.* 38, 375–386. doi: 10.1016/j.tins.2015.04.005

Ramírez-Barrantes, R., Cordova, C., Poblete, H., Muñoz, P., Marchant, I., Wianny, F., et al. (2016). Perspectives of TRPV1 function on the neurogenesis and neural plasticity. *Neural Plasticity* 2016, 1–12. doi: 10.1155/2016/1568145

Robinson, T. (1993). The neural basis of drug craving: an incentive-sensitization theory of addiction. *Brain Res. Rev.* 18, 247–291. doi: 10.1016/0165-0173(93)90013-P

Robinson, T. E., and Becker, J. B. (1986). Enduring changes in brain and behavior produced by chronic amphetamine administration: a review and evaluation of animal models of amphetamine psychosis. *Brain Res. Rev.* 11, 157–198. doi: 10.1016/0165-0173(86)90002-0

Roeper, J. (2013). Dissecting the diversity of midbrain dopamine neurons. *Trends Neurosci.* 36, 336–342. doi: 10.1016/j.tins.2013.03.003

Rubinstein, M., Muschietti, J. P., Gershanik, O., Flawia, M. M., and Stefano, F. J. (1990). Adaptive mechanisms of striatal D1 and D2 dopamine receptors in response to a prolonged reserpine treatment in mice. *J. Pharmacol. Exp. Ther.* 252, 810–816.

Salamone, J. D., and Correa, M. (2012). The mysterious motivational functions of mesolimbic dopamine. *Neuron* 76, 470–485. doi: 10.1016/j.neuron.2012.10.021

Scherrer, G., Low, S. A., Wang, X., Zhang, J., Yamanaka, H., Urban, R., et al. (2010). VGLUT2 expression in primary afferent neurons is essential for normal acute pain and injury-induced heat hypersensitivity. *Proc. Natl. Acad. Sci. U.S.A.* 107, 22296–22301. doi: 10.1073/pnas.1013413108

Schultz, W. (2016). Dopamine reward prediction-error signalling: a two-component response. *Nat. Rev. Neurosci.* 17, 183–195. doi: 10.1038/nrn.2015.26

Sulzer, D., Chen, T. K., Lau, Y. Y., Kristensen, H., Rayport, S., and Ewing, A. (1995). Amphetamine redistributes dopamine from synaptic vesicles to the cytosol and promotes reverse transport. *J. Neurosci.* 15, 4102–4108. doi: 10.1523/JNEUROSCI.15-05-04102.1995

Sulzer, D., and Rayport, S. (1990). Amphetamine and other psychostimulants reduce ph gradients in midbrain dopaminergic neurons and chromaffin granules: a mechanism of action. *Neuron* 5, 797–808. doi: 10.1016/0896-6273(90)90339-H

Szallasi, A., Cortright, D. N., Blum, C. A., and Eid, S. R. (2007). The vanilloid receptor TrpV1: 10 years from channel cloning to antagonist proof-of-concept. *Nat. Rev. Drug Dis.* 6, 357–372. doi: 10.1038/nrd2280

Tiklová, K., Björklund, ÅK., Lahti, L., Fiorenzano, A., Nolbrant, S., Gillberg, L., et al. (2019). Single-cell RNA sequencing reveals midbrain dopamine neuron

diversity emerging during mouse brain development. *Nat. Commun.* 10:581. doi: 10.1038/s41467-019-08453-1

Trudeau, L. E., Hnasko, T. S., Wallén-Mackenzie, A., Morales, M., Rayport, S., and Sulzer, D. (2014). The multilingual nature of dopamine neurons. *Prog. Brain Res.* 211, 141–164. doi: 10.1016/B978-0-444-63425-2.00006-4

Trudeau, L. E., and El Mestikawy, S. E. (2018). Glutamate cotransmission in cholinergic, gabaergic and monoamine systems: contrasts and commonalities. *Front. Neural Circ.* 12:113. doi: 10.3389/fncir.2018.00113

Viereckel, T., Dumas, S., Smith-Anttila, C. J. A., Vlcek, B., Bimpisidis, Z., Lagerström, M. C., et al. (2016). Midbrain gene screening identifies a new mesoaccumbal glutamatergic pathway and a marker for dopamine cells neuroprotected in Parkinson's disease. *Sci. Rep.* 6:35203. doi: 10.1038/srep35203

Wang, D. V., Viereckel, T., Zell, V., Konradsson-Geuken, Å, Broker, C. J., Talishinsky, A., et al. (2017). Disrupting glutamate co-transmission does not affect acquisition of conditioned behavior reinforced by dopamine neuron activation. *Cell Rep.* 18, 2584–2591. doi: 10.1016/j.celrep.2017.02.062

Wang, Y. M., Gainetdinov, R. R., Fumagalli, F., Xu, F., Jones, S. R., Bock, C. B., et al. (1997). Knockout of the vesicular monoamine transporter 2 gene results in neonatal death and supersensitivity to cocaine and amphetamine. *Neuron* 19, 1285–1296. doi: 10.1016/S0896-6273(00)80419-5

Watabe-Uchida, M., Zhu, L., Ogawa, S. K., Vamanrao, A., and Uchida, N. (2012). Whole-brain mapping of direct inputs to midbrain dopamine neurons. *Neuron* 74, 858–873. doi: 10.1016/j.neuron.2012.03.017

Conflict of Interest: SD is the owner of Oramacell, Paris.

The remianing authors declare that the research was conducted in the absence of any commercial or financial relationships that could be construed as a potential conflict of interest.

Publisher's Note: All claims expressed in this article are solely those of the authors and do not necessarily represent those of their affiliated organizations, or those of the publisher, the editors and the reviewers. Any product that may be evaluated in this article, or claim that may be made by its manufacturer, is not guaranteed or endorsed by the publisher.

Copyright © 2021 Serra, Guillaumin, Dumas, Vlcek and Wallén-Mackenzie. This is an open-access article distributed under the terms of the Creative Commons Attribution License (CC BY). The use, distribution or reproduction in other forums is permitted, provided the original author(s) and the copyright owner(s) are credited and that the original publication in this journal is cited, in accordance with accepted academic practice. No use, distribution or reproduction is permitted which does not comply with these terms.

frontiers in Neural Circuits

ORIGINAL RESEARCH
published: 19 November 2021
doi: 10.3389/fncir.2021.769342

Dendritic Architecture Predicts *in vivo* Firing Pattern in Mouse Ventral Tegmental Area and Substantia Nigra Dopaminergic Neurons

Trinidad Montero[1†], Rafael Ignacio Gatica[1†], Navid Farassat[2], Rodrigo Meza[1], Cristian González-Cabrera[1], Jochen Roeper[2] and Pablo Henny[1]*

[1] Laboratorio de Neuroanatomía, Departamento de Anatomía, and Centro Interdisciplinario de Neurociencia, NeuroUC, Escuela de Medicina, Pontificia Universidad Católica de Chile, Santiago, Chile, [2] Institute of Neurophysiology, Goethe University, Frankfurt, Germany

The firing activity of ventral tegmental area (VTA) and substantia nigra pars compacta (SNc) dopaminergic (DA) neurons is an important factor in shaping DA release and its role in motivated behavior. Dendrites in DA neurons are the main postsynaptic compartment and, along with cell body and axon initial segment, contribute to action potential generation and firing pattern. In this study, the organization of the dendritic domain in individual VTA and SNc DA neurons of adult male mice, and their relationship to *in vivo* spontaneous firing, are described. In comparison with dorsal VTA DA neurons, ventrally located VTA neurons (as measured by cell body location) possess a shorter total dendritic length and simpler dendritic architecture, and exhibit the most irregular *in vivo* firing patterns among DA neurons. In contrast, for DA neurons in the SNc, the higher irregularity of firing was related to a smaller dendritic domain, as measured by convex hull volumes. However, firing properties were also related to the specific regional distribution of the dendritic tree. Thus, VTA DA neurons with a larger extension of their dendritic tree within the parabrachial pigmented (PBP) nucleus fired more regularly compared with those with relatively more dendrites extending outside the PBP. For DA neurons in the SNc, enhanced firing irregularity was associated with a smaller proportion of dendrites penetrating the substantia nigra pars reticulata. These results suggest that differences in dendritic morphology contribute to the *in vivo* firing properties of individual DA neurons, and that the existence of region-specific synaptic connectivity rules that shape firing diversity.

Keywords: dopamine, substantia nigra, ventral tegmental area, dendritic morphology, firing properties, neuronal tracing

OPEN ACCESS

Edited by:
Jean-Francois Poulin, McGill University, Canada

Reviewed by:
John T. Williams, Oregon Health & Science University, United States
Qian Li, Washington University School of Medicine in St. Louis, United States

***Correspondence:**
Pablo Henny
pablohenny@uc.cl

† These authors have contributed equally to this work and share first authorship

Received: *01 September 2021*
Accepted: *12 October 2021*
Published: *19 November 2021*

Citation:
Montero T, Gatica RI, Farassat N, Meza R, González-Cabrera C, Roeper J and Henny P (2021) Dendritic Architecture Predicts in vivo Firing Pattern in Mouse Ventral Tegmental Area and Substantia Nigra Dopaminergic Neurons. Front. Neural Circuits 15:769342. doi: 10.3389/fncir.2021.769342

INTRODUCTION

Dopaminergic neurons of the substantia nigra pars compacta (SNc) and ventral tegmental area (VTA) are involved in important brain functions, such as movement, behavioral reinforcement, and learning (Wise, 2004; Schultz, 2007; Fahn, 2008; Redgrave et al., 2008; Berke, 2018). Dopaminergic (DA) neurons exhibit an autonomous, pacemaker-type of firing that depends on

intrinsic membrane properties and is typically responsible for the observed regular or tonic firing of DA neurons in the absence of synaptic input (Gantz et al., 2018). On the other hand, excitatory synaptic activity can lead to phasic and/or irregular firing, as typically observed *in vivo*, and, conversely, afferent inhibitory activity produces a decrease or halt in firing (Paladini and Roeper, 2014; Gantz et al., 2018). While tonic, regular activity contributes to the maintenance of a basal level of dopamine release in targeted regions such as the striatum (Schultz, 2007; Sulzer et al., 2016), phasic increase or decrease in DA release, on the other hand, may allow for plastic changes in postsynaptic structures in association to preference or avoidance learning (Schultz, 2007; Chang et al., 2015, 2018).

Anatomical studies demonstrated that in SNc and VTA DA neurons the vast majority of synaptic inputs occurs in the dendritic field (Rinvik and Grofová, 1970; Bolam and Smith, 1990; Bayer and Pickel, 1991; Henny et al., 2012) as compared with less frequent innervation of somatic (Rinvik and Grofová, 1970) or axon initial segment (González-Cabrera et al., 2017) compartments. This is also in line with evidence from single cell reconstructions that show dendrites account for up to 90% of the somatodendritic surface in nigral neurons (Meza et al., 2018). Considering the role that synaptic inputs play in the firing behavior of DA neurons, understanding how the dendritic domain is organized in this population and how it relates to single cell behavior *in vivo* is a critical issue to examine.

The role that dendrites, more specifically dendritic spatial organization, plays in the *in vivo* firing behavior of DA neurons has only been partially examined. For instance, we have previously shown that in rat SNc DA neurons the likelihood of firing to decrease or pause after nociceptive stimulation is associated with the extension of dendrites that penetrate the underlying substantia nigra pars reticulata (SNr) (Henny et al., 2012). Because SNr penetrating dendrites receive a much denser afferent inhibitory innervation than those located in the SNc, they may be thought as a distinctive compartment involved in mediating inhibition (Hajós and Greenfield, 1994; Henny et al., 2012). We have also examined recently the role that the somatic and dendritic domains play in *in vivo* spontaneous firing frequency in mouse nigral DA neurons and found that, in this case, spontaneous firing frequency did not seem to depend strongly on somatodendritic surface (the vast majority of which corresponds to dendrites, as indicated above). In contrast, the firing rate is related much more strongly with axon initial segment size or position (Meza et al., 2018).

With these antecedents in mind, we set out a study to (1) quantitatively describe the dendritic organization of mouse SNc and VTA DA neurons at the individual cell level, with special attention to the course of dendrites across substantia nigra and VTA regional subdivisions (Fu et al., 2012) and to (2) assess the relationship between the dendritic organization and firing pattern. For that, we performed *in vivo* juxtacellular labeling and vector-based 3D reconstruction (Henny et al., 2014; Meza et al., 2018; Farassat et al., 2019) of the complete somatodendritic domain of 15 SNc and 15 VTA DA neurons of adult mice, and analyzed in 25 of these neurons spontaneous firing rate and firing pattern.

Our results suggest that individual neuron morphology and heterotopic extension of dendrites across adjacent anatomical subdivisions within substantia nigra and VTA play an important role in shaping *in vivo* firing pattern, and suggest region-specific anatomical rules underlying firing diversity.

MATERIALS AND METHODS

Animals

The reported experimental procedures and results were obtained from 25 adult male C57BL/6J mice. The animals were obtained from the animal house at the Faculty of Biological Sciences, Pontificia Universidad Católica de Chile, and were approved by the Ethics Committees of the School of Medicine of the Pontificia Universidad Católica de Chile which conform to the guidelines of the Comisión Nacional de Investigación Científica y Tecnológica (CONICYT) and the United States National Institutes of Health (NIH). Experimental procedures for a further five adult male C57BL/6N mice were performed at Goethe University, Germany and approved by German Regierungspraesidium Darmstadt (V54-19c20/15-F40/28), as also reported in Farassat et al. (2019).

Recording and Labeling of Single Neurons

Ten SNc neuronal reconstructions came from a pool of neurons that had their electrophysiology, general dendritic arrangement, and axon initial segment described (Meza et al., 2018), and were selected for this study because their mediolateral (ML), dorsoventral (DV), and anteroposterior (AP) localization within the SNc could be unambiguously determined, thus making them suitable for the localization analysis reported here. Additionally, using the same methodological approach, two recently labeled and reconstructed SNc DA neurons from two adult mice (23–30 g) were added. These 12 SNc neurons were used in this study for anatomical and physiological analysis. Three further SNc DA neurons came from a pool of neurons recently characterized (Farassat et al., 2019) and were selected only for the anatomical analysis included in this study based on the quality and completeness of their dendritic labeling, which allowed for a complete reconstruction of their somatodendritic domain. As a result, 12 SNc neurons were used for anatomical and physiological analysis (see below), and three others for purely anatomical analysis. Regarding the VTA, 13 neurons were recorded, labeled, and completely filled with tracer, and their somatodendritic domain was 3D reconstructed. These 13 neurons were used in this study for anatomical and physiological analysis. Two further VTA DA neurons came from a pool of neurons recently characterized (Farassat et al., 2019) and were deemed suitable for a complete reconstruction of their dendritic tree by the quality and completeness of their dendritic labeling.

Anesthesia was initially induced with isoflurane (Isoflurano USP; Baxter Healthcare, USA) and maintained with urethane (1.5 g per kg, i.p., ethyl carbamate; Sigma, Germany). The animals were placed in a rat stereotaxic frame adapted to mice using a MA-6N head-holding adaptor (Narishige, Japan). Body temperature was maintained at 37°C using a homeothermic

heating device (ATC 1000; World Precision Instruments, USA). Anesthesia levels were assessed by examination of the electrocorticogram (ECoG) and by testing reflexes to cutaneous pinch or gentle corneal stimulation. Topical benzocaine (20%, Mayon) and a PBS solution with pH 7.4 were applied to all surgical incisions to prevent pain and dehydration, respectively. Extracellular recordings of single-unit activity were made using borosilicate glass electrodes (1–1.5 μm diameter, tip resistance 10–15 MΩ or < 1 μm diameter and tip resistance 35–45 MΩ depending on the labeling method used (see below); World Precision Instruments), and obtained using a vertical puller (PC-10 model; Narishige Scientific Instrument Laboratory, Japan). Pipettes were filled with a solution consisting of 0.5 M NaCl or 0.25 M K + -gluconate and 1.7% neurobiotin (w/v; Vector Laboratories, USA). A single-axis *in vivo* micromanipulator (IVM-1000; Scientifica, United Kingdom) connected to an ultralow noise IU controller rack was used to descend electrodes in the z-axis into the brain. Stereotaxic coordinates for VTA single-unit recording were derived from Franklin and Paxinos (2007) (AP: −3.1 mm, ML: 0.4 mm, see Meza et al. (2018) for the description of experiments for SNc DA neurons labeling). Following single cell recordings, the neurons were labeled with the juxtacellular method (Pinault, 1996) or through intracellular access. Briefly, in the first method, the electrode was advanced slowly toward the neurons while a microiontophoretic square current was applied (2–10 nA positive current, 200 ms duration, 50% duty cycle). The optimal position of the electrode was identified when the firing of the neuron was robustly modulated by the positive current injection. Modulation was performed for at least 5 min to obtain reliable labeling. In the second protocol, for VTA DA neurons, after the extracellular recordings were made, using a 35–50-ΩM electrode, AC pulses were given in order to gain intracellular access. The amount of current in each AC pulse was progressively increased, and the electrode moved closer in 2 μm steps until the intracellular medium was accessed (evidenced by spike waveform change from biphasic to monophasic and a small negative shift in potential measured by the electrode; 5 to 25 mV). Then, if necessary, the electrode was moved up to 2 μm closer to the cell, and the recording was stabilized by the negative current. For labeling, a micro square current was applied (0.4–1 nA positive current, 200 ms duration, 50% duty cycle) for 10–20 min. In both protocols, after the current injection, the neurobiotin was left to transport along neuronal processes for at least 2 h. After the labeling sessions, the animals were perfuse-fixed with 25 ml of PBS, pH 7.4, followed by 50 ml 4% paraformaldehyde (w/v) in phosphate buffer, pH 7.4. Finally, the brains were post-fixed in 4% paraformaldehyde in PBS overnight, maintained in 30% sucrose in distilled water for 48 h, and sectioned.

Electrophysiological Analysis

Electrophysiological analysis was carried out for the 25 (12 SNc and 13 VTA, see above) DA neurons that were recorded under urethane anesthesia. The other five neurons (three SNc and two VTA) were not analyzed as they came from a pool of neurons previously characterized using an alternative anesthetic regime (Farassat et al., 2019), which made direct electrophysiological comparisons difficult. Measurements of spike firing rate (FR), coefficient of variation (CV), coefficient of variation 2 (CV2), and percentage of spikes in bursts (% SIB) were taken from 3–15 min of spontaneous activity before the labeling session. Following spontaneous activity and before labeling, a strong somatosensory stimulus challenge was applied to the hind paw, the analysis of which will be reported elsewhere. To determine FR, the spontaneous activity train was binned into 0.5 s bins, and frequency was determined for each bin and averaged. CV was calculated as the standard deviation divided by the mean of the inter-spike intervals (ISI). CV2 was calculated for every single spike in the time series. As such, the standard deviation of the two adjacent ISIs was calculated and then divided by their mean and finally multiplied by $\sqrt{2}$. The overall reported CV2 is the average of every spike CV2 (Holt et al., 1996). The percentage of spikes in burst (% SIB) was determined from a suitable open access script developed by CED to interface with Spike2[1]. Bursts were composed of at least three spikes, and the classical criteria outlined by Grace and Bunney (1984) were used: a burst begins when two action potentials occur within 80 ms of each other and ends when an ISI greater than 160 ms occurs.

Neuronal Identification

The brains were cut in the coronal plane on a freezing-stage microtome (Reichert–Jung Hn-40) at 25 or 40 μm. All midbrain-containing sections were incubated with Cy3-conjugated streptavidin (1:1,000; Jackson ImmunoResearch, USA) for 2–3 h to reveal the neurobiotin. After mounting, the sections were examined with an epifluorescent microscope (Nikon Eclipse Ci; Nikon, Japan) to confirm that the neurons were completely filled with tracer. One or two sections were selected, blocked with 3% normal horse serum (NHS) in PBS (v/v; Jackson ImmunoResearch), and incubated with a guinea pig anti-tyrosine hydroxylase (TH) antibody (1:1,000; Synaptic Systems, Germany) in PBS, 3% NHS, and.3% Triton-X overnight at room temperature. They were then incubated in Alexa Fluor 488 or Dylight 405-conjugated donkey anti-guinea pig antibody (1:1,000; Jackson ImmunoResearch). Three to four 8-min washes were performed in between and after incubation in streptavidin or antibodies. Labeling for neurobiotin and colocalization of neurobiotin-labeled processes with TH was assessed. Only neurons that were neurochemically identified as DA neurons by immunoreactivity for TH were analyzed further. An almost identical protocol was used for SNc DA neuron identification [see Meza et al. (2018) for further details]. Three SNc and two VTA DA neurons were identified as previously described in Farassat et al. (2019).

Microscopy and Imaging

For the 13 VTA and 12 SNc DA neurons, fluorescence imaging for all neurobiotin-labeled profiles across sections was performed with one of the following three laser-scanning confocal microscopes: Nikon Eclipse C2, using the NIS-Elements C program (Nikon software) to acquire and export images (12 SNc and 3 VTA neurons), Zeiss LSM 700, using the ZEN2012

[1]http://ced.co.uk/downloads

program (Zeiss software) (2 VTA neurons), and Olympus FV1000 using the Fluoview program (Olympus software) (7 VTA neurons). Low-magnification images were acquired with appropriate 10× and 20× objectives. High-magnification and z-stack images were acquired with a 60× oil or water immersion objective (1.3–1.4 numerical aperture). Images taken for 3D neuronal reconstruction were 512 pixels × 512 pixels in size with a resolution of 0.19 (2 VTA neurons) or 0.41 μm/pixel (12 SNc and 11 VTA neurons) and taken in z-stacks of 0.5 μm steps between images. To ensure the best signal-to-noise ratio in all the stack images, maximum and minimum intensity pixels were established independently in each channel and for each z-stack acquired during the acquisition sessions using the appropriate software [see also Meza et al. (2018)]. For the three SNc and two VTA DA neurons, high magnification z-stacks of juxtacellularly labeled neurons were acquired with a 60× oil immersion objective (1.4 numerical aperture) using a laser-scanning microscope (Nikon Eclipse90i, Nikon GmbH) and the NIS-Elements C program (Nikon software) with a 1,024 pixel × 1,024 pixel size [for further details see Farassat et al. (2019)].

Neuronal Reconstructions

The dendritic domain of neurons selected for digital reconstruction was completely filled, and all of the dendrites extended to natural tapering ends. The axon was traced as it branched off from a proximal dendrite or cell body (Meza et al., 2018), did not exhibit local collaterals, and was followed until it eventually joined the nigrostriatal or medial forebrain bundle pathways, where its signal usually started to fade out. Neurons were reconstructed in three dimensions from all the z-stack images taken with the confocal microscope using Neurolucida (MBF Bioscience, USA). Neuronal fragments from every section were traced onto a corresponding digital section using the Serial Section Manager in Neurolucida (Henny et al., 2014). For the entire somatodendritic domain, a correction factor in the z-axis was applied to account for the shrinkage that follows dehydration and histological processing, which, in 25 cases, was approximately 50% and in five cases (from Farassat et al., 2019) was 34%. Quantitative data for anatomical parameters were obtained using the Neurolucida Explorer software.

Morphological Analyses

To determine the location of each reconstructed SNc and VTA DA neuron, double immunostaining for TH and neurobiotin was performed in the section containing the soma or dendrite. The SNc and VTA were delimited in the TH-stained cell body section and compared with the sections provided by Franklin and Paxinos (2007) and Fu et al. (2012). Then, a virtual 3D map of the substantia nigra [SN, including pars compacta (SNc), pars lateralis (SNl), and pars reticulata (SNr)], all VTA constituent nuclei [including rostral VTA (VTAR), parabrachial pigmented (PBP), paraintrafascicular (PIF), paranigral (PN), infrascapular (IF), and caudal (CLi) and rostral (RLi) linearis], and relevant landmark tracts, was created in Neurolucida based on a recent study that re-assessed the boundaries and cyto-architecture of DA cluster groups (Fu et al., 2012). We decided to aggregate, in a single subdivision (SNc), all the SNc clusters defined by Fu et al. (2012), except the SNl, which we left apart as a different nucleus. Individual neuronal reconstructions were placed in the 3D map according to the ML, DV, and AP locations of the cell body obtained from the TH immunostaining. The neuronal reconstructions were further tilted-corrected by matching the position of the furthest dendritic tips to anatomical landmarks, to the best of our possibilities. Reconstructions of neurons labeled in the left hemisphere were vertically flipped and projected onto the right hemisphere. To predict the proportion of dendrites in a given subdivision, the entire neuronal reconstruction and 3D map were observed in the 3D module of Neurolucida, and rotated until the approximate location of a dendrite as it coursed through an adjacent subdivision was determined. Dendrites were detached from the main reconstruction and analyzed separately. Physical and topological data of dendrites and entire dendritic domains were taken from the Neurolucida Explorer software.

Statistical Analysis

To assess whether data sets were normally distributed, we performed single-sample Kolmogorov–Smirnov test or, if the n was too small, Shapiro–Wilk normality test in all the data sets. For parametric data, unpaired *t*-test was performed (**Figure 4**). Non-parametric tests were performed on non-normally distributed data; two-tailed Mann–Whitney U tests (**Figure 4**) and Spearman correlation were performed (**Figures 2**, **4–7** and **Supplementary Tables 1, 3–5**). Significance for all the statistical tests was set at $p < 0.05$. Boxplots are explained in **Figure 4** legend. All the statistical analyses were performed using GraphPad Prism 7.

RESULTS

Given the role of the dendritic domain in the afferent connectivity and activity of a neuron, two main questions guided this study. First: what are the architectural characteristics that define the dendritic domain of individual mouse SNc and VTA DA neurons? And, second: does the dendritic domain architecture relate to *in vivo* spontaneous firing activity at the individual cell level? To address these questions, we reconstructed the somatodendritic domain of DA neurons in 3D. We used the juxtacellular technique to label one neuron per hemisphere, either in the SNc or the VTA (Meza et al., 2018; Farassat et al., 2019) and subsequently identified them as DA by the expression of the catecholamine synthetic enzyme tyrosine hydroxylase (TH) (**Figure 1A**). We determined the ML, DV and AP locations of the cell bodies of reconstructed neurons in relation to the standard map of Fu et al. (2012). The cell bodies of labeled neurons located across the SNc (15 neurons) and VTA (15 neurons) (**Figures 1B,C**). In the case of SNc, cell bodies located at the central (in relation to mediolateral coordinates) and slightly posterior locations. In the case of the VTA, the cell bodies tended to locate at the more medial and anterior locations. In the VTA, 13 cell bodies located at various DV depths in the PBP (**Figure 1C**), and two others located in the PN and a VTAR, near the PBP (**Figure 1C**).

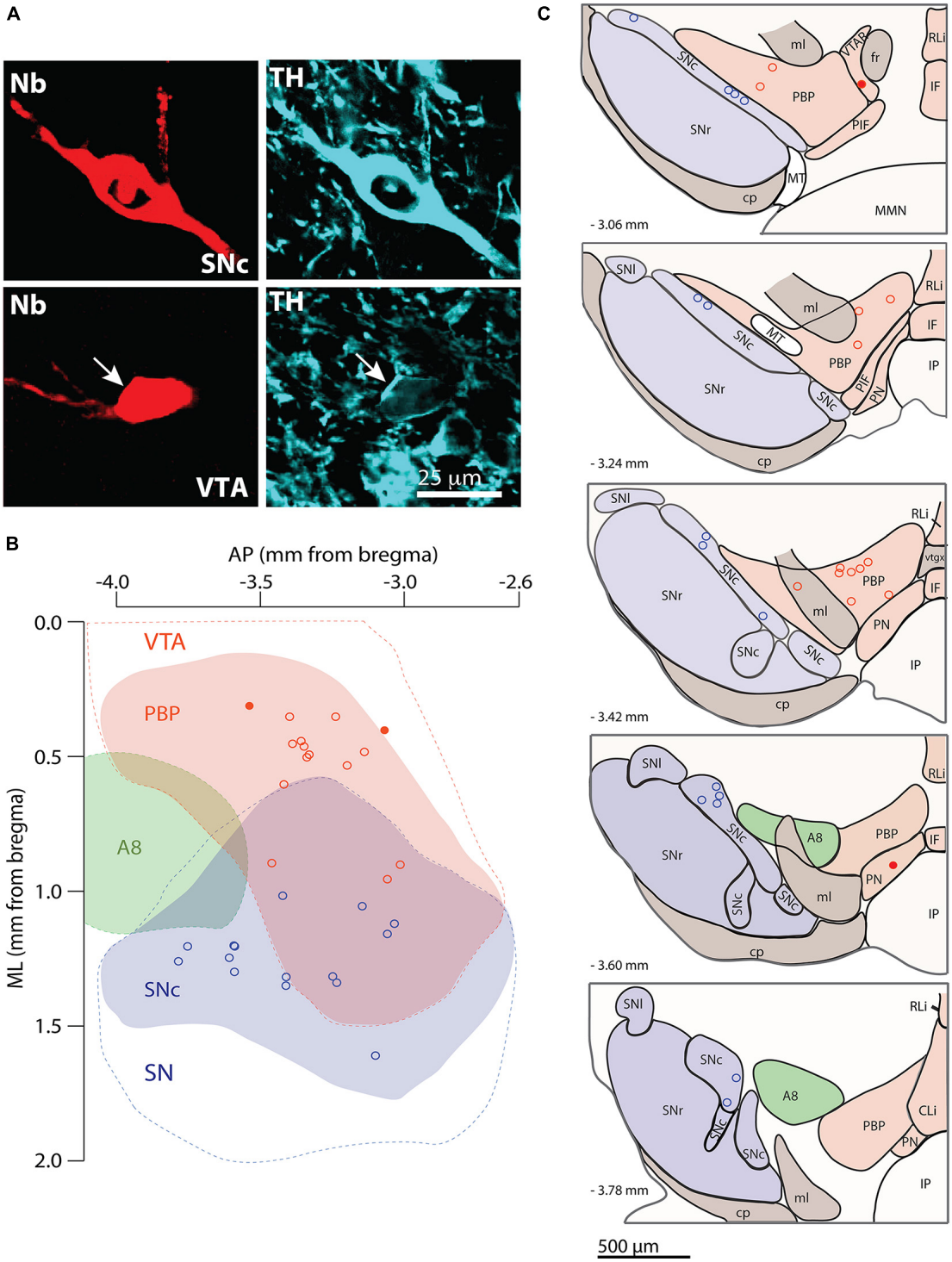

FIGURE 1 | Labeling, identification, and cell body localization of dopaminergic (DA) neurons. **(A)** SNc (top) and VTA (bottom, arrow) neurons were labeled with neurobiotin (red, left) and expressed tyrosine hydroxylase immunoreactivity (cyan, right, arrow in bottom image). **(B,C)** Location of cell bodies of the 15 SNc and 15 VTA DA neurons used in this study in one **(B)** dorsal and five **(C)** frontal views. Blue, red, and green shades indicate the SNc, PBP, and A8 groups, respectively. Blue and red dashed lines indicate the substantia nigra and VTA regions, respectively in panel **(B)**. AP, anteroposterior; ML, mediolateral; CLi, caudal linear nucleus; cp, cerebral peduncle; fr, fasciculus retroflexus; IF, interfascicular nucleus; IP, interpeduncular nucleus; ml, medial lemniscus; MMN, medial mammillary nuclei; MT, medial terminal nucleus; PBP, parabrachial pigmented nucleus; PIF, parainterfascicular nucleus; PN, paranigral nucleus; RLi, rostral linear nucleus; SN, substantia nigra; SNc, substantia nigra pars compacta; SNl, substantia nigra compacta pars lateralis; SNr, substantia nigra pars reticulata; VTAR, rostral VTA.

Physical and Topological Characteristics of Mouse Dopaminergic Neurons

We examined whether the architectural features of the dendritic tree differ between SNc and VTA DA neurons and, more generally, whether cell body position in these areas was a good predictor of dendritic tree architecture. To do that, the dendritic tree of labeled SNc and VTA DA neurons were reconstructed and analyzed by its physical and topological characteristics. For physical characteristics, we analyzed total dendritic length (the actual tortuous length, as taken from reconstructions) and convex hull volume [which corresponds to the polygon connecting the most distant dendritic tips or inflections of the dendritic domain of a neuron, as if a "plastic sheet (was) wrapped around the entire neuron"[2]], and used these characteristics as a proxy for volumetric maximal extension of the dendritic domain (Gertler et al., 2008; Vrieler et al., 2019). For topological characteristics, we analyzed number of primary trees, maximum dendritic branch order, and number of dendritic segments (the latter is closely related to number of dendritic nodes and ends). Quantitative analysis showed differences of up to 4 or 5 times in dendritic length and topological parameters between neurons, and over 10 times in convex hull volumes in both SNc (Meza et al., 2018) and VTA (**Figure 2** and **Table 1**) populations. Regional comparisons showed that the SNc and VTA neurons did not differ in physical or topological characteristics (**Table 1**).

Because previous studies have reported that cell bodies of physiologically distinctive or projection-specific subpopulations aggregate at certain locations in the SNc or VTA (Lammel et al., 2008; Brischoux et al., 2009; Farassat et al., 2019), we wonder whether the dendritic morphology of neurons could also depend on cell body location within these regions. In the case of SNc neurons, we found that morphological characteristics did not relate to the position in the DV (**Figures 2B,C1,D1**), ML and AP axes (**Supplementary Table 1**). In the VTA, on the other hand, we found a positive correlation among DV position and dendritic length (**Figure 2B2**), number of dendritic segments (**Figure 2C2**), and maximum dendritic order (**Supplementary Table 1**), in that the dendritic tree of neurons whose cell bodies locate more dorsally shows longer dendrites that are arranged in a more complex manner. A positive relationship between DV position and maximum dendritic order (**Supplementary Table 1**) and number of segments (**Figure 2C3**) was also found when the SNc and VTA neurons were pooled together. Dendritic domain convex hull volumes did not correlate with cell body position for SNc, VTA, or the entire population. In summary, the results show that dendritic morphological diversity is related to cell body position in the VTA and entire population, in that the dendritic length and complexity of VTA neurons increase toward more dorsal positions. They also indicate that morphological diversity could be a factor underlying differences in electrophysiological profile across neurons within the VTA and substantia nigra regions.

[2]https://www.mbfbioscience.com/help/nx11/Content/Analyses/Convex_Hull_Analysis.htm

Course of Individual Neuron Dendritic Tree Across SNc and VTA Regions and Subdivisions

Because the substantia nigra and the VTA encompass several cytoarchitectonic subdivisions (Fu et al., 2012), that in the case of substantia nigra are well characterized to be neurochemically and hodologically distinctive (Bolam and Smith, 1990; Bolam et al., 1991; Comoli et al., 2003; Henny et al., 2012) we estimated the dendritic extension across different subdomains for individual neurons. To do that, we created a common 3D map of the substantia nigra, VTA, and respective subdivisions. Then we placed the reconstructions inside according to the location of their cell bodies (**Figure 3**) and in-tissue confirmed orientation of the dendritic tree (see section "Materials and Methods"). In general, most SNc neurons had dendrites descending into the SNr (**Figure 3A**), and some toward adjacent VTA (**Figure 3B**) and other nearby regions. In the case of PBP-located VTA neurons, the neurons extended dendrites into the underlying PIF and PN subdivisions (**Figure 3A**), and sometimes into the substantia nigra (**Figure 3B**). We quantified for each SNc neuron the proportion of dendrites in different nuclei and found that in the SNc neurons, an average of 39% of dendrites stayed in the SNc, over 33% in SNr, and the rest toward other adjacent regions, namely, dorsal tegmentum and adjacent lateral limb of the PBP (**Supplementary Table 2**). In the case of the VTA neurons, which in our sample included 13 neurons in the PBP and 2 in adjacent PN and VTAR, most dendrites located in the PBP (73%) and adjacent PIF and PN, or midline VTA nuclei (11%). We also observed occasional crossing-over to the adjacent substantia nigra (7%) (**Supplementary Table 2**). Given that subdivisions are characterized not only because of cytoarchitectural features of the resident neuronal somata (Fu et al., 2012) but also the specific pattern of afferent innervation and neurochemistry (Bolam and Smith, 1990; Bolam et al., 1991; Comoli et al., 2003; Henny et al., 2012), the results indicate the capacity of neurons to sample and integrate inputs arriving at differentiated loci. From a cellular point of view, these results also show that the dendritic tree of DA neurons can be seen as a multicompartmental domain, as it is the case for rat SNc neurons (Hajós and Greenfield, 1994; Henny et al., 2012) and may play a role in physiological diversity.

Cell Body Position and Spontaneous *in vivo* Activity

In order to examine the relationship between single cell dendritic morphology and spontaneous activity, we analyzed the firing behavior of 25 out of the 30 neurons (12 from SNc and 13 from VTA, see section "Materials and Methods"). We chose these 25 neurons because they all had been recorded under the same anesthetic regime (urethane). We found that spontaneous firing rate did not differ between the SNc and VTA neurons [$t(23) = 1.625$, $p = 0.1177$ unpaired t-test, **Figures 4A,B**], which could in part be explained by the large firing rate variability in the VTA group (**Figure 4B**). On the other hand, we found that the SNc neurons fired significantly more regularly than the VTA neurons, as evidenced by lower CV and CV2 values [CV: $U = 36.5$, $p = 0.028$ Mann–Whitney test; CV: $t(23) = 2.84$,

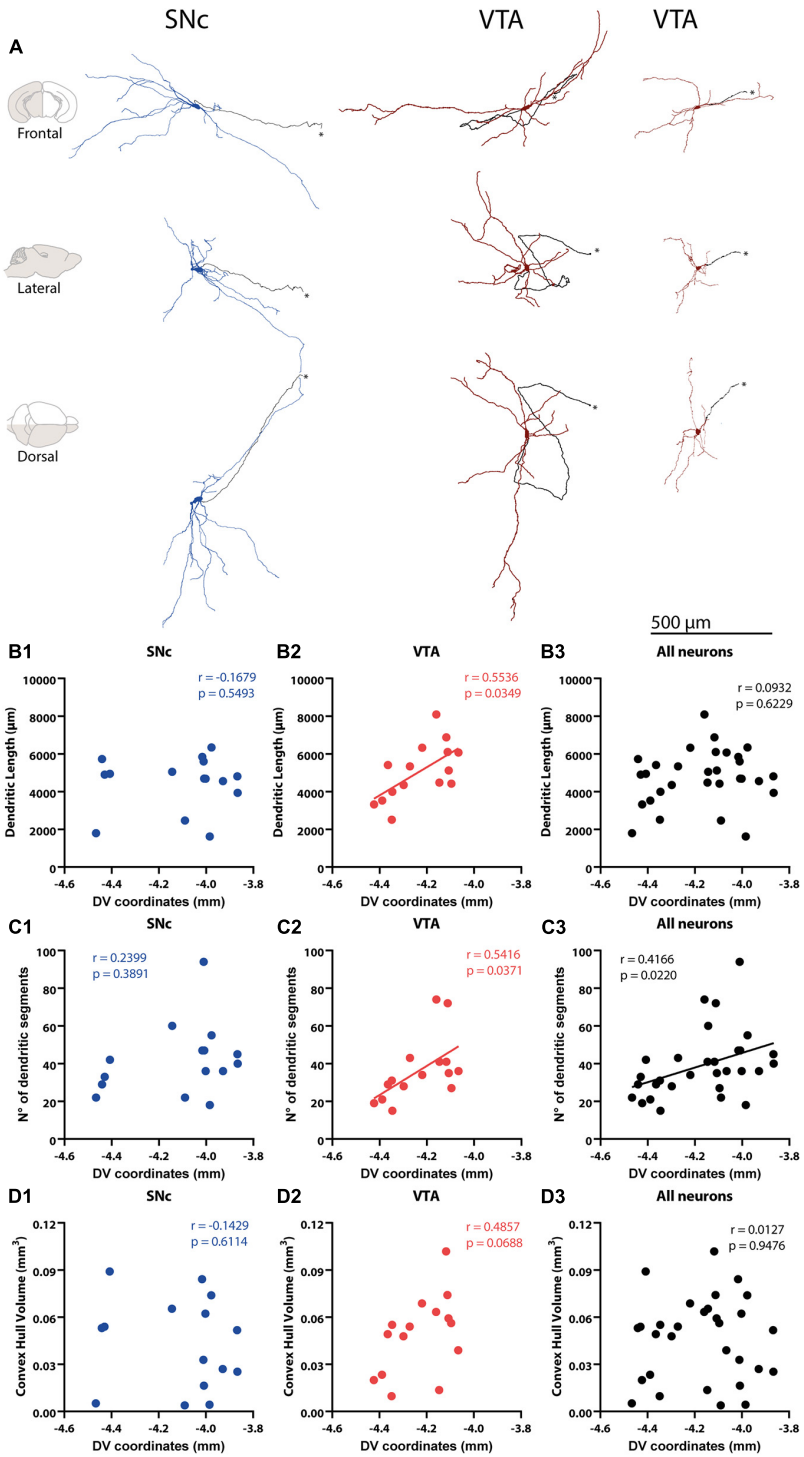

FIGURE 2 | Reconstruction and correlation between morphological characteristics and cell body localization. **(A)** Identified SNc and VTA DA neuron 3D reconstructions. Arranged in columns, one SNc, and two VTA DA neurons are shown from the frontal (top), lateral (middle), and dorsal (bottom) views. Axons are shown in black in all panels and pinpointed with an *. Brain diagrams to the left indicate hemisphere depicted (in gray) and view. **(B1–D3)** Correlations between physical (dendritic length, convex hull) and topological (number of dendritic segments) measures and cell body position of 3D reconstructed SNc and VTA DA neurons. A positive correlation was found between total dendritic length and DV coordinates of VTA neurons **(B2)**, but this was not observed for SNc **(B1)** or all DA neurons pooled together **(B3)**. Number of dendritic segments and DV coordinates were positively correlated in VTA **(C2)**, and when all neurons were pooled together **(C1)** with no correlation observed for SNc DA neurons **(C2)**. No correlation was found between convex hull volume and DV position with all DA neurons **(D1)**, or for SNc **(D2)**, VTA **(D3)** for all DA neurons **(D1)**. Figure only shows correlations between morphology and DV position. Refer to the Results section and **Supplementary Table 1** for correlations between morphology and mediolateral (ML) and anteroposterior (AP) axis positions.

TABLE 1 | Cell body and dendritic arbor size and complexity measures in ventral tegmental area (VTA) and substantia nigra pars compacta (SNc) reconstructed neurons.

Parameter	SNc (n = 15)			VTA (n = 15)		
	Average	SEM	Range	Average	SEM	Range
Dendritic Length (μm)	4,463	370	1,618–6,339	5,062	383	2,508–8,094
Soma Surface Area (μm^2)	1,692	200	765–3,168	1,359	152	670–2,927
Convex Hull volume (mm^3)	0.0432	0.0075	0.0038–0.0890	0.0490	0.0064	0.0097–0.1019
Dendritic Trees N°	5.4	0.43	2–8	4.90	0.36	2–7
Max. Dendritic order	6.4	0.63	3–13	6.08	0.50	3–9
Number of segments	41.7	4.86	18–94	36.50	4.37	15–74

Depending on the distribution of the data-sets, an unpaired t-test or Mann–Whitney test was performed, and no significant differences were found between groups in the parameters tested.

p = 0.0093 unpaired t-test, **Figures 4A,C**]. We did not find a significant difference between groups at the level of bursting activity, computed as the percentage of spikes in burst (SFB) [$t(23)$ = 1.629, p = 0.117 unpaired t-test]. We did notice, however, that the number of neurons showing at least one burst event was larger in the VTA sample (10 out of 13 neurons) than in the SNc sample (6 out of 12). We noticed that the overall incidence of bursting activity in neurons appeared low, which, in part, could be explained by the use of urethane that, as shown for SNc neurons, reduces bursting activity (Tepper et al., 1995).

We checked whether cell body localization correlated with electrophysiological characteristics (**Figures 4E,F** and **Supplementary Table 3**). We found that firing rate increased toward dorsal positions when we pooled both the SNc and VTA neurons together (r = 0.4223, p = 0.0365 Spearman correlation, **Figure 4E3**), although this relation was lost when observed in each region separately (SNc: r = 0.4545, p = 0.1404, VTA: r = 0.3187, p = 0.2286 Spearman correlation, **Figures 4E1,E2** and **Supplementary Table 3**). We also found that firing irregularity increased toward more ventral positions when all the neurons were pooled together, reflected in larger CV at deeper DV positions (r = −0.5457, p = 0.0048 Spearman correlation, **Figure 4F3**). That relationship was maintained for the VTA neurons alone (r = −0.6593, p = 0.0171 Spearman correlation, **Figure 4F2** and **Supplementary Table 3**) although not for the SNc neuron (r = −0.0982, p = 0.7613 Spearman correlation, **Figure 4F1** and **Supplementary Table 3**) values. Firing activity was also studied in relation to location of the cell body in the ML and AP axes. When considering all neurons, a negative relationship between the ML position and CV (also CV2) values was found (CV: r = 0.4491, p = 0.0243 Spearman; CV2: r = 0.4047, p = 0.0448 Spearman correlation, **Supplementary Table 3**), in that more lateral neurons fired more regularly, reflecting the already mentioned significant difference in regularity between the SNc and VTA neurons (**Figures 4C,D**). We also found that the neurons fired more irregularly at posterior positions (CV2: r = 0.4359, p = 0.0294 Spearman correlation, **Supplementary Table 3**). Finally, we observed that more anterior localization was associated to faster firing in the case of SNc neurons (r = −0.6993, p = 0.0145 Spearman correlation, **Supplementary Table 3**) and more bursting activity in the case of VTA neurons (SIB: r = 0.6630, p = 0.0135 Spearman correlation, **Supplementary Table 3**). In summary, cell body position was a good, although complex, predictor of spontaneous firing behavior in DA neurons.

Dendritic Domain Morphology as a Correlate of *in vivo* Activity

Given that cell body localization was a good predictor of spontaneous activity (**Figure 4**) and that cell body position itself is also associated to differences in physical and topological characteristics of dendritic trees (**Figure 2**), we examined how these morphological and electrophysiological characteristics are related to each other (**Figure 5** and **Supplementary Table 4**). In the case of SNc neurons, no relationship between electrophysiological (firing rate, CV, CV2 or SIB) and morphological (dendritic length, number of dendritic segments, maximum branch order) variables was found (**Figure 5** and **Supplementary Table 4**). On the other hand, however, we found that larger dendritic volumetric space (larger convex hull volumes) values correlated positively with firing regularity (CV: r = −0.5930, p = 0.0421 Spearman correlation, **Figure 5**), although not with firing rate or SIB (firing rate: r = 0.1329, p = 0.6834; SIB: r = −0.4703, p = 0.1229 Spearman correlation, **Figure 5** and **Supplementary Table 4**). In the case of VTA neurons, firing rate, CV2, or SIB did not relate to morphological variables (**Figures 5C2,D2** and **Supplementary Table 4**). However, CV values in VTA neurons negatively correlated to number of dendritic segments (r = −0.575, p = 0.0398 Spearman correlation, **Figure 5** and **Supplementary Table 4**), in that a more complex architecture relates to more regular firing. We did not find that the convex hull volume of VTA neurons related to any electrophysiological variable (**Figure 5** and **Supplementary Table 4**). Finally, when the entire population was considered, we found that neither firing rate nor SIB (**Supplementary Table 4**) related to dendritic length, maximum dendritic order, number of segments, or convex hull volume (**Supplementary Table 4**). However, the CV and CV2 values related to maximum dendritic order and number of segments (**Supplementary Table 4**). In summary, morphological features of the dendritic domain relate to electrophysiological characteristics in individual DA neurons in that a more extensive dendritic space (in the case of SNc neurons) or a more complex architecture (in

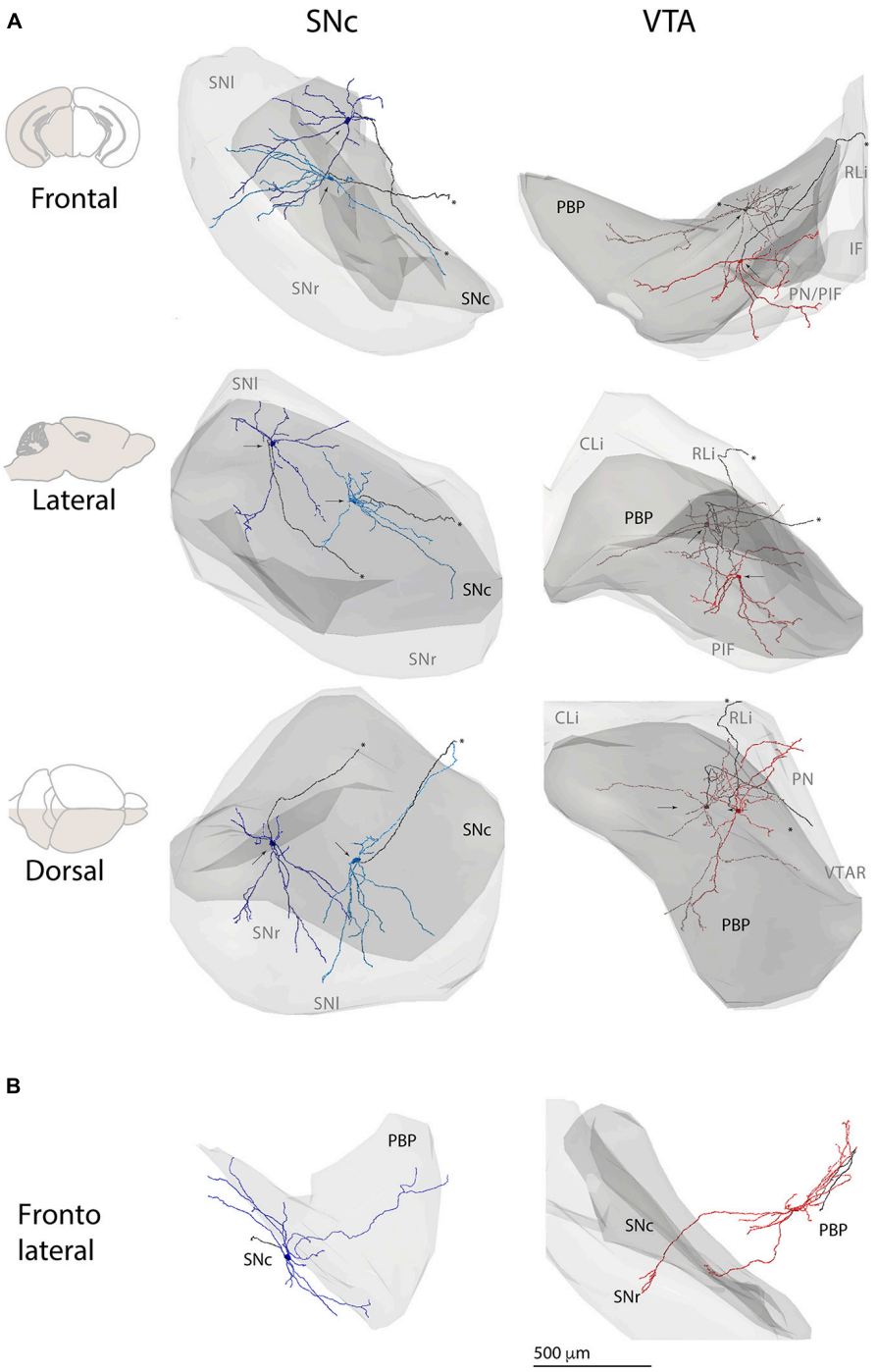

FIGURE 3 | Cell body and dendritic domain of individual substantia nigra and VTA neurons within and between respective regions. **(A)** 3D reconstructions of two SNc (left column) and two VTA (right column) DA neurons and respective regions. Neurons were placed inside 3D renderings of substantia nigra and VTA, as part of a common reference map based on Fu et al. (2012). Depicted in light gray is the substantia nigra (left) or the VTA (right) and in darker gray is the SNc or PBP. Gray text indicates the projected location of SN or VTA subdivisions. Arrows indicate the position of cell bodies. Axons are in black and marked with an *. For SNc DA neurons, note the extension of dendrites outside the boundaries of SNc into the SNr (frontal and dorsal views). For the VTA DA neuron depicted in bright red, note the extension of dendrites outside the boundaries of the PBP, into more ventral VTA subdivisions PIF and PN (frontal and dorsal views). **(B)** 3D reconstructions of one SNc (left) and one VTA DA neurons (right) depicting dendritic extensions onto PBP and SN, respectively. Only PBP (left) and SNc-SNr (right) contours are shown. CLi, caudal Linear nucleus; IF, interfascicular nucleus; PBP, parabrachial pigmented nucleus; PIF, parainterfascicular nucleus; PN, paranigral nucleus; RLi, rostral linear nucleus; SN, substantia nigra; SNc, substantia nigra pars compacta; SNl, substantia nigra compacta pars lateralis; SNr, substantia nigra pars reticulata; VTAR, rostral VTA.

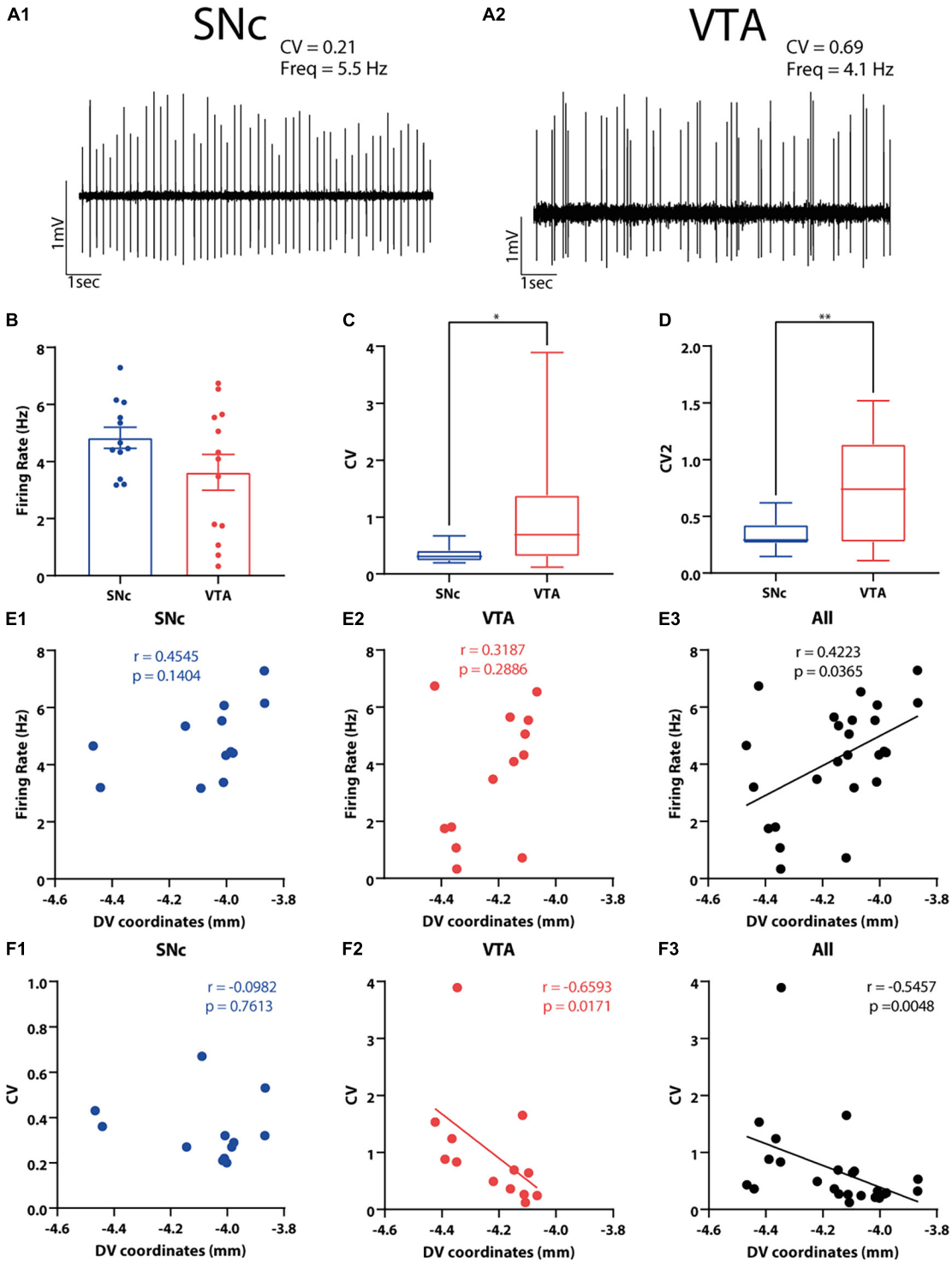

FIGURE 4 | *In vivo* electrophysiological characteristics of SNc and VTA DA neurons and their correlation with cell body position in the DV axis. **(A1,A2)** Examples of *in vivo* extracellular recordings of **(A1)** SNc and **(A2)** VTA neurons. **(B–D)** Electrophysiological properties of SNc and VTA DA neurons were compared. Firing rate **(B)** and the firing regularity measures **(C)** CV and **(D)** CV2 are shown. $*p < 0.05$, $**p < 0.01$, unpaired *t*-test (CV2) or Mann–Whitney *U* test (CV). **(E1–F3)** Correlations between electrophysiological variables and DV cell body position of 3D-reconstructed SNc and VTA DA neurons. Positive correlation was found between firing rate and DV coordinates when all neurons were analyzed together **(E3)**, but this was not observed in each area separately **(E1,E2)**. Negative correlation was observed between CV and DV coordinates used and for VTA **(F2)** and for all neurons **(F3)** but not for SNc DA neurons **(F1)**. Figure only shows correlations between electrophysiological variables and DV position. Refer to the Results section and **Supplementary Table 3** for correlations between electrophysiological variables and ML and AP axes position.

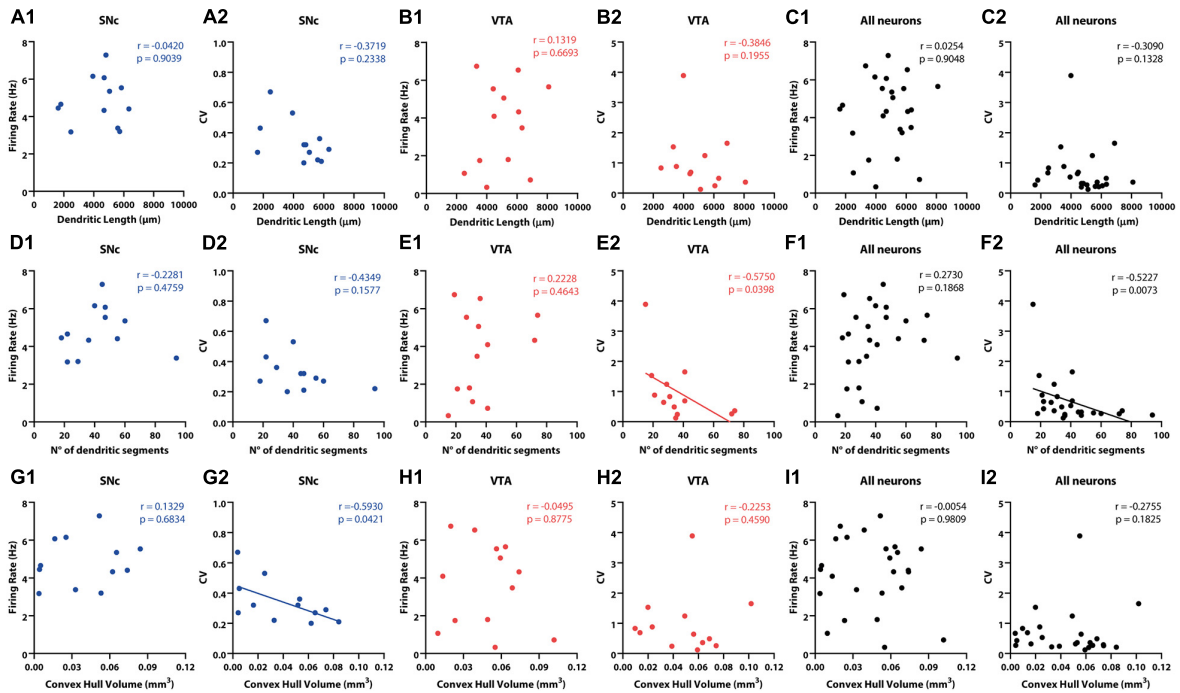

FIGURE 5 | Correlation between *in vivo* electrophysiological and morphological characteristics of SNc and VTA DA neurons. **(A1,B1,C1)** No significant correlation between dendritic length and firing rate was found for **(A1)** SNc, **(B1)** VTA, or all **(C1)** DA neurons. **(A2,B2,C2)**. No significant correlations were found between CV and dendritic length for **(A2)** SNc, **(B2)** VTA, or all **(C2)** DA neurons. No significant correlation between number of dendritic segments and firing rate was observed for **(D1)** SNc, **(E1)** VTA, or all **(F1)** DA neurons. **(D2)** No correlation was found between CV and number of dendritic segments for SNc neurons. On the other hand, a negative correlation was found for **(E2)** VTA and for **(F2)** all neurons. Finally, no correlation between convex hull volume and firing rate was found for **(G1)** SNc, **(H1)** VTA, or all **(I1)** DA neurons. Negative correlation was found between convex hull volume and CV in **(G2)** SNc neurons, but not in panel **(H2)** VTA or all **(I2)** DA neurons. See Results and **Supplementary Tables** for further physiological and anatomical correlations.

the case of VTA neurons or the entire population), leads to more regular firing.

Dendritic Compartmental Organization as a Correlate of *in vivo* Activity

Having found that dendritic tree organization relates to *in vivo* spontaneous activity diversity (above), and that an important property of the dendritic organization is the presence of dendrites across multiple SN or VTA subdivisions (**Figure 3** and **Supplementary Table 2**), we examined whether the presence of dendrites across different SN or VTA subdivisions could also relate to spontaneous activity in individual neurons. For that, we tested whether absolute or proportional dendritic length in different subdivisions (**Supplementary Table 2**) correlated with basal electrophysiological parameters (**Figures 6**, **7** and **Supplementary Table 5**). In SNc neurons, the presence of dendrites in the SNr subdivision did not correlate with firing rate or SIB (**Supplementary Table 5**). On the other hand, baseline firing regularity values (CV and CV2) were negatively correlated with dendritic length (CV: $r = -0.6819$, $p = 0.0146$; CV2: $r = -0.718$, $p = 0.0085$ Spearman correlation, **Figure 6A1**) and dendritic length percentage (CV: $r = -0.6784$, $p = 0.0153$; CV2: $r = -0.7321$, $p = 0.0068$, **Figure 6A2**) in SNr (**Supplementary Table 5**). Hence, neurons with more dendrites in SNr fired more regularly (**Figure 6B1**), and neurons with little or no dendrites in SNr were more irregular (**Figure 6B2**). No relationship was found between the extension of dendrites in SNc, PBP, or tegmentum above SNc and electrophysiological parameters (**Supplementary Table 5**). Neurons also presented dendrites in the retrorubral field ($n = 5$) and in SNl ($n = 1$) but were few, and the dendritic length was proportionally very small; thus, we did not evaluate correlations regarding dendrites in these areas.

In VTA neurons, total dendritic length (or percentage) inside or outside the PBP subdivision did not correlate with firing rate or SIB either (**Supplementary Table 5**). On the other hand, firing regularity did relate to dendritic distribution in different subdivisions. Specifically, we found a negative correlation between absolute dendritic length (or dendritic length percentage) in the PBP and CV or CV2 values, in that neurons with a larger percentage of dendrites located in PBP fired more regularly (CV: $r = -0.7386$, $p = 0.0039$; CV2: $r = -0.7165$, $p = 0.0059$ Spearman correlation, **Figures 7A1–B2** and **Supplementary Table 5**), and that those with a lower proportion of dendrites in PBP fired more irregularly (**Figure 7B2**). Several VTA DA neurons also had dendrites in the more ventrally located PIF and PN subdivisions of the VTA, and we found a positive correlation with either dendritic length or length percentage

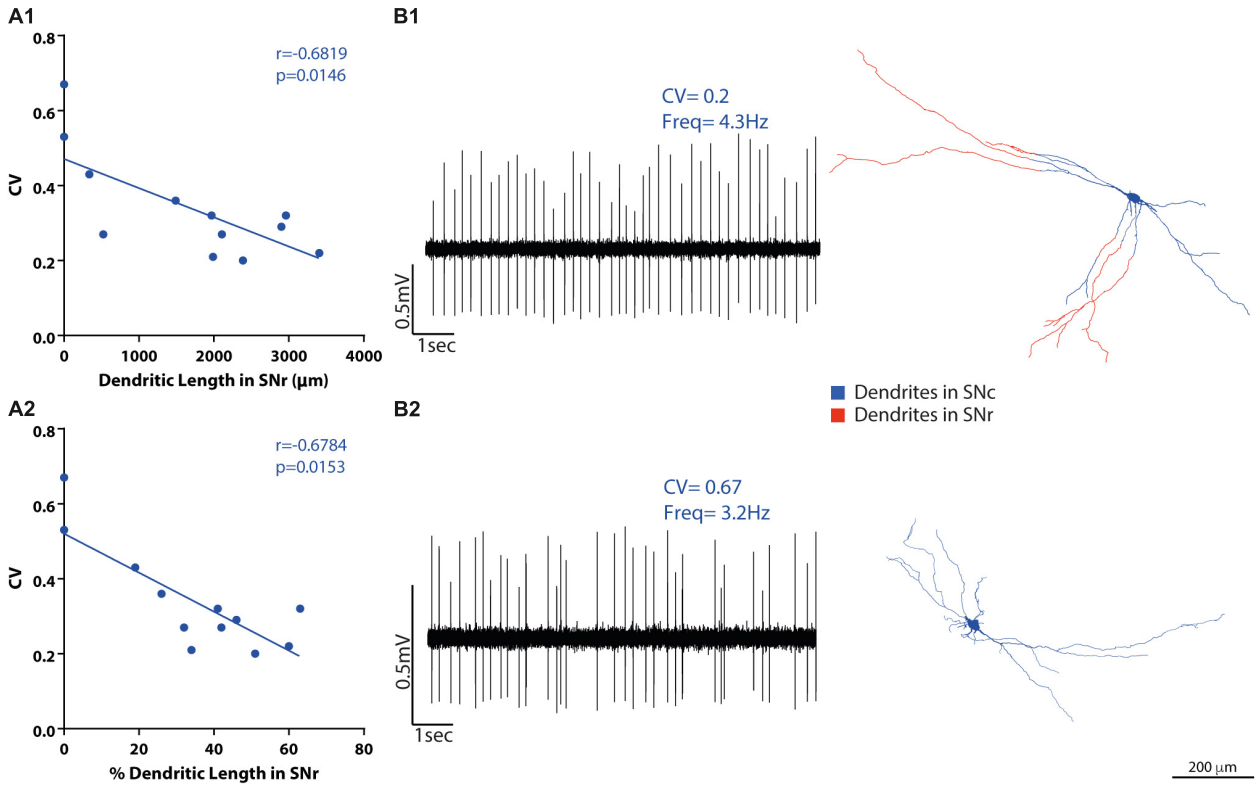

FIGURE 6 | SNc DA neuron heterotopic distribution of dendrites correlates with the electrophysiological activity of the neurons. **(A1-2)** Firing regularity (coefficient of variation, CV) correlations with the proportion of dendritic length in panel **(A1)** SNr, but not in panel **(A2)** SNc. **(B1-2)** Raw data examples of firing traces of SNc DA neurons and their matching 3D reconstructions. Examples of one [**(B1)**-top] regular and one [**(B2)**-bottom] irregular SNc raw baseline recordings (10 s) with their respective dendritic reconstructions [**(B1,B2)**, right] showing dendrites inside SNr in red and their dendrites inside SNc (and other subdivisions, not shown) in blue. Scale bar = 200 µm.

in PIF/PN and CV or CV2 values (% dendritic length, CV: $r = 0.7048$, $p = 0.0071$; CV2: $r = 0.663$, $p = 0.0135$ Spearman correlation, **Figure 7A2** and **Supplementary Table 5**). Additionally, some neurons had dendrites in the tegmentum dorsal to the VTA (mRF/p1RF); however, there were no significant correlations of CV or CV2 with the total dendritic length (or the percentage (**Supplementary Table 5**). Very few neurons had dendrites in the A8 field ($n = 1$), VTAR ($n = 4$), ml ($n = 1$), thus, their dendritic extension in those areas was not evaluated for correlation with baseline electrophysiological measurements.

DISCUSSION

Mouse DA neuron dendritic domains show a considerable architectural diversity. Some of that diversity is explained by a dorsoventral gradient of further smaller and simpler dendritic domains at ventral positions, particularly evident in the VTA. Single cell dendritic architecture also predicts differences in spontaneous firing patterns. In the SNc, firing irregularity relates to smaller dendritic space, as quantified by convex hull volumes, and a smaller proportion of SNr-projecting dendrites. In the VTA, instead, irregularity is associated to cell body ventral localization, topologically simpler dendritic domains, and a smaller proportion of dendrites within the PBP.

Morphology of Mouse SNc and VTA Dopaminergic Neurons

This study conforms to classical descriptions of single cell dendritic morphology in the rat SNc, characterized by extensive dendritic fields, relatively simple bifurcation patterns, and contingents of SNr-projecting dendrites (Juraska et al., 1977; Grace and Bunney, 1983; Tepper et al., 1987). It also follows descriptions of identified DA (Grace and Onn, 1989) or Golgi-stained VTA neurons (Phillipson, 1979) in rats that report extensive, overlapping, and radially oriented dendrites. In this study, we quantitatively analyzed single cell dendritic domains and found a considerable architectural diversity.

We did not find that diverse dendritic architectures of SNc neurons associated with the DV, ML, or AP cell body position. In contrast, VTA DA neurons, being similarly diverse, exhibited a dorsoventral gradient of reduced size and complexity of dendritic domains, in line with the study of Philipson showing ventral PN neurons that appeared smaller than dorsal PBP ones (Phillipson, 1979). We acknowledge that our sampling may fall short of revealing subtler subregional differences in morphology. Future

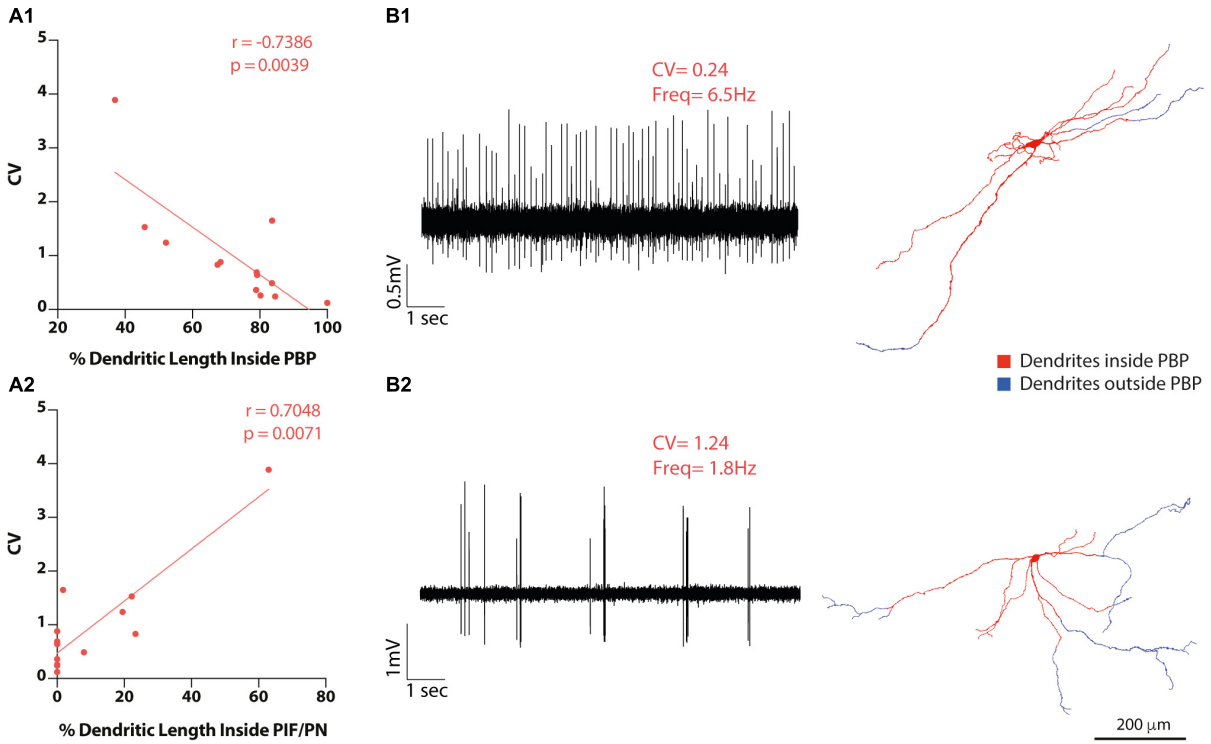

FIGURE 7 | VTA DA neuron heterotopic distribution of dendrites correlates with baseline electrophysiological activity. **(A1-2)** Firing regularity (CV) correlations with the proportion of dendritic length inside PBP **(A1)** or inside PIF/PN subdivisions. **(B1-2)** Raw data examples of firing traces of VTA DA neurons and their matching 3D reconstructions. Examples of one [**(B1)**-top] regular and one [**(B2)**-bottom] irregular VTA DA neuron raw baseline recordings (10 s) with their respective dendritic reconstructions [**(B1,B2)**, right] showing dendrites inside PBP in red and their dendrites outside PBP in blue. Neuron in B2 is also shown in **Figure 3**. Scale bar = 200 µm.

studies that will perform more systematic and extensive sampling, as carried out in other brain areas (Benavides-Piccione et al., 2006; Vrieler et al., 2019), may provide beneficial in this respect.

We wondered whether single cell morphological diversity could also relate to the course of dendrites within substantia nigra and VTA cytoarchitectonic subdivisions. We confirmed that a proportion of SNc neurons project dendrites to the SNr. Similar to what we described in the rat (Henny et al., 2012), we failed to observe a clear association between ventral or dorsal tiers cell body location with exhibiting, or not, SNr-projecting dendrites, as previously reported (Gerfen et al., 1987; Grace and Onn, 1989). In fact, the cell bodies of most SNc neurons in this study, such as those exhibiting SNr-projecting dendrites, locate in what would correspond to the neurochemically and hodologically defined mouse SNc dorsal tier (Fu et al., 2012; **Figure 1**). We also observed (**Figures 2**, **3**) that SNr-projecting dendrites usually originate from multiple primary dendrites and course across the SNr in various directions, and that they do not from a single thick *apical* dendrite, as sometimes reported (Juraska et al., 1977; Gerfen et al., 1987; Yung et al., 1991). As also evident from the long dendritic extension of VTA neurons (**Figure 3**), we show that dendrites course across subdivisions of the VTA. The functional consequences of such heterotopic distribution of dendrites should be interpreted in relation to the segregated distribution of input into different subdivisions, as demonstrated for SNc versus SNr (Gerfen et al., 1985; Bolam and Smith, 1990; Bolam et al., 1991). This is a much more difficult challenge for VTA neurons, for the segregation of inputs to different subdivision of the VTA seems to be minimal, as described in rats (Geisler and Zahm, 2005).

Activity Correlates of Neuron Localization and Dendritic Domain Architecture

We described a dorsoventral gradient of increased firing irregularity for VTA (and SNc-VTA) DA neurons. Interestingly, a recent study has also reported an effect of DV cell body positioning in *in vivo* firing frequency of identified mouse VTA DA neurons, in that lateral nucleus accumbens-projecting neurons (which locate dorsally in the VTA and include medial SNc neurons) were faster than medial nucleus accumbens-projecting neurons (located ventrally in the VTA) (Farassat et al., 2019). We also found that anterior cell body locations associated with more bursting activity in the VTA, but failed to find differences in mediolateral positioning, contrasting with evidence that dorsolateral striatum (DLS)-projecting lateral SNc neurons are burstier than DLS-projecting medial SNc neurons (Farassat et al., 2019). Although these differences may, in part, be due to the smaller sample in this study or anesthetic regime, it is

also likely that other anatomical principles underlie functional diversity beyond cell body position, and may include projection target (Farassat et al., 2019), axon initial segment size (González-Cabrera et al., 2017; Meza et al., 2018), size and organization of somatodendritic or proximal dendritic domains (Jang et al., 2014; Meza et al., 2018; Moubarak et al., 2019) or, as shown in this study, the organization of the dendritic domain.

In fact, regularity of firing in SNc neurons is correlated with dendritic extension, as measured by convex hulls. One could assume that total dendritic length, which may affect convex hull size, could also relate to regularity, but it does not. Regularity of discharge, instead, was associated specifically with the proportion of SNr-projecting dendrites, indicating that it is not dendritic extension *per se* that underlies regularity but specific properties of SNr-projecting dendrites. A crucial difference between SNr-projecting versus SNc dendrites is the denser GABAergic input in the former (Henny et al., 2012). It has been previously recognized for cortical integrate-fire neurons that firing regularity is tuned by changes in synaptic excitation/inhibition (E/I) balance (Hamaguchi et al., 2011). Therefore, an enhanced inhibitory tone onto SNr-projecting dendrites might promote regularity, an interpretation consistent with the role of inhibition in suppressing excitation-mediated firing irregularity and bursting activity (Tepper et al., 1995; Celada et al., 1999). In addition, enhanced inhibition might boost the role of subthreshold conductances such as T-type calcium channels and coupled Ca2 + activated SK channels, which themselves further promote regular discharge (Wolfart and Roeper, 2002). This is not to say, however, that inhibition should always promote regularity and emergence of regular pacemaking firing in DA neuronal subtypes. Indeed, a recent report showed that some DA neurons may exhibit *in vivo* hyperpolarization-initiated rebound bursting (Otomo et al., 2020) in line with previous *ex vivo* evidence showing that rebound excitation may also depend on T-type channels in calbindin-negative SNc DA neurons (Evans et al., 2017; Gantz et al., 2018).

In VTA DA neurons, regularity was predicted by the dorsal positioning of the cell body, and dendritic domain complexity and extension within the PBP. Again, it is noticeable that regularity was not related to dendritic size *per se*, but tree complexity and heterotopic distribution. As mentioned earlier, evidence shows that, at least when considering the entire population of inputs to the VTA, they do not seem to segregate according to subdivisions (Geisler and Zahm, 2005) (their Figure 14). One plausible, although highly speculative, hypothesis that could explain a regional effect on firing regularity may be that somata and dendrites located in the PBP receive a high inhibitory-to-excitatory innervation ratio from local or extrinsic afferents (Omelchenko and Sesack, 2009; Faget et al., 2016), therefore mimicking the high inhibitory-to-excitatory innervation ratio seen in SNr-projecting dendrites.

Functional Compartmentalization in Proximal and Distal Dendritic Domains

Previous studies have shown the role that dendrites play in synaptically mediated phenomena such as burst firing (Wilson and Callaway, 2000; Komendantov et al., 2004; Blythe et al., 2007; Gantz et al., 2018; Lopez-Jury et al., 2018) and firing inhibition or pauses (Hajós and Greenfield, 1994; Henny et al., 2012; Paladini and Roeper, 2014). Our data support this role and suggest that dendritic organization influences firing pattern by allowing irregular and burst firing to emerge (which we assume reflects excitatory volleys of activity reaching the dendritic domain), or, following afferent inhibitory activity, to enhance regularity or rebound bursting (Otomo et al., 2020).

The influence of the dendritic domain on firing pattern, on the other hand, sharply contrasts with the null correlation between dendritic domain (size, complexity, extension, heterotopic distribution) and firing frequency (**Figure 5** and **Supplementary Tables 4**, **5**). This supports the contention that DA neurons could be seen as functionally compartmentalized structures with different degrees of influence on firing pattern (e.g., its dendritic domain) or firing frequency [e.g., its more proximal subcellular compartments such as cell body, proximal dendrites (Jang et al., 2014), and axon initial segment (Meza et al., 2018)]. In fact, we have shown that axon initial segment size strongly correlates with *in vivo* spontaneous firing frequency but not with irregular or burst firing (Meza et al., 2018). In SNc neurons, compartmentalization should also extend to functionally and synaptically differentiated dendrites that locate either in the SNc or SNr. Due to a strong GABAergic influence, SNr dendrites could promote regular firing (see above) while also facilitating the concerted action of inhibitory inputs during aversive stimulation (Henny et al., 2012; Paladini and Roeper, 2014). Conversely, due to a higher proportion of excitatory glutamatergic and cholinergic synapses on SNc dendrites (Bolam et al., 1991; Henny et al., 2012), they could be better suited to mediate phasic bursting and/or irregular firing. Regarding the VTA, recent evidence has reported differences in excitability between axon-bearing and non-axon bearing dendrites (Engel and Seutin, 2015), supporting a compartmentalized view of VTA neurons proximal dendritic domain. Future studies that will describe differences in afferent innervation of VTA subdivisions or the distribution of inputs in the somatodendritic domain of individual neurons may shed light onto this subject. Finally, approaches aimed to test the role of different compartments in firing pattern, such as those that use subcellular specific expression of channel rhodopsins (Greenberg et al., 2011; Baker et al., 2016; Mahn et al., 2018), which could be coupled to focal illumination of opsins (Sun et al., 2014; Stahlberg et al., 2019), would help to test the causal relationship between morphological characteristics of different compartments of DA neurons and firing properties of the cell.

DATA AVAILABILITY STATEMENT

The raw data supporting the conclusions of this article will be made available by the authors, without undue reservation.

ETHICS STATEMENT

The animal study was reviewed and approved by Ethics Committees of the School of Medicine of the

Pontificia Universidad Católica de Chile and German Regierungspraesidium Darmstadt.

AUTHOR CONTRIBUTIONS

TM, NF, RM, and CG-C performed the experiments. TM, RG, NF, and PH contributed to the data analysis. TM, RG, JR, and PH contributed to the manuscript writing. All authors approved the submitted version.

FUNDING

This study was supported by CONICYT-PFCHA Doctorado Nacional 2015-21150324 to TM and Fondecyt Regular grants 1141170 and 1191497, Conicyt-Anillo initiative 1109, and Conicyt/ANID REDES 180207 to PH.

ACKNOWLEDGMENTS

We would like to thank Gonzalo Marin for insightful comments during the early stages of this study, and Marcia Gaete for executive coaching during the writing process.

SUPPLEMENTARY MATERIAL

The Supplementary Material for this article can be found online at: https://www.frontiersin.org/articles/10.3389/fncir.2021.769342/full#supplementary-material

REFERENCES

Baker, C. A., Elyada, Y. M., Parra, A., and Bolton, M. M. L. (2016). Cellular resolution circuit mapping with temporal-focused excitation of soma-targeted channelrhodopsin. *Elife* 5:e14193. doi: 10.7554/eLife.14193

Bayer, V. E., and Pickel, V. M. (1991). GABA-labeled terminals form proportionally more synapses with dopaminergic neurons containing low densities of tyrosine hydroxylase-immunoreactivity in rat ventral tegmental area. *Brain Res.* 559, 44–55. doi: 10.1016/0006-8993(91)90285-4

Benavides-Piccione, R., Hamzei-Sichani, F., Ballesteros-Yáñez, I., Defelipe, J., and Yuste, R. (2006). Dendritic size of pyramidal neurons differs among mouse cortical regions. *Cereb. Cortex* 16, 990–1001. doi: 10.1093/cercor/bhj041

Berke, J. D. (2018). What does dopamine mean? *Nat. Neurosci.* 21, 787–793. doi: 10.1038/s41593-018-0152-y

Blythe, S. N., Atherton, J. F., and Bevan, M. D. (2007). Synaptic activation of dendritic AMPA and NMDA receptors generates transient high-frequency firing in substantia nigra dopamine neurons in vitro. *J. Neurophysiol.* 97, 2837–2850. doi: 10.1152/jn.01157.2006

Bolam, J. P., Francis, C. M., and Henderson, Z. (1991). Cholinergic input to dopaminergic neurons in the substantia nigra: A double immunocytochemical study. *Neuroscience* 41, 483–494. doi: 10.1016/0306-4522(91)90343-M

Bolam, J. P., and Smith, Y. (1990). The GABA and substance P input to dopaminergic neurones in the substantia nigra of the rat. *Brain Res.* 529, 57–78. doi: 10.1016/0006-8993(90)90811-O

Brischoux, F., Chakraborty, S., Brierley, D. I., and Ungless, M. A. (2009). Phasic excitation of dopamine neurons in ventral VTA by noxious stimuli. *Proc. Natl. Acad. Sci. U.S.A.* 106, 4894–4899. doi: 10.1073/pnas.0811507106

Celada, P., Paladini, C. A., and Tepper, J. M. (1999). GABAergic control of rat substantia nigra dopaminergic neurons: Role of globus pallidus and substantia nigra pars reticulata. *Neuroscience* 89, 813–825. doi: 10.1016/S0306-4522(98)00356-X

Chang, C. Y., Esber, G. R., Marrero-Garcia, Y., Yau, H. J., Bonci, A., and Schoenbaum, G. (2015). Brief optogenetic inhibition of dopamine neurons mimics endogenous negative reward prediction errors. *Nat. Neurosci.* 19, 111–116. doi: 10.1038/nn.4191

Chang, C. Y., Gardner, M. P. H., Conroy, J. C., Whitaker, L. R., and Schoenbaum, G. (2018). Brief, but not prolonged, pauses in the firing of midbrain dopamine neurons are sufficient to produce a conditioned inhibitor. *J. Neurosci.* 38, 8822–8830. doi: 10.1523/JNEUROSCI.0144-18.2018

Comoli, E., Coizet, V., Boyes, J., Bolam, J. P., Canteras, N. S., Quirk, R. H., et al. (2003). A direct projection from superior colliculus to substantia nigra for detecting salient visual events. *Nat. Neurosci.* 6, 974–980. doi: 10.1038/nn1113

Engel, D., and Seutin, V. (2015). High dendritic expression of Ih in the proximity of the axon origin controls the integrative properties of nigral dopamine neurons. *J. Physiol.* 593, 4905–4922. doi: 10.1113/JP271052

Evans, R. C., Zhu, M., and Khaliq, Z. M. (2017). Dopamine inhibition differentially controls excitability of substantia nigra dopamine neuron subpopulations through T-type calcium channels. *J. Neurosci.* 37, 3704–3720. doi: 10.1523/JNEUROSCI.0117-17.2017

Faget, L., Osakada, F., Duan, J., Ressler, R., Johnson, A. B., Proudfoot, J. A., et al. (2016). Afferent Inputs to Neurotransmitter-Defined Cell Types in the Ventral Tegmental Area. *Cell Rep.* 15, 2796–2808. doi: 10.1016/j.celrep.2016.05.057

Fahn, S. (2008). The history of dopamine and levodopa in the treatment of Parkinson's disease. *Mov. Disord.* 23, S497–S508. doi: 10.1002/mds.22028

Farassat, N., Costa, K. M., Stojanovic, S., Albert, S., Kovacheva, L., Shin, J., et al. (2019). In vivo functional diversity of midbrain dopamine neurons within identified axonal projections. *Elife* 8:e48408. doi: 10.7554/eLife.48408

Franklin, K. B. J., and Paxinos, G. (2007). *The Mouse Brain in Stereotaxic Coordinates*. Cambridge: Academic press.

Fu, Y. H., Yuan, Y., Halliday, G., Rusznák, Z., Watson, C., and Paxinos, G. (2012). A cytoarchitectonic and chemoarchitectonic analysis of the dopamine cell groups in the substantia nigra, ventral tegmental area, and retrorubral field in the mouse. *Brain Struct. Funct.* 217, 591–612. doi: 10.1007/s00429-011-0349-2

Gantz, S. C., Ford, C. P., Morikawa, H., and Williams, J. T. (2018). The Evolving Understanding of Dopamine Neurons in the Substantia Nigra and Ventral Tegmental Area. *Annu. Rev. Physiol.* 80, 219–241. doi: 10.1146/annurev-physiol-021317-121615

Geisler, S., and Zahm, D. S. (2005). Afferents of the ventral tegmental area in the rat-anatomical substratum for integrative functions. *J. Comp. Neurol.* 490, 270–294. doi: 10.1002/cne.20668

Gerfen, C. R., Baimbridge, K. G., and Miller, J. J. (1985). The neostriatal mosaic: Compartmental distribution of calcium-binding protein and parvalbumin in the basal ganglia of the rat and monkey. *Proc. Natl. Acad. Sci. U.S.A.* 82, 8780–8784. doi: 10.1073/pnas.82.24.8780

Gerfen, C. R., Baimbridge, K. G., and Thibault, J. (1987). The neostriatal mosaic: III. Biochemical and developmental dissociation of patch-matrix mesostriatal systems. *J. Neurosci.* 7, 3935–3944. doi: 10.1523/jneurosci.07-12-03935.1987

Gertler, T. S., Chan, C. S., and Surmeier, D. J. (2008). Dichotomous anatomical properties of adult striatal medium spiny neurons. *J. Neurosci.* 28, 10814–10824. doi: 10.1523/JNEUROSCI.2660-08.2008

González-Cabrera, C., Meza, R., Ulloa, L., Merino-Sepúlveda, P., Luco, V., Sanhueza, A., et al. (2017). Characterization of the axon initial segment of mice substantia nigra dopaminergic neurons. *J. Comp. Neurol.* 525, 3529–3542. doi: 10.1002/cne.24288

Grace, A. A., and Bunney, B. S. (1983). Intracellular and extracellular electrophysiology of nigral dopaminergic neurons-2. Action potential generating mechanisms and morphological correlates. *Neuroscience* 10, 321–331. doi: 10.1016/0306-4522(83)90136-7

Grace, A. A., and Bunney, B. S. (1984). The control of firing pattern in nigral dopamine neurons: Burst firing. *J. Neurosci.* 4, 2877–2890. doi: 10.1523/jneurosci.04-11-02877.1984

Grace, A. A., and Onn, S. P. (1989). Morphology and electrophysiological properties of immunocytochemistry identified rat dopamine neurons recorded in vitro. *J. Neurosci.* 9, 3463–3481. doi: 10.1523/jneurosci.09-10-03463.1989

Greenberg, K. P., Pham, A., and Werblin, F. S. (2011). Differential Targeting of Optical Neuromodulators to Ganglion Cell Soma and Dendrites Allows Dynamic Control of Center-Surround Antagonism. *Neuron* 69, 713–720. doi: 10.1016/j.neuron.2011.01.024

Hajós, M., and Greenfield, S. A. (1994). Synaptic connections between pars compacta and pars reticulata neurones: electrophysiological evidence for functional modules within the substantia nigra. *Brain Res.* 660, 216–224. doi: 10.1016/0006-8993(94)91292-0

Hamaguchi, K., Riehle, A., and Brunel, N. (2011). Estimating network parameters from combined dynamics of firing rate and irregularity of single neurons. *J. Neurophysiol.* 105, 487–500. doi: 10.1152/jn.00858.2009

Henny, P., Brown, M. T. C., Micklem, B. R., Magill, P. J., and Bolam, J. P. (2014). Stereological and ultrastructural quantification of the afferent synaptome of individual neurons. *Brain Struct. Funct.* 219, 631–640. doi: 10.1007/s00429-013-0523-9

Henny, P., Brown, M. T. C., Northrop, A., Faunes, M., Ungless, M. A., Magill, P. J., et al. (2012). Structural correlates of heterogeneous in vivo activity of midbrain dopaminergic neurons. *Nat. Neurosci.* 15, 613–619. doi: 10.1038/nn.3048

Holt, G. R., Softky, W. R., Koch, C., and Douglas, R. J. (1996). Comparison of discharge variability in vitro and in vivo in cat visual cortex neurons. *J. Neurophysiol.* 75, 1806–1814. doi: 10.1152/jn.1996.75.5.1806

Jang, J., Um, K. B., Jang, M., Kim, S. H., Cho, H., Chung, S., et al. (2014). Balance between the proximal dendritic compartment and the soma determines spontaneous firing rate in midbrain dopamine neurons. *J. Physiol.* 592, 2829–2844. doi: 10.1113/jphysiol.2014.275032

Juraska, J. M., Wilson, C. J., and Groves, P. M. (1977). The substantia nigra of the rat: A golgi study. *J. Comp. Neurol.* 172, 585–599. doi: 10.1002/cne.901720403

Komendantov, A. O., Komendantova, O. G., Johnson, S. W., and Canavier, C. C. (2004). A Modeling Study Suggests Complementary Roles for GABAA and NMDA Receptors and the SK Channel in Regulating the Firing Pattern in Midbrain Dopamine Neurons. *J. Neurophysiol.* 91, 346–357. doi: 10.1152/jn.00062.2003

Lammel, S., Hetzel, A., Häckel, O., Jones, I., Liss, B., and Roeper, J. (2008). Unique Properties of Mesoprefrontal Neurons within a Dual Mesocorticolimbic Dopamine System. *Neuron* 57, 760–773. doi: 10.1016/j.neuron.2008.01.022

Lopez-Jury, L., Meza, R. C., Brown, M. T. C. C., Henny, P., Canavier, C. C., López-Jury, L., et al. (2018). Morphological and biophysical determinants of the intracellular and extracellular waveforms in nigral dopaminergic neurons: A computational study. *J. Neurosci.* 38, 8295–8310. doi: 10.1523/JNEUROSCI.0651-18.2018

Mahn, M., Gibor, L., Patil, P., Cohen-Kashi Malina, K., Oring, S., Printz, Y., et al. (2018). High-efficiency optogenetic silencing with soma-targeted anion-conducting channelrhodopsins. *Nat. Commun.* 9, 1–15. doi: 10.1038/s41467-018-06511-8

Meza, R. C., López-Jury, L., Canavier, C. C., and Henny, P. (2018). Role of the axon initial segment in the control of spontaneous frequency of nigral dopaminergic neurons in vivo. *J. Neurosci.* 38, 733–744. doi: 10.1523/JNEUROSCI.1432-17.2017

Moubarak, E., Enge, D., Dufour, M. A., Tapia, M., Tell, F., and Goaillard, J. M. (2019). Robustness to axon initial segment variation is explained by somatodendritic excitability in rat substantia nigra dopaminergic neurons. *J. Neurosci.* 39, 5044–5063. doi: 10.1523/JNEUROSCI.2781-18.2019

Omelchenko, N., and Sesack, S. R. (2009). Ultrastructural analysis of local collaterals of rat ventral tegmental area neurons: GABA phenotype and synapses onto dopamine and GABA cells. *Synapse* 63, 895–906. doi: 10.1002/syn.20668

Otomo, K., Perkins, J., Kulkarni, A., Stojanovic, S., Roeper, J., and Paladini, C. A. (2020). In vivo patch-clamp recordings reveal distinct subthreshold signatures and threshold dynamics of midbrain dopamine neurons. *Nat. Commun.* 11, 1–15. doi: 10.1038/s41467-020-20041-2

Paladini, C. A., and Roeper, J. (2014). Generating bursts (and pauses) in the dopamine midbrain neurons. *Neuroscience* 282, 109–121. doi: 10.1016/j.neuroscience.2014.07.032

Phillipson, O. T. (1979). A Golgi study of the ventral tegmental area of Tsai and interfascicular nucleus in the rat. *J. Comp. Neurol.* 187, 99–115. doi: 10.1002/cne.901870107

Pinault, D. (1996). A novel single-cell staining procedure performed in vivo under electrophysiological control: Morpho-functional features of juxtacellularly labeled thalamic cells and other central neurons with biocytin or Neurobiotin. *J. Neurosci. Methods* 65, 113–136. doi: 10.1016/0165-0270(95)00144-1

Redgrave, P., Gurney, K., and Reynolds, J. (2008). What is reinforced by phasic dopamine signals? *Brain Res. Rev.* 58, 322–339. doi: 10.1016/j.brainresrev.2007.10.007

Rinvik, E., and Grofová, I. (1970). Observations on the fine structure of the substantia nigra in the cat. *Exp. Brain Res.* 11, 229–248. doi: 10.1007/BF01474384

Schultz, W. (2007). Behavioral dopamine signals. *Trends Neurosci.* 30, 203–210. doi: 10.1016/j.tins.2007.03.007

Stahlberg, M. A., Ramakrishnan, C., Willig, K. I., Boyden, E. S., Deisseroth, K., and Dean, C. (2019). Investigating the feasibility of channelrhodopsin variants for nanoscale optogenetics. *Neurophotonics* 6:015007. doi: 10.1117/1.nph.6.1.015007

Sulzer, D., Cragg, S. J., and Rice, M. E. (2016). Striatal dopamine neurotransmission: regulation of release and uptake. *Basal Ganglia* 6, 123–148. doi: 10.1016/j.baga.2016.02.001.Striatal

Sun, Q. Q., Wang, X., and Yang, W. (2014). Laserspritzer: A simple method for optogenetic investigation with subcellular resolutions. *PLoS One* 9:e101600. doi: 10.1371/journal.pone.0101600

Tepper, J. M., Martin, L. P., and Anderson, D. R. (1995). GABA(A) receptor-mediated inhibition of rat substantia nigra dopaminergic neurons by pars reticulata projection neurons. *J. Neurosci.* 15, 3092–3103. doi: 10.1523/jneurosci.15-04-03092.1995

Tepper, J. M., Sawyer, S. F., and Groves, P. M. (1987). Electrophysiologically identified nigral dopaminergic neurons intracellularly labeled with HRP: light-microscopic analysis. *J. Neurosci.* 7, 2794–2806. doi: 10.1523/jneurosci.07-09-02794.1987

Vrieler, N., Loyola, S., Yarden-Rabinowitz, Y., Hoogendorp, J., Medvedev, N., Hoogland, T. M., et al. (2019). Variability and directionality of inferior olive neuron dendrites revealed by detailed 3D characterization of an extensive morphological library. *Brain Struct. Funct.* 224, 1677–1695. doi: 10.1007/s00429-019-01859-z

Wilson, C. J., and Callaway, J. C. (2000). Coupled oscillator model of the dopaminergic neuron of the substantia nigra. *J. Neurophysiol.* 83, 3084–3100. doi: 10.1152/jn.2000.83.5.3084

Wise, R. A. (2004). Dopamine, learning and motivation. *Nat. Rev. Neurosci.* 5, 483–494. doi: 10.1038/nrn1406

Wolfart, J., and Roeper, J. (2002). Selective Coupling of T-Type Calcium Channels to SK Potassium Channels Prevents Intrinsic Bursting in Dopaminergic Midbrain Neurons. *J. Neurosci.* 22, 3404–3413. doi: 10.1523/jneurosci.22-09-03404.2002

Yung, W. H., Häusser, M. A., and Jack, J. J. (1991). Electrophysiology of dopaminergic and non-dopaminergic neurones of the guinea-pig substantia nigra pars compacta in vitro. *J. Physiol.* 436, 643–667. doi: 10.1113/jphysiol.1991.sp018571

Conflict of Interest: The authors declare that the research was conducted in the absence of any commercial or financial relationships that could be construed as a potential conflict of interest.

Publisher's Note: All claims expressed in this article are solely those of the authors and do not necessarily represent those of their affiliated organizations, or those of the publisher, the editors and the reviewers. Any product that may be evaluated in this article, or claim that may be made by its manufacturer, is not guaranteed or endorsed by the publisher.

Copyright © 2021 Montero, Gatica, Farassat, Meza, González-Cabrera, Roeper and Henny. This is an open-access article distributed under the terms of the Creative Commons Attribution License (CC BY). The use, distribution or reproduction in other forums is permitted, provided the original author(s) and the copyright owner(s) are credited and that the original publication in this journal is cited, in accordance with accepted academic practice. No use, distribution or reproduction is permitted which does not comply with these terms.

frontiers in Neural Circuits

ORIGINAL RESEARCH
published: 28 January 2022
doi: 10.3389/fncir.2021.799688

Uncovering the Connectivity Logic of the Ventral Tegmental Area

*Pieter Derdeyn[1], May Hui[2], Desiree Macchia[2] and Kevin T. Beier[2,3,4,5,6]**

[1] Program in Mathematical, Computational, and Systems Biology, University of California, Irvine, Irvine, CA, United States, [2] Department of Physiology and Biophysics, University of California, Irvine, Irvine, CA, United States, [3] Department of Neurobiology and Behavior, University of California, Irvine, Irvine, CA, United States, [4] Department of Biomedical Engineering, University of California, Irvine, Irvine, CA, United States, [5] Department of Pharmaceutical Sciences, University of California, Irvine, Irvine, CA, United States, [6] Center for the Neurobiology of Learning and Memory, University of California, Irvine, Irvine, CA, United States

Decades of research have revealed the remarkable complexity of the midbrain dopamine (DA) system, which comprises cells principally located in the ventral tegmental area (VTA) and substantia nigra pars compacta (SNc). Neither homogenous nor serving a singular function, the midbrain DA system is instead composed of distinct cell populations that (1) receive different sets of inputs, (2) project to separate forebrain sites, and (3) are characterized by unique transcriptional and physiological signatures. To appreciate how these differences relate to circuit function, we first need to understand the anatomical connectivity of unique DA pathways and how this connectivity relates to DA-dependent motivated behavior. We and others have provided detailed maps of the input-output relationships of several subpopulations of midbrain DA cells and explored the roles of these different cell populations in directing behavioral output. In this study, we analyze VTA inputs and outputs as a high dimensional dataset (10 outputs, 22 inputs), deploying computational techniques well-suited to finding interpretable patterns in such data. In addition to reinforcing our previous conclusion that the connectivity in the VTA is dependent on spatial organization, our analysis also uncovered a set of inputs elevated onto each projection-defined VTA^{DA} cell type. For example, $VTA^{DA}\rightarrow$NAcLat cells receive preferential innervation from inputs in the basal ganglia, while $VTA^{DA}\rightarrow$Amygdala cells preferentially receive inputs from populations sending a distributed input across the VTA, which happen to be regions associated with the brain's stress circuitry. In addition, $VTA^{DA}\rightarrow$NAcMed cells receive ventromedially biased inputs including from the preoptic area, ventral pallidum, and laterodorsal tegmentum, while $VTA^{DA}\rightarrow$mPFC cells are defined by dominant inputs from the habenula and dorsal raphe. We also go on to show that the biased input logic to the VTA^{DA} cells can be recapitulated using projection architecture in the ventral midbrain, reinforcing our finding that most input differences identified using rabies-based (RABV) circuit mapping reflect projection archetypes within the VTA.

Keywords: VTA (ventral tegmental area), rabies, circuit mapping, dopamine, inputs and outputs, high dimension datasets, spatial patterning

OPEN ACCESS

Edited by:
Talia Newcombe Lerner, Northwestern University, United States

Reviewed by:
Mitsuko Watabe-Uchida, Harvard University, United States
David Bortz, University of Pittsburgh, United States

***Correspondence:**
Kevin T. Beier
kbeier@uci.edu

Received: *21 October 2021*
Accepted: *14 December 2021*
Published: *28 January 2022*

Citation:
Derdeyn P, Hui M, Macchia D and Beier KT (2022) Uncovering the Connectivity Logic of the Ventral Tegmental Area. Front. Neural Circuits 15:799688. doi: 10.3389/fncir.2021.799688

INTRODUCTION

The VTA plays a central role in a variety of both adaptive and pathological motivated behaviors, principally through cells that release the neurotransmitter DA (Morales and Margolis, 2017). These cells direct motivated behaviors by release of DA into downstream brain structures such as the nucleus accumbens (NAc), dorsal striatum (DStr), and medial prefrontal cortex (mPFC) (Beier et al., 2015). Activation of DA cells as a population is highly reinforcing, as animals will robustly self-administer stimulation of DA neurons (Olds and Milner, 1954). DA cells have also been implicated in reward-prediction error (RPE), or the difference between the received and anticipated value of an outcome (Schultz, 1998). While much of the data fit the RPE model, some do not. For example, an aversive stressful experience or a painful stimulus such as a foot pinch triggers DA release into forebrain structures (Navratilova et al., 2015). One recent study suggested that physiological DA release in the NAc only relates to outcomes predicted by RPE within a limited number of scenarios and instead broadly signals perceived salience (Kutlu et al., 2021). Other studies pointed to the existence of subsets of DA cells that not only project to different forebrain sites, but also have unique transcriptional, electrophysiological, and response properties to various stimuli (Lammel et al., 2008, 2011; Kim et al., 2016). We now know that the VTA is comprised of heterogenous cell types: DA cells comprise roughly 50% of VTA cells in the rat, fewer than the >70% previously estimated (Margolis et al., 2006); another ∼40% of cells in the VTA are GABAergic. Many of these GABAergic cells inhibit VTA^{DA} neurons, and their activation has the opposite effect of DA cell stimulation (Bouarab et al., 2019). In addition to locally inhibiting DA cells, VTA^{GABA} neurons also project to a variety of forebrain sites, including the NAc and lateral habenula (LHb). Many VTA^{GABA} cells can also co-transmit glutamate (Root et al., 2014). Additionally, many NAc-projecting midbrain DA cells co-transmit glutamate, and some can also synthesize and transmit GABA through a non-canonical pathway (Tritsch et al., 2012; Kim et al., 2015). This complexity makes it difficult to definitively disentangle the roles that various cells play in adaptive and maladaptive behaviors.

To date, DA cells have typically been differentiated based on output site. For example, Lammel et al. (2008) injected fluorescent microspheres into different forebrain sites and showed that the DA cells in the midbrain that took up the microspheres were largely distinct, as these cell populations differed in their expression of dopamine transporter, DAT, and in their electrophysiological properties. They later showed that these cells were differentially modulated by experience, as the synapses onto some cells and not others were modulated by either a cocaine (rewarding) or formalin (aversive) experience (Lammel et al., 2011). These results suggested that these cells are integrated into separate circuits that are differentially involved in either reward or aversion learning. The same investigators then showed that VTA^{DA} cells projecting to the NAc preferentially received inputs from the laterodorsal tegmentum (LDT) and signaled reward, whereas VTA^{DA} cells projecting to the mPFC preferentially received inputs from the LHb and signaled aversion (Lammel et al., 2012). These studies provided a simplified framework through which VTA^{DA} neurons could encode both reward and aversion-related signals through separate forebrain projections. Subsequent studies have largely supported this framework, with some modifications. We, therefore, wanted to explore the global anatomical organization of these cells and examine how connectivity logic may help to explain the roles different DA cells play in behavior. As midbrain DA cells have been shown to receive direct monosynaptic inputs from over 100 anatomically defined brain regions (Watabe-Uchida et al., 2012), our goal has been to create comprehensive input-output connectivity maps of discrete DA populations to compare the inputs and outputs of these cells.

To unambiguously define input-output relationships of midbrain DA cells, we developed an intersectional viral-genetic method to tag cells defined by both gene expression and output site, termed cell type-specific Tracing the Relationship of Inputs and Outputs (cTRIO) (Beier et al., 2015; Schwarz et al., 2015). In our initial study, we characterized the input-output relationships of VTA^{DA} cells projecting to the nucleus accumbens (NAcMed and NAcLat), medial prefrontal cortex (mPFC), and Amygdala (Beier et al., 2015). cTRIO revealed separate sub-circuits centered on midbrain DA cells that had biased inputs and discrete outputs. We then performed a more detailed characterization of the connectivity relationships of these populations (Beier et al., 2019), finding that the spatial location of starter cells in the VTA was the main determinant of the inputs that each population received while the neurotransmitters that the cells released did not strongly influence input patterns. However, relating the center of mass (COM) of "starter" neurons that initiate RABV tracing to input fraction using a simple linear regression only explained significant variance for about half of the input sites examined, suggesting that this level of analysis was not sufficient to explain the full complexity of input patterning to the VTA. Quantitative techniques have been adopted in other fields to reveal patterns in high dimensional data. In this study we aim to introduce such techniques to neural circuit mapping. We revisit previously published datasets describing the inputs and outputs of VTA^{DA} cells and find new patterns and rules underlying their connectivity.

RESULTS

VTA^{DA} Neurons Segregate by Projection Condition With Characteristic Output Patterns

Lammel et al. (2008) first used retrobead injections into different forebrain regions in the mouse to show that DA cells projecting to different forebrain sites were physically located in different domains of the VTA or SNc. These results suggested that DA cells largely project to one forebrain site and not others. Recently, we used a more sensitive method that enabled brain-wide analysis of the entire axonal arbor of each DA cell subpopulation to show that each cell population in fact does send collaterals to other brain sites, but that the collateralization patterns are largely unique for each subpopulation, and thus the overall projection

pattern of each population is largely distinct (Beier et al., 2015, 2019). We also were the first to perform brain-wide input mapping analysis from projection-defined DA populations in the VTA and the adjacent SNc (Beier et al., 2015, 2019; Lerner et al., 2015; Menegas et al., 2015). In contrast to the largely discrete output patterns of these cells, we and others observed that midbrain DA cells receive quantitatively similar inputs from most brain regions, with several biases in the contributions of these inputs onto defined DA cell types. These input biases between conditions may influence the differential role these cells play in subsequent behavioral output, for example in reinforcement behavior (Beier et al., 2015). Given that we have collected whole-brain quantitative datasets of the inputs and outputs of $VTA^{DA}\rightarrow$NAcMed, $VTA^{DA}\rightarrow$NAcLat, $VTA^{DA}\rightarrow$mPFC, and $VTA^{DA}\rightarrow$Amygdala cells, we wanted to perform a more in-depth analysis to identify factors that differentiated the inputs and outputs of different DA cell types. We previously performed hierarchical clustering on bootstrapped data and demonstrated that VTA^{DA} cells projecting to NAcMed, NAcLat, mPFC, or Amygdala clustered separately based on their output projections to 10 forebrain sites (Beier et al., 2019), indicating that their global output patterns were distinct. We also demonstrated the existence of four groups of output sites with high levels of covariance in our dataset, suggesting that each set of output regions may be preferentially targeted by one DA cell population. However, we did not rigorously identify how these conditions differed and which output sites most contributed to differentiating the projection pattern of each DA cell population.

To explore this dataset in greater detail, we first used Principal Component Analysis (PCA) to dimensionally reduce the output data (**Figures 1A,B**). The output data consist of 18 brain samples from 4 different output-defined conditions (n = 5 for NAcMed and mPFC; n = 4 for NAcLat and Amygdala). Each sample has 10 measurements, one for each of the output regions quantified. PCA is a linear dimensionality reduction technique that finds a lower dimensional representation of the data that maximizes variance for each principal component (PC). The first PC is a linear combination of the feature space that leads to the highest degree of variance in the data. Each component after makes the same optimization with the remaining dimensions. We found that three components are sufficient to explain ∼70% of the variance in the output data, indicating that these data have a relatively simple structure (**Figure 1C**). PC1 separates $VTA^{DA}\rightarrow$NAcLat cells, PC2 separates $VTA^{DA}\rightarrow$NAcMed cells, PC3 separates $VTA^{DA}\rightarrow$Amygdala cells, and a combination of PC2 and PC3 separates $VTA^{DA}\rightarrow$mPFC cells (**Figures 1D,E**). Thus, three PCs were sufficient to separate each condition.

Next, we wanted to explore how each output region contributed to each PC. For example, PC1, which separated $VTA^{DA}\rightarrow$NAcLat cells, is driven by NAcLat, nucleus accumbens core (NAcCore), dorsomedial striatum (DMS), and dorsolateral striatum (DLS; **Figure 1F**). The finding that the NAcLat as an output site helps to differentiate $VTA^{DA}\rightarrow$NAcLat cells is consistent with the biased projections of each midbrain DA cell population. Additionally, the contribution of other regions in the striatum (except for NAcMed) is consistent with the overall arborization pattern of these cells (Beier et al., 2015). This cell population had the most distinct overall arborization pattern and thus positive weights of these four regions were sufficient to differentiate it. PC2, which separates $VTA^{DA}\rightarrow$NAcMed cells, is primarily made up of the NAcMed, with smaller contributions from the NAcCore and negative contributions from the mPFC, bed nucleus of the stria terminalis (BNST), and central amygdala (CeA). These negative contributions mean that $VTA^{DA}\rightarrow$NAcMed cells do not prominently project to the mPFC, BNST, or CeA. Lastly, PC3, which separated $VTA^{DA}\rightarrow$Amygdala cells, is made up of positive contributions from the ventral pallidum (VP), BNST, and CeA, and negative contributions from the mPFC and septum. The overall arborization patterns of NAcMed-, mPFC-, and Amygdala-projecting VTA^{DA} cells are more similar to one another than to NAcLat-projecting VTA^{DA} cells (Beier et al., 2019); thus in PC2, the negative contributions from the mPFC, CeA, and BNST differentiate NAcMed-projectors from Amygdala- and mPFC-projectors, and in PC3, the negative contributions from the mPFC and septum, which are the brain regions most enhanced in the output targets of $VTA^{DA}\rightarrow$mPFC cells, differentiate $VTA^{DA}\rightarrow$mPFC and $VTA^{DA}\rightarrow$Amygdala cells.

While PCA is useful due to its interpretability, Uniform Manifold Approximation and Projection (UMAP) is better optimized for finding clusters in high dimensional data. Indeed, we find it is much more effective at clustering conditions by output site (**Figure 1G**; McInnes et al., 2018). As UMAP uses non-linear transformations to achieve clustering, it does not provide us the same detailed information about which output regions are differentiating these clusters. However, we can compute the transpose of the output data and take the z-score to look at how output scores per region vary across samples. Z-scoring normalizes the data such that high and low count regions that have the same variance will have similar values. We used UMAP on these z-scores and found two clusters of output sites with similar variance (**Figure 1H**). The bottom left cluster contains the four regions that show up in PC1: NAcLat, NAcCore, DMS, and DLS. These data provide confirmation that these four regions vary as a module across these four conditions and serve as a common set of brain sites targeted by the same cell population ($VTA^{DA}\rightarrow$NAcLat) whereas the other three cell populations share more overlap in their overall projection patterns. This visualization serves as a complement to previous analysis of these data, where hierarchical clustering of the output regions' covariances found the same organization, highlighting both the robustness of this result and these methods.

To ensure these results were not biased by outputs to the injected projection sites, we removed the projection sites from the output counts and performed the same analysis as before on just the collaterals. We largely see the same clustering behaviors as before (**Supplementary Figure 1**). The main difference is that the $VTA^{DA}\rightarrow$NAcMed and $VTA^{DA}\rightarrow$mPFC brains are harder to separate (**Supplementary Figures 1B,C,E**). Previously, PC2–now PC3–separated these two conditions the strongest (**Figure 1D**). This principal component previously had large contributions from three of the projection targets, so it is not surprising that the differences between these conditions are weakened along with the principal component (**Figure 1F** and

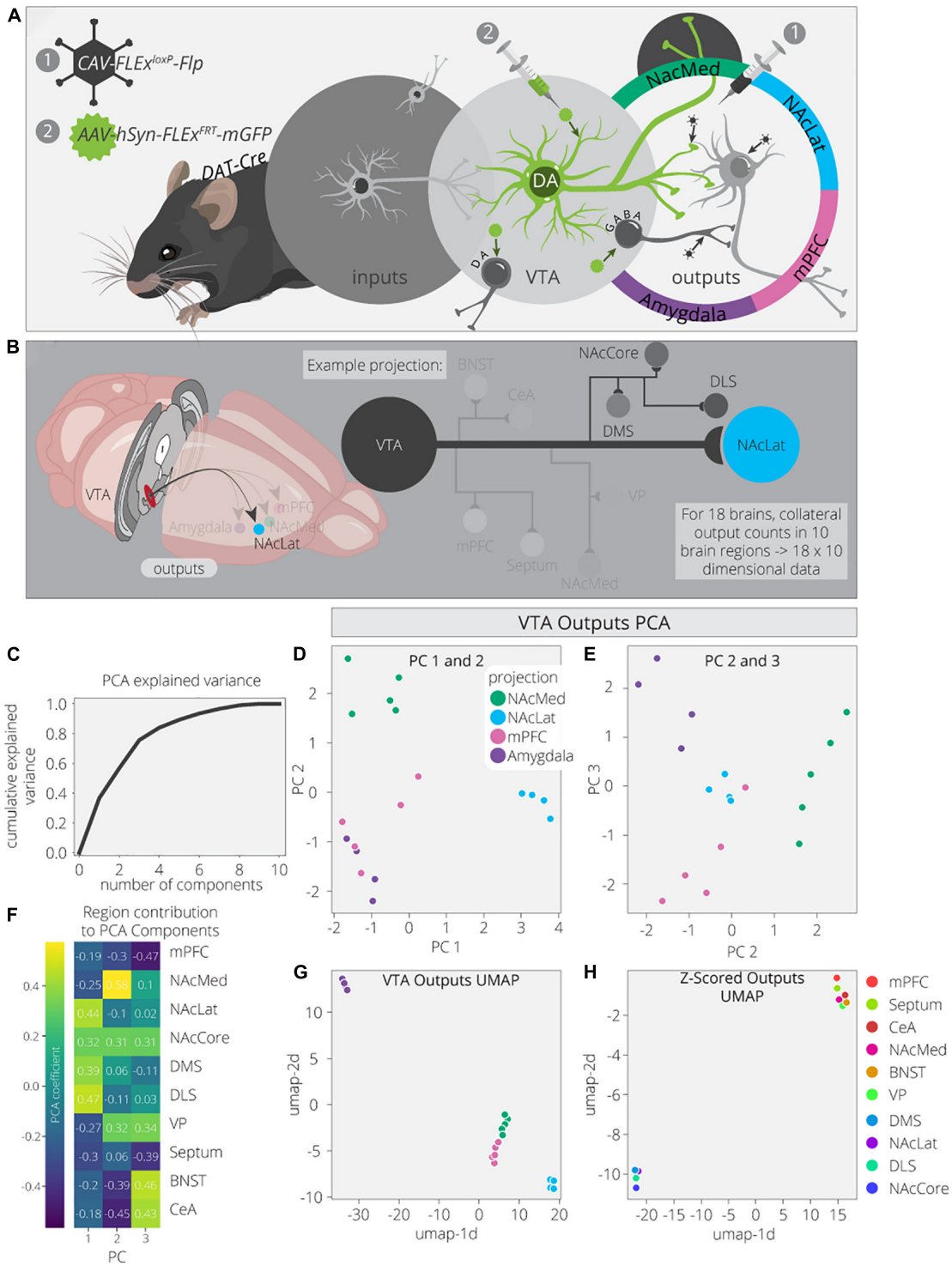

FIGURE 1 | VTA^{DA} outputs are organized by four core projections. **(A)** Schematic for axonal arborization experiments. Viral injections were performed in *DAT-Cre* mice to label collaterals to VTA^{DA} neurons projecting to a specified target. **(B)** Collaterals of VTA projections to the NAcMed, NAcLat, mPFC, and Amygdala were quantified in 10 brain regions across 18 mice. The NAcLat and its major collaterals are highlighted. **(C)** Cumulative explained variance from each principal component. **(D)** Brains are plotted in PCA space for the 1st and 2nd components, colored by projection. **(E)** Brains are plotted in PCA space for the 2nd and 3rd components, colored by projection. **(F)** Heatmap of each output region's contribution to the first three principal components. **(G)** Brains are plotted in UMAP space, colored by projection. **(H)** Output regions are plotted in UMAP space, embedded with respect to z-scores across mouse brains. Clusters represent outputs with similar patterns of variation across the cohort.

Supplementary Figure 1D). Altogether, this analysis confirms that the clustering of projection conditions does not completely depend on including the main projection targets.

VTA^{DA} Neuron Inputs Do Not Cluster as Cleanly by Projection Site

We and others used intersectional viral-genetic methods to map global inputs to output-defined DA cells (Beier et al., 2015; Lerner et al., 2015; Menegas et al., 2015). While the exact relationships of inputs and outputs varied slightly between different studies, the common finding was that different DA cell populations largely shared common input patterns, with some quantitative differences. We more recently performed a comprehensive mapping of input-output relationships of different cell types in the VTA and reported that (1) the spatial location of cells in the VTA explained a significant amount of variation between conditions for about half of the input sites, (2) cell type did not explain much variation in the inputs between cell populations, and (3) the projection site explained about as much input variation as did spatial position of starter cells in the VTA (Beier et al., 2019). To account for neurons that co-release multiple neurotransmitters, for example glutamate and dopamine, we included the percentage of starter cell immunostaining for tyrosine hydroxylase (TH), a marker of DA neurons, in our linear regression analysis and found it had very little predictive value compared to spatial location (Beier et al., 2019). These observations suggested that the quantitative contribution of inputs a given population of cells receives depends heavily on the physical location of the starter cells in the brain, but not on the identify of what neurotransmitters (e.g., DA, GABA, glutamate) these starter cells release.

Here we used PCA and UMAP to dimensionally reduce and explore patterns in the input data. These data consist of 76 brains with counts across 22 input regions (Beier et al., 2019). These brains cover a variety of cTRIO and TRIO conditions as well as non-output-defined tracing, resulting in a mix of output and cell-type specifications (**Figures 2A,B**). A PCA analysis of these data found that three components explained only about 40% of the variance (**Figure 2C**). This is rather low compared to the output data, even considering the difference in dimensionality, and implies that this dataset is more complex. In the PCA embedding, cell types defined by Cre expression (*DAT-Cre*, *GAD2-Cre*, *vGluT2-Cre*, no Cre) mix together but cells projecting to a common output target do show some organization (**Figures 2D,E** and **Supplementary Figure 2**). For example, VTA→NAcLat cells have more positive values in the 1st PC and more negative values in the 2nd PC (**Figure 2E**). These coordinates reflect higher contributions from brain regions in the basal ganglia which include the NAc, dorsal striatum (DStr), and global pallidus external segment (GPe), as well as lower contributions from the VP and preoptic area (PO) (**Figure 2F**). Notably, the non-output-defined condition is most similar to the VTA→NAcLat condition, which is expected given that VTA→NAcLat cells comprise the majority of cells in the VTA (Beier et al., 2015).

We next used UMAP to look for any additional clustering behavior between the inputs mapped in different brains in order to assess the similarities and differences between conditions (**Figures 2G,H**). When defining conditions by Cre expression (*DAT-Cre*, *GAD2-Cre*, *vGluT2-Cre*, no Cre), there are some local neighborhoods within the same conditions, but none are very well-separated into clusters. However, when defining conditions based on output site, the VTA→NAcLat conditions segregate relatively well (**Figure 2H**). These results are consistent with our previously published analysis (Beier et al., 2019). We then performed a UMAP analysis on the input region z-scores to identify regions with similar variation across conditions (**Figure 2I**). We found one cluster (cluster 1) made up of inputs from the NAc, DStr, GPe, and cortex. Almost all these regions follow a pattern of contributing positively to the 1st PC and negatively to the 2nd PC (**Figure 2F**). Thus, these regions provide a stronger fractional innervation to VTA→NAcLat cells than other VTA cells, as observed previously (Beier et al., 2015, 2019). In addition to cluster 1, we observed two other clusters of inputs; one included the CeA, parabrachial nucleus (PBN), zona incerta (ZI), entopeduncular nucleus (EP), and deep cerebellar nuclei (DCN; cluster 2), while the other included all the other regions: VP, PO, LDT, BNST, dorsal raphe (DR), medial habenula (MHb), lateral habenula (LHb), paraventricular nucleus of the hypothalamus (PVH), extended amygdala (EAM), lateral hypothalamus (LH), and septum (cluster 3). These clusters were not readily apparent in our previous analyses of our RABV tracing data, suggesting that there may be additional organization in the input patterns that we had overlooked previously.

Lateral or Medial Biases of Starter Cells Accounts for Some but Not All VTA^{DA} Input-Output Variation

We previously analyzed the spatial influence of starter neurons in the VTA on the fractional contribution of inputs by using a linear regression test with the medial-lateral and dorsal-ventral coordinates of the starter cell center of mass (COM) (Beier et al., 2019). Since the cells were counted on coronal slices, we do not have nearly as good resolution for the anterior-posterior axis as the ML and DV axes, and for the most part we focus our analyses on these axes. We observed that the medial-lateral coordinate of the COM explained a significant level of variance for about one half of the brain regions across conditions, about the same contribution as the output site and significantly more than the Cre line used to mark starter cells. These results suggested that many inputs to the VTA are biased along the medial/lateral axis in their projections to the VTA, and that the location of the starter cells, as defined by a single point in space, was significantly linked to the fraction of inputs from various brain regions those cells received.

To further explore the spatial organization of VTA inputs, we plotted each sample according to the starter cell COM and colored them according to their PC values, as calculated in **Figure 2** (**Figures 3A–E**). PC1 has an increasing spatial gradient from the medial to the lateral VTA (**Figure 3B**). This principal component in general is made up of input populations that project more laterally in the VTA, or to the adjacent SNc/substantia nigra pars reticulata (SNr) (Oh et al., 2014;

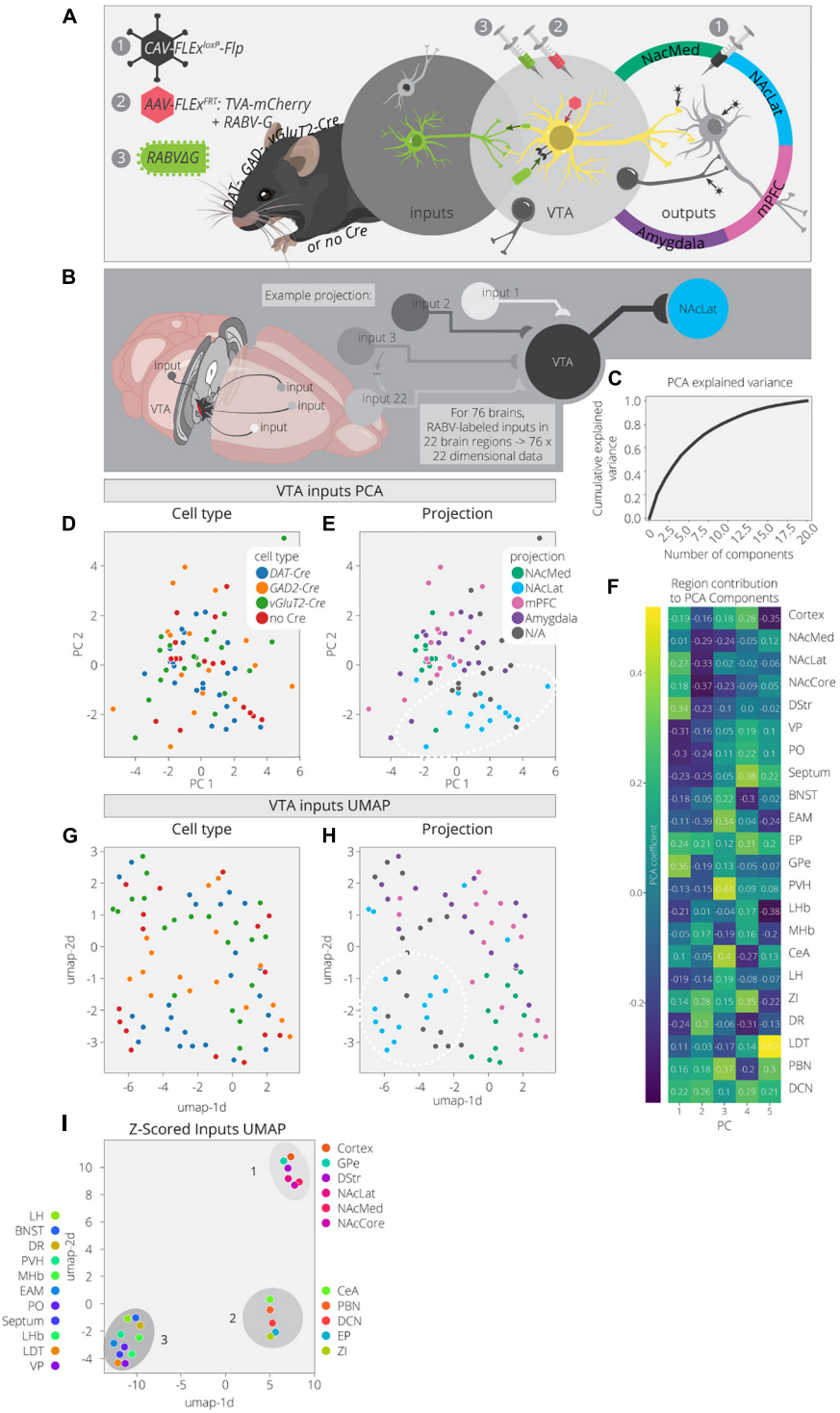

FIGURE 2 | Clusters of VTA inputs revealed by dimensional reduction. **(A)** Schematic for RABV input labeling experiments. *DAT-*, *GAD-*, *vGlut2-Cre*, and non-Cre-expressing mice were used to identify specific (or non-specific) VTA cell types. Injections of *CAV* were used to define output sites. **(B)** Input labeling experiments provided maps of inputs to VTA cells for a combination of different cell-type and projection specifications. Cohort includes 76 brains and 22 input regions counted. **(C)** Cumulative explained variance from each principal component. **(D)** Brains are plotted in PCA space for the 1st and 2nd components, colored by cell type. **(E)** Brains are plotted in PCA space for the 1st and 2nd components, colored by projection. **(F)** Heatmap of each input region's contribution to the first five principal components. **(G)** Brains are plotted in UMAP space, colored by cell type. **(H)** Brains are plotted in UMAP space, colored by projection. **(I)** Input regions are plotted in UMAP space, embedded with respect to z-scores across mouse brains. Clusters represent inputs with similar patterns of variation across the cohort.

Beier et al., 2019). This result agrees with the previous finding that the medial-lateral coordinate is related to the fractional contribution from about one half of the input sites examined (Beier et al., 2019). Furthermore, we can compare this spatial organization with the location of VTA→NAcLat starter cells (**Figure 3F**). The VTA→NAcLat cells are biased toward the lateral side of the VTA, same as the +PC1 cell populations. As PC1 captures the most variation across the data, this means that the primary axis of variation in VTA inputs is whether or not the inputs are biased onto VTA→NAcLat cells, and hence whether the starter cells are located laterally within the VTA or not. PC2 has a mild spatial gradient that increases in the dorsal direction (**Figure 3C**). PC3, on the other hand, does not have much of a clear spatial bias in the medial-lateral or dorsal-ventral axes (**Figure 3D**). Rather, starter cell populations with +PC3 span the VTA across the two axes, suggesting that a lack of clear spatial bias in the VTA characterizes this PC. A linear regression analysis confirmed these observations: PC1 was found to have a significant slope in the lateral direction and PC2 in the dorsal direction, while other slopes were not found to be significant after correction for multiple comparisons (**Table 1**).

Our analysis with PCA and UMAP separated VTA→NAcLat cells by inputs, but largely failed to differentiate VTA→NAcMed, VTA→mPFC, or VTA→Amygdala cells from one another. To explore the input-output features most specific to each VTA cell type, we stitched together the average input and output counts for each region. We then took the z-score of these values to see how enriched or diminished connections are for that region compared to the other conditions. For each projection condition, we found a unique set of enriched inputs and outputs (**Figure 3G** and **Supplementary Figure 3**). Many of these were found significant, even when corrected for multiple comparisons (**Table 2**). We observed some evidence for reciprocal connectivity: for example, inputs from NAcLat are enriched onto VTA→NAcLat cells, and inputs from the Amygdala and BNST are enriched onto VTA→Amygdala cells that collateralize principally to the BNST, both of which were found to be significant. However, this was not equally clear for all populations, as the NAcMed input was approximately equal onto VTA^{DA}→NAcLat and VTA^{DA}→NAcMed cells, and we did not observe a preference for cortical inputs onto VTA^{DA}→mPFC cells (Beier et al., 2019), suggesting that while some reciprocal connections may exist in the VTA, they may not be universal for all brain regions (**Figure 3G**).

The input and output sites enriched onto VTA^{DA}→NAcLat cells consist of those previously identified (Beier et al., 2015, 2019) and shown in **Figures 1**, **2**. However, we also found a number of brain sites enriched as inputs to or outputs from VTA^{DA}→Amygdala cells that we did not previously identify. These outputs include preferential projections to the Amygdala and BNST, as previously described (Beier et al., 2019), as well as inputs from the CeA, PBN, ZI, PVH, BNST, EAM, DCN, LH, and MHb. Many of these brain regions, including the CeA, PBN, PVH, BNST, and EAM, are in the extended amygdala and are principally involved in stress and anxiety-related behaviors (Bernard and Besson, 1988; Han et al., 2015; Chou et al., 2018; Zhou et al., 2018; Chiang et al., 2019). These same regions are also the strongest positive contributors to PC3 (**Figure 2F**). Furthermore, the location of starter cell COM with a +PC3 (**Figure 3D**) most closely mirrored the distribution of VTA→Amygdala cells, which are distributed broadly throughout the VTA with a centroid in approximately the middle of the structure (**Figure 3F**). These visualizations therefore provide further evidence of the spatial organization of inputs on the VTA that we reported previously, and they also suggest the existence of subpopulations of VTA cells that receive preferential inputs from key brain regions involved in the brain's stress response.

To explore how starter cell COM and RABV input cells distinguish the various projection conditions, we trained logistic regression models to predict each condition. Logistic regression can be used for multiclass classification, in which a logistic regression model is trained for each condition, and the condition with the highest probability is assigned to a given observation. We used the first five principal components as features representing the inputs to the VTA, to reduce overfitting our dataset and to simplify the model to increase the model's interpretability. We trained models on the principal components and the starter cell COMs separately, and on both combined. Unsurprisingly, projection conditions already grouped together in the PCA plots were well-predicted by the principal components, for example the VTA→NAcLat and VTA→Amygdala cell populations (**Table 3**). Additionally, projection conditions that appeared to have a spatial bias achieved higher scores when predicted by COMs, for example the VTA→NAcLat and VTA→mPFC. VTA→NAcMed was predicted greater than chance across each individual set of features. It also ends up with one of the highest prediction scores when both PCs and COMs are considered. This result suggests that a combination of input features and spatial location is needed to encode the identity of this population. Logistic regression models are highly interpretable, as each feature is assigned a coefficient which models the increased or decreased likelihood of a label given a higher or lower value of the feature. These coefficients largely recapitulate observations we have already made. For example, PC1 is useful for predicting VTA→NAcLat, PC3 is useful for predicting VTA→Amygdala (**Supplementary Figure 4A**), and the medial-lateral coordinate is useful for predicting VTA→NAcLat and VTA→mPFC populations (**Supplementary Figure 4B**). In the model incorporating both PCs and COMs, we found that a combination of PC1 with the dorsal and anterior coordinates can predict the VTA→NAcMed condition (**Supplementary Figure 4C**). These analyses imply that while the most striking aspect of VTA input connectivity is the presence of spatial gradients, there may be some interesting connectivity relationships that are not uniquely delineated by a medial-lateral or dorsal-ventral gradient.

Spatial Analysis of Allen Mouse Connectivity Atlas Data Finds Archetypal Projection Patterns to the Ventral Tegmental Area

Using publicly available data from the Allen Mouse Brain Connectivity Atlas, we had previously investigated the spatial

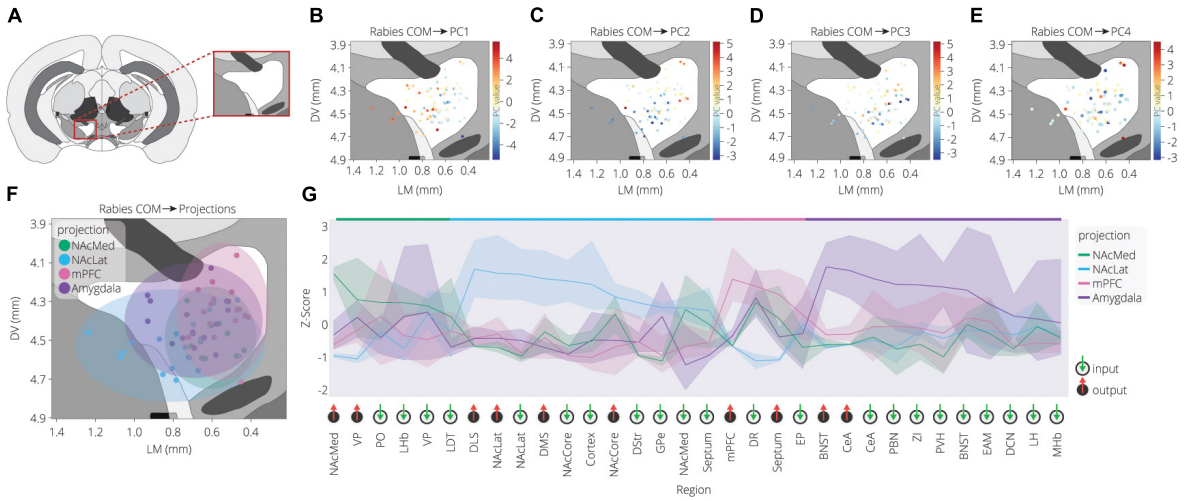

FIGURE 3 | Spatial location of targeted cells in the VTA influences both inputs and outputs. **(A)** Context for coronal slice of VTA used in analysis is shown. **(B)** Brains are plotted by starter cell center of mass (COM), colored by PC1 value. **(C)** Brains are plotted by starter cell COM, colored by PC2 value. **(D)** Brains are plotted by starter cell COM, colored by PC3 value. **(E)** Brains are plotted by starter cell COM, colored by PC4 value. **(F)** Brains are plotted by starter cell COM, colored by projection specification. Ellipsoids are drawn for each condition and have radii of five standard deviations for both dorsoventral and lateromedial axes. **(G)** Z-scores of average input and output counts for each projection condition. Inputs are marked with a green down arrow and outputs with a red up arrow. All inputs and outputs quantified are shown. Inputs and outputs are sorted according to the projection in which they receive the highest z-score. Samples include inputs to and outputs from DA cells only. *p*-values are listed in **Table 2**.

TABLE 1 | Linear regression scores predicting starter cell location from principal components.

PC#	Score	Lateral slope	Significance	Corrected *p*	Dorsal slope	Significance	Corrected *p*
PC1	0.359	8.08	1e-3	1e-2	–2.06	0.175	0.617
PC2	0.299	–2.29	0.031	0.172	–5.36	1e-3	1e-2
PC3	0.0759	0.26	0.81	0.963	–3.08	0.018	0.119
PC4	0.0102	0.04	0.97	0.97	–1.05	0.401	0.871
PC5	0.122	0.4	0.634	0.951	2.9	0.005	0.039

Corrected *p*-value < 0.05

Uncorrected *p*-value < 0.05

Slope and p-value for lateral and dorsal coefficients in linear regression models predicting each principal component. p-value is the probability of the coefficient being 0 given the observed data.

organization of projections to the VTA. We had found that the relative projection ratio across some inputs varied across the lateral-medial axis and that was related to the relative ratio of inputs received by different VTA^{DA} cell populations, linking the density of projections from a given input site to RABV-labeled inputs (Beier et al., 2019). However, this analysis was done with a limited set of brain regions, focused only on the medial-lateral gradient along the VTA, and only explored the link between input density and DA neurons in the VTA. Here we wanted to explore this question with a broader perspective and assess the relationship between projections throughout the ventral midbrain from each of the input sites that we quantified in our previous studies. We wanted to assess globally how closely spatial projection patterns throughout the ventral midbrain relate to RABV input mapping datasets.

For each input region, we selected three experiments from the Allen Mouse Brain Connectivity Atlas and took the average projection into the ventral midbrain. The NAcLat was excluded as an input site, as the Atlas does not contain injections into this site. We also used injections in the infralimbic/prelimbic (IL/PL) and orbitofrontal cortex (Orb) to represent two distinct regions of the anterior cortex. We then mapped these projections onto a coronal slice of the ventral midbrain to facilitate visualization. We used an extended spatial domain that allowed us to assess projections within the VTA as well as to adjacent structures. As before, we used PCA to reduce the dimensions of this space. The first principal component is a weighted combination of the projections from the 22 input sites that maximizes variance across the ventral midbrain window. This weighted combination can then be visualized in the original spatial dimensions. By comparing the PC projection patterns with the region contributions to the PCs (**Figure 4A**), we can see what the archetypal projection patterns are and how input region projections are similar or dissimilar. For example, we computed and plotted the archetypal projection of four regions that provide

TABLE 2 | Sample mean comparison tests for input and output z-scores.

Enriched projection	Region	*p*-value	Corrected *p*-value
NAcMed	NAcMed output	3.31E-09	1.06E-07
NAcMed	VP output	4.93E-02	5.31E-01
NAcMed	PO input	1.50E-01	8.80E-01
NAcMed	LHb input	1.55E-01	8.80E-01
NAcMed	VP input	2.25E-01	8.99E-01
NAcMed	LDT input	6.07E-01	9.74E-01
NAcLat	DLS output	7.43E-07	2.23E-05
NAcLat	NAcLat output	2.57E-05	6.94E-04
NAcLat	NAcLat input	3.00E-04	7.76E-03
NAcLat	DMS output	4.69E-04	1.17E-02
NAcLat	NAcCore input	2.47E-03	5.54E-02
NAcLat	Cortex input	6.15E-03	1.27E-01
NAcLat	NAcCore output	6.09E-02	5.85E-01
NAcLat	DStr input	1.57E-01	8.80E-01
NAcLat	GPe input	2.69E-01	9.19E-01
NAcLat	NAcMed input	2.78E-01	9.19E-01
NAcLat	Septum input	3.64E-01	9.34E-01
mPFC	mPFC output	8.87E-06	2.48E-04
mPFC	DR input	9.29E-03	1.62E-01
mPFC	Septum output	1.51E-02	2.28E-01
mPFC	EP input	5.19E-01	9.74E-01
Amygdala	BNST output	3.35E-08	1.04E-06
Amygdala	CeA output	2.93E-06	8.50E-05
Amygdala	CeA input	1.23E-03	2.91E-02
Amygdala	PBN input	6.24E-03	1.27E-01
Amygdala	ZI input	7.06E-03	1.32E-01
Amygdala	PVH input	1.14E-02	1.86E-01
Amygdala	BNST input	2.15E-02	2.93E-01
Amygdala	EAM input	1.97E-01	8.89E-01
Amygdala	DCN input	5.69E-01	9.74E-01
Amygdala	LH input	7.01E-01	9.74E-01
Amygdala	MHb input	8.77E-01	9.74E-01

Corrected *p*-value < 0.05
Uncorrected *p*-value < 0.05

Significance tests comparing projections for each input and output. For each input and output, the sample mean of the most enriched projection was compared against the remaining projections with a T-test. p-values are corrected for multiple comparisons using a Bonferroni correction.

TABLE 3 | Logistic regression scores predicting projection conditions from starter cell location and principal components.

Projection	3 PCs	5 PCs	COMs	5 PCs + COMs
NAcLat	0.8125	0.875	0.6875	0.8125
NAcMed	0.5	0.333333	0.5	0.75
mPFC	0.375	0.4375	0.625	0.625
Amygdala	0.625	0.625	0.4375	0.75
None	0.5625	0.4375	0.125	0.6875

Score > 0.8
Score > 6
Score > 0.4

Logistic regression model scores predicting each condition using RABV input principal components and/or starter cell location, using multi-class classification.

preferential inputs onto VTA→NAcLat cells: The NAcMed, NAcCore, DStr, and GPe. This archetype shows a projection to the lateral VTA, where the VTA→NAcLat cells are located, as expected (**Figure 4B**).

PC1 includes projections that relatively uniformly innervate the entire VTA, with little bias (**Figures 4C–E**). This marks the +PC1 pixels, and thus we would expect the regions with positive contributions to this PC to have higher projections over this space. Some example input sites with this pattern include the PO, BNST, EAM, PVH, and LH (**Figure 4C**). Interestingly, these regions all fall within cluster 3 of our RABV data (**Figure 2I**) and have inputs that are enriched onto VTA→Amygdala cells (**Figure 3G**). Another characteristic of PC1 is that its negative values are ventral and lateral to the VTA. We therefore expect -PC1 pixels to have higher projections from the -PC1 regions and lower projections from the +PC1 regions. The DStr and GPe both do not project much to the VTA directly, but they do have strong projections lateral to the VTA (**Figure 4E**). Likewise, the +PC1 regions – PO, BNST, EAM, PVH, and LH – tend not to project at all to this area lateral and ventral to the VTA, but rather project broadly throughout the VTA. Thus, the primary axis of variation that PC1 seems to capture contains the regions that are projecting with little bias to the VTA, and those that are projecting lateral and ventral to the VTA (**Figures 4D,F**). This projection primarily innervates VTA→Amygdala cells that are distributed throughout the VTA (**Figure 3F**).

+PC2 receives the strongest weights from the septum, LDT, PO, MHb, and LHb, while -PC2 is composed primarily of the VP, GPe, CeA, PBN, and DCN (**Figure 4C**). This PC appears to have a medial/ventral bias, as the brain regions with the strongest weights project primarily to the medial and ventral portion of the VTA, while the GPe, CeA, PBN, and DCN all project laterally/dorsally (**Figures 4G–H**). Given that the VTA→NAcMed cells are located the furthest in the ventromedial portion of the VTA (**Figure 3F**), we would expect that VTA^{DA}→NAcMed cells receive preferential input from these brain regions. Indeed, the PO, LHb, and LDT preferentially connect to VTA^{DA}→NAcMed cells, while the septum connects approximately equally to VTA→NAcMed and VTA→NAcLat cells (**Figure 3G**). Notably, -PC2 receives a relatively strong negative weight from the DR (**Figure 4C**).

+PC3 is primarily composed of inputs from the basal ganglia (NAcMed, NAcCore, DStr, GPe), and the two cortical regions, IL/PL and Orb, while –PC3 is composed primarily of the EP, ZI, and DCN (**Figure 4C**). +PC3 corresponds to inputs that project ventrolateral to the VTA (**Figures 4I,J**), and primarily innervate VTA→NAcLat cells (**Figures 2H**, **3G**). The brain regions that contribute to -PC3 project dorsal to the VTA.

+PC4 has strong contributions from the LHb, MHb, and DR, while -PC4 is primarily composed of the septum, PVH, and ZI (**Figure 4C**). Of the positive contributors, the LHb and MHb are also present in +PC2 as they broadly project to the medial VTA, which also is where VTA^{DA}→NAcMed cells are located. In contrast, the DR contributes mostly to +PC4 and +PC1. This combination of PCs describes the DR's

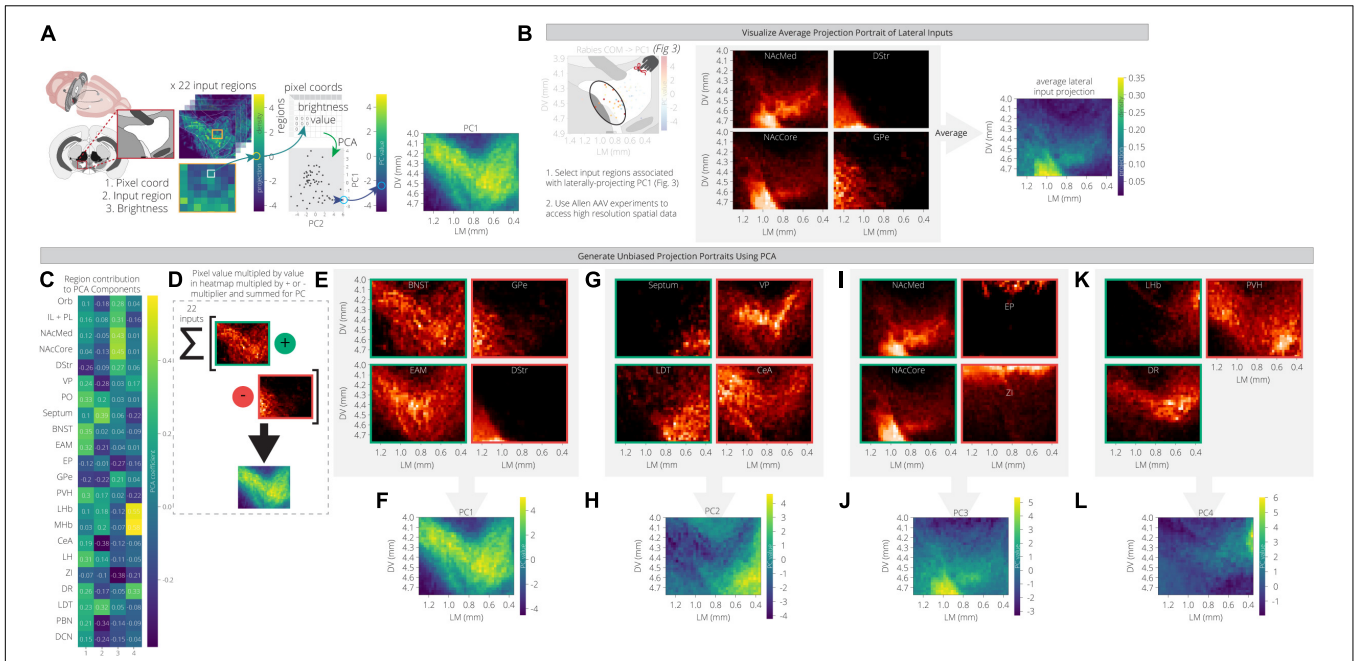

FIGURE 4 | PCA of data from the Allen Mouse Brain Connectivity Atlas reveals projection archetypes across different input groups. **(A)** Schematic of analysis. Sample projections to the VTA were pulled from the Allen Mouse Connectivity Atlas for 22 input regions. Pixel values representing projection density were pulled from the coronal slice for each region to generate a table of 2,058 pixel coordinates x 22 regions. PCA found a linear combination of input regions that maximizes variation across the pixels. Each pixel is then visualized on a coronal slice of the VTA with its PC value, revealing the most common projection portrait. **(B)** Brain regions that preferentially provide inputs to VTA→NAcLat cells were selected as a test case to see if they might have a common projection pattern. Sample projections from these regions to the VTA are shown from the Allen data, along with their average projection portrait. **(C)** Heatmap of each input region's contribution to the first four principal components. **(D)** Positive and negative contributing regions to each principal component are summed according to their sign in order to generate the principal component projection portrait. **(E–L)** Example projection portraits are shown for the major positive and negative contributing regions for each of the first four principal components. The projection archetypes corresponding with these principal components are shown in panels **(F,H,J,L)**.

broad projection to the dorsal VTA with a strong bias to the dorsomedial VTA. +PC4's archetypal projection is also to the dorsomedial VTA (**Figures 4K,L**), a region that most prominently includes VTA^{DA}→mPFC neurons (**Figure 3F**). Accordingly, the DR preferentially innervates VTA^{DA}→mPFC cells (**Figure 3G**) and thus is the main input brain region that differentiates VTA^{DA}→NAcMed from VTA^{DA}→mPFC cells.

These data demonstrate that the first four PCs using data from the Allen Mouse Brain Connectivity Atlas correspond to the input biases of the four VTA populations that we examined here. Therefore, our conclusion is that we can recapitulate the principal differences in inputs to different cell populations in the VTA solely by identifying the archetypal projections into the VTA using open-source data from the Allen Institute.

Patterns of Input Innervation Are Conserved Between RABV Mapping and Allen Projection Data

Our analysis of the Allen's projection data suggests that we can recapitulate the variance in RABV mapping experiments by decomposing the Allen's projection data into principal components. As we previously mentioned, UMAP is better optimized for identifying the relationship between variables in high-dimensional space. We therefore wanted to assess the relationship between input sites to the VTA, defined either through their covariance in our RABV mapping data or spatial similarity in Allen projection data. We demonstrated earlier that the input sites in RABV mapping experiments segregate into three clusters (**Figures 2H**, **5A**). As UMAP embeddings can be somewhat stochastic because they rely on initial seeding conditions, we computed the distance between points relative to the maximum distance between any two points in each embedding, over 20 embeddings, then averaged across all embeddings (**Figures 5A–D**). In both cases, we identified three clusters of brain regions. Cluster 1 contained perfect correspondence between RABV and Allen datasets, and included regions in the frontal cortex (either anterior cortex or both the IL/PL and Orb), NAcMed, NAcCore, DStr, and GPe (the NAcLat was not included in the Allen dataset). While clusters 2 and 3 in the RABV and Allen datasets did not perfectly align, they did have similar structures. RABV cluster 2 included the CeA, EP, ZI, PBN, and DCN. These regions also clustered together in the Allen data, but were joined by the VP, EAM, LHb, MHb, and DR that split from cluster 3. The remainder of the brain regions (septum, BNST, PO, PVH, LH, LDT) are in cluster 3 for both datasets. Notably, the distance between clusters 2 and 3 in the Allen data is much smaller than to cluster 1 and thus, Allen clusters 2 and 3 have a more similar projection profile to each other than to cluster 1. Overall, we observed substantial similarity between RABV and

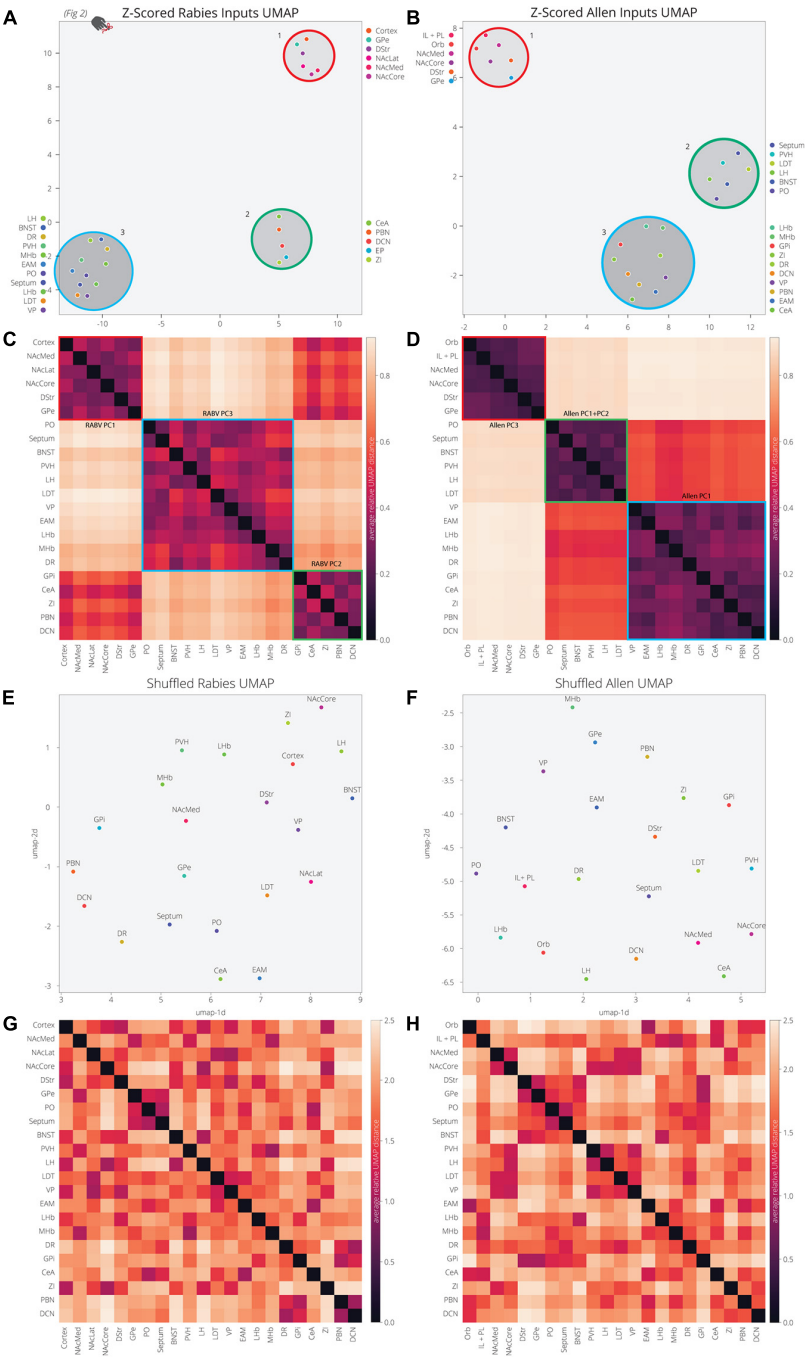

FIGURE 5 | UMAP dimensional reduction of RABV and Allen data reveal common clusters of VTA inputs. **(A)** Input regions are plotted in UMAP space, embedded with respect to z-scores from the RABV input mapping data. Clusters represent inputs with similar patterns of variation across the cohort. **(B)** Input regions are plotted in UMAP space, embedded with respect to z-scores across pixels in the Allen data. **(C)** Heatmap of pairwise distances (averaged across 20 UMAP embeddings) for the RABV input data. Regions are grouped according to hierarchical clusters. Clusters are highlighted to match the clusters above in the UMAP plot; they are also annotated according to which principal components to which the regions contribute. Regions are grouped to line up with the Allen clusters. **(D)** Heatmap of pairwise distances (averaged across 20 UMAP embeddings) for the Allen input data. **(E–H)** Same plots as panels **(A–D)**, but UMAP was run on scrambled data. For each region, z-score values were scrambled across mouse brains for RABV data, or pixel coordinate for the Allen data.

Allen datasets, suggesting that the covariance in input labeling using RABV mapping can be largely attributed to differences in axonal innervation from input sites and thus, the information can be gleaned through parsing open-source projection datasets. To demonstrate that these associations were not attributed to chance, we scrambled the association of the COM with fraction

of inputs labeled in the RABV dataset, or the order of z-scores for pixel intensity for each input site. UMAP was unable to identify clusters or significant levels of co-variance in either scrambled dataset (**Figures 5E–H**), demonstrating that the high covariance between selected input brain sites is highly significant and similar between both RABV and Allen datasets.

DISCUSSION

Our detailed observations of input and output datasets of VTA cells revealed several interesting findings. The largest contributor to variance in our input tracing dataset is the medial-lateral gradient in the VTA, which differentiates the VTA^{DA}→NAcLat cells from the other three subpopulations. The VTA^{DA}→NAcLat cells also had the most distinct collateralization pattern of the four VTA^{DA} subpopulations studied. These results confirm our previous analyses (Beier et al., 2015, 2019). However, here we were able to further differentiate the VTA^{DA} projections to the NAcMed, mPFC, and Amygdala by inputs as well as outputs with an integrated spatial analysis of several high dimensional datasets. By exploring the z-scores of input counts in different brain regions, we found that the PO, LHb, VP, and LDT inputs were elevated for VTA^{DA}→NAcMed cells, DR and EP inputs are elevated for VTA^{DA}→mPFC cells, and CeA, PBN, ZI, PVH, BNST, EAM, DCN, LH, and MHb inputs are elevated for VTA^{DA}→Amygdala cells (**Figure 6**). The z-score normalization allowed us to find elevations in inputs and outputs whose fractional counts were smaller in magnitude than other regions. Logistic regression models demonstrated how RABV inputs and starter cell location contributed to differentiating these conditions. Investigation of the projection patterns of inputs to the VTA revealed that VTA input populations can be differentiated into several projection archetypes—projections to the VTA broadly, projections to regions around but not including the VTA, and projections to

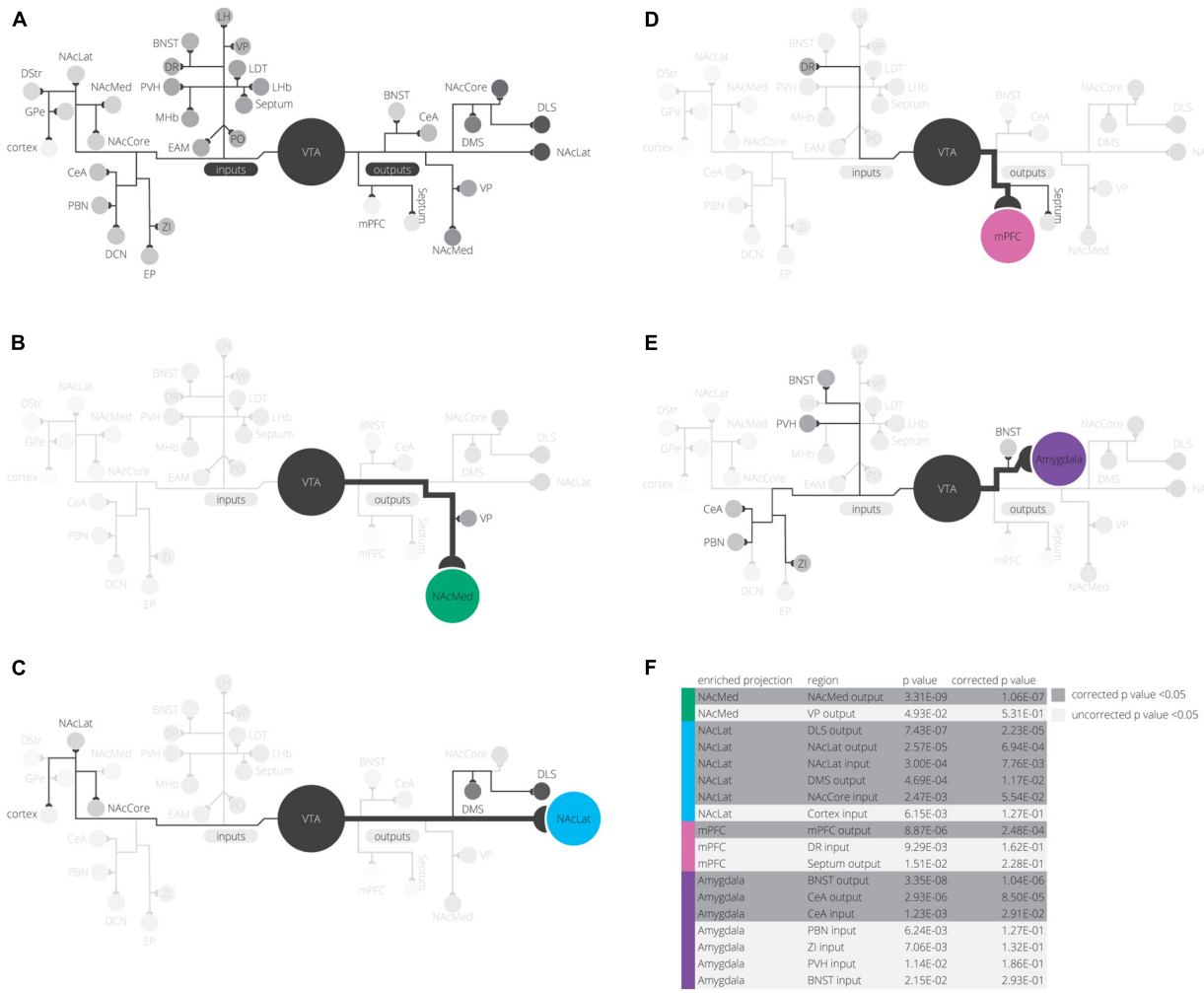

FIGURE 6 | Summary of findings. **(A)** All inputs and outputs we mapped in our experiments are shown, grouped in their clusters from UMAP analysis. **(B–E)** For each projection, elevated inputs and outputs are shown (according to **Figure 3G**). **(F)** Inputs or outputs significantly elevated in any projection condition are shown grouped by projection. *p*-values are corrected for multiple comparisons using a Bonferroni correction.

subdomains of the VTA. Lastly, we showed that the patterns of these projection archetypes mirror input differences to VTA subpopulations. These data together demonstrate that the location of different DA cell populations determines the quantitative contribution from different inputs and, thus, the signals that these cells receive.

Comprehensive Quantitative Analysis Enables Differentiation of Four VTA^{DA} Cell Populations

Our goal in this study was to identify input and output factors that differentiate VTA^{DA} neurons. Previous studies have shown that subpopulations of VTA^{DA} cells differ in their forebrain projections, electrophysiological properties, and behavioral functions (Lammel et al., 2008, 2011; Kim et al., 2016). Comprehensive input-output mapping studies from us and several other groups suggested that DA cell populations received inputs from the same brain regions in quantitatively similar proportions, with some biases. Of note, we previously found that VTA^{DA} cells projecting to the NAcLat received more inputs from the striatum and globus pallidus external segment than the other VTA^{DA} cells that we examined (Beier et al., 2015, 2019). This is likely because the VTA^{DA}→NAcLat cells are located the most laterally within the VTA, and most of the basal ganglia inputs project most strongly to the adjacent SNr (Beier et al., 2015, 2019). While our previous analyses comparing the fractional contribution from 22 input sites to 4 different VTA^{DA} cell populations were able to differentiate VTA^{DA}→NAcLat cells, VTA^{DA} cells projecting to the NAcMed, mPFC, or Amygdala appeared highly similar. Here, by exploring the z-scored input and output data, we identified sets of inputs and outputs elevated for each cell type.

First, we observed that some VTA^{DA} cell types may be preferentially reciprocally connected, including the predominant VTA^{DA}→NAcLat subpopulation. While this was not the case for all our observed cell populations, as VTA^{DA}→mPFC cells received fewer mPFC inputs than did VTA^{DA}→NAcLat cells (Beier et al., 2019), it does suggest that the hypothesis of reciprocal connectivity cannot entirely be discarded. A model of reciprocal connectivity was proposed long ago (Swanson, 1982; Alheid and Heimer, 1988; Zahm, 2006; Yetnikoff et al., 2014), but a recent viral-genetic mapping study failed to find evidence for this reciprocal connectivity in the VTA (Menegas et al., 2015). By comparing the average percent of inputs arising from individual identified brain regions across animals, we also failed to observe statistically significant evidence of reciprocity (Beier et al., 2015, 2019). However, our z-scored analysis gave better visualizations of the lower fractional inputs, supporting the possibility that some preferential reciprocal connectivity may exist in the VTA. This observation argues that a detailed and higher powered investigation into reciprocal connections in RABV mapping datasets may be necessary to reveal the true connectivity relationships in the brain. It is also possible that reciprocal connections may be more present in certain structures and projections than others. It is however noteworthy that in order for these analyses to achieve significance, comparatively larger datasets like ours may be needed, whereas the majority of RABV mapping studies use only a handful of animals (typically 6 or fewer) per condition.

Second, input regions that are integrated into common circuits and have been implicated in common behavioral functions tend to provide preferential innervation onto one particular VTA^{DA} cell type. For example, striatal and globus pallidus inputs that comprise key components of the basal ganglia preferentially provide input to VTA^{DA}→NAcLat cells that project back into the striatum. We also found that several regions in the extended amygdala that have been implicated in stress-related behaviors preferentially provide input onto VTA^{DA}→Amygdala cells. Several studies have been published in the past few years about the role of VTA^{DA}→Amygdala cells in reward and aversion learning, fear learning, as well as anxiety (Lutas et al., 2019; Lin et al., 2020; Tang et al., 2020). The CeA, PBN, ZI, PVH, BNST, and EAM all play key roles in aversion and anxiety behaviors (Bernard and Besson, 1988; Han et al., 2015; Chou et al., 2018; Zhou et al., 2018; Chiang et al., 2019), and interestingly, all contain neurons that express CRF, a neuropeptide that modulates DA cells in the midbrain and DA responses in downstream structures (Ungless et al., 2003; Wanat et al., 2008; Lemos et al., 2012). While each of these brain regions participates in behaviors other than fear learning and anxiety, it is interesting that each of these regions, which are distributed throughout the brain, has a similar projection pattern in the VTA. This suggests that these regions may work in concert to facilitate behavioral outcomes associated with stress and aversion/fear learning through VTA^{DA}→Amygdala cells. The preferential inputs from basal ganglia regions to VTA^{DA}→NAcLat cells and stress-related inputs to VTA^{DA}→Amygdala cells is likely due to the fact that inputs with common functions form particular projection archetypes. This means that inputs with a similar function may share a set of factors that govern their connectivity, an idea that we explore further below.

Third, variance in our input and output data can be explained by differences in the location of starter cells within the VTA. The input regions that provided preferential innervation to particular VTA^{DA} cell populations preferentially innervated regions of the VTA that matched the spatial location or distribution of the corresponding VTA^{DA} cell type. These results reinforce our previous conclusion that organization within the VTA is largely spatial, with cell type providing little influence on the inputs that those cells receive (Beier et al., 2019). However, they also highlight that additional dimensions of spatial pattern exist within the VTA beyond the medial-lateral gradient that we identified earlier and that these patterns underlie differences in inputs that each cell population receives. For example, we found that while VTA^{DA}→NAcMed and VTA^{DA}→mPFC cells were both located medially in the VTA, inputs that were ventrally biased in the medial VTA preferred VTA^{DA}→NAcMed cells, and inputs that were dorsally biased preferred VTA^{DA}→mPFC cells. These results indicate that these spatial preferences matched the relative ventral or dorsal bias of these VTA^{DA} subpopulations, respectively (**Figure 3**). We also found that VTA^{DA}→Amygdala cells had the broadest medial-lateral distribution and were

located the most centrally in the VTA. Inputs to these cells also lacked clear medial-lateral biases. Altogether, our conclusions in this study are entirely consistent with our previous conclusions, while also extending them by identifying more subtle differences in the location of DA cells within the VTA as well as the location of input projections throughout the VTA.

Specificity of RABV Transmission and Implications for Rules Governing Connectivity

As we noted above, comparing the averages between the percentage of inputs received from different brain regions across animals was sufficient only to reveal the largest differences between conditions. In our dataset, this was sufficient to differentiate $VTA^{DA}\rightarrow$NAcLat cells from the rest, but insufficient to parse apart $VTA^{DA}\rightarrow$NAcMed, $VTA^{DA}\rightarrow$mPFC, and $VTA^{DA}\rightarrow$Amygdala cells from one another. Notably, the method of comparing averages across animals is the standard method of analysis of RABV mapping datasets. Beyond being the simplest approach to analyzing these data, most mapping datasets likely contain too few samples to effectively perform PCA or UMAP analyses of their data. This is likely because RABV mapping experiments are labor intensive and typically not performed on the scale that ours was. In the case of our 76-brain dataset, it took years of viral generation, mouse breeding, stereotaxic injection, brain sectioning, imaging, and manual quantification to obtain it. That it is currently a one-of-a-kind dataset has provided a unique opportunity to explore connectivity within the VTA as well as assess the merit of different analyses of RABV mapping datasets.

It is also worth assessing what RABV mapping studies can tell us and what they cannot. The prevailing viewpoint among those who use RABV circuit mapping is that RABV transmits between neurons in a synapse-specific fashion. We have argued that the evidence for synaptic-exclusive transmission of RABV is weak (Beier, 2019, 2021; Rogers and Beier, 2021). The fact that the results from RABV mapping experiments such as we conducted in the VTA can be largely recapitulated only from anterograde mapping experiments such as those from the Allen Brain Institute, notably ones that do not differentiate axons of passage from axons that functionally innervate cells in the VTA, could be an additional argument that RABV can spread non-specifically. However, we previously performed an experiment in the VTA that showed that RABV transmission from one cell to another is quite different from direct injection of RABV (Beier et al., 2019). This result was also seen in a similar set of experiments carried out in the DMS (Wall et al., 2013). That a quantitatively different set of inputs was obtained from tracing experiments utilizing different modes of RABV administration provides a strong argument that one-step RABV mapping is not equivalent to directly administering RABV into the brain.

Our observation thus is that RABV mapping does not reveal cell type-specific connectivity, as defined by spatially intermingled cells defined by neurochemical identity. In assessing the implications of this finding, it is worthwhile to consider our state of knowledge regarding spatial patterning and mechanisms that govern connectivity between neurons in the brain. Spatial patterning within the brain during development has been extensively studied, and the roles of families of patterning molecules such as ephrins, netrins, slits, and semaphorins have been well documented (Yu and Bargmann, 2001; Bashaw and Klein, 2010). Other surface proteins such as Teneurins, Tolls, DIPs, and Dprs may play roles in regulating connectivity at the cellular level (Hong et al., 2012; Ward et al., 2015; Barish et al., 2018). However, our understanding of the exact roles that these surface proteins play in dictating whether or not two neurons form connections, particularly in the rodent brain, is limited. It is important to note that we do not know the biases that RABV may have for spread to particular cell types in the brain, and it is possible that these biases are similar for all cell types and outweigh any actual differences in connectivity. Advances in RABV mapping technology, for example the development of a genetically barcoded RABV, may enable the exploration of the role that classes of surface proteins may play in defining connections between neurons (Saunders et al., 2021). However, it is also possible that the lack of cell type-specific connectivity revealed by RABV may be biologically meaningful. Such random connectivity patterns would then have implications for how connections at both the macro and micro-scales influence circuit output and animal behavior.

FUTURE DIRECTIONS

We and others have extensively mapped inputs and outputs of cells in the ventral midbrain and have detailed the role of spatial location in determining input patterns between different cell types (Beier et al., 2015, 2019; Lerner et al., 2015; Menegas et al., 2015). Our analysis in this study extends our previous observations. One next step is to determine if this finding applies to brain regions outside of the VTA. The observation that spatially intermingled cell populations tend to receive inputs from the same brain regions in quantitatively similar proportions supports the hypothesis that spatial location is the major determinant of global input patterns, at least as measured by one-step RABV mapping. However, the sources of spatial patterning of inputs and projection archetypes remain unknown. That brain regions sharing a common behavioral role have a similar projection pattern throughout the ventral midbrain suggests that these regions likely follow similar rules of patterning in the ventral midbrain, and this patterning in turn guides their preferential connectivity into particular cell types within the ventral midbrain. The identification of patterning molecules expressed during development and synapse formation through single cell RNA sequencing, for example, would help to elucidate what molecular pathways dictate projection patterns. It would also be interesting to test how ubiquitous this phenomenon of projection archetypes is throughout the brain and if it relates to projection-defined cells in a similar way as in the VTA. If so, the definition of projection archetypes during development along with spatial localization of projection-defined cell types may be one important generator of specificity in circuit connectivity in the brain.

MATERIALS AND METHODS

RABV Input and Axonal Arborization Output Tracing

Input and output mapping from VTA cells was described previously (Beier et al., 2015, 2019). Briefly, *DAT-Cre*, *GAD2-Cre*, *vGluT2-Cre*, and wild type C57Bl/6 mice were obtained and housed with 12 hour light/dark cycles and food and water *ad libitum* (Beier et al., 2019). Viral vectors were prepared as previously described (Schwarz et al., 2015). For TRIO experiments, *CAV-Cre* was injected into an output site, and Cre-dependent AAVs expressing the avian TVA protein as well as the rabies glycoprotein, RABV-G, were injected into the VTA. Two weeks later, EnvA-pseudotyped rabies virus (RABV) was injected into the VTA. These TRIO experiments thus labeled the inputs to VTA neurons with a specified output. We also performed cell-type specific TRIO (cTRIO) experiments. This included injecting a *CAV-FLEx^{loxP}-Flp* into a target output site and Flp-dependent AAVs expressing TVA and RABV-G into the VTA, and EnvA-pseudotyped RABV 2 weeks later. These cTRIO experiments labeled inputs to VTA neurons of a specific cell-type with a specified output. Rabies labeling experiments were also performed to cover conditions without an output target specified.

Axonal arborization experiments labeled the axons of VTA neurons with projections to a specified target. We performed similar CAV and AAV injections to the above, but rather than TVA and RABV-G we expressed a membrane-targeted GFP in targeted cells. This allowed us to view the entire axonal arbor of these cells. After 2 months, animals were perfused with PBS and 4% formaldehyde. For inputs, cells were counted manually using preselected regions. For both inputs and outputs, data were normalized by the total counts in each brain, accounting for differing levels of viral infection. Detailed protocols for input tracing and axon arborization can be found in previous publications (Beier et al., 2015, 2019).

Region Selection

Regions were selected for RABV input and axonal arborization output tracing according to previous publications (Beier et al., 2015, 2019). Notably, for VTA inputs we subdivided the global pallidus into the global pallidus external (GPe) and the entopeduncular nucleus (EP), the rodent equivalent of the GPi. For outputs, we subdivided the dorsal striatum into the dorsal lateral striatum (DLS) and dorsal medial striatum (DMS). Since the DLS does not substantially project to the VTA, and since the divide between the DMS and DLS is somewhat arbitrary, we did not subdivide the DStr for inputs. Here and previously we binned the anterior cortex into a single region. We previously subdivided the cortex into its composite regions, but did not find biased projections onto VTA cells according to cell type or projection (Beier et al., 2019). We did explore some substructures in the Allen Mouse Brain Connectivity Atlas analysis, including the orbital cortex, and the combined infralimbic and prelimbic cortical regions. For the amygdalar regions, we analyzed the central amygdala as an input site. For the projection site, we targeted the CeA, but we were not confident that our injections were completely restricted to this site, and hence we call these amygdala-projecting cells. It is likely that our VTA injections did not substantially induce DA cells located in the retrorubal field (RRF), where some have detected projections to amygdalar structures (Zahm et al., 2011).

Groupings of brain regions are listed below, in alphabetical order:

CeA–central amygdala lateral, medial, and capsular nuclei
Cortex–anterior cingulate cortex (ACC); infralimbic cortex (IL); insular cortex (Ins); motor cortex (MO; anterior portion); orbital cortex (Orb); prelimbic cortex (PL); somatosensory cortex (SS, anterior portion). This is the same composite structure as called the anterior cortex in Beier et al. (2015, 2019).
DR–as defined in Weissbourd et al. (2014).
EAM–anterior amygdaloid area, basomedial amygdala, anterior cortical amygdaloid nucleus, cortex-amygdala transition zone
LDT–laterodorsal tegmental area, dorsomedial tegmental area, dorsal tegmental nucleus, Barrington's nucleus, ventral tegmental nucleus, subpeduncular tegmental nucleus
PO–medial preoptic area, lateral preoptic area, lateral anterior hypothalamic area, anterior hypothalamic area, striohypothalamic nucleus
Septum–triangular septal nucleus, lateral septum, dorsal fornix, septofimbrial nucleus, medial septum, septohypothalamic nucleus, septohippocampal nucleus, lambdoid septal zone
VP–interstitial nucleus of posterior limb of anterior commissure (IPAC), substantia innominata, horizontal diagonal band, nucleus of the vertical diagonal band

Abbreviations for brain regions made throughout the paper are listed below, in alphabetical order:

BNST–bed nucleus of the stria terminalis
CeA–central amygdala
DCN–deep cerebellar nucleus
DR–dorsal raphe
DStr–dorsal striatum
EAM–extended amygdala
EP–entopeduncular nucleus (GPi)
GPe–globus pallidus (GPe)
LDT–laterodorsal tegmentum
LH–lateral hypothalamus
LHb–lateral habenula
MHb–medial habenula
NAcCore- nucleus accumbens, core
NAcMed–nucleus accumbens, medial shell
NAcLat–nucleus accumbens, lateral shell
PBN–parabrachial nucleus
PO–pre-optic area
PVH–paraventricular hypothalamus
VP–ventral pallidum
VTA–ventral tegmental area
ZI–zona incerta

Dimensional Reduction of Output and RABV Input Data

Principal Component Analysis (PCA) was used to dimensionally reduce both axon arborization output and RABV input data. PCA is a linear dimensional reduction technique that finds the maximal axes of variation through a dataset. Once a PCA embedding is found, each principal component can be unpacked to find out what linear combination of features (output sites or input sites), or weights, comprise it. Input and output counts per brain region were converted to fraction data to account for variation in total number of cells across brains. Fraction data were scaled so that variations in larger regions do not provide oversized contributions to PCA, compared to smaller regions. Analyses were performed in Python using Scikit-learn's PCA implementation (Pedregosa et al., 2011).

Uniform Manifold Approximation and Projection (UMAP) was used as a non-linear dimensional reduction technique on output and input data. UMAP is better optimized for finding local and global structures in high dimensional data than PCA, but it is far less interpretable. Analyses were performed using the official UMAP library (McInnes et al., 2018). The fractional counts data were z-scored to compare variation in output and input sites across regions with different magnitudes of counts. Z-scored data were dimensionally reduced with UMAP to find clusters of output and input sites with similar patterns of variation. UMAP parameters were tuned manually to optimize stability of clusters.

Regression Analysis of RABV Input Data

Linear regression was used to quantify the relationship of starter cell COM with the RABV input principal components. Slopes returned from the analysis reflect to what degree lateral and dorsal location increase, decrease, or have no effect on principal components. *p*-values give the probability of these slopes being 0 given the observed data. The statsmodels Python library was used to train these models and examine the slopes (Seabold and Perktold, 2010).

Logistic regression was used to classify the different projection conditions based on the RABV starter cell COMs and the RABV input principal components. To build a model for multiclass classification, we trained a separate logistic regression model to classify each projection condition. When evaluated against a given brain, the model prediction with the highest probability was used. Logistic regression coefficients represent the increased or decreased likelihood of the model prediction given a higher or lower value of a given feature. For example, a positive coefficient for Feature A means the model prediction increases in likelihood for higher values of Feature A and decreases for lower values. A negative coefficient has the opposite relationship; the model prediction increases in likelihood for lower values and decreases for higher values. The higher magnitude of the coefficient, the higher the importance of that feature on the prediction. The Scikit-learn implementation of logistic regression in Python was used for our analysis (Pedregosa et al., 2011).

Principal Component Analysis of Allen Mouse Brain Connectivity Data

For each of the input regions considered in the RABV experiments, we manually selected corresponding samples from the Allen Mouse Brain Connectivity Data. Experiments were selected based on whether or not the experiment contained labeled projections to the ventral midbrain. NAcLat was not included as an input site, as there were no samples that contained injections that were specific to NAcLat that also projected to the ventral midbrain. Cortex was subdivided into the orbital area and the combined infralimbic and prelimbic areas since our original quantification of RABV inputs included a broad spatial domain not encompassed by any single set of injections. The ID and hyperlink of each sample selected is provided in **Supplementary Table 1**. For each input region, the sample projections to the VTA were averaged together. Projections were sliced into a 42 pixel x 49 pixel rectangle to capture the largest coronal section of the VTA along with some of the surrounding area. PCA was used to find linear combinations of input regions that maximize variation across the pixels of this rectangle. PC values for each pixel were visualized on the original rectangular space to see how this variation is organized spatially within and around the VTA. These spatial projection "archetypes," revealed by each principal component's visualization, were compared to the primary regions that comprise them. Allen samples were accessed using the allensdk python library,[1] and PCA was performed using Scikit-learn (Pedregosa et al., 2011).

Allen and RABV Input Clustering Comparison

Clustering of input regions was compared between the RABV input data and the Allen Mouse Brain Connectivity Data (**Figures 5C,D,G,H**). Z-scoring was performed as before on the input data, capturing variation for each input across the samples. Z-scored data were dimensionally reduced with UMAP to find clusters of inputs with similar variations in each dataset. To account for variability in embeddings, we ran these embeddings 20 times for each dataset and took the average relative pairwise distance between each region. These pairwise distances were computed relative to the maximum distance between any two points in each embedding. Regions were hierarchically clustered based on this distance matrix and compared across datasets.

In order to assess how much clustering we might expect in a random dataset with a similar distribution, we shuffled both RABV and Allen datasets. The z-scored input values were shuffled independently for each region across samples. This eliminated any association between input values for each sample across regions. The clustering comparison analysis was repeated as above.

[1] https://github.com/AllenInstitute/AllenSDK

DATA AVAILABILITY STATEMENT

All code and data used to complete the analysis and generate the figures in this paper are publicly available in a repository on GitHub: https://github.com/pderdeyn/vtada-network.

ETHICS STATEMENT

The animal study was reviewed and approved by the University of California IACUC and the Stanford University IACUC.

AUTHOR CONTRIBUTIONS

PD performed computational analyses. MH made figures. KB organized the results and led manuscript writing and submission. All authors contributed to writing the manuscript.

FUNDING

This work was funded by NIH T32-GM136624 and NSF GRFP DGE-1839285 to PD, NIH DP2-AG067666, R00-D041445, R01-DA054374, TRDRP T31KT1437, and T31IP1426, One Mind OM-5596678, Alzheimer's Association AARG-NTF-20-685694, New Vision Research CCAD2020-002, and ADPA APDA-5589562 to KB, and NIH T32-GM008620 and TRDRP T31DT1729 to MH.

ACKNOWLEDGMENTS

We would like to thank Katrina Bartas for sharing code used to access the allensdk.

SUPPLEMENTARY MATERIAL

The Supplementary Material for this article can be found online at: https://www.frontiersin.org/articles/10.3389/fncir.2021.799688/full#supplementary-material

Supplementary Figure 1 | VTA^{DA} outputs without the four targeted projection sites. **(A)** Cumulative explained variance from each principal component. **(B)** Samples are plotted in PCA space for the 1st and 2nd components, colored by projection. **(C)** Samples are plotted in PCA space for the 1st and 3rd components, colored by projection. **(D)** Heatmap of each output region's contribution to the first three principal components. **(E)** Brains are plotted in UMAP space, colored by projection. **(F)** Output regions are plotted in UMAP space, embedded with respect to z-scores across mouse brains. Clusters represent outputs with similar patterns of variation across the cohort.

Supplementary Figure 2 | VTA input dimensional reduction without non-Cre and projection-undefined conditions. **(A)** Brains are plotted in PCA space for the 1st and 2nd components, colored by cell type. **(B)** Brains are plotted in PCA space for the 1st and 2nd components, colored by projection. **(C)** Brains are plotted in UMAP space, colored by cell type. **(D)** Brains are plotted in UMAP space, colored by projection.

Supplementary Figure 3 | Input and output z-scores stitched together for all cell types. **(A)** Z-scores of average input and output counts for each projection condition. Inputs are marked with a green down arrow and outputs with a red up arrow. Regions are sorted according to the projection in which they receive the highest rank.

Supplementary Figure 4 | Revealing RABV input PCs and starter cell locations that predict projection conditions. **(A)** Logistic regression coefficients for five principal components. Positive coefficients predict this condition when the feature is higher. Negative coefficients predict this condition when the feature is lower. Model scores are provided in **Table 3**. **(B)** Logistic regression coefficients for starter cell location. **(C)** Logistic regression coefficients for five principal components and starter cell location.

Supplementary Figure 5 | Projection portraits for all inputs from the Allen Brain Connectivity Atlas. All regions are in the same order as index from **Figure 4C**.

REFERENCES

Alheid, G. F., and Heimer, L. (1988). New perspectives in basal forebrain organization of special relevance for neuropsychiatric disorders: the striatopallidal, amygdaloid, and corticopetal components of substantia innominata. *Neuroscience* 27, 1–39. doi: 10.1016/0306-4522(88)90217-5

Barish, S., Nuss, S., Strunilin, I., Bao, S., Mukherjee, S., Jones, C. D., et al. (2018). Combinations of DIPs and Dprs control organization of olfactory receptor neuron terminals in *Drosophila*. *PLoS Genetics* 14:e1007560. doi: 10.1371/journal.pgen.1007560

Bashaw, G. J., and Klein, R. (2010). Signaling from axon guidance receptors. *Cold Spring Harb. Perspect. Biol.* 2, 1–16.

Beier, K. T. (2019). Hitchhiking on the neuronal highway?: mechanisms of transsynaptic specificity. *J. Chem. Neuroanat.* 99, 9–17. doi: 10.1016/j.jchemneu.2019.05.001

Beier, K. T. (2021). The Serendipity of viral trans-neuronal specificity: more than meets the eye. *Front. Cell. Neurosci.* 15:720807. doi: 10.3389/fncel.2021.720807

Beier, K. T., Gao, X. J., Xie, S., DeLoach, K. E., Malenka, R. C., Luo, L., et al. (2019). Topological organization of ventral tegmental area connectivity revealed by viral-genetic dissection of input-output relations. *Cell Rep.* 26, 159–167.e6. doi: 10.1016/j.celrep.2018.12.040

Beier, K. T., Steinberg, E. E., DeLoach, K. E., Xie, S., Miyamichi, K., Schwarz, L., et al. (2015). Circuit architecture of VTA dopamine neurons revealed by systematic input-output mapping. *Cell* 162, 622–634. doi: 10.1016/j.cell.2015.07.015

Bernard, J., and Besson, J. (1988). Convergence of nociceptive information on the parabrachio-amygdala neurons in the rat. *C R. Acad. Sci. III* 307, 841–847.

Bouarab, C., Thompson, B., and Polter, A. M. (2019). VTA GABA neurons at the interface of stress and reward. *Front. Neural Circuits* 13:78. doi: 10.3389/fncir.2019.00078

Chiang, M. C., Bowen, A., Schier, L. A., Tupone, D., Uddin, O., and Heinricher, M. M. (2019). Parabrachial complex: a hub for pain and aversion. *J. Neurosci.* 39, 8225–8230. doi: 10.1523/jneurosci.1162-19.2019

Chou, X. L., Wang, X., Zhang, Z.-G., Shen, L., Zingg, B., Huang, J., et al. (2018). Inhibitory gain modulation of defense behaviors by zona incerta. *Nat. Commun.* 9:1151. doi: 10.1038/s41467-018-03581-6

Han, S., Soleiman, M., Soden, M., Zweifel, L., and Palmiter, R. D. (2015). Elucidating an affective pain circuit that creates a threat memory. *Cell* 162, 363–374. doi: 10.1016/j.cell.2015.05.057

Hong, W., Mosca, T. J., and Luo, L. (2012). Teneurins instruct synaptic partner matching in an olfactory map. *Nature* 484, 201–207.

Kim, C. K., Yang, S. J., Pichamoorthy, N., Young, N. P., Kauvar, I., Jennings, J. H., et al. (2016). Simultaneous fast measurement of circuit dynamics at multiple sites across the mammalian brain. *Nat. Methods* 13, 325–328. doi: 10.1038/nmeth.3770

Kim, J. I., Ganesan, S., Luo, S. X., Wu, Y. W., Park, E., Huang, E. J., et al. (2015). Aldehyde dehydrogenase 1a1 mediates a GABA synthesis pathway in midbrain dopaminergic neurons. *Science* 350, 102–106. doi: 10.1126/science.aac4690

Kutlu, M. G., Zachry, J. E., Melugin, P. R., Cajigas, S. A., Chevee, M. F., Kelley, S. J., et al. (2021). Dopamine release in the nucleus accumbens core signals perceived saliency. *Curr. Biol.* 31, 4748–4761.e8. doi: 10.1016/j.cub.2021.08.052.

Lammel, S., Hetzel, A., Häckel, O., Jones, I., Liss, B., and Roeper, J. (2008). Unique properties of mesoprefrontal neurons within a dual mesocorticolimbic dopamine system. *Neuron* 57, 760–773. doi: 10.1016/j.neuron.2008.01.022

Lammel, S., Ion, D. I., Roeper, J., and Malenka, R. C. (2011). Report projection-specific modulation of dopamine neuron synapses by aversive and rewarding stimuli. *Neuron* 70, 855–862. doi: 10.1016/j.neuron.2011.03.025

Lammel, S., Lim, B. K., Ran, C., Huang, K. W., Betley, M. J., Tye, K. M., et al. (2012). Input-specific control of reward and aversion in the ventral tegmental area. *Nature* 491, 212–217. doi: 10.1038/nature11527

Lemos, J. C., Wanat, M. J., Smith, J. S., Reyes, B. A. S., Hollon, N. G., Van Bockstaele, E. G., et al. (2012). Severe stress switches CRF action in the nucleus accumbens from appetitive to aversive. *Nature* 490, 402–406. doi: 10.1038/nature11436

Lerner, T. N., Shilyansky, C., Davidson, T. J., Evans, K. E., Beier, K. T., Zalocusky, K. A., et al. (2015). Intact-Brain analyses reveal distinct information carried by SNc dopamine subcircuits. *Cell* 162, 635–647. doi: 10.1016/j.cell.2015.07.014

Lin, R., Liang, J., Wang, R., Yan, T., Zhou, Y., Liu, Y., et al. (2020). The raphe dopamine system controls the expression of incentive memory. *Neuron* 106, 498–514.e8.

Lutas, A., Kucukdereli, H., Alturkistani, O., Carty, C., Sugden, A. U., Fernando, K., et al. (2019). State-specific gating of salient cues by midbrain dopaminergic input to basal amygdala. *Nat. Neurosci.* 22, 1820–1833. doi: 10.1038/s41593-019-0506-500

Margolis, E. B., Lock, H., Hjelmstad, G. O., and Fields, H. L. (2006). The ventral tegmental area revisited: is there an electrophysiological marker for dopaminergic neurons? *J. Physiol.* 577, 907–924.

McInnes, L., Healy, J., Saul, N., and Großberger, L. (2018). UMAP: uniform manifold approximation and projection. *J. Open Source Softw.* 3:861.

Menegas, W., Bergan, J. F., Ogawa, S. K., Isogai, Y., Umadevi Venkataraju, K., Osten, P., et al. (2015). Dopamine neurons projecting to the posterior striatum form an anatomically distinct subclass. *eLife* 4:e10032. doi: 10.7554/eLife.10032

Morales, M., and Margolis, E. B. (2017). Ventral tegmental area: cellular heterogeneity, connectivity and behaviour. *Nat. Rev. Neurosci.* 18, 73–85.

Navratilova, E., Atcherley, C. W., and Porreca, F. (2015). Brain circuits encoding reward from pain relief. *Trends Neurosci.* 38, 741–750.

Oh, S. W., Harris, J. A., Ng, L., Winslow, B., Cain, N., Mihalas, S., et al. (2014). A mesoscale connectome of the mouse brain. *Nature* 508, 207–214.

Olds, J., and Milner, P. (1954). Positive reinforcement produced by electrical stimulation of septal area and other regions of rat brain. *J. Comp. Physiol. Psychol.* 47, 419–427. doi: 10.1037/h0058775

Pedregosa, F., Varoquaux, G., Gramfort, A., Michel, V., Thirion, B., Grisel, O., et al. (2011). Scikit-learn: machine learning in python. *J. Mach. Learn. Res.* 12, 2825–2830. doi: 10.1080/13696998.2019.1666854

Rogers, A., and Beier, K. T. (2021). Can transsynaptic viral strategies be used to reveal functional aspects of neural circuitry? *J. Neurosci. Methods* 348:109005. doi: 10.1016/j.jneumeth.2020.109005

Root, D. H., Mejias-Aponte, C. A., Zhang, S., Wang, H. L., Hoffman, A. F., Lupica, C. R., et al. (2014). Single rodent mesohabenular axons release glutamate and GABA. *Nat. Neurosci.* 17, 1543–1551.

Saunders, A., Huang, K. W., Vondrak, C., Hughes, C., Smolyar, K., Sen, H., et al. (2021). Ascertaining cells' synaptic connections and RNA expression simultaneously with massively barcoded rabies virus libraries. *bioRxiv [preprint]* doi: 10.1101/2021.09.06.459177

Schultz, W. (1998). Predictive reward signal of dopamine neurons. *J. Neurophysiol.* 80, 1–27. doi: 10.1152/jn.1998.80.1.1

Schwarz, L. A., Miyamichi, K., Gao, X., Beier, K., Charles Weissbourd, B., Deloach, K. E., et al. (2015). Viral-genetic tracing of the input–output organization of a central noradrenaline circuit. *Nature* 524, 88–92. doi: 10.1038/nature14600

Seabold, S., and Perktold, J. (2010). "Statsmodels: econometric and statistical modeling with python," in *Proceedings of the 9th Python in Science Conference* (Austin, TX), 92–96. doi: 10.25080/majora-92bf1922-011

Swanson, L. W. (1982). The projections of the ventral tegmental area and adjacent regions: a combined fluorescent retrograde tracer and immunofluorescence study in the rat. *Brain Res. Bull.* 9, 321–353. doi: 10.1016/0361-9230(82)90145-9

Tang, W., Kochubey, O., Kintscher, M., and Schneggenburger, R. (2020). A VTA to basal amygdala dopamine projection contributes to signal salient somatosensory events during fear learning. *J. Neurosci.* 40, 3969–3980. doi: 10.1523/jneurosci.1796-19.2020

Tritsch, N. X., Ding, J. B., and Sabatini, B. L. (2012). Dopaminergic neurons inhibit striatal output through non-canonical release of GABA. *Nature* 490, 262–266. doi: 10.1038/nature11466

Ungless, M. A., Singh, V., Crowder, T. L., Yaka, R., Ron, D., and Bonci, A. (2003). Corticotropin-releasing factor requires CRF binding protein to potentiate NMDA receptors *via* CRF receptor 2 in dopamine neurons. *Neuron* 39, 401–407. doi: 10.1016/s0896-6273(03)00461-6

Wall, N. R., De La Parra, M., Callaway, E. M., and Kreitzer, A. C. (2013). Differential innervation of direct- and indirect-pathway striatal projection neurons. *Neuron* 79, 347–360. doi: 10.1016/j.neuron.2013.05.014

Wanat, M. J., Hopf, F. W., Stuber, G. D., Phillips, P. E. M., and Bonci, A. (2008). Corticotropin-releasing factor increases mouse ventral tegmental area dopamine neuron firing through a protein kinase C-dependent enhancement of Ih. *J. Physiol.* 586, 2157–2170. doi: 10.1113/jphysiol.2007.150078

Ward, A., Hong, W., Favaloro, V., and Luo, L. (2015). Toll receptors instruct axon and dendrite targeting and participate in synaptic partner matching in a drosophila olfactory circuit. *Neuron* 85, 1013–1028. doi: 10.1016/j.neuron.2015.02.003

Watabe-Uchida, M., Zhu, L., Ogawa, S. K., Vamanrao, A., and Uchida, N. (2012). Whole-Brain mapping of direct inputs to midbrain dopamine neurons. *Neuron* 74, 858–873. doi: 10.1016/j.neuron.2012.03.017

Weissbourd, B., Ren, J., DeLoach, K. E., Guenthner, C. J., Miyamichi, K., Luo, L., et al. (2014). Presynaptic partners of dorsal raphe serotonergic and GABAergic neurons. *Neuron* 83, 645–662. doi: 10.1016/j.neuron.2014.06.024

Yetnikoff, L., Lavezzi, H. N., Reichard, R. A., and Zahm, D. S. (2014). An update on the connections of the ventral mesencephalic dopaminergic complex. *Neuroscience* 282, 23–48. doi: 10.1016/j.neuroscience.2014.04.010

Yu, T. W., and Bargmann, C. I. (2001). Dynamic regulation of axon guidance. *Nat. Neurosci.* 4, 1169–1176. doi: 10.1038/nn748

Zahm, D. S. (2006). The evolving theory of basal forebrain functional - anatomical 'macrosystems'. *Neurosci. Biobehav. Rev.* 30, 148–172. doi: 10.1016/j.neubiorev.2005.06.003

Zahm, D. S., Cheng, A. Y., Lee, T. J., Ghobadi, C. W., Schwartz, Z. M., Geisler, S., et al. (2011). Inputs to the midbrain dopaminergic complex in the rat, with emphasis on extended amygdala-recipient sectors. *J. Comp. Neurol.* 519, 3159–3188. doi: 10.1002/cne.22670

Zhou, M., Liu, Z., Melin, M. D., Ng, Y. H., Xu, W., Südhof, T. C., et al. (2018). A central amygdala to zona incerta projection is required for acquisition and remote recall of conditioned fear memory. *Nat. Neurosci.* 21, 1515–1519. doi: 10.1038/s41593-018-0248-4

Conflict of Interest: The authors declare that the research was conducted in the absence of any commercial or financial relationships that could be construed as a potential conflict of interest.

Publisher's Note: All claims expressed in this article are solely those of the authors and do not necessarily represent those of their affiliated organizations, or those of the publisher, the editors and the reviewers. Any product that may be evaluated in this article, or claim that may be made by its manufacturer, is not guaranteed or endorsed by the publisher.

Copyright © 2022 Derdeyn, Hui, Macchia and Beier. This is an open-access article distributed under the terms of the Creative Commons Attribution License (CC BY). The use, distribution or reproduction in other forums is permitted, provided the original author(s) and the copyright owner(s) are credited and that the original publication in this journal is cited, in accordance with accepted academic practice. No use, distribution or reproduction is permitted which does not comply with these terms.

Advantages of publishing in Frontiers

OPEN ACCESS
Articles are free to read for greatest visibility and readership

FAST PUBLICATION
Around 90 days from submission to decision

HIGH QUALITY PEER-REVIEW
Rigorous, collaborative, and constructive peer-review

TRANSPARENT PEER-REVIEW
Editors and reviewers acknowledged by name on published articles

Frontiers
Avenue du Tribunal-Fédéral 34
1005 Lausanne | Switzerland

Visit us: www.frontiersin.org
Contact us: frontiersin.org/about/contact

REPRODUCIBILITY OF RESEARCH
Support open data and methods to enhance research reproducibility

DIGITAL PUBLISHING
Articles designed for optimal readership across devices

FOLLOW US
@frontiersin

IMPACT METRICS
Advanced article metrics track visibility across digital media

EXTENSIVE PROMOTION
Marketing and promotion of impactful research

LOOP RESEARCH NETWORK
Our network increases your article's readership